НАУЧНО-ПРАКТИЧЕСКИЙ ЖУРНАЛ

БЮЛЛЕТЕНЬ СИБИРСКОЙ МЕДИЦИНЫ

ISSN 1682-0363 (print)
ISSN 1819-3684 (online)

BULLETIN OF SIBERIAN MEDICINE

Том 25
№ 2. 2026

СИБИРСКИЙ ГОСУДАРСТВЕННЫЙ МЕДИЦИНСКИЙ УНИВЕРСИТЕТ

ТОМСКИЙ НАЦИОНАЛЬНЫЙ ИССЛЕДОВАТЕЛЬСКИЙ МЕДИЦИНСКИЙ ЦЕНТР РОССИЙСКОЙ АКАДЕМИИ НАУК

НИИ фармакологии и регенеративной медицины им. Е.Д. Гольдберга

ВСЕРОССИЙСКАЯ КОНФЕРЕНЦИЯ С МЕЖДУНАРОДНЫМ УЧАСТИЕМ «ПАТОФИЗИОЛОГИЯ: ПРОШЛОЕ, НАСТОЯЩЕЕ И БУДУЩЕЕ», ПОСВЯЩЕННАЯ 80-ЛЕТИЮ СО ДНЯ РОЖДЕНИЯ АКАДЕМИКА РАН ВЯЧЕСЛАВА ВИКТОРОВИЧА НОВИЦКОГО

г. Томск, 23-24 сентября 2026 года

Сибирский государственный медицинский университет
НИИ фармакологии и регенеративной медицины имени Е.Д. Гольдберга
Томского НИМЦ

Глубокоуважаемые коллеги!

Сибирский государственный медицинский университет (СибГМУ) совместно с НИИ фармакологии и регенеративной медицины имени Е.Д. Гольдберга Томского НИМЦ (НИИФиРМ им. Е.Д. Гольдберга Томского НИМЦ) проводит Всероссийскую конференцию с международным участием «Патофизиология: прошлое, настоящее и будущее», посвященную 80-летию со дня рождения академика РАН Вячеслава Викторовича Новицкого – одного из ярчайших представителей отечественной медицинской науки, лидера томской научной школы специалистов по общей патологии и патофизиологии, почетного гражданина города Томска.

Конференция будет охватывать широкий спектр вопросов патологической физиологии, отражающих вклад учёного в развитие науки и медицины.

ОСНОВНЫЕ НАПРАВЛЕНИЯ:

1. Исторический экскурс в прошлое патофизиологии в Томске и роль академика РАН В.В. Новицкого в развитии томской научной школы патофизиологов;
2. Патофизиология в медицинской практике: тенденции и междисциплинарные подходы в изучении болезней;
3. Перспективы развития патофизиологии в условиях современных технологий: глобальные вызовы и пути их преодоления.

Данная конференция призвана объединить исследователей для обсуждения ключевых аспектов патофизиологии, её истории, текущего состояния и перспектив дальнейшего развития.

КОНТАКТЫ

634050, Томская область, г. Томск, Московский тракт, 2
ФГБОУ ВО Сибирский государственный
медицинский университет Минздрава России
+7 (903) 913-14-83
заведующий кафедрой патофизиологии СибГМУ,
член-корр. РАН
Ольга Ивановна Уразова
e-mail: pathophysiologist80org@ya.ru

BULLETIN OF SIBERIAN MEDICINE

Peer-reviewed scientific-practical journal
Issued quarterly

Volume 25, No. 2, 2026

ISSN 1682-0363 (print)
ISSN 1819-3684 (online)

FOUNDER AND PUBLISHER:
Siberian State Medical University, Ministry of Healthcare of the Russian Federation

Registered by the Ministry of Mass Media and Communications of the Russian Federation
Certificate of registration
No. 77-7366 of 26.03.2001

The journal "Bulletin of Siberian Medicine" is included in the list of peer-reviewed scientific journals and publications issued in the Russian Federation, which should publish main scientific results of doctoral and Candidate of Sciences theses

Bulletin of Siberian Medicine is indexed in:
Scopus (2018–2023)
Web of Science (WoS (ESCI))
Science Index
RSCI
Ulrich's International Periodicals Directory
Cyberleninka
DOAS

Editorial Board Office:
107 Lenina Ave., 634050 Tomsk, Russian Federation
Telephone: +7-(382-2)-51-41-53.
http://bulletin.ssmu.ru
E-mail: bulletin.tomsk@mail.ru

Publisher: Siberian State Medical University.
2 Moskovsky trakt, Tomsk, 634050,
Russian Federation.
Editors: E.E. Stepanova, Yu.P. Gotfrid
Translators: E.Yu. Skvortsova, M.E. Chirikova
Electronic makeup, cover design: L.D. Krivtsova

Printed in Litburo LLC,
4 Koroleva St., Tomsk, 634055 Russian Federation

Signed to print on 26.06.2026
Format 60 × 84/8. Offset print.
Coated paper. Times font.
P.s. 24,25. C.p.s. 24.
500 copies. Order No. 388.

The price – free.
Date of publication 30.06.2026.

БЮЛЛЕТЕНЬ СИБИРСКОЙ МЕДИЦИНЫ

Научно-практический журнал
Выходит 4 раза в год

Том 25, № 2, 2026

ISSN 1682-0363 (print)
ISSN 1819-3684 (online)

УЧРЕДИТЕЛЬ И ИЗДАТЕЛЬ:
ФГБОУ ВО «Сибирский государственный медицинский университет» Минздрава России

Журнал основан в 2001 году
Зарегистрирован в Министерстве РФ по делам печати, телерадиовещания и средств массовых коммуникаций
Свидетельство регистрации ПИ № 77-7366 от 26.03.2001 г.

Журнал входит в Перечень ведущих рецензируемых научных журналов и изданий, выпускаемых в РФ, в которых должны быть опубликованы основные научные результаты диссертаций на соискание ученой степени доктора и кандидата наук

Индексация:
Scopus (годы охвата: 2018–2023)
Web of Science (WoS (ESCI))
РИНЦ (Science Index)
RSCI
Ulrich's International Periodicals Directory
Cyberleninka
DOAS

Редакция:
634050, г. Томск, пр. Ленина, 107.
Тел.: (382-2)-51-41-53.
http://bulletin.ssmu.ru
E-mail: bulletin.tomsk@mail.ru

Оригинал-макет:
Издательство СибГМУ.
634050, г. Томск, Московский тракт, 2.
Редакторы: Е.Е. Степанова, Ю.П. Готфрид
Перевод: Е.Ю. Скворцова, М.Е. Чирикова
Электронная верстка, дизайн обложки: Л.Д. Кривцова

Отпечатано в ООО «Литбюро»,
634055, г. Томск, ул. Королёва, 4.

Подписано в печать 26.06.2026 г.
Формат 60 × 84/8. Печать офсетная.
Бумага мелованная. Гарнитура «Times».
Печ. л. 24,25. Усл. печ. л. 24.
Тираж 500 экз. Заказ 388.

Цена – свободная.
Дата выхода в свет 30.06.2026.

СОДЕРЖАНИЕ

CONTENTS

ОРИГИНАЛЬНЫЕ СТАТЬИ

ORIGINAL ARTICLES

УДК 616.12-005.4:616.399:615.27
https://doi.org/10.20538/1682-0363-2026-2-5-12

Effects of Metformin on Ceramide Production in Local Fat Depots in Patients with Coronary Artery Disease

Dyleva Yu.A.[1], Gorbatovskaya E.E.[1, 2], Dolmatova S.E.[1, 2], Ivanov S.V.[1], Fanaskova E.V.[1], Gruzdeva O.V.[1, 2]

[1] *Research Institute for Complex Issues of Cardiovascular Diseases*
6 Academician Barbarash Blvd., 650002 Kemerovo, Russian Federation

[2] *Kemerovo State Medical University*
22a Voroshilov St., 650029 Kemerovo, Russian Federation

ABSTRACT

Aim. To evaluate the effects of metformin on the expression level of ceramide synthesis enzyme genes, and on the total content and spectrum of ceramides in local fat depots in patients with coronary heart disease (CHD).

Materials and methods. The study included 41 patients with CHD, who were scheduled to undergo coronary artery bypass grafting. Samples of subcutaneous, epicardial, and perivascular adipose tissue (SAT, EAT, and PVAT) were obtained during surgery, adipose tissue adipocytes were isolated and cultured for 24 hours with the addition of metformin (Sigma-Aldrich, USA) at concentrations of 1 and 10 mmol/l. The expression characteristics of *de novo* ceramide synthesis enzymes were assessed by quantitative polymerase chain reaction on a ViiA 7 amplifier (Applied Biosystems, USA). The total content and spectrum of ceramides (Cer) were determined by high-performance liquid chromatography with mass spectrometry (HPLC-MS/MS). Statistical processing of the results was performed using the STATISTICA 12 software package.

Results. Metformin at a concentration of 1 mmol/l statistically significantly decreased the gene expression of the enzymes serine palmitoyltransferase-1 (SPTLC1) in SAT, EAT and PVAT, ceramide synthase-2 (CERS2) in EAT and SAT, ceramide synthase-4 (CERS4) in EAT and PVAT, and increased dihydroceramide desaturase (DEGS1) in EAT and SAT. Metformin at a concentration of 10 mmol/l decreased the level of SPTLC1 and CERS2 mRNA in EAT, CERS4 in EAT and PVAT. A significant decrease in the content of Cer d18:1/16:0 in EAT at a metformin concentration of 1 mmol/l, and Cer d18:1/18:0 in EAT and PVAT, Cer d18:1/20:0 in SAT and EAT at concentrations of 1 and 10 mmol/l was revealed.

Conclusion. Thus, the potential ability of metformin to inhibit *de novo* ceramide synthesis in isolated SAT, EAT and PVAT adipocytes and to reduce the content of ceramides associated with adverse cardiovascular events in fat cells was demonstrated in *in vitro* experiments.

Keywords: ceramides, metformin, adipose tissue, coronary heart disease

Conflict of interest. The authors declare the absence of obvious or potential conflicts of interest related to the publication of this manuscript.

Source of financing. This study was supported by the Complex Program of Basic Research under the Siberian Branch of the Russian Academy of Sciences within the Basic Research Topic of the Research Institute for Complex Issues of Cardiovascular Diseases No. 0419-2022-0002 “Development of Innovative Models for Managing the Risk of Developing Diseases of the Circulatory System, Taking into Account Comorbidity Based on the Study of Fundamental, Clinical, and Epidemiological Mechanisms and Organizational Technologies of Medical Care in the Industrial Region of Siberia”.

Conformity with the principles of ethics. All individuals signed an informed consent to participate in the study. The study was approved by the Ethics Committee of the Research Institute for Complex Issues of Cardiovascular Diseases (Minutes No. 12 dated March 20, 2023).

✉ *Gorbatovskaya Evgeniya E.,* eugenia.tarasowa@yandex.ru

For citation: Dyleva Yu.A., Gorbatovskaya E.E., Dolmatova S.E., Ivanov S.V., Fanaskova E.V., Gruzdeva O.V. Effects of Metformin on Ceramide Production in Local Fat Depots in Patients with Coronary Artery Disease. *Bulletin of Siberian Medicine.* 2026;25(2):5–12. https://doi.org/10.20538/1682-0363-2026-2-5-12.

Эффекты метформина на продукцию церамидов в локальных жировых депо у пациентов с ишемической болезнью сердца

Дылева Ю.А.[1], Горбатовская Е.Е.[1, 2], Долматова С.Е.[1, 2], Иванов С.В.[1], Фанаскова Е.В.[1], Груздева О.В.[1, 2]

[1] *Научно-исследовательский институт комплексных проблем сердечно-сосудистых заболеваний (НИИ КПССЗ)*
Россия, 650002, г. Кемерово, б-р им. академика Л.С. Барбараша, стр. 6

[2] *Кемеровский государственный медицинский университет*
Россия, 650056, г. Кемерово, ул. Ворошилова, 22а

РЕЗЮМЕ

Цель: оценить эффекты метформина на уровень экспрессии генов ферментов синтеза церамидов и общее содержание и спектр церамидов в локальных жировых депо у пациентов с ишемической болезнью сердца (ИБС).

Материалы и методы. В исследование включен 41 пациент с ИБС, которому планировалось проведение аортокоронарного шунтирования. Образцы подкожной, эпикардиальной и периваскулярной жировой ткани (ПЖТ, ЭЖТ и ПВЖТ) были получены во время оперативного вмешательства, адипоциты ЖТ изолировали и культивировали в течение суток с добавлением метформина (Sigma-Aldrich, США) в концентрациях 1 и 10 ммоль/л. Оценку экспрессии ферментов синтеза церамидов *de novo* проводили методом количественной полимеразной цепной реакции на амплификаторе ViiA 7 (Applied Biosystems, США). Общее содержание и спектр церамидов (Cer) устанавливали методом высокоэффективной жидкостной хроматографии с масс-спектрометрическим детектированием (ВЭЖХ-МС/МС). Статистическую обработку результатов осуществляли с использованием программного пакета Statistica 12.

Результаты. Метформин в концентрации 1 ммоль/л статистически значимо снижал генную экспрессию ферментов серинпальмитоилтрансферазы-1 (SPTLC1) в ПЖТ, ЭЖТ и ПВЖТ, церамидсинтазы-2 (CERS2) в ЭЖТ и ПЖТ, церамидсинтазы-4 (CERS4) в ЭЖТ и ПВЖТ и повышал экспрессию ферментов дигидроцерамиддесатуразы (DEGS1) в ЭЖТ и ПЖТ. Метформин в концентрации 10 ммоль/л снижал уровень мРНК SPTLC1 и CERS2 в ЭЖТ, CERS4 в ЭЖТ и ПВЖТ. Выявлено снижение содержания Cer d18:1/16:0 в ЭЖТ при концентрации метформина 1 ммоль/л и Cer d18:1/18:0 в ЭЖТ и ПВЖТ, Cer d18:1/20:0 в ПЖТ и ЭЖТ при концентрациях 1 и 10 ммоль/л.

Заключение. Показана потенциальная способность метформина в экспериментах *in vitro* ингибировать синтез церамидов *de novo* в изолированных адипоцитах ПЖТ, ЭЖТ и ПВЖТ и снижать содержание в жировых клетках церамидов, ассоциированных с неблагоприятными сердечно-сосудистыми событиями.

Ключевые слова: церамиды, метформин, жировая ткань, ишемическая болезнь сердца

Конфликт интересов. Авторы декларируют отсутствие явных и потенциальных конфликтов интересов, связанных с публикацией настоящей статьи.

Источник финансирования. Исследование выполнено в рамках фундаментальной темы НИИ КПССЗ № 0419-2022-0002 «Разработка инновационных моделей управления риском развития болезней системы кровообращения с учетом коморбидности на основе изучения фундаментальных, клинических, эпидемиологических механизмов и организационных технологий медицинской помощи в условиях промышленного региона Сибири».

Соответствие принципам этики. Все лица подписали информированное согласие на участие в исследовании. Исследование одобрено локальным этическим комитетом НИИ КПССЗ (протокол № 12 от 20.03.2023).

Для цитирования: Дылева Ю.А., Горбатовская Е.Е., Долматова С.Е., Иванов С.В., Фанаскова Е.В., Груздева О.В. Эффекты метформина на продукцию церамидов в локальных жировых депо у пациентов с ишемической болезнью сердца. *Бюллетень сибирской медицины.* 2026;25(2):5–12. https://doi.org/10.20538/1682-0363-2026-2-5-12.

INTRODUCTION

Metformin is the oldest first-line oral hypoglycemic agent for patients with type 2 diabetes mellitus (T2DM). Over the past two decades, metformin has demonstrated a number of beneficial effects beyond its efficacy in the context of hypoglycemic therapy, both in experimental models and in clinical trials.

Among the drug's most significant pleiotropic effects are its cardioprotective properties [1] and its impact on modifiable cardiovascular risk factors, such as dyslipidemia, obesity, and insulin resistance [2–4], suppression of oxidative stress in vascular cells, and reduction of inflammatory responses [5–7]. Furthermore, there is growing evidence demonstrating the efficacy of metformin in secondary cardiovascular prevention [8]. Pleiotropic effects are likely mediated, as demonstrated in studies, through the drug's ability to suppress adipocyte differentiation and modulate their functional activity, reducing adipose tissue inflammation, thereby potentially reducing the risk of cardiac fibrosis, which leads to structural changes and systolic and diastolic myocardial dysfunction.

Using untargeted and targeted lipidomics methods, a comprehensive and advanced analytical approach to studying lipidome changes, the effect of metformin on the serum lipidome in obesity and diabetes mellitus was assessed. The drug demonstrated positive effects by significantly reducing certain lipid classes, the role of which has been demonstrated in the development of obesity, diabetes mellitus, and cardiovascular disease [9–12]. Furthermore, adipose tissue (AT) of the heart and blood vessels can also act as a potential source of complex lipids, as its epicardial and perivascular compartments are located in close proximity to atherosclerotic lesions.

In this regard, the class of sphingolipids, especially ceramides, is of particular interest, as experimental and clinical studies have shown their association with the development and progression of atherosclerosis [13, 14]. Currently, the question remains open as to whether metformin is capable of modulating the functional activity of local cardiac fat depots and regulating the synthesis of ceramides associated with coronary diseases.

This study aimed to evaluate the effect of metformin on the level of expression of enzyme-encoding genes responsible for *de novo* synthesis of ceramides and the total content and spectrum of ceramides in local fat depots in patients with coronary heart disease (CHD).

MATERIALS AND METHODS

The inclusion criteria for the study were the presence of stable CHD and indications for coronary artery bypass grafting (CABG). Exclusion criteria were as follows: age over 75 years, myocardial infarction, carbohydrate metabolism disorders (T1DM and T2DM), and the presence of clinically significant comorbidities (renal failure, liver failure, anemia, acute oncological and infectious and inflammatory diseases, and autoimmune diseases).

Thus, the study included 41 patients meeting the inclusion and exclusion criteria. The study was approved by the local Ethics Committee of the Research Institute for Complex Issues of Cardiovascular Diseases (Minutes No. 12 dated March 20, 2023) and complied with the principles of good clinical practice and the principles of the World Medical Association's Declaration of Helsinki, taking into account the amendments adopted in 2013, as well as the "Rules of Clinical Practice in the Russian Federation" (Order of the Ministry of Health of the Russian Federation No. 266 dated June 19, 2003).

All patients had their medical history taken upon admission to the hospital, their height (m) and weight (kg) were measured, and their body mass index (BMI, kg/m^2) was calculated. The clinical characteristics of the patients are presented in Table 1.

Table 1

Clinical Characteristics of Patients with Coronary Heart Disease

Parameter	CHD patients, $n = 41$
Male gender, *n* (%)	27 (66)
Age, years, *Me* (Q_{25}; Q_{75})	66.2 (48.5;70.3)
Body mass index, kg/m^2, *Me* (Q_{25}; Q_{75})	26.9 (22.1;29.7)
History of myocardial infarction, *n* (%)	30 (73)
History of CHD, *n* (%)	21 (56)
Arterial hypertension, *n* (%)	25 (61)
Dyslipidemia, *n* (%)	20 (49)
Smoking, *n* (%)	21 (56)
Acute cerebrovascular accident, *n* (%)	3 (7)
Atherosclerosis of one coronary artery, *n* (%)	6 (15)
Atherosclerosis of two coronary arteries, *n* (%)	7 (17)
Atherosclerosis of three or more coronary arteries, *n* (%)	28 (68)
Atherosclerosis of other vascular basins, *n* (%)	8 (20)
Class I heart failure, *n* (%)	28 (68)

End of table 1

Parameter	CHD patients, $n = 41$
Class II heart failure, *n* (%)	13 (32)
Class III heart failure, *n* (%)	0
Class IV heart failure, *n* (%)	0
No angina pectoris, *n* (%)	3 (7)
Class I angina pectoris, *n* (%)	0
Class II angina pectoris, *n* (%)	14 (34)
Class III angina pectoris, *n* (%)	24 (57)
Class IV angina pectoris, *n* (%)	0
Ejection fraction, %, *Me* (Q_{25}; Q_{75})	53.6 (46.3;58.9)
Aspirin, *n* (%)	38 (93)
Clopidogrel, *n* (%)	6 (15)
β-blockers, *n* (%)	37 (90)
Angiotensin-converting enzyme inhibitors, *n* (%)	31 (76)
Statins, *n* (%)	41 (100)
Ca-channel blockers, *n* (%)	31 (76)
Nitrates, *n* (%)	1 (2)
Diuretics, *n* (%)	33 (81)

Note. Class is functional class according to NYHA.

Patients' medical histories often included cardiovascular risk factors, such as hypertension, dyslipidemia, and smoking. Left ventricular ejection fraction calculated according to the Teicholz formula was preserved. During their hospital stay, patients received standard medications in accordance with the guidelines of the Ministry of Health of the Russian Federation (2020) and the European Society of Cardiology (2020) (Table 1).

Obtaining cardiac adipose tissue samples and isolating adipocytes were performed according to a previously described method [15]. To assess the effect of the drug on the functional activity of adipocytes in subcutaneous, epicardial, and perivascular adipose tissue (SAT, EAT, and PVAT, respectively), the cells were cultured for 24 hours with the addition of metformin (Sigma-Aldrich, USA) at concentrations of 1 and 10 mmol/l. To obtain the required concentrations, metformin was diluted with complete culture medium M199 containing a glucose solution at a concentration of 5.3 mmol/l and dexamethasone 10^{-9}M. These substances are necessary to create a state of adipocytes in the body that is as close as possible to the physiological state.

Next, 2 x 106 adipocytes were added to the wells of a sterile 24-well plate (Greiner, Germany) and brought to a volume of 1 ml with complete M199 culture medium containing glucose at a final concentration of 5.3 mmol/l, dexamethasone 10^{-9}M, and metformin at the specified concentration. The cells were cultured for 24 hours in a CO_2 incubator (CB-53, BINDER, Germany) at 37°C and 5% CO_2. After the incubation period, the cultured cells were carefully removed for subsequent gene expression determination.

The expression of ceramide synthesis enzymes in isolated adipocytes was assessed by quantitative polymerase chain reaction on a ViiA 7 amplifier (Applied Biosystems, USA) using primers (Eurogen, Russia) indicated in Table 2.

Table 2

Nucleotide Sequences in the Primers of Enzymes Involved in *de novo* Ceramide Synthesis

Gene	Sequence Direction	Sequence (5'->3')	Primer Length
Serine palmitoyltransferase long chain base subunit 1 *(SPTLC1)*	Forward primer	aggaagcggctaactatggc	20
	Reverse primer	ccagaggatcagaatcccttcc	22
Ceramide synthase 2 *(CERS2)*	Forward primer	ggacgtgtctacgccaaagc	20
	Reverse primer	atgttcaagagggcagccagt	21
Ceramide synthase 4 *(CERS4)*	Forward primer	caggacttgttggcagccct	20
	Reverse primer	cgttgggcttcacttgcctc	20
Delta 4-desaturase, sphingolipid 1 *(DEGS1)*	Forward primer	ccactgagctggagtttcct	20
	Reverse primer	caggaattgtagtgagggaggt	22

The total content and spectrum of ceramides (Cer) in adipocytes were assessed by high-performance liquid chromatography with mass spectrometry to identify precursor ions of the fragment with m/z 264 in the mass/charge ratio range from 500 to 700 (HPLC-MS). First, liquid–liquid extraction was performed using chloroform, methanol, and water. Calculation of ceramide concentrations was performed using calibration standards (ng/ml). The HPLC-MS/MS system consisted of a Sciex QTRAP 5500 tandem triple quadrupole mass spectrometric detector (ab Sciex, USA) and an Agilent 1260

Infinity liquid chromatograph (Agilent Technologies, USA). For chromatographic determination of ceramides in adipose tissue adipocytes, a ZORBAX Eclipse XDB-C18 column, 2.1 × 100 mm, 1.8 μm (Agilent Technologies, USA) with a Security Guard precolumn (Phenomenex, USA) was used. Ceramide identification was performed using LipidMatch scripts and the LipidMaps lipid nomenclature.

Statistical processing was performed using the Statistica 12 software package. Quantitative data were presented as the median and the interquartile range *Me* (Q_{25}; Q_{75}), while qualitative data were presented as frequency indices in absolute and relative units *n* (%). Intergroup differences were determined using nonparametric tests. Three dependent groups were compared using the Friedman test, and pairwise comparisons were performed using the Wilcoxon test. Using the Bonferroni correction, the critical level of significance was taken to be $p \leq 0.017$ when comparing three study groups; when comparing two groups, differences were considered as statistically significant at $p < 0.05$.

RESULTS

Metformin was found to modulate the functional activity of cardiac adipose tissue adipocytes. Concentrations of 1 and 10 mmol/l metformin had consistent effects on the gene expression of *de novo* ceramide synthesis enzymes in cultured subcutaneous, epicardial, and perivascular adipocytes from individuals with CHD. However, the effect of the drug at a concentration of 1 mmol/l was more pronounced than at 10 mmol/l. Among patients with coronary heart disease, decreased gene expression of the enzyme encoding the first step in *de novo* ceramide synthesis, serine palmitoyltransferase-1 *(SPTLC1)*, was observed in SAT, EAT, and PVAT (Figure).

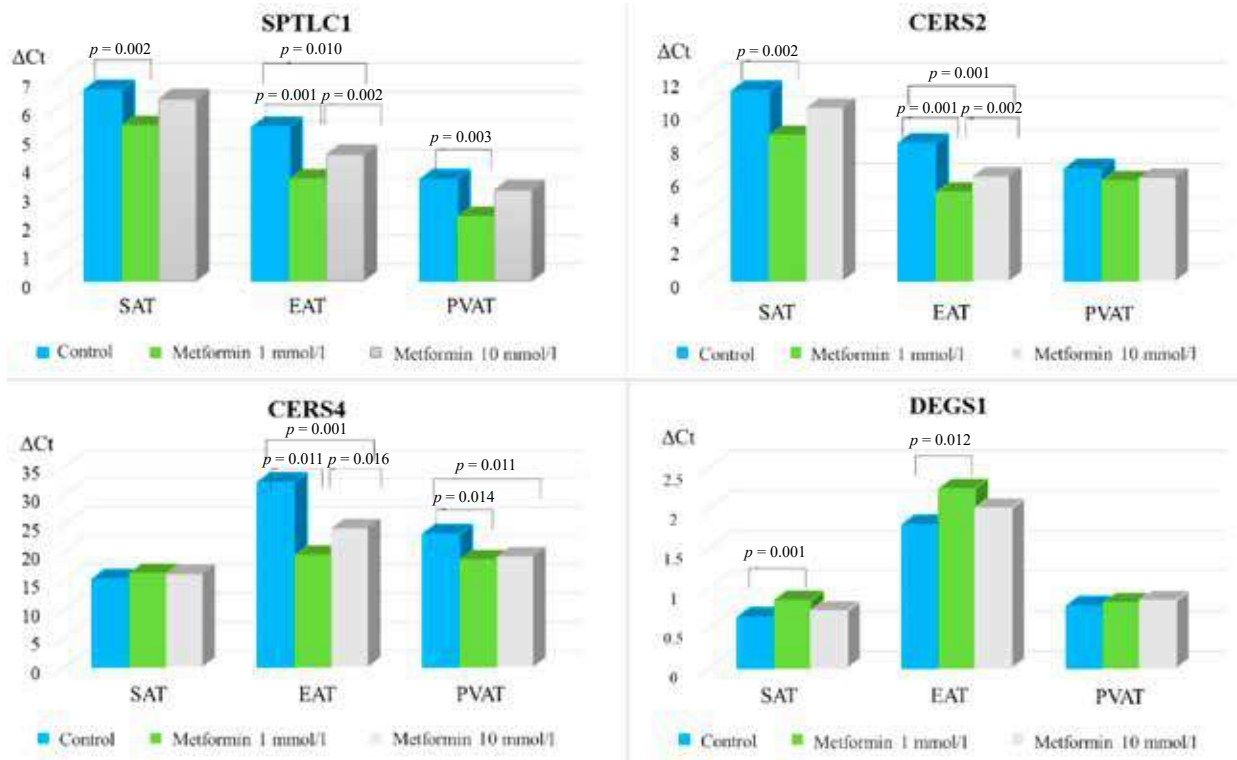

Figure. Evaluation of the effect of metformin on the expression levels of serine palmitoyltransferase-1 *(SPTLC1),* ceramide synthase 2 *(CERS2),* ceramide synthase 4 *(CERS4),* and delta 4-desaturase, sphingolipid 1 *(DEGS1)* in adipocytes of various locations in patients with coronary heart disease. ΔCt (delta Ct) is the difference between the threshold cycles (Ct) for the gene under study and the reference gene in the same sample

In patients with CHD, metformin at a concentration of 1 mmol/l suppressed the expression of genes encoding enzymes responsible for ceramide species diversity: ceramide synthase-4 *(CERS4*) in EAT and PVAT, and ceramide synthase-2 *(CERS2*) in EAT and SAT, which synthesize ceramides with a long hydrocarbon chain of C16-C24. Furthermore, metformin at a concentration of 1 mmol/l increased

the expression level of the delta 4-desaturase, sphingolipid 1 *(DEGS1)* gene, an enzyme involved in the final stage of *de novo* ceramide synthesis in EAT and SAT.

Ceramides containing saturated fatty acid residues were detected in patients with CHD: Cer d18:1/16:0, Cer d18:1/18:0, Cer d18:1/20:0, and Cer d18:1/24:0. Metformin at concentrations of 1 and 10 mmol/l was shown to modulate ceramide levels in adipocytes. The effects of metformin were consistent with the identified patterns of changes in gene expression of enzymes involved in *de novo* ceramide synthesis. Metformin had a unidirectional effect regardless of concentration. However, the effect of the drug at a concentration of 1 mmol/l on the levels of some ceramides was more pronounced.

Adipocytes in the epicardial region were most susceptible to the effects of metformin. A significant decrease in the content of Cer d18:1/16:0, Cer d18:1/18:0, and Cer d18:1/20:0 in EAT was observed. In perivascular adipocytes, only the level of Cer d18:1/18:0 decreased, while in subcutaneous adipocytes, Cer d18:1/20:0 decreased. Metformin had no statistically significant effect on the production of Cer d18:1/24:0 (Table 3).

Table 3

Evaluation of Ceramide Concentration in Adipocytes of Local Fat Depots of Patients with Coronary Heart Disease with the Addition of Metformin, *Me* (Q_{25}; Q_{75})

Ceramides, ng/ml	SAT			EAT			PVAT		
	C	1 mmol/l	10 mmol/l	C	1 mmol/l	10 mmol/l	C	1 mmol/l	10 mmol/l
	1	2	3	4	5	6	7	8	9
Cer d18:1/16:0	42.18 (21.07; 49.28)	44.20 (22.03; 50.32)	45.16 (22.21; 51.2)	75.33 (53.07; 87.25)	60.07 (47.82; 79.45)	71.21 (51.17; 86.02)	37.67 (32.13; 51.04)	35.61 (29.53; 49.81)	36.35 (28.44; 45.22)
	$p_{Ft} \geq 0.05$			$p_{Ft} = 0.012$ $p_{Wt4,5} = 0.021$			$p_{Ft} \geq 0.05$		
Cer d18:1/18:0	12.04 (9.22; 15.91)	13.00 (9.27; 16.42)	13.03 (9.32; 16.63)	25.27 (17.15; 30.37)	15.32 (10.22; 19.54)	19.63 (11.53; 21.64)	18.75 (11.03; 23.68)	15.13 (10.30; 20.63)	15.60 (10.61; 23.21)
	$p_{Ft} \geq 0.05$			$p_{Ft} = 0.015$ $p_{Wt4,5} = 0.003$ $p_{Wt4,6} = 0.018$			$p_{Ft} = 0.001$ $p_{Wt7,8} = 0.014$ $p_{Wt7,9} = 0.027$		
Cer d18:1/20:0	22.01 (18.11; 30.11)	16.93 (11.31; 22.49)	19.83 (12.98; 23.83)	15.95 (9.35; 21.80)	10.30 (8.38; 13.11)	12.26 (8.57; 18.95)	13.04 (9.11; 19.50)	10.13 (8.01; 12.53)	12.15 (8.38; 17.44)
	$p_{Ft} = 0.001$ $p_{Wt1,2} = 0.003$			$p_{Ft} = 0.001$ $p_{Wt4,5} = 0.002$ $p_{Wt4,6} = 0.009$ $p_{Wt5,6} = 0.011$			$p_{Ft} \geq 0.05$		
Cer d18:1/24:0	60.54 (33.78; 71.24)	59.55 (34.19; 67.51)	60.05 (32.55; 69.33)	45.85 (24.51; 53.22)	45.97 (24.88; 58.04)	45.92 (24.61; 58.31)	42.03 (21.32; 52.12)	41.29 (23.08; 50.76)	43.53 (22.14; 53.35)
	$p_{ft} \geq 0.05$			$p_{Ft} \geq 0.05$			$p_{Ft} \geq 0.05$		

Note. C – control, SAT – subcutaneous adipose tissue, PVAT – perivascular adipose tissue, EAT – epicardial adipose tissue. The levels of statistical significance: *p*Ft – the level when comparing three groups using the Friedman method, *p*Wt – the level when comparing two groups using the Wilcoxon method, and 1 mmol/l and 10 mmol/l – metformin concentration.

DISCUSSION

Metformin is a widely used biguanide with antihyperglycemic properties. However, its potential uses have long extended beyond the treatment of T2DM. The beneficial effects of metformin on cardiovascular health are being increasingly discussed.

The mechanisms of this phenomenon are not fully understood and are related to metformin's ability to modulate lipid homeostasis, but the molecular and genetic aspects require further clarification [16]. Ceramides are key molecules in sphingolipid metabolism and are considered to be important modulators of various cells and tissues, including cardiac and vascular adipose tissue [17]. According to experimental data, metformin inhibits the synthesis of ceramides and other complex lipids in animal skeletal muscle [18, 19], significantly reduces the

levels of certain lipid classes in the myocardium, as well as the expression of genes encoding enzymes that synthesize them, and regulates fatty acid composition [20].

The obtained results indicate the ability of metformin to regulate ceramide metabolism *in vitro* in epicardial and perivascular adipocytes to a greater extent than in subcutaneous ones, among patients with CHD. The pleiotropic effect of metformin was expressed in the ability to regulate the pathways of ceramide synthesis in cardiac adipocytes. Thus, at a low concentration (1 mmol/l), metformin more effectively suppressed the *de novo* ceramide synthesis from palmitoyl-CoA and serine at the stage of the first enzymatic reaction, as evidenced by a reduced expression of *SPTLC1*. Metformin suppressed the expression of genes of some ceramide synthases *CERS2* and *CERS4* in epicardial and perivascular adipocytes responsible for the synthesis of ceramides containing C-16, C-18, C-20, and C-24 residues of fatty acids associated with cardiovascular diseases [21]. At the same time, the drug increased the expression of the gene encoding the enzyme for the final reaction of *de novo* ceramide synthesis (*DEGS1*).

Based on the obtained results, it was established that the use of metformin *in vitro* promotes changes in ceramide concentrations in adipocytes, primarily in EAT and PVAT, in patients with CHD. Moreover, the drug effect was more pronounced at a concentration of 1 mmol/l compared to 10 mmol/l. Thus, ceramide levels, which are closely linked to the development and progression of cardiovascular disease, decreased in EAT and PVAT.

The pronounced effect of metformin in patients with CHD is likely due to the fact that one of the drug pleiotropic effects is the ability to suppress adipocyte differentiation and hypertrophy and reduce AT inflammation [22]. Therefore, metformin has the potential to reduce the ceramide-producing capacity of adipocytes. The reduction in ceramide production is achieved through the regulation of gene expression of enzymes synthesizing ceramides *de novo*, thereby inhibiting the accumulation of Cer in the ventricular tract of the heart and coronary vessels, which have adverse cardiovascular effects.

CONCLUSION

The potential ability of metformin to inhibit *de novo* ceramide synthesis in isolated adipocytes (SAT, EAT, and PVAT) and to reduce the content of ceramides associated with adverse cardiovascular events in fat cells was demonstrated in *in vitro* experiments.

REFERENCES

1. Drzewoski J., Hanefeld M. The current and potential therapeutic use of metformin-the good old drug. *Pharmaceuticals (Basel)*. 2021;14(2):122. DOI: 10.3390/ph14020122.
2. Miklankova D., Markova I., Hüttl M., Zapletalova I., Poruba M., Malinska H. Metformin affects cardiac arachidonic acid metabolism and cardiac lipid metabolite storage in a prediabetic rat model. *Int. J. Mol. Sci*. 2021;22(14):7680. DOI: 10.3390/ijms22147680.
3. Seifarth C., Schehler B., Schneider H.J. Effectiveness of metformin on weight loss in non-diabetic individuals with obesity. *Exp. Clin. Endocrinol. Diabetes*. 2013;121(1):27–31. DOI: 10.1055/s-0032-1327734.
4. Halabi A., Sen J., Huynh Q., Marwick T.H. Metformin treatment in heart failure with preserved ejection fraction: a systematic review and meta-regression analysis. *Cardiovasc. Diabetol*. 2020;19(1):124. DOI: 10.1186/s12933-020-01100-w.
5. Lascu A., Ionică L.N., Merce A.P., Dănilă M.D., Petrescu L., Sturza A. et al. Metformin Acutely Mitigates Oxidative Stress in Human Atrial Tissue: A Pilot Study in Overweight Non-Diabetic Cardiac Patients. *Life (Basel)*. 2022;12(12):2058. DOI: 10.3390/life12122058.
6. Bai B., Chen H. Metformin: a novel weapon against inflammation. *Front. Pharmacol.* 2021;12:622262. DOI: 10.3389/fphar.2021.622262.
7. Kristófi R., Eriksson J.W. Metformin as an anti-inflammatory agent: a short review. *J. Endocrinol.* 2021;251(2):R11–R22. DOI: 10.1530/JOE-21-0194.
8. Bu Y., Peng M., Tang X., Xu X., Wu Y., Chen A.F., et al. Protective effects of metformin in various cardiovascular diseases: Clinical evidence and AMPK-dependent mechanisms. *J. Cell Mol. Med*. 2022;26(19):4886–4903. DOI: 10.1111/jcmm.17519.
9. Aleidi S.M., Dahabiyeh L.A., Gu X., Al Dubayee M., Alshahrani A., Benabdelkamel H. et al. Obesity connected metabolic changes in type 2 diabetic patients treated with metformin. *Front. Pharmacol.* 2021;11:616157. DOI: 10.3389/fphar.2020.616157.
10. Dahabiyeh L.A., Mujammami M., Arafat T., Benabdelkamel H., Alfadda A.A., Abdel Rahman A.M. A metabolic pattern in healthy subjects given a single dose of metformin: a metabolomics approach. *Front. Pharmacol.* 2021;12:705932. DOI: 10.3389/fphar.2021.705932.
11. Dahabiyeh L.A., Mujammami M., AlMalki R.H., Arafat T., Benabdelkamel H., Alfadda A.A. et al. Lipids alterations associated with metformin in healthy subjects: an investigation using mass spectrometry shotgun approach. *Int. J. Mol. Sci*. 2022;23(19):11478. DOI: 10.3390/ijms231911478.

12. Mujammami M., Aleidi S.M., Buzatto A.Z., Alshahrani A., AlMalki R.H., Benabdelkamel H. et al. Lipidomics profiling of metformin-induced changes in obesity and type 2 diabetes mellitus: insights and biomarker potential. *Pharmaceuticals (Basel)*. 2023;16(12):1717. DOI: 10.3390/ph16121717.
13. Zietzer A., Düsing P., Reese L., Nickenig G., Jansen F. Ceramide metabolism in cardiovascular disease: a network with high therapeutic potential. *Arterioscler. Thromb. Vasc. Biol*. 2022;42(10):1220–1228. DOI: 10.1161/ATVBAHA.122.318048.
14. Zhu Q., Scherer P.E. Ceramides and atherosclerotic cardiovascular disease: a current perspective. *Circulation*. 2024;149(21):1624–1626. DOI: 10.1161/CIRCULATIONAHA.123.065409.
15. Gruzdeva O.V., Akbasheva O.E., Dyleva Y.A., Antonova L.V., Matveeva V.G., Uchasova E.G. et al. Adipokine and cytokine profiles of epicardial and subcutaneous adipose tissue in patients with coronary heart disease. *Bull. Exp. Biol. Med*. 2017;163(5):608–611. DOI: 10.1007/s10517-017-3860-5.
16. Turkistani A., Al-Kuraishy H.M., Al-Gareeb A.I., Alexiou A., Papadakis M., Bahaa M.M. et al. Pharmacological characterization of the antidiabetic drug metformin in atherosclerosis inhibition: A comprehensive insight. *Immun. Inflamm. Dis*. 2024;12(8):e1346. DOI: 10.1002/iid3.1346.
17. Delcheva G., Stefanova K., Stankova T. Ceramides-emerging biomarkers of lipotoxicity in obesity, diabetes, cardiovascular diseases, and inflammation. *Diseases*. 2024;12(9):195. DOI: 10.3390/diseases12090195.
18. Zabielski P., Chacinska M., Charkiewicz K., Baranowski M., Gorski J., Blachnio-Zabielska A.U. Effect of metformin on bioactive lipid metabolism in insulin-resistant muscle. *J. Endocrinol*. 2017;233(3):329–340. DOI: 10.1530/JOE-16-0381.
19. Grycel S., Markowski A.R., Hady H.R., Zabielski P., Kojta I., Imierska M. et al. Metformin treatment affects adipocytokine secretion and lipid composition in adipose tissues of diet-induced insulin-resistant rats. *Nutrition*. 2019;63-64:126–133. DOI: 10.1016/j.nut.2019.01.019.
20. Miklankova D., Markova I., Hüttl M., Zapletalova I., Poruba M., Malinska H. Metformin affects cardiac arachidonic acid metabolism and cardiac lipid metabolite storage in a prediabetic rat model. *Int. J. Mol. Sci*. 2021;22(14):7680. DOI: 10.3390/ijms22147680.
21. Hilvo M., Vasile V.C., Donato L.J., Hurme R., Laaksonen R. Ceramides and ceramide scores: clinical applications for cardiometabolic risk stratification. *Front. Endocrinol. (Lausanne)*. 2020;11:570628. DOI: 10.3389/fendo.2020.570628.
22. Fujita K., Iwama H., Oura K., Tadokoro T., Hirose K., Watanabe M. et al. Metformin-suppressed differentiation of human visceral preadipocytes: Involvement of microRNAs. *Int. J. Mol. Med.* 2016;38(4):1135–1140. DOI: 10.3892/ijmm.2016.2729.

Author Contribution

Dyleva Yu.A. – conception and design, drafting of the manuscript. Gorbatovskaya E.E. – preparation of illustrations, drafting of the manuscript. Dolmatova S.E. – data analysis and interpretation. Ivanov S.V., Fanaskova E.V. – data collection and processing. Gruzdeva O.V. – critical revision for important intellectual content, final approval of the manuscript for publication.

Author Information

Dyleva Yulia A. – Cand. Sci. (Med.), Senior Researcher, Laboratory for Homeostasis Research, Research Institute for Complex Problems of Cardiovascular Diseases, Kemerovo, dyleva87@yandex.ru, https://orcid.org/0000-0002-6890-3287

Gorbatovskaya Evgeniya E. – Cand. Sci. (Med.), Junior Researcher, Laboratory for Homeostasis Research, Research Institute for Complex Problems of Cardiovascular Diseases; Senior Lecturer of the Department of Medical Biochemistry, Kemerovo State Medical University, Kemerovo, eugenia.tarasowa@yandex.ru, https://orcid.org/0000-0002-0500-2449

Dolmatova Sofya E. – Research Laboratory Assistant, Laboratory for Homeostasis Research, Research Institute for Complex Problems of Cardiovascular Diseases; Post-graduate Student of the Department of Pathological Physiology, Assistant of the Department of Medical Biochemistry, Kemerovo State Medical University, Kemerovo, soniad_30_09@mail.ru, https://orcid.org/0009-0008-2997-4497

Ivanov Sergey V. – Dr. Sci. (Med.), Leading Researcher, Laboratory of X-ray Endovascular and Reconstructive Surgery of the Heart and Vascular System, Research Institute for Complex Problems of Cardiovascular Diseases, Kemerovo, https://orcid.org/0000-0002-9070-5527

Fanaskova Elena V. – Cand. Sci. (Med.), Head of the Transfusion Department, Research Institute for Complex Problems of Cardiovascular Diseases, Kemerovo, fanaskova70@mail.ru, https://orcid.org/0000-0003-2705-3252

Gruzdeva Olga V. – Dr. Sci. (Med.), Professor, Professor of the Russian Academy of Sciences, Head of the Laboratory for Homeostasis Research, Research Institute for Complex Problems of Cardiovascular Diseases; Head of the Department of Medical Biochemistry, Kemerovo State Medical University, Kemerovo, o_gruzdeva@mail.ru, https://orcid.org/0000-0002-7780-829X

(✉) **Gorbatovskaya Evgeniya E.,** eugenia.tarasowa@yandex.ru

Received on July 3, 2025;
approved after peer review on October 20, 2025;
accepted on October 30, 2025

УДК 616.831-092.9:576.7:615.214
https://doi.org/10.20538/1682-0363-2026-2-13-20

Morphological Changes in Cortical Neurons and Glia of Rats in the Context of Global Cerebral Ischemia – Reperfusion Injury and its Treatment with p-Tyrosol

Zhdankina A.A.[1], Osipenko A.N.[1], Chernysheva G.A.[2], Smolyakova V.I.[2], Logvinov S.V.[1], Potapov A.V.[1], Gerasimov A.V.[1], Lasukova T.V.[1], Gereng E.A.[1], Akbasheva O.E.[1], Tikhonovskaya O.A.[1], Plotnikov M.B.[2]

[1] *Siberian State Medical University*
2 Moscovsky trakt, 634050 Tomsk, Russian Federation

[2] *E.D. Goldberg Research Institute of Pharmacology and Regenerative Medicine, Tomsk National Research Medical Center (NRMC) of the Russian Academy of Sciences*
3 Lenin Ave., 634028 Tomsk, Russian Federation

ABSTRACT

Aim. To investigate morphological alterations in neurons and glial cells in the cerebral cortex using a rat model of total transient global cerebral ischemia (GCI) and to evaluate the neuroprotective effects of *p*-tyrosol.

Materials and methods. Experiments were performed on Wistar rats (n = 30), randomly divided into three groups: sham-operated, GCI control, and GCI with *p*-tyrosol treatment. The glioneuronal elements of the cerebral cortex were analyzed by light and transmission electron microscopy combined with a quantitative morphometric assessment.

Results. In the GCI group, a significant reduction in neuron density was observed. Surviving neurons showed a marked decrease in the relative volume of membrane-bound organelles, accompanied by an increase in lipofuscin, lysosomes, and vacuoles. Administration of *p*-tyrosol after GCI enhanced neuronal survival.

Conclusion. For the first time in this rat model of GCI, structural and ultrastructural changes of cortical neurons and glial cells in rats were characterized, confirming the validity of the model. Neuroprotective effects of *p*-tyrosol in the context of GCI were demonstrated at both the light-microscopic and ultrastructural levels.

Keywords: brain, ischemia, light microscopy, electron microscopy, tyrosol, neuroprotection

Conflict of interest. The authors declare the absence of obvious or potential conflicts of interest related to the publication of this article.

Source of financing. The authors state that they received no funding for the study.

Conformity with the principles of ethics. The study was approved by the Bioethics Committee at Siberian State Medical University (Minutes No. 2203201 dated 22.12.2014).

For citation: Zhdankina A.A., Osipenko A.N., Chernysheva G.A., Smolyakova V.I., Logvinov S.V., Potapov A.V., Gerasimov A.V., Lasukova T.V., Gereng E.A., Akbasheva O.E., Tikhonovskaya O.A., Plotnikov M.B. Morphological Changes in Cortical Neurons and Glia of Rats in the Context of Global Cerebral Ischemia – Reperfusion Injury and its Treatment with p-Tyrosol. *Bulletin of Siberian Medicine.* 2026;25(2):13–20. https://doi.org/10.20538/1682-0363-2026-2-13-20.

✉ *Zhdankina Anna A.,* annazhdank@yandex.ru

Морфологические изменения нейронов и глии коры головного мозга крыс в условиях глобальной церебральной ишемии-реперфузиии их коррекция п-тирозолом

Жданкина А.А.[1], Осипенко А.Н.[1], Чернышева Г.А.[2], Смольякова В.И.[2], Логвинов С.В.[1], Потапов А.В.[1], Герасимов А.В.[1], Ласукова Т.В.[1], Геренг Е.А.[1], Акбашева О.Е.[1], Тихоновская О.А.[1], Плотников М.Б.[2]

[1] *Сибирский государственный медицинский университет (СибГМУ)*
Россия, 634050, г. Томск, Московский тракт, 2

[2] *Научно-исследовательский институт фармакологии и регенеративной медицины (НИИФиРМ) Томского национального исследовательского медицинского центра (НИМЦ) Российской академии наук*
Россия, 634028, г. Томск. пр. Ленина, 3

РЕЗЮМЕ

Цель. Изучить морфологические изменения нейронов и глии коры больших полушарий на модели тотальной транзиторной ишемии головного мозга (ТТИГМ) у крыс и на фоне коррекции *n*-тирозолом.

Материалы и методы. Опыты проведены на крысах линии Вистар (n = 30). Животные были разделены случайным образом на три группы – ложнооперированные, контрольные с воспроизведением ТТИГМ, опытные с моделью ТТИГМ и введением *n*-тирозола. Глионейрональный комплекс коры больших полушарий изучали при помощи световой и электронной микроскопии с применением морфоколичественного анализа.

Результаты. В группе животных с ТТИГМ отмечено значимое снижение численной плотности нейронов. В сохранившихся нейронах происходило значительное уменьшение удельного объема мембранных органелл, а также повышение удельного объема липофусцина, лизосом и вакуолей. У животных, получавших *n*-тирозол после ТТИГМ, отмечалось усиление выживаемости нейронов.

Заключение. Впервые на данной модели ТТИГМ охарактеризованы структурные и ультраструктурные изменения нейронов и глии коры больших полушарий у крыс, которые свидетельствуют о состоятельности модели. В условиях ТТИГМ впервые продемонстрированы нейропротективные эффекты *n*-тирозола на светомикроскопическом и ультраструктурном уровнях.

Ключевые слова: головной мозг, ишемия, световая микроскопия, электронная микроскопия, *n*-тирозол, нейропротекция

Конфликт интересов. Авторы декларируют отсутствие явных и потенциальных конфликтов интересов, связанных с публикацией настоящей статьи.

Источник финансирования. Авторы заявляют об отсутствии источника финансирования при проведении исследования.

Соответствие принципам этики. Исследование одобрено комиссией по биоэтике СибГМУ (протокол № 2203201 от 22.12.2014).

Для цитирования: Жданкина А.А., Осипенко А.Н., Чернышева Г.А., Смольякова В.И., Логвинов С.В., Потапов А.В., Герасимов А.В., Ласукова Т.В., Геренг Е.А., Акбашева О.Е., Тихоновская О.А., Плотников М.Б. Морфологические изменения нейронов и глии коры головного мозга крыс в условиях глобальной церебральной ишемии-реперфузиии их коррекция п-тирозолом. *Бюллетень сибирской медицины.* 2026;25(2):13–20. https://doi.org/10.20538/1682-0363-2026-2-13-20.

INTRODUCTION

According to the WHO, stroke is the second leading cause of death in Russia and most other countries [1], with ischemic strokes predominating. Acute cerebral ischemia – reperfusion causes massive death of neuronal and glial cells and leads to severe neurological deficits [2], creating a need for neuroprotection [3]. Due to the leading role of oxidative stress during ischemia – reperfusion injury, the use of neuroprotective agents with antioxidant effects is relevant [4]. One such neuroprotective

agent is *p*-tyrosol, a naturally occurring phenol with high bioavailability for brain tissue [5].

To study the pathogenesis of ischemia – reperfusion injury and to carry out a preclinical evaluation of neuroprotection, a total transient global cerebral ischemia (GCI) rat model was used [6]. We developed a modified variant of the model proposed by N.S. Shcherbak et al., with low morbidity and mortality in animals [7]. The pharmaceutical substance *p*-tyrosol (99.5% purity) was provided by the Institute for Problems of Chemical and Energy Technologies, Siberian Branch of the Russian Academy of Sciences (Biysk, Russia).

The aim of the study was to investigate morphological changes in cortical neurons and glia using a rat model of GCI and after treatment with *p*-tyrosol.

MATERIALS AND METHODS

The study involved 30 outbred Wistar rats weighing 220–240 g. The animals were divided into three groups (10 each): a sham-operated group (sham control), a group with GCI induction (control), and a group with GCI induction and *p*-tyrosol administration (experimental). The GCI model was reproduced using the three-vessel occlusion method [7]. Shamoperated animals underwent the same surgical procedure, but without application of arterial occluders. Rats in the experimental group received *p*tyrosol intraperitoneally at a dose of 20 mg/kg body weight for 5 days starting from the time of GCI induction. Rats in the control group received distilled water according to the same regimen.

At the end of the experiment, the animals were euthanized under isoflurane anesthesia, and the brains were removed. All procedures complied with the Directive 2010/63/EU. The study was approved by the Bioethics Committee at Siberian State Medical University (Minutes No. 2203201 dated).

For morphological studies, the brains of the experimental animals were fixed by transcardial perfusion with a mixture of 4% paraformaldehyde and 1% glutaraldehyde for 15–20 minutes at 90 mm Hg. After fixation, the brains were removed and post-fixed in a similar fixative mixture. For light microscopy, the material was embedded in paraffin. Thin serial frontal sections of the whole brain at the level of the sensorimotor cortex were then obtained and stained with hematoxylin – eosin and Nissl stain (cresyl violet). The sections were viewed and photographed using the Carl Zeiss Axiostar plus microscope.

For electron microscopy, the sensorimotor cortex (areas Fpa and Fpp) was isolated using stereotaxic atlases. Slices of the sensorimotor cortex (five from each hemisphere) were then post-fixed in 2% OsO_4, dehydrated in graded alcohols, and embedded in the Epon – Araldite mixture. Semithin sections were cut on the LKB4 ultratome (Sweden) and stained with 0.1% toluidine blue. Ultrathin sections were mounted on copper grids and contrasted with uranyl acetate and lead citrate.

In the paraffin sections stained with cresyl violet, we counted the percentage of neurons with focal and total chromatolysis, hyperchromic and pycnomorphic neurons in layers II, IV, and V of the cerebral cortex per 500 neurons in each layer from each animal. We also determined the numerical density of neurons per section plane (Ns), the mean number of neurons, and the total number of glial cells and perineuronal glia within an ocular frame of 0.029 mm² and calculated the glia-to-neuron ratio (GNR). Using the ImageJ software (NIH, USA) and electron micrographs, we calculated the specific total area of mitochondria, endoplasmic reticulum, Golgi complex (GC), vacuoles, and lipofuscin in layer V neurons.

The statistical significance of differences between the groups was assessed using the nonparametric Kruskal – Wallis test, followed by pairwise comparisons with the Mann – Whitney test. A Bonferroni correction was applied to account for multiple comparisons; the adjusted significance level was 0.01, with a baseline significance level of 0.05. Differences were considered statistically significant at $p < 0.01$. Results were presented as the median and the interquartile range Me (Q_1–Q_3).

RESULTS

Due to ischemia, the numerical density of neurons in cortical layers IV and V decreased by 29 and 22%, respectively ($p < 0.01$) compared to the sham-operated animals. The numerical density of total glial cells also significantly decreased, but the numerical density of perineuronal glia remained at the control level, indicating a pronounced progressive proliferative glial response. The analysis of glial – neuronal interactions revealed a significant increase in the GNR in cortical layers IV and V in the control group by 19 and 35%, respectively ($p < 0.01$; Table 1).

Table 1

Quantitative Characteristics of Glial and Neuronal Elements in Layers II, IV, and V of the Rat Occipital Cortex after Experimental Global Cerebral Ischemia – Reperfusion with and without *p*Tyrosol Treatment, *Me* (Q_1–Q_3)

Animal groups		Neuron density (per 1 mm² of slice)	Total glia density (per 1 mm² of slice)	Numerical density of perineuronal glia (per 1 mm² of slice)	Gliato-neuron ratio
Sham-operated animals	Layer II	2,142.39 (2,095.67–2,151.71)	1,040.54 (1,025.03–1,133.89)	385.24 (377.46–409.11)	0.18 (0.18–0.19)
	Layer IV	2,149.61 (2,140.12–2,171.22)	1,195.64 (1,195.58–1,208.57)	352.37 (348.87–371.53)	0.17 (0.16–0.17)
	Layer V	1,972.8 (1,872.8–2,041.46)	975.17 (969.45–982.54)	294.44 (259.73–316.58)	0.13 (0.13–0.19)
Control	Layer II	2,028.16 (1,916.77–2,132.14)	922.28* (902.26–944.47)	373.29 (351.54–374.49)	0.18 (0.17–0.20)
	Layer IV	1,506.50 (1,449.76–1,675.83)*	844.18* (827.38–881.27)	329.14 (311.58–331.59)	0.21 (0.19–0.24)*
	Layer V	1,338.67 (1,330.65–1,338.81)*	976.68 (793.98–893.59)	276.30 (221.87–278.91)	0.20 (0.17–0.21)*
p-Tyrosol	Layer II	1,992.51 (1,991.98–2,132.18)	999.29 (914.94–1,171.46)	396.22 (373.93–429.14)	0.19 (0.18–0.22)
	Layer IV	2,116.55 (2,092.19–2,126.80)^	931.87 (931.53–966.87)	338.84 (325.37–369.45)	0.17 (0.15–0.18)
	Layer V	1,743.45 (1,642.22–1,748.28)^	1,071.07 (1,007.17–1,078.49)	316.44 (316.43–316.45)	0.18*^ (0.18–0.19)

Here and in Table 2, 3: * $p < 0.01$ compared to the sham-operated animals; ^ $p < 0.01$ compared to the control group.

p-Tyrosol (20 mg/kg) promoted normalization of the cytoarchitecture in the examined cortical regions, as evidenced by preservation of the numerical density of neurons and glial cells in cortical layers IV and V at levels comparable to those in the sham-operated rats, along with normalization of the GNR (Table 1).

Among the surviving neurons in cortical layers II, IV, and V in the GCI group, a substantial proportion exhibited chromatolysis of varying severity, as well as dark-stained changes with nuclear pyknosis and a decrease in cytoplasmic volume.

Quantitative analysis showed that chromatolysis was more pronounced in cortical layers II and IV of the control group, whereas dark-stained neuronal changes with nuclear pyknosis and increased osmiophilic cytoplasmic inclusions predominated in layer V (Table 2).

Administration of *p*-tyrosol after ischemia attenuated the development of reversible and irreversible changes in cortical neurons compared to the rats in the control group. Moreover, neuronal integrity was approximately equal in all studied layers; the indices of neuronal damage were 1.5–2-fold lower than in the control group ($p < 0.01$), but they remained significantly higher than in the sham-operated group (Table 2).

Table 2

Morphological Changes in Cortical Neurons of Rats from Different Experimental Groups, %, *Me* (Q_1–Q_3)

Animal groups		Neurons with focal chromatolysis	Neurons with total chromatolysis	Hyperchromic neurons without shrinkage	Hyperchromic neurons with shrinkage
Sham-operated animals	Layer II	0.82 (0.82–0.88)	0.97 (0.83–1.11)	1.23 (0.94–1.34)	1.40 (1.02–1.57)
	Layer IV	1.2 (0.39–1.26)	0.78 (0.42–0.88)	1.39 (1.32–1.41)	1.34 (1.31–1.62)
	Layer V	2.23 (2.15–2.29)	0.47 (0.45–0.57)	10.06 (9.82–10.23)	4.66 (3.31–5.10)
Control	Layer II	58.22* (54.27–59.36)	7.84* (7.17–10.23)	7.15* (6.88–8.91)	3.43* (2.57–3.85)
	Layer IV	58.21* (58.11–58.40)	10.67* (9.15–11.81)	7.04* (6.94–8.45)	2.78* (2.36–3.04)
	Layer V	12.91* (11.42–15.16)	3.36* (3.31–4.44)	13.88 (12.40–14.21)	7.41* (7.41–7.54)
p-Tyrosol	Layer II	42.57 *^ (27.44–43.98)	3.45 *^ (3.13–3.81)	7.77 (7.31–8.70)	2.67 (2.53–2.69)
	Layer IV	35.02*^ (34.43–37.42)	4.94* (4.18–5.16)	9.11 (8.07–9.64)	1.90^ (1.65–2.12)
	Layer V	10.63*^ (10.62–11.29)	2.55*^ (2.41–2.86)	6.59*^ (6.50–6.90)	4.94^ (4.53–5.76)

Electron microscopy of the cerebral cortex in the rats with GCI revealed a marked reduction in the number of rough endoplasmic reticulum (RER) cisternae throughout the cytoplasm, with only isolated polysomes and free ribosomes remaining. A significant reduction in the number of mitochondria was noted; the remaining mitochondria were swollen, with matrix clearing and destruction of cristae. Increased vacuolization was observed in a substantial proportion of neurons. The nuclei of surviving neurons often had an irregular outline, with deep invaginations of the karyolemma and localized expansion of the perinuclear space. In some neurons, the nucleolus was enlarged, which may be interpreted as a compensatory and adaptive response of neurons to injury (Fig. 1, *a*).

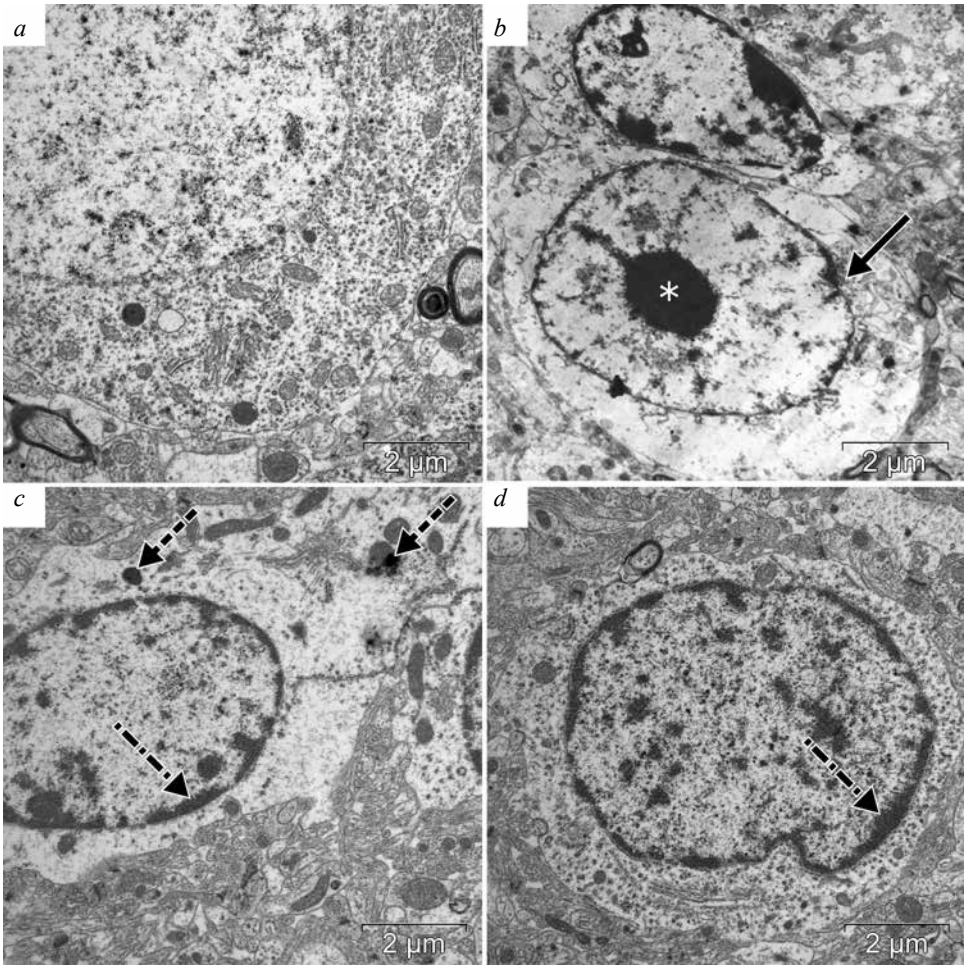

Fig. 1. Layer IV of the cerebral cortex of rats from different experimental groups: *a* – unchanged cortical neuron from a sham-operated rat; *b, c* – cortical neurons from rats in the control group. Disintegration of RER, with isolated RER fragments in the cytoplasm (black arrows), the appearance of lipofuscin granules (dashed arrow), condensation of the neuron nucleolus (asterisk), and peripheral chromatin fragmentation in the nucleus (dotted – dashed arrows); *d* – cortical neuron from a rat in the experimental group. Preservation of organelles, marginal condensation of chromatin in the nucleus (dotted – dashed arrows). Electron micrographs, × 4,500

Quantitatively, in the ischemia – reperfusion group, the specific volume of RER, mitochondria, and the GC decreased 4.4-fold, 1.9-fold, and by 21.4%, respectively, compared to the sham-operated animals ($p < 0.01$). In the meantime, a ten-fold increase in the specific volume of lipofuscin and lysosomes and a five-fold increase in the specific volume of vacuoles were detected ($p < 0.01$; Table 3).

Table 3

Specific Area of Organelles in the Cytoplasm of Cortical Pyramidal Neurons of Layer V in Rats from Different Experimental Groups, %, *Me* (Q_1–Q_3)

Animal groups	RER	Mitochondria	Lysosomes	Golgi complex	Vacuoles
Sham-operated animals	24.33 (19.52–27.21)	9.67 (8.72–11.51)	1.38 (1.12–1.72)	2.34 (2.15–3.29)	1.8 (1.6–2.3)
Control	5.48* (4.97–5.86)	5.09* (4.089–5.14)	13.9* (12.15–15.02)	1.84 * (1.7–2.05)	8.82* (8.12–9.91)
p-Tyrosol	10.15*^ (9.58–11.51)	6.85*^ (6.15–7.71)	7.1*^ (6.88–7.65)	1.86* (1.85–2.52)	8.9* (8.1–9.65)

Administration of *p*-tyrosol to the rats after GCI significantly prevented the development of the ultrastructural neuronal abnormalities described above. The specific volume of organelles remained 1.9- and 1.4-fold greater than in the control group, respectively ($p < 0.01$), but was 1.6-fold smaller than in the sham-operated group. *p*-Tyrosol also prevented the accumulation of lipofuscin and lysosomes in the neuronal perikarya: their specific volume value was almost two-fold lower than in the control group ($p < 0.01$; Table 3).

Neuronal death during GCI promoted activation of perineuronal glia, whose cytoplasm contained numerous vacuoles, phagosomes, and myelin-like bodies. Satellite glial cells were frequently observed, indicating the onset of neuronophagia. Activation of microglia was also evident: the cells lost their processes, became rounded, the nucleolus was clearly visible within the nucleus, and there was marked development of the GC and, consequently, of the vacuolar apparatus in the cytoplasm (Fig. 2).

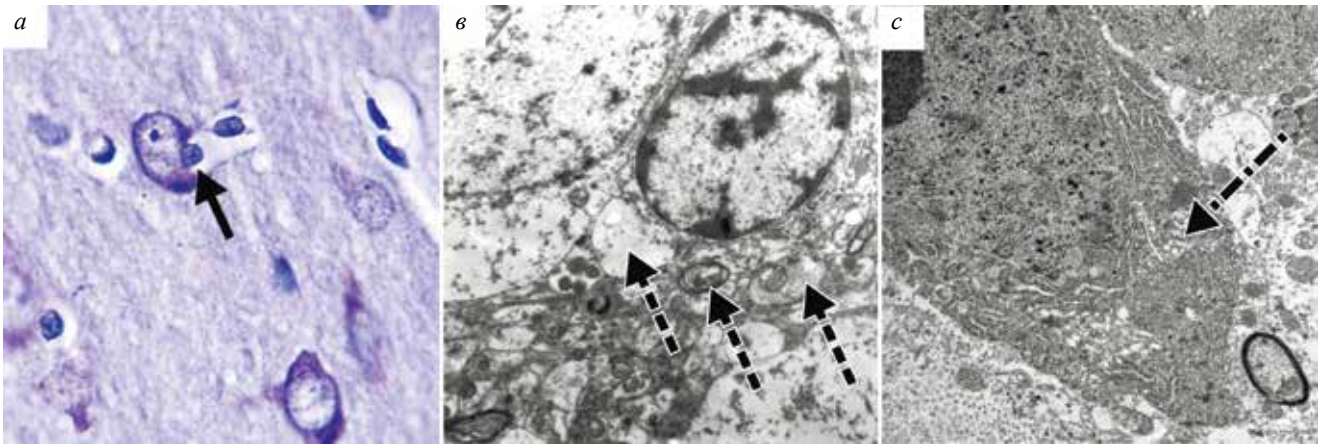

Fig. 2. Glial – neuronal interactions in the cerebral cortex of rats with total transient cerebral ischemia: *a* – neuronophagia: invagination of a satellite glial cell into the neuronal cytoplasm (arrow); Nissl staining with methylene blue; × 1,000; *b* – vacuoles, phagosomes, myelin-like bodies in the cytoplasm of a glial cell (dashed arrows); *c* – activated microglial cell (dotted – dashed arrow). Electron micrographs, × 5,000

DISCUSSION

The comprehensive analysis of layers II, IV, and V of the sensorimotor cortex in the rats subjected to GCI revealed marked alterations in the structure and number of neurons and glial cells during hemodynamic disturbances. Neurons showed hyperchromia and varying degrees of chromatolysis, and postischemic neuronal death was noted. By day 5, focal chromatolysis manifested as peripheral and segmental dissolution of the chromatophilic substance, which is considered as the most typical response to hypoxia [8]. Total chromatolysis was characterized by uniform dissolution of chromatophilic clumps throughout the perikarya and dendrites, and its extreme stage (ghost cells) is regarded as irreversible neuronal destruction [9]. According to various authors, hyperchromia may result either from increased nucleocytoplasmic RNA transport or from suppressed protein synthesis, the latter coinciding with activation of hydrolytic processes and indicating irreversible neuronal damage [8]. Electron microscopy confirmed the morphometric data: after GCI, layer V neurons exhibited degranulation of RER, dilation of RER and GC cisternae, and destruction of membranous organelles with formation of vacuoles. Quantitatively, this was reflected in a decrease in the specific volume of RER, mitochondria, and GC and an increase in the specific volume of lipofuscin, lysosomes, and vacuoles. In surviving neurons, GC cisternae were dilated and fragmented, and the number of lysosomes, lipid inclusions, and lipofuscin granules increased. These findings are consistent with other GCI models [10–12].

Glial – neuronal interactions normally support axonal conduction and synaptic transmission [13]. The study revealed a progressive neuroglial response: increased GNR, more frequent contacts between neurons and glial cell bodies and processes, and an increased number of satellite cells, all of which are characteristic of the early postischemic period [8].

At the same time, the numerical density of glial cells in the GCI control group decreased, reflecting predominant death of astrocytes.

Oxidative stress during ischemia – reperfusion injury damages erythrocyte membranes and vascular endothelium, thereby impairing microcirculation and reducing oxygen availability to tissues [14]. The previously described antioxidant effects of *p*-tyrosol in cerebral ischemia [5] may also explain its neuroprotective effects under GCI conditions. Administration of *p*-tyrosol reduced neuronal loss in all layers, decreased the proportion of neurons with focal and total chromatolysis in layers II and IV, and reduced the proportion of pycnomorphic neurons in layer V. Similarly, in models of focal ischemia, *p*tyrosol was shown to reduce free radical levels, prevent necrosis and apoptosis, decrease the size of the ischemic core, and increase neuronal survival in the prefrontal cortex and hippocampus [15].

At the ultrastructural level, preservation of RER and mitochondria and a smaller number of lysosomes were observed in the *p*-tyrosol-treated animals compared to the GCI control group. In addition to its antioxidant effect, the hemorheological properties of *p*-tyrosol are important: increased erythrocyte deformability, reduced erythrocyte aggregation, and decreased wholeblood and plasma viscosity [16]. These effects probably improve microcirculation and oxygen delivery and thereby limit damage to neurons and glial cells.

CONCLUSION

Therefore, *p*-tyrosol exhibits neuroprotective effects, reducing neuronal loss in the cerebral cortex and decreasing the proportion of neurons with pathomorphological changes after transient total cerebral ischemia – reperfusion. These effects are associated with preservation of neuronal membrane organelles, normalization of neuronal – glial interactions, and improvement of microcirculation. The efficacy of *p*-tyrosol in cerebral ischemia – reperfusion demonstrated in these preclinical trials is an important prerequisite for conducting clinical trials of this drug in the treatment of ischemic lesions of the central nervous system.

REFERENCES

1. Vos T., Lim S.S., Abbafati C., Abbas K.M., Abbasi M., Abbasifard M., Abbasi-Kangevari M. et al. Global burden of 369 diseases and injuries in 204 countries and territories, 1990–2019: a systematic analysis for the Global Burden of Disease Study 2019. *The Lancet*. 2020;17;396(10258):1204–1222. DOI: 10.1016/S0140-6736(20)30925-9.
2. Sekhon M.S., Ainslie P.N., Griesdale D.E. Clinical pathophysiology of hypoxic ischemic brain injury after cardiac arrest: a "two-hit" model. *Crit. Care*. 2017;21(1):90. DOI: 10.1186/s13054-017-1670-9.
3. Dammavalam V., Lin S., Nessa S., Daksla N., Stefanowski K., Costa A., Bergese S. Neuroprotection during thrombectomy for acute ischemic stroke: a review of future therapies. *Int. J. Mol. Sci*. 2024;25(2):891. DOI: 10.3390/ijms25020891.
4. George P.M., Steinberg G.K. Novel stroke therapeutics: unraveling stroke pathophysiology and its impact on clinical treatments. *Neuron*. 2015;87(2):297–309. DOI: 10.1016/j.neuron.2015.05.041.
5. Plotnikov M.B., Plotnikova T.M. Tyrosol as a Neuroprotector: Strong effects of a "weak" antioxidant. *Curr. Neuropharmacol*. 2021;19(4):434–448. DOI: 10.2174/1570159X18666200507082311.
6. Neuhaus A.A., Couch Y., Hadley G., Buchan A.M. Neuroprotection in stroke: the importance of collaboration and reproducibility. *Brain*. 2017;140(8):2079–2092. DOI: 10.1093/brain/awx126.
7. Atochin D.N., Chernysheva G.A., Aliev O.I., Smol'yakova V.I., Osipenko A.N., Logvinov S.V. et al. An improved three-vessel occlusion model of global cerebral ischemia in rats. *Brain Res. Bull*. 2017;132:213–221. DOI: 10.1016/j.brainresbull.2017.06.005.
8. Bogolepov N.N. Ultrastructure of the Brain under Hypoxia. M.: Meditsina, 1979:167. (In Russ.).
9. Yarygin N.E. Pathological and Adaptive Changes of the Neuron. M.: Meditsina, 1973:190. (In Russ.).
10. Chan P.H. Mitochondria and neuronal death/survival signaling pathways in cerebral ischemia. *Neurochem. Res*. 2004;29(11):1943–1949. DOI: 10.1007/s11064-004-6869-x.
11. Rafols J.A., Daya A.M., O'Neil B.J., Krause G.S., Neumar R.W., White B.C., Global brain ischemia and reperfusion: Golgi apparatus ultrastructure in neurons selectively vulnerable to death. *Acta Neuropathologica*. 1995;90(1):17–30. DOI: 10.1007/BF00294455.
12. Bon L.I., Maksimovich N.Ye., Zimatkin S.M. Morphological Changes in the Rats' Parietal Cortex after Subtotal Cerebral Ischemia and on the Background of L-NAME Administration. *Vitebsk Medical Journal*. 2019;18(1):14–20. (In Russ.). DOI: 10.22263/2312-4156.2019.1.14.
13. Hatton G.I. Glial-neuronal interactions in the mammalian brain. *Advances in Physiology Education*. 2002;26(4):225–237. DOI: 10.1152/advan.00038.2002.
14. Stoltz J.F., Donner M. New trends in clinical hemorheology: an introduction to the concept of the hemorheological profile. *Schweiz. Med. Wochenschr. Suppl*. 1991;43:41–49.
15. Bu Y., Rho S., Kim J., Kim M.Y., Lee D.H., Kim S.Y. et al. Neuroprotective effect of tyrosol on transient focal cerebral ischemia in rats. *Neurosci. Lett*. 2007;414(3):218–221. DOI: 10.1016/j.neulet.2006.08.094.
16. Osipenko A.N., Plotnikova T.M., Chernysheva G.A., Smolyakova V.I. The Mechanisms of Neuroprotective Action of p-Tyrosol after the Global Cerebral Ischemia in Rats. *Bulletin of Siberian Medicine*. 2017;16(1):65–72. (In Russ.). DOI: 10.1016/j.phymed.2016.03.015.

Author Contribution

Zhdankina A.A., Plotnikov M.B. – conception and design. Gereng E.A., Akbasheva O.E. – methodology. Chernysheva G.A., Smolyakova V.I. – experiment design. Osipenko A.N. – data analysis and interpretation. Lasukova T.V. – validation. Logvinov S.V., Gerasimov A.V., and Tikhonovskaya O.A.– critical revision of the manuscript for important intellectual content. Potapov A.V., Akbasheva O.E. – final approval of the manuscript for publication.

Author Information

Zhdankina Anna A. – Dr. Sci. (Med.), Professor, Histology, Embryology and Cytology Division, Siberian State Medical University, Tomsk, annazhdank@yandex.ru, https://orcid.org/0000-0002-4954-7416

Osipenko Anton N. – Teaching Assistant, Division of Pharmacology, Siberian State Medical University, Tomsk, osipenko-an@mail.ru, https://orcid.org/0000-0002-4763-3214

Chernysheva Galina A. – Dr. Sci. (Med.), Senior Researcher, Laboratory for Circulatory Pharmacology, Goldberg Research Institute of Pharmacology and Regenerative Medicine, Tomsk NRMC, Tomsk, bona2711@mail.ru, https://orcid.org/0000-0002-6438-5734

Smolyakova Vera I. – Dr. Sci. (Med.), Senior Researcher, Laboratory for Circulatory Pharmacology, Goldberg Research Institute of Pharmacology and Regenerative Medicine, Tomsk NRMC, Tomsk, light061265@mail.ru, https://orcid.org/0000-0001-9501-4664

Logvinov Sergey V. – Dr. Sci. (Med.), Professor, Head of the Histology, Embryology and Cytology Division, Siberian State Medical University, Tomsk, logvinov.sv@ssmu.ru, https://orcid.org/0000-0002-9876-6957

Potapov Alexey V. – Dr. Sci. (Med.), Professor, Histology, Embryology and Cytology Division, Siberian State Medical University, Tomsk, potapov.av@ssmu.ru, https://orcid.org/0000-0002-0468-3959

Gerasimov Alexander V. – Dr. Sci. (Med.), Professor, Histology, Embryology and Cytology Division, Siberian State Medical University, Tomsk, gerasimov.av@ssmu.ru, https://orcid.org/0000-0002-8526-6187

Lasukova Tatiana V. – Dr. Sci. (Biology), Professor, Normal Physiology Division, Siberian State Medical University, Tomsk, lasukova.tv**@ssmu.ru, https://orcid.org/0000-0003-3274-6010**

Gereng Elena A. – Dr. Sci. (Med.), Associate Professor, Morphology and General Pathology Division, Siberian State Medical University, Tomsk, gereng.ea@ssmu.ru, https://orcid.org/0000-0001-7226-0328

Akbasheva Olga E. – Dr. Sci. (Med.), Associate Professor, Biochemistry and Molecular Biology Division, Siberian State Medical University, Tomsk, akbasheva.oe@ssmu.ru, https://orcid.org/0000-0003-0680-8249

Tikhonovskaya Olga A. – Dr. Sci. (Med.), Professor, Obstetrics and Gynecology Division, Siberian State Medical University, Tomsk, tikhonovskaya.oa@ssmu.ru, https://orcid.org/0000-0003-4309-5831

Plotnikov Mark B. – Dr. Sci. (Biology), Professor, Chief Researcher at the Laboratory for Circulatory Pharmacology, Goldberg Research Institute of Pharmacology and Regenerative Medicine, Tomsk NRMC, Tomsk, mbp2001@mail.ru, https://orcid.org/0000-0002-0548- 6586

(✉) **Zhdankina Anna A.,** annazhdank@yandex.ru

Received on August 26, 2025;
approved after peer review on October 16, 2025;
accepted on October 30, 2025

УДК 616.136.7:616.61-073.75-047.58
https://doi.org/10.20538/1682-0363-2026-2-21-31

Mathematical Modeling of the Intrarenal Arterial Bed Structure Using Regression Models and a Graph Neural Network

Zenin O.K.[1], Gorbachenko V.I.[1], Gribkov D.N.[1], Sergienko A.A.[1], Ilias Miltiadis[2]

[1] *Penza State University (PSU)*
40 Krasnaya St., 440026 Penza, Russian Federation

[2] *The University of Palermo*
61 Piazza Marina St., 90133 Palermo, Italy

ABSTRACT

The aim was to develop models for numerical modeling of the diameters and lengths of bifurcation segments, structural units of the intrarenal arterial bed (IAB).

Materials and methods. The study is based on previously obtained morphometric data on the structure of 9,642 arterial bifurcations (AB) of 60 corrosion casts of the IAB. AB is a section of the IAB consisting of a proximal arterial segment (AS) (D), two distal AS (with a larger (d_{max}) and smaller (d_{min}) internal diameter) and a branching point. Regression models were used for numerical modeling of the AS diameters, while a graph attention network (GAT) was used for the lengths of AS.

Results. The developed models demonstrate high prediction accuracy: for AS diameters with a larger value (d_{max}), the training set reached an R^2 value of 0.89, for AS with a smaller value (d_{min}) – R^2 = 0.8. For the length of the AS with a larger diameter, the training set reached an R^2 value of 0.75, and the test set reached an R^2 value of 0.74; for the length of the AS with a smaller diameter, the training set reached an R^2 value of 0.77, and the test set reached an R^2 value of 0.73.

Conclusion. The proposed models can be used for numerical modeling of the IAB structure and assessment of the adequacy of renal blood supply.

Keywords: intrarenal arterial bed, arterial bifurcation, numerical modeling, neural networks

Conflict of interest. The authors declare the absence of obvious or potential conflicts of interest related to the publication of this article.

Source of financing. The authors state that they received no funding for the research.

For citation: Zenin O.K., Gorbachenko V.I., Gribkov D.N., Sergienko A.A., Ilias Miltiadis. Mathematical Modeling of the Intrarenal Arterial Bed Structure Using Regression Models and a Graph Neural Network. *Bulletin of Siberian Medicine.* 2026;25(2):21–31. https://doi.org/10.20538/1682-0363-2026-2-21-31.

✉ *Zenin Oleg K.,* zen.olegz@gmail.com

Математическое моделирование структуры внутрипочечного артериального русла с помощью регрессионных моделей и графовой нейронной сети

Зенин О.К.[1], Горбаченко В.И.[1], Грибков Д.Н.[1], Сергиенко А.А.[1], Ilias Miltiadis[2]

[1] *Пензенский государственный университет (ПГУ)*
Россия, 440026, г. Пенза, ул. Красная, 40

[2] *Университет Палермо*
Италия, 90133, г. Палермо, ул. Пиацца Марина, 61

РЕЗЮМЕ

Цель – разработать модели для численного моделирования диаметров и длин сегментов бифуркаций – структурных единиц внутрипочечного артериального русла (ВАР).

Материалы и методы. Исследование основано на ранее полученных морфометрических данных о структуре 9 642 артериальных бифуркаций (АБ) 60 коррозионных препаратов ВАР. Артериальная бифуркация – участок ВАР, состоящий из проксимального артериального сегмента (АС) (D), двух дистальных АС (с большей (d_{max}) и меньшей (d_{min}) величиной внутреннего диаметра) и точки ветвления. Для численного моделирования диаметров (АС) использовали регрессионные модели, для моделирования длин АС – графовую нейронную сеть внимания (GAT).

Результаты. Разработаны модели, которые демонстрируют высокую точность прогнозирования: для диаметров АС с d_{max} обучающий набор достиг значения $R^2 = 0{,}89$, для АС с d_{min} – $R^2 = 0{,}8$. Для длины АС с d_{max} обучающий набор достигал значения $R^2 = 0{,}75$, а тестовый набор – $R^2 = 0{,}74$; для длины АС с d_{min} обучающий набор достиг значения $R^2 = 0{,}77$, а тестовый набор – $R^2 = 0{,}73$.

Заключение. Предложенные модели могут быть использованы для численного моделирования структуры ВАР и оценки адекватности почечного кровоснабжения.

Ключевые слова: внутрипочечное артериальное русло, артериальная бифуркация, численное моделирование, нейронные сети

Конфликт интересов. Авторы декларируют отсутствие явных и потенциальных конфликтов интересов, связанных с публикацией настоящей статьи.

Источник финансирования. Авторы заявляют об отсутствии источника финансирования при проведении исследования.

Для цитирования: Зенин О.К., Горбаченко В.И., Грибков Д.Н., Сергиенко А.А., Ilias Miltiadis. Математическое моделирование структуры внутрипочечного артериального русла с помощью регрессионных моделей и графовой нейронной сети. *Бюллетень сибирской медицины.* 2026;25(2):21–31. https://doi.org/10.20538/1682-0363-2026-2-21-31.

INTRODUCTION

The prevalence of kidney disease is steadily increasing every year [1–3]. Recently, the P4 medicine – personalized, predictive, preventive, and participatory – has become increasingly important in modern medicine, including the fight against kidney disease [4]. Modern digital *in vivo* imaging technologies offer new opportunities for diagnosis [5, 6], predicting the results of angioplasty [7], and solving educational problems related to the anatomy and pathology of the intrarenal arterial bed (IAB) [8, 9]. Despite many studies, these problems remain unresolved, which, in our opinion, is largely due to the lack of a digital model adequately describing the structure of the IAB.

Previous attempts at numeric modeling and creating a digital model of the IAB described its structure as a fractal system. This system consists of arterial bifurcations (ABs), which include a parent (D) and two daughter arterial segments (ASs), with larger (d_{max}) and smaller ((d_{min}) internal

diameters. This issue was first addressed in the doctoral dissertation of the German anatomist and embryologist Wilhelm Roux [10]. On the basis of his observations, he concluded that the structure of AB resembles the shape of a jet of liquid flowing out of a tube opening. He was the first to establish a connection between the AB branching angle and the diameters of the lumen of the parent and daughter ASs [10]. This issue was subsequently studied by C.D. Murray [11], H.B. Uylings [12], M. Kretowski et al. [13], F. Cassot et al. [14], P.J. Blanco et al. [15], T. Fredrich et al. [16], F.M. Kashkooli et al. [17], and P. Li et al. [18].

Nevertheless, an adequate quantitative (numerical) description of IAB remains an unsolved problem for two main reasons. Firstly, the channel covers a wide range of AS diameters – from several micrometres to several millimeters [19], which is undeservedly ignored by most authors. Secondly, the complexity of visualizing and obtaining reliable information about AS lengths, which is extremely necessary for their numerical modeling.

The aim was to develop models for numerical modeling of the diameters and lengths of bifurcation segments – structural units of IAB.

MATERIALS AND METHODS

The material for the study was previously obtained from the morphometry of 60 corrosion casts of IAB [20]. This method allows for the measurement of ASs with an inner diameter of 0.1 mm with accuracy of 0.01 mm. IABs are considered to be fractal systems consisting of interconnected ABs (Fig. 1, *a, b*).

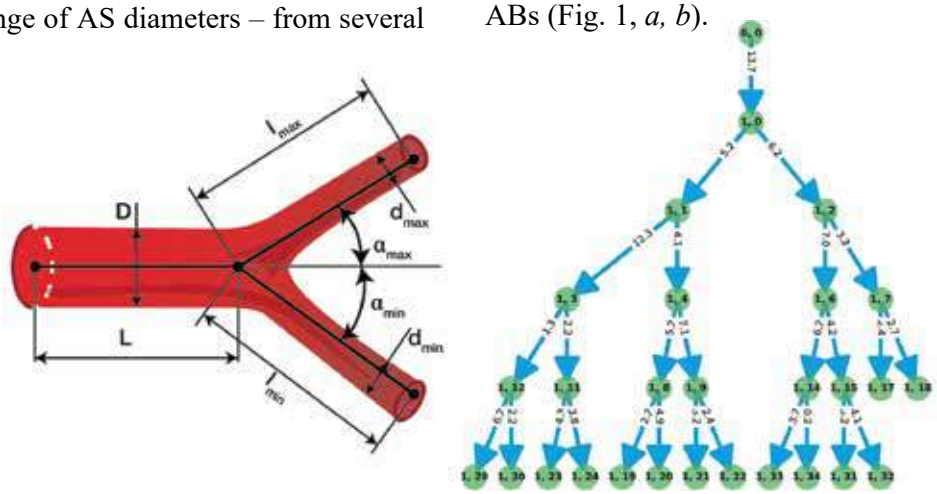

Fig. 1. Diagram of IAB as a fractal system: *a* – AB IAB diagram; *b* – graphical representation of the protocol; 1 – unique numbers are indicated at the graph nodes, and the edges indicate the lengths of AS. *D* – diameter of the proximal segment; d_{max} – diameter of the distal segment with a larger value; d_{min} – diameter of the distal segment with a smaller value; *L* – length of the proximal segment; l_{max} – length of the distal segment with a larger diameter; l_{min} – length of the distal segment with a smaller diameter; α_{max} – branching angle between the distal segment with a larger diameter and the proximal segment; α_{min} – branching angle between the distal segment with a smaller diameter and the proximal segment

The study included 9,642 ABs located at 22 division levels (*i*) and 60 corrosive IAB preparations. The ABs were divided into the following groups: two sex-based groups (male or female ABs); two age groups: middle-aged (men aged 36–60 years, women aged 36–55 years) and elderly individuals (men aged 61–75 years, women aged 56–75 years) (Classification of the USSR Academy of Medical Sciences (1965)); as well as ABs belonging to the corrosion preparations of the left and right kidneys. Previous studies have revealed morphological differences in the arterial bed of the kidneys in individuals of different sexes [21], as well as in the left and right kidneys [22].

The following indicators were used to describe this structure numerically: *i* – serial number of the division level – newly formed AS series; *D* – diameter of the parent proximal AS located at the initial division level; d_{max} – diameter of the daughter distal AS with a larger value; d_{min} – diameter of the daughter distal AS with a smaller value; *L* – length of the parent proximal AS located at the initial division level, distance between the nearest branching points; l_{max} – length of the daughter distal AS with a larger diameter; l_{min} – length of the daughter distal AS with a smaller diameter.

For the diameters of the AB IAB segments, calculations and comparisons of several regression model options were performed. A formal description of the model in statistics assumes the presence of observations, a set of all measured pairs of features – responses, expressed as $\{(\mathbf{x}_i, y_i)\}_{(i=1)}^{n}$, where the observation vector x_i is one element of the sample. In our case, this is one row of the available database [20], where *i* is the observation index, x_i is the value of the predictor (feature) for the i-th observation, and y_i is the response value for this observation.

When a simple linear regression model is applied, the observation vector contains only one element x_i. From a mathematical point of view, simple linear regression has the form represented as $y_i = \alpha + \beta x_i + \varepsilon_i$, where α is the intercept (free term) common to all observations, which does not depend on *x*; β is the slope coefficient, which describes how *y* changes on average when *x* changes by one unit, assuming that the relationship is linear (straight); ε_i is a random error (noise), i.e., the part of the variation in *y* that is not explained by the linear relationship.

The regression problem was solved via the method of least squares. The accuracy of each predicted value is measured by the square of its residual (the vertical distance between the data point and the constructed line), and the goal of the method is to minimize the sum of these squares of deviations. In the case of simple linear regression, the method of least squares leads to a system of two linear equations, the solutions of which are the coefficients α and β.

We also employed a multiple linear regression model that uses a vector of features $x_i = [x_{i1}\, x_{i2} \ldots x_{ip}]^{\mathrm{T}}$ for *p* features, in contrast to simple linear regression, which relies on a single variable. Then, the regression equation takes the form $y_i = \sum_{j=0}^{p} a_j x_{ji}$, where $x_{0i} = 1$. In matrix form, the regression equation takes the form **Xa** = y, where $y = [y_1\, y_2 \ldots y_n]^{\mathrm{T}}$ is the vector of dependent variable values, T is the transpose symbol, and $a = [a_0\, a_1, \ldots, a_k]^{\mathrm{T}}$ is the vector of regression coefficients:

$$X = \begin{bmatrix} 1\, x_{11} \ldots x_{1k} \\ 1\, x_{21} \ldots x_{2k} \\ \vdots\ \vdots \quad\ \vdots \\ 1\, x_{n1} \ldots x_{nk} \end{bmatrix}$$

is the matrix of independent variables (design matrix).

In modern libraries, the regression equation is solved via the singular value decomposition method rather than the method of least squares.

In addition, we explored the use of polynomial regression of degrees 2 and 3. It is a linear model in the space of extended basis features obtained by raising the initial variables to power and multiplying them together. From a mathematical point of view, the general form of polynomial regression is represented as $y = \beta_0 + \beta_1 x + \beta_2 x^2 + \ldots + \beta_n x^n + \varepsilon$, where *y* is the dependent variable response, β_n are unknown terms, ε is noise, and *n* is the degree of the polynomial. In general, the matrix form is $\vec{y} = X\vec{\beta} + \vec{\varepsilon}$, and the solution is $\hat{\vec{\beta}} = (\mathbf{X}^{\mathrm{T}}\mathbf{X})^{-1}\mathbf{X}^{\mathrm{T}}\vec{y}$.

For regression modeling of diameters, the dataset was divided into a training set (7,710 samples, 80 %) and a test set (1,930 samples, 20%). In a simple linear regression approach, the diameter of the parent segment was used as the only predictor. For all other models, a complete set of features was used, including the diameter of the parent vessel, sex, age, and division level.

The following metrics were selected to verify the quality of the results. R^2 is the coefficient of determination. An R^2 close to 1 indicates that the model almost completely explains the variation. An R^2 of 0 means that the model does not explain the variance any better than the mean, while a negative R^2 suggests the model's predictions are worse than simply using the mean as a forecast. The coefficient is calculated by subtracting from one the ratio of the residual sum of squares to the total sum of squares: $R^2 = 1 - \frac{\sum_{i=1}^{n}(y_i - \hat{y}_i)^2}{\sum_{i=1}^{n}(y_i - \bar{y})^2}$, where y_i are the actual values, $\hat{y}_i$ are the predicted values, and $\bar{y} = \frac{1}{n}\sum_{i=1}^{n} y_i$ is the average value of the observed data.

The RMSE and MAE metrics were used to evaluate the accuracy of the forecasts. The RMSE is the root mean squared error, measured in the same units as the target variable. The formula is as follows: $RMSE = \sqrt{\frac{1}{n}\sum_{i=1}^{n}(y_i - \hat{y}_i)^2}$, where n is the number of observations and $\hat{y}_i$ is the predicted value. The MAE is the mean absolute error , which is less sensitive to outliers than the RMSE: $MAE = \frac{1}{n}\sum_{i=1}^{n}\left|y_i - \hat{y}_i\right|$.

The models were implemented in Python version 3.11.11 in the Ubuntu 24.04 software environment via the scikit-learn library version 1.7.2. The forecasts were visualized via the matplotlib library version 3.10.6. The same linear regression models were used for forecasting $l_{max}$and l_{min} as for d_{max} and d_{min}. The only change for simple linear regression was that the dependence of the daughter length on a single predictor L – vessel length – was investigated, whereas for multiple regression and polynomial regression, the set of features was expanded with the parameters for d_{max} and d_{min}.

RESULTS

Mathematical modeling of AB as a structural element of the fractal system IAB is a difficult task. To construct an accurate digital model of ABs, four tasks were solved simultaneously. Specifically, the following were determined: 1. Diameters d_{max} of distal ASs with large values; 2. Diameters d_{min} of distal ASs with smaller values; 3. Lengths l_{max} of distal ASs with large diameters; 4. Lengths l_{min} of distal ASs with smaller diameters.

The results of the calculations for d_{max} and d_{min} are presented in Table 1 and Figure 2, *a*:

Table 1

Model Quality Indicators for Predicting d_{max} and d_{min}

Model/metrics	Prediction			Prediction		
		RMSE, mm	MAE, mm		RMSE, mm	MAE, mm
Linear regression	0.87	0.21	0.15	0.78	0.22	0.15
Multiple linear regression	0.87	0.21	0.15	0.78	0.21	0.14
Second-degree polynomial regression	0.88	0.20	0.15	0.78	0.21	0.14
Third-degree polynomial regression	0.83	0.24	0.17	0.75	0.23	0.16

Note. Here and in Tables 2 and 3: d_{max} – diameter of the distal AS with a larger value; d_{min} – diameter of the distal AS with a smaller value; R^2 – coefficient of determination; RMSE – root mean squared error; MAE – mean absolute error.

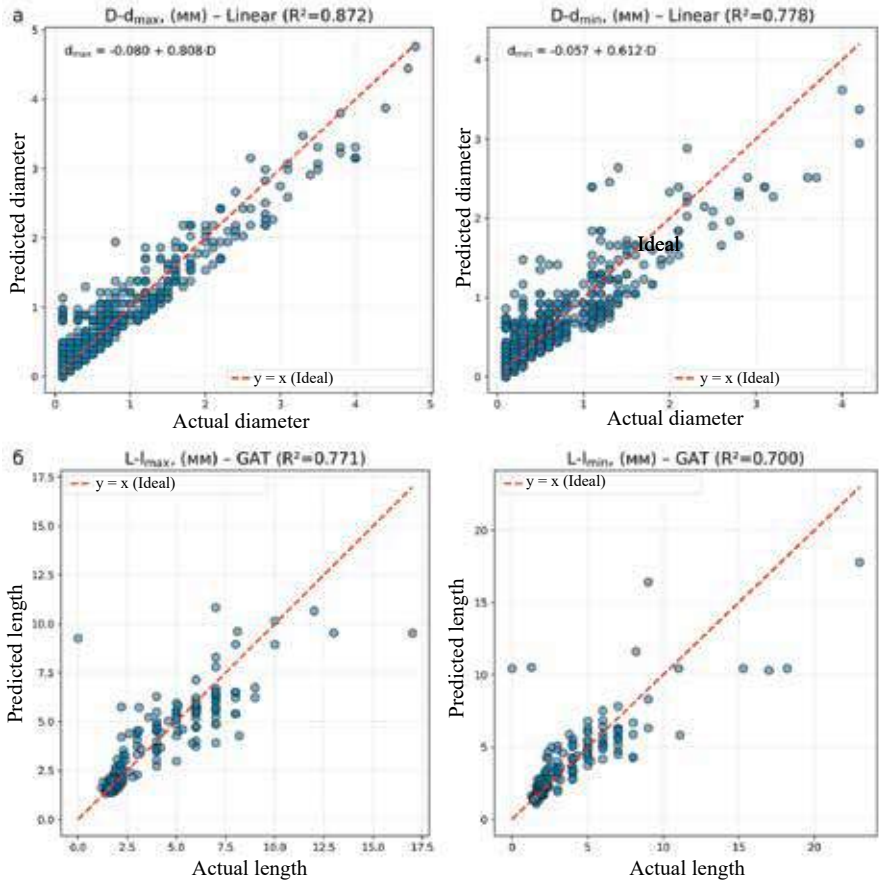

Fig. 2. Predicted/actual graphs for: *a* – simple linear regression for d_{max} and d_{min} of the relationship equations: $d_{max} = –0.080 + 0.808D$ $(R^2 = 0.87)$ and $d_{min} = –0.057 + 0.612D$ $(R^2 = 0.77)$; b – GAT for l_{max} and l_{min}: the coefficient of determination for l_{max} is $R^2 = 0.77$ and l_{min} is $R^2 = 0.70$

As shown above (Table 1 and Fig. 2, *a*), all the models yield good results ($R^2 \geq 0.70$), with both linear regression and second-degree polynomial regression showing the best results. The third-degree polynomial regression models are overfit: R^2 decreases to 0.83 (for d_{max}) and 0.75 (for d_{min}), and the RMSE increases by approximately 10–15% (Table 1).

The results of the calculations for l_{max} and l_{min} are presented in Table 2.

Table 2

Model Quality Indicators for Predicting l_{max} and l_{min}

Model/metrics	Prediction			Prediction		
		RMSE, mm	MAE, mm		RMSE, mm	MAE, mm
Linear regression	0.55	1.43	0.93	0.42	1.48	0.88
Multiple linear regression	0.57	1.40	0.90	0.51	1.35	0.86
Second-degree polynomial regression	0.58	1.38	0.85	0.55	1.31	0.79
Third-degree polynomial regression	0.56	1.41	0.85	0.56	1.30	0.77

The results of regression analysis show that for simple linear regression, the dependence is too complex to detect. As the complexity of the regression model increases, the results improve, but even for second- and third-degree polynomial regressions, the results do not exceed 58%. In this context, the use of neural networks, which can approximate arbitrarily complex functions [23] and capture hidden dependencies between variables that are not accessible to standard regressors [24], has been proposed.

This was the prerequisite for using a neural network approach to solve these problems. The first architecture used was the basis and progenitor of all other networks – a multilayer perceptron [24]. The advantages of a multilayer perceptron are its simplicity of implementation, fast training, and easy integration into the workflow pipeline (as well as into regressors). The main limitation is the inability to account for the structure of the input data (for example, temporal or graph data).

The main idea of a multilayer perceptron is that each neuron of layer l is connected to all the neurons of the previous layer $l-1$. This connection defines a linear transformation, which is usually followed by nonlinear activation. From a mathematical point of view, this can be represented as $\mathbf{z}^{(l)} = \mathbf{W}^{(l)}\mathbf{a}^{(l-1)} + \mathbf{b}^{(l)}$, $\mathbf{a}^{(l)} = \mathbf{f}(\mathbf{z}^{(l)})$, , where $\mathbf{W}^{(l)}$ is the weight matrix of layer l, $\mathbf{b}^{(l)}$ is the bias vector of layer l, $\mathbf{f}(\mathbf{z}^{(l)})$ is a nonlinear activation function (ReLU, tanh, sigmoid, etc.), $\mathbf{a}^{(l-1)}$ is the activation vector of the previous layer, and $\mathbf{a}^{(l)}$ is the activation vector of the current layer. MLP training is implemented via the backpropagation algorithm, which calculates the gradients of the loss function across the network parameters. Parameter optimization is performed via stochastic gradient descent methods or their modern adaptive variants, such as Adam. The choice of loss function depends on the task at hand; MSE is often used for regression.

The next architecture chosen was a recurrent neural network LSTM [25] (long short-term memory network). The choice was made because segments of the vascular system are represented as sequences, the characteristics of which can potentially be predicted by LSTM. The main advantage of LSTM is the preservation of long-term dependencies in memory and resistance to vanishing gradients (unlike conventional recurrent networks). When applied to the vascular structure, each individual AB segment can be represented as a time series, where a daughter vessel grows from a larger vessel, and so on. In vascular bed modeling, the level of vascular bed division acts as an analog of the time series step.

The disadvantages of LSTM include the high computational cost of training and limitations in parallelization. The main advantage of LSTM is its ability to store information effectively over many steps, solving the problem of gradient decay. This allows the network to identify long-term dependencies in the data, which is impossible for conventional recurrent networks. This is achieved by introducing a memory cell that transmits information in steps and three control gates that regulate the flow of information. The gates are fully connected layers

with sigmoid activation functions that output values close to 0 ("closed") and 1 ("open").

At step t, the LSTM components work as follows. The forget gate (f_t) determines what proportion of information from the previous state of the cell (c_{t-1}) needs to be "forgotten." The forget gate is described by the expression $\mathbf{f}_t = \sigma(\mathbf{W}_f[\mathbf{h}_{t-1}, \mathbf{x}_t] + \mathbf{b}_f)$, where $[\mathbf{h}_{t-1}, \mathbf{x}_t]$ is the concatenation of the previous hidden state ($\mathbf{h}_{t-1}$) and the current input ($\mathbf{x}_t$), and $\mathbf{b}_f$ is the bias vector. The input gate ($\mathrm{i}_t = \sigma(\mathbf{W}_f[\mathbf{h}_{t-1}, \mathbf{x}_t] + \mathbf{b}_i)$)) determines which part of the new information to update, and the candidate value creates new candidate values that can be added to the cell ($\hat{\mathbf{c}}_t = \tanh(\mathbf{W}_{\hat{c}}[\mathbf{h}_{t-1}, \mathbf{x}_t] + \mathbf{b}_{\hat{c}}$). The cell state update is performed by combining the forgetting of old information and the addition of a new $\mathbf{c}_t = \mathbf{f}_t \odot \mathbf{c}_{t-1} + \mathbf{i}_t \odot \hat{\mathbf{c}}_t$, where the symbol $\odot$ denotes element-wise multiplication. Old information is multiplied by the "forgetting" coefficient, and new information is multiplied by the "input" coefficient. The output gate determines which part of the updated cell state ($\mathbf{c}_t$) will be used to form the output signal $\mathbf{o}_t = \sigma(\mathbf{W}_o[\mathbf{h}_{t-1}, \mathbf{x}_t] + \mathbf{b}_o$. The new hidden state is formed according to the formula

$$\mathbf{h}_t = \mathbf{o}_t \odot \tanh(\mathbf{c}_t).$$

LSTM training, like other recurrent networks, is performed via the backpropagation through time (BPTT) algorithm. The key mechanism of LSTM, additive state updates through gates, allows gradients to propagate without attenuation. This enables the network to remember information over many steps, as the model itself learns to decide when to "open" or "close" the gates.

For comparison with the multilayer perceptron, we selected the Kolmogorov–Arnold Network (KAN), a novel neural network architecture [26]. The KAN architecture is based on the Kolmogorov–Arnold theorem, which states that any continuous function of many variables can be represented as a finite superposition of continuous functions of a single variable. For the input vector $\mathrm{x} = (x_1 x_2, \ldots, x_n)$ KAN, the regression problem for predicting vessel diameters is described by the expression

$$y = \sum_{j=1}^{2n+1} \Phi_j \left(\sum_{i=1}^{n} \varphi_{ij}(x_i) \right),$$

where φ_{ij} are B-splines (approximating basis functions), and Φ_j are nonlinear functions of the output layer (B-splines). The network has two layers with activations on the edges rather than on the nodes. B-splines with trainable coefficients are used as activation functions. The main advantage of Kolmogorov–Arnold networks is their high accuracy with fewer parameters.

Since the AS components of AB in the IAB system can be represented as a graph, the use of graph neural networks [27] to predict vessel diameters has been proposed. The best results were obtained via graph attention networks (GAT) [28]. In this work, PyTorch Geometric (PyG), a specialized PyTorch extension for working with graph neural networks, was used to implement the graph attention network [29].

Let us consider the implementation of a GAT, taking into account the features of PyG. The graph at the input of the graph neural network was represented by two matrices: a vertex matrix and an adjacency matrix. The vertex matrix is a concatenation (combination) of vectors (embeddings) describing the vertices. Considering the bifurcations of the daughter vessel length , they were represented in the node embeddings, which made it possible to exclude the edge matrix. The adjacency matrix, as is customary in graph theory, is a binary matrix in which the element (i, j) is equal to one if the vertex i is connected to the vertex j. Since the adjacency matrix is sparse, PyG is represented as an array of edges containing the indices of the graph edges.

A multi-headed graph attention network is a GAT architecture in which each node of the graph is trained to dynamically weigh the importance of its neighbors simultaneously in several independent projections of the feature space («attention heads»). Multi-headed attention uses K independent attention mechanisms («heads») in parallel to improve stability and expressiveness. Each head k has its own trainable weight matrix $\mathbf{W}^k$ of size $f \times f$, where f is the dimension of the node embeddings at the layer input, and a trainable attention matrix $\mathbf{A}_{\text{att}}^k$ of size $n \times n$, where n is the number of graph nodes. The attention matrix shares structure with the graph adjacency matrix, but the elements of the adjacency matrix are constant and equal to 0 or 1, whereas the elements of the attention matrix are trainable and capture the varying degrees of influence of neighboring nodes. Each attention head performs the following operations (in PyG, the operations are vectorized and performed in parallel).

Linear transformation $\mathbf{H}^k = \mathbf{X}\mathbf{W}^k$ for $k = 1, \ldots K$, where $\mathbf{X}$ is the matrix of input embeddings of the layer with size $n \times f$.

Calculation of attention matrices $\mathbf{A}_{\text{att}}^k$.

Aggregation $\mathbf{Z}^k = A_{\text{att}}^k \mathbf{H}^k$ for $k = 1, \ldots, K$.

The results of all heads are combined. For the hidden layers, concatenation is used $\mathbf{X}'$ = Concat $[\sigma(\mathbf{Z}^1), \sigma(\mathbf{Z}^2), .., \sigma(\mathbf{Z}^K)]$, where σ is the activation function, usually ReLU. The output dimension of the network layer increases $n \times (K \cdot f)$. In the input layer, averaging

$$\mathbf{X}' = \frac{1}{K}\sum_{k=1}^{K}\sigma(\mathbf{Z}^k)$$

is used, and the output dimension of the network becomes equal to the dimension of the input embedding array. Since the regression problem is being solved, a linear activation function is used in the output layer.

The embeddings of nodes in a single layer of a multi-headed attention graph network consider the properties of neighboring nodes. The perception area (how far the influence spreads) is controlled by the number of layers in the network. A graph network with m layers will aggregate information from nodes at a distance of up to m transitions.

To implement neural networks, the cuda library version 12.8 is added to the above information, together with the PyTorch library for implementing neural networks in Python version 2.7.0. Pycan library version 0.0.2 was used to implement KAN. Owing to the limitations of this library, KAN training was also performed on the CPU via the PyTorch library. PyTorch-Geometric library version 2.6.1 [29] was used to implement the GAT graph model.

Each of the four neural networks was trained on an identical dataset. All the networks used a single set of features: parent diameter, diameter of the larger and smaller daughter ASs, parent AS length, sex, age, and division level. The target data were the lengths of the larger and smaller daughter ASs. For each of the trained networks, the Adam optimizer and MSE validation for early stopping were used to prevent overfitting on the training set. The MLP is represented by a single hidden layer with a dimension of 128 with a ReLU activation function and a learning rate of 0.0005. The LSTM is represented by four layers, with 1,024 hidden neurons, at the output of a linear layer for compressing the output data into one neuron, with a learning rate of 0.005. The KAN consists of two hidden layers with two neurons in each, the grid size (number of "nodes" in each function) is 5, the grid range is from –5 to 5, and a learning rate of 0.01. The GAT is represented by two layers with 1,024 neurons, one attention head, a learning rate of 0.001, and weight decay (L2 regularization) of 0.00001.

The graph models (GATs) demonstrate the best prediction quality for both the maximum length of IAB AS (l_{max}) and the minimum length of IAB AS (l_{min}). This confirms the idea that the relationships between individual ASs play a key role in assessing the morphology of the vascular system: at l_{max}, it outperforms all other models on all the metrics; for l_{min}, the GAT retains the best explanatory power (R^2 = 0.70) and the lowest MAE, but its RMSE (1.46 mm) is slightly greater than that of the MLP. This may indicate that when predicting shorter lengths (l_{min}), the model is more sensitive to "outliers" in the data, whereas the MLP is more stable on average; the poor performance of the LSTM indicates that the current dataset does not have a clearly defined sequential structure that can be used by a recurrent architecture.

Neural networks use nonlinear transformations that cannot be written as fixed analytical formulas without fully disclosing all the weights and biases. Therefore, the article presents a structural description of the models, their hyperparameters, and results, which fully meets the requirements of a scientific publication and allows the experiment to be reproduced. In neural networks, prediction is a sequence of matrix multiplication and nonlinear activation functions with many parameters (weights and biases). It is meaningless to write them down as a few formulas; instead, the architecture, hyperparameters, and metric results are published, allowing other researchers to reproduce the model.

The results are presented in Table 3 and Fig.2, *b*.

Table 3

Neural Network Training Results l_{max} and l_{min}

Model/metrics	Prediction			Prediction		
		RMSE, mm	MAE, mm		RMSE, mm	MAE, mm
MLP neural network	0.61	1.32	0.79	0.61	1.21	0.73
LSTM neural network	0.43	1.59	0.95	0.34	1.51	0.93
KAN	0.63	1.28	0.78	0.55	1.29	0.77
GAT neural network	0.77	1.11	0.56	0.70	1.45	0.66

DISCUSSION

Two models were trained to find the diameters of daughter ASs with larger and smaller values. For practical implementation, simple linear regression equations can be used: $d_{max} = -0.080 + 0.808\ D$ ($R^2 = 0.87$) and $d_{min} = -0.057 + 0.612\ D$ ($R^2 = 0.77$) (Fig. 2, *a*). Two models were trained to find the length of AS with larger and smaller diameters, both of which solve the regression problem (Fig. 2, *b*). The training used features that were explicitly known or could be accurately calculated, including the following: current AS diameter; AS diameters with larger values; AS diameters with smaller values; division level (*i*); sex; age group; and current AS length.

Studies have shown that using the organ position (i.e., right or left) impairs the predictive power of the models. Using AS lengths with larger and smaller diameter values increases the accuracy of the model's predictions, but these characteristics cannot be used because of their uncertainty in predicting distal AS lengths.

As a result of the experiments, the best solution was a graph network consisting of two layers of GAT and two attention heads, implemented in the PyTorch Geometric library [29]. The best results were obtained via the Adam optimizer [32], with a learning rate of 0.001 and weight_decay of 0.00001. Retraining was controlled by monitoring the values of R^2 for the test sample: if there was no improvement in the indicator by a delta of 0.01 within 100 epochs, training was stopped.

For accurate modeling of the geometry of the IAB, it is necessary to combine the developed neural network models to determine the distal ASs with maximum and minimum diameters. The results of testing the program were presented in the form of model training quality metrics. The coefficient of determination R^2 was used to evaluate quality. For the length of the distal segment with a large diameter, the training set reached a value of $R^2 = 0.75$, and the test set reached a value of $R^2 = 0.74$. The mean square error function was used as the loss function.

Similar metrics and loss functions were used for the length of the distal segment with a calculation model of a smaller diameter. The training set achieves a value of $R^2 = 0.77$, and the test set achieves a value of $R^2 = 0.73$. The results of our study confirm that the use of a GNN for modeling AB IAB is a promising approach. In particular, the GAT demonstrated high prediction accuracy, which is consistent with other studies in the field of vascular structure modeling [33, 34].

The results obtained coincide with the results of previous studies, such as those by P.J. Blanco et al., which showed that digital models and computer simulations can accurately describe vascular beds. However, unlike these studies, the present study focuses on neural networks, which allows for the consideration of more complex relationships between the AS parameters that make up the AB. Moreover, the neural network approach made it possible for the first time to quantitatively predict the model of the IAB structure – to determine the values of the AS length for each AB, which makes it possible to conduct a more in-depth study and perform numerical modeling of hemodynamics within the IAB.

The use of the GAT offers several advantages over traditional modeling methods. First, graph networks consider the topology of the IAB, which is crucial for modeling complex bifurcation structures [35]. Second, the use of GAT mechanisms allows for more accurate consideration of the importance of AS (edges) and AB (nodes) connections in the graph, as GAT calculates trainable attention coefficients for each AS that determine how important a neighboring AB is to the current one, thereby improving the quality of prediction [28].

Despite these promising results, the study has several limitations. Firstly, the accuracy of predictions depends on the quality of the input data and model parameters. Secondly, the use of neural networks requires significant computational resources, which may limit their application in clinical practice. Further improvements will focus on using more accurate data and optimizing training algorithms.

CONCLUSION

Thus, models were developed for numerical simulation of the diameters and lengths of AB segments, i.e., structural units of IAB. The first module consisting of two regression equations allows the diameters of two daughter (distal) ASs to be calculated on the basis of the diameter of the parent (proximal) AS. The second module, a graph neural attention network, allows for the calculation of the lengths of two daughter (distal) ASs on the

basis of the length of the parent (proximal) AS to determine the lengths of the AB segments of the IAB. The use of a graph attention network has made it possible to achieve high prediction accuracy, opening new opportunities for clinical applications, including preoperative modeling and assessment of whether renal blood supply is normal.

The developed two-module model can serve as a basis for creating methods for the numerical prediction of the volume and area of the kidney region supplied by a given artery. This will help in planning and performing surgical interventions, as well as evaluating their results. Further improvements will focus on using more accurate data and optimizing training algorithms.

REFERENCES

1. Borg R., Carlson N., Søndergaard J., Persson F. The growing challenge of chronic kidney disease: an overview of current knowledge. *Int. J. Nephrol*. 2023:9609266. DOI: 10.1155/2023/9609266.
2. Eckardt K.U., Delgado C., Heerspink H.J.L., Pecoits-Filho R., Ricardo A.C., Stengel B. et al. Trends and perspectives for improving quality of chronic kidney disease care: conclusions from a kidney disease: Improving Global Outcomes (KDIGO) Controversies Conference. *Kidney Int.* 2023;104(5):888–903. DOI: 10.1016/j.kint.2023.05.013.
3. Eckardt K.U., Coresh J., Devuyst O., Johnson R.J., Köttgen A., Levey A.S. et al. Evolving importance of kidney disease: from subspecialty to global health burden. *Lancet*. 2013;382(9887):158–169. DOI: 10.1016/S0140-6736(13)60439-0.
4. Jenkins S.L., Ma'ayan A. Systems pharmacology meets predictive, preventive, personalized and participatory medicine. *Pharmacogenomics*. 2013;14(2):119–122. DOI: 10.2217/pgs.12.186.
5. Tsai S.H., Chu S.J., Chen S.J., Fan Y.M., Chang W.C., Wu C.P. et al. Acute renal infarction: a 10-year experience. *Int. J. Clin. Pract*. 2007;61(1):62–67. DOI: 10.1111/j.1742-1241.2006.01136.x
6. Siegel R.L., Miller K.D., Jemal A. Cancer statistics, 2018. *CA Cancer J. Clin.* 2018;68(1):7–30. DOI: 10.3322/caac.21442.
7. Heuer R., Gill I.S., Guazzoni G., Kirkali Z., Marberger M., Richie J.P. et al. A critical analysis of the actual role of minimally invasive surgery and active surveillance for kidney cancer. *Eur. Urol*. 2010;57(2):223–232. DOI: 10.1016/j.eururo.2009.10.023.
8. Pather N., Blyth P., Chapman J.A., Dayal M.R., Flack N.A.M.S., Fogg Q.A. et al. Forced disruption of anatomy education in Australia and New Zealand: an acute response to the Covid-19 pandemic. *Anat. Sci. Educ*. 2020;13(3):284–300. DOI: 10.1002/ase.1968.
9. Baptiste Y.M. Digital feast and physical famine: the altered ecosystem of anatomy education due to the Covid-19 pandemic. *Anat. Sci. Educ*. 2021;14(4):399–407. DOI: 10.1002/ase.2098.
10. Roux W. Ueber die verzweigungen der blutgefsse. *Eine morphologische Studie*. *Z Naturwiss.* 1878;12:205–266.
11. Murray C.D. The physiological principle of minimum work applied to the angle of branching of arteries. *J. Gen. Physiol*. 1926;9(6):835–841. DOI: 10.1085/jgp.9.6.835.
12. Uylings H.B. Optimization of diameters and bifurcation angles in lung and vascular tree structures. *Bull. Math. Biol*. 1977;39(5):509–520. DOI: 10.1007/BF02461198.
13. Kretowski M., Rolland Y., Bézy-Wendling J., Coatrieux J.L. Physiologically based modeling of 3-D vascular networks and CT scan angiography. *IEEE Trans. Med. Imaging*. 2003;22(2):248–257. DOI: 10.1109/TMI.2002.808357.
14. Cassot F., Lauwers F., Fouard C., Prohaska S., Lauwers-Cances V. A novel three-dimensional computer-assisted method for a quantitative study of microvascular networks of the human cerebral cortex. *Microcirculation*. 2006;13(1):1–18. DOI: 10.1080/10739680500383407.
15. Blanco P.J., de Queiroz R.A., Feijóo R.A. A computational approach to generate concurrent arterial networks in vascular territories. *Int. J. Numer. Method Biomed. Eng*. 2013;29(5):601–614. DOI: 10.1002/cnm.2547.
16. Fredrich T., Welter M., Rieger H. Tumorcode: A framework to simulate vascularized tumors. *Eur. Phys. J. E. Soft Matter*. 2018;41(4):55. DOI: 10.1140/epje/i2018-11659-x.
17. Kashkooli F.M., Abazari M.A., Soltani M., Ghazani M.A., Rahmim A. A spatiotemporal multi-scale computational model for FDG PET imaging at different stages of tumor growth and angiogenesis. *Sci. Rep*. 2022;12(1):10062. DOI: 10.1038/s41598-022-13345-4.
18. Li P., Pan Q., Jiang S., Yan M., Yan J., Ning G. Development of novel fractal method for characterizing the distribution of blood flow in multi-scale vascular tree. *Front. Physiol*. 2021;12:711247. DOI: 10.3389/fphys.2021.711247.
19. Montino Pelagi G., Regazzoni F., Huyghe J.M., Baggiano A., Alì M., Bertoluzza S. et al. Modeling cardiac microcirculation for the simulation of coronary flow and 3D myocardial perfusion. *Biomech. Model. Mechanobiol*. 2024;23(6):1863–1888. DOI: 10.1007/s10237-024-01873-z.
20 Database Registration Certificate No. 2021620982 Russian Federation. Quantitative Anatomy of the Intrarenal Arterial Bed in the Human Kidney : No. 2021620806 : applied on April 27, 2021 : published on May 18, 2021 / Zenin O.K., Dmitriev A.V., Miltykh I.S., Yurchenko O.O.; applicant: Federal State Budgetary Educational Institution of Higher Education Penza State University. (In Russ.) EDN JDPUFN.
22. Kolsanov A.V., Nazaryan A.K., Voronin A.S., Gelashvili O.A. Variant Anatomy of the Renal Arteries: a Computed Tomography Angiography Study. *Journal of Anatomy and Histopathology*. 2020;9(1):43–48. (In Russ.). DOI: 10.18499/2225-7357-2020-9-1-43-48
23. Liu C., Tan Z., He M. Overview of Artificial Intelligence in Medicine. In: Raz M., Nguyen T.C., Loh E. Artificial intelligence in medicine: applications, limitations and future directions. Singapore: Springer, 2022: 23–34. DOI: 10.1007/978-981-19-1223-8_2.
24. Aggarwal C.C. Neural networks and deep learning: a textbook, 2nd ed. Switzerland: Springer International Publishing AG, 2023:553. DOI: 10.1007/978-3-031-29642-0_13.

25. Nielsen A. Practical time series analysis: prediction with statistics and machine learning. Sebastopol: O'Reilly Media, Inc., 2019:504.
26. Wu Y., Su T., Du B., Hu S., Xiong J., Pan D. Kolmogorov–Arnold network made learning physics laws simple. *J. Phys. Chem. Lett*. 2024;15(50):12393–12400. DOI: 10.1021/acs.jpclett.4c02589.
27. Wu L., Cui P., Pei J., Zhao L. Graph Neural networks: foundations, frontiers, and applications. Singapore: Springer Nature, 2022:725. DOI: 10.1007/978-981-16-6054-2.
28. Veličković P., Cucurull G., Casanova A., Romero A., Liò P., Bengio Y. Graph Attention Networks. Published as a conference paper at ICLR, 2018:12. arXiv:1710.10903v3 [stat.ML].
29. PyG documentation. URL: https://pytorch-geometric.readthedocs.io/en/latest/#.
30. Hagberg A.A., Schult D.A., Swart P.J. Exploring Network Structure, Dynamics, and Function using NetworkX. Proceedings of the 7th Python in Science Conference. Pasadena, CA USA. 2008:11–15. URL: https://aric.hagberg.org/papers/hagberg-2008-exploring.pdf
31. Harris C.R., Millman K.J., van der Walt S.J., Gommers R., Virtanen P., Cournapeau D. et al. Array programming with NumPy. *Nature*. 2020;585(7825):357–362. DOI: 10.1038/s41586-020-2649-2.
32. Kingma D.P., Ba J. Adam: A method for stochastic optimization. Published as a conference paper at the 3rd International Conference for Learning Representations, San Diego. 2017. DOI: 10.48550/arXiv.1412.6980.
33. Zhang S., Yang G., Qian J., Xiaomei Zh., L J., Li Pu. et al. A novel 3D deep learning model to automatically demonstrate renal artery segmentation and its validation in nephron-sparing surgery. *Front. Oncol.* 2022;12:997911. DOI: 10.3389/fonc.2022.997911.
34. Xu P., Holstein-Rathlou N.H., Søgaard S.B., Gundlach C., Sørensen C.M., Erleben K. et al. A hybrid approach to full-scale reconstruction of renal arterial network. *Sci. Rep.* 2023;13(1):7569. DOI: 10.1038/s41598-023-34739-y.
35. Thomas S.R. Mathematical models for kidney function focusing on clinical interest. *Morphologie*. 2019;103(343):161–168. DOI: 10.1016/j.morpho.2019.10.043.

Author Contribution

Zenin O.K. — conception and design, final approval of the manuscript for publication. Gorbachenko V.I. — analysis and interpretation of the data. Gribkov D.N. — software development, analysis and interpretation of the data. Sergienko A.A. — critical revision for important intellectual content. Ilias Miltiadis — justification of the manuscript.

Author Information

Zenin Oleg K. – Dr. Sci. (Med.), Professor, Professor of Human Anatomy Department, Penza State University, Penza, zen.olegz@gmail.com, https://orcid.org/0000-0002-5447-1989

Gorbachenko Vladimir I. – Dr. Sci. (Tech.), Professor, Head of Computer Technologies Department, Penza State University, Penza, gorvi@mail.ru, https://orcid.org/0000-0002-1012-8855

Gribkov Dmitry N. – Postgraduate Student, Computer Technologies Department, Penza State University, Penza, rororol23@mail.ru, https://orcid.org/0000-0003-4728-5923

Sergienko Anna A. – Postgraduate Student, Human Anatomy Department, Penza State University, Penza, anya.gurieva00@mail.ru, https://orcid.org/0009-0005-1380-8767

Ilias Miltiadis – Graduate Student, University of Palermo, Palermo, Italy, contact@miltykh.com, https://orcid.org/0000-0002-9130-3255

(✉) **Zenin Oleg K.,** zen.olegz@gmail.com

Received on June 30, 2025;
approved after peer review on October 25, 2025;
accepted on October 30, 2025

УДК 616-022.854.2:616.155.34
https://doi.org/10.20538/1682-0363-2026-2-32-37

Spontaneous Neutrophil Extracellular Trap Formation During Pollinosis Exacerbation

Kazimirskii A.N., Salmasi J.M., Poryadin G.V., Panina M.I., Kim A.E., Kim T.E., Turishcheva O.O.

Pirogov Russian National Research Medical University (Pirogov University)
1 Ostrovityanov St., 117997 Moscow, Russian Federation

ABSTRACT

Aim. To study the morphological structure and functional activity of neutrophil extracellular traps in patients with seasonal allergic rhinitis during the exacerbation period.

Materials and methods. The study included 12 patients with seasonal allergic rhinitis during the exacerbation period. We studied the morphological structure and functional activity of neutrophil extracellular traps (NET) in pollinosis patients. Fluorescence microscopy with SYBR Green dye was used to visualize NETs.

Results. The study of neutrophils from allergic patients during the exacerbation period showed spontaneous NETs formation in the morphological form of neutrophil networks. The number of NETs during 1 hour of incubation is 10 [8.3–14] %, and their size was 28 [17.5–35] μm. Culturing neutrophils from allergic patients for 2 hours does not increase the number of NETs, but the size of NETs doubles, and 10% of NETs form as single threads and fibers. Neutrophil networks have a high functional activity.

Conclusion. The results specify that during the exacerbation of seasonal allergic rhinitis, there is an NET formation similar to that observed during infectious inflammation, which is combined with high functional activity of neutrophil networks.

Keywords: pollinosis, seasonal allergic rhinitis, exacerbation period, neutrophil extracellular traps, neutrophil networks, allergy

Conflict of interest. The authors declare the absence of obvious or potential conflicts of interest related to the publication of this article.

Source of financing. The authors state that they received no funding for the study.

Conformity with the principles of ethics. All individuals signed a written consent to participate in the study. The study was approved by the local Ethics Committee of Pirogov Russian National Research Medical University (Minutes No. 239 of April 15, 2024).

For citation: Kazimirskii A.N., Salmasi J.M., Poryadin G.V., Panina M.I., Kim A.E., Kim T.E., Turishcheva O.O. Spontaneous Neutrophil Extracellular Trap Formation During Pollinosis Exacerbation. *Bulletin of Siberian Medicine.* 2026;25(2):32–37. https://doi.org/10.20538/1682-0363-2026-2-32-37.

✉ *Kazimirskii Alexander N.,* alnica10@mail.ru

Обострение поллиноза сопровождается спонтанным формированием нейтрофильных экстраклеточных ловушек в морфологической форме нейтрофильных сетей

Казимирский А.Н., Салмаси Ж.М., Порядин Г.В., Панина М.И., Ким А.Э., Ким Т.Э., Турищева О.О.

Российский национальный исследовательский медицинский университет (РНИМУ) им. Н.И. Пирогова (Пироговский университет)
Россия, 117997, г. Москва, ул. Островитянова, 1

РЕЗЮМЕ

Цель. Исследование морфологической структуры и функциональной активности нейтрофильных экстраклеточных ловушек у больных сезонным аллергическим ринитом в период обострения заболевания.

Материалы и методы. В исследование включены 12 больных с поллинозом период обострения заболевания. Исследовали морфологическую структуру и функциональную активность нейтрофильных экстраклеточных ловушек (НЭЛ) у больных поллинозом. Для визуализации НЭЛ использовали флуоресцентную микроскопию с красителем SYBR Green.

Результаты. Исследование нейтрофилов больных в период обострения заболевания показало спонтанное формирование НЭЛ в морфологической форме нейтрофильных сетей. Количество НЭЛ в течение 1 ч инкубации составляет 10 [8,3–14]%, а их размеры – 28 [17,5–35] мкм. Культивирование нейтрофилов аллергических пациентов в течение 2 ч не увеличивает численность НЭЛ, размеры НЭЛ увеличиваются в 2 раза, при этом происходит формирование 10% НЭЛ в форме одиночных нитей и волокон. Нейтрофильные сети имеют высокую функциональную активность.

Заключение. Результаты свидетельствуют, что при обострении поллиноза наблюдается образование НЭЛ, подобное развивающемуся при инфекционном воспалении, сочетающееся с высокой функциональной активностью нейтрофильных сетей.

Ключевые слова: поллиноз, сезонный аллергический ринит, период обострения заболевания, нейтрофильные экстраклеточные ловушки, нейтрофильные сети, аллергия

Конфликт интересов. Авторы декларируют отсутствие явных и потенциальных конфликтов интересов, связанных с публикацией настоящей статьи.

Источник финансирования. Авторы заявляют об отсутствии источника финансирования при проведении исследования.

Соответствие принципам этики. Все лица подписали информированное согласие на участие в исследовании. Исследование одобрено этическим комитетом РНИМУ им. Н.И. Пирогова (протокол № 239 от 15.04.2024).

Для цитирования: Казимирский А.Н., Салмаси Ж.М., Порядин Г.В., Панина М.И., Ким А.Э., Ким Т.Э., Турищева О.О. Обострение поллиноза сопровождается спонтанным формированием нейтрофильных экстраклеточных ловушек в морфологической форме нейтрофильных сетей. *Бюллетень сибирской медицины.* 2026;25(2):32–37. https://doi.org/10.20538/1682-0363-2026-2-32-37.

INTRODUCTION

The rapid development of immunology has led to the creation of many new biological drugs for the treatment of allergic diseases, including anti-immunoglobulin E (anti-IgE), anti-interleukin-5 (anti-IL-5), and anti-thymic stromal lymphopoietin (anti-TSLP/IL-4), but the initiation of the allergic (atopic) process is still unclear [1]. The dysfunction of the immune system in allergic (atopic) diseases is associated with changes in the functioning of the body's defense.

One of the possible mechanisms is associated with the disruption of the protective functions of neutrophils as participants in the innate immunity. This particular pathogen link was identified during the examination of patients suffering from

hay fever (chronic allergic rhinitis) [2], where it was demonstrated that the neutrophils of these patients had impaired adhesion to plastic, reduced chemotaxis, and decreased bactericidal activity. An increased level of neutrophils in nasal mucosa biopsies was recorded in patients with allergies during the blooming season, compared to healthy individuals. Studies have shown that neutrophils in patients with seasonal allergic rhinitis are partially activated [3] and can, in turn, activate T-cells and enhance the migration of eosinophils.

Recently, researchers have gradually come to understand that in order to develop effective treatment strategies that take into account the complex interaction between immune system cells and pathogens, it is necessary to study in depth the mechanisms of neutrophil extracellular trap (NET) formation in allergic (atopic) diseases. It can be reasonably assumed that NETs can serve as potential biomarkers and therapeutic targets.

The aim was to study the morphological structure and functional activity of neutrophil extracellular traps in patients with seasonal allergic rhinitis during the exacerbation period.

MATERIALS AND METHODS

The study included 12 patients with hay fever during the exacerbation period. The inclusion criterion was the absence of other acute diseases at the time of the study and indications of other chronic diseases in history. The exclusion criterion was acute infectious diseases within a month before the day of the study.

The blood samples were analyzed at the Department of Pathophysiology and Clinical Pathophysiology, Institute of Biology and Human Pathology, Pirogov Russian National Research Medical University. All procedures were performed in accordance with the ethical standards of the WMA Helsinki Declaration (as revised in 2004) and the written informed consent of the patients. The study was approved by the local Ethics Committee of Pirogov University (Minutes No. 239 dated April 15, 2024).

Neutrophil isolation from EDTA-treated venous blood of patients was carried out as described by us before [4]. Immunofluorescence study of NETs to determine their morphological structure, as well as the study of the functional activity of neutrophil extracellular structures using a cell culture of *Klebsiella pneumoniae* (ATCC 700603) was carried out using the method [5].

Statistical data processing was carried out using STATISTICA 12.0 software packages (StatSoft, USA). Descriptive statistics are presented in the form of continuous quantitative data: for normal distributions, in the form of the mean value (M) ± standard error (m), and for distributions that differ from normal, as the median of the interquartile range Me [Q_1–Q_3]. Comparison of quantitative variables was performed using the Mann–Whitney test. The difference was considered to be statistically significant at a two-tailed p value of < 0.05.

RESULTS AND DISCUSSION

The study of neutrophils in patients with allergic rhinitis during the exacerbation period showed spontaneous formation of NETs in the morphological form of neutrophil networks.

The number of neutrophil networks during 1 hour of incubation was 10 [8.3–14] %, and their size was 28 [17.5–35] μm. Culturing neutrophils from allergic patients for 2 hours did not increase the number of NETs, but the size of neutrophil extracellular traps increased by almost 2 times (Table 1).

Table 1

Parameters of Neutrophil Extracellular Traps (NETs) in Patients with Seasonal Allergic Rhinitis (n = 12) during the Exacerbation Period, Me [Q_1–Q_3]

Number of NETs, %	NET size, microns	NET structure
Spontaneous formation of extracellular structures (1 hour of incubation)		
10 [8.3–14]	28 [17.5–35]	Networks
Spontaneous formation of extracellular structures (2 hours of incubation)		
11.1 [8.3–21]	52.5 [35–70]*	Networks, single strands, fibers

*$p < 0.05$ compared to cell incubation for 1 hour

The peculiarity of the NET formation in patients with seasonal allergic rhinitis during the exacerbation period is that, in addition to neutrophil networks, single strands, and fibers are detected during longer neutrophil cultivation (for 2 hours). The number of these abnormal structures is small and does not exceed 10% of the total number of neutrophil networks.

NET formation in the morphological form of neutrophil networks (Fig. 1), combined with single strands and fibers, confirms that the neutrophils of allergic patients are already pre-activated [3].

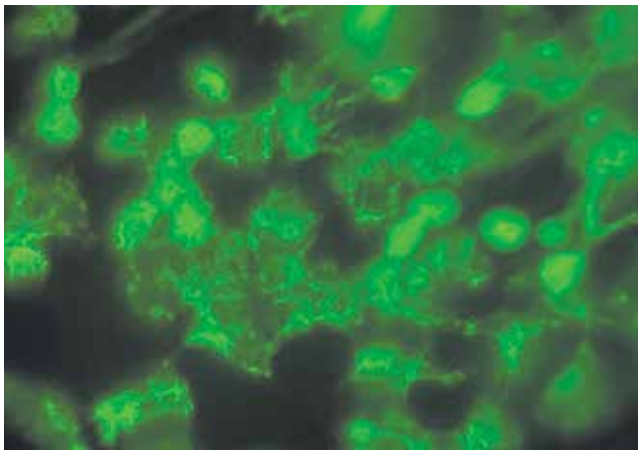

Fig. 1. Neutrophil networks in patients with seasonal allergic rhinitis during the exacerbation period. Incubation time 1 h. CYBR Green staining. Magnification × 1 000

These two morphological structures (neutrophil networks and single strands) may indicate two forms of neutrophil activation during the exacerbation period and may be caused by two different processes. Neutrophil network formation in patients with seasonal allergic rhinitis during the exacerbation period may be induced by both contact interactions with pathogens [5] and the action of IL-8, which can induce the production of free radicals and the formation of extracellular traps [6].

In severe infectious complications/sepsis, it was found that the IL-8 concentration in the patients' blood plasma was closely related to the NET formation, and the inhibition of IL-8 using monoclonal antibodies significantly weakened the formation of NETs [7]. Epithelial cells stimulated by pollen extracts release IL-8, as well as a number of pro-inflammatory cytokines, including IL-1, IL-6, and TNFα [8]. The secretion of pro-allergic alarmins (thymic stromal lymphopoietin TSLP, IL-33; and IL-25) contributes to a Th2-dominated immune response and the development of sensitization.

For that reason, the neutrophil network formation in the patients we examined is likely to be caused by the action of IL-8. However, as we have previously shown, the neutrophil network formation is a manifestation of the body's readiness to trigger protective anti-infective reactions [5]. The detection of NETs in the morphological form of single strands can be interpreted as a neutrophil response to contact interactions with damaged vascular endothelium [9].

The central neutrophil extracellular structure found in patients with seasonal allergic rhinitis during the exacerbation period is neutrophil networks. Functional activity study of these neutrophil structures showed that, despite the relatively small size of the neutrophil networks – 52.5 [35–70] microns, upon incubation for 2 hourthe pathogen *Klebsiella pneumoniae* in these extracellular structures is quite high (Table 2).

Table 2

Functional Activity of Neutrophil Networks, Single Strands, and Fibers in Patients with Seasonal Allergic Rhinitis (n = 12) during the Exacerbation Period, after Incubation for 2 hours, *Me* [Q_1-Q_3]

NET structure	NET size, microns	NET conversion after interaction with a pathogen	Capture of pathogen cells Klebsiella pneumoniae
Neutrophil networks	52.5 [35–70]	Neutrophil veils	50 [40–60]
Single strands, fibers	130 [112.5–157.5]	Single strands, fibers	0.00

Each neutrophil network binds 50 [40–60] pathogen cells. At the same time, the structure of the neutrophil network changes – it undergoes morphofunctional transformation, i.e., it transforms into a veil-like structure (Fig. 2).

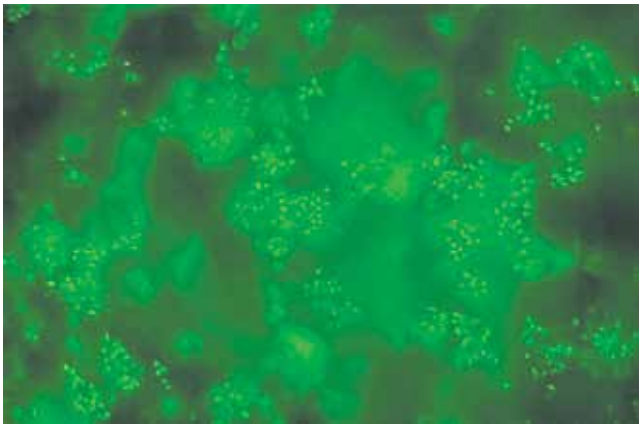

Fig. 2. Neutrophil networks of patients with seasonal allergic rhinitis during exacerbation capture and bind the cells of the pathogen *Klebsiella pneumoniae*.

We previously described such morphofunctional transformation of neutrophil networks during contact interactions with a pathogen in patients with infectious inflammation in the abdominal area [10].

It should be noted that during the neutrophil activation in healthy individuals, each neutrophil network is capable of capturing and retaining an average of 80 [60–100] *Klebsiella pneumoniae* cells. In patients with inflammatory diseases of the abdominal cavity (appendicitis, cholecystitis, and pancreatitis), the functional activity of NETs is reduced by several times compared to healthy donors in the postoperative period.

In these patients, neutrophil extracellular structures capture and bind an average of no more than 20 cells of the test microorganism, and some of the infectious pathogen cells remain unbound by the extracellular neutrophil structures, which increases the risk of postoperative infectious complications in these patients [9].

The functional activity of spontaneous neutrophil networks in patients with seasonal allergic rhinitis during the exacerbation period is 1.6 times lower than the activity of induced NETs in healthy donors, but 2.5 times higher than the same parameter in patients with inflammatory diseases of the abdominal cavity.

CONCLUSION

The results of a study of the morphological structure and functional activity of neutrophil extracellular traps in patients with hay fever (seasonal allergic rhinitis) during the exacerbation period indicate that during the exacerbation of hay fever, the NET formation is similar to that observed during infectious inflammation, accompanied by relatively high functional activity of neutrophil networks. The conducted research suggests that neutrophil extracellular trap formation in the morphological form of neutrophil networks is a universal response of neutrophils to pathogens.

REFERENCES

1. Wang J., Zhou Y., Zhang H., Hu L., Liu J., Wang L., et al. Pathogenesis of allergic diseases and implications for therapeutic interventions. *Sig Transduct Target Ther.* 2023;8(1):138. https://doi.org/10.1038/s41392-023-01344-4
2. Lianou P., Fortis A., Papadopoulos N., Trakas N. Defective neutrophil function in patients with perennial allergic rhinitis. *Allergology International.* 2001;50(1):15–20 DOI https://doi.org/10.1046/j.1440-1592.2001.00196.x
3. Arebro J, Ekstedt S, Hjalmarsson E, Winqvist O, Kumlien Georén S, et al. A possible role for neutrophils in allergic rhinitis revealed after cellular subclassification. *Sci Rep*. 2017;7:43568. doi:10.1038/srep43568
4. Kazimirskii A.N., Salmasi J.M., Poryadin G.V., Panina M.I., Kim A.E., Chakhalian A.G., et al. DNA-Containing Extracellular Structures of Tumor Cells Inhibit the Formation of Neutrophil Extracellular Traps *in vitro*. *Bulletin of Siberian Medicine*. 2025;24(2):36-43. (In Russ.) https://doi.org/10.20538/1682-0363-2025-2-36-43
5. Kazimirskii A.N., Salmasi J.M., Poryadin G.V., Panina M.I., Stupin V.A., Kim A.E., et al. Neutrophil extracellular traps in the anti-infectious defense of human organism. *Bulletin of Siberian Medicine*. 2024;23(1):56-63. (In Russ.) https://doi.org/10.20538/1682-0363-2024-1-56-63
6. Keshari R.S., Jyoti A., Dubey M., Kothari N., Kohli M., Bogra J., et al. Cytokines induced neutrophil extracellular traps formation: implication for the inflammatory disease condition. *PloS one*, 2012;*7*(10), e48111. https://doi.org/10.1371/journal.pone.0048111
7. Abrams S.T., Morton B., Alhamdi Y., Alsabani M., Lane S., Welters I.D., et al. A Novel Assay for Neutrophil Extracellular Trap Formation Independently Predicts Disseminated Intravascular Coagulation and Mortality in Critically Ill Patients. *American journal of respiratory and critical care medicine*, 2019;*200*(7), 869–880. https://doi.org/10.1164/rccm.201811-2111OC
8. Hosoki K, Brasier AR, Kurosky A, Boldogh I, Sur S. Reply: protease plays a role in ragweed pollen-induced neutrophil recruitment and epithelial barrier disruption. *Am J Respir Cell Mol Biol*. 2017;56(2):272–273. DOI: 10.1165/rcmb.2016-0281LE.
9. Kazimirskii A.N., Salmasi J.M., Poryadin G.V., Panina M.I., Kim A.E., Rogozhina L.S. Neutrophil extracellular traps as markers of infectious and aseptic inflammation. *Russian Journal of Infection and Immunity = Infektsiya i immunitet.* 2024;14(3): 505–510 (In Russ.) DOI: 10.15789/2220- 7619-NET-16602
10. Kazimirskii A.N., Salmasi J.M., Poryadin G.V., Panina M.I., Kim A.E., Rogozhina L.S. Transformation of NETs under the effect of pathogens and IgG. *Bulletin of Siberian Medicine*. 2024;23(4):22-30 (In Russ.) https://doi.org/10.20538/1682-0363-2024-4-22-30

Author Contribution

Poryadin G.V., Salmasi J.M. – conception and design. Kazimirskii A.N., Kim A.E., Kim T.E. – experimental studies. Kazimirskii A.N., Turishcheva O.O. – preparation of illustrative material. Panina M.I. – statistical processing of the material. Kazimirskii A.N. – drafting of the manuscript. Panina M.I., Salmasi J.M. – editing of the manuscript. The contribution of the authors is equivalent.

Author Information

Kazimirskii Alexander N. – Dr. Sci. (Biol.), Associate Professor, Professor of the Department of Pathophysiology and Clinical Pathophysiology at the Institute of Human Biology and Pathology, Leading Researcher at the Department of Molecular Technologies at the Research Institute of Translational Medicine, Pirogov Russian National Research Medical University (Pirogov University), Moscow, alnica10@mail.ru, https://orcid.org/0000-0002-3079-4089

Salmasi Jean M. – Dr. Sci. (Med.), Professor, Head of the Department of Pathophysiology and Clinical Pathophysiology at the Institute of Human Biology and Pathology, Pirogov Russian National Research Medical University (Pirogov University), Moscow, profjms@yandex.ru, https://orcid.org/0000-0001-8524-0019

Poryadin Gennady V. – Corresponding Member of the Russian Academy of Sciences, Dr. Sci. (Med.), Professor, Department of Pathophysiology and Clinical Pathophysiology at the Institute of Human Biology and Pathology, Pirogov Russian National Research Medical University (Pirogov University), Moscow, poryadin_GV@rsmu.ru, https://orcid.org/0000-0003-2010-3296

Panina Marina I. – Dr. Sci. (Med.), Professor, Professor of the Department of Pathophysiology and Clinical Pathophysiology of the Institute of Human Biology and Pathology, Pirogov Russian National Research Medical University (Pirogov University), Moscow, panmar@list.ru, https://orcid.org/0000-0002-7651-0037

Kim Anna E. – Senior Lecturer, Department of Pathophysiology and Clinical Pathophysiology, Institute of Human Biology and Pathology, Pirogov Russian National Research Medical University (Pirogov University), Moscow, infoany@mail.ru, https://orcid.org/0000-0001-8119-772X

Kim Tatiana E. – Assistant, Department of Pathophysiology and Clinical Pathophysiology, Institute of Human Biology and Pathology, Pirogov Russian National Research Medical University (Pirogov University), Moscow, kimtany@gmail.com, https://orcid.org/0009-0000-0677-9076

Turishcheva Olga O. – Cand. Sci. (Med.), Associate Professor, Department of Pathophysiology and Clinical Pathophysiology, Institute of Human Biology and Pathology, Pirogov Russian National Research Medical University (Pirogov University), Moscow, turishevaolia@mail.ru, https://orcid.org/0009-0009-6000-9131

(✉) **Kazimirskii Alexander N.,** alnica10@mail.ru

Received on December 22, 2025;
approved after peer review on January 13, 2026;
accepted on January 22, 2026

УДК 616.351-006.6-033.2:576.311.347
https://doi.org/10.20538/1682-0363-2026-2-38-48

Morphological Features of Mitochondria Isolated from Tumor and Apparently Healthy Tissue of the Rectum in Patients Depending on the Presence of Metastases

Kit O.I.[1], Shikhlyarova A.I.[1], Frantsiyants E.M.[1], Ilchenko S.A.[1], Neskubina I.V.[1], Kirichenko E.Yu.[2], Logvinov A.K.[3], Rodkin S.V.[2], Cheryarina N.D.[1], Kolesnikov E.N.[1], Kozhushko M.A.[1], Anisimov A.E.[1], Legenko N.N.[1]

National Medical Research Centre for Oncology
63 14th Liniya, 344037 Rostov-on-Don, Russian Federation

Don State Technical University
1 Gagarin Sq., 344000 Rostov-on-Don, Russian Federation

Southern Federal University
105/42 B. Sadovaya St., 344006 Rostov-on-Don, Russian Federation

ABSTRACT

Aim. To examine the ultrastructural characteristics of mitochondria isolated from rectal adenocarcinoma tissue and apparently healthy tissue along the tumor resection line in patients of both sexes, depending on the presence or absence of metastases.

Materials and methods. The study encompassed the analysis of 28 patients diagnosed with rectal cancer, classified as T2–3N0M0 and T2–3N1–3M1, with tumor differentiation grade G2. Mitochondria were isolated from tumor and intestinal tissue cells via differential centrifugation. The mitochondrial suspension was then placed in a fixative solution containing formaldehyde and glutaraldehyde, followed by immersion in pure Epon-812 resin (SPI Inc., USA). The resin was allowed to cure for a period of 72 hours at a temperature of 70° C. Standard methodologies were employed to prepare the sections, which were then examined using a Jeol JEM-1011 electron microscope (JEOL Inc., Japan). The mitochondrial perimeter on images obtained by electron microscopy was determined using the Fiji program.

Results. A comprehensive ultrastructural study and statistical analysis of the perimeter size of mitochondria isolated from rectal adenocarcinoma in patients of both sexes were conducted. The results indicated that there were no statistically significant intergroup differences in mitochondrial size, categorized as conditionally small (0–1 μm), medium (1–2 μm), and large (>2 μm), depending on the presence or absence of metastases. In contrast to the tumor tissue, in apparently healthy tissue along the rectal resection line, the proportion of mitochondria with a perimeter of > 2 μm, characterized by the most pronounced dysfunction, decreased by 3.6 times in women and by 4.8 times in men without metastases compared to the indicators in all patients with metastases ($p < 0.05$).

Conclusion. The significance of differences in the perimeter dimensions of mitochondria isolated from apparently healthy tissue at the resection line of rectal adenocarcinoma, regardless of gender differences in patients, indicated the possibility of a morphofunctional relationship between processes occurring at the ultrastructural mitochondrial level and metastasis of rectal cancer.

Keywords: rectal adenocarcinoma, mitochondria, metastasis

Conflict of interest. The authors declare the absence of obvious or potential conflicts of interest related to the publication of this article.

Source of financing. The authors state that they received no funding for the study.

Conformity with the principles of ethics. All patients signed an informed consent to collection and transfer of biological material and to carrying out of studies and state assignments for socially sensitive purposes. The study

✉ *Neskubina Irina V.,* neskubina.irina@mail.ru

was approved by the Ethics Committee at N.N. Blokhin Russian Cancer Research Center (Minutes No. 1 dated 30.01.2023).

For citation: Kit O.I., Shikhlyarova A.I., Frantsiyants E.M., Ilchenko S.A., Neskubina I.V., Kirichenko E.Yu., Logvinov A.K., Rodkin S.V., Cheryarina N.D., Kolesnikov E.N., Kozhushko M.A., Anisimov A.E., Legenko N.N. Morphological Features of Mitochondria Isolated from Tumor and Apparently Healthy Tissue of the Rectum in Patients Depending on the Presence of Metastases. *Bulletin of Siberian Medicine.* 2026;25(2):38–48. https://doi.org/10.20538/1682-0363-2026-2-38-48.

Морфологические особенности митохондрий, изолированных из опухоли и условно здоровой ткани прямой кишки, у пациентов в зависимости от наличия метастазов

Кит О.И.[1], Шихлярова А.И.[1], Франциянц Е.М.[1], Ильченко С.А.[1], Нескубина И.В.[1], Кириченко Е.Ю.[2], Логвинов А.К.[3], Родькин С.В.[2], Черярина Н.Д.[1], Колесников Е.Н.[1], Кожушко М.А.[1], Анисимов А.Е.[1] Легенько Н.Н.[1]

[1] *Национальный медицинский исследовательский центр (НМИЦ) онкологии*
Россия, 344037, г. Ростов-на-Дону, ул. 14-я Линия, 63

[2] *Донской государственный технический университет (ДГТУ)*
Россия, 344000, г. Ростов-на-Дону, пл. Гагарина, 1

[3] *Южный федеральный университет(ЮФУ)*
Россия, 344006, г. Ростов-на-Дону, пр. Стачки 194/1

РЕЗЮМЕ

Цель. Изучение ультраструктурных особенностей митохондрий, изолированных из ткани аденокарциномы прямой кишки и условно здоровой ткани по линии резекции опухоли, у пациентов обоего пола в зависимости от наличия или отсутствия метастазов.

Материалы и методы. В исследование включены результаты, полученные от 28 больных раком прямой кишки T2–3N0M0 и T2–3N1–3M1, степень дифференцировки опухоли – G2. Митохондрии из клеток тканей опухоли и кишки выделяли с применением дифференциального центрифугирования. Взвесь митохондрий помещали в фиксирующий раствор, содержащий формальдегид и глутаральдегид, далее в чистую смолу Epon-812 (SPI Inc., США) и отверждали в течение 72 ч при 70 °C. Применяли стандартные методы подготовки срезов, которые исследовали с помощью электронного микроскопа Jeol JEM-1011 (JEOL Inc., Япония). Определение периметра митохондрий на изображениях, полученных методом электронной микроскопии, проводилось с использованием программы FiJi.

Результаты. На основе ультраструктурного исследования и статистического анализа размерности периметра митохондрий, изолированных из аденокарциномы прямой кишки пациентов обоего пола, было установлено, что показатели условно малых (0–1 мкм), средних (1–2 мкм) и больших (> 2 мкм) размеров митохондрий не имели межгрупповых статистически значимых различий в зависимости от наличия или отсутствия метастазов. В отличие от опухоли, в условно здоровой ткани по линии резекции прямой кишки доля митохондрий с периметром более 2 мкм, характеризующихся наиболее выраженной дисфункциональностью, снижалась в 3,6 раза у женщин и в 4,8 раза у мужчин без метастазов по сравнению с показателями у всех пациентов с метастазами ($p < 0,05$).

Заключение. Значимость различий в показателях размерности периметра митохондрий, изолированных из условно здоровой ткани на линии резекции аденокарциномы прямой кишки, независимо от гендерных различий пациентов указывала на возможность морфофункциональной взаимосвязи процессов, протекающих на ультраструктурном митохондриальном уровне и метастазированием рака прямой кишки.

Ключевые слова: аденокарцинома прямой кишки, митохондрии, метастазирование

Конфликт интересов. Авторы декларируют отсутствие явных и потенциальных конфликтов интересов, связанных с публикацией настоящей статьи.

Источник финансирования. Авторы заявляют об отсутствии источника финансирования при проведении исследования.

Соответствие принципам этики. Все пациенты подписали информированное согласие на взятие и передачу биологического материала для проведения научных исследований, государственных заданий в общественно и социально полезных целях. Исследование одобрено этическим комитетом НМИЦ онкологии (протокол № 1 от 30.01.2023).

Для цитирования: Кит О.И., Шихлярова А.И., Франциянц Е.М., Ильченко С.А., Нескубина И.В., Кириченко Е.Ю., Логвинов А.К., Родькин С.В., Черярина Н.Д., Колесников Е.Н., Кожушко М.А., Анисимов А.Е., Легенько Н.Н. Морфологические особенности митохондрий, изолированных из опухоли и условно здоровой ткани прямой кишки, у пациентов в зависимости от наличия метастазов. *Бюллетень сибирской медицины.* 2026;25(2):38–48. https://doi.org/10.20538/1682-0363-2026-2-38-48.

INTRODUCTION

The principle of the unbreakable link between structure and function, that has long been developed in Russian science by the flagship of morphofunctional unity, Academician D.S. Sarkisov, has currently reached full understanding within the global community with the recognition of the equivalence of concepts previously considered as polar opposites at the fine ultrastructural level of mitochondria [1]. In major world publications, such as *Nature*, *Nat. Metabolism*, *Redox Biology*, and many others, hundreds of relevant articles and literature reviews have been published over the past 10 years, presenting a new paradigm regarding the versatility of mitochondria and declaring the expansion of mitochondrial science beyond the scope of function and dysfunction [2–5].

The tight link between mitochondrial structure and function led to the emergence of the concept of "morphofunctionality" of mitochondria [6], which included "morphofunctional analysis of mitochondria" as the "simultaneous quantitative determination of morphological and functional parameters of mitochondria." T.T. Renault et al. (2015) showed that both mitochondrial hyperfusion and hyperfragmentation protected cells from BAX-mediated apoptosis, suggesting that a specific mitochondrial shape is required for BAX to induce mitochondrial outer membrane permeabilization [7].

Furthermore, it was established that in response to low ADP concentrations, the structure of the inner mitochondrial membrane (IMM) changed: the mitochondrial matrix contracted and condensed ("condensed state"), and then became less dense and more stretched ("orthodox state"), which was associated with a more compact arrangement of the cristae [8]. A study by Y. Wang et al. (2017) demonstrated that mitochondrial fragmentation allowed for the release of Ca2+ from the endoplasmic reticulum into the cytosol, which promoted phagocytosis by stimulating Ca2+-mediated vesicle transport [9]. Mitochondrial structure has been shown to influence the cell cycle phase, and vice versa [10].

For example, cyclin-dependent kinase 5 (CDK5) inhibits dynamin-related protein 1 (DRP1) via phosphorylation [11], and mitochondria form a hyperfused network during the transition from the G1 to the S phase, associated with cyclin E accumulation [12]. The latter study also showed that $\Delta\psi$ depolarization at the onset of G1 prevented cell cycle progression into the S phase [12].

One of the most important aspects of mitochondrial research is associated with their unique and indispensable role in oncogenesis and cancer progression [5, 13, 14]. Although the mechanisms of mitochondrial reprogramming in cancer have recently received closer attention, the specifics of organelle adaptation during this process have not been widely considered [15–17]. Meanwhile, the microenvironment in which a tumor grows is extremely unfavorable for mitochondria, as unstable oxygen concentrations and oxidative radicals can disrupt organelle integrity, disintegrate the regulation of numerous mitochondrial functions, and activate cell death [18]. Questions regarding how mitochondria cope with the loss of their "functional shape" and what the impact of low-quality or damaged mitochondria is on tumor characteristics, including the transfer of malignant information, remain poorly understood and understudied [19].

In early 2025, Guidelines for the Nomenclature and Characterization of Mitochondrial Transfer developed by more than 30 scientists from different

countries around the world were published [20]. These guidelines significantly eased the complex task of describing all forms of mitochondria, whether structurally damaged, intact, or fragmented. They indicate the necessity for mitochondria to be characterized, at a minimum, in terms of size, as this is a physical characteristic that can be measured using various methods. Thus, studies at the level of mitochondria isolated from tissues can contribute not only to expanding the understanding of the link between functional and morphological aspects but also to determining the role of mitochondrial dimensions in tumor progression, particularly in the processes of metastasis.

The aim of this study was to investigate the ultrastructural features of isolated mitochondria derived from rectal adenocarcinoma tissue and apparently healthy tissue along the tumor resection line in patients of both sexes, depending on the presence or absence of metastases.

MATERIALS AND METHODS

The study included results obtained from 28 patients with rectal cancer classified as T2–3N0M0 and T2–3N1–3M1, with a median age of 66 (58–73) years. None of the patients included in the study received neoadjuvant treatment prior to surgery. The tumor differentiation grade in all patients corresponded to G2. Rectal resection of the affected organ was performed with the removal of the malignant tumor.

Mitochondria were isolated from tumor cells and apparently healthy rectal tissue using differential centrifugation on the Avanti J-E high-speed refrigerated centrifuge (BECKMAN COULTER, USA) according to generally accepted methods [21, 22]. To disrupt intercellular bonds, cell walls, and plasma membranes, mechanical tissue processing was used, including mincing with scissors and homogenization in a glass homogenizer with a Teflon pestle (Potter-Elvehjem homogenizer). For each gram of tissue, 10 ml of sterile isolation medium was added (0.22 M mannitol, 0.3 M sucrose, 1 mM EDTA, 2 mM TRIS-HCl, 10 mM HEPES, pH 7.4).

Tissues were homogenized and centrifuged for the first time for 10 min at 1,000 g at 0–2° C; the second and third centrifugations were performed at 20,000 g for 20 min at 0–2° C. Between centrifugations, the mitochondrial pellet was resuspended in the isolation medium. Mitochondria were further purified from lysosomes, peroxisomes, melanosomes, etc. by centrifuging in a 23% Percoll gradient. The suspension of subcellular structures was layered onto the Percoll gradient and centrifuged for 15 min at 21,000 g; after this, separation into 3 phases was observed, the bottom layer of mitochondria was retained and resuspended with the isolation medium. The next purification of the mitochondria was carried out by centrifugation for 10 min at 15,000 g at 0–2° C.

A portion of the intestinal tissues and the mitochondrial suspension isolated from the tumor and apparently healthy rectal tissue were immediately placed in a fixative solution containing formaldehyde and glutaraldehyde. After pre-treatment, the tissue sample was embedded in pure Epon-812 resin (SPI Inc., USA) and cured for 72 hours at 70° C. Ultrathin 90-nm sections were obtained using an ultramicrotome equipped with a diamond knife. The sections were mounted on copper slot grids and stained with a 2% aqueous solution of uranyl acetate for 40 min and lead citrate for 2 min. The sections were examined and photographed using the Jeol JEM-1011 electron microscope (JEOL Inc., Japan).

Mitochondrial perimeters were determined on electron microscopy images using Fiji software. Before starting the analysis, the image scale was manually set using the scale bar present on each micrograph. Mitochondria were selected using the Freehand Selection tool. When necessary, contrast correction and image smoothing were also performed to improve the visualization of mitochondrial boundaries. After tracing each mitochondrion, the result was saved as a region of interest (ROI), and the obtained contours were added to the ROI Manager. Based on these selections, the software automatically calculated the perimeter of each mitochondrion. To increase the reproducibility and transparency of the analysis, a markup map was created for each image: files with the applied mitochondrial contours were saved separately, which allowed for subsequent verification of the accuracy of object identification.

Statistical analysis of the results was performed using the Statistica 10.0 software package. Normality distribution was assessed using the Shapiro – Wilk test (for small samples). Quantitative data in groups (independent samples) were compared using the Student's *t*-test and the Mann – Whitney *U*-test. A value of $p < 0.05$ was considered as the limit of statistical significance. Data in tables were presented

as $M \pm m$, where M is the arithmetic mean, and m is the standard error of the mean (SEM).

RESULTS

In all patients with rectal adenocarcinoma, morphological signs of dysfunction of mitochondria isolated from the tumor were noted on ultrathin serial sections, which was manifested by a significant variation in the size and shape of the organelles, ranging from ovoid and rounded to polygonal (Fig. 1). The electron micrograph shows that a significant part of the mitochondrial population (over 40%) with large and medium perimeters is in a swollen state. Total mitochondrial swelling could indicate greater coupling and increased ATP synthesis within them, i.e., the probability of a high metabolic rate. According to the literature, the intensity of mitochondrial respiration in pathological conditions can double, but without a significant change in the efficiency of oxidative phosphorylation [23, 24].

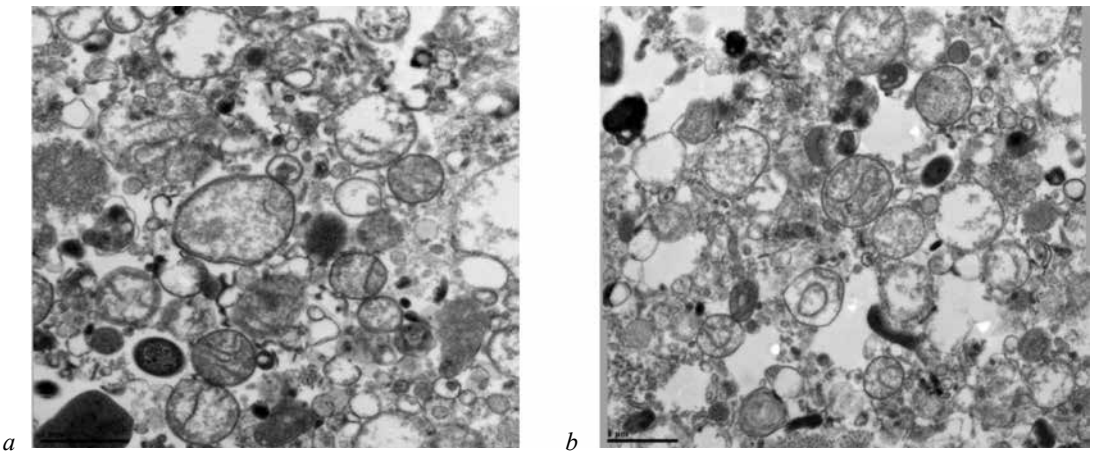

Fig. 1. Electron micrograph of mitochondria isolated from rectal adenocarcinoma in men: *a* – with detected metastases; *b* – without metastases. Manifestation of local swelling (left arrow) and the granular osmiophilic component (right arrow); × 50,000

It was noted that in swollen, enlarged mitochondria, the structure of the cristae was substantially deformed and limited to single elongated or shortened invaginations of the inner membrane, oriented radially with an increase in the intermembrane space.

The ultrastructure of mitochondria in rectal adenocarcinoma of men without metastases and with metastases was similar in heterogeneity and was supplemented by data on the state of the mitochondrial matrix, which was completely or partially filled with inclusions of increased electron density. The matrix filling was heterogeneous, since the inclusions either filled the entire matrix or formed clumps in the marginal zones closer to the IMM (Fig. 1, *b*). On ultrathin sections, the outer membrane of the mitochondria was clearly contoured, in most cases retaining its integrity or having small ruptures. The pathological presentation of mitochondrial heterogeneity of the tumor in men without metastases was supplemented by the manifestation of local swelling and a slight deposition of the granular osmiophilic component inside individual organelles (indicated by arrows in Fig. 1, *b*).

In women with metastatic rectal adenocarcinoma, similar morphological signs of dysfunction of mitochondria isolated from the tumor were noted on ultrathin serial sections, as were observed in men (Fig. 2).

A pronounced variety in the size and shape of the organelles was observed: ovoid, rounded, and less commonly, polygonal. In more than 50% of cases, mitochondrial swelling with deformation or absence of cristae was noted. Single mitochondria were identified with relatively uniform cristae striation, high osmiophilic activity of inclusions, and increased electron optical density of the matrix. Marginal deposits in the matrix of rounded fragments of the osmiophilic component, associated with deformed cristae, could be of a lipid nature.

When analyzing electron micrographs of mitochondria isolated from rectal adenocarcinoma cells in women without detected metastases (Fig. 2, *b*), no distinctive features of the ultrastructure were noted compared to previous studies.

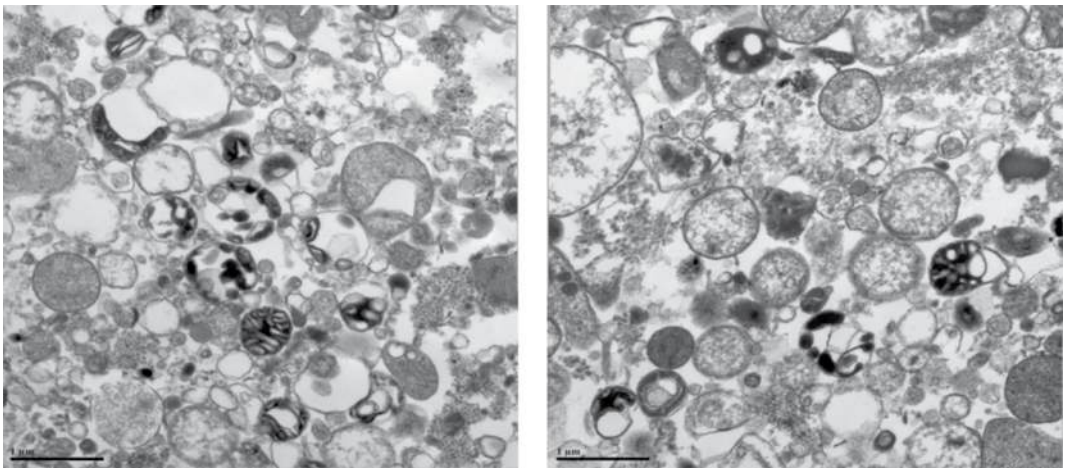

a *b*

Fig. 2. Electron micrograph of mitochondria isolated from rectal adenocarcinoma in women: *a* – with detected metastases; *b* – without metastases; × 50,000

Thus, the microscopic presentation of mitochondria isolated from tumor cells in men and women, regardless of the presence of metastases, was characterized by comparatively similar features: heterogeneity of shape and enlarged size, total mitochondrial swelling with significant deformation of the cristae, altered electron density, and osmiophilic deposits in the matrix and cristae.

Upon studying the apparently healthy rectal tissue along the resection line in men and women with or without metastases, the infiltration of unaffected tissue by tumor mitochondria was revealed (Fig. 3).

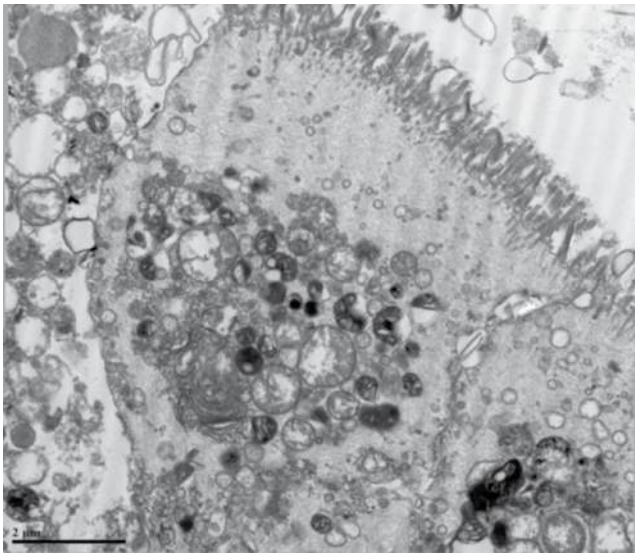

Fig. 3. Electron micrograph demonstrating the variation in the size and shape of mitochondria in apparently healthy rectal tissue along the tumor resection line; × 25,000

As an example, we present a micrograph that convincingly demonstrates the ability of tumor mitochondria to translocate into the areas adjacent to the resection line, which were visually (by light microscopy) unaffected by the tumor process.

Electron microscopy of mitochondria isolated from apparently healthy rectal tissue in men with metastatic adenocarcinoma revealed the entire spectrum of morphological disorders. The micrograph (Fig. 4, *a*) shows swollen organelles of various size clusters, predominantly with increased electron density of the matrix and single elongated as well as multiple shortened cristae.

The outer mitochondrial membrane largely retained its integrity; however, fragmented areas of damage were also detected, including splitting of the outer and inner membranes with filling of the intermembrane space. The presence of process-like inclusions with high osmiophilic activity, associated with the cristae, within the mitochondria was notable. Pathological forms of mitochondria isolated from apparently healthy rectal tissue cells were also noted in men without metastases. However, the microscopic presentation changed somewhat, highlighting the predominance of small forms. With reduced mitochondrial dimensions, the mitochondrial matrix was characterized by moderate and low optical density, the membrane retained its integrity, and a cristae structure of varying visualization intensity and configuration was revealed.

A similar discrepancy in mitochondrial size was visualized in apparently healthy rectal tissue among

women, depending on the presence or absence of adenocarcinoma metastases. It is important to emphasize that a fundamental condition was met during all studies of mitochondrial ultrastructure for the adequate comparison of their sizes: an identical electron microscope magnification of ×50,000, which allowed for the standardization of their dimensions.

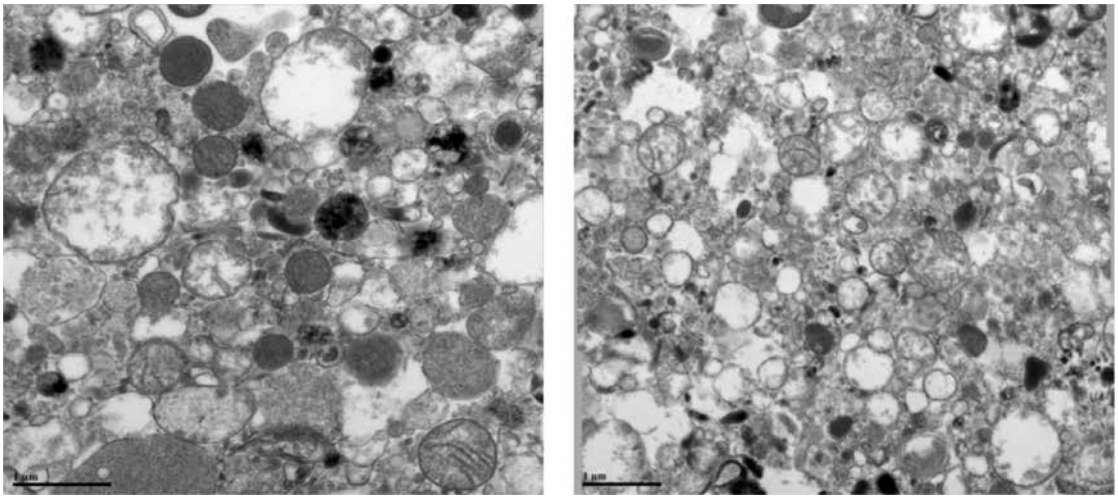

a *b*

Fig. 4. Electron micrograph of mitochondria isolated from apparently healthy tissue along the resection line in men: *a* – with detected metastases; *b* – without metastases; × 50,000

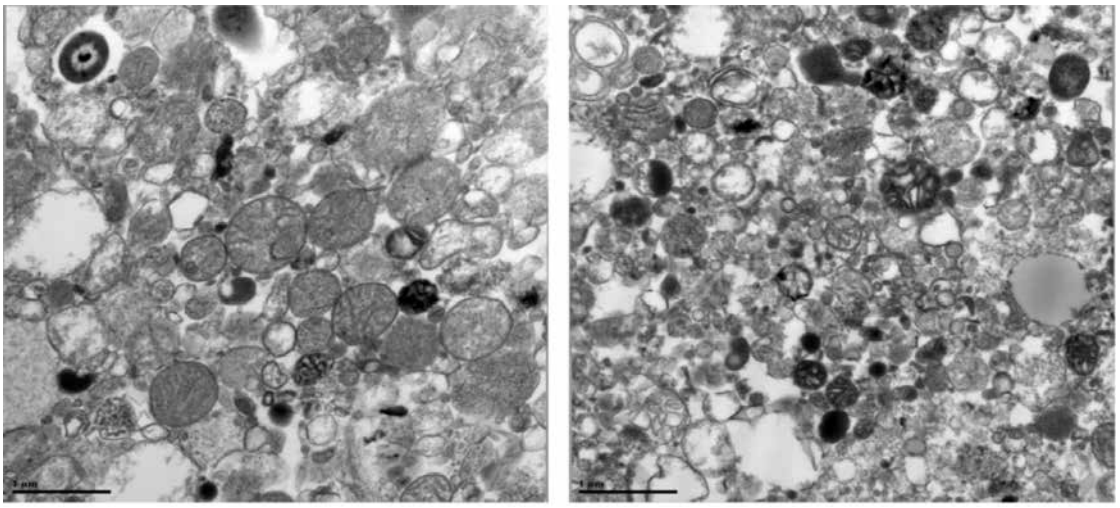

a *b*

Fig. 5. Electron micrograph of mitochondria isolated from apparently healthy rectal tissue along the tumor resection line in women: *a* – with detected adenocarcinoma metastases; *b* – without metastases; × 50,000

Mitochondria isolated from apparently healthy tissue along the tumor resection line in women with metastases appeared larger compared to mitochondria without metastases (Fig. 5*, a*, *b*). Nevertheless, in both cases, swelling and a pronounced cristae structure were noted, associated to a greater or lesser extent with inclusions of high osmiophilic activity. The outer mitochondrial membranes generally maintained their integrity; however, thinning or even blurring of mitochondrial boundaries could be observed, as well as membrane splitting with the gap filled by the active medium resulting from mitochondrial metabolism.

Given the significant variation in mitochondrial sizes, we formed clusters of conditionally small (0–1 μm), medium (1–2 μm), and large (>2 μm)

mitochondria. Their perimeters were measured, followed by statistical processing of the results and calculation of the occurrence frequency of these mitochondrial dimensions in women and men with the presence and absence of metastases (Table).

Table

Occurrence Frequency (%) and Perimeter (μm) of Mitochondria Isolated from Tumor Cells and Apparently Healthy Rectal Tissue of Male and Female Patients with or without Metastases, $M \pm m$

Patient groups	Tumor			Apparently healthy tissue		
	0–1	1–2	> 2	0–1	1–2	> 2
Women with metastases, $n = 7$	65.5 ± 5.1% 0.63 ± 0.009 $n = 272$	22.9 ± 2.0% 1.46 ± 0.03 $n = 95$	11.6 ± 1.4% 2.43 ± 0.05 $n = 48$	50.6 ± 4.9% 0.69 ± 0.01 $n = 167$	35.2 ± 2.9% 1.45 ± 0.03 $n = 116$	14.2 ± 1.7% 2.41 ± 0.06 $n = 47$
Women without metastases, $n = 7$	49.6 ± 4.4% 0.69 ± 0.01 $n = 130$	36.3 ± 3.1% 1.45 ± 0.03 $n = 95$	14.1 ± 1.6% 2.43 ± 0.06 $n = 37$	61.5 ± 5.4% 0.68 ± 0.01 $n = 220$	34.6 ± 2.7% 1.32 ± 0.02 $n = 124$	3.9 ± 0.5% * 2.32 ± 0.06 $n = 14$
Men with metastases, $n = 7$	58.1 ± 5.3% 0.68 ± 0.01 $n = 122$	27.1 ± 2.2% 1.41 ± 0.04 $n = 57$	14.8 ± 1.9% 2.65 ± 0.12 $n = 31$	42.5 ± 3.9% 0.69 ± 0.02 $n = 119$	42.5 ± 3.7% 1.41 ± 0.03 $n = 119$	15.0 ± 1.6% 2.63 ± 0.09 $n = 42$
Men without metastases, $n = 7$	55.9 ± 4.9% 0.7 ± 0,02 $n = 85$	32.3 ± 2.7% 1.4 ± 0.04 $n = 49$	11.8 ± 1.5% 2.5 ± 0.08 $n = 18$	64.5 ± 5.1% 0.76 ± 0.01 $n = 82$	32.4 ± 2.5% 1.37 ± 0.03 $n = 71$	3.1 ± 0.2% * 2.48 ± 0.16 $n = 19$

* differences between the frequency of detection of the maximum mitochondrial dimension in the apparently healthy tissue of patients with and without metastases are statistically significant ($p < 0.05$).

The calculations revealed that in all patient groups across the three mitochondrial perimeter dimension clusters isolated from the tumor, the conventional ratio of perimeter values was maintained, with a predominance of small mitochondria (0–1 μm) (Table). Perimeter values of mitochondria > 2 μm in women and men with and without rectal adenocarcinoma metastases showed no significant intergroup differences and varied with an insignificant difference of 3%. Meanwhile, the relative content of small organoid forms (perimeter of 0–1 μm) exceeded the proportion of large forms by 5.6–3.1 times. The relative number of mitochondria belonging to the medium perimeter dimension of 1–2 μm occupied an intermediate position between the large and small mitochondria.

Upon the analysis of the perimeter values of mitochondria isolated from apparently healthy tissue cells, statistically significant differences were found in both women and men, depending on the presence or absence of metastases. These differences were characteristic only of the conditionally large mitochondrial cluster.

Thus, while the proportion of isolated mitochondria with a perimeter > 2 μm from apparently healthy tissue cells in women and men with metastases showed no statistically significant differences either between one another or compared to the mitochondria isolated from the tumor, a completely different situation was revealed in patients without metastases. In women without rectal adenocarcinoma metastases, the frequency of occurrence of mitochondria with a perimeter > 2 μm isolated from apparently healthy tissue decreased by 3.6 times compared to the mitochondria of the same dimension in women with detected metastases ($p < 0.05$). Simultaneously, a reciprocal increase in the proportion of small-dimension mitochondria (0–1 μm) was observed together with a decrease in the proportion of large organoids; however, the differences in the values were not significant in the context of detected metastases.

A similar pattern of changes was observed in men without metastases: against the background of an increase in the frequency of detecting organoids with a small perimeter (0–1 μm), the content of mitochondria with a perimeter > 2 μm isolated from apparently healthy tissue was 4.8 times smaller compared to the values when metastases were present ($p < 0.05$). In other words, the statistical significance of differences in the indicators of the large-perimeter mitochondrial cluster pointed to the possibility of a morphofunctional interrelation between processes occurring at the ultrastructural level and rectal cancer metastasis. A question arose as to what might cause this kind of determination of

mitochondrial morphogenesis in apparently healthy rectal tissue with metastasis?

DISCUSSION

We believe that the causal chain of events may be primarily linked to the specific characteristics of mitochondrial dysfunction during carcinogenesis. Large mitochondria represent the most unfavorable, yet effective, form of dysfunctional mitochondria, the excessive presence of which in the tumor poses a high risk of its death. What is this associated with? The increase in mitochondrial size, including the perimeter, is associated with swelling processes, which intensify when the production of Bcl-2, Bax, and Bak increases within the cell. These very apoptotic signals cause mitochondrial swelling and the formation of a special pore for the exit of biologically active molecules into the medium: cytochrome C, flavoproteins, reactive oxygen species (ROS), and mtDNA, which, upon entering the cytosol, trigger the program of cell death [25].

Based on this fundamental process, the following can be hypothesized. The statistically significant increase in the frequency of detection of mitochondria with perimeter > 2 μm in the apparently healthy rectal tissue of patients with metastases, compared to the same perimeter dimension in cases without metastases, may be related to various metabolic changes in the surrounding cellular environment. First and foremost, this may be due to the release of factors involved in the pathological reprogramming of genetic and metabolic processes, including ROS, acting as mediators of targeted mitochondrial transfer [26, 27].

Additionally, cancer-associated fibroblasts (CAFs), which participate in the metabolic reprogramming of cancer cells and promote tumor progression, may also contribute to this [28]. Consequently, the morphological differences in mitochondria observed by us in the apparently healthy rectal tissue of patients with metastases may indirectly indicate involvement in the processes of metastasis. These prerequisites may be associated with the accumulation of unfavorable factors in the form of enlarged, deformed mitochondria, whose dysfunction is combined with the ability to actively translocate in media and tissues and which possess potent signaling regulation of structural and metabolic processes during tumor growth.

As noted previously, the present study was aimed at identifying the ultrastructural features of mitochondria isolated from rectal adenocarcinoma tissue and apparently healthy tissue along the tumor resection line in patients of both sexes, depending on the presence or absence of metastases.

However, this problem is much broader than just the morphological aspects and may encompass many more unaccounted factors. These include violations of mitophagy, an increase in extracellular vesicles (EVs) which can engulf large mitochondria and facilitate their transfer to the extracellular space [29, 30]. In this regard, it should be noted that a population of mitochondria-derived extracellular vesicles (EV-Mitos) plays an important role in the realization of mitochondrial dysfunction toward metastasis. These vesicles contain numerous mitochondrial components (the mitochondrial cargo), the composition of which reflects changes in the parent cell.

It is fundamentally important to consider that metastasis is a complex, multi-stage process dependent not only on intracellular changes but also on angio- and lymphangiogenesis, expression of adhesion molecules, EMT, and features of the immune microenvironment. For more detailed investigation, control of variables, such as tumor stage, level of invasion, tumor mutational profile, tumor microenvironment, Ki-67 index, etc., is required. The present study represents only a limited portion of changes at the subcellular level within the multifaceted processes of rectal cancer metastasis.

Nevertheless, considering the strategic role of mitochondria in the processes of carcinogenesis, one cannot but to note that even the observed morphological changes in these organoids already at the tumor resection line may manifest events related to the implementation of the tumor progression program. An increase in the number of dysfunctional, enlarged mitochondria in the zone relatively close to the tumor may serve as one of the significant signals on the path to metastasis.

CONCLUSION

Morphological differences were revealed when comparing the spatial dimension of mitochondria isolated from adenocarcinoma and apparently healthy rectal tissue in patients of both sexes with or without metastases. These differences were associated with a statistically significant increase in the population of large-dimension mitochondria

(perimeter > 2 μm) only in the apparently healthy tissue along the tumor resection line in cases where metastasis was detected, compared to their content in the absence of metastases ($p < 0.05$). The increase in mitochondrial dimension, coupled with morphological signs of dysfunction, characterizes an increase in the malignant potential of apparently healthy rectal tissue, which may contribute to the progression of the tumor process.

REFERENCES

1. Sarkisov D.S. Structural Basics of Adaptation and Compensation of Impaired Functions. M.: Meditsina, 1987:448. (In Russ.).
2. Wallace D.C. A mitochondrial paradigm of metabolic and degenerative diseases, aging, and cancer: a dawn for evolutionary medicine. *Annu. Rev. Genet*. 2005;39:359–407. DOI: 10.1146/annurev.genet.39.110304.095751.
3. Monzel A.S., Enriquez J.A., Picard M. Multifaceted mitochondria: moving mitochondrial science beyond function and dysfunction. *Nat. Meta.* 2023;5:546–562. DOI: 10.1038/s42255-023-00783-1.
4. Conroy G. Cells are swapping their mitochondria. What does this mean for our health? *Nature*. 2025;640(8058):302–304. DOI: 10.1038/d41586-025-01064-5.
5. Kit O.I., Frantsiyants E.M., Shikhlyarova A.I., Neskubina I.V. Mitochondrial Transplantation: New Challenges for Cancer. *South Russian Journal of Cancer*. 2024;5(1):60–70. (In Russ.). DOI: 10.37748/2686-9039-2024-5-1-7.
6. Benard G., Rossignol R. Mitochondrial ultrastructure and its impact on function and bioenergetics. *Antioxid. Redox Signal*. 2008;10(8):1313–1342. DOI: 10.1089/ars.2007.2000.
7. Renault T.T., Floros K.V., Elkholi R., Corrigan K.A., Kushnareva Y., Wieder S.Y. et al. Mitochondrial shape governs BAX-induced membrane permeabilization and apoptosis. *Mol. Cell*. 2015;57(1):69–82. DOI: 10.1016/j.molcel.2014.10.028.
8. Hackenbrock C.R. Ultrastructural bases for metabolically linked mechanical activity in mitochondria. I. Reversible ultrastructural changes with change in metabolic steady state in isolated liver mitochondria. *J. Cell Biol*. 1966;30(2):269–297. DOI: 10.1083/jcb.30.2.269.
9. Wang Y., Subramanian M., Yurdagul A. Jr., Barbosa-Lorenzi V.K., Tsai B., de Juan-Saens H. et al. Mitochondrial fission promotes further macrophage clearance of apoptotic cells. *Cell*. 2017;171(2):331–345. DOI: 10.1016/j.cell.2017.08.041.
10. Horbay R., Bily R. Mitochondrial dynamics during the cell cycle. *Apoptosis.* 2016;21(12):1327–1335. DOI: 10.1007/s10495-016-1295-5.
11. Cho B., Cho H.M., Kim H.J., Jeong J., Park S.K., Hwang E.M. et al. CDK5-dependent inhibitory phosphorylation of Drp1 during neuronal maturation. *Exp. Mol. Med*. 2014;46(7):e105. DOI: 10.1038/emm.2014.36.
12. Mitra K., Vander S., Roysam B., Lin G., Lippincott-Schwartz J. A hyperfused mitochondrial state achieved in G1-S regulates cyclin E accumulation and entry into S phase. *Proc. Natl. Acad. Sci. USA*. 2009;106(29):11960–11965. DOI: 10.1073/pnas.0904875106.
13. Grasso D., Zampieri L.X., Capelôa T., Van de Velde J.A., Sonveaux P. Mitochondria in cancer. *Cell Stress*. 2020;4(6):114–146. DOI: 10.15698/cst2020.06.221.
14. Frantsiyants E.M., Neskubina I.V., Cheryarina N.D., Surikova E.I., Shikhlyarova A.I., Bandovkina V.A. et al. Functional State of Cardiomyocyte Mitochondria in Malignant Process in Presence of Comorbid Pathology in Experiment. *South Russian Journal of Cancer*. 2021;2(3):13–22. (In Russ.). DOI: 10.37748/2686-9039-2021-2-3-2.
15. Jia D., Park J.H., Jung K.H., Levine H., Kaipparettu B.A. Elucidating the metabolic plasticity of cancer: mitochondrial reprogramming and hybrid metabolic states. *Cells*. 2018;7(3):21. DOI: 10.3390/cells7030021.
16. Li J., Agarwal E., Bertolini I., Seo J.H., Caino M.C., Ghosh J.C. et al. The mitophagy effector FUNDC1 controls mitochondrial reprogramming and cellular plasticity in cancer cells. *Sci. Signal*. 2020;13(642):eaaz8240. DOI: 10.1126/scisignal.aaz8240.
17. Kit O.I., Vodolazhsky D.I., Kutilin D.S., Maleyko M.L., Dvadnenko K.V., Enin Y.S. et al. The Copy Number of Genes *GSTP1, NFKB1* and Hypervariable Region 2 of Mitochondrial DNA in Some Histological Types of Gastric Cancer. *Advances in Current Natural Sciences.* 2015;1(6):918–921. (In Russ.).
18. Damaghi M., West J., Robertson-Tessi M., Xu L., Ferrall-Fairbanks M.C., Stewart P.A. et al. The harsh microenvironment in early breast cancer selects for a Warburg phenotype. *Proc. Natl. Acad. Sci. USA*. 2021;118(3):e2011342118. DOI: 10.1073/pnas.2011342118.
19. Humpton T.J., Alagesan B., DeNicola G.M., Lu D., Yordanov G.N., Leonhardt C.S. et al. Oncogenic KRAS induces NIX-mediated mitophagy to promote pancreatic cancer. *Cancer Discov*. 2019;9(9):1268–1287. DOI: 10.1158/2159-8290.
20. Brestoff J.R., Singh K.K., Aquilano K., Becker L.B., Berridge M.V., Boilard E. et al. Recommendations for mitochondria transfer and transplantation nomenclature and characterization. *Nat. Metab*. 2025;7(1):53–67. DOI: 10.1038/s42255-024-01200-x.
21. Egorova M.V., Afanas`ev S.A. Isolation of Mitochondria from Animal and Human Cells and Tissues: Modern Methodological Techniques. *Siberian Medical Journal*. 2011;26(1-1):22–28. (In Russ.).
22. Gureev A.P., Kokina A.V., Syromyatnikova M.Yu., Popov V.N. Optimization of Methods for Isolating Mitochondria from Different Mouse Tissues. *Bulletin of VSU. Chemistry, Biology, Pharmacy*. 2015;4:61–65. (In Russ.).
23. Belosludceva N.V., Pavlik L.L, Goryacheva N.A., Mironova G.D. Electron Microscopy of Forming Lamellar Bodies in Liver Mitochondria in a Rat Model of Hyperthyroidism. *Modern Issues in Medicine and Natural Sciences.* 2018;7:19–22. (In Russ.).
24. Shears S.B., Bronk J.R. Ion transport in liver mitochondria from normal and thyroxine-treated rats. *J. Bioenerg. Biomembr*.1980;12(5-6):379–393.
25. Santhanam S., Dianne L., Kalimuthusamy N. Inter and Intracellular mitochondrial trafficking in health and disease. *Ageing Research Reviews*. 2020;62:101128. DOI: 10.1016/j.arr.2020.101128.

26. Bonnay F., Veloso A., Steinmann V., Köcher T., Abdusselamoglu M.D., Bajaj S. et al. Oxidative metabolism drives immortalization of neural stem cells during tumorigenesis. *Cell*. 2020;182(6):1490–1507. DOI: 10.1016/j.cell.2020.07.039.
27. Sessions D.T., Kashatus D.F. Mitochondrial dynamics in cancer stem cells. *Cell Life Science*. 2021;78(8):3803–3816. DOI: 10.1007/s00018-021-03773-2.
28. Ippolito L., Morandi A., Taddei M.L., Parri M., Comito G., Iscaro A. et al. Cancer-associated fibroblasts promote prostate cancer malignancy via metabolic rewiring and mitochondrial transfer. *Oncogene.* 2019;38:5339–5355. DOI: 10.1038/s41388-019-0805-7.
29. Davis C.-H.O., Kim K.-Y., Bushong E.A., Mills E.A., Boassa D., Shih T. et al. Transcellular degradation of axonal mitochondria. *Proc. Natl. Acad. Sci. USA*. 2014;111:9633–9638. DOI: 10.1073/pnas.1404651111.
30. Ikeda H., Kawase K., Nishi T., Watanabe T., Takenaga K., Inozume T. et al. Immune evasion through mitochondrial transfer in the tumour microenvironment. *Nature.* 2025;638:225–236. DOI: 10.1038/s41586-024-08439-0.

Author Contribution

Kit O.I., Kolesnikov E.N. – final approval of the manuscript for publication. Shikhlyarova A.I., Ilchenko S.A. – substantiation of the manuscript and critical revision of the manuscript for important intellectual content. Neskubina I.V., Cheryarina N.D., Kozhushko M.A., Anisimov A.E. – critical revision of the manuscript for important intellectual content. Kirichenko E.Yu., Logvinov A.K., Legenko N.N. – analysis and interpretation of the data. Rodkin S.V., Frantsiyants E.M. – conception and design.

Author Information

Kit Oleg I. – Dr. Sci. (Med.), Professor, Academician of the Russian Academy of Sciences, Director General, National Medical Research Centre for Oncology, Rostov-on-Don, super.gormon@ya.ru, https://orcid.org/0000-0003-3061-6108

Shikhlyarova Alla I. – Dr. Sci. (Biology), Professor, Senior Researcher, Laboratory of Malignant Tumor Pathogenesis Study, National Medical Research Centre for Oncology, Rostov-on-Don, shikhliarova.a@mail.ru, https://orcid.org/0000-0003-2943-7655

Frantsiyants Elena M. – Dr. Sci. (Biology), Professor, Deputy Director General for Science, National Medical Research Centre for Oncology, Rostov-on-Don, super.gormon@yandex.ru, http://orcid.org/0000-0003-3618-6890

Ilchenko Sergey A. – Cand. Sci. (Med.), Oncologist, Abdominal Oncology Department No. 1, Deputy Director General for Educational Activities, National Medical Research Centre for Oncology, Rostov-on-Don, ilchenkosergei@mail.ru, https://orcid.org/0000-0002-0796-3307

Neskubina Irina V. – Dr. Sci. (Biology), Senior Researcher, Laboratory of Malignant Tumor Pathogenesis Study, National Medical Research Centre for Oncology, Rostov-on-Don, neskubina.irina@mail.ru, https://orcid.org/0000-0002-7395-3086

Kirichenko Evgeniya Yu. – Dr. Sci. (Biology), Acting Head of the Department of Bioengineering, Don State Technical University, Rostov-on-Don, kiriche.evgeniya@yandex.ru, http://orcid.org/0000-0003-4703-1616

Logvinov Aleksandr K. – Cand. Sci. (Biology), Research Fellow, Laboratory of Molecular Neurobiology, Southern Federal University, Rostov-on-Don, a.k.logvinov@yandex.ru, https://orcid.org/0000-0002-8873-3625

Rodkin Stanislav V. – Cand. Sci. (Biology), Associate Professor, Department of Bioengineering, Don State Technical University, Rostov-on-Don, rodkin_stas@mail.ru, https://orcid.org/0000-0003-4036-5410.

Cheryarina Natalia D. – Laboratory Assistant, Laboratory of Malignant Tumor Pathogenesis Study, National Medical Research Centre for Oncology, Rostov-on-Don, scalolas.92@yandex.ru, http://orcid.org/0000-0002-3711-8155

Kolesnikov Evgeniy N. – Dr. Sci. (Med.), Head of the Department of Abdominal Oncology No.1, National Medical Research Centre of Oncology, Rostov-on-Don, super.gormon@ya.ru, http://orcid.org/0000-0002-8436-7250

Kozhushko Mikhail A. – Cand. Sci. (Med.), Oncologist, Abdominal Oncology Department No.1, Deputy Director General for Educational Activities, National Medical Research Centre for Oncology, Rostov-on-Don, Kozhushko.misha@ yandex.ru, http://orcid.org/0000-0001-6866-475X

Anisimov Alexander E. – Cand. Sci. (Med.), Oncologist, Abdominal Oncology Department No.1, Deputy Director General for Educational Activities, National Medical Research Centre for Oncology, Rostov-on-Don, anisimovaleksan1992@gmail.com, http://orcid.org/0000-0003-1891-9528

Legenko Nikolay N. – Resident, Abdominal Oncology Department No.1, Deputy Director General for Educational Activities, National Medical Research Centre for Oncology, Rostov-on-Don, prostaff64@yandex.ru, http://orcid.org/0009-0005-6923-802X

(✉) **Neskubina Irina V.,** neskubina.irina@mail.ru

Received on May 27, 2025;
approved after peer review on September 22, 2025;
accepted on October 30, 2025

УДК 616.895.8–07:616.89–008.441.44
https://doi.org/10.20538/1682-0363-2026-2-49-57

The Role of Systemic Inflammatory Indices in Predicting Carotid Atherosclerosis in Patients with Rheumatoid Arthritis

Kononykhin A.A.[1, 3], Zhdanova E.V.[1, 2]

[1] *National Ilizarov Medical Research Center for Traumatology and Orthopedics*
6 M. Ulyanov St., 640014 Kurgan, Russian Federation

[2] *Tyumen State Medical University*
54 Odesskaya St., 625023 Tyumen, Russian Federation

[3] *Kurgan Regional Clinical Hospital*
63 Tomin St., 640002 Kurgan, Russian Federation

ABSTRACT

Aim. To determine the prognostic significance of systemic inflammatory indices for the development of carotid artery (CA) atherosclerosis in patients with rheumatoid arthritis (RA).

Materials and methods. A single-center, observational, cross-sectional study was conducted, which included 52 male and female patients with RA. The average age of the study participants was 59.5 ± 6.7 years. All patients underwent carotid duplex ultrasound. The intima – media thickness was recorded at ≥ 0.9 mm. A hemodynamically significant atherosclerotic plaque (AP) was considered to be a CA thickening of more than 50% compared to adjacent tissues. Based on the complete blood count data, the systemic inflammatory response index (SIRI), the aggregate index of systemic inflammation (AISI), the systemic immune – inflammation index (SII), the neutrophil-to-lymphocyte ratio (NLR), the lymphocyte-to-monocyte ratio (LMR), the platelet-to-lymphocyte ratio (PLR), and the Reis leukocyte index of intoxication were calculated. Binary logistic regression was used to develop a prognostic model.

Results. Based on the results of the carotid duplex ultrasound, the patients were divided into 2 groups: 32 patients (61.5%) with the presence of AP in the CA and 20 patients (38.5%) without AP. Patients with AP in the CA had higher values of NLR, SII, SIRI, and the Reis leukocyte index of intoxication. During the study, threshold values for these indices were determined, and a prognostic model for the probability of developing atherosclerosis of the CA in patients with RA was developed, in which the predictors were the values of the Reis index, SIRI, low-density lipoproteins, and age.

Conclusion. In RA, high activity of systemic inflammation is associated with the development of atherosclerotic arterial lesions, which should be taken into account when determining the tactics of managing these patients.

Keywords: rheumatoid arthritis, atherosclerosis, NLR, SIRI, SII, systemic inflammation

Conflict of interest. The authors declare the absence of obvious or potential conflicts of interest related to the publication of this article.

Source of financing. The authors state that they received no funding for the study.

Conformity with the principles of ethics. All patients signed informed consent to participate in the study. The study was approved by the local Ethics Committee of the National Ilizarov Medical Research Center for Traumatology and Orthopedics (Minutes No. 1 (76) dated November 29, 2024).

For citation: Kononykhin A.A., Zhdanova E.V. The Role of Systemic Inflammatory Indices in Predicting Carotid Atherosclerosis in Patients with Rheumatoid Arthritis. *Bulletin of Siberian Medicine.* 2026;25(2):49–57. https://doi.org/10.20538/1682-0363-2026-2-49-57.

✉ *Kononykhin Alexey A.,* kononykhin.al98@mail.ru

Роль системных воспалительных индексов в прогнозировании атеросклероза сонных артерий у пациентов с ревматоидным артритом

Кононыхин А.А.[1, 3], Жданова Е.В.[1, 2]

[1] *Национальный медицинский исследовательский центр (НМИЦ) травматологии и ортопедии им. акад. Г.А. Илизарова (Центр Илизарова)*
Россия, 640014, г. Курган, ул. М. Ульяновой, 6

[2] *Тюменский государственный медицинский университет (ТюмГМУ)*
Россия, 625023, г. Тюмень, ул. Одесская, 54

[3] *Курганская областная клиническая больница (КОКБ)*
Россия, 640002, г. Курган, ул. Томина, 63

РЕЗЮМЕ

Цель. Определить прогностическую значимость системных воспалительных индексов для развития атеросклероза сонных артерий (СА) у пациентов с ревматоидным артритом (РА).

Материалы и методы. Проведено одноцентровое обсервационное кросс-секционное исследование, в которое были включены 52 пациента с РА. Средний возраст участников составил 59,5 ± 6,7 лет. Всем пациентам выполнено ультразвуковое дуплексное сканирование (УЗДС) СА. Утолщение комплекса интима-медиа фиксировали при значениях 0,9 мм и более. За гемодинамически значимую атеросклеротическую бляшку (АСБ) принимали утолщение СА свыше 50% в сравнении с близлежащими тканями. Проведен анализ наличия факторов риска сердечно-сосудистых заболеваний. На основании данных общего анализа крови рассчитывали индекс системного воспалительного ответа (SIRI), совокупный индекс системного воспаления (AISI), индекс системного воспаления (SII), нейтрофильно-лимфоцитарное соотношение (NLR), лимфоцито-моноцитарное соотношение (LMR), тромбоцитарно-лимфоцитарное соотношение (PLR), а также индекс Рейса. Для разработки прогностической модели использован метод бинарной логистической регрессии.

Результаты. По результатам УЗДС СА пациенты были разделены на две группы: 32 пациента (61,5%) с наличием АСБ в СА и 20 пациентов (38,5%) без АСБ. Пациенты с наличием АСБ в СА имели более высокие значения NLR, SII, SIRI, индекса Рейса. В ходе исследования определены пороговые значения для данных индексов, а также разработана прогностическая модель вероятности развития атеросклероза СА у пациентов с РА, в которой предикторами являлись значения индекса Рейса, SIRI, липопротеиды низкой плотности и возраст.

Заключение. При РА высокая активность системного воспаления ассоциирована с развитием атеросклеротического поражения артерий, что следует учитывать при разработке тактики ведения данных пациентов.

Ключевые слова: ревматоидный артрит, атеросклероз, NLR, SIRI, SII, системное воспаление

Конфликт интересов. Авторы декларируют отсутствие явных и потенциальных конфликтов интересов, связанных с публикацией настоящей статьи.

Источник финансирования. Авторы заявляют об отсутствии источника финансирования при проведении исследования.

Соответствие принципам этики. Все пациенты подписали информированное согласие на участие в исследовании. Исследование одобрено локальным этическим комитетом Национального медицинского исследовательского центра травматологии и ортопедии им. академика Г.А. Илизарова (протокол № 1 (76) от 29.11.2024).

Для цитирования: Кононыхин А.А., Жданова Е.В. Роль системных воспалительных индексов в прогнозировании атеросклероза сонных артерий у пациентов с ревматоидным артритом. *Бюллетень сибирской медицины.* 2026;25(2):49–57. https://doi.org/10.20538/1682-0363-2026-2-49-57.

INTRODUCTION

Rheumatoid arthritis (RA) is a chronic autoimmune disease that affects joints and internal organs [1]. In 2020, there were over 17.6 million patients with RA worldwide, and the prevalence of the disease was 208.8 cases per 100,000 population, which is 14.1% more than in 1990. According to projections, by 2050, the global prevalence of RA will reach 31.7 million [2]. The prevalence of RA in the Russian Federation is 0.61% [3].

Patients with RA have an increased cardiovascular risk (CVR), which significantly contributes to overall cardiovascular mortality. This is primarily due to systemic inflammation, which is an independent factor in the development and progression of atherosclerosis. According to the World Health Organization, cardiovascular diseases (CVD) annually cause 17.9 million (32%) of all deaths worldwide [3]. Acute myocardial infarction (AMI) and stroke, which are most often caused by atherosclerosis, are the most significant causes of cardiovascular mortality [4].

The presence of atherosclerotic plaques (AP) in the carotid arteries (CA) is known to be a risk factor for ischemic stroke. According to the data of a systematic review and meta-analysis conducted by P. Ambrosino et al., patients with RA had higher values of the intima-media thickness (IMT) of the CA based on the results of carotid duplex ultrasound and also more often AP were detected in the CA (odds ratio (OR): 3.57; 95% confidence interval (95% CI): 1.69, 7.51; $p = 0.0008$) compared to the general population [5]. D.A. Galarza-Delgado et al. indicate that in RA, AP in the CA are formed more often than in the general population (30.0% versus 11.7%, $p = 0.013$), while bilateral AP are also detected significantly more often (8.3% versus 3.3%, $p = 0.008$) [6]. According to data from various studies in the Russian cohort, AP in the CA were detected in 59.5% (L.N. Eliseeva et al.) [7], 77% (O.A. Fomicheva et al.) [8], and 11% (E.V. Gerasimova et al.) of patients with RA [9].

The development and progression of atherosclerotic arterial lesions in RA are largely determined by the influence of systemic inflammation. Increased production of interleukin-1 (IL-1), IL-6, and tumor necrosis factor alpha (TNFα) in RA induces the expression of adhesion molecules (vascular cell adhesion molecule 1 (VCAM-1), intercellular adhesion molecule 1 (ICAM-1), and E-selectin) on the surface of CA endothelial cells, which leads to a decrease in the production and bioavailability of nitric oxide (NO), an increase in the synthesis of endothelin-1, and hyperproduction of reactive oxygen species, contributing to increased oxidative stress and endothelial activation [10]. In addition, TNFα and IL-6 suppress the activity of lipoprotein lipase and lecithin cholesterol acyltransferase, which contributes to the formation of a proatherogenic lipid profile in RA, the development of oxidative modifications of low-density lipoproteins (LDL), and an increase in the production of dysfunctional high-density lipoproteins (HDL), leading to the progression of atherosclerotic lesions of the CA [11, 12]. Under conditions of systemic inflammation in RA, T-lymphocytes and monocytes are activated, which, under the influence of VCAM-1 and ICAM-1, migrate to the CA intima and infiltrate the AP, where they contribute to increased expression of proinflammatory cytokines and the development of AP instability [13].

The significant influence of inflammation on the development of carotid atherosclerosis and the contribution of the latter to the increase in CVR in patients with RA determine the special clinical significance of the search for predictors of this vascular lesion, which can be considered as systemic inflammatory indices based on the indicators of a complete blood count: the systemic inflammatory response index (SIRI), the aggregate index of systemic inflammation (AISI), the systemic immune – inflammation index (SII), the neutrophil-to-lymphocyte ratio (NLR), the lymphocyte-to-monocyte ratio (LMR), the platelet-to-lymphocyte ratio (PLR), the Reis leukocyte index of intoxication. Currently, the possibility of using systemic inflammatory indices in predicting atherosclerosis and CVR is being actively studied worldwide [14].

The aim of the study was to determine the prognostic significance of systemic inflammatory indices for the development of CA atherosclerosis in patients with RA.

MATERIALS AND METHODS

A single-center, observational, cross-sectional study was conducted, including 52 male and female patients (mean age 59.5 ± 6.7 years) with RA. Inclusion criteria were as follows: age from 35 to 75 years; RA diagnosis established in accordance

with the criteria of the American College of Rheumatology/European Alliance of Associations for Rheumatology (ACR/EULAR). Patients meeting one of the following criteria were excluded from the study: coronary artery disease (CAD), chronic heart failure, acute or exacerbated chronic infection, cancer or history of cancer, and type 1 or type 2 diabetes mellitus. Patients underwent a general clinical examination in accordance with the 2024 Clinical Guidelines for Rheumatoid Arthritis of the Russian Association of Rheumatologists. All patients received basic anti-inflammatory therapy with one of the following medications: methotrexate, sulfasalazine, or leflunomide.

A carotid duplex ultrasound was performed for all patients by a single specialist – a functional diagnostics doctor – once during inpatient treatment in a specialized Rheumatology Unit. The carotid duplex ultrasound was performed using a Samsung RS85 ultrasound machine (South Korea). The linear transducer used in the study emitted a frequency of 7.5 MHz. The IMT of the CA was measured in mm at three points: the first point is the area of the general CA at a distance of 10 mm from the bulb; the second point is 5–10 mm cranial to the beginning of the bulb; the third point is the internal CA, 10 mm after the bifurcation on both sides. The maximum values of the IMT obtained during the study were analyzed. IMT was recorded at values of 0.9 mm or more. A hemodynamically significant AP was defined as a CA thickening over 50% compared to adjacent tissues [15, 16].

Total cholesterol (TC) was analyzed enzymatically, LDL and HDL were analyzed using a direct enzymatic colorimetric method, and triglycerides (TG) were analyzed using an enzymatic colorimetric method. A complete blood count was performed on a MINDRAY BC-6000 hematology analyzer (China). The erythrocyte sedimentation rate (ESR) was determined using the Westergren method. C-reactive protein (CRP) and IgM rheumatoid factor (RF) levels were analyzed using an immunoturbidimetric method on an ILab Taurus automated biochemical analyzer (USA). An enzyme-linked immunosorbent assay was used to determine the concentration of antibodies to cyclic citrullinated peptide (anti-CCP) in the serum.

Systemic inflammatory indices were calculated using the following formulas: SIRI = neutrophils x monocytes / lymphocytes [17]; AISI = neutrophils × monocytes × platelets / lymphocytes [18]; SII = neutrophils × platelets / lymphocytes [19]; NLR = neutrophils / lymphocytes [20]; PLR = platelets / lymphocytes [20]; LMR = lymphocytes / monocytes [21]; Reis index = (myelocytes + metamyelocytes + band neutrophils + segmented neutrophils) / (monocytes + lymphocytes + eosinophils) [22]. Absolute values of the number of formed elements in the blood were used for the calculation.

Microsoft Excel was used to create the study database. Statistical analysis was performed using STATISTICA 9 (StatSoft, USA). The normality of distribution of quantitative variables was assessed using the Shapiro – Wilk test, as well as analysis of the asymmetry and kurtosis coefficients. Data corresponding to a normal distribution were presented as the arithmetic mean (M) and standard deviation (SD). Indicators with a distribution different from the normal one were described using the median and interquartile range, Me [Q_1; Q_3]. Categorical variables were described as absolute values (n) and percentages (%).

Comparison of two independent groups for a quantitative indicator, the distribution of which in each of the groups corresponded to the normal one, under the condition of equal variances was performed using Student's t-test; in case of unequal variances, Welch's t-test was used. A comparison of two independent groups based on quantitative variables with non-normal distributions was performed using the non-parametric Mann – Whitney U-test. ROC analysis was used to assess the predictive value and discriminatory ability of quantitative variables for the target outcome. Classification quality was assessed based on the area under the ROC curve (AUC) with a 95% confidence interval. The cutoff value of the quantitative variable was determined by the highest value of the Youden's index. A predictive model for the probability of a specific outcome was constructed using logistic regression. Statistical significance of differences was determined at a significance level of $p < 0.05$.

RESULTS

Based on carotid duplex ultrasound data, all patients were divided into two groups: those with CA AP (n = 32; 61.5%) and those without them (n = 20; 38.5%). Patients in the study groups did not differ in

gender, age, disease duration and stage, CVD risk factors, or the proportion of patients receiving statins and glucocorticosteroids. No significant differences in lipid profile parameters were found between the patient groups. The presence of CA AP was statistically significantly more often associated with anti-CCP status and higher ESR and CRP values (Table 1). Systemic inflammation indices were higher in the presence of CA AP, while NLR, SII, SIRI, and Reis index values also differed statistically significantly (Table 2).

As a result of the ROC analysis conducted to assess the risk of the formation of AP in the CA, the threshold values of the studied indices of systemic inflammation were determined (Table 3, Figure).

Table 1

Comparative Characteristics of Patients with and without Carotid Artery Atherosclerosis

Indicator	Patients with the presence of AP in the carotid arteries (n = 32)	Patients without AP in the carotid arteries (n = 20)	p
Age, years, $M \pm SD$	60.4±6.5	58.6±7.1	0.06
Gender (male), n (%)	9 (28.1)	6 (30)	0.07
Duration of disease, years, Me [Q_1; Q_3]	11.9 [7.4; 14.3]	10.8 [6.1; 13.9]	0.21
Disease stage, early/advanced/late, n (%)	5 (15.6) / 11 (34.4) / 16 (50)	3 (15) / 3 (15) / 14 (70)	0.19
Positive RF, n (%)	25 (78.1)	16 (80)	0.44
Positive anti-CCP, n (%)	23 (71.8)	13 (65)	0.03
Hypertension, n (%)	14 (43.8)	8 (40)	0.29
Statin therapy, n (%) Atorvastatin, n (%) Average dose, mg, $M \pm SD$ Rosuvastatin, n (%) Average dose, mg, $M \pm SD$	15 (46.9) 8 (25) 26.25±8.5 7 (21.9) 10.7±3.5	9 (45) 6 (30) 20±6.5 3 (15) 13.3±4.2	0.36 0.08 0.25 0.07 0.23
Glucocorticosteroid therapy, n (%)	6 (18.8)	3 (15)	0.22
Smoking, n (%)	7 (21.8)	4 (20)	0.17
Family history of CVD, n (%)	6 (18.8)	5 (25)	0.06
Antirheumatic therapy: Methotrexate Leflunomide Sulfasalazine, n (%)	 15 (46.8) 8 (25) 9 (28.2)	 9 (45) 6 (30) 5 (25)	 0.54 0.19 0.12
TC, mmol/l, $M \pm SD$	5.21±1.22	5.03±0.98	0.11
LDL, mmol/l, Me [Q_1; Q_3]	3.31 [2.2; 3.98]	3.12 [2.11; 3.77]	0.09
HDL, mmol/l, Me [Q_1; Q_3]	0.89 [0.68; 1.01]	0.78 [0.65; 0.99]	0.078
TG, mmol/l, $M \pm SD$	1.77±0.33	1.71±0.41	0.15
ESR, mm/h, Me [Q_1; Q_3]	27 [22; 31]	20 [16; 25]	0.03
CRP, mg/l, $M \pm SD$	6.28±1.17	3.22±1.12	0.02

Note. AP – atherosclerotic plaque; RF – rheumatoid factor; anti-CCP – antibodies to cyclic citrullinated peptide; CVD – cardiovascular disease; TC – total cholesterol; LDL – low-density lipoprotein; HDL – high-density lipoprotein; TG – triglycerides; ESR – erythrocyte sedimentation rate; CRP – C-reactive protein; p – level of statistical significance of differences.

Table 2

Values of Systemic Inflammation Indices in Patients with and without Carotid Artery Atherosclerosis, Me [Q_1; Q_3]

Index	Patients with the presence of AP in the carotid arteries (n = 32)	Patients without AP in the carotid arteries (n = 20)	p
NLR	2.31 [1.72; 3.59]	1.48 [1.21; 2.21]	0.01
LMR	4.78 [2.9; 6.1]	4.01 [2.76; 5.8]	0.17
PLR	178.9 [129.7; 213.24]	159 [109.3; 179.9]	0.29
Reis index	1.64 [1.21; 2.11]	1.26 [1.11; 1.43]	0.002
SII	794.2 [440.5; 1,090.8]	411.11 [360.06; 582.93]	0.004
SIRI	1.35 [0.77; 1.57]	0.74 [0.53; 0.89]	0.01
AISI	255.3 [199.1; 279.2]	219.8 [165; 231.5]	0.059

Note. AP – atherosclerotic plaque; LMR – lymphocyte-monocyte ratio; PLR – platelet-lymphocyte ratio; NLR – neutrophil-lymphocyte ratio; SII – systemic immune-inflammation index; SIRI – systemic inflammatory response index; AISI – aggregate inflammation systemic index; p – level of statistical significance of differences.

Table 3

Results of ROC Analysis for Determining Threshold Values of Systemic Inflammatory Indices Associated with the Presence of AP in the CA

Index	Threshold value	AUC	95% CI for AUC	*p*
NLR	>1.756	0.754	0.583–0.926	0.029
SII	>585.29	0.751	0.577–0.926	0.021
SIRI	>1.04	0.768	0.599–0.937	0.022
AISI	>247.4	0.699	0.577–0.874	0.032
Reys index	>1.57	0.791	0.698–0.897	0.007

Note. AUC – area under the curve.

As a result of the analysis conducted using binary logistic regression, a prognostic model was developed for assessing the risk of AP formation in the CA in patients with RA. The model includes a set of independent predictors statistically significantly associated with the outcome under study (the presence of AP in the CA in patients with RA) and allows for calculating the personalized probability of this complication.

The observed dependence was described by the equation: $P = 1 / (1 + e^{-z})$; $z = -4.710 + 1.374 \times$ (Reis index) + $0.745 \times$ (SIRI) − $0.331 \times$ (LDL) + $0.057 \times$ (age), where P is the risk assessment of AP formation in the CA in patients with RA, and *z* is the value of the logistic function. The discriminatory ability of the regression model was assessed using ROC analysis, during which the threshold P value was defined as 0.615. The probability of the presence of AP in the CA in patients with RA was predicted by a P value greater than or equal to this value. The sensitivity and specificity of the developed model were 78.9% and 81.8%, respectively.

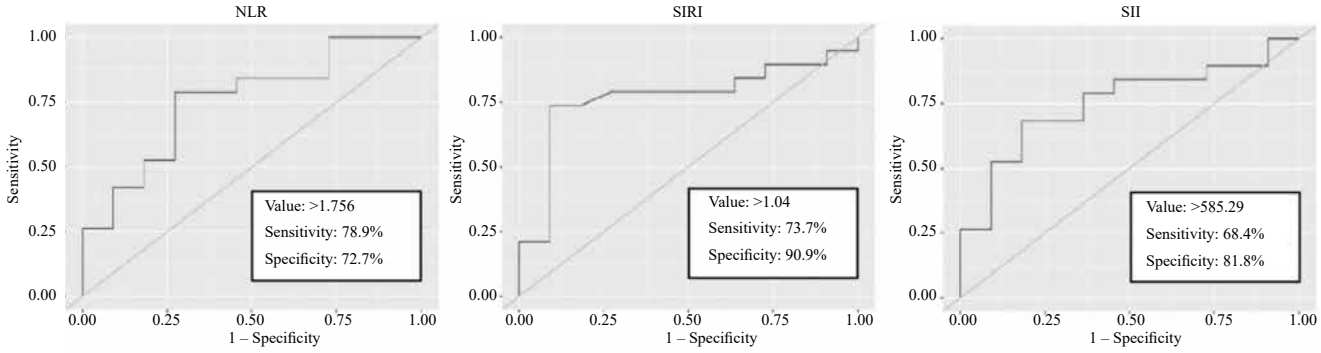

Figure. ROC curve characteristics of the threshold values of systemic inflammatory indices (NLR, SIRI, and SII) for optimal binary classification of the presence or absence of carotid artery atherosclerosis in patients with rheumatoid arthritis. ROC analysis: NLR – neutrophil-to-lymphocyte ratio, SIRI – systemic inflammatory response index, SII – systemic immune-inflammation index. The ordinate axis shows sensitivity (%), the abscissa axis – 1 minus specificity (%). The rectangles show sensitivity and specificity estimates, as well as the threshold values of the systemic inflammatory indices

DISCUSSION

Data from cohort studies indicate an association between peripheral blood leukocyte levels and their major subpopulations (neutrophils, lymphocytes, and monocytes) and an increased risk of stroke, CAD, and all-cause mortality. The simplicity and accessibility of this analysis have facilitated the active study of calculated leukocyte indices (LMR, NLR, and PLR) as markers of systemic inflammation. Numerous studies confirm that these indices have a higher predictive power for overall and cardiovascular mortality compared to the use of absolute leukocyte count alone [23].

Systemic inflammatory indices (SII, SIRI, and AISI) are expanded versions of indices calculated based on leukocyte differential parameters. Although the importance of systemic inflammatory indices for predicting the course and outcome of various diseases has only recently been studied, and the accumulated scientific data are still insufficient, a number of publications indicate their potential clinical significance in oncological, infectious, autoimmune, and cardiovascular pathologies [24].

Y. Xia et al. found that patients with SII >655.56 had significantly higher rates of overall mortality (OR = 1.29; 95% CI): 1.18–1.41) and CVD mortality (OR = 1.33; 95% CI: 1.11–1.59) compared to the SII group (<335.36). Similarly, the risk of all-cause (OR = 1.39; 95% CI: 1.26–1.52) and CVD mortality (OR = 1.39; 95% CI: 1.14–1.68) was increased in the group with SIRI >1.43 relative to the group with SIRI <0.68 [25].

Of particular interest are the data of V.A. Schwartz et al., who found that in patients without RA, the threshold levels of systemic inflammatory indices associated with atherosclerosis were equal for NLR >2.05, for SIRI >1.05, and for SII >368 [26]. E. Zhou et al. found that in patients with RA with an NLR value >3.28, the risk of death from all causes (relative risk (RR) = 2.02, 95% CI: 1.53–2.66) and from cardiovascular pathology (RR = 2.48, 95% CI: 1.34–4.57) was higher than in patients with a lower value of this index [27]. According to X. Yin et al., in RA, a higher SII level was associated with a 1.48-fold increase in the risk of all-cause mortality (RR = 1.48, 95% CI: 1.21–1.81) and a 1.51-fold increase in the risk of cardiovascular mortality (RR = 1.51, 95% CI: 1.04–2.18) compared to lower SII [28]. The SIRI inflammatory index also demonstrated a positive correlation with all-cause and CVD mortality in patients with RA [29]. According to M. González-Sierra et al., in patients with RA, the values of the SIRI, NLR, and PLR indices were not associated with CA atherosclerosis, but they had a positive correlation with the CVR assessed by the SCORE2 scale [30].

According to our data, the threshold values that were statistically significantly associated with the presence of AP in the CA in patients with RA were: for SII >585.29; for SIRI >1.04; for NLR >1.756; and for AISI >247.4. The increase in the values of systemic inflammation indices is due to characteristic changes in the leukocyte formula and platelet component: an increase in the absolute number of neutrophils, monocytes and platelets against the background of a decrease in the number of lymphocytes. In RA, high levels of TNFα, IL-1, and IL-6 stimulate the production of neutrophils, and increased concentrations of chemokines (CXCL1, CXCL2, CXCL5, etc.) secreted by synovial fibroblasts, macrophages, and other cells at the site of inflammation cause the migration of neutrophils from the bloodstream into the synovial membrane and other tissues, which is accompanied by a compensatory increase in the production of neutrophils by the bone marrow [31].

IL-6 plays a central role in the pathogenesis of reactive thrombocytosis in RA: it induces increased synthesis of thrombopoietin, a key hormonal regulator of thrombopoiesis in hepatocytes, and simultaneously has a direct stimulating effect on megakaryocytic progenitor cells and mature megakaryocytes in the bone marrow, activating the JAK/STAT (janus kinase/signal transducer and activator of transcription proteins) and MAPK (mitogen-activated protein kinase) signaling pathways, which leads to increased proliferation, accelerated differentiation, increased ploidy of megakaryocytes, and, as a consequence, increased platelet release [32]. Increased platelet counts and activation are considered as factors potentially contributing to increased CVR and persistent inflammation in the vascular bed, as well as in the synovial lining of joints in RA.

Lymphocytopenia in patients with RA is a common hematological manifestation reflecting profound immune dysregulation and having a multifactorial nature. Key proinflammatory cytokines (TNFα, IL-6, etc.) enhance the expression of the Fas receptor (CD95) on lymphocytes and increase the level of soluble Fas ligand (sFasL), triggering the caspase cascade and activation-induced cell death [33]. Hypoxia and the Warburg effect in the synovium cause competition for glucose and the accumulation of lactate, which suppresses lymphocyte function and induces their apoptosis by disrupting the PI3K/Akt/mTOR (Phosphoinositide 3-kinases/Protein kinase B/mammalian target of rapamycin) survival signaling pathways.

In addition, the presence of antilymphocyte autoantibodies and increased expression of inhibitory receptors (PD-1, programmed cell death protein 1; CTLA-4, cytotoxic T-lymphocyte associated protein 4) on chronically activated T cells lead to their lysis, opsonization, or a state of functional exhaustion with an increased tendency to apoptosis [33]. Limitations of the present study included its single-center and cross-sectional nature, as well as a small sample size of patients.

CONCLUSION

This study demonstrates that in patients with RA, elevated systemic inflammatory indices are significantly associated with the presence and severity of atherosclerosis. These indices, easily calculated using routine clinical blood tests, reflect the intensity and imbalance of the systemic immune inflammatory process underlying RA, making them accessible, noninvasive, and cost-effective biomarkers of elevated CVR in patients with RA.

Monitoring systemic inflammatory indices can complement traditional CVR assessment scales (SCORE, SCORE2, etc.) and facilitate the early identification of patients requiring more intensive preventive strategies. Persistently elevated values of these indices may indirectly indicate a more aggressive course of RA with a pronounced systemic inflammatory component directly damaging the vascular wall.

Determining optimal cutoff values for each index in patients with RA and assessing their additional diagnostic and prognostic value compared to existing markers (CRP, ESR) and assessment tools (carotid duplex ultrasound and coronary artery calcium levels) are a pressing scientific challenge. Randomized controlled trials are needed to establish a causal relationship and determine the prognostic value of changes in systemic inflammatory indices in relation to atherosclerosis progression and the occurrence of cardiovascular events (myocardial infarction, stroke) in patients with RA.

Of equal importance is the study of how various RA treatment strategies (especially therapy with biological disease-modifying antirheumatic drugs and targeted synthetic disease-modifying antirheumatic drugs) influence the changes in systemic inflammatory indices and, consequently, the risk of atherosclerosis and cardiovascular events. The development and validation of clinically applicable algorithms integrating these indices into routine CVR assessment and preventive therapy decision-making in patients with RA is of significant scientific interest.

REFERENCES

1. Lyubimova L.V., Pchelova N.N., Nikolaev N.S., Preobrazhenskaya E.V., Lyubimov E.A. Periprosthetic Joint Infection in Patients with Rheumatoid Arthritis: Case Series. *Genij Ortopedii*. 2024;30(4):552–560. (In Russ.). DOI: 10.18019/1028-4427-2024-30-4-552-560.
2. Black R.J., Cross M., Haile L.M., Culbreth G.T., Steinmetz J.D., Hagins H. et al. Global, regional, and national burden of rheumatoid arthritis, 1990–2020, and projections to 2050: a systematic analysis of the Global Burden of Disease Study 2021. *Lancet Rheumatol.* 2023;5:e594–e610. DOI: 10.1016/s2665-9913(23)00211-4.
3. Galushko E.A., Nasonov E.L. Prevalence of Rheumatic Diseases in Russia. *Almanac of Clinical Medicine*. 2018;46(1):32–39. (In Russ.). DOI: 10.18786/2072-0505-2018-46-1-32-39.
4. Roth G.A., Abate D., Abate K.H., Abay S.M., Abbafati C., Abbasi N. et al. Global Health Metrics. Global, regional, and national age-sex-specific mortality for 282 causes of death in 195 countries and territories, 1980-2017: a systematic analysis for the global burden of disease study 2017. *Lancet.* 2018;392(10159):1736–1788. DOI: 10.1016/S0140-6736(18)32203-7.
5. Ambrosino P., Lupoli R., Di Minno A., Tasso M., Peluso R., Di Minno M.N. Subclinical atherosclerosis in patients with rheumatoid arthritis. A meta-analysis of literature studies. *Thromb. Haemost.* 2015;113(5):916–30. DOI: 10.1160/TH14-11-0921.
6. Galarza-Delgado D.A., Azpiri-Lopez J.R., Guajardo-Jauregui N., Cardenas-de la Garza J.A., Garza-Cisneros A.N., Garcia-Heredia A. et al. Carotid atherosclerosis in the first five years since rheumatoid arthritis diagnosis: a cross sectional study. *Adv. Rheumatol.* 2023;63(1):36. DOI: 10.1186/s42358-023-00319-x.
7. Eliseeva L.N., Otarova Zh.Z., Zhdamarova O.I., Davydova A.F. Clinical Efficacy of a Method for Identifying Patients at High Risk of Carotid Atherosclerosis in Rheumatoid Arthritis. *South Russian Journal of Therapeutic Practice*. 2022;3(4):70–76. (In Russ.). DOI: 10.21886/2712-8156-2022-3-4-70-76.
8. Fomicheva O.A., Popkova T.V., Krugly L.B., Gerasimova E.V., Novikova D.S., Pogorelova O.A. et al. Factors of Progression and Occurrence of Atherosclerosis in Rheumatoid Arthritis. *Kardiologiia*. 2021;61(1):12–21. (In Russ.). DOI: 10.18087/cardio.2021.1.n1331.
9. Gerasimova E.V., Popkova T.V., Shalygina M.V., Kirillova I.G., Gerasimova D.A., Glukhova S.I. et al. Subclinical Atherosclerosis of the Carotid Arteries in Patients with Rheumatoid Arthritis with Low Cardiovascular Risk. *Terapevticheskii Arkhiv*. 2023;95(5):375–379. (In Russ.). DOI: 10.26442/00403660.2023.05.202203.
10. England B.R., Thiele G.M., Anderson D.R., Mikuls T.R. Increased cardiovascular risk in rheumatoid arthritis: mechanisms and implications. *BMJ.* 2018;361:k1036. DOI: 10.1136/bmj.k1036.
11. Feingold K.R., Grunfeld C. Effect of inflammation on HDL structure and function. *Curr. Opin. Lipidol.* 2016;27(5):521–530. DOI: 10.1097/MOL.0000000000000333.
12. Chang C.K., Chiang E.I., Chang K.H., Tang K.T., Chen P.K., Yip H.T. et al. The sizes and composition of HDL-cholesterol are significantly associated with inflammation in rheumatoid arthritis patients. *Int. J. Mol. Sci.* 2023;24(13):10645. DOI: 10.3390/ijms241310645.
13. Certo M., Rahimzadeh M., Mauro C. Immunometabolism in atherosclerosis: a new understanding of an old disease. *Trends. Biochem. Sci.* 2024;49(9):791–803. DOI: 10.1016/j.tibs.2024.06.003.
14. Jin Z., Wu Q., Chen S., Gao J., Li X., Zhang X. et al. The Associations of Two Novel Inflammation Indexes, SII and SIRI with the Risks for Cardiovascular Diseases and All-Cause Mortality: A Ten-Year Follow-Up Study in 85,154 Individuals. *J. Inflamm. Res.* 2021; 14:131–40. DOI:10.2147/JIR.S283835.
15. Johri A.M., Nambi V., Naqvi T.Z., Feinstein S.B., Kim E.SH., Park M.M. et al. Recommendations for the assessment of carotid arterial plaque by ultrasound for the characterization of atherosclerosis and evaluation of cardiovascular risk: from the American Society of Echocardiography. *J. Am. Soc. Echocardiogr.* 2020;33(8):917–933. DOI: 10.1016/j.echo.2020.04.021.

16. Chernyavsky M.A., Irtyuga O.B., Yanishevsky S.N., Alieva A.S., Samochernykh K.A., Abramov K.B. et al. Russian Consensus Statement on the Diagnosis and Treatment of Patients with Carotid Stenosis. *Russian Journal of Cardiology*. 2022;27(11):5284. (In Russ.). DOI: 10.15829/1560- 4071-2022-5284.
17. Qi Q., Zhuang L., Shen Y., Geng Y., Yu S., Chen H. et al. A novel systemic inflammation response index (SIRI) for predicting the survival of patients with pancreatic cancer after chemotherapy. *Cancer.* 2016;122(14):2158–67. DOI: 10.1002/cncr.30057.
18. Xiu J., Lin X., Chen Q., Yu P., Lu J., Yang Y. et al. The aggregate index of systemic inflammation (AISI): a novel predictor for hypertension. *Front. Cardiovasc. Med.* 2023;10:1163900. DOI: 10.3389/fcvm.2023.1163900.
19. Hu B., Yang X.R., Xu Y., Sun Y.F., Sun C., Guo W. et al. Systemic immune-inflammation index predicts prognosis of patients after curative resection for hepatocellular carcinoma. *Clin. Cancer. Res.* 2014;20(23):6212–22. DOI: 10.1158/1078-0432.CCR-14-0442.
20. Diem S., Schmid S., Krapf M., Flatz L., Born D., Jochum W. et al. Neutrophil-to-Lymphocyte ratio (NLR) and Platelet-to-Lymphocyte ratio (PLR) as prognostic markers in patients with non-small cell lung cancer (NSCLC) treated with nivolumab. *Lung Cancer.* 2017;111:176–181. DOI: 10.1016/j.lungcan.2017.07.024.
21. Abe S., Kawai K., Nozawa H., Hata K., Kiyomatsu T., Morikawa T. et al. LMR predicts outcome in patients after preoperative chemoradiotherapy for stage II-III rectal cancer. *J. Surg. Res.* 2018;222:122–131. DOI: 10.1016/j.jss.2017.09.053.
22. Grebennikova I.V., Lidokhova O.V., Makeeva A.V., Bolotrskikh V.I., Berdnikov A.A., Savchenko A.P. et al. Clinical and Pathogenetic Significance of Leukocyte Indices in COVID-19: a Restrospective Study. *Bashkortostan Medical Journal.* 2022;17(3):10–14. (In Russ.).
23. Joshi A., Bhambhani A., Barure R., Gonuguntla S., Sarathi V., Attia A.M. Neutrophil-lymphocyte ratio and platelet-lymphocyte ratio as markers of stable ischemic heart disease in diabetic patients: An observational study. *Medicine.* 2023;102(5):e32735. DOI: 10.1097/MD.0000000000032735.
24. Cheng Q., Liu C., Zhong H., Wang Z., Zhou S., Sun J. et al. Comparison of systemic immunoinflammatory biomarkers for assessing severe abdominal aortic calcification among US adults aged ≥40 years: A cross-sectional analysis from NHANES. *PLoS One*. 2025;20(6):e0325949. DOI: 10.1371/journal.pone.0325949.
25. Xia Y., Xia C., Wu L., Li Z., Li H., Zhang J. Systemic Immune Inflammation Index (SII), System Inflammation Response Index (SIRI) and Risk of All-Cause Mortality and Cardiovascular Mortality: A 20-Year Follow-Up Cohort Study of 42,875 US Adults. *J. Clin. Med.* 2023;12(3):1128. DOI: 10.3390/jcm12031128.
26. Schwartz V.A., Talibova S.M., Sokolskaya M.A, Ispiryan A.Yu., Shvarts E.N., Petrosyan A.D. et al. Association of Novel Biomarkers of Systemic Inflammation with Atherosclerosis and its Severity. *Russian Journal of Cardiology*. 2024;29(8):6025. (In Russ.). DOI: 10.15829/1560-4071-2024-6025.
27. Zhou E., Wu J., Zhou X., Yin Y. The neutrophil-lymphocyte ratio predicts all-cause and cardiovascular mortality among U.S. adults with rheumatoid arthritis: results from NHANES 1999–2020. *Front. Immunol.* 2023;14:1309835. DOI: 10.3389/fimmu.2023.1309835.
28. Yin X., Zhang Y., Zou J., Yang J. Association of the systemic immune-inflammation index with all-cause and cardiovascular mortality in individuals with rheumatoid arthritis. *Sci. Rep.* 2024;14(1):15129. DOI: 10.1038/s41598-024-66152-4.
29. Wang W., Yao W., Tang W., Li Y., Lv Q., Ding W. Systemic inflammation response index is associated with increased all-cause and cardiovascular mortality in US adults with rheumatoid arthritis. *Prev. Med.* 2024;185:108055. DOI: 10.1016/j.ypmed.2024.108055.
30. González-Sierra M., Quevedo-Rodríguez A., Romo-Cordero A., González-Chretien G., Quevedo-Abeledo J.C., de Vera-González A. et al. Relationship of blood inflammatory composite markers with cardiovascular risk factors and subclinical atherosclerosis in patients with rheumatoid arthritis. *Life (Basel).* 2023;13(7):1469. DOI: 10.3390/life13071469.
31. Karmakar U., Vermeren S. Crosstalk between B cells and neutrophils in rheumatoid arthritis. *Immunology*. 2021;164(4):689–700. DOI: 10.1111/imm.13412.
32. Harifi G., Sibilia J. Pathogenic role of platelets in rheumatoid arthritis and systemic autoimmune diseases. Perspectives and therapeutic aspects. *Saudi Med. J.* 2016;37(4):354–60. DOI: 10.15537/smj.2016.4.14768.
33. Wang Y., Su R., Li B., Guo Q., Hu F., Yu X. et al. Reduction of peripheral regulatory T cells in active rheumatoid arthritis patients with coronary artery disease. *BMC Immunol.* 2021;22(1):76. DOI: 10.1186/s12865-021-00466-0.

Author Information

Kononykhin Alexey A. – Postgraduate Student, National Ilizarov Medical Research Center for Traumatology and Orthopedics, Kurgan; Rheumatologist, Kurgan Regional Clinical Hospital, Kurgan, kononykhin.al98@mail.ru, http://orcid.org/0000-0002-9404-712X

Zhdanova Ekaterina V. – Dr. Sci. (Med.), Professor, Head of the Department of Pathological Physiology, Tyumen State Medical University, Tyumen; Professor of the Traumatology, Orthopedics and Allied Disciplines Department, National Ilizarov Medical Research Center for Traumatology and Orthopedics, Kurgan, zhdanova.e.v@bk.ru, http://orcid.org/0004-0002-7938-5470

(✉) **Kononykhin Alexey A.,** kononykhin.al98@mail.ru

Received on September 5, 2025;
approved after peer review on September 29, 2025;
accepted on October 30, 2025

УДК 616.895.8–07:616.89–008.441.44
https://doi.org/10.20538/1682-0363-2026-2-58-64

Constitutional and Morphological Predisposition to Suicidal Behavior in Schizophrenia

Kornetov A.N., Galkin S.A., Mednova I.A., Petkun D.A., Kornetova E.G.

Mental Health Research Institute, Tomsk National Research Medical Center (NRMC), Russian Academy of Sciences
4 Aleutskaya St., 634014 Tomsk, Russian Federation

ABSTRACT

Aim. To study the relationship of constitutional and morphological features of patients with schizophrenia with suicidal behavior.

Materials and methods. We examined 215 patients with schizophrenia. Information about the age of the patients, the age of manifestation and duration of the disease, and the history of suicide attempts was acquired through structured clinical interviews and examination of medical records. Additionally, the Beck Hopelessness Inventory was used. The anthropometric examination was carried out according to V.V. Bunak's method, modified by V.P. Chitetsov. Constitutional and morphological body types and somatic sexual differentiation were determined based on the calculation of the Rees – Eysenck index and the Tanner index.

Results. The $\chi 2$ test revealed significant differences in the distribution frequencies of the main constitutional and morphological types between the groups of patients with and without suicide attempts ($p = 0.033$). Following a pairwise comparison, significant differences were found only in the frequency of asthenic constitutional and morphological type ($p = 0.018$). Also, when comparing the frequencies of the distribution of constitutional and morphological types between patients with and without hopelessness, significant differences were found ($p = 0.035$). In the group of patients with hopelessness, the asthenic constitutional and morphological type prevailed ($p = 0.045$). The network analysis made it possible to identify two independent suicide risk factors in patients with schizophrenia: clinical and anthropometric.

Conclusion. The results of the study clearly confirm the importance of the constitution as an independent risk factor for suicidal behavior in patients with schizophrenia. The data obtained open up prospects for early detection of predisposition to suicidal thoughts and actions in this group of patients.

Keywords: schizophrenia, suicidal risk, parasuicide, hopelessness, constitution, anthropometry, Rees – Eysenck index, Tanner index

Conflict of interest. The authors declare the absence of obvious or potential conflicts of interest related to the publication of this article.

Source of financing. The study was supported by the Russian Science Foundation grant No. 25-15-00344 "Constitutional and biological predictors of suicidal behavior risk in patients with schizophrenia".

Conformity with the principles of ethics. All patients signed an informed consent to participate in the study. The study was approved by the local Ethics Committee at Mental Health Research Institute, Tomsk NMRC (Minutes No. 185 dated 16.06.2025).

For citation: Kornetov A.N., Galkin S.A., Mednova I.A., Petkun D.A., Kornetova E.G. Constitutional and Morphological Predisposition to Suicidal Behavior in Schizophrenia. *Bulletin of Siberian Medicine.* 2026;25(2):58–64. https://doi.org/10.20538/1682-0363-2026-2-58-64.

✉ *Kornetov Alexander N.,* alkornetov@gmail.com

Конституционально-морфологическая предиспозиция суицидального поведения при шизофрении

Корнетов А.Н., Галкин С.А., Меднова И.А., Петкун Д.А., Корнетова Е.Г.

Научно-исследовательский институт (НИИ) психического здоровья
Томского национального исследовательского медицинского центра (НИМЦ) Российской академии наук
Россия, 634014, г. Томск, ул. Алеутская, 4

РЕЗЮМЕ

Цель. Изучить связь конституционально-морфологических особенностей больных шизофренией с суицидальным поведением.

Материалы и методы. Обследовано 215 пациентов с диагнозом шизофрении. Возраст пациентов, возраст манифестации и продолжительность заболевания, история суицидальных попыток были получены путем структурированного клинического интервью и изучения медицинских карт. Дополнительно использовалась Шкала безнадежности Бека (Beck Hopelessness Inventory). Антропометрическое обследование проводилось по методике В.В. Бунака в модификации В.П. Чтецова. Конституционно-морфологические типы телосложения и соматическая половая дифференциация определялись на основании расчета индекса Rees-Eysenk и индекса Tanner.

Результаты. По критерию $\chi 2$ были обнаружены статистически значимые различия частот распределения основных конституционально-морфологических типов между группами пациентов с суицидальными попытками и без ($p = 0{,}033$). При попарном сравнении значимые различия были выявлены только по частоте встречаемости астенического конституционально-морфологического типа ($p = 0{,}018$). Также при сравнении частот распределения конституционально-морфологических типов между пациентами с наличием и отсутствием безнадежности обнаружены статистически значимые различия ($p = 0{,}035$), в группе пациентов с безнадежностью преобладал астенический конституционально-морфологических тип ($p = 0{,}045$). Проведенный сетевой анализ позволил выделить два независимых друг от друга фактора суицидального риска у пациентов с шизофренией: клинический и антропометрический.

Заключение. Результаты исследования наглядно подтверждают значимость конституции в качестве независимого фактора риска суицидального поведения у пациентов с шизофренией. Полученные данные открывают перспективы для раннего выявления предрасположенности к суицидальным мыслям и действиям у данной группы больных.

Ключевые слова: шизофрения, суицидальный риск, парасуицид, безнадежность, конституция, антропометрия, индекс Rees-Eysenk, индекс Tanner

Конфликт интересов. Авторы декларируют отсутствие явных и потенциальных конфликтов интересов, связанных с публикацией настоящей статьи.

Источник финансирования. Исследование выполнено за счет гранта Российского научного фонда № 25-15-00344 «Конституционально-биологические предикторы риска суицидального поведения у больных шизофренией».

Соответствие принципам этики. Все пациенты подписали информированное согласие на участие в исследование. Исследование одобрено локальным этическим комитетом НИИ психического здоровья Томского НИМЦ (протокол № 185 от 16.06.2025).

Для цитирования: Корнетов А.Н., Галкин С.А., Меднова И.А., Петкун Д.А., Корнетова Е.Г. Конституционально-морфологическая предиспозиция суицидального поведения при шизофрении. *Бюллетень сибирской медицины.* 2026;25(2):58–64. https://doi.org/10.20538/1682-0363-2026-2-58-64.

INTRODUCTION

According to the World Health Organization (WHO), approximately 800,000 people die by suicide each year globally, with suicide attempts estimated to be 20 times more frequent [1, 2]. Mental disorders are a leading cause of suicidal behavior [3, 4]. Among individuals with schizophrenia, the lifetime risk of suicide death is approximately 5%, while the likelihood of a suicide attempt ranges from 25 to 50% [5, 6]. A literature search in the PubMed database using the keywords “schizophrenia” and

"suicide" indicates that scholarly publications on this topic have increased 3.5-fold over the past two decades. This growing attention is warranted, as suicide remains a leading cause of premature mortality in patients with mental disorders [7].

Retrospective studies reveal that schizophrenia is diagnosed in 8.8 to 15.4% of psychiatric patients hospitalized following a suicide attempt [8, 9]. In outpatient settings, however, the proportion of individuals with schizophrenia who have attempted suicide is significantly higher, reaching 55.6% [10, 11]. Key risk factors for this population include a family history of mental illness, suicide among relatives, feelings of loneliness, and alcohol abuse [11].

Currently, the primary focus of research lies in identifying various biological markers of suicide risk in schizophrenia [12–15]. However, despite significant progress in studying the genetic and neurobiological foundations of schizophrenia and suicidal behavior, as well as in investigating the clinical aspects of these conditions, a notable gap remains in the analysis of a patient biotype. The biotype encompasses parameters such as phenotypic traits, morphophenotypic characteristics, and constitutional type, which serves as a structural biomarker of body reactivity that remains largely stable throughout adulthood. In healthy individuals, it is linked to the functional state of organs and systems [16]. In individuals with various pathologies, reactivity influences the nature of the illness.

The most detailed and comprehensive research in this area has been conducted on schizophrenia. Based on the obtained data, N.A. Kornetov, in his works from 1989 and 2008, formulated an anthropological paradigm that revised previous notions about the role of constitutional predisposition to certain diseases [17, 18]. This paradigm demonstrated that constitutional features influence not so much the likelihood of developing a particular pathology, but rather its course and outcome. This approach has opened new prospects for forecasting the pathokinesis of diseases and developing more personalized treatment methods.

The aim of the study was to establish the relationship between the constitutional and morphological status of patients with schizophrenia and suicidal behavior.

MATERIALS AND METHODS

The study was carried out at two clinical sites: the Department of Endogenous Disorders at the Clinic of Mental Health Research Institute, Tomsk NRMC and Tomsk Clinical Psychiatric Hospital. The study sample comprised 215 patients (121 men (56.3%) and 94 women (43.7%)) with a verified diagnosis of schizophrenia (F20 in the ICD-10), confirmed through a clinical interview by an expert psychiatrist from the research team.

Inclusion criteria:

– diagnosis of schizophrenia according to ICD-10 criteria (F20);

– age between 18 and 50 years (inclusive);

– absence of congenital or acquired skeletal disorders;

– absence of organic disorders, including symptomatic mental disorders;

– absence of neurological diseases;

– absence of severe somatic-symptom disorders leading to organ or system failure (including conditions directly related to prior suicide attempts).

Exclusion criteria:

– dependence on psychoactive substances (with the exception of tobacco dependence, which is highly prevalent in this population in Russia [19]);

– use of clozapine within the six months prior to enrollment in the study, due to its demonstrated effect on reducing suicidal behavior [20].

Data on patient age, age of onset, duration of the mental disorder, and history of suicide attempts were collected from medical records and a structured clinical interview.

The severity of symptoms was assessed using the Positive and Negative Syndrome Scale (PANSS) [21]. As all participants were native Russian speakers, the Russian version of the Structured Clinical Interview for PANSS (SCI-PANSS), adapted for use in Russia by S.N. Mosolov [22], was applied. Suicide risk was evaluated using the Beck Hopelessness Inventory (BHI) [23], which demonstrates high sensitivity and specificity in assessing suicide risk in patients with schizophrenia [24, 25]. Consequently, we employed the original 20-item version of the scale [23]. Its Russian adaptation, originally developed by A.A. Gorbatkov [26], was derived from an earlier version [27] and was used in this study.

An anthropometric examination was performed by measuring height as well as transverse, biacromial,

and bicristal chest diameters using the modified V.P. Chtetsov method [28]. Measurements were taken using a medical stadiometer and a large sliding caliper. Constitutional and morphological types and somatic sexual differentiation were determined using the Rees – Eysenck index and Tanner index, respectively. Reference ranges for these indices were established based on data from a comparison group of 100 healthy volunteers, matched to the study group by sex and age. The cutoff values were defined as follows. The hypersthenic constitutional and morphological type had values < 95.1 in men and < 96.8 in women, mesosthenic – 95.1–105.7 in men and 96.8–110.8 in women, asthenic – > 105.7 in men and > 110.8 in women. For gynecomorphic somatic sexual differentiation, the values were < 87 in men and < 75 in women, for mesomorphic – 87–93.5 in men and 75–81 in women, for andromorphic – > 93.5 in men and > 81 in women.

Statistical data processing was performed using Statistica 12 (Copyright© StatSoft, Inc. 1984-2014) and the R 4.5.2 software packages. All obtained variables were presented in absolute (n) and relative (%) units. Frequency analysis was performed using the $\chi 2$ test. The Statnet R package was used for network analysis.

RESULTS

Of the entire patient sample, 70 individuals had suicide attempts (parasuicides), which constituted 32.6%. A comparative analysis of the frequencies of distribution of constitutional and morphological types between patients with and without a history of suicidal behavior is presented in Table 1.

Table 1

Comparison of the Distribution Frequencies of Constitutional and Morphological Types in Patient Subgroups, *n* (%)

Constitutional and morphological type	Patients with parasuicides	Patients without parasuicides	*p*
Asthenic	34 (48.6)	45 (31)	0.018**
Mesosthenic	29 (41.4)	74 (51)	0.239**
Hypersthenic	7 (10)	26 (18)	0.190**
Total	70 (100)	145 (100)	0.033*

Here and in Tables 2–4: * results of the $\chi 2$ test; ** results of the pairwise comparison.

The $\chi 2$ test revealed significant differences in the distribution frequencies of the main constitutional and morphological types between the patient groups ($p = 0.033$). The pairwise comparison revealed significant differences only in the frequency of the asthenic body type ($p = 0.018$).

Comparison of the di stribution of somatic sexual differentiation types between the subgroups (Table 2) did not reveal any significant differences ($p = 0.581$), nor did pairwise comparison of these parameters ($p > 0.05$).

Table 2

Comparison of the Distribution Frequencies of Different Types of Somatic Sexual Differentiation in Patient Subgroups, *n* (%)

Type of somatic sexual differentiation	Patients with parasuicides	Patients without parasuicides	*p*
Andromorphic	24 (34.3)	53 (36.6)	0.862**
Mesomorphic	25 (35.7)	58 (40)	0.648**
Gynecomorphic	21 (30)	34 (23.4)	0.387**
Total	70 (100)	145 (100)	0.581*

Hopelessness, i.e., the degree of a person's negative attitude toward their own future, is used as an indirect marker of a suicide risk. Therefore, the level of hopelessness in the study group of patients with schizophrenia was analyzed. Most patients reported mild (41.4%) or no (35.8%) hopelessness, while moderate (16.2%) and severe (6.6%) conditions were significantly less common. When comparing the frequencies of body type distribution among the patients depending on the presence and absence of hopelessness (Table 3), statistically significant differences were revealed ($p = 0.035$).

Table 3

Comparison of the Distribution Frequencies of Constitutional and Morphological Types between Patient Subgroups with and without Hopelessness, *n* (%)

Constitutional and morphological type	Hopelessness		*p*
	Presence	Absence	
Asthenic	58 (42)	21 (27,3)	0.045**
Mesosthenic	64 (46.4)	39 (50.6)	0.646**
Hypersthenic	16 (11.6)	17 (22.1)	0.064**
Total	138 (100)	77 (100)	0.035*

The pairwise comparison of the resulting groups revealed significant differences for the asthenic constitutional and morphological type ($p = 0.045$).

Similarly, the frequencies of the distribution of somatic sexual differentiation types in patients were compared based on the presence or absence of hopelessness. The comparison revealed no significant differences ($p > 0.05$) (Table 4).

Table 4

Comparison of the Distribution Frequencies of Somatic Sexual Differentiation Types Depending on the Presence and Absence of Hopelessness, *n* (%)

Type of somatic sexual differentiation	Hopelessness		*p*
	Presence	Absence	
Andromorphic	54 (39.1)	23 (29.9)	0.226**
Mesomorphic	48 (34.8)	35 (45.4)	0.163**
Gynecomorphic	36 (26.1)	19 (24.7)	0.948**
Total	138 (100)	77 (100)	0.261*

Next, a graph (network model) of suicide risk was constructed for the patients included in the study. Two groups of parameters (clinical and anthropometric) served as nodes in the network model. Statistically significant ($p > 0.05$) correlations identified served as edges (Figure).

The resulting network model contained 8 nodes and 11 undirected edges. The network analysis also allowed to identify two independent factors (clusters) of suicide risk in schizophrenia.

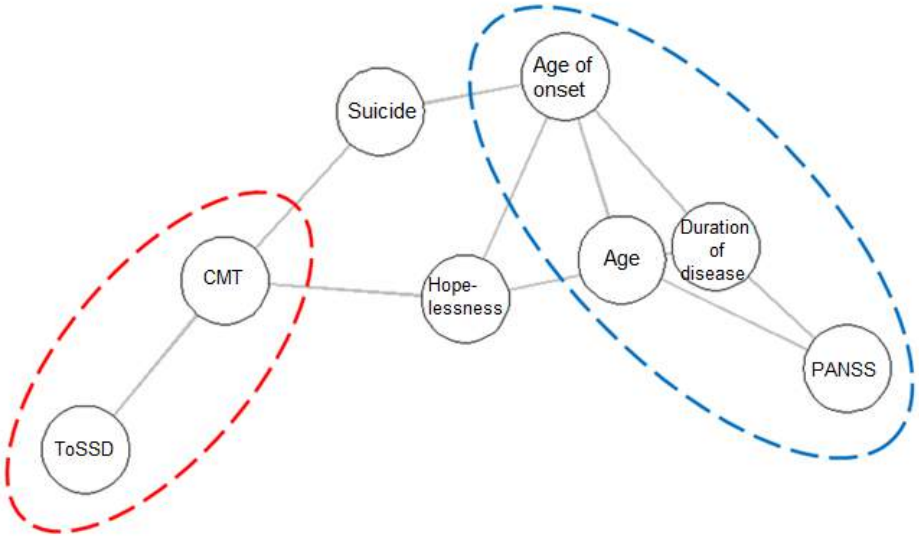

Figure. Network model of a suicide risk in schizophrenia. CMT – constitutional and morphological type; ToSSD – type of somatic sexual differentiation.

DISCUSSION

The incidence of documented suicide attempts in the studied sample of patients with schizophrenia was 32.6%. This rate aligns with findings from a number of other studies [3–6] and reflects the average trend observed in this patient population. The high frequency of suicide attempts among individuals with schizophrenia represents a serious challenge, necessitating a comprehensive approach to treatment and rehabilitation. It is crucial to address not only the management of psychotic symptoms but also the treatment of comorbid conditions, such as depression, anxiety, and substance use disorders, as these can significantly elevate suicide risk [11].

In addition to retrospective data, the study included an observational component in a cross-sectional design. Hopelessness was analyzed as a potential risk factor for suicidal behavior, revealing relatively high prevalence among patients with schizophrenia: 64.2% of patients exhibited varying degrees of hopelessness. Hopelessness, as a hallmark of depressive symptom severity, significantly impacts a patient's understanding of mental illness, its consequences, and recognition of a need for treatment and adherence to medical recommendations [26, 29].

Previously, our research group has presented data on somatomorphological predictors of negative symptom development in schizophrenia [30, 31], as well as on the adverse effects of antipsychotic therapy [32, 33]. However, the role of anthropometric characteristics in suicidal behavior has remained unclear. The significant overrepresentation of the asthenic constitutional and morphological type identified in the present study (both among patients with parasuicide and those with high hopelessness values) raises the question of whether constitutional and morphological predisposition to suicidal behavior in schizophrenia should be delineated.

Given two key dimensions of suicidal behavior (a history of parasuicide and current hopelessness), we performed a network analysis to model suicide risk in schizophrenia. The resulting network delineated two distinct and independent clusters central to shaping

this risk. The first cluster encompasses clinical characteristics related to disease development, progression, and the severity of psychopathological symptoms. The second, anthropometric cluster is defined by constitutional physical parameters that may predispose individuals to suicidal ideations. This integrative approach allows for a comprehensive assessment of inter-variable relationships and facilitates the development of more targeted strategies for suicide risk prevention at early stages of schizophrenia.

CONCLUSION

The study results confirm the significance of the constitutional status as an independent risk factor for suicidal behavior in patients with schizophrenia. These findings offer potential for early identification of suicidal ideations in this patient group, which could, in turn, significantly reduce the adverse outcomes of schizophrenia and facilitate the development of tailored approaches to psychological counseling, psychotherapy, and rehabilitation.

REFERENCES

1. Lovero K.L., Dos Santos P.F., Come A.X., Wainberg M.L., Oquendo M.A. Suicide in global mental health. *Curr. Psychiatry Rep*. 2023;25(6):255–262. DOI: 10.1007/s11920-023-01423-x.
2. Bachmann S. Epidemiology of suicide and the psychiatric perspective. *Int. J. Environ. Res. Public Health.* 2018;15(7):1425. DOI: 10.3390/ijerph15071425.
3. Sutar R., Kumar A., Yadav V. Suicide and prevalence of mental disorders: A systematic review and meta-analysis of world data on case-control psychological autopsy studies. *Psychiatry Res.* 2023;329:115492. DOI: 10.1016/j.psychres.2023.115492.
4. Kim H., Jung J.H., Han K., Jeon H.J. Risk of suicide and all-cause death in patients with mental disorders: a nationwide cohort study. *Mol. Psychiatry.* 2025;30(7):2831–2839. DOI: 10.1038/s41380-025-02887-4.
5. Cassidy R.M., Yang F., Kapczinski F., Passos I.C. Risk Factors for Suicidality in Patients With Schizophrenia: A Systematic Review, Meta-analysis, and Meta-regression of 96 Studies. *Schizophr. Bull.* 2018;44(4):787–797. DOI: 10.1093/schbul/sbx131.
6. Berardelli I., Rogante E., Sarubbi S., Erbuto D., Lester D., Pompili M. The importance of suicide risk formulation in schizophrenia. *Front. Psychiatry*. 2021;12:779684. DOI: 10.3389/fpsyt.2021.779684.
7. Song I.A., Park H.Y., Oh T.K. Suicide Risk in Individuals With Psychiatric Disorder: Population-Based Cohort Study. *Psychiatry Investig*. 2025;22(12):1422–1429. DOI: 10.30773/pi.2025.0195.
8. Mekhtiev E.S., Abbasova S.E., Kasimov O.G., Dnov K.V. Clinical Characteristics of People of Different Nationalities Who Have Committed Suicide Attempts and Were Hospitalized in Psychiatric Hospital. *Bulletin of the Russian Military Medical Academy*. 2018;63(3):114–118. (In Russ.).
9. De Leo D., Klieve H. Communication of suicide intent by schizophrenic subjects: data from the Queensland Suicide Register. *Int. J. Ment. Health Syst*. 2007;1(1):6. DOI: 10.1186/1752-4458-1-6.
10. Deisenhammer E.A., Behrndt-Bauer E.M., Kemmler G., Haring C., Miller C. Suicide in Psychiatric Inpatients – A Case-Control Study. *Front. Psychiatry*. 2020;11:591460. DOI: 10.3389/fpsyt.2020.591460.
11. Ivanov O.V. Comparative Characteristics of the Main Socio-demographic Indicators in Mentally Suicidal Patients. *The Eurasian Union of Scientists*. 2015;19(10-1):27–32. (In Russ.).
12. Kibitov A.O., Shumskaya D.S. Modern Genome-wide Association Studies of Mental Disorders: Focus on the Mechanisms of Inflammation. *Siberian Bulletin of Psychiatry and Narcology.* 2024;125(4):56–65. (In Russ.). DOI: 10.26617/1810-3111-2024-4(125)-56-65.
13. Garcia Fernandez A., Martínez-Cao C., Couce-Sánchez M., González-Blanco L., Sáiz P., García-Portilla P. Relation between biomarkers and suicide attempts in patients with schizophrenia. *Eur. Psychiatry*. 2024;67(Suppl. 1):S125. DOI: 10.1192/j.eurpsy.2024.293.
14. Zakharova N.V., Bravve L.V., Mamedova G.S., Kaydan M.A., Ershova E.S., Martynov A.V. et al. Telomere length as a marker of suicidal risk in schizophrenia. *Consortium Psychiatricum*. 2022;3(2):37–47. DOI: 10.17816/CP171.
15. Dickerson F., Adamos M., Katsafanas E., Khushalani S., Origoni A., Savage C. et al. The association between immune markers and recent suicide attempts in patients with serious mental illness: A pilot study. *Psychiatry Res*. 2017;255:8–12. DOI: 10.1016/j.psychres.2017.05.005
16. Garganeeva N.P., Taminova I.F., Kalyuzhin V.V., Kalyuzhina E.V., Smirnova I.N., Sarycheva T.V. Anthropometric Features and Functional State of the Cardiovascular System in Qualified Athletes of Various Sports. *Russian Journal of Cardiology.* 2023;28(11):5538. (In Russ.). DOI: 10.15829/1560-4071-2023-5538.
17. Kornetov N.A. Study of Somatic Sexual Maturation Based on Various Anthropometric Indicators. *S.S. Korsakov Journal of Neurology and Psychiatry.* 1989;89(5):97–102. (In Russ.).
18. Kornetov N.A. The Concept of Clinical Anthropology in Medicine. *Bulletin of Siberian Medicine.* 2008;7(1):7–31. (In Russ.). DOI: 10.20538/1682-0363-2008-1-7-31.
19. Svetlichnaya T.G., Voronov V.A., Smirnova E.A. Patterns of Smoking and Alcoholic Addiction in Inpatients with Schizophrenia: Medical and Sociological Study. *Psychiatry*. 2020;18(4):51–62. (In Russ.). DOI: 10.30629/2618-6667-2020-18-4-51-62
20. Khokhar J.Y., Henricks A.M., Sullivan E.D.K., Green A.I. Unique effects of clozapine: a pharmacological perspective. *Adv. Pharmacol*. 2018;82:137–162. DOI: 10.1016/bs.apha.2017.09.009.
21. Kay S.R., Fiszbein A., Opler L.A. The positive and negative syndrome scale (PANSS) for schizophrenia. *Schizophr. Bull*. 1987;13(2):261–276. DOI: 10.1093/schbul/13.2.261.

22. Mosolov S.N. Psychometric Assessment Scales for Schizophrenia Symptoms and the Concept of Positive and Negative Disorders. Moscow: Novyj tsvet, 2001:238. (In Russ.).
23. Beck A.T., Weissman A., Lester D., Trexler L. The measurement of pessimism: the hopelessness scale. *J. Consult. Clin. Psychol*. 1974;42(6):861–865. DOI: 10.1037/h0037562.
24. Aloba O., Esan O., Alimi T. Adaptation of the Beck Hopelessness Scale as a suicide risk screening tool among Nigerian patients with schizophrenia. *Int. J. Psychiatry Clin. Pract*. 2018;22(1):19–24. DOI: 10.1080/13651501.2017.1356928
25. Rueda-Jaimes G.E., Castro-Rueda V.A., Rangel-Martínez-Villalba A.M., Moreno-Quijano C., Martinez-Salazar G.A., Camacho P.A. Validation of the Beck Hopelessness Scale in patients with suicide risk. *Rev. Psiquiatr. Salud. Ment. (Engl. Ed.).* 2018;11(2):86–93. DOI: 10.1016/j.rpsm.2016.09.004.
26. Gorbatkow A.A. Beck Hopelessness Scale: Dimensional Structure and Its Determinants. *Russian Psychological Journal*. 2007;4(2):26–34. (In Russ.).
27. Czapiński J. Psychologia szczęścia. Przegląd badań i zarys teorii cebulowej. Warszawa: Akademos, 1992:38. (In Pol.).
28. Chtetsov V.P., Negasheva M.A., Lapshina N.E. The Study of Body Composition in the Adult Population: Methodological Aspects. *Bulletin of the Moscow University. Episode 23: Anthropology.* 2012;(2):43–52. (In Russ.).
29. Han H., Midorikawa A. Depression accompanied by hopelessness is associated with more negative future thinking. *Healthcare (Basel).* 2024;12(12):1208. DOI: 10.3390/healthcare12121208.
30. Kornetova E.G., Galkin S.A., Kornetov A.N., Petkun D.A., Kazennykh T.V., Bokhan N.A. The Influence of Constitutional and Morphological Features of Patients with Schizophrenia on the Severity of Neurocognitive Deficit. *Social and Clinical Psychiatry.* 2024;34(1):26–34. (In Russ.).
31. Mikilev F.F., Kornetova E.G., Lobacheva O.A., Kornetov A.N., Semke A.V. Psychometric Evaluation of Symptoms and Clinical Dynamics of Schizophrenia Depending on Constitutional and Morphological Type of the Patients. *Bulletin of Siberian Medicine.* 2016;15(2):58–64. (In Russ.). DOI: 10.20538/1682-0363-2016-2-58-64.
32. Goncharova A.A., Kornetova E.G., Kornetov A.N., Semke A.V. Is there Constitutional and Morphological Predisposition to Akathisia in Schizophrenic Patients Receiving Antipsychotic Therapy? *Bulletin of Siberian Medicine.* 2019;18(4):36–43. (In Russ.). DOI: 10.20538/1682-0363-2019-4-36-43.
33. Galkin S.A., Kornetova E.G., Mednova I.A., Tiguntsev V.V., Kornetov A.N. Prevalence and Risk Factors of QT Prolongation Syndrome in Patients with Schizophrenia while Taking Antipsychotics. *Modern Therapy of Mental Disorders.* 2024;(2):32–39. (In Russ.). DOI: 10.21265/PSYPH.2024.31.31.004

Author Contribution

Kornetov A.N. – conception and design, editing of the manuscript. Galkin S.A. – data analysis and initial drafting of the manuscript. Mednova I.A. – anthropometric examination and database management. Petkun D.A. – clinical, psychopathological and psychometric examination and database management. Kornetova E.G. – critical revision of the manuscript for important intellectual content, final approval of the manuscript for publication.

Author Information

Kornetov Alexander N. – Dr. Sci. (Med.), Leading Researcher, Department of Affective States, Mental Health Research Institute, Tomsk NRMC of RAS, Tomsk, alkornetov@gmail.com, http://orcid.org/0000–0002–2342–7504

Galkin Stanislav A. – Cand. Sci. (Med.), Senior Researcher, Department of Addictive Disorders, Mental Health Research Institute, Tomsk NRMC of RAS, Tomsk, s01091994@yandex.ru, http://orcid.org/0000–0002–7709–3917

Mednova Irina A. – Cand. Sci. (Med.), Researcher, Mental Health Research Institute, Tomsk NRMC of RAS, Tomsk, irinka145@yandex.ru, http://orcid.org/0000-0002-8057-3305

Petkun Dmitry A. – Psychiatrist, Researcher, Department of Endogenous Disorders, Mental Health Research Institute, Tomsk NRMC of RAS, Tomsk, substantia_p@mail.ru, http://orcid.org/0009-0008-1878-5084

Kornetova Elena G. – Dr. Sci. (Med.), Head of the Department of Endogenous Disorders, Mental Health Research Institute, Tomsk NRMC of RAS, Tomsk, ekornetova@outlook.com, http://orcid.org/0000–0002–5179–9727

(✉) **Kornetov Alexander N.,** alkornetov@gmail.com

Received on December 30, 2025;
approved after peer review on January 14, 2026;
accepted on January 22, 2026

УДК 616.716.4-08:611.018.4:615.382]-092.9
https://doi.org/10.20538/1682-0363-2026-2-65-72

Content of Bone Morphogenetic Proteins in Blood Plasma of Rats with Metabolic Syndrome during Mandibular Defect Restoration

Makarova M.V.[1], Tsygan V.N.[2], Lyashev Yu.D.[1], Brusentsova A.Ye.[1]

[1]Kursk State Medical University (KSMU)
3 Karl Marx St., 305041 Kursk, Russian Federation

[2]Kirov Military Medical Academy
6G Academician Lebedev St., 194044 Saint-Petersburg, Russian Federation

ABSTRACT

The aim was to study the concentration of bone morphogenetic proteins-2 (BMP) and -7 in the blood plasma of rats with metabolic syndrome during reparative osteogenesis in mandibular defect.

Materials and methods. The experiments were carried out on male Wistar rats, which were divided into 4 groups: 1) native; 2) control (with mandibular defect); 3) metabolic syndrome; 4) experimental (with metabolic syndrome and mandibular defect). Metabolic syndrome was simulated by replacing standard feed with a high-fat and high-carbohydrate diet. The development of metabolic syndrome was confirmed by changes in body weight, glucose and triacylglycerides concentrations in blood plasma. The mandibular defect was formed in rats according to the method proposed by Grigoryan et al. The content of BMP-2 and BMP-7 in blood plasma was determined by the enzyme-linked immunoassay on days 7, 14, 21, and 28 after the surgery. We calculated the median and the interquartile range *Me* [Q_1; Q_3] and applied the Mann – Whitney *U*-test and the Bonferroni correction. Differences in indicators were considered to be significant at $p < 0.025$.

Results. A significant increase in the content of the studied proteins in the blood plasma was determined in the group metabolic syndrome compared to the naïve group. BMP-2 and BMP-7 concentration in rats of the control group was higher throughout the experiment compared to the naïve group ($p < 0.025$). In the experimental group, a decrease in the concentration of BMP-2 (on days 7, 14, and 28) and BMP-7 (on days 7–28) was found compared to the control group ($p < 0.025$). An increase in the concentration of BMP-2 and BMP-7 was detected in the experimental group compared to the metabolic syndrome group ($p < 0.025$) on day 7 and on days 7–14, respectively.

Conclusion. A significant decrease in BMP-2 and BMP-7 concentration in the blood plasma was found in rats with metabolic syndrome during mandibular reparative osteogenesis compared to animals without metabolic disorders.

Keywords: metabolic syndrome, mandibular defect, reparative osteogenesis, bone morphogenetic proteins

Conflict of interest. The authors declare the absence of obvious or potential conflicts of interest related to the publication of this article.

Source of financing. The authors state that they received no funding for the study.

Conformity with the principles of ethics. The study was approved by the Regional Ethics Committee of KSMU (Minutes No. 4 of December 15, 2022).

For citation: Makarova M.V., Tsygan V.N., Lyashev Yu.D., Brusentsova A.Ye. Content of Bone Morphogenetic Proteins in Blood Plasma of Rats with Metabolic Syndrome during Mandibular Defect Restoration. *Bulletin of Siberian Medicine.* 2026;25(2):65–72. https://doi.org/10.20538/1682-0363-2026-2-65-72.

✉ *Makarova Marina V.,* marina-golovina@inbox.ru

Содержание костных морфогенетических белков в плазме крови крыс с метаболическим синдромом при восстановлении дефекта нижней челюсти

Макарова М.В.[1], Цыган В.Н.[2], Ляшев Ю.Д.[1], Брусенцова А.Е.[1]

[1] *Курский государственный медицинский университет (КГМУ)*
Россия, 305041, г. Курск, ул. Карла Маркса, 3

[2] *Военно-медицинская академия (ВМА) им. С.М. Кирова*
Россия, 194044, г. Санкт-Петербург, ул. Академика Лебедева, 6Ж

РЕЗЮМЕ

Цель – изучение концентрации костных морфогенетических белков (КМБ) 2 и 7 в плазме крови крыс с метаболическим синдромом в процессе репаративного остеогенеза при дефекте нижней челюсти.

Материалы и методы. Работа выполнена на самцах крыс линии Вистар, из которых сформировали четыре группы: 1) интактная; 2) контрольная – дефект нижней челюсти; 3) метаболический синдром; 4) опытная – метаболический синдром и дефект нижней челюсти. Метаболический синдром моделировали заменой стандартного корма высокожировой и высокоуглеводной диетой. О наличии метаболического синдрома судили по изменениям массы тела, концентрации глюкозы и триацилглицеридов в плазме крови. Дефект нижней челюсти формировали по методу А.С. Григорьяна и соавт. На 7-, 14-, 21- и 28-е сут после операции в плазме крови определяли содержание КМБ-2 и -7 методом иммуноферментного анализа. Рассчитывали медиану и интерквартильный размах Me [Q_1; Q_3], использовали U-критерий Манна – Уитни и поправку Бонферрони. Различия показателей считали значимыми при $p < 0{,}025$.

Результаты. В группе «метаболический синдром» установлено увеличение в плазме содержания исследуемых белков по сравнению с интактной группой. Концентрация КМБ-2 и КМБ-7 у крыс контрольной группы был выше на всем протяжении эксперимента по сравнению с интактной группой ($p < 0{,}025$). В опытной группе установлено снижение концентрации КМБ-2 (на 7-, 14- и 28-е сут) и КМБ-7 (на 7–28 сут) по сравнению с контрольной группой ($p < 0{,}025$). Показано увеличение содержания КМБ-2 на 7-е сут, а КМБ-7 на 7–14 сут в опытной группе по сравнению с группой «метаболический синдром» ($p < 0{,}025$).

Заключение. У крыс с метаболическим синдромом установлено значимое снижение концентрации в плазме крови КМБ-2 и КМБ -7 при заживлении дефекта нижней челюсти по сравнению с животными без метаболических нарушений.

Ключевые слова: метаболический синдром, дефект нижней челюсти, репаративный остеогенез, костные морфогенетические белки

Конфликт интересов. Авторы декларируют отсутствие явных и потенциальных конфликтов интересов, связанных с публикацией настоящей статьи.

Источник финансирования. Авторы заявляют об отсутствии финансирования при проведении исследования.

Соответствие принципам этики. Исследование одобрено региональным этическим комитетом КГМУ (протокол № 4 от 15.12.2022).

Для цитирования: Макарова М.В., Цыган В.Н., Ляшев Ю.Д., Брусенцова А.Е. Содержание костных морфогенетических белков в плазме крови крыс с метаболическим синдромом при восстановлении дефекта нижней челюсти. *Бюллетень сибирской медицины.* 2026;25(2):65–72. https://doi.org/10.20538/1682-0363-2026-2-65-72.

INTRODUCTION

Bone morphogenetic proteins (BMPs) belong to the transforming growth factor β superfamily, with BMP-1 being the exception [1]. Currently, more than 20 types of BMPs have been identified, which play a key role in the processes of morphogenesis, cell differentiation, apoptosis, and tissue repair [2]. BMPs are synthesized by osteopregenitor cells, osteoblasts, chondrocytes, platelets, and endothelial cells in various tissues [3]. BMPs stimulate different stages of bone tissue development and the restoration of its integrity after damage [3]. BMPs-2, -4, -5, -6, -7, and -9 exhibit high osteogenic activity, interacting with two types of receptors [2]. The main pathways for the implementation of BMP regulatory effects are Smad-dependent, RUNX2, MKK-ERK1/2, and MKK-ERK1/2 [2]. It is generally accepted that BMP-2 and BMP-7 are the most active stimulators of osteogenic differentiation of mesenchymal stem cells in *in vitro* and *in vivo* models [4]. The transcription factors Runx2 and Dlx5 control the enhancement of osteoblast formation from mesenchymal stem cells [3].

Metabolic disorders alter the production of osteogenesis inducers, which stimulate the restoration of bone integrity following damage [5]. Studies have demonstrated increased activity of the osteopontin and osteoprotegerin genes in experimental type 2 diabetes mellitus in rats [6] and resistance to erythropoietin, which activates osteogenesis [7] in patients with metabolic syndrome (MS) on hemodialysis [8]. Decreased production of BMP-6 by bone callus cells has been observed in rats with streptozotocin-induced type 1 diabetes mellitus [9].

Recently, an alteration of the reparative osteogenesis process in the mandibular defects in MS rats has been demonstrated, manifested by a slowdown in the formation of new bone tissue and its remodeling [10]. However, there are no literature data on the MS effect on BMP production. Therefore, an analysis of BMP levels in MS rats during bone integrity restoration is of interest.

The aim was to study BMP-2 and BMP-7 concentration in the blood plasma of MS rats during reparative osteogenesis in the mandibular defects.

MATERIALS AND METHODS

The experiments were performed on 81 male Wistar rats weighing 200–230 g from the Stolbovaya branch of the Scientific Center for Biomedical Technologies of the Federal Medical and Biological Agency. The experiments were conducted in the preclinical drug research laboratory of the Research Institute of Experimental Medicine of Kursk State Medical University (KSMU), adhering to ethical principles for the handling of laboratory animals [11, 12]. The study was conducted in compliance with the European Convention for the Protection of Vertebrate Animals used for Experimental and Other Scientific Purposes (CETS No. 123, as amended by ETS No. 170), GOST R 33647-2015 "Principles of Good Laboratory Practice (GLP), Terms and Definitions (as amended)" (Order of the Ministry of Health of the Russian Federation No. 199n of April 1, 2016), and GOST R 33216-2014 "Guidelines for the Care and Housing of Laboratory Animals. Rules for the Care and Housing of Laboratory Rodents and Rabbits (Reissue)".

The experimental protocol for this dissertation research was approved by the Regional Ethics Committee of KSMU (Minutes No. 4 of the Preclinical Research Section meeting of December 15, 2022).

Four groups of experimental animals were formed: 1) naïve – without the mandibular defect and metabolic syndrome ($n = 6$); 2) control – the simulation of the mandibular defect ($n = 33$); 3) metabolic syndrome – metabolic syndrome simulation ($n = 5$); 4) experimental – the simulation of metabolic syndrome and the mandibular defect ($n = 37$).

MS was simulated in the rats of groups 3 and 4 by replacing the standard feed with a high-fat, high-carbohydrate diet (HFHCD) consisting of a mixture of standard feed (65.75%) with the addition of animal fat (lard 17%), fructose (17%), cholesterol (0.25%) and drinking water with a 20% fructose solution (total caloric content 4,400 kcal/kg, 54% of energy from fat) for 12 weeks *ad libitum* at the first stage of the experiment (weeks 1–12) [13, 14]. Rats of the naïve and control groups (groups 1 and 2) received standard dry granulated feed complying with GOST 34566-2019 "Complete Compound Feeds for Laboratory Animals", as well as water *ad libitum* for 12 weeks. MS development was assessed by changes in body weight, concentration of glucose and triacylglycerides (TAG) in blood plasma, which were measured using standard kits (Vector-Best, Russia) "Glucose GOD" (cat. No. B-8056) and "Triglycerides" (cat. No. B-8322) on a BA-400 biochemical automatic analyzer (BioSystems, Spain)

in animals consuming HFHCD (groups 3 and 4), and compared to the rats of groups 1 and 2.

The mandibular defect was simulated in 37 rats of the experimental group (after 12 weeks of HFHCD administration) and 33 animals of the control group using the method developed by A.S. Grigoryan et al. at the second stage of experiment (13–16 weeks) [15]. A 3-mm-diameter perforation hole was formed with a portable drill in the body of the right lower jaw in the molar area (with cooling with normal saline) using chloralhydrate narcosis (at a dose of 400 mg/kg). Rats of groups 2 and 4 were administered ceftriaxone intramuscularly at a dose of 100 mg/kg of body weight once a day for 2 days to prevent complications. The operated rats of the fourth group consumed HFHCD until the withdrawal from the experiment. Three rats from the experimental group and one animal from the control group died after the surgery. Animals of groups 2 and 4 with the mandibular defects were sacrificed on day 7, 14, 21, and 28 after surgery by chloral hydrate overdose. Two rats of group 4 (experimental group) were revealed to have muscle tissue interposition in the area of the mandibular defect and were excluded from further experiment. Animals of groups 1 and 3 were sacrificed by chloral hydrate overdose on day 85 (12 weeks + 1 day) after the experiment beginning.

The levels of BMP-2 (catalog number SEA013Ra) and BMP-7 (catalog number SEA799Ra) in the blood plasma were determined by enzyme-linked immunosorbent assay (ELISA) using standard kits from Cloud-Clone Corp. (China) on a Lazurit automated ELISA analyzer (Dynex Technologies, USA) according to the included instructions in the animals of all groups.

Distribution normality was assessed using the Shapiro – Wilk test, and variance homogeneity was assessed using Levene's test for statistical analysis of the results. The data are presented as the median and interquartile range Me [Q_1; Q_3]. Statistical hypotheses were tested by pairwise comparison using the nonparametric Mann – Whitney U-test to detect statistically significant differences between groups and the Bonferroni correction to address the problem of multiple comparisons. Parameter differences were considered to be significant at $p < 0.025$. The use of nonparametric statistics was due to the small sample size, different distribution patterns in the variation series, and unequal variances in comparing groups. Statistical processing was performed using Statistica version 13 software.

RESULTS

Increased body weight, plasma glucose, and TAG levels were detected in Wistar rats of the experimental and MS groups compared to animals of the naïve and control groups ($p < 0.025$), which confirms MS development in the rats that received HFHCD for 12 weeks (Table 1).

Table 1

Dynamics of Body Weight, Glucose and Triacylglycerides Concentrations in Blood Plasma of Rats with and without Metabolic Syndrome, Me [Q_1; Q_3]

Group	Body weight, g		Glucose concentration, mmol/l		Triacylglyceride concentration, mmol/l	
	At the beginning of the experiment	At the end of the experiment (12 weeks after)	At the beginning of the experiment	At the end of the experiment (12 weeks after)	At the beginning of the experiment	At the end of the experiment (12 weeks after)
Naïve (n = 6)	215.0 [210.0; 225.0]	400.0 [385.0; 415.0]	3.7 [3.6; 3.8]	3.8 [3.6; 3.9	1.8 [1.8; 1.9]	1.9 [1.8; 1.9]
Control (n = 33)	220.0 [210.0; 225.0], ^{x}p = 0.3698	420.0 [390.0; 435.0], ^{x}p = 0.3115	3.8 [3.7; 3.9], ^{x}p = 0.3023	3.8 [3.7; 3.9], ^{x}p = 0.2844	1.7 [1.6; 1.8], ^{x}p = 0.2540	1.8 [1.7; 1.9], ^{x}p = 0.3023
Metabolic syndrome (n = 5)	215.0 [210.0; 220.0], ^{x}p = 1.00, $^{*}p$ = 0.6502	470.0 [460.0; 480.0] ^{x}*, ^{x}p = 0.0081, $^{*}p$ = 0.0004	3.8 [3.7; 3.9], ^{x}p = 0.6481, $^{*}p$ = 0.6043	5.8 [5.6; 5.9]^{x}*, ^{x}p = 0.0081, $^{*}p$ = 0.0004	1.8 [1.7; 1.8], ^{x}p = 0.3613 $^{*}p$ = 0.2900	3.9 [3.9; 4.1]^{x}*, ^{x}p = 0.0081, $^{*}p$ = 0.0004
Experimental (n = 37)	215.0 [210.0; 220.0], ^{x}p = 0.9163, ^{y}p = 0.8007, $^{*}p$ = 0.4791	485.0 [460.0; 510.0] ^{x}*, ^{x}p = 0.0002, ^{y}p = 0.3822, $^{*}p$ = 0.0001	3.8 [3.7; 3.9], ^{x}p = 0.2620 ^{y}p = 0.7413, $^{*}p$ = 0.8612	5.8 [5.6; 5.9]^{x}*, ^{x}p = 0.0001 ^{y}p = 0.7267, $^{*}p$ = 0.0001	1.8 [1.7; 1.8], ^{x}p = 0.1458, ^{y}p = 0.7857, $^{*}p$ = 0.4240	3.8 [3.7; 3.9]^{x*}, ^{x}p = 0.0001, ^{y}p = 0.1620, $^{*}p$ = 0.0001

$^{x}p < 0.025$ compared to the naïve group; $^{y}p < 0.025$ compared to the metabolic syndrome group; * $p < 0.025$ compared to control group.

MS simulation was accompanied by a significant increase in plasma BMP-2 and BMP-7 levels compared to the naïve group ($p = 0.0081$) (Table 2).

An increase in BMP-2 concentrations was detected in the rats of the control group compared to the naïve animals on day 7 of the experiment ($p = 0.0024$). The levels of both BMPs in this group decreased compared to day 7 ($p = 0.0009$) fourteen days after the simulation of the mandibular defect; however, both values were higher than in the rats of the naïve group ($p = 0.0024$).

A decrease in the concentration of the studied BMPs in rats of the control group was also observed on day 21 compared to the previous period of the experiment, but the content of BMP-2 and BMP-7 three weeks after the simulation of the mandibular defect was significantly higher than in the naïve group ($p = 0.0024$). The content of both BMPs in rats of the control group remained virtually unchanged on day 28 after the mandibular surgery compared to that on day 21, and it was significantly higher than in rats of the naïve group ($p = 0.0024$).

Table 2

Results of Measuring BMP-2 and BMP-7 Concentration in the Blood Plasma of the Rats of the Naïve Group, the Metabolic Syndrome Group, the Control Group (Mandibular Surgery), and the Experimental Group (Metabolic Syndrome + Mandibular Surgery), *Me* [Q_1; Q_3]

Group	Experiment period	BMP-2 concentration in blood plasma, pg/ml	BMP-7 concentration in blood plasma, pg/ml
Naïve ($n = 6$)		46.0 [45.0; 48.0]	43.5 [43.0; 45.0]
Metabolic syndrome ($n = 5$)		50.0 [49.0; 50.0]^x, $p = 0.0081$	49.0 [47.0; 49.0]^x, $p = 0.0081$
Control ($n = 8$)	day 7	182.0 [125.5; 257.5]^x, $p = 0.0024$	88.5 [76.5; 107.0]^x, $p = 0.0024$
	day 14	64.0 [62.0; 68.5]^{xz}, $^x p = 0.0024$, $^z p = 0.0009$	68.5 [65.5; 72.0]^{xz}, $^x p = 0.0024$, $^z p = 0.0009$
	day 21	51.5 [50.0; 57.0]^{xz}, $^x p = 0.0024$, $^z p = 0.0009$	57.0 [53.0; 60.5]^{xz}, $^x p = 0.0024$, $^z p = 0.0016$
	day 28	52.0 [51.5; 52.0]^x, $p = 0.0024$	55.0 [51.0; 56.5]^x, $p = 0.0024$
Experimental ($n = 8$)	day 7	84.0 [82.0; 92.0]^y*, $^y p = 0.0043$, $*p = 0.0009$	66.5 [61.0; 67.5]^y*, $^y p = 0.0043$, $*p = 0.0009$
	day 14	50.5 [50.0; 55.5]*, $*p = 0.0009$	54.0 [51.0; 55,5]^y*, $^y p = 0.0068$, $*p = 0.0009$
	day 21	51.5 [50.5; 53.5]	49.0 [49.0; 51.0]*, $*p = 0.0039$
	day 28	48.0 [47.0; 48.5]*, $*p = 0.0019$	49.5 [49.0; 51.0]*, $*p = 0.0209$

$^x p < 0.025$ compared to the naïve group; $^y p < 0.025$ compared to the metabolic syndrome group; * $p < 0.025$ compared to the control group; $^z p < 0.025$ compared to the previous experiment period in the group

The content of both BMPs on day 7 of the experiment was significantly higher in rats of the experimental group (MS + mandibular surgery) than in animals of the metabolic syndrome group ($p = 0.0043$). BMP-7 concentration alone was higher compared to the MS group ($p = 0.0068$) on day 14 after the mandibular defect simulation. BMP-2 and BMP-7 concentrations did not differ significantly from the same indices in the MS group on days 21–28 ($p > 0.05$).

It was established that the BMP-2 content was significantly lower in the rats of the experimental group on day 7 ($p = 0.0009$), day 14 ($p = 0.0009$), and day 28 of the experiment ($p = 0.0019$) compared to the control groups. A decrease in the BMP-7 concentration in animals of the experimental group was revealed at all stages of the experiment ($p = 0.0009$–0.0029) compared to the control group.

Thus, the study allowed to establish an increase in the concentration of BMP-2 and BMP-7 in the MS simulation in rats, as well as a decrease in the BMP content in the process of reparative osteogenesis in the case of the mandibular defect in animals with MS compared to the group without metabolic disorders.

DISCUSSION

The study demonstrated that the MS development is accompanied by increased BMP-2 and -7 plasma levels. This was likely due to the development of metainflammation in MS – a chronic, low-grade inflammation of adipose tissue manifested by increased plasma levels of proinflammatory interleukins (ILs): IL-1, IL-6, and TNFα – in both patients and rats with experimental MS [16, 17]. Proinflammatory ILs stimulate the BMP-producing cells activity, particularly platelets and endothelial cells [18].

An increase in the BMP-2 and BMP-7 content in the blood plasma during reparative osteogenesis in the rats of the control (throughout the experiment) and experimental (BMP-2 alone on day 7, BMP-7 on days 7–14) groups. However, this increase was less

pronounced at almost all stages of the experiment in MS animals. In our opinion, this is explained by the depletion of BMP reserves due to the metainflammation development in the osteopregenitor cells, platelets, and endothelial cells during reparative osteogenesis, as well as a decrease in the osteoblast number in the area of the mandibular defect in MS rats, as shown in our previous study [10].

Literature data on the effect of carbohydrate metabolism disorders on the BMP-2 content are contradictory. Simulation of streptozotocin-induced type 1 diabetes mellitus in Sprague-Dawley rats was accompanied by a decrease in the expression of BMP-2 mRNA in the tissue of the upper jaw [19]. In contrast, an increase in the expression of BMP-2 mRNA, BMP-7, and the type II BMP receptor in the aorta was revealed in mice with experimental type 1 diabetes mellitus [20]. The authors explain this effect by an increase in endothelin activity, which has a regulatory effect on BMP production. Enhanced BMP production by endothelial cells, which was previously shown in a study of BMP-4 secretion [21], may be one of the mechanisms explaining the increase in the blood plasma levels of BMP-2 and BMP-7 in experimental animals, as established in our study.

BMP-2 and BMP-7 play a key role in the osteoinductive process and have a stimulating effect on the osteogenic differentiation of mesenchymal stem cells (MSCs) [22]. It has been established that one of the biologically active substances stimulating the production of BMP-2 during reparative osteogenesis is fibroblast growth factor-21 (FGF-21). The study has shown an increase in BMP-dependent protein transcription, alkaline phosphatase activity, and bone matrix mineralization under the influence of FGF-21, which is associated with the Smad activation, but not with that of p44/42MAPK proteins [23]. The combined administration of FGF-21 and BMP-2 in a hydrogel has a stimulating effect on the osteogenic differentiation of mesenchymal stromal cells and vascular growth in newly formed bone [24].

It has previously been shown that high BMP concentrations promote the differentiation of MSCs into osteogenic cells, while low concentrations activate the formation of adipocytes from MSCs [3]. A significant increase in BMP-2 and -7 levels increase in the control group was observed on day 7 after the mandibular defect simulation, while these values were significantly lower in the rats of the experimental group. These data suggest that the slowdown in the development of newly formed bone tissue in MS rats, which we demonstrated previously [10], is explained by the insufficient effect of low BMP-2 and BMP-7 concentrations on osteogenic differentiation and the conversion of a certain proportion of MSCs into adipocytes, among other things.

It is known that BMP-2 interaction with specific type I receptors activates the MSCs conversion into adipocytes, and the activation of specific type II receptors stimulates the osteogenic MSC differentiation [3]. It is possible that the MS development is accompanied by an increase in type I receptors specific to BMP and a decrease in type II receptors, which disrupts the osteoblasts formation and slows down the formation of newly formed bone tissue in MS rats.

A stimulating effect of BMP-2 on angiogenesis during periodontal bone tissue regeneration has been established [25], which promotes the bone remodeling process in the control group of rats and explains low intensity of this process in the experimental group. BMP-2 and FGF-21 enhance the polarization of M2-phenotype macrophages, which immunomodulatory effect enhances osteogenic differentiation of stem cells during periodontal bone defect restoration [25].

CONCLUSION

This study demonstrated a statistically significant increase in BMP-2 and BMP-7 plasma levels in male Wistar MS rats. The analysis of the mandibular integrity restoration revealed a decrease in BMP-7 concentrations in the experimental group of rats throughout the experiment, and a decrease in BMP-2 concentrations on days 7, 14, and 28, compared to the control group. These data suggest that the decreased BMP-2 and BMP-7 plasma levels may be some of the mechanisms explaining the slowdown in reparative osteogenesis in MS rats. The results presented in this study support the administration of BMP-2 and BMP-7 analogs to stimulate the mandibular integrity restoration in MS.

REFERENCES

1. Ahmad P., Della Bella E., Stoddart M.J. Applications of Bone Morphogenetic Proteins in Dentistry: A Bibliometric Analysis. *BioMed Res. Int*. 2020;2020:5971268. DOI: 10.1155/2020/5971268.
2. Lukača N., Katavića V., Novakc S., Šućura A., Filipovića M., Kalajzić I. et al. What do we know about bone morphoge-

netic proteins and osteochondroprogenitors in inflammatory conditions? *Bone.* 2020;137:115403. DOI: 10.1016/j.bone.2020.115403.
3. Carreira A.C., Alves G.G., Zambuzzi W.F., Sogayar M.C., Granjeiro J.M. Bone morphogenetic proteins: structure, biological function and therapeutic applications. *Archives of Biochemistry and Biophysics.* 2014;561:64-73. DOI: 10.1016/j.abb.2014.07.011.
4. Stokovic N., Ivanjko N., Maticic D., Luyten F.P., Vukicevic S. Bone morphogenetic proteins, carriers, and animal models in the development of novel done regenerative therapies. *Materials.* 2021;14(13):3513. DOI: 10.3390/ma14133513.
5. Takematsu E., Murphy M., Hou S., Steininger H., Alam A., Ambrosi T.H. et al. Optimizing delivery of therapeutic growth factors for bone and cartilage regeneration. *Gels.* 2023;9(5):377. DOI: 10.3390/gels9050377.
6. Janbozorgi M., Hosseinzadeh M., Taheri A., Ghafaripur S. Impact of aerobic exercise on expression of OPN and OPG genes and bmal1 protein in the done tissue of diabetic rats during two phases of light and dark circadian rhythm. *Research Results in Biomedicine.* 2024;10(4):520–531. DOI: 10.18413/2658-6533-2024-10-4-0-3.
7. Nadezhdina N.A., Gudyrev O.S., Nadezhdin S.V., Danilenko L.M., Dolzhikov A.A., Kremleva K.K. et al. Epoetin-alfa-induced osteogenesis in the bone organoid model. *Research Results in Pharmacology.* 2024;10(4):29–41. DOI: 10.18413/rrpharmacology.10.517.
8. Kotb E., El Mancy I.M., Mohamed I.G.R., Ayoub H.S.A., Rashed A.M., El-Nasser W.S. et al. Relation between erythropoietin resistance and metabolic syndrome in hemodialysis patients: A multicentric propensity score matched analysis. *Journal of Investigative Medicine.* 2023;71(7):753–759. DOI: 10.1177/10815589231171405.
9. Rodríguez-Merchán E.C. A Review of Recent Developments in the Molecular Mechanisms of Bone Healing. *International Journal of Molecular Science.* 2021;22(2):767. DOI: 10.3390/ijms22020767.
10. Makarova M.V., Lyashev Yu.D., Solin A.V., Serikov V.S., Klevtsov S.A. Features of Reparative Osteogenesis in Mandibular Defects in Rats with Experimental Metabolic Syndrome. *Bulletin of Experimental Biology and Medicine.* 2025;179(6):762–767. (In Russ.). DOI: 10.47056/0365-9615-2025-179-6-762-767.
11. Lipatov V.A., Kryukov A.A., Severinov D.A., Saakyan A.R. Ethical and Legal Aspects of In Vivo Experimental Biomedical Research. Part I. *I.P. Pavlov Russian Medical Biological Herald.* 2019;27(1):80–92. (In Russ.). DOI: 10.23888/PAVLOVJ201927180-92.
12. Lipatov V.A., Kryukov A.A., Severinov D.A., Saakyan A.R. Ethical and Legal Aspects of In Vivo Experimental Biomedical Research. Part II. *I.P. Pavlov Russian Medical Biological Herald.* 2019;27(2):245–257. (In Russ.). DOI: 10.23888/PAVLOVJ2019272245-257.
13. Birulina Yu.G., Ivanov V.V., Buyko E.E., Bykov V.V., Smagliy L.V., Nosarev A.M. et al. High-fat, High-carbohydrate Diet-induced Experimental Model of Metabolic Syndrome in Rats. *Bulletin of Siberian Medicine*. 2020;19(4):14–20. (In Russ.). DOI: 10.20538/1682-0363-2020-4-14-20.
14. Wong S.K., Chin K.Y., Suhaimi F.H., Ahmad F., Ima-Nirvana S. The effects of a modified high-carbohydrate high-fat diet on metabolic syndrome parameters in male rats. *Experimental and Clinical Endocrinology and Diabetes.* 2018;126(3):205–212. DOI: 10.1055s-0043-109352.
15. Grigoryan A.S., Orlov A.A., Saburina I.N., Zurina I.M., Sysoev S.D. Dynamics of Osteogenesis Associated with Inoculation of Autologous Stromal Cells from Rat Adipose Tissue (Experimental-Morphological Study). *Pathological Physiology and Experimental Therapy.* 2015;59(2):4–11. (In Russ.).
16. Voronkova O.V., Birulina Yu.G., Ivanov V.V., Buyko E.E., Esimova I.E., Grigorieva A.V. et al. Features of the Cytogram and Cytokine Profile of Bronchoalveolar Lavage Fluid in Experimental Metabolic Syndrome. *Bulletin of Siberian Medicine*. 2022;21(4):29–36. (In Russ.). DOI: 10.20538/1682-0363-2022-4-29-36.
17. Rossi J.L.S., Barbalho S.M., de Araujo R.R., Bechara M.D., Sloan K.P., Sloan L.A. Metabolic syndrome and cardiovascular diseases: Going beyond traditional risk factors. *Diabetes Metabolism Research and Reviews.* 2022;38(3):e3502. DOI: 10.1002/dmrr.3502.
18. Li. M., Willey J. The interplay between inflammation and thrombosis in COVID-19: Mechanisms, therapeutic strategies, and challenges. *Thrombosis Update.* 2022;8:100117. DOI: 10.1016/j.tru.2022.100117.
19. Wang M., Qiu Y., Gao L., Qi F., Bi L. The impact of IGF-1 on alveolar bone remodeling and BMP-2 expression in orthodontic tooth movement in diabetic rats. *Advances in Clinical and Experimental Medicine.* 2023;32(3):349–356. DOI: 10.17219/acem/153956.
20. Nett P.C., Ortmann J., Celeiro J., Haas E., Hofmann-Lehmann R., Tornillo L. et al. Transcriptional regulation of vascular bone morphogenetic protein by endothelin receptors in early autoimmune diabetes mellitus. *Life Science.* 2006;78(19):2213–2218. DOI: 10.1016/j.lfs.2005.09.026.
21. Cai B., Du J. Role of bone morphogenetic protein-4 in gestational diabetes mellitus-related hypertension. *Experimental and Therapeutic Medicine.* 2021;22(1):762. DOI: 10.3892/etm.2021.10194.
22. Carreira A.C.O., Zambuzzi W.F., Rossi M.C., Filho R.A., Sogayar M.C., Granjeiro J.M. Bone morphogenetic proteins: promising molecules for bone healing, bioengineering, and regenerative medicine. *Vitamins and Hormones.* 2015;99:293–322. DOI: 10.1016/bs.vh.2015.06.002.
23. Ishida K., Haudenschild D.R. Interactions between FGF21 and BMP-2 in osteogenesis. *Biochemical and Biophysical Research Communications.* 2013;432(4):677–682. DOI: 10.1016/j.bbrc.2013.02.019.
24. Zhou X., Chen J., Sun X., Wang F., Wang Y., Zhang Z. et al. Spatiotemporal regulation of angiogenesis/osteogenesis emulating natural bone healing cascade for vascularized bone formation. *Journal of Nanobiotechnology.* 2021;19(1):420. DOI: 10.1186/s12951-021-01173-z.
25. Ding T., Kang W., Li J., Yu L., Ge S. An in situ tissue engineering scaffold with growth factors combining angiogenesis and osteoimmunomodulatory functions for advanced periodontal bone regeneration. *Journal of Nanobiotechnology.* 2021;19(1):247. DOI: 10.1186/s12951-021-00992-4.

Author Contribution

Makarova M.V. – conception and design, analysis and interpretation of data, justification of the manuscript or critical revision for important intellectual content. Tsygan V.N., Lyashev Yu.D. – conception and design, justification of the manuscript, critical revision for important intellectual content, and final approval of the manuscript for publication. Brusentsova A.Ye. – analysis and interpretation of data, justification of the manuscript or critical revision for important intellectual content.

Author Information

Makarova Marina V. – Assitant, Department of Therapeutic Dentistry, KSMU, Kursk, marina-golovina@inbox.ru, http://orcid.org/0009-0005-5431-3760

Tsygan Vasily N. – Dr. Sci. (Med.), Professor, Head of the Department of Pathological Physiology, Kirov Military Medical Academy, Saint Petersburg, vn-t@mail.ru, http://orcid.org/0000-0003-1199-0911

Lyashev Yuri D. – Dr. Sci. (Med.), Professor, Professor of the Department of Pathological Physiology, KSMU, Kursk, ylyashev@yandex.ru, http://orcid.org/0000-0003-0536-923X

Brusentsova Anna Ye. – Cand. Sci. (Med.), Associate Professor, Department of Therapeutic Dentistry, KSMU, Kursk, brusentsovaanna81@yandex.ru, http://orcid.org/0000-0002-3353-272X

(✉) **Makarova Marina V.,** marina-golovina@inbox.ru

Received on July 22, 2025;
approved after peer review on October 21, 2025;
accepted on October 30, 2025

УДК 616-022-056.43:613.287.5:613.953.13
https://doi.org/10.20538/1682-0363-2026-2-73-83

Efficacy and Safety of Amino Acid-based Formulas in the Management of Infants with Cow's Milk Protein Allergy: an Open-label Prospective Controlled Study

Novik G.A.[1], Tamrazova O.B.[2, 3], Sukhotina A.G.[3], Tamrazova A.V.[4], Zhdanova M.V.[1]

[1] *Saint-Petersburg State Pediatric Medical University (SPbSPMU)*
2 Litovskaya St., 194100 Saint-Peterburg, Russian Federation

[2] *Russian Medical Academy of Continuing Professional Education (RMACPE)*
2/1 Barrikadnaya St., 125993 Moscow, Russian Federation

[3] *Z.A. Bashlyaeva Children Hospital*
28 Geroev Panfilovtsev St., 125373 Moscow, Russian Federation

[4] *Central State Medical Academy (CSMA)*
19/1A Marshala Timoshenko St., 121359 Moscow, Russian Federation

ABSTRACT

Aim. To determine the efficacy and safety of long-term use of an amino acid-based formula in children with cow›s milk protein allergy (CMPA) and moderate to severe atopic dermatitis (AD).

Materials and methods. The study included 60 children under 12 months of age with CMPA presenting with cutaneous symptoms (moderate or severe AD according to the oSCORAD) and/or gastrointestinal symptoms. Prior to the study, all patients were prescribed an extensively hydrolyzed formula (EHF) for 4 weeks. Patients with no or incomplete response to EHF ($n = 30$) were assigned to Group 1, receiving an amino acid-based formula (AAF) for 12 months. The 30 patients who showed a positive response to EHF were assigned to Group 2.

Results. Children in Group 1 showed greater gains in weight and height during the first 6 months compared to children in Group 2 ($p < 0.001$). The resolution of gastrointestinal symptoms in children receiving AAF was observed within 14 days along with an improvement in the clinical picture of AD within 3–5 days. Also, both groups showed a decrease in oSCORAD and EASI scores; however, children receiving AAF had a significantly smaller number of exacerbations ($p = 0.041$) and a lower impact of dermatosis on daily activities ($p = 0.002$). After 6 months of therapy, 53.3% of children in Group 1 developed tolerance to cow's milk proteins, compared to only 23.3% in Group 2 ($p = 0.017$). After 2 years of follow-up, tolerance was noted in all children who received AAF versus 87.7% of those fed with EHF.

Conclusion. The use of AAF in children with CMPA is an effective dietary management method that leads to faster resolution of gastrointestinal symptoms, improvement in the course of atopic dermatitis, and prolongation of its remission. It shortens the period for tolerance development, has a positive effect on the child›s physical development, and contributes to a significant improvement in the quality of life of both patients and their parents.

Keywords: CMPA, food allergy, casein, atopic dermatitis, extensively hydrolyzed formula, amino acid-based formula

Conflict of interest. The authors declare the absence of obvious and potential conflicts of interest related to the publication of this article.

Source of financing. The authors state that they received no funding for the study.

Conformity with the principles of ethics. All legal representatives of the patients signed an informed consent to participate in the study. The study was approved by the Ethics Committee at SPbSPMU.

✉ *Novik Gennady A.,* ga_novik@mail.ru

For citation: Novik G.A., Tamrazova O.B., Sukhotina A.G., Tamrazova A.V., Zhdanova M.V. Efficacy and Safety of Amino Acid-based Formulas in the Management of Infants with Cow's Milk Protein Allergy: an Open-label Prospective Controlled Study. *Bulletin of Siberian Medicine.* 2026;25(2):74–84. https://doi.org/10.20538/1682-0363-2026-2-74-84.

Эффективность и безопасность применения аминокислотных смесей у детей первого года жизни с аллергией к белкам коровьего молока: открытое проспективное контролируемое исследование

Новик Г.А.[1], Тамразова О.Б.[2, 3], Сухотина А.Г.[3], Тамразова А.В.[4], Жданова М.В.[1]

[1] Санкт-Петербургский государственный педиатрический медицинский университет (СПбГПМУ)
Россия, 194100, г. Санкт-Петербург, ул. Литовская, 2

[2] Российская медицинская академия непрерывного профессионального образования (РМАНПО)
Россия, 125993, г. Москва, ул. Баррикадная, 2/1, стр. 1

[3] Детская городская клиническая больница им. З.А. Башляевой (ДГКБ им. З.А. Башляевой)
Россия, 125373, г. Москва, ул. Героев Панфиловцев, 28

[4] Центральная государственная медицинская академия (ЦГМА)
Россия, 121359, г. Москва, ул. Маршала Тимошенко, 19, стр. 1а

РЕЗЮМЕ

Цель: определить эффективность и безопасность длительного применения аминокислотной смеси у детей с аллергией на белок коровьего молока (АБКМ) и атопическим дерматитом (АтД) умеренной или тяжелой степени тяжести.

Материалы и методы. Дети ($n = 60$) в возрасте до 12 мес с АБКМ с кожными (АтД умеренной или тяжелой степенью тяжести по шкале oSCORAD) и (или) гастроинтестинальными симптомами. Всем пациентам до начала исследования была назначена высокогидролизная смесь (ВГС) в течение 4 нед. Пациенты с отсутствием или неполным ответом на ВГС ($n = 30$) были определены в группу 1, получающую аминокислотную смесь (АКС) в течение 12 мес, 30 пациентов с положительным эффектом на ВГС вошли в группу 2.

Результаты. У детей из группы 1 отмечались более высокие прибавки в показателях массы и роста в течение первых 6 мес по сравнению с детьми из группы 2 ($p < 0,001$). Исчезновение гастроинтестинальных симптомов у детей, получавших АКС, наблюдалось в течение 14 сут, а улучшение клинической картины АтД – в течение 3–5 сут. Также в обоих группах отмечалось снижение индексов oSCORAD и EASI, однако у детей, получавших АКС, наблюдалось значительно более низкое число обострений ($p = 0,041$) и влияние дерматоза на повседневную деятельность ($p = 0,002$). Через 6 мес терапии 53,3% детей из группы 1 сформировали толерантность к белкам коровьего молока, в то время как в группе 2 лишь 23,3% ($p = 0,017$). Через 2 года наблюдения толерантность отмечалась у всех детей, получавших АКС, против 87,7% – на ВГС.

Заключение. Использование АКС у детей с АБКМ является эффективным методом диетотерапии, который в более короткие сроки приводит к разрешению гастроинтестинальных явлений, улучшению течения атопического дерматита и продлению его ремиссии, сокращает период формирования толерантности, оказывает положительное влияние на физическое развитие ребенка и способствует значительному улучшению качества жизни пациентов и их родителей.

Ключевые слова: АБКМ, пищевая аллергия, казеин, атопический дерматит, высокогидролизная смесь, аминокислотная смесь

Конфликт интересов. Авторы декларируют отсутствие явных и потенциальных конфликтов интересов, связанных с публикацией настоящей статьи.

Источники финансирования. Авторы заявляют об отсутствии финансирования при проведении исследования.

Соответствие принципам этики. Все законные представители пациентов подписали информированное согласие на участие в исследовании. Исследование одобрено этическим комитетом СПбГПМУ.

Для цитирования: Новик Г.А., Тамразова О.Б., Сухотина А.Г., Тамразова А.В., Жданова М.В. Эффективность и безопасность применения аминокислотных смесей у детей первого года жизни с аллергией к белкам коровьего молока: открытое проспективное контролируемое исследование. *Бюллетень сибирской медицины.* 2026;25(2):73–83. https://doi.org/10.20538/1682-0363-2026-2-73-83.

INTRODUCTION

Cow's milk protein allergy (CMPA) is an adverse immune-mediated reaction to one or more cow's milk proteins (CMP), the most common of which are casein (α1, α2, β, and κ-casein) and whey proteins (α-lactalbumin and β-lactoglobulin) [1].

Currently, there is an increase in the incidence of food allergies, including CMPA among children under 3 years of age [2]. The incidence of CMPA during the first year of life, according to epidemiological studies, ranges from 2 to 7.5%, which decreases to less than 1% after 6 years of age [3]. Sensitization can occur in children who are exclusively breastfed, or in children who received a mixed diet (with the introduction of cow's milk protein). The peak incidence occurs at the age of 5–6 months, which may coincide with the introduction of complementary foods into the diet [1, 4].

It is believed that breastfeeding during the first 4–6 months of life is one of the main methods for preventing the development of CMPA, however, even in such children, allergy symptoms are observed in 0.5% of cases, which is associated with the penetration of CMPs into breast milk 4–6 hours after consuming dairy products [5]. Moreover, modern studies indicate that proteins transmitted through the placenta can form neonatal tolerance or lead to sensitization (for example, if there is a genetic predisposition to the development of allergic diseases) [6].

The clinical manifestations of CMPA presented in Table 1 are multifaceted and depend both on the type of immune mechanisms (IgE-dependent allergic reaction, non-IgE-dependent reaction, or mixed type) and on the patient's age [7]. Thus, infants are more likely to have disorders of the gastrointestinal tract, while older children more commonly have skin or gastrointestinal symptoms [8].

Diagnosis of CMPA is primarily based on medical history, clinical manifestations, and the elimination effect. The methods of laboratory diagnosis of sensitization include determination of specific antibodies of the IgE class (sIgE), including component-resolved diagnosis of allergy, determination of the basophil activation rate, as well as mast cell degranulation (MCD) reaction. Skin tests (skin prick test, scarification tests) can also be used in the diagnosis. The combination of an oral provocation test and an elimination diet remains the gold standard for the diagnosis of CMPA [9]. The disadvantages of these methods are the risks of adverse reactions, as well as dependence on parental compliance, which creates prerequisites for the search for new diagnostic methods to improve the accuracy and reliability of allergen detection in children under the age of 2 years [10].

Table 1

Clinical Manifestations of IgE- and Non-IgE-associated Allergy to Cow's Milk. Adapted from [7]

IgE-dependent manifestations	Skin and mucous membranes: urticaria, angioedema, erythema
	Cardiovascular system: tachycardia, dizziness, hypotension, loss of consciousness
	Anaphylaxis: severe, life-threatening, rapidly developing hypersensitivity reaction
	Respiratory organs: asthma and rhinitis caused by ingestion or inhalation of MG, itching, sneezing, nasal congestion, hoarseness of voice
	Organs of the gastrointestinal tract: oral allergy syndrome, cramping abdominal pain, nausea, vomiting, diarrhea
Non-IgE-dependent manifestations	Food protein-induced enterocolitis syndrome: recurrent vomiting and diarrhea, severe course
	Food protein-induced enteropathy: growth retardation, diarrhea, mucus in the stool
	Food protein-induced colitis/proctocolitis: diarrhea with blood in the stool, sometimes the presence of mucus
	Heiner syndrome (a rare form of pulmonary hemosiderosis induced by CMPs): infiltrates in the lungs, chronic cough, shortness of breath, obstruction, fever, anemia, eosinophilia, failure to thrive
Mixed (IgE + non-IgE)	Eosinophilic gastroenteritis: obstruction, ascites, weight loss
	Atopic dermatitis: moderate or severe
	Esophagitis: reflux, dysphagia, vomiting, eating disorders/obstruction

The basis of the disease-modifying treatment is exclusion of foods containing CMPs from the diet (Clinical recommendations: Food Allergy.

Developer: The Union of Pediatricians of Russia, the Russian Association of Allergologists and Clinical Immunologists. 2025). The duration of the elimination diet depends on the severity of the course of food allergies, on the need to exclude products with cross-reactivity, as well as on individual characteristics and ranges from 6 to 18 months [11, 12]. The introduction of soy, goat, or other animal milk into the diet is not recommended, which is either due to a lower content of nutritional components or a trend toward cross-sensitization with cow's milk [13].

According to domestic and foreign regulatory documents for young children with manifestations of CMPA, in order to relieve allergic symptoms and maintain normal physical development, it is recommended to replace cow's milk and dairy products with an extensively hydrolyzed formula (EHF) or an amino acid-based formula (AAF) [11]. The EHF uses enzymatic processing to break down cow's milk powder proteins into smaller peptide chains and free amino acids, the former retaining allergenicity, which limits its effectiveness in a number of patients [14]. The AAF is created by artificial splitting of proteins into amino acids to eliminate peptide chains and consists exclusively of amino acids, which makes it the most effective in CMPA therapy [14].

The aim of the study was to determine the efficacy and safety of AAFs in children with CMPA and moderate or severe AD using clinical and laboratory parameters, as well as the quality of life.

MATERIALS AND METHODS

This study was single-center, prospective, parallel, controlled, and open. The study duration was 24 months and included 60 patients (37 boys and 23 girls) aged 3 to 12 months with moderate or severe AD and cooccurring CMPA, accompanied by gastrointestinal symptoms and positive elimination and provocation tests. The severity of AD, given the very young age of patients and their inability to independently assess itching and sleep disorders, was determined using the **o**SCORAD (Objective SCORing Atopic Dermatitis) score, a modification of the SCORAD score which excludes subjective symptoms.

At the selection stage, all patients underwent elimination therapy using the EHF for 4 weeks to confirm CMPA. The study included patients with moderate and severe AD, according to the oSCORAD index, and confirmed CMPA, accompanied by gastrointestinal symptoms. On day 1 of the study, all patients underwent laboratory testing: complete blood count, fecal occult blood test, determination of sIgE to CMPs, MCD test, and the basophil activation rate to CMPs. The children were examined and their anthropometric parameters were recorded. The oSCORAD and EASI (Eczema Area and Severity Index) indices were determined, and the IDQoL (Infants' Dermatitis Quality of Life) index was calculated (via a specialized questionnaire to assess the quality of life of children with AD under 4 years of age). The following treatment was prescribed: Group 1 (n = 30) was prescribed the EHF, Group 2 (n = 30) – the AAF.

During subsequent visits, laboratory tests were also performed, anthropometric parameters were recorded, the severity of AD was determined according to the oSCORAD and EASI indices, and the IDQoL questionnaire was filled out by legal representatives.

The hypothesis of the study (the use of the AAF in children with AD and CMPA leads to a significant reduction in the number of exacerbations, improvement of the clinical presentation and quality of life of patients and their parents) was tested by the statistical analysis of the results obtained.

Inclusion criteria:

– full-term infants under the age of 12 months;

– moderate or severe AD according to the oSCORAD (Objective Scoring Atopic Dermatitis) index;

– presence of gastrointestinal symptoms: food protein-induced proctocolitis, enterocolitis, enteropathy;

– patients with CMPA confirmed by anamnestic data, elimination diet, and oral food allergy challenge;

an informed consent signed by a legal representative to participate in the study and to subsequently publish the data following confidentiality rules;

– for the AAF group: persistent symptoms or incomplete effect in the context of EHF use for 4 weeks, severe manifestations of food allergies and CMPA, sensitization to multiple allergens, malabsorption.

Criteria for non-inclusion:

– the presence of concomitant pathologies that limit the possibility of participating in the study (severe infectious diseases, cancer, somatic-symptom disorders);

– mild AD (oSCORAD index < 15);

– use of systemic anti-inflammatory or gene therapy during the study and one month before inclusion;

– refusal of legal representatives to participate in the study.

Exclusion criteria:

– non-compliance with the therapies prescribed by the study design, violation of the elimination diet;

– voluntary desire of legal representatives to complete the study ahead of schedule;

– detection of adverse reactions or appearance of severe concomitant somatic-symptom disorders or infectious diseases that require discontinuation of the study.

The examination of the patients corresponded to the ethical standards of the Declaration of Helsinki (2008). All legal representatives of the patients signed an informed consent. The study was conducted at the Department of Pediatric Diseases named after Professor I. M. Vorontsov of Saint-Petersburg State Pediatric University from September 2023 to January 2026 and consisted of four control time points: on day 1 of the study (before treatment), after 6 months, after 12 months, and after 24 months and included six visits every two months. In addition to the visits, telephone communication was conducted with legal representatives to register skin, gastrointestinal, and other symptoms. The study was approved by the Ethics Committee at

Group 1 received Nutrilak Premium ProAllergy AMINO AAF for 12 months. During the study, Group 2 received the EHF for 12 months. Prescribing complementary foods to patients suffering from food allergies adhered to current clinical guidelines (Methodological recommendations "Program for optimizing the feeding of infants in the first year of life in the Russian Federation, Moscow, 2019). Also, regular use of emollients (at least 2 times a day, starting from 200 g/week) was prescribed to all patients as a baseline therapy for AD and to reduce the number of exacerbations caused by skin xerosis. When exacerbations of AD happened during the study, it was recommended by a dermatovenerologist to use topical glucocorticoids, topical calcineurin inhibitors, and antihistamines, depending on the intensity and clinical form of AD manifestations.

The required sample size was not calculated. The statistical analysis was performed using the StatTech v. 4.11.2 software (Stattech LLC, Russia). Descriptive statistics for quantitative variables were presented as the median and interquartile interval (Me [Q_1–Q_3]) or as the mean and the standard deviation ($M \pm SD$), depending on the type of data distribution. For intergroup comparisons of quantitative variables, nonparametric methods were used: the Mann – Whitney U-test (independent samples), the Wilcoxon test (two related groups), and the Friedman test (three or more dependent populations). The percentages in the analysis of four-field contingency tables were compared using the Pearson's chi-square test and the Fisher's exact test. The comparison of binary parameters characterizing two related populations was performed using the McNemar test, and those characterizing more than two populations were compared using the Cochran's Q-test. The differences were considered statistically significant at $p < 0.05$.

RESULTS

The study included 37 boys, the average age was 6 [6–8] months, the average weight was 8,123 [7,685–8,543] g, the average height was 68 [66–69.4] cm, and 23 girls aged 6 [4.55–8] months, weighing 7,254 [5,914.5–7,920.5] g with the height of 65 [61–69] cm. All children included in the study were full-term and had normal birth weight and height: height 49.06 ± 2.27 (48.07–50.04) cm for girls and 51.28 ± 1.36 (50.82–51.73) cm for boys and weight 3,212 [3,022–3,340] and 3,487 [3,421–3,689] g for girls and boys, respectively. Anamnestic data: sensitization to food, medication, household or seasonal allergens in both parents was noted in 21.7% of cases and at least in one parent – in 68.3%. Seventeen (28.3%) patients had moderate AD (the oSCORAD index 15–40), whereas 43 (71.7%) patients had severe AD (oSCORAD index > 40). Gastrointestinal symptoms (constipation, diarrhea, mucus in the stool, hemocolitis, regurgitation, colic in children) were observed in 55% ($n = 33$) of patients.

Despite the fact that the elimination and provocation test was positive in all (100%) of the study participants, the determination of sIgE, MCD reaction, and basophil activation index to CMP yielded positive results only in 28.3, 51.6, and 58.3% of cases, respectively, indicating limited capabilities of laboratory methods in the diagnosis of CMPA (Fig.1).

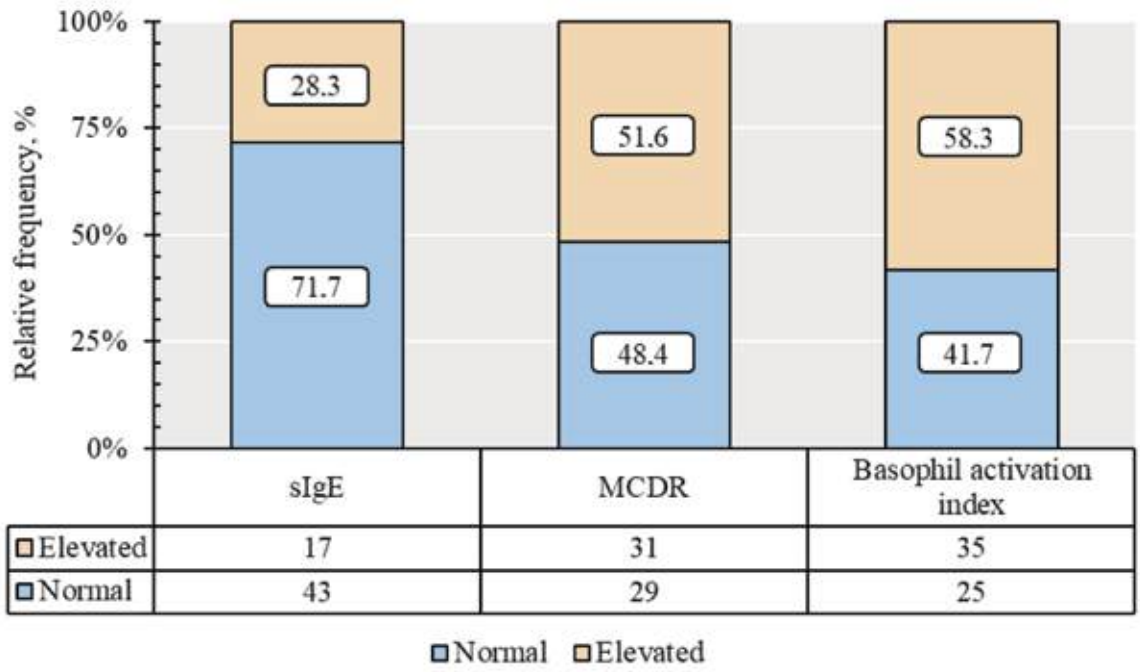

Fig. 1. Results of diagnostic tests in the patients included in the study

The patients were divided into groups of 30 people: Group 1 included children with symptoms of CMPA / incomplete clinical effect during 4 weeks of EHF application, and Group 2 included children with a positive response to EHF. The full characteristics of the study participants are presented in Table 2.

Table 2

Characteristics of the Study Participants

Parameters		Group 1	Group 2	*p*
Gender, abs. (%)	Girls	9 (30.0%)	14 (46.7%)	0.184
	Boys	21 (70.0%)	16 (53.3%)	
Age, months, *Me* [Q_1–Q_3]		6.00 [4.70–8.75]	6.50 [6.00–8.00]	0.691
Weight, g, *Me* [Q_1–Q_3]		7,312.5[5,808.25–7,672.25]	7,893[7,098–8,220.25]	0.049*
Height, cm,*Me* [Q_1–Q_3]		64 [60.1–66.82]	66.85 [64.17–69]	0.041*
Parental sensitization in the medical history, abs. (%)	No	6 (20.0%)	13 (43.3%)	0.254
	Mother	4 (13.3%)	4 (13.3%)	
	Father	12 (40.0%)	8 (26.7%)	
	Both parents	8 (26.7%)	5 (16.7%)	
Parents have a history of CMPA, abs. (%)	No	6 (20.0%)	13 (43.3%)	0.274
	Mother	6 (20.0%)	4 (13.3%)	
	Father	16 (53.3%)	12 (40.0%)	
	Both parents	2 (6.7%)	1 (3.3%)	
Complementary foods, abs. (%)	No	17 (56.7%)	13 (43.3%)	0.302
	Yes	13 (43.3%)	17 (56.7%)	
History of gastrointestinal symptoms, abs (%)	No	12 (40.0%)	15 (50.0%)	0.436
	Yes	18 (60.0%)	15 (50.0%)	
Milk sIgE, abs. (%)	Normal/Questionable result	21 (70.0%)	22 (73.3%)	1.000
	Elevated	9 (30.0%)	8 (26.7%)	
MCDR, milk, abs. (%)	Normal/Questionable result	12 (40.0%)	17 (56.7%)	0.196
	Elevated	18 (60.0%)	13 (43.3%)	
Basophil activation index, milk, abs. (%)	Normal/Questionable result	12 (40.0%)	13 (43.3%)	0.793
	Elevated	18 (60.0%)	17 (56.7%)	

End of table 2

Parameters	Group 1	Group 2	*p*
oSCORAD score, *Me* [Q_1–Q_3]	29 [20.50–48.75]	22 [18–34.5]	0.143
EASI score, *Me* [Q_1–Q_3]	14 [10.25–24]	11 [9–17.75]	0.285
IDQoL score, $M \pm SD$ (95% CI)	10 [8–15]	10 (8.25–14.75)	0.994

* differences in parameters are statistically significant ($p < 0.05$)

During the therapy, all children showed a significant increase in height and weight after both 6 and 12 months ($p < 0.001$). After 6 months, body weight gain in Group 1 was estimated at 2,772 [2,233.75–2,972.00] g, and in Group 2 – at 1,571.00 [851.25–1,787] g ($p < 0.001$), which is primarily due to lower baseline weight values in children who were prescribed AAF (Fig.2).

However, despite the fact that the baseline weight values in children from Group 1 were significantly lower ($p = 0.049$), the use of AAF allowed them to gain weight comparable to Group 2 ($p = 0.130$) by month 6 of therapy. Similarly to body weight, the patients' height had the same dynamics (Fig. 3). By the end of the study, the anthropometric parameters of all children were within the normal range according to the WHO standards, however, there were no significant differences between the two groups in either weight ($p = 0.554$) or height ($p = 0.734$).

Twelve months after the start of the study, 90% of children fed with AAF had a basophil activation rate within the normal range, while only 63.3% of children receiving EHF exhibited normalization of this parameter ($p = 0.030$) (Fig.4). The median basophil activation index in Group 1 after one year of the study changed from 1.18 [0.80–1.96] to 0.76 [0.65–0.98], in Group 2 – from 1.18 [0.68–2.04] to 0.90 [0.80–1.23], thereby demonstrating a more significant decrease ($p = 0.009$).

By the end of therapy, 76.7% ($n = 23$) of patients from Group 1 had normalized results of the MCD reaction, which is almost twice as many as before the start of the study ($p < 0.001$). There were no significant changes in Group 2: normalization in the parameter values occurred in only three patients ($p = 0.083$).

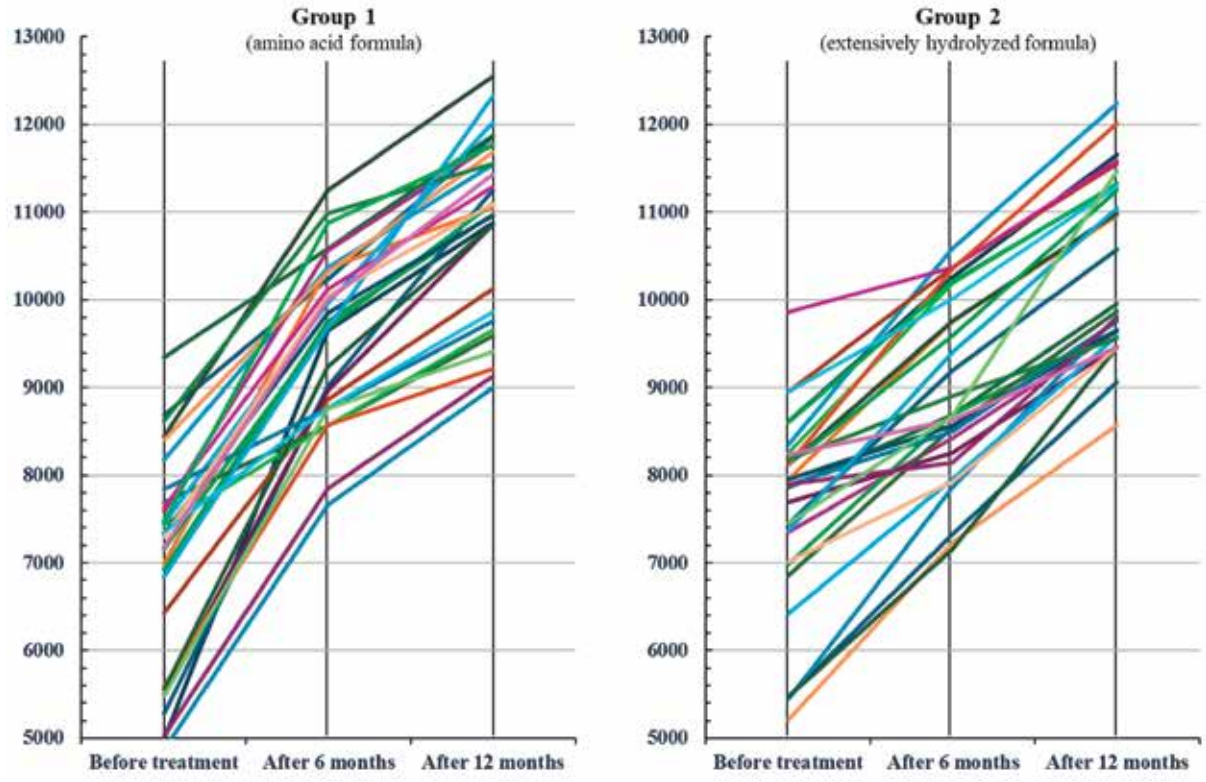

Fig. 2. Body weight dynamics in children of both groups at the beginning of the study, after 6 and 12 months

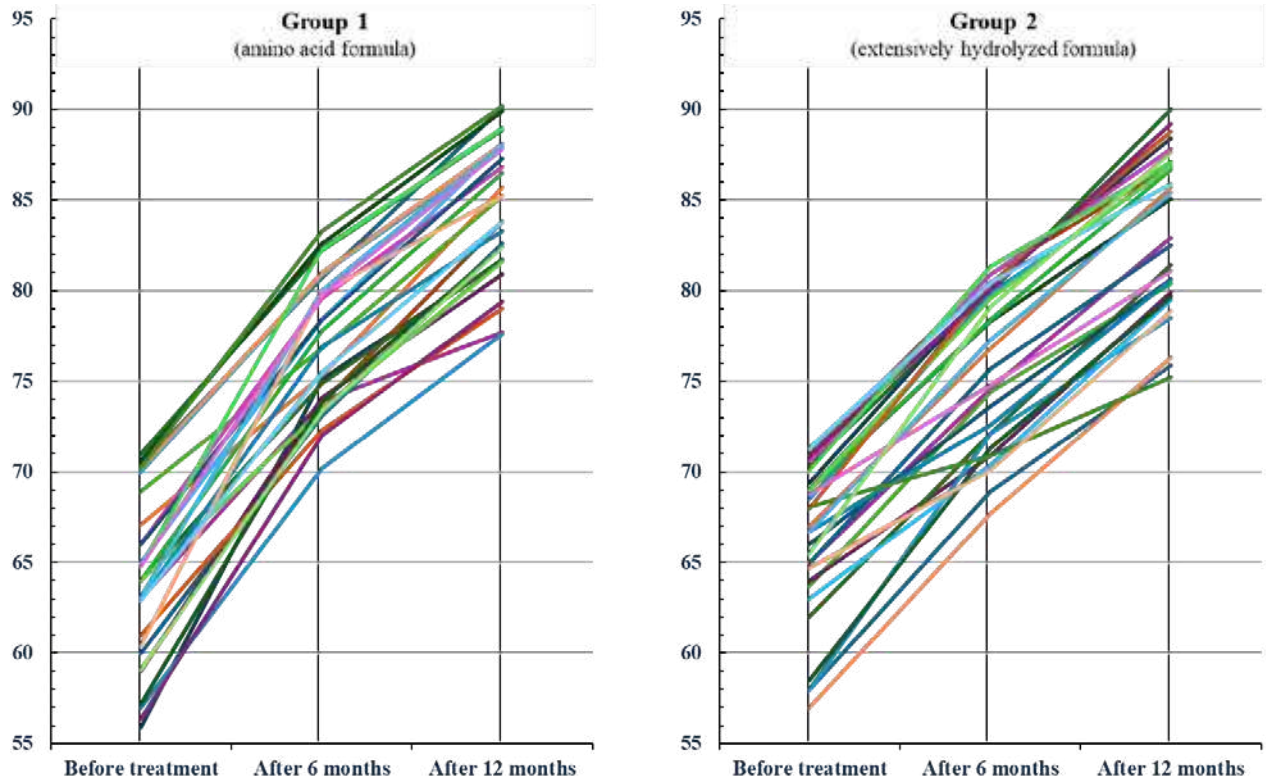

Fig. 3. Growth dynamics in children of both groups at the beginning of the study, after 6 and 12 months

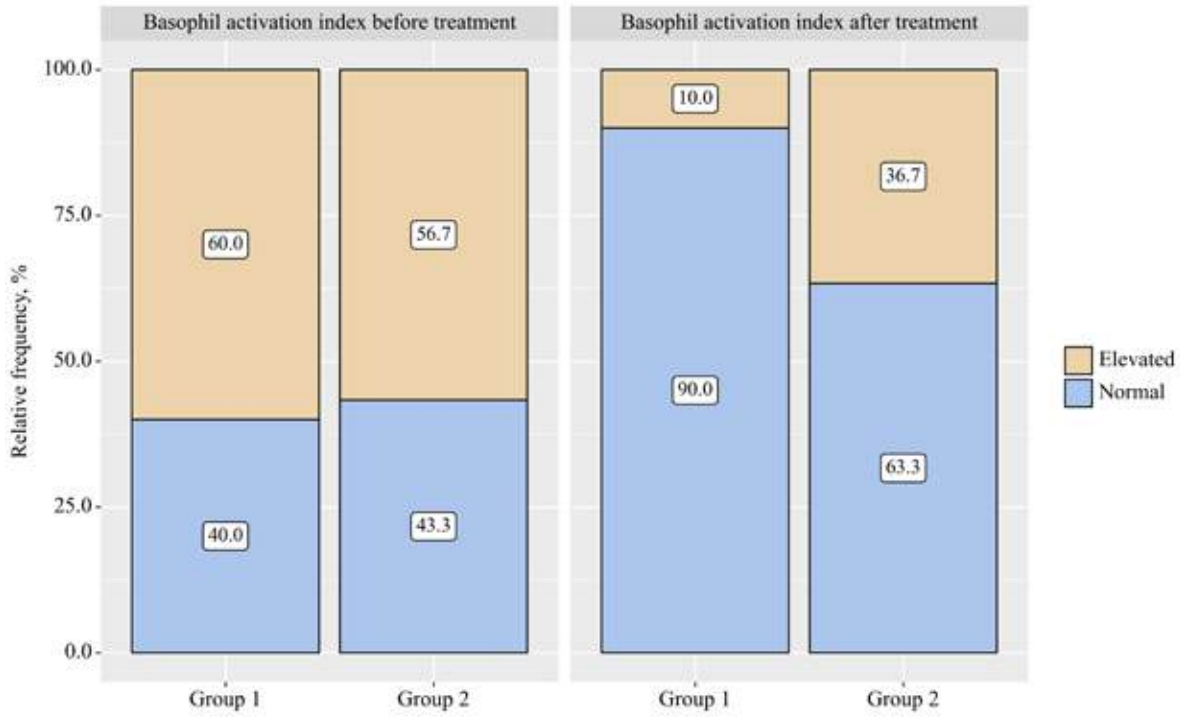

Fig. 4. Dynamics of the basophil activation index after 12 months of therapy

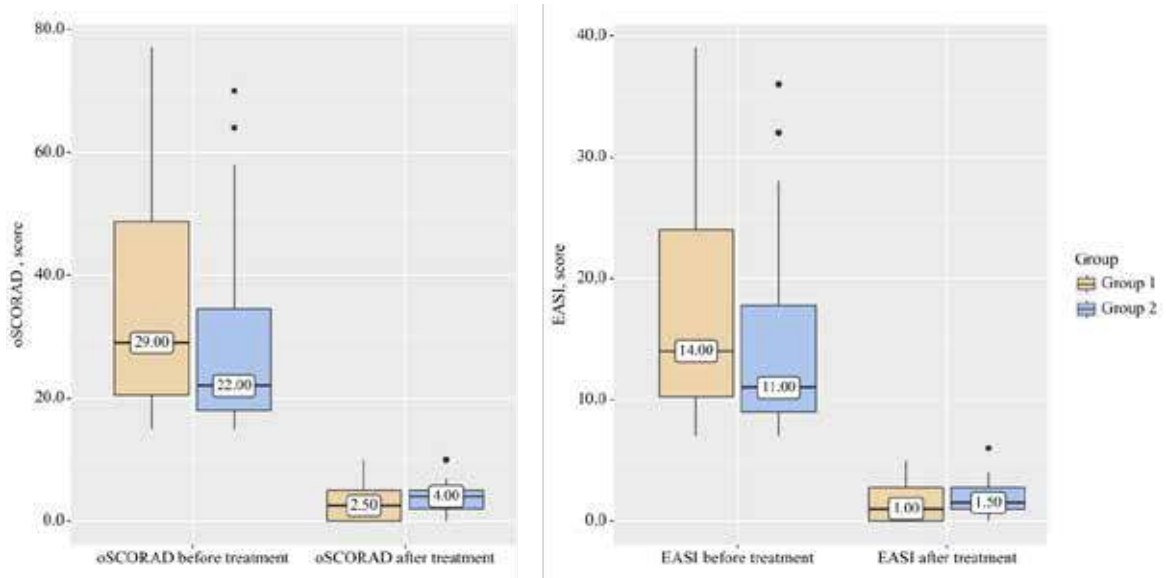

Fig. 5. Dynamics of the oSCORAD and EASI indices depending on the group

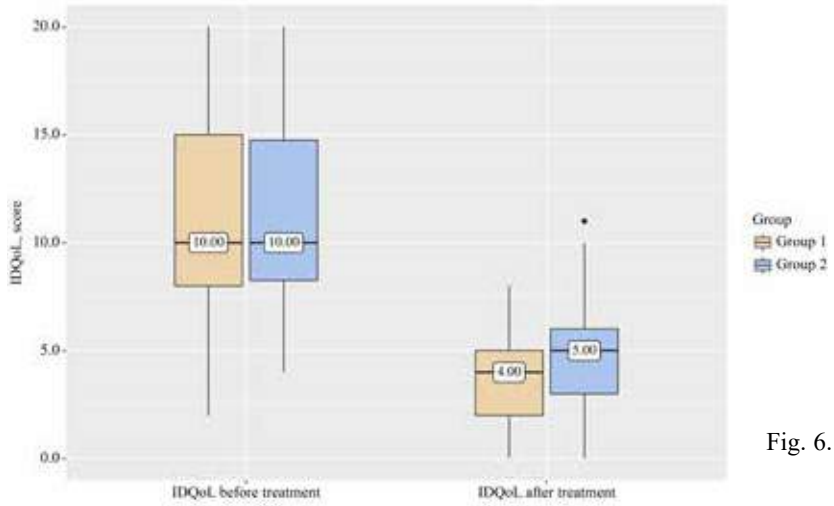

Fig. 6. Dynamics of the IDQoL index before and after treatment in both groups

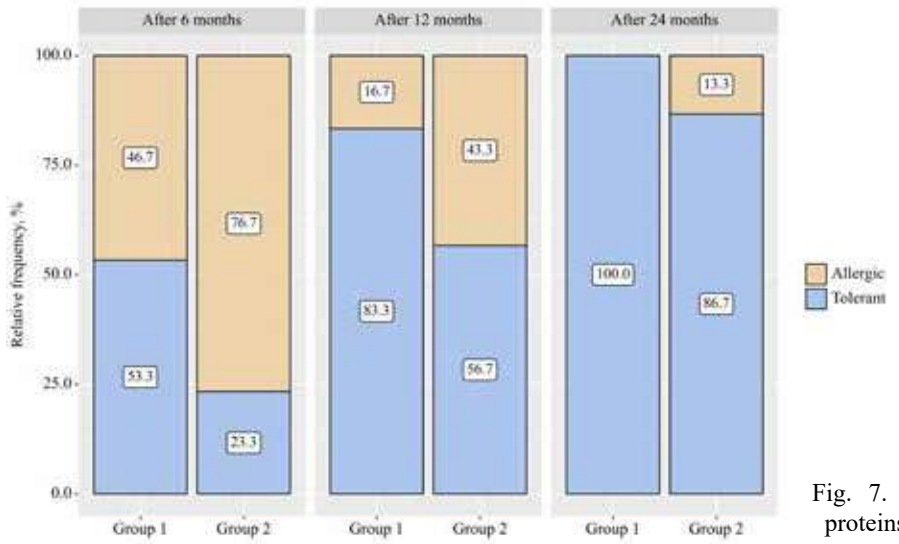

Fig. 7. Formation of tolerance to cow's milk proteins in the groups after 6, 12, and 24 months

In Group 1, the use of AAF led to a relief of gastrointestinal symptoms (colic, vomiting/regurgitation, hemocolitis) within 3–4 days. Complete normalization of stool with the disappearance of mucous impurities was achieved after an average of 2 weeks of therapy. A comparison between the groups was not carried out in this case, since in children from Group 2, these symptoms were stopped at the preclinical stage of the study following the diagnostic use of EHF for a month. According to retrospective data, the disappearance of gastrointestinal symptoms in Group 2 patients occurred within 7–10 days.

The clinical manifestations of AD had similar dynamics. In Group 1, an improvement in symptoms was observed on day 3–5 after the initiation of AAF therapy, while in Group 2 – on day 7–9 after the start of EHF administration with the use of adequate external and systemic therapy for dermatosis. The complete disappearance of AD symptoms varied in both groups, which is associated with the multifactorial pathogenesis of the disease, the role of food allergies in which has not been fully established.

The number of AD exacerbations in Group 1 within 12 months of follow-up was significantly smaller than in Group 2: 4 [3–5] versus 5.5 [3–6.75], respectively (p = 0.041). By the end of the study, there was a positive trend in the course of AD in both groups, but there were no significant differences in the severity of the clinical presentation of dermatosis for either the oSCORAD index (p = 0.328) or the EASI index (p = 0.223) after 12 months (Fig.5). The absence of differences may be due to the length of follow-up and the small number of control points for recording clinical manifestations at the time of exacerbation.

*The box-and-whisker plot displays five key statistical parameters: the minimum value is the end of the lower whisker, the first quartile is the bottom edge of the central box, the median is the line dividing the box into two parts, the third quartile is the top edge of the central box, the maximum value is the end of the upper whisker; the individual points in the figure indicate outliers – data that are very different from the total sample.

When assessing the quality of life using the IDQoL questionnaire, a decrease in the effect of dermatosis on daily activities was revealed (p < 0.001). However, in the group of patients receiving AAF, thE value of this parameter was lower than in the group receiving EHF: 4 [2–5] and 5 [3–6], respectively (p = 0.002) (Fig. 6).

* The box-and-whisker plot displays five key statistical parameters: the minimum value is the end of the lower whisker, the first quartile is the bottom edge of the central box, the median is the line dividing the box into two parts, the third quartile is the top edge of the central box, the maximum value is the end of the upper whisker; the individual points in the figure indicate outliers – data that are very different from the total sample.

After six months of therapy, 53.3% (n = 16) of children from Group 1 developed tolerance to CMPs, compared to only 23.3% (n = 7) in Group 2 (p = 0.017), which indicates more pronounced effectiveness of AAF in reducing sensitization to CMPs compared to EHF (Fig.7). When assessing the long-term results of therapy, 24 months after the start of follow-up, all children from Group 1 had no sensitization to CMPs compared to 87.7% (n = 26) in Group 2.

During the study, there were no adverse events (allergic reactions, diarrhea, vomiting, regurgitation, intestinal colic) that led to the discontinuation of AAF. The adaptation to the new formula took place within 1–2 weeks and did not require discontinuation of its use. Special attention should be paid to the organoleptic properties of the formula, as 83.3% of parents (n = 25) of children who received AAF reported satisfactory taste.

CONCLUSION

The results of this study confirm compliance of AAF with current criteria of efficacy and safety in patients with moderate or severe AD and gastrointestinal forms of CMPA. The use of AAF promotes faster resolution of skin and gastrointestinal symptoms, reduces the number of AD exacerbations, and improves the quality of life of patients and their parents. In the context of AAF use, normalization of laboratory parameters (basophil activation index and MCD reaction) is noted, which contributes to the formation of tolerance in most patients after six months of therapy.

REFERENCES

1. Hao L., Wang S., Ji W. Cow's milk protein allergy: A comprehensive review of epidemiology, pathogenesis, clinical manifestations, diagnostics, and management strategies. *Asia Pac. J. Clin. Nutr*. 2025;34(3):298–307. DOI: 10.6133/apjcn.202506_34(3).0004.

2. Warren C.M., Sehgal S., Sicherer S.H., Gupta R.S. Epidemiology and the growing epidemic of food allergy in children and adults across the globe. *Curr. Allergy Asthma Rep*. 2024;24(3):95–106. DOI: 10.1007/s11882-023-01120-y.
3. Ribes-Koninckx C., Amil-Dias J., Espin B., Molina M., Segarra O., Diaz-Martin J.J. The use of amino acid formulas in pediatric patients with allergy to cow's milk proteins: Recommendations from a group of experts. *Front. Pediatr.* 2023;11:1110380. DOI: 10.3389/fped.2023.1110380.
4. Onizawa Y., Noguchi E., Okada M., Sumazaki R., Hayashi D. The association of the delayed introduction of cow's milk with ige-mediated cow's milk allergies. *J Allergy Clin. Immunol. Pract*. 2016;4(3):481–488.e2. DOI: 10.1016/j.jaip.2016.01.012.
5. Zhu J., Dingess K.A. the functional power of the human milk proteome. *Nutrients*. 2019;11(8):1834. DOI: 10.3390/nu11081834.
6. Fujimura T., Lum S.Z.C., Nagata Y., Kawamoto S., Oyoshi M.K. Influences of maternal factors over offspring allergies and the application for food allergy. *Front. Immunol.* 2019;10:1933. DOI: 10.3389/fimmu.2019.01933.
7. Giannetti A., Toschi Vespasiani G., Ricci G., Miniaci A., di Palmo E., Pession A. Cow's milk protein allergy as a model of food allergies. *Nutrients*. 2021;13(5):1525. DOI: 10.3390/nu13051525.
8. Kubala S.A., Young F.D., Callier V., Rasooly M.M., Dempsey C., Brittain E. et al. Key factors that influence quality of life in patients with IgE-mediated food allergy vary by age. *Allergy.* 2024;79(10):2812–2825. DOI: 10.1111/all.16253.
9. Eiwegger T., Hung L., San Diego K.E., O'Mahony L., Upton J. Recent developments and highlights in food allergy. *Allergy.* 2019;74(12):2355–2367. DOI: 10.1111/all.14082.
10. Koletzko S., Niggemann B., Arato A., Miniaci A., di Palmo E., Pession A. Diagnostic approach and management of cow's-milk protein allergy in infants and children: ESPGHAN GI Committee practical guidelines. *J. Pediatr. Gastroenterol. Nutr*. 2012;55(2):221–229. DOI: 10.1097/MPG.0b013e31825c9482.
11. Meyer R., Venter C., Bognanni A., Szajewska H., Shamir R., Nowak-Wegrzyn A. et al. World Allergy Organization (WAO) Diagnosis and Rationale for Action against Cow's Milk Allergy (DRACMA) Guideline update – VII – milk elimination and reintroduction in the diagnostic process of cow's milk allergy. *World Allergy Organ J*. 2023;16(7):100785. DOI: 10.1016/j.waojou.2023.100785.
12. Coppola S., Carucci L., Oglio F., Di Sarra C., Ozen G., Berni Canani R. Nutritional strategies for the prevention and management of cow's milk allergy in the pediatric age. *Nutrients.* 2023;15(15):3328. DOI: 10.3390/nu15153328.
13. Skypala I., Vlieg-Boerstra B. Food intolerance and allergy: increased incidence or contemporary inadequate diets? *Curr. Opin. Clin. Nutr. Metab. Care*. 2014;17(5):442–447. DOI: 10.1097/MCO.0000000000000086.
14. Harijani A.M., Fatahi S., Guimarães N.S., Shidfar F. A Comparison of Amino Acid-Based, Hydrolyzed, and Soy-Based Formulas on Growth of Pediatric Patients with Cow's Milk Allergy: A Systematic Review and Meta-Analysis of Clinical Trials. *Breastfeed Med.* 2025;20(5):288–295. DOI: 10.1089/bfm.2024.0252.

Author Contribution

Novik G.A., Tamrazova O.B., Sukhotina A.G. – conception and design. Sukhotina A.G., Tamrazova A.V. – analysis and interpretation of the data. Zhdanova M.V. – critical revision of the manuscript for important intellectual content. Novik G.A., Tamrazova O.B. – final approval of the manuscript for publication.

Author Information

Novik Gennady A. – Dr. Sci. (Med.), Professor, Head of the Department of Pediatrics named after Professor I.M. Vorontsov, SPbSPMU, Saint-Petersburg, ga_novik@mail.ru, http://orcid.org/0000-0002-7571-5460

Tamrazova Olga B. – Dr. Sci. (Med.), Professor of the Russian Academy of Sciences, Professor at the Department of Pediatric Infectious Diseases, RMACPE, Moscow; Head of the Pediatric Dermatology Department, Z.A. Bashlyaeva Children Hospital, Moscow, anait_tamrazova@mail.ru, http://orcid.org/0000-0003-3261-6718

Sukhotina Alexandra G. – Dermatovenereologist, Z.A. Bashlyaeva Children Hospital, Moscow, aleksandra170697@mail.ru, http://orcid.org/0000-0001-7394-6575

Tamrazova Anait V. – Cand. Sci. (Med.), Associate Professor at the Department of Dermatovenereology and Cosmetology, CSMA, Moscow, anaittamrazova@gmail.com, http://orcid.org/0000-0002-4672-697X

Zhdanova Marina V. – Cand. Sci. (Med.), Associate Professor, Head of the Academic Department, Department of Pediatrics named after Professor I.M. Vorontsov, SPbSPMU, Saint-Petersburg, zhdanova-marina@rambler.ru, http://orcid.org/0000-0001-7035-0100

(✉) **Novik Gennady A.,** ga_novik@mail.ru

Received February 24, 2026;
approved after peer review March 5, 2026;
accepted March 19, 2026

УДК 618.36-073.584
https://doi.org/10.20538/1682-0363-2026-2-84-90

The Influence of Preanalytical Factors on the Algorithm of Multiplex Spectroscopy of Placental Samples

Rodionov V.E.[1,2], Avdalyan A.M.[1], Nichiporov A.I.[1], Chernov I.A.[2], Kukushkin V.I.[3], Avraamova S.T.[4], Kirillov Yu.A.[1,2,5]

[1] *Moscow Multidisciplinary Clinical Center "Kommunarka"*
8/3 Sosensky Stan St., 108814 Kommunarka village, Moscow, Russian Federation

[2] *Tyumen State Medical University*
54 Odesskaya St., 625023 Tyumen, Russian Federation

[3] *Institute of Solid State Physics, Russian Academy of Sciences*
2 Academician Osipyan St., 142432 Chernogolovka, Moscow Region, Russian Federation

[4] *The First Sechenov Moscow State Medical University*
8/2 Trubetskaya St., 119992 Moscow, Russian Federation

[5] *Avtsyn Research Institute of Human Morphology, Petrovsky National Research Centre of Surgery*
3 Tsyurupy St., 117418 Moscow, Russian Federation

ABSTRACT

Aim. To evaluate the effect of preanalytical processing of placental samples on the results of Raman spectroscopy.

Materials and methods. Thirty placental samples were prospectively studied. The samples were examined using the InSpectr M spectrometer at three stages of preanalytical processing of the material: native tissue, after fixation in formalin, after deparaffinization of the section. Statistical analysis included descriptive statistics, the Shapiro – Wilk test, the Friedman test with the post-hoc analysis, and the Spearman's rank correlation.

Results. The analysis of the samples revealed 33 Raman peaks (415–2,915 cm^{-1}), most of which were distributed abnormally (Shapiro – Wilk test, $p < 0.05$). The Friedman test with the Durbin – Conover post-hoc analysis revealed a group of stable analytes: 19 analytes retained intensity after fixation, 6 – after deparaffinization, and 10 – at all processing stages. The Spearman's rank correlation revealed selective relationships between processing stages for individual analytes (890; 1,117; 1,204; 753, 830, and 2,225 cm^{-1}).

Conclusion. The study revealed a significant effect of preanalytical sample processing on the spectral characteristics of placental tissue, the prospects for the clinical use of Raman spectroscopy, and the need to develop standardized protocols.

Keywords: Raman spectroscopy, placenta, limiting factors, preanalytical material processing, spectral profile

Conflict of interest. The authors declare the absence of obvious or potential conflicts of interest related to the publication of this article.

Source of financing. The authors declare that they received no funding for this study.

Conformity with the principles of ethics. The protocol of this study was approved by the Ethics Committee at Moscow Multidisciplinary Clinical Center "Kommunarka" (Minutes No.6 dated August 8, 2023).

For citation: Rodionov V.E., Avdalyan A.M., Nichiporov A.I., Chernov I.A., Kukushkin V.I., Avraamova S.T., Kirillov Yu.A. The Influence of Preanalytical Factors on the Algorithm of Multiplex Spectroscopy of Placental Samples. *Bulletin of Siberian Medicine.* 2026;25(2):84–90. https://doi.org/10.20538/1682-0363-2026-2-84-90.

✉ *Rodionov Vladimir E.,* rodionovforever@mail.ru

Влияние преаналитических факторов на алгоритм мультиплексного спектроскопического анализа образцов плаценты

Родионов В.Э.[1, 2], Авдалян А.М.[1], Ничипоров А.И.[1], Чернов И.А.[2], Кукушкин В.И.[3], Авраамова С.Т. [4], Кириллов Ю.А.[1, 2, 5]

[1] Московский многопрофильный клинический центр (ММКЦ) «Коммунарка» Департамента здравоохранения города Москвы (ДЗМ)
Россия, 108814, г. Москва, п. Коммунарка, ул. Сосенский Стан, 8/3

[2] Тюменский государственный медицинский университет (ГМУ)
Россия, 625023, г. Тюмень, ул. Одесская, 54

[3] Институт физики твердого тела им. Ю.А. Осипьяна Российской академии наук (ИФТТ РАН)
Россия, 142432, Московская обл., г. Черноголовка, ул. Академика Осипьяна, 2

[4] Первый Московский государственный медицинский университет им. И.М. Сеченова (Сеченовский Университет)
Россия, 119048, г. Москва, ул. Трубецкая, 8/2

[5] Научно-исследовательский институт морфологии человека (НИИМЧ) им. акад. А.П. Авцына, Российский научный центр хирургии (РНЦХ) им. акад. Б.В. Петровского
Россия, 117418, г. Москва, ул. Цюрупы, 3

РЕЗЮМЕ

Цель. Оценка влияния преаналитической подготовки плаценты на результаты рамановской спектроскопии.

Материалы и методы. Проспективно исследованы 30 образцов плаценты. Образцы исследовались при помощи спектрометра «ИнСпектр М» (ООО «РамМикс», Россия) на трех этапах преаналитической обработки материала: нативная ткань, после фиксации в формалине, после депарафинирования среза. Статистический анализ включал описательную статистику, тест Шапиро – Уилка, тест Фридмана с пост-хок тестом и корреляцию Спирмена.

Результаты. Исследование образцов выявило 33 рамановских пика (415–2915 $см^{-1}$), большинство из которых распределялись ненормально (критерий Шапиро – Уилка, $p < 0,05$). Тест Фридмана с пост-хок тестом Дурбина – Коновера выявил группу стабильных аналитов: 19 аналитов сохранили интенсивность после фиксации, 6 – после депарафинирования, а 10 – на всех этапах обработки. Тест Спирмена выявил избирательные взаимосвязи между этапами обработки для отдельных аналитов (890, 1117, 1204, 753, 830 и 2225 $см^{-1}$).

Заключение. Исследование выявило значительное влияние преаналитической подготовки образцов на спектральные характеристики плацентарной ткани, перспективность клинического использования рамановской спектроскопии и необходимость разработки стандартизированных протоколов.

Ключевые слова: рамановская спектроскопия, плацента, ограничивающие факторы, преаналитическая обработка материала, спектральный профиль

Конфликт интересов. Авторы декларируют отсутствие явных и потенциальных конфликтов интересов, связанных с публикацией настоящей статьи

Источники финансирования. Авторы заявляют об отсутствии финансирования при проведении исследования.

Соответствие принципам этики. Исследование одобрено комитетом по этике при ММКЦ «Коммунарка» ДЗМ (протокол № 6 от 08.08.2023).

Для цитирования: Родионов В.Э., Авдалян А.М., Ничипоров А.И., Чернов И.А., Кукушкин В.И., Авраамова С.Т., Кириллов Ю.А. Влияние преаналитических факторов на алгоритм мультиплексного спектроскопического анализа образцов плаценты. *Бюллетень сибирской медицины.* 2026;25(2):84–90. https://doi.org/10.20538/1682-0363-2026-2-84-90.

INTRODUCTION

The placenta is a unique, temporary, multifunctional organ that plays a critical role in ensuring normal fetal development. In recent years, researchers have increasingly focused on the potential of using data from physicochemical metabolic processes occurring in the placenta, which constitute the essence of its metabolome, as informative biomarkers and predictors of pathological conditions during pregnancy and its consequences [1, 2]. However, traditional histopathological examination methods have several limitations, including the subjectivity of visual assessment, the lack of data on metabolic pathologies, and significant time requirements.

Raman spectroscopy (RS) represents a promising alternative to classical morphological methods, providing detailed information on the conformation of macro- and micromolecules, making it a suitable tool for identifying analytes of pathological conditions in real time. Despite the widespread use of RS in oncology and other areas of medicine, its use in placental medicine [3–6] is limited to only a few pathological conditions [7–9]. Of particular interest is the potential use of RS for diagnosing inflammatory processes in placental tissue.

A key issue limiting the widespread adoption of this method in clinical practice, despite the obtained approval of the device for clinical use, is the presence of factors that can influence the outcome. These include the purity of the sample material, the presence of non-biological contaminants in the samples, background fluorescence, Gaussian noise, and preanalytical processing, which creates significant difficulties in interpreting results, especially when working with archival histological samples [10-12]. A particular methodological challenge is the need for prospective collection and analysis of a large number of samples followed by histological verification, which is associated with significant time and material costs. The influence of these limiting factors makes it impossible to extrapolate the results of a retrospective study to the data obtained in real time.

The aim of this study was to evaluate the effect of the stages of preanalytical processing of placental tissue on the RS results.

MATERIALS AND METHODS

The protocol for the study was reviewed and approved by the Ethics Committee at Moscow Multidisciplinary Clinical Center "Kommunarka" (Minutes No. 6 dated August 8, 2023).

Thirty placental tissue samples were prospectively randomized for the study. The mothers ranged in age from 19 to 43 years (median (*Me*) – 30.5 years); gestational age was 36 to 41 weeks (*Me* 39 weeks); birth order was 1 to 5 (*Me* 2); the fetal health status according to the Apgar scale at the first and fifth minutes of life, respectively, ranged from 1/3 to 9/10 (*Me* 8/9), the newborns' weight was 2,580 to 4,400 g (*Me* 3,510 g), and the placenta weight was 269 to 650 g (*Me* 437.5 g). Eighteen mothers delivered spontaneously through the birth canal, three had medically induced vaginal deliveries, and nine had cesarean deliveries.

The spectroscopic examination of each placental tissue sample was performed at three preanalytical stages: without fixation in media (native material) (stage 1); after fixation in 10% neutral buffered formalin for 24 hours (stage 2); and after deparaffinization of a 20-μm-thick section (standard histological processing) (stage 3). We used the InSpektr M spectrometer, version M-532 (RU No. RZN 2015/2419 dated June 18, 2021, manufacturer: RamMix LLC, Russia), consisting of an Olympus CX41 optical microscope and a spectrometer unit with the excitation wavelength of 532 nm. The laser spot diameter at the focal point was 10 μm, and the laser power was 10 mW. Instrument control, spectral recording, and data acquisition were performed using the specialized InSpektr software (RamMix LLC, Russia).

Data processing was performed using the Jamovi software (version 2.6.26, The jamovi project (2024)) – a freely distributed, open-source program for statistical analysis. Statistical analysis methods included descriptive statistics, testing for normality using the Shapiro – Wilk test, the nonparametric Friedman test (presumably rejecting the hypothesis of normal data distribution for most analytes) for comparing related samples followed by the post-hoc analysis (Durbin – Conover pairwise comparisons), and Spearman's rank correlation to assess the monotonic relationship between pairs of processing steps for each analyte. Data visualization was also performed using the Jamovi software.

RESULTS

The spectroscopic studies revealed that the spectra of placental samples were characterized by the presence of Raman peaks in the spectral range of 415–2,915 cm^{-1} and contained fluorescence intensity

values for 33 vibrational modes (components/analytes) (Table 1).

Table 1

Grouping of Placental Raman Peaks by Functional Classes with Shifts Indicated (cm^{-1})

Raman shift (cm^{-1})	Components/analytes*
1. Lipids and lipid components	
415; 533; 628; 1,300; 1,304; 1,445; 1,463; 2,915	Phosphatidylinositol, cholesterol ester, glycerol, (CH_2)-lipids, fatty acids, CH_2 deformation (lipids), phospholipids, collagen, CH_3, CH stretching of lipids
2. Proteins and amino acids	
641; 753; 830; 890; 933; 1,002; 1,174; 1,204; 1,365; 1,445; 1,554; 1,627; 2,554	Tyrosine, tryptophan, proline, hydroxyproline, tumor structural proteins, collagen, phenylalanine, amide III, glycine, amide II, amide I (β-form), methionine (S–H)
3. Nucleic acids (DNA/RNA)	
720; 810; 830; 1,230; 1,287; 1,304; 1,361; 1,609	DNA, phosphodiester (Z-marker), PO_2^- (nucleic acids), antisymmetric phosphate stretch, cytosine, adenine, guanine (N7, B/Z-marker)
4. Carbohydrates and glycans	
1,048; 1,117; 1,370	Glycogen, glucose, saccharides
5. Pigments and specialized metabolites	
957; 1,157; 1,528	Carotenoid, cholesterol, β-carotene (C=C)
6. Mineral components	
957	Hydroxyapatite
7. Combined/Overlapping Modes	
1,445–1,463; 2,225	CH_2/CH_3 deformations, C≡N

* the complete list of 33 components/analytes is provided in [13].

Analysis of the fluorescence intensity distribution for 33 analytes revealed that some shifts did not follow a normal distribution (Shapiro – Wilk test, $p < 0.05$). The greatest number of deviations from a normal distribution was observed for the native material (30 Raman shifts). After fixation in formalin, the number of anomalously distributed shifts decreased to 13. A limited number of deviations (19 Raman shifts) were also observed for the deparaffinized samples.

Due to the rejection of the hypothesis on a normal data distribution for a larger number of analytes, nonparametric methods were used for further statistical analysis.

Given the exploratory nature of the analysis of 33 analytes to identify potentially stable markers, rather than to confirm strict hypotheses, and the high risk of false-negative results when adjusting for 99 comparisons (33 analytes, 3 stages of preanalytical material processing), the Bonferroni correction was not applied. Unadjusted *p*-values are provided below, with an explicit indication that further validation is needed.

The analysis of differences in fluorescence intensity between the stages (Friedman test with the Durbin – Conover post-hoc analysis) showed that the group of analytes (Raman shifts at 753; 830; 890; 957; 1,002; 1,117; 1,174; 1,204; 1.230; 1,300; 1,304; 1,361; 1,365; 1,370; 1,445; 1,463; 1,528; 1,609; 1,627 cm^{-1}) did not show statistically significant differences in fluorescence intensity between stages 1 and 2. Analytes corresponding to Raman shifts of 1,048; 1,361; 1,370; 1,528; 2,225; 2,554 cm^{-1} did not have differences in fluorescence intensity between stages 2 and 3. A group of analytes (Raman shifts of 933; 1,157; 1,230; 1,304; 1,365; 1,370; 1,528; 1,554; 1,609; 1,627 cm^{-1}) maintained the stability of fluorescence intensity between stages 1 and 3. The most stable were analytes with Raman shifts of 1,230; 1,361; 1,365; 1,370; 1,528; 1,609; 1,627 cm^{-1}, which did not exhibit significant changes between at least two pairs of stages ($p > 0.05$), among which 2 analytes (1,370 and 1,528 cm^{-1}) did not have significant changes at all three stages (Tables 2, 3).

Table 2

Repeated Measures ANOVA for the 1,370 cm^{-1} Analyte

Pairwise comparisons (Durbin – Conover post-hoc analysis)	Statistics	*p*
1,370 (stage 1) – 1,370 (stage 2)	1.913	0.061
1,370 (stage 1) – 1,370 (stage 3)	0.137	0.892
1,370 (stage 2) – 1,370 (stage 3)	1.776	0.081

Note. $\chi^2 = 4.36$; df = 2; $p = 0.113$ (Friedman test).

Table 3

Repeated Measures ANOVA for the 1,528 cm^{-1} Analyte

Pairwise comparisons (Durbin – Conover post-hoc analysis)	Statistics	*p*
1,528 (stage 1) – 1,528 (stage 2)	0.136	0.892
1,528 (stage 1) – 1,528 (stage 3)	1.701	0.095
1,528 (stage 2) – 1,528 (stage 3)	1.565	0.123

Note. $\chi^2 = 3.48$; df = 2; $p = 0.176$ (Friedman test).

The Spearman's correlation demonstrated that correlation between the stages was observed only for a limited number of analytes. The 890- (Table 4) and 1,117 cm^{-1} analytes demonstrated significant correlation between stages 1 and 2, the 1,204 cm^{-1} analyte – between stages 2 and 3, and the 753, 830, 1,204 (Table 5), and 2,225 cm^{-1} analytes – between stages 1 and 3.

Table 4

Spearman's Rank Correlation Matrix for the 890 cm^{-1} Analyte

Parameter	890 (stage 1)	890 (stage 2)	890 (stage 3)
890 (stage 1) Spearman's ρ (rho)	–	–	–
df (degrees of freedom)	–	–	–

End of table 4

Parameter	890 (stage 1)	890 (stage 2)	890 (stage 3)
p	–	–	–
890 (stage 2) Spearman's ρ (rho)	0.570**	–	–
df (degrees of freedom)	26	–	–
p	0.002	–	–
890 (stage 3) Spearman's ρ (rho)	0.007	0.072	–
df (degrees of freedom)	26	26	–
p	0.972	0.717	–

Table 5

Spearman's Rank Correlation Matrix for the 1,204 cm^{-1} Analyte

Parameter	1,204 (stage 1)	1,204 (stage 2)	1,204 (stage 3)
1,204 (stage 1) Spearman's ρ (rho)	–	–	–
df (degrees of freedom)	–	–	–
p	–	–	–
1,204 (stage 2) Spearman's ρ (rho)	–0.051	–	–
df (degrees of freedom)	26	–	–
p	0.797	–	–
1,204 (stage 3) Spearman's ρ (rho)	–0.386*	0.430*	–
df (degrees of freedom)	26	26	–
p	0.042	0.023	–

DISCUSSION

RS of 30 placental samples (native material, samples fixed in 10% neutral buffered formalin for 24 hours, and deparaffinized sections from paraffin blocks) revealed significant changes in spectral characteristics reflecting changes in the biochemical composition of the placental tissue. The data obtained demonstrated that each sample preparation method had a significant effect on the placental spectral profile.

The greatest variability in spectral characteristics was observed in native samples, where 30 of 33 analytes did not follow a normal distribution. This could be due to either the natural heterogeneity of placental tissue or the initial degradation of biomolecules (lipids, proteins) after cessation of blood supply [13]. Moreover, the high coefficient of variation in labile analytes, including lipid and protein components, confirmed their sensitivity to post-extraction changes.

Fixation in formalin resulted in significant stabilization of the spectral profile, manifested by a decrease in the number of anomalously distributed shifts to 13. This is apparently due to formalin ability to form cross-links between proteins, which reduces macromolecular degradation. At the same time, a significant decrease in the correlation between native and fixed samples indicated profound biochemical changes caused by protein denaturation and modification of lipid structures [14].

The deparaffinization process caused a repeated increase in the number of deviations from the normal distribution (19 anomalously distributed shifts) and, as a result, a discrepancy between these spectral profiles and those of the fixed samples. The correlation between fixed and deparaffinized samples was maintained for only one analyte (1,204 cm^{-1}) and indicated both a change in formalin-induced shifts and a pronounced effect of paraffin on the lipid and alcohol content and on hydrophobic components [15].

The Friedman test with post-hoc analysis allowed us to divide all analytes into three groups: labile, partially stable (showing stability of fluorescence intensity between one or two pairs of stages), and absolutely stable (analytes at 1.370 and 1,528 cm^{-1}), whose fluorescence intensity was stable across all three stages. Based on this, these vibrational modes can be further considered as potential reference markers for the analysis of materials with different preanalytical histories.

A limitation of the study was a relatively small sample size (n = 30) and the exploratory nature of the multiple comparison analysis without strict adjustments. However, the identified patterns provide a basis for targeted research with pre-formulated hypotheses.

CONCLUSION

This study demonstrates that preanalytical processing of placental tissue significantly affects its biochemical composition and spectral characteristics. Native tissue differs radically from processed tissue; its spectra cannot be directly compared with fixed/deparaffinized samples without adjustments. Machine learning methods are necessary to compare spectral data from native and processed tissue due to the nonlinear nature of changes. Thus, Raman spectroscopy can be used to monitor changes in placental tissue, but it requires consideration of the influence of preanalytical factors on data interpretation and the development of standardized protocols, with the potential for retrospective studies and implementation of the method in clinical practice.

REFERENCES

1. Gromova O.A., Torshin I.Yu., Chuchalin A.G., Lazebnik L.B. Ferritin as a Biomarker of Multiple Organ Pathology: Anti-in-

flammatory and Antioxidant Peptides of Standardized Human Placenta Hydrolysate. *Experimental and Clinical Gastroenterology.* 2024;(8):113–122. (In Russ.). DOI: 10.31146/1682-8658-ecg-228-8-113-122.
2. Chernyshova A.L., Chernyakov A.A., Truschuk Yu.M., Yunusova N.V., Sevostyanova N.V., Arkhipova Ya.I. et al. Molecular Genetic and Biochemical Profiles of Malignant Neoplasms during Pregnancy. *Advances in Molecular Oncology.* 2024;11(3):32–40. (In Russ.). DOI: 10.17650/2313-805X-2024-11-3-32-40.
3. Zhuang Z., Zhu M., Huang Y., Liu J., Guo Z., Xiong K. et al. Study of molecule variation in various grades of human nuclear cataracts by confocal micro-Raman spectroscopy. *Appl. Phys. Lett.* 2012;101(17):173701. DOI: 10.1063/1.4762838.
4. Zhuang Z., Li N., Guo Z., Zhu M., Xiong K., Chen S. Study of molecule variations in renal tumor based on confocal micro-Raman spectroscopy. *J. Biomed. Opt.* 2012;18(3):031103. DOI: 10.1117/1.JBO.18.3.031103.
5. Zhuo S., Chen J., Wu G., Xie S., Zheng L., Jiang X. et al. Quantitatively linking collagen alteration and epithelial tumor progression by second harmonic generation microscopy. *Appl. Phys. Lett.* 2010;96(21):213704. DOI: 10.1063/1.3441337.
6. Zheng-Fei Z., Han-Ping L., Zhou-Yi G., Shuang-Mu Z., Bi-Ying Y., Xiao-Yuan D. Second-harmonic generation as a DNA malignancy indicator of prostate glandular epithelial cells. *Chinese Physics B.* 2010;19(4):049501. DOI: 10.1088/1674-1056/19/4/049501.
7. Chen S.J., Zhang Y., Ye X.P., Hu K., Zhu M.F., Huang Y.Y. et al. Study of the molecular variation in pre-eclampsia placenta based on micro-Raman spectroscopy. *Archives of Gynecology and Obstetrics.* 2014;290(5):943–946. DOI: 10.1007/s00404-014-3282-9.
8. Pielesz A., Bobiński R., Biniaś D., Gawłowski A., Waksmańska W., Ulman-Włodarz I. et al. FT Raman spectroscopy in the evaluation of biomarkers of normal and pathological placenta tissue. *Molecular and Cellular Biochemistry.* 2019;458(1):125–132. DOI: 10.1007/s11010-019-03536-5.
9. Başar G., Parlatan U., Şeninak Ş., Günel T., Benian A., Kalelioğlu İ. Investigation of Preeclampsia Using Raman Spectroscopy. *Journal of Spectroscopy.* 2012;27(4):376793. DOI: 10.1155/2012/376793.
10. Monaghan J.F., Cullen D., Wynne C., Lyng F.M., Meade A.D. Effect of pre-analytical variables on Raman and FTIR spectral content of lymphocytes. *Analyst.* 2023;148(21):5422–5434. DOI: 10.1039/D3AN00686G.
11. Bocklitz T., Walter A., Hartmann K., Rösch P., Popp J. How to pre-process Raman spectra for reliable and stable models? *Analytica Chimica Acta.* 2011;704(1):47–56. DOI: 10.1016/j.aca.2011.06.043.
12. Campanella B., Legnaioli S., Onor M., Benedetti E., Bramanti E. The role of the preanalytical step for human saliva analysis via vibrational spectroscopy. *Metabolites.* 2023;13(3):393. DOI: 10.3390/metabo13030393.
13. Movasaghi Z., Rehman, S., Rehman Ihtesham U. Raman spectroscopy of biological tissues. *Applied Spectroscopy Reviews*. 2007;42(5):493–541. DOI: 10.1080/05704920701551530.
14. Roy A., Mantay M., Brannan C., Griffiths S. Placental tissues as biomaterials in regenerative medicine. *BioMed Research International.* 2022;2022(1):6751456. DOI: 10.1155/2022/6751456.
15. Howat W.J., Wilson B.A. Tissue fixation and the effect of molecular fixatives on downstream staining procedures. *Methods.* 2014;70(1):12–19. DOI: 10.1016/j.ymeth.2014.01.022.
16. Alturkistani H., Faris T., Zuhair M. Histological Stains: A Literature Review and Case Study. *Global Journal of Health Science.* 2015;8:72–72. DOI: 10.5539/gjhs.v8n3p72.

Author Contribution

Rodionov V.E. – conception and design, analysis and interpretation of the data, substantiation of the manuscript or critical revision of the manuscript for important intellectual content. Avdalyan A.M – conception and design. Nichiporov A.I., Kukushkin V.I., Chernov I.A. – analysis and interpretation of the data. Avraamova S.T. – substantiation of the manuscript or critical revision of the manuscript for important intellectual content. Kirillov Yu.A. – conception and design, substantiation of the manuscript or critical revision of the manuscript for important intellectual content, final approval of the manuscript for publication.

Author Information

Rodionov Vladimir E. – Pathologist, Moscow Multidisciplinary Clinical Center "Kommunarka", Moscow; Lecturer, Department of Pathological Anatomy and Forensic Medicine, Tyumen State Medical University, Tyumen, rodionovforever@mail.ru, https://orcid.org/0000-0003-0842-4169

Avdalyan Ashot M. – Dr. Sci. (Med.), Head of the Pathological Anatomy Department, Moscow Multidisciplinary Clinical Center "Kommunarka", Moscow, ashot_avdalyan@mail.ru, https://orcid.org/0000-0002-2229-1713

Nichiporov Andrey I. – Laboratory Research Assistant, Moscow Multidisciplinary Clinical Center "Kommunarka", Moscow, andrei.ni4iporov@yandex.ru, https://orcid.org/0009-0006-6895-5278

Chernov Igor A. – Cand. Sci. (Biology), Associate Professor, Head of the Department of Pathological Anatomy and Forensic Medicine, Tyumen State Medical University, Tyumen, Chernov@tyumsmu.ru, https://orcid.org/0000-0002-6475-5731

Kukushkin Vladimir I. – Cand. Sci. (Physics and Mathematics), Senior Researcher, Laboratory of Non-equilibrium Electronic Processes, Institute of Solid State Physics, Russian Academy of Sciences, Chernogolovka, kukushvi@mail.ru, https://orcid.org/0000-0001-6731-9508

Avraamova Sofia T. – Cand. Sci. (Med.), Associate Professor, Institute of Clinical Morphology and Digital Pathology, The First Sechenov Moscow State Medical University, Moscow, avraamovast@mail.ru, https://orcid.org/0000-0001-9704-5915

Kirillov Yuri A. – Dr. Sci. (Med.), Professor, Pathologist, Moscow Multidisciplinary Clinical Center "Kommunarka", Moscow; Leading Researcher, Clinical Morphology Laboratory, A.P. Avtsyn Research Institute of Human Morphology, B.V. Petrovsky Russian Scientific Center of Surgery, Moscow; Professor, Department of Pathological Anatomy and Forensic Medicine, Tyumen State Medical University, Tyumen, youri_kirillov@mail.ru, https://orcid.org/0000-0003-3555-0902

(✉) **Rodionov Vladimir E.,** rodionovforever@mail.ru

Received on June 18, 2025;
approved after peer review on November 06, 2025;
accepted on November 20, 2025

УДК 618.19-006.6:577.217
https://doi.org/10.20538/1682-0363-2026-2-91-100

The Potential Application of the Random Forest Method to Explore the Association between MicroRNAs and Tissue and Molecular Genetic Biomarkers of Breast Cancer

Studenikina A.A.[1, 2], Mihailovsky M.A.[3], Timofeev V.S.[3], Arkhipov S.A.[1, 2], Autenshlyus A.I.[1, 2]

[1] *Novosibirsk State Medical University*
52 Krasny Ave., 630091 Novosibirsk, Russian Federation

[2] *Institute of Molecular Biology and Biophysics, Federal Research Center of Fundamental and Translational Medicine*
2 Timakova St., 630060 Novosibirsk, Russian Federation

[3] *Novosibirsk State Technical University*
20 Karl Marx Ave., 630073 Novosibirsk, Russian Federation

ABSTRACT

Aim. Exploring the potential of using a random forest method (RFM) to identify associations between serum levels of microRNAs miR-181a and miR-25 and the expression of the following markers: E-cadherin (CDH1), type II collagen (CII), integrin beta-1 (ITGB1), cyclin D1 (CCND1), and T-lymphocyte costimulator (CD86), as well as their relationship with clinically relevant molecular genetic markers (ER, PR, HER2, Ki-67) in patients with breast cancer (BC).

Materials and methods. We recruited 44 BC patients with invasive ductal carcinoma who had not received neoadjuvant treatment. Serum levels of miR-181a and miR-25 were measured using digital droplet PCR, and the expression of CDH1, CII, ITGB1, CCND1, CD86, ER, PR, HER2, and Ki-67 in tumor tissue samples was assessed via immunohistochemistry. Spearman's correlation analysis and the RFM were applied to assess associations between variables.

Results. Spearman's correlation analysis did not reveal any significant linear relationships between the studied parameters ($p > 0.05$). However, the RFM identified nonlinear associations: for miR-181a, the optimal predictive model included CDH1 and CCND1 (MAE = 4.267); for miR-25, ITGB1 and CCND1 (MAE = 16.255). Among clinical and pathological characteristics, statistically significant positive correlations were found between CII and ER ($r = 0.498$; $p = 0.001$) and PR ($r = 0.354$; $p = 0.018$). The RFM models demonstrated the highest accuracy in predicting the HER2 status (82.6%) when using a combination of ITGB1, miR-181a, and CDH1.

Conclusion. The RFM revealed complex nonlinear associations between microRNAs and tissue markers of tumor progression that were not detected by conventional statistical methods. These findings are exploratory in nature and provide a foundation for further research aimed at validating these biomarkers and elucidating their role in the pathogenesis of various breast cancer subtypes.

Keywords: breast cancer, HER2, microRNA, machine learning, random forest, molecular markers, epithelial – mesenchymal transition

Conflict of interest. The authors declare the absence of obvious or potential conflict of interest related to the publication of this article.

Source of financing. The study was conducted within the state assignment of Novosibirsk State Medical University, Ministry of Health of the Russian Federation (Registration No. 115060410035), and the research project of the Federal Research Center for Fundamental and Translational Medicine, Research Institute of Molecular Biology and Biophysics (Registration No. 125031203556-7).

✉ *Studenikina Anastasiia A.,* aastudenikina@frcftm.ru

Conformity with the principles of ethics. All patients signed an informed voluntary consent to participate in the study. The study was approved by the Ethics Committee at the Research Institute of Molecular Biology and Biophysics of the Federal Research Center for Fundamental and Translational Medicine (Minutes No. 28 dated September 27, 2023).

For citation: Studenikina A.A., Mihailovsky M.A., Timofeev V.S., Arkhipov S.A., Autenshlyus A.I. The Potential Application of the Random Forest Method to Explore the Association between MicroRNAs and Tissue and Molecular Genetic Biomarkers of Breast Cancer. *Bulletin of Siberian Medicine.* 2026;25(2):91–100. https://doi.org/10.20538/1682-0363-2026-2-91-100.

Возможность использования метода «случайного леса» для поиска взаимосвязи микроРНК с тканевыми и молекулярно-генетическими маркерами рака молочной железы

Студеникина А.А.[1, 2], Михайловский М.А.[3], Тимофеев В.С.[3], Архипов С.А.[1, 2], Аутеншлюс А.И.[1, 2]

[1] *Новосибирский государственный медицинский университет (НГМУ)*
Россия, 630091, г. Новосибирск, Красный пр., 52

[2] *Научно-исследовательский институт молекулярной биологии и биофизики (НИИМББ), Федерального исследовательского центра фундаментальной и трансляционной медицины (ФИЦ ФТМ)*
Россия, 630060, г. Новосибирск, ул. Тимакова, 2

[3] *Новосибирский государственный технический университет (НГТУ)*
Россия, 630073, г. Новосибирск, пр. Карла Маркса, 20

РЕЗЮМЕ

Цель. Поиск возможности выявления с помощью метода «случайного леса» (МСЛ) взаимосвязи между уровнем микроРНК miR-181a, miR-25 и экспрессией маркеров: Е-кадгерина (CDH1), коллагена II (CII), интегрина бета-1 (ITGB1), циклина D1 (CCND1) и белка-костимулятора Т-лимфоцитов (CD86), а также их ассоциации с клинически значимыми молекулярно-генетическими маркерами (ER, PR, HER2, Ki-67) у пациенток с раком молочной железы (РМЖ).

Материалы и методы. У 44 пациенток с инвазивной протоковой карциномой молочной железы (без неоадъювантной терапии) определяли экспрессию микроРНК miR-181a и miR-25 в сыворотке крови, используя цифровую капельную полимеразную цепную реакцию (ПЦР). Экспрессию CDH1, CII, ITGB1, CCND1, CD86, ER, PR, HER2 и Ki-67 анализировали с помощью иммуногистохимии в образцах опухолевой ткани. Для анализа взаимосвязей использовали корреляционный анализ Спирмена и алгоритм МСЛ.

Результаты. Корреляционный анализ не выявил статистически значимых линейных взаимосвязей между исследуемыми параметрами ($p > 0,05$). Метода «случайного леса» показал наличие нелинейных ассоциаций: для miR-181a оптимальная прогностическая модель включала CDH1 и CCND1 (MAE = 4,267), для miR-25 – ITGB1 и CCND1 (MAE = 16,255). Из клинико-патологических характеристик статистически значимые положительные корреляции выявлены для CII с ER ($r = 0,498$; $p = 0,001$) и PR ($r = 0,354$; p = 0,018). Модели МСЛ продемонстрировали наибольшую точность предсказания HER2-статуса (82,6%) при использовании комбинации ITGB1, miR-181a и CDH1.

Заключение. Алгоритм МСЛ выявил сложные нелинейные взаимосвязи между miR-181a, miR-25 и тканевыми маркерами опухолевой прогрессии, которые ранее не обнаружены стандартными статистическими методами. Полученные результаты носят поисковый характер и формируют основу для дальнейших исследований по валидации данных биомаркеров и их роли в патогенезе различных подтипов РМЖ.

Ключевые слова: рак молочной железы, HER2, микроРНК, машинное обучение, метод «случайного леса», молекулярные маркеры, эпителиально-мезенхимальный переход

Конфликт интересов. Авторы декларируют отсутствие явных и потенциальных конфликтов интересов, связанных с публикацией настоящей статьи.

Источник финансирования. Исследование выполнено в рамках темы государственного задания ФГБОУ ВО «Новосибирский государственный медицинский университет» Министерства здравоохранения Российской Федерации (регистрационный номер 115060410035) и в рамках темы НИР ФГБНУ «Федеральный исследовательский центр фундаментальной и трансляционной медицины», Научно–исследовательский институт молекулярной биологии и биофизики (регистрационный номер 125031203556-7).

Соответствие принципам этики. Все пациенты подписали информированное согласие на участие в исследовании. Исследование одобрено этическим комитетом НИИМББ, НИЦ АТМ (протокол № 28 от 27.09.2023).

Для цитирования: Студеникина А.А., Михайловский М.А., Тимофеев В.С., Архипов С.А., Аутеншлюс А.И. Возможность использования метода «случайного леса» для поиска взаимосвязи микроРНК с тканевыми и молекулярно-генетическими маркерами рака молочной железы. *Бюллетень сибирской медицины.* 2026;25(2):91–100. https://doi.org/10.20538/1682-0363-2026-2-91-100.

INTRODUCTION

Breast cancer (BC) annually claims the lives of thousands of women, underscoring the need for an in-depth study of the molecular mechanisms of its pathogenesis. Particular attention should be paid to analyzing the association of potential markers with classical molecular genetic indicators: estrogen receptors (ER), progesterone receptors (PR), human epidermal growth factor receptor 2 (HER2), and the Ki-67 proliferation index.

MicroRNAs (miRs) are small non-coding RNAs that regulate gene expression at the post-transcriptional level [1]. They function as both oncogenes and tumor suppressors, affecting mRNA stability and translation. Dysregulation of microRNAs is associated with various types of cancer [2]. Specifically, miR-181a and miR-25 are involved in proliferation, invasion, and modulation of the immune response [3, 4]. It is known that miR-181a can reduce ER expression in BC cell culture, and its high level correlates with low PR expression, HER2 overexpression, and a high Ki-67 index [5–7]. MiR-25, in turn, is involved in modulating ER and PR signaling pathways [5].

The study by J. Feng et al. confirms that abnormal microRNA expression is accompanied by the development of cellular transformation towards carcinogenesis, which is also associated with the ability of microRNAs to promote epithelial – mesenchymal transition (EMT) [8]. This process is characterized by a decrease in the expression of epithelial markers, such as E-cadherin (CDH1), and the activation of mesenchymal markers, including integrin beta-1 (ITGB1) [9]. During this process, tumor cells lose intercellular connections and acquire increased mobility and invasiveness, which is associated with a higher degree of malignancy and metastasis to lymph nodes [10]. According to A.H. Ali et al., low CDH1 expression was characteristic of patients with negative ER and HER2 status [11].

We previously showed that BC patients had elevated levels of miR-181a, miR-25, CD86, ITGB1, and cyclin D1 (CCND1) along with reduced CDH1 expression compared to patients with benign breast diseases [12–14]. However, no statistically significant relationships were found between these biomarkers, indicating the need for more sophisticated analytical tools. It should be emphasized that each of these biomarkers plays an important role in BC pathogenesis. CCND1 is a key regulator of the cell cycle and can increase the transcriptional activity of ER, contributing to the formation of resistance to endocrine therapy [15]. CD86 is a co-stimulatory molecule involved in T-lymphocyte activation and the formation of an anti-tumor immune response [16]. Type II collagen (CII), as a major component of the cartilage matrix, may be involved in extracellular matrix remodeling and the creation of metastatic niches in BC [17]. Despite the fact that CCND1, CD86, and CII are not classic inducers of EMT, their influence on key signaling pathways, such as TGF-β, Wnt/β-catenin, and integrin-dependent signaling, suggests their indirect role in EMT progression [17, 18].

Machine learning algorithms offer objective and reproducible tools for identifying hidden patterns and relationships between biomarkers that may be overlooked by traditional analysis, which is a promising direction for studying the molecular mechanisms of the development and progression of oncological diseases [19]. The Random Forest Method (RFM) is a machine learning algorithm based

on constructing an ensemble of decision trees, each of which is built on its own unique subset of data and features (bootstrap sample), and then averaging their predictions. This significantly reduces prediction variance and the tendency to overfit compared to single trees [20].

The first step is to form the training sample $D = \{(X_i, y_i)\}_{t=1}^{N}$, where N is the number of objects, X_i is a set of k features for the i-th observation, and y_i is the value of the target variable. Then, a function that calculates the final prediction of the values of the variable of interest is sought. An ensemble of T regression trees, $\{h_t\}_{t=1}^{T}$, is formed, where h_t is an individual decision tree. Next, a bootstrap sample is formed for each tree h_t: from the training sample D , a training set D_t is created by random sampling of N observations; some observations will appear in D_t several times, and some will not appear at all. The construction of a regression decision tree on D_t begins with the root node, which contains the entire sample D_t . Then, for each node, a subset of features is randomly selected from all features, and among the selected features, the best feature and the best split value (point) are found to maximize the reduction of the variance of the target variable y in the two child nodes. The criterion is the minimization of the Mean Squared Error (MSE):

$$MSE = \frac{1}{n}\sum_{i=1}^{n}(y_i - \hat{y}_i)^2,$$

where $\hat{y}_i$ is the obtained prediction of the target variable, and n is the number of observations. The sample is then split into two based on the found point and features. The splitting procedure is recursively repeated for each child node until one of the stopping criteria is met (maximum tree depth reached, split does not reduce MSE sufficiently, etc.). When the stopping criterion is reached, the prediction in that node becomes the average value of the target variable y of all training observations that fell into that node. The prediction of the trained model for a new observation x is obtained by finding the terminal node for x in each tree h_t of the ensemble. The terminal node is found by following the splitting rules compiled during the training of the decision tree. The prediction of the terminal node is considered as the model's prediction. The final RFM prediction is found by averaging the predictions of all trees:

$$\hat{y} = \frac{1}{T}\sum_{t=1}^{T} h_t.$$

RFM has shown promising results in predicting the risk of BC development, early detection of recurrences, and predicting a response to chemotherapy [21–23].

The present study is exploratory in nature and aims at determining the possibility of effectively using machine learning algorithms to analyze the relationships between microRNAs and molecular tumor markers in the context of a limited sample size.

The aim of the study was to explore the potential of using the RFM algorithm to identify the association between the levels of miR-181a, miR-25 and the expression of the molecular markers CDH1, CII, ITGB1, CCND1, and CD86, as well as their association with key clinicopathological characteristics (ER, PR, HER2, Ki-67) in BC patients.

MATERIALS AND METHODS

The study involved 44 female patients with the diagnosis of ductal breast carcinoma of no special type, aged 23 to 72 years (mean age 55 years), who received treatment at the Breast Tumor Department of City Clinical Hospital (CCH) No. 1 (Novosibirsk). Inclusion criteria: primary BC without neoadjuvant therapy; histologically confirmed diagnosis of ductal breast carcinoma of no special type; histological tumor grade G2. Exclusion criteria: concomitant malignant neoplasms; acute infectious diseases or exacerbation of chronic infections; distant metastases. The expression of ER, PR, HER2, and Ki-67 was determined according to standard clinical protocols of CCH No. 1 and provided in patient charts. A detailed description of the patients is presented in Table 1.

Table 1

Clinical and Pathological Characteristics of BC Patient Tumors

Parameter	Category	Abs. Number (n)	Share (%)
Tumor Size (T)	T1 (<2 cm)	13	29.5
	T2 (2–5 cm)	31	70.5
Lymph Node Involvement (N)	N0	28	63.6
	N1	12	27.3
	N2	4	9.1
Estrogen Receptors (ER)	ER+ (≥1%)	25	56.8
	ER– (<1%)	19	43.2
Progesterone Receptors (PR)	PR+ (≥1%)	22	50.0
	PR– (<1%)	22	50.0
Human Epidermal Growth Factor Receptor 2 (HER2)	3+	9	20.5
	0 or 1+	35	79.5
Ki-67 Proliferative Index	<20%	18	40.9
	≥20%	26	59.1

MicroRNAs were isolated from 300 µl of blood serum using the NucleoSpin miRNA Plasma Kit (Macherey–Nagel, Germany). M–MuLV–RH (Biolabmix, Russia) and miR-specific primers were used for reverse transcription. Detailed primer characteristics were presented in a previously published work [16]. Quantitative expression was assessed by digital droplet PCR on the QX200 AutoDG system (Bio–Rad, USA) with TaqMan detection. U6 small nuclear RNA served as an internal control sample.

Immunohistochemistry. The expression of the studied markers was determined on deparaffinized tumor tissue sections using monoclonal antibodies: Anti-E-Cadherin (Cat. No. 610181, BD Biosciences, USA), Anti-CD29/Clone 18 (Cat. No. 610467, BD Transduction Laboratories, USA), Anti-CII (COL2A1/M2139, Cat. No. sc-52658, Santa Cruz Biotechnology, Inc., USA), Anti-Cyclin D1 and Anti-B7–2 (PAA585Hu01, Cloud–Clone Corp., China). Visualization was performed using the VECTASTAIN ABC Kit (Vector Laboratories, USA) and analyzed with the ImageJ software (National Instruments Corporation, USA). Marker expression levels were calculated as the percentage of positively stained cells, using at least 10 fields of view at ×400 magnification for each patient.

The expression levels of Her2/neu, estrogen (ER) and progesterone (PR) receptors, as well as the Ki-67 proliferation marker were assessed in BC samples according to the methods [24] recommended for determining molecular genetic subtypes of BC (Gallen International Expert Consensus, 2011). The receptor status for ER and PR was determined using the ER/PR pharmDx Kit (K4071, Dako). The Ultra View Universal DAB Detection Kit (4B5 antibodies) was used to determine the HER2/neu status. The Ki-67 protein (MIB-1 clone) was detected using a set of diagnostic antibodies from Dako. All antibodies were used at a dilution of 1:100. ER and PR expression levels were assessed using the Allred scoring system [25]. Her2/neu expression levels were assessed using the generally accepted scoring system (from 0 to 3+).

Data processing was carried out using the Python programming language (version 3.12). The Scikit – learn package (version 1.4.0) for Data Science and Machine Learning was used to calculate Spearman's rank correlation coefficients (r) and develop the RFM model. Normality of distribution was checked using the Shapiro – Wilk test. The non-parametric Mann – Whitney U-test was used to assess differences in marker expression levels between the patient groups. Data were presented as the median, the 25th and the 75th percentiles Me (Q_{25}; Q_{75}). Differences were considered to be statistically significant at $p < 0.05$.

The quality of RFM regression models was assessed using the Mean Absolute Error (MAE), which indicates the average deviation of predicted values from actual values. The smaller the MAE, the more accurately the model describes the data [26]. MAE is expressed in the same units as the target variable. The MAE formula is:

$$\mathrm{MAE} = \frac{1}{n}\sum_{i=1} |y_i - \hat{y}_i|,$$

where y_i is the true value, $\hat{y}_i$ is the predicted value, and n is the number of observations. For RFM classification tasks, the precision metric was used, calculated as the ratio of correctly predicted positive cases to the total number of predicted positive cases.

Given the limited sample size ($n = 44$), which did not allow for splitting the data into training and test subsets without losing statistical representativeness, RFM model training and validation were performed on the entire dataset. The relatively small number of predictors (molecular markers) allowed for finding the most suitable model to describe the existing relationships through complete enumeration of all predictor combinations. For each possible combination of predictors, 500 models with different randomness parameters were built, and the quality was assessed by averaging the MAE across all models.

RESULTS

Initial analysis using the Spearman's rank correlation coefficient did not reveal significant relationships between the levels of miR-181a, miR-25, and markers of adhesion, proliferation, and immune response (Table 2, $p > 0.05$ for all comparisons). This indicated the absence of simple linear dependencies and the need for more complex analytical approaches.

Table 2

Correlations between MicroRNA Levels and Molecular Markers

Marker	miR-181a		miR-25	
	r	*p*	*r*	*p*
CDH1	– 0.049	0.753	– 0.018	0.910
ITGB1	0.036	0.815	– 0.071	0.648

End of table 2

Marker	miR-181a		miR-25	
	r	*p*	*r*	*p*
CCND1	0.006	0.970	– 0.124	0.421
CII	0.069	0.657	– 0.091	0.557
CD86	– 0.081	0.600	0.053	0.731

The RFM was used to identify more complex nonlinear associations. The optimal model corresponded to the combination of predictors yielding the smallest MAE. For miR-181a, the best predictive model included the combination of markers CDH1 and CCND1 (MAE = 4.267). For miR-25, the optimal set of predictors was ITGB1 and CCND1 (MAE = 16.255). Figure presents a comparison of predicted and actual values for both models, demonstrating their ability to detect hidden patterns in the data.

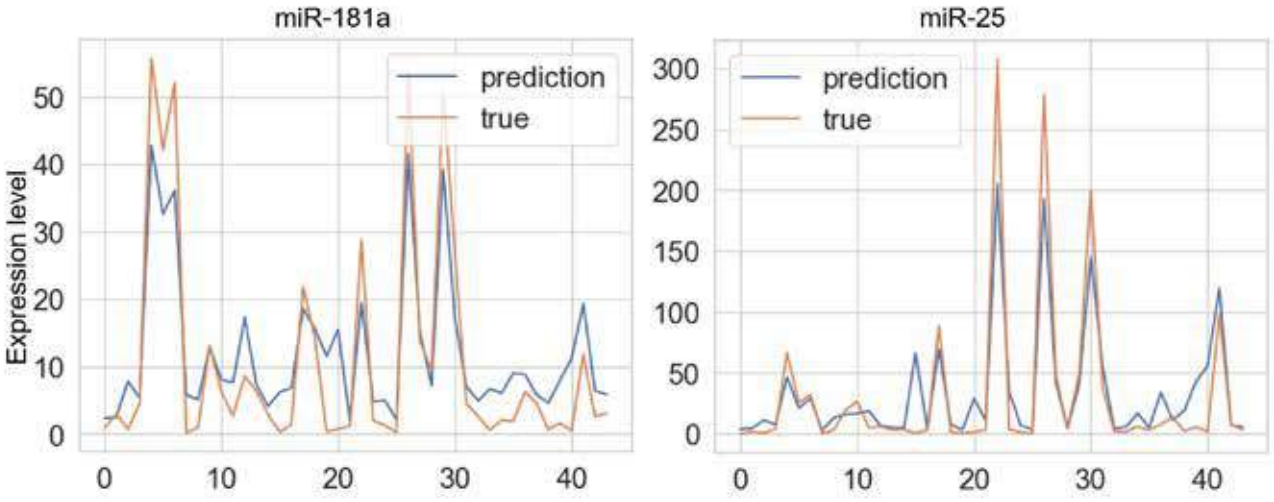

Figure. Comparison of predicted and actual levels of miR-181a and miR-25: X-axis: patients, $n = 44$; Y-axis: microRNA concentration

The analysis of the relationships between the studied biomarkers and key clinicopathological tumor parameters (ER, PR, HER2, Ki-67) showed statistically significant correlations only for CII. Moderate positive correlations were found between CII expression and estrogen receptor status ($r = 0.498$; $p = 0.001$) and progesterone receptor status ($r = 0.354$; $p = 0.018$, Table 3).

Table 3

Correlation between MicroRNA Levels, Molecular Markers, and Molecular Genetic Tumor Parameters

Marker		ER	PR	HER2	Ki-67
miR-181a	*r*	– 0.156	– 0.036	0.150	0.176
	p	0.311	0.819	0.330	0.253
miR-25	*r*	– 0.166	– 0.007	0.057	0.300
	p	0.282	0.967	0.712	0.048
CDH1	*r*	0.089	0.047	0.024	– 0.051
	p	0.568	0.763	0.879	0.744
ITGB1	*r*	0.326	0.180	0.168	– 0.121
	p	0.031	0.243	0.275	0.433
CII	*r*	0.498*	0.354*	0.076	– 0.196
	p	0.001	0.018	0.623	0.202
CCND1	*r*	– 0.016	0.118	0.076	– 0.164
	p	0.917	0.446	0.622	0.288
CD86	*r*	0.030	– 0.058	– 0.277	0.204
	p	0.846	0.708	0.069	0.183

*$p < 0.05$.

Further analysis of marker level differences between the patient groups showed that CII expression was statistically significantly higher in tumors with positive hormone receptor status (Table 4). In ER-positive samples, the *Me* expression level was 20.3% compared to 6.9% in ER-negative samples ($p = 0.010$). A similar trend was noted for the PR status: 20.2% in PR-positive versus 9.8% in PR-negative tumors ($p = 0.016$). For ITGB1, there was a trend toward higher expression in ER-positive tumors (*Me* 18.8% vs. 11.5%), but the difference did not reach statistical significance ($p = 0.052$).

The application of the RFM for predicting the BC receptor status showed varying levels of accuracy depending on the marker. The best result was achieved for the HER2 status (82.6% accuracy) using the combination of ITGB1, miR-181a, and CDH1.

Table 4

Analysis of the Expression of the Studied Markers Depending on Molecular Genetic Tumor Parameters, *Me* (Q_{25}; Q_{75})

Parameters	ER–, *n* = 19	ER+, *n* = 25	PR–, *n* = 22	PR+ *n* = 22	HER2–0 или 1+, *n* = 35	HER2+ 3+, *n* = 9	Ki-67 <20%, *n* = 18	Ki-67 ≥20%, *n* = 26
miR-181a	2.9 (1.6–14.4)	3.0 (0.8–11.3)	3.0 (1.5–18.0)	2.9 (0.9–10.3)	2.9 (1.0–9.4)	3.1 (1.4–52.8)	2.6 (0.8–18.1)	4.5 (1.6–13.1)
	p = 0.414		*p* = 0.438		*p* = 0.383		*p* = 0.557	
miR-25	5.0 (3.1–26.7)	3.3 (1.3–25.8)	3.6 (2.2–28.1)	4.5 (1.3–24.2)	3.6 (1.8–25.5)	5.0 (0.8–49.2)	3.3 (1.0–16.6)	5.5 (3.1–38.6)
	p = 0.337		*p* = 0.656		*p* = 0.977		*p* = 0.162	
CDH1	81.5 (30.8–94.0)	90.3 (59.5–96.4)	84.0 (36.8–94.5)	89.4 (67.1–96.3)	88.5 (58.9–94.8)	74.1 (31.4–96.3)	88.5 (49.3–95.4)	86.4 (38.8–94.8)
	p = 0.507		*p* = 0.664		*p* = 0.942		*p* = 0.925	
ITGB1	11.5 (5.4–19.1)	18.8 (10.5–80.6)	12.0 (6.1–20.4)	18.5 (8.2–80.1)	13.5 (6.3–46.1)	16.5 (9.8–24.9)	14.3 (5.9–26.4)	16.4 (7.4–46.1)
	p = 0.052		*p* = 0.236		*p* = 0.827		*p* = 0.690	
CII	6.9 (6.3–15.7)	20.3 (12.7–30.0)	9.8 (6.4–15.9)	20.2 (11.2–27.3)	14.4 (6.4–26.5)	14.4 (9.0–18.5)	15.7 (8.4–27.2)	14.4 (6.5–20.5)
	p = 0.010*		*p* = 0.016*		*p* = 0.942		*p* = 0.259	
CCND1	93.9 (77.1–97.2)	93.9 (83.1–97.6)	93.9 (74.6–96.8)	93.9 (85.8–97.7)	93.9 (80.7–97.3)	93.9 (87.9–97.4)	93.9 (83.1–98.0)	93.9 (77.1–96.7)
	p = 0.849		*p* = 0.451		*p* = 0.759		*p* = 0.207	
CD86	21.1 (10.9–26.4)	19.9 (15.2–29.2)	21.3 (10.9–27.3)	19.0 2.4–29.0)	20.7 (12.8–30.2)	19.0 (8.9–23.6)	20.7 (11.2–29.2)	19.9 (16.1–26.4)
	p = 0.924		*p* = 0.673		*p* = 0.244		*p* = 0.991	

The accuracy for the ER status was 69.5% using miR-25, CDH1, and CII. The accuracy for the PR status was 66.3% with predictors miR-181a, ITGB1, and CCND1. In contrast, predicting the Ki-67 level using miR-25 and CCND1 was the least accurate, indicated by high mean absolute error (MAE = 30.411).

DISCUSSION

The obtained data demonstrate the complex nature of the associations between the expression of miR-25, miR-181a and molecular markers in BC. The ability of the RFM algorithm to detect nonlinear associations that were not detectable by traditional correlation analysis methods emphasizes the potential of machine learning in studying the molecular mechanisms of carcinogenesis.

The identified association of miR-181a with CDH1 and CCND1 has a biological rationale. MiR-181a can influence E-cadherin by activating TGF-β/Smad-dependent mechanisms, promoting EMT [27]. Furthermore, miR-181a activates the PI3K-Akt signaling pathway, which enhances cell growth and proliferation, thereby influencing CDH1 expression [28]. The involvement of both CCND1 and CDH1 in regulating the Wnt/β-catenin signaling pathway may explain their joint inclusion in the predictive model for miR-181a [29]. A study on multiple myeloma by X. Yan et al. outlined the mechanisms underlying the regulation of the cell cycle by miR-181a through influencing CCND1 expression [30].

The connection of miR-25 with ITGB1 and CCND1 also finds confirmation at the molecular level. MiR-25 is involved in activating the Wnt/β-catenin pathway, promoting the nuclear accumulation of β-catenin and enhancing the transcription of target genes, including CCND1 [31]. ITGB1 is involved in the ILK-Akt signaling pathway, which enhances EMT, potentially indicating common regulatory mechanisms with miR-25 [32].

The statistically significant associations of CII with hormonal receptors (ER and PR) are of particular interest, as this marker is not well-studied in the context of BC. In breast cancer, different types of collagen demonstrate varied expression profiles [33]. It has been shown that different types of collagen have varying effects on the development of malignant growth, particularly BC, by impacting crucial cellular processes, including apoptosis, proliferation, and metastasis [33, 34]. For example, in triple-negative BC, decreased expression of COL2A1 (CII) is associated with an increased grade of tumor malignancy, metastasis, poor prognosis, and decreased survival [33]. Conversely, a decrease in COL1A1 expression may be associated with a decrease in BC malignancy. It has been established that COL1A1 expression is linked to ER/PR expression and metastasis status. In patients with ER-positive BC, higher COL1A1 expression correlates with aggressive cellular behavior and poor prognosis [34]. Our findings of increased CII expression in hormone-positive tumors may reflect

specific characteristics of extracellular matrix remodeling in luminal BC subtypes, which requires further investigation.

The high accuracy of HER2 status prediction (over 80%) using the combination of ITGB1, miR-181a, and CDH1 points to their potential diagnostic significance. This combination likely reflects the biological characteristics of the aggressive HER2-positive BC subtype comprehensively. ITGB1 enhances tumor aggressiveness through cellular remodeling, while miR-181a further amplifies proliferation and invasive potential by suppressing CDH1 expression. In contrast, the models for ER and PR status showed only moderate accuracy. This is most likely due to the significant heterogeneity of luminal BC subtypes, which vary greatly in both molecular characteristics and clinical behavior.

It should be emphasized that this study is exploratory in nature and has several significant limitations that must be considered when interpreting the results. The main limitations are the relatively small sample size and its heterogeneity in terms of clinical, morphological, and molecular genetic parameters. Due to the small number of observations, we did not split the data into training and test samples, which increases the risk of model overfitting and limits the generalizability of the results. Therefore, the findings should be considered as preliminary, requiring validation in larger and independent patient cohorts.

CONCLUSION

The obtained data demonstrate that the application of the random forest machine learning method is an effective approach for identifying complex, nonlinear associations between circulating microRNAs and markers in breast tumor tissue. The established associations (specifically between miR-181a, CDH1, and CCND1, as well as between miR-25, ITGB1, and CCND1) were not detected using standard correlation analysis methods. These results are of fundamental importance as they allow for the hypothesis of coordinated regulation of key processes in tumor progression: loss of cell adhesion (CDH1), enhanced migration (ITGB1), and disruption of the cell cycle (CCND1). Although the resulting models are not intended for direct clinical application at this stage, they represent an important starting point for future research in this direction. The findings underscore the potential of biomarker combinations for patient stratification and prediction of molecular BC subtypes, especially the HER2 status.

REFERENCES

1. Rani V., Sengar R.S. Biogenesis and mechanisms of microRNA-mediated gene regulation. *Biotechnol. Bioeng*. 2022;119 (3):685–692. DOI: 10.1002/bit.28029.
2. Kumar S., Ranga A. Role of miRNAs in breast cancer development and progression: Current research. *BioFactors*. 2025;51(1):e2146. DOI: 10.1002/biof.2146.
3. Zhai Z., Mu T., Zhao L., Li Y., Zhu D., Pan Y. MiR-181a-5p facilitates proliferation, invasion, and glycolysis of breast cancer through NDRG2-mediated activation of PTEN/AKT pathway. *Bioengineered*. 2022;13(1):83–95. DOI: 10.1080/21655979.2021.2006974.
4. Zhao T., Meng W., Chin Y., Gao L., Yang X., Sun S. et al. Identification of miR-25-3p as a tumor biomarker: Regulation of cellular functions via TOB1 in breast cancer. *Mol. Med. Rep*. 2021; 23(6):406. DOI: 10.3892/mmr.2021.12045.
5. Kalinina T.S., Kononchuk V.V., Alekseenok E.Y., Obukhova D., Sidorov S.V., Strunkin D. et al. Expression of estrogen receptor- and progesterone receptor-regulating microRNAs in breast cancer. *Genes*. 2021;12(4):582. DOI: 10.3390/genes12040582.
6. Andreeva O.E., Sorokin D.V., Mikhaevich E.I., Bure I.V., Shchegolev Y.Y., Nemtsova M.V. et al. Towards unravelling the role of ERα-targeting miRNAs in the exosome-mediated transferring of the hormone resistance. *Molecules*. 2021;26(21):6661. DOI: 10.3390/molecules26216661.
7. Gilam A., Shai A., Ashkenazi I., Sarid L.A., Drobot A., Bickel A. et al. MicroRNA Regulation of Progesterone Receptor in Breast Cancer. *Oncotarget*. 2017;8(16):25963–25976. DOI: 10.18632/oncotarget.15657.
8. Feng J., Hu S., Liu K., Sun G., Zhang Y. The role of microRNA in the regulation of tumor epithelial-mesenchymal transition. *Cells*. 2022;11(13):1981. DOI: 10.3390/cells11131981.
9. Mendez M.J., Hoffman M.J., Cherry E.M., Lemmon C.A., Weinberg S.H. Cell fate forecasting: a data-assimilation approach to predict epithelial-mesenchymal transition. *Biophys. J.* 2020;118(7): 1749–1768. DOI: 10.1016/j.bpj.2020.02.011.
10. Manfioletti G., Fedele M. Epithelial-mesenchymal transition (EMT). *Int. J. Mol. Sci.* 2023;24(14):11386. DOI: 10.3390/ijms241411386.
11. Ali A.H., Haider G., Ahmed K., Hashmi M., Kerio P., Irshad R. Correlation between e-cadherin and hormone receptor status among breast cancer patients. *Journal of the College of Physicians and Surgeons Pakistan*. 2020;30(10):1030–1034. DOI: 10.29271/jcpsp.2020.10.1030.
12. Autenshlyus A.I., Perepechaeva M.L., Studenikina A.A., Grishanova A.Y., Lyakhovich V.V. Serum miR-181a and miR-25 Levels in Patients with Breast Cancer or Benign Breast Disease. *Dokl. Biochem. Biophys.* 2023;512(1):279–283. DOI: 10.1134/S1607672923700436.
13. Studenikina A.A., Arkhipov S.A., Varaksin N.A., Proskura A.V., Autenshlyus A.I. Breast Biomarkers for the Detection of Malignancy in Benign Diseases in Women. *Russian Jour-*

nal of Preventive Medicine. 2024;27(1):63–66. (In Russ.). DOI: 10.17116/profmed20242701163.
14. Studenikina A.A., Arkhipov S.A., Zhurakovsky I.P., Proskura A.V., Autenshlyus A.I. Expression of Markers of Epithelial – Mesenchymal Transition in Breast Cancer. *Archive of Pathology*. 2023;85(4):12–17. (In Russ.). DOI: 10.17116/patol20238504112.
15. Jeffreys S.A., Becker T.M., Khan S., Soon P., Neubauer H., de Souza P. et al. Prognostic and predictive value of CCND1/Cyclin D1 Amplification in Breast Cancer with a Focus on Postmenopausal Patients: A Systematic Review and Meta-Analysis. *Frontiers in Endocrinology*. 2022;13:895729. DOI: 10.3389/fendo.2022.895729.
16. Wennhold K., Thelen M., Lehmann J., Schran S., Preugszat E., Garcia-Marquez M. et al. CD86+ antigen-presenting B cells are increased in cancer, localize in tertiary lymphoid structures, and induce specific T-cell responses. *Cancer Immunol. Res*. 2021;9(9):1098–1108. DOI: 10.1158/2326-6066.CIR-20-0949.
17. Yang H.L., Tsai Y.C., Korivi M., Chang C.T., Hseu Y.C. Lucidone Promotes the cutaneous wound healing process via activation of the PI3K/AKT, Wnt/β-catenin and NF-κB signaling pathways. *Biochimica et Biophysica Acta - Molecular Cell Research*. 2017;1864(1):151–168. DOI: 10.1016/j.bbamcr.2016.10.021.
18. Li X., Jin Y., Xue J. Unveiling collagen's role in breast cancer: insights into expression patterns, functions and clinical implications. *International Journal of General Medicine*. 2024;17:1773–1787. DOI: 10.2147/IJGM.S463649.
19. Khan M.J., Singh A.K., Sultana R., Singh P.P., Khan A., Saxena S. Breast cancer: A comparative review for breast cancer detection using machine learning techniques. *Cell Biochem. Funct.* 2023;41(8):996–1007. DOI: 10.1002/cbf.3868.
20. Breiman L. Random forests. Mach. Learn. 2001;45:5–32. DOI: 10.1023/A:1010933404324.
21. Zuo D., Yang L., Jin Y., Qi H., Liu Y., Ren L. Machine learning-based models for the prediction of breast cancer recurrence risk. *BMC Med. Inform. Decis. Mak.* 2023;23(1):276. DOI: 10.1186/s12911-023-02377-z.
22. Jin Y., Lan A., Dai Y., Jiang L., Liu S. Development and testing of a random forest-based machine learning model for predicting events among breast cancer patients with a poor response to neoadjuvant chemotherapy. *Eur. J. Med. Res.* 2023;28(1):394. DOI: 10.1186/s40001-023-01361-7.
23. Arika R.N., Mindila A., Cheruiyo W. Machine learning algorithms for breast cancer diagnosis: challenges, prospects and future research directions. *J. Oncol.* 2023;5(1):1–31. DOI: 10.30564/jor.v5i1.4977.
24. Kondov B., Milenkovikj Z., Kondov G., Petrushevska G., Basheska N., Bogdanovska-Todorovska M. et al. Presentation of the molecular subtypes of breast cancer detected by immunohistochemistry in surgically treated patients. *J. Med. Sci.* 2018;6(6): 961–967. DOI: 10.3889/oamjms.2018.231.
25. Yumpu [Internet]. ER/PR PharmDx Interpretation Manual. – Dako. URL: https://www.yumpu.com/en/document/read/18500132/er-pr-pharmdxtm-interpretation-manual-dako. Available at: 09.20.2013.
26. Willmott C.J., Matsuura K. Advantages of the mean absolute error (MAE) over the root mean square error (RMSE) in assessing average model performance. *Clim. Res.* 2005;30(1):79–82. DOI: 10.3354/cr030079.
27. Li L., Xu Q.H., Dong Y.H., Li G.X., Yang L., Wang L.W. et al. MiR-181a upregulation is associated with epithelial-to-mesenchymal transition (EMT) and multidrug resistance (MDR) of ovarian cancer cells. *Eur. Rev. Med. Pharmacol. Sci.* 2016;20(10):2004–2010.
28. Strotbek M., Schmid S., Sánchez-González I., Boerries M., Busch H., Olayioye M.A. miR-181 elevates Akt signaling by co-targeting PHLPP2 and INPP4B phosphatases in luminal breast cancer. *Int. J. Cancer.* 2017;140(10):2310–2320. DOI: 10.1002/ijc.30661.
29. Govatati S., Singamsetty G.K., Nallabelli N., Malempati S., Rao P.S., Madamchetty V.K.K. et al. Contribution of cyclin D1 (CCND1) and E-cadherin (CDH1) alterations to colorectal cancer susceptibility: a case-control study. *Tumor Biol.* 2014;35(12):12059–12067. DOI: 10.1007/S13277-014-2505-9.
30. Yan X., Gao M., Zhang P., Ouyang G., Mu Q., Xu K. MiR-181a functions as an oncogene by regulating CCND1 in multiple myeloma. *Oncol. Lett.* 2020;20(1):758–764. DOI: 10.3892/OL.2020.11579.
31. Yao J., Li G., Liu M., Yang S., Su H., Ye C. lnc-MICAL2 1 sponges miR 25 to regulate DKK3 expression and inhibits activation of the Wnt/β catenin signaling pathway in breast cancer. *Int. J. Mol. Med.* 2022;49(2):23. DOI: 10.3892/ijmm.2021.5078.
32. Jiang X., Wang J., Zhang K., Tang S., Ren C., Chen Y. The role of ITGB1-ILK-Akt signaling-mediated epithelial-mesenchymal transition of liver epithelial cells and chemoresistance and radioresistance in hepatocellular carcinoma cells. *Med. Oncol.* 2015;32(5):141. DOI: 10.1007/S12032-015-0595-X.
33. Vora H., Gavali M., Patel N. A Study of Col2A1 expression in triple-negative brest cancer patients. *Glob. J. Clinic. Medici. Medica. Res.* 2023;1:1–5.
34. Li X., Jin Y., Xue J. Unveiling collagen's role in breast cancer: insights into expression patterns, functions and clinical implications. *Int. J. Gen. Med.* 2024;17:1773–1787. DOI: 10.2147/IJGM.S463649.

Author Contribution

Studenikina A.A. – carrying out of the experiments, discussion of the results of the studies, drafting of the article. Mihailovsky M.A. – carrying out of the experiments, discussion of the results of the studies. Timofeev V.S., Autenshlyus A.I. – conception of the study, supervision of the work, discussion of the results of the studies, editing of the article. Arkhipov S.A. – carrying out of the experiments, discussion of the results of the studies, editing of the article.

Author Information

Studenikina Anastasiia A. – Cand. Sci. (Med.), Senior Researcher, Central Research Laboratory, Novosibirsk State Medical University, Novosibirsk; Researcher, Institute of Molecular Biology and Biophysics, Federal Research Center of Fundamental and Translational Medicine, Novosibirsk, aastudenikina@frcftm.ru, https://orcid.org/0000-0003-3936-1316

Mihailovsky Michael A. – Bachelor's Degree Student, Novosibirsk State Technical University, Novosibirsk, maihailovsky18@mail.ru, https://orcid.org/0009-0009-2272-6295

Timofeev Vladimir S. – Dr. Sci. (Engineering), Professor, Department of Theoretical and Applied Computer Science, Dean of the Faculty of Applied Mathematics and Computer Science, Novosibirsk State Technical University, Novosibirsk, v.timofeev@corp.nstu.ru, https://orcid.org/0000-0002-6352-3218

Arkhipov Sergey A. – Dr. Sci. (Biology), Leading Researcher, Central Research Laboratory, Novosibirsk State Medical University, Novosibirsk; Senior Researcher, Institute of Molecular Biology and Biophysics, Federal Research Center of Fundamental and Translational Medicine, Novosibirsk, arhipowsergei@yandex.ru, https://orcid.org/ 0000-0002-1390-4426

Autenshlyus Aleksandr I. – Dr. Sci. (Biology), Professor, Head of the Central Research Laboratory, Novosibirsk State Medical University, Novosibirsk; Chief Researcher, Institute of Molecular Biology and Biophysics, Federal Research Center of Fundamental and Translational Medicine, Novosibirsk, lpciip@211.ru, https://orcid.org/0000-0001-7180-010X

(✉) **Studenikina Anastasiia A.,** aastudenikina@frcftm.ru

Received on June 23, 2025;
approved after peer review on September 22, 2025;
accepted on October 30, 2025

УДК 546.82-034.24:576.343:544.032.65
https://doi.org/10.20538/1682-0363-2026-2-101-114

Metabolic Reaction of Cells to Changes in the Physical and Chemical State of the Nitinol Surface Induced by Ultraviolet Laser Radiation with a Wavelength of 266 nm

Khlusov I.A.[1, 2], Kokorev O.V.[1], Gorokhova A.V.[1, 2], Nasibov T.F.[1, 2], Krivoshchekov S.V.[1], Chebodaeva V.V. [2, 3], Brazovsky K.S.[1], Khlusova M.Yu.[1], Sablina T.Yu.[2], Kandaurova M.Yu.[2], Zyatikov I.A.[2], Panchenko Yu.N.[2]

[1] *Siberian State Medical University*
2 Moskovsky trakt, 634050 Tomsk, Russian Federation

[2] *Institute of High Current Electronics, Siberian Branch of the Russian Academy of Sciences (IHCE SB RAS)*
2/3 Akademichesky Ave., 634055 Tomsk, Russian Federation

[3] *Institute of Strength Physics and Materials Science, Siberian Branch of the Russian Academy of Sciences (ISPMS SB RAS)*
2/4 Akademichesky Ave., 634055 Tomsk, Russian Federation

ABSTRACT

Aim. MTT (methylthiazolyldiphenyl-tetrazolium bromide) viability assessment of the *in vitro* cellular response to changes in the physicochemical properties (zeta potential, wettability, topography) of the nitinol surface after treatment with ultraviolet (UV) laser radiation (UV-LR) with a wavelength of 266 nm.

Materials and methods. The MCF-7 cell culture was incubated with nitinol-based alloy plates for 24 hours, before and after exposure to UV light (wavelength 266 nm, energy density 0.1 J/cm²) with a Q-smart 850 pulsed Nd:YAG laser. The samples were then analyzed for roughness (*Ra*) (GOST 2789-73) and surface contact angle with water. Zeta (ζ) potentials were also measured for both nitinol-based alloy substrates (SurPASS 3) and MCF-7 cells (Litesizer DLS 500). Metabolic activity of the cells was assessed using the MTT test, as recommended by GOST ISO 10993-5-2023 for the *in vitro* assessment of the cytotoxicity of medical materials and devices. Bioinformatics *in silico* analysis of intracellular signaling and metabolic pathways was conducted using the WikiPathways database.

Results. Surface modification caused by UV-LR significantly reduced the toxic response (decrease in metabolic activity) of MCF-7 cells to the nitinol-based alloy substrate. UV-LR did not affect the zeta potential (±10 mV from the isoelectric point), but it significantly decreased the water contact angle (from 75 to 8.7°) and increased the *Ra* index of surface roughness (from 71.5 nm to 93.9 nm). *In silico* mechanotransduction analysis revealed that the roughness and hydrophilicity/hydrophobicity of nitinol can independently induce gene expression in MCF-7 cells, as well as through cross-talking molecular mechanisms. At the same time, several signaling pathways (WP5504, WP3680, WP5477, WP3941, WP5046, and WP2435) were found to be close to those involved in the reduction of the MTT reagent, which is used as a marker for the cell death program induced by metabolic imbalance in MCF-7 cells.

Conclusion. UV-LR promotes an increase in hydrophilicity and/or nanoroughness of the nitinol-based alloy surface, but it does not affect the zeta potential. This may initiate a cascade of molecular mechanisms regulating cellular and tissue responses to implanted materials. These events can include inflammation, hemostasis activation, angiospasm, vessel regeneration, and metabolic activity of target cells.

Keywords: MCF-7 cells, MTT test, *in vitro*, stent substrates, zeta-potential, wettability, roughness, *in silico* modeling

✉ *Khlusov Igor A.,* khlusov63@mail.ru

Conflict of interest. The authors declare the absence of obvious or potential conflict of interest related to the publication of this article.

Source of financing. The study was carried out with support from the Russian Science Foundation grant No. №25-79-31008.

For citation: Khlusov I.A., Kokorev O.V., Gorokhova A.V., Nasibov T.F., Krivoshchekov S.V., Chebodaeva V.V., Brazovsky K.S., Khlusova M.Yu., Sablina T.Yu., Kandaurova M.Yu., Zyatikov I.A., Panchenko Yu.N. Metabolic Reaction of Cells to Changes in the Physical and Chemical State of the Nitinol Surface Induced by Ultraviolet Laser Radiation with a Wavelength of 266 nm. *Bulletin of Siberian Medicine.* 2026;25(2):101–114. https://doi.org/10.20538/1682-0363-2026-2-101-114.

Метаболическая реакция клеток на изменение физико-химического состояния поверхности никелида титана, индуцированное ультрафиолетовым лазерным излучением с длиной волны 266 нм

Хлусов И.А.[1, 2], Кокорев О.В.[1], Горохова А.В.[1, 2], Насибов Т.Ф.[1, 2], Кривощеков С.В.[1], Чебодаева В.В.[2, 3], Бразовский К.С.[1], Хлусова М.Ю.[1], Саблина Т.Ю.[2], Кандаурова М.Ю.[2], Зятиков И.А.[2], Панченко Ю.Н.[2]

[1] *Сибирский государственный медицинский университет (СибГМУ)*
Россия, 634050, г. Томск, Московский тракт, 2

[2] *Институт сильноточной электроники Сибирского отделения Российской академии наук (ИСО СО РАН)*
Россия, 634055, г. Томск, пр. Академический, 2/3

[3] *Институт физики прочности и материаловедения Сибирского отделения Российской академии наук (ИФПМ СО РАН)*
Россия, 634055, г. Томск, пр. Академический, 2/4

РЕЗЮМЕ

Цель: оценка с помощью 3-[4,5-диметилтиазол-2-ил]-2,5-дифенилтетразолия бромида (MTT) клеточной реакции *in vitro* на изменение физико-химического состояния (дзета-потенциала, смачиваемости, топографии) поверхности сплава на основе никелида титана (нитинола) после обработки ультрафиолетовым лазерным излучением (УФ-ЛИ) с длиной волны 266 нм.

Материалы и методы. Клеточную культуру MCF-7 инкубировали в течение 24 ч с пластинами из сплава на основе никелида титана, до и после обработки УФ-ЛИ (плотность энергии 0,1 Дж/см^2). На образцах измеряли индекс шероховатости *Ra* (ГОСТ 2789-73) и контактный угол смачивания поверхности водой. Дзета-потенциалы поверхности подложек из нитинола и MCF-7 клеток определяли с использованием анализаторов для плоских образцов (SurPASS 3) и частиц (Litesizer DLS 500) соответственно. Метаболическую активность клеточной культуры определяли с помощью MTT-теста, рекомендуемого ГОСТ ISO 10993-5-2023 для оценки *in vitro* цитотоксичности медицинских материалов и изделий. Биоинформатический *in silico* анализ внутриклеточных сигнальных и метаболических путей осуществляли в базе данных WikiPathways.

Результаты. Модификация поверхности УФ-ЛИ статистически значимо снижала токсический отклик (падение метаболической активности) MCF-7 клеток на контакт с подложкой из нитинола. Обработка УФ-ЛИ не влияла на величину дзета-потенциала, но существенно уменьшала контактный угол смачивания водой (с 75 до 8,7°), а также повышала *Ra* поверхности образцов (с 71,5 до 93,9 нм). Анализ *in silico* с позиций механотрансдукции показал, что шероховатость и гидрофильность (гидрофобность) нитинола могут индуцировать экспрессию генов в MCF-7 клетках независимо друг от друга, а также через перекрестные молекулярные механизмы. При этом некоторые сигнальные пути (WP5504, WP3680, WP5477, WP3941, WP5046, WP2435) близки к системам, участвующим в редукции MTT-реагента как маркера программы клеточной смерти, индуцированной метаболическим дисбалансом MCF-7 клеток.

Заключение. Обработка УФ-ЛИ способствует увеличению гидрофильности и (или) наношероховатости, но не дзета-потенциала поверхности подложек из нитинола. Это может инициировать каскад молекулярных механизмов, регулирующих клеточно-тканевые реакции на имплантируемые материалы, включая индукцию воспаления, активацию гемостаза, ангиоспазм и регенерацию кровеносного русла, а также метаболическую активность клеток-мишеней.

Ключевые слова: MCF-7 клетки, МТТ-тест, *in vitro*, подложки для стентов, дзета-потенциал, смачиваемость, шероховатость, *in silico* моделирование

Конфликт интересов. Авторы декларируют отсутствие явных и потенциальных конфликтов интересов, связанных с публикацией настоящей статьи.

Источники финансирования. Исследование выполнено при поддержке гранта Российского научного фонда № 25-79-31008.

Для цитирования: Хлусов И.А., Кокорев О.В., Горохова А.В., Насибов Т.Ф., Кривощеков С.В., Чебодаева В.В., Бразовский К.С., Хлусова М.Ю., Саблина Т.Ю., Кандаурова М.Ю., Зятиков И.А., Панченко Ю.Н. Метаболическая реакция клеток на изменение физико-химического состояния поверхности никелида титана, индуцированное ультрафиолетовым лазерным излучением с длиной волны 266 нм. *Бюллетень сибирской медицины.* 2026;25(2):101–114. https://doi.org/10.20538/1682-0363-2026-2-101-114.

INTRODUCTION

Cardiovascular diseases are the leading cause of mortality worldwide [1]. The primary method of urgent minimally invasive therapy for coronary artery disease, one of the most common circulatory system pathologies, is stenting of arteries affected by atherosclerosis and arterial hypertension. Currently, there are more than 400 types of stents, differing in material composition, dimensions, design, coating for the blood-contacting surface, delivery system into the blood vessel, etc.

For some time, it was believed that the main challenges of stenting (thrombosis and arterial restenosis) would be solved by composite drug-eluting stents (DES). However, due to the high risk of late (occurring 6 months after implantation) thromboses associated with DES [2], preference is commonly given to metal stents, which hold a definitive clinical niche [3]. Nitinol alloy attracts the attention of researchers and clinicians due to its superelastic behavior, which allows implants to deform congruently with blood vessel walls over a long period, as well as to withstand the cyclic fatigue resistance threshold for cardiovascular devices, which is 15 million cycles in mechanical tests [4].

However, the high (up to 57 wt.%) concentration of nickel (Ni) in nitinol poses a threat of its release into the bloodstream and penetration into the vascular wall due to stent corrosion. Ni exhibits pronounced toxicity (Hazard Class 1–2; GOST 32419-2022), allergenicity, and carcinogenicity [5]. To improve the corrosion resistance of nitinol, various surface modification methods are being proposed, including those utilizing ion – plasma technologies [5] and concentrated energy flows (electron beam, laser radiation).

Recently, laser processing of nitinol-based alloys has attracted researchers' attention as a method that allows for the wide-ranging modification of the physicochemical properties of the surface layer without affecting the beneficial functional properties of the medical device [6, 7]. The team from the Gas Lasers Laboratory at ISE SB RAS is developing a laser surface modification method for nitinol using ultraviolet (UV) laser radiation ($\lambda < 400$ nm) [8, 9], which requires investigation of the biocompatibility of the modified devices.

In this regard, the aim of the study was to perform the MTT assessment of the *in vitro* cellular response to changes in the physical and chemical state (zeta (ζ) potential, wettability, topography) of the nitinol surface after treatment with UV laser radiation.

MATERIALS AND METHODS

Plates measuring 10 × 10 × 1 mm^3 (length × width × thickness) made of a nitinol-based alloy were used for the study. The material was developed at the Research Institute of Medical Materials and Shape Memory Implants (Tomsk, Russia). Pre-treatment of the sample surface (grinding, polishing, and ultrasonic cleaning), measurement of the contact wettability angle, and surface topography were performed as described in [8]. The average surface

roughness index *Ra* was measured in accordance with GOST 2789-73.

UV (wavelength 266 nm) laser modification of the nitinol sample surfaces was carried out using a Q-smart 850 pulsed Nd:YAG laser (Quantel, France) generating pulses with a duration of 5 ns and a frequency of 10 Hz (Fig.1). The laser beam diameter was d = 5 mm, the step between scanning lines was h_y = 0.25 cm, the energy density was j = 0.1 J/cm², and the scanning speed was V_x = 375 μm/s.

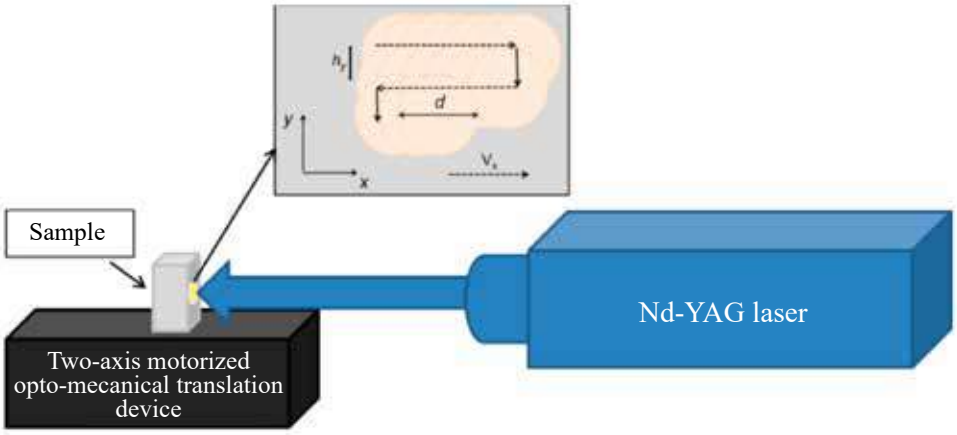

Fig. 1. Schematic diagram of the UV-laser surface processing of samples and the laser scanning principle

The ζ-potential of the nitinol sample surfaces before and after UV laser treatment was determined using a SurPASS 3 electrokinetic analyzer for flat samples (Anton Paar GmbH, Austria) in accordance with the manufacturer's instructions. The samples were mounted pairwise (opposite each other) in an adjustable gap cell with a gap width of up to 100 μm (98 μm in the current experiment). A 0.001 M KCl solution with pH ~7 was used as the background electrolyte. The pH of the electrolyte varied within the range of 3.0 – 8.5 units at a pressure of 200–600 mbar by adding 0.05 M KOH or HCl to the background electrolyte. The SurPASS 3 software calculated the ζ-potentials using the Helmholtz – Smoluchowski equation, as described previously [10].

The ζ-potential of MCF-7 cells was determined using a Litesizer DLS 500 particle analyzer (Anton Paar GmbH, Austria) with its integrated software in accordance with the manufacturer's instructions. A cell suspension at a concentration of 50×10^4 per 1 ml of the RPMI-1640 medium with low calcium content at pH = 7.0–7.2 was placed into the instrument measurement cell. The automated measurement cycle relative to a reference electrolyte (phosphate buffered saline) comprised 100–1,000 cells to achieve a normal distribution of the variable (Fig.2).

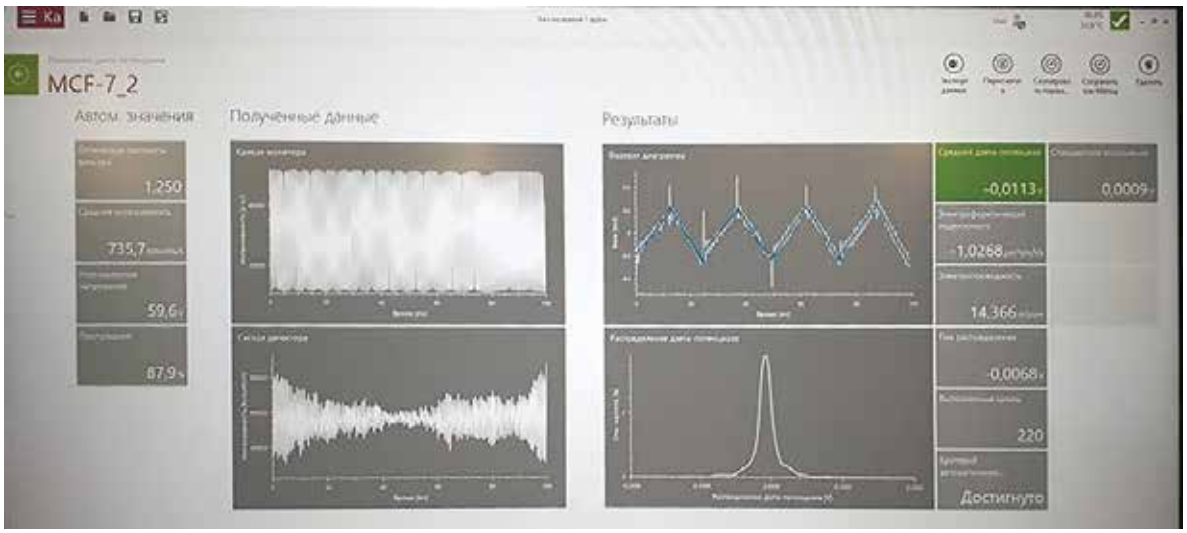

Fig. 2. Interface of the particle analyzer software during the measurement of the ζ-potential of MCF-7 cells

To determine the cellular response upon contact with the nitinol samples (plates measuring 10 × 10 × 1 mm^3), which were preliminarily sterilized by dry heat at 180 °C for 60 minutes, the MCF-7 cells of human invasive ductal adenocarcinoma (Institute of Cytology, Russian Academy of Sciences, St. Petersburg) were employed.

The cells were co-cultured with the test objects for 24 hours in 24-well flat-bottom plates (Orange Scientific, Braine-l'Alleud, Belgium) at a concentration of 50×10^4 viable cells per 1 ml of the nutrient medium with the following composition: 90% Dulbecco's Modified Eagle Medium (DMEM) (Servicebio, China), 10% fetal bovine serum (Technozero, Russia), antibiotics (100 units/ml penicillin and 100 μg/ml streptomycin, Capricon Scientific, Germany), and 2 mM L-glutamine (PanEco, Russia).

Four hours prior to the end of the cultivation period, the cell cultures were detached from the plastic surface of the culture plates. The *in vitro* cytotoxicity index (CI) for the control (cell culture without nitinol substrates) and the test group (cells + nitinol samples) was determined, as described in [11], using a 0.5% solution of 3-[4,5-dimethylthiazol-2-yl]-2,5-diphenyltetrazolium bromide (MTT) (NeoFroxx, Germany), as recommended by GOST ISO 10993-5-2023.

The bioinformatics *in silico* analysis of signaling and metabolic pathways, as well as associated genes potentially expressed in the MCF-7 cells in response to stimuli (keywords: "surface roughness", "surface wettability") was performed using the open-access GeneCards database (https://www.genecards.org/). Subsequently, an over-representation analysis (ORA) was conducted for each resulting gene list according to the algorithm described in [12, 13]. Common metabolic pathways relevant to the study focus were then identified.

Statistical data analysis was performed using the R programming language (version 4.5.1) with the MVN [14], PMCMRplus [15], and brunnermunzel [16] packages. The compliance of quantitative variables with a normal distribution was assessed using the Shapiro – Wilk test with the Royston's correction [17]. Quantitative, normally distributed variables were described as the mean and the standard deviation ($M \pm SD$). Quantitative variables that were not normally distributed and ordinal variables were described as the median and the interquartile range ($Me\ [Q_1; Q_3]$).

For comparing the means of two samples with a normal distribution, the Welch's *t*-test [21–23] was used as a more powerful test that does not require equality of variances, unlike the classical Student's *t*-test [18–20].

For comparing two independent samples that did not comply with a normal distribution, the Brunner – Munzel test [27, 28] was applied as a more robust and versatile method compared to the Mann – Whitney *U*-test, since it does not require assumptions about the equality of distributions and/or variances [29, 30].

For multiple comparisons of groups with a normal distribution but unequal variances, the Welch's analysis of variance (Welch's ANOVA) was employed, which does not require preliminary testing for homogeneity of variances [31, 32] and controls the type I error rate [32–35]. Subsequent pairwise comparisons were performed using the Games – Howell post-hoc test due to its robustness to violations of homoscedasticity and high statistical power [36, 37].

RESULTS

MCF-7 cells adhere to plastic, exhibit variable sizes (up to 50 μm), and display variable morphology (rounded or fibroblast-like) (Fig.3).

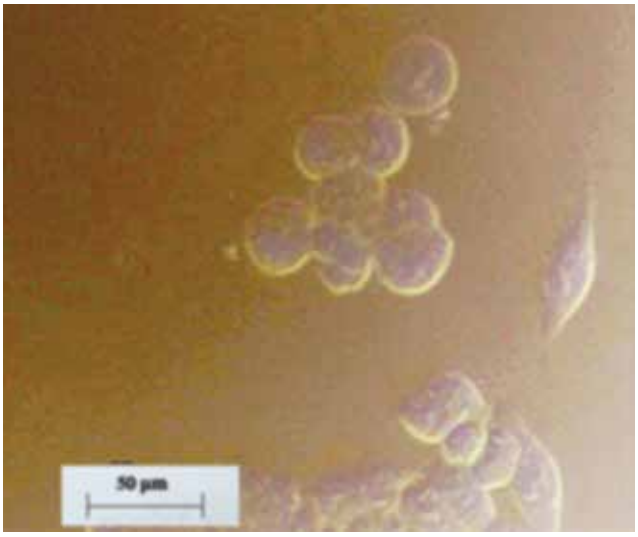

Fig. 3. Morphology of adherent MCF-7 cells after 24 hours of cultivation. Unstained native preparation, dark-field microscopy. Scale bar: 50 μm.

The MTT test showed (Fig.4) that during short-term *in vitro* contact of the cell suspension with the

studied nitinol substrates, which simulate the surface state of vascular stents, a decrease in the metabolic activity of the cells was observed. This was recorded by reduced (relative to the control culture) formation of the colored metabolite (formazan) from the MTT reagent. Such a result is interpreted as a marker of cell death at a median CI of 33%. This value slightly exceeds the threshold (30%) recommended by GOST ISO 10993-5-2023 as conditionally safe for determining the *in vitro* cytotoxicity of medical materials and devices. The physicochemical modification of the surface with UV laser radiation statistically significantly (Brunner – Munzel test, $p < 0.001$) reduced the toxic cell response upon contact with the test device to the 30% recommended by the regulatory document (Fig.4). This indicates less significant inhibition of the metabolic activity of the MCF-7 cells upon contact with the modified metal substrate.

From a fundamental perspective, the probable cause-and-effect relationships underlying this phenomenon are of interest.

To better understand the physicochemical changes in the surface state induced by UV laser radiation, the ζ-potential of the samples was investigated (Fig.5). The experimental electrokinetic curves (Fig.5, *a*) showed that across a wide pH range for both types of nitinol surface (initial and laser-treated), the measured potential amplitude varied mainly within ±10 mV from the isoelectric point. For the statistical assessment of the effect of laser surface modification, the pH range of 6–8 was selected for

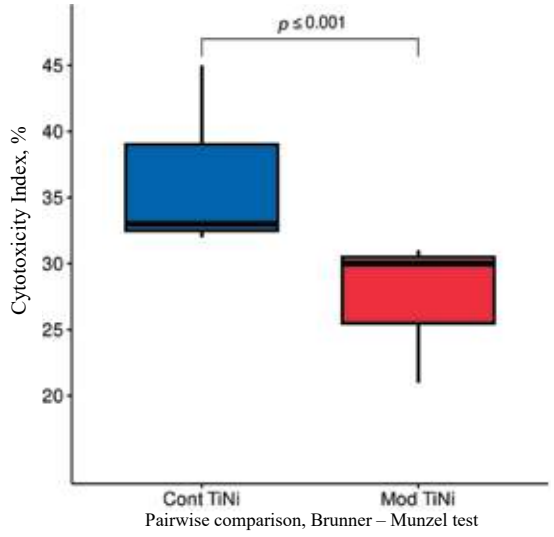

Fig.4. Results of the MTT test after 24-hour cultivation of the MCF-7 cells on unmodified (control, Cont nitinol) and modified (Mod nitinol) with UV laser radiation nitinol substrates. The X-axis, – group names; and the Y-axis – CI, %, *Me* [Q_1; Q_3] (pairwise comparison, Brunner – Munzel test, $p < 0.001$)

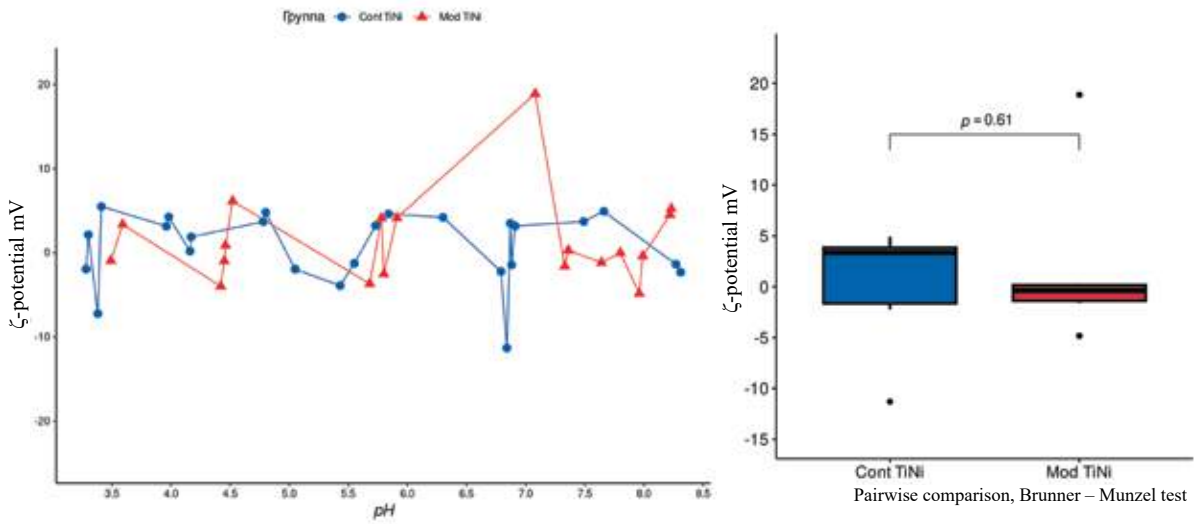

Fig. 5. Dependence of the amplitude and sign of the zeta potential on the tested nitinol samples on the pH of the solutions: *a* – pH = 3–8.5 (the X-axis – pH values, the Y-axis – ζ-potential, mV); *b* – pH = 6–8 (the X-axis – group names, the Y-axis – ζ-potential values, mV); *Me* [Q_1; Q_3], Brunner – Munzel test, $p = 0.61$

the following reasons: 1) in this region of electrolyte ionic strength, the maximum overshoots of the ζ-potentials with opposite charge signs occurred (Fig.5, *a*); 2) according to GOST R 52770-2016, the permissible change in the solvent pH after contact with the test device should not exceed ±1 unit from the physiological level of pH ~7–7.4.

The median values did not show a statistically significant effect of UV laser irradiation on the amplitude of the electrokinetic potential of the samples (Fig.5, *b*). In the meantime, the MCF-7 cells carried a negative surface charge with a potential amplitude of 11.3–11.6 mV (Fig.6).

Based on the obtained result, it was hypothesized that the change in the metabolic activity of the MCF-7 cells (Fig.4) was not associated with the ζ-potential of the modified nitinol surface under the selected mode of UV laser treatment. Nitinol in both study groups maintains an electrically neutral surface when exposed to a flow of the model electrolyte. The MTT molecule carries a positive charge [38] and can therefore penetrate the cytoplasmic membrane of MCF-7 cells, which carry a negative surface charge, via an electrostatic mechanism [39]. The identical charge and amplitude of the ζ-potential on the surface of both the initial and modified nitinol samples apparently do not affect the interaction between the reagent and the cell population.

Fig. 7 shows the result of the change in the contact wettability angle of the nitinol sample surfaces before and after UV-laser processing. Laser modification led to a drastic increase in the hydrophilicity of the samples; the contact angle decreased to 8.7°, which is 8.5 times smaller (Welch's *t*-test, $p < 0.001$) than the baseline value (Fig. 7). This corresponds to a superhydrophilic surface state, where the water contact angle approaches 0° [40].

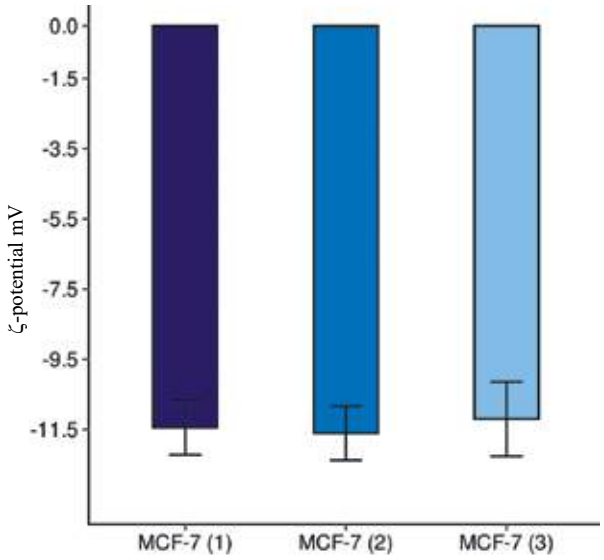

Fig. 6. Amplitude and sign of the zeta potential of the MCF-7 cells in the pH range of 6–8; the X-axis – cell line name and sample numbers, the Y-axis – ζ-potential values, mV; $M \pm SD$ (multiple comparison, one-way Welch's ANOVA, $p = 0.91$)

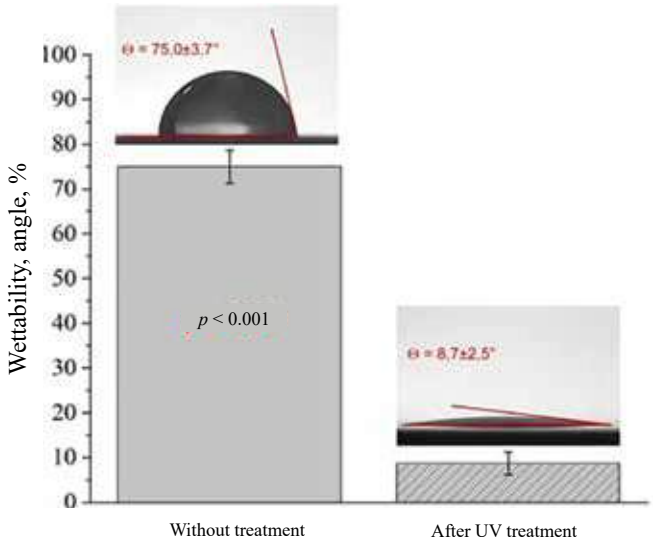

Fig. 7. Contact wettability angle and characteristic images of water droplets on the surface of nitinol samples before and after surface modification: the X-axis – group names, the Y-axis – wettability angle, °, $M \pm SD$ (5 measurements for each group, pairwise comparison, Welch's *t*-test, $p < 0.001$)

Surface wettability is influenced by its phase and elemental composition, as well as its topography (texture and roughness) [41–43]. The measured average roughness value *Ra* for the sample in its initial state was 71.5 ± 6.3 nm (class 11 of surface roughness according to GOST 2789-73) (Fig.8). After laser treatment (at an energy density of $j = 0.1$ J/cm^2), the surface profile did not change (Fig.8, *a*). However, it became more textured, and the average *Ra* value increased to 93.9 ± 9.6 nm (Welch's *t*-test, $p = 0.0041$), which corresponds to class 10 surface irregularity range (Fig.8, *b*).

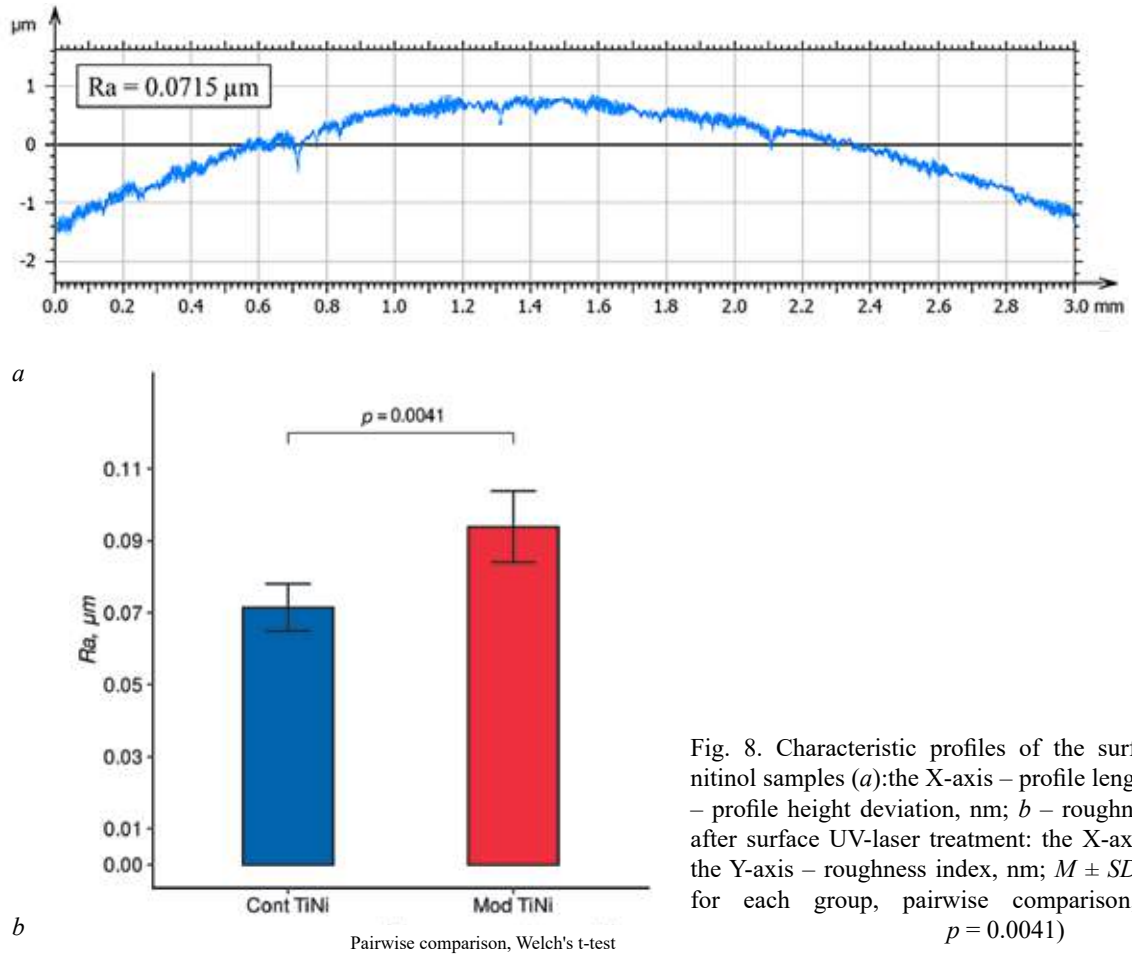

Fig. 8. Characteristic profiles of the surface of the tested nitinol samples (*a*):the X-axis – profile length, mm, the Y-axis – profile height deviation, nm; *b* – roughness *Ra* before and after surface UV-laser treatment: the X-axis – group names, the Y-axis – roughness index, nm; $M \pm SD$ (5 measurements for each group, pairwise comparison, Welch's *t*-test, $p = 0.0041$)

DISCUSSION

The MCF-7 cell line is widely used for determining the *in vitro* cytotoxicity of substances, scaffolds, and various medical materials and devices [11, 44–48], including stents for cardiovascular surgery [49]. Furthermore, the metabolism and signaling pathways of MCF-7 cells have been studied in considerable detail. For instance, a PubMed search for "MCF-7 cell metabolism" yielded 33,360 results, starting from the year 1975.

The MTT test is considered to be the gold standard for assessing cytotoxicity [50] based on the metabolic activity of the tested cells and is recommended by GOST ISO 10993-5-2023 for this purpose. The reduction of the MTT reagent into formazan granules is visualized in various cellular compartments (mitochondria, cytoplasm, nucleus, cytoplasmic membrane, microsomes) and is mediated by various enzymatic systems, including glycolysis and the mitochondrial respiratory chain [38].

A modern mechanotransduction theory postulates the translation of diverse stressors ((bio)physical and (bio)chemical forces (signals) from the macro- and microenvironments) into the cell nucleus via the cytoskeleton and intracellular signaling pathways [51–53]. Accordingly, diverse physicochemical signals from external stimuli are converted into variants of a cellular response through feedback mechanisms that regulate the expression of specific gene groups [53].

The intimate molecular (metabolic) processes underlying the functioning of the mechanotransduction system ("stressor – pathway – gene expression – cellular response") remain largely unelucidated. Nevertheless, certain properties of the natural and synthetic (scaffolds) extracellular matrix (ECM) that are capable of initiating signal transduction, thereby regulating cell behavior, are already known to varying degrees. These can be conditionally divided into (bio)physical (charge sign and ζ-potential amplitude, topography dimensionality), (bio)mechanical (elasticity/stiffness, compliance), and (bio)chemical (wettability (hydrophilicity or hydrophobicity), free energy, chemical composition,

solubility) stimuli [54–56], including in the context of the cardiovascular system [57–59].

For ECM and implants contacting blood, the sign of the surface charge and the amplitude of the electrostatic (in air) and electrokinetic potential are of great importance [60], since most cells in the body carry a negative surface charge [61], including blood cells [62], as well as the vascular endothelium [62, 63] and MSCs [64].

Thus, the ζ-potential value on human umbilical vein endothelial cells (HUVEC) is –17.1 ± 1.7 mV [65]. The amplitudes we measured for MCF-7 cells varied from –11.3 to –11.6 mV (Fig.6), which, according to the results of [65], is close to the values for another tumor cell line (–13.2 ± 1.2 mV, HeLa cells). In this regard, the MCF-7 cells of adenocarcinoma isolated from human breast ducts can be an adequate tool for modeling the interaction of cells with the surface of materials developed for cardiovascular stents.

Furthermore, such studies are beneficial because inflammation of the vascular wall, which inevitably occurs in the stent area [66], may promote the chemotaxis and tissue invasion of tumor cells circulating in the blood. Another possible scenario is the emigration of malignant cells from a tumor into the blood, induced by the implanted device. In this regard, studying the mechanisms of tumor cell adhesion to vascular implants is significant for the advancement of not only cardiovascular surgery but also oncology.

Artificial surfaces with ζ-potential fluctuations ranging from –10 mV to +10 mV are considered to be electrically neutral. According to [67], such materials will be bioinert towards circulating blood provided they possess high hydrophilicity. UV laser modification did not affect the neutral ζ-potential values (Fig.5).

Based on this fact, a hypothesis was put forward that the increased cell survival on nitinol after laser treatment (Fig.4) might be associated with the resulting superhydrophilic state of the modified surface (Fig.7). It is believed that mammalian cells prefer to adhere to hydrophilic substrates [68]. However, cells (for example, L-929 fibroblasts) can exhibit enhanced adhesion to both hydrophilic (after exposure to UV laser radiation) [69] and hydrophobic surfaces [70] of biomaterials.

The topography of the ECM undoubtedly influences the behavior of various cells (endothelial cells, smooth muscle cells, platelets) [71]. However, in each specific case, research results are ambiguous. On the one hand, MCF-7 cells adhere better and increase cell mass on rougher, bioinert gold electrode surfaces [72]. On the other hand, according to [73], an increase in the *Ra* value of the nano relief on a polymer surface (polyethylene terephthalate, PET) from 3.5 nm to 19 nm, conversely, stimulates apoptosis of MCF-7 cells. The surface chemistry and wettability of gold and PET differ significantly. Our results on nitinol suggest an improvement in the viability (metabolic activity) of MCF-7 cells on the rougher, hydrophilic surface induced by UV laser radiation (Fig.7, 8).

Next, a bioinformatics approach (Table) was used to predict potential intracellular mediators capable of transforming the action of physicochemical stimuli into gene expression and the corresponding cellular response. For MCF-7 cells, the ORA detected 358 target pathways for the query “surface roughness” and 39 for the keyword “surface wettability”, which does not seem surprising, given greater publication activity on the influence of topography on cell behavior.

We conditionally divided the found metabolic pathways into groups that may be relevant to the cellular and tissue reactions of the blood system to implantable materials (Table), including the induction of inflammation, activation of hemostasis, angiospasm and regeneration of the vascular bed, and metabolic activity. On one hand, the roughness and wettability of nitinol can induce a response in MCF-7 cells via their own signaling pathways. On the other hand, the search engine predicted several molecular mechanisms common to both stressors (WP453, WP5088, WP98, WP5036, and WP5158; Table), which can be interpreted as potential synergism or antagonism between roughness and wettability (hydrophilicity/hydrophobicity) regarding the ultimate response of MCF-7 cells.

Also of interest in Table is the group of pathways “Metabolic Activity and Cell Behavior”, where some entries (WP5504, WP3680, WP5477, WP3941, WP5046, WP2435) are related to the signaling and enzymatic intracellular systems involved in the reduction of the MTT reagent [39] as a marker of the cell death program [74] caused by a metabolic imbalance in MCF-7 cells.

In terms of discussion, it should be emphasized that both hydrophilicity and hydrophobicity are considered as beneficial biomedical/functional properties for medical devices contacting blood [75, 76].

Table

Target Intracellular Metabolic Pathways of MCF-7 Cells for Extracellular Matrix Mechanotransduction Factors (Roughness, Wettability) according to *in silico* Modeling Using the WikiPathways Database Search Engine

ID	Pathway name	Number of target genes	q-value < 0.05 for stressors		Common pathway for stressors
			Wettability	Roughness	
	Inflammation				
WP453	Inflammatory response	2/3	0.0033	0.0026	+
WP5088	Prostaglandin signaling	8	–	<0.001	
WP98	Prostaglandin synthesis and regulation	3	–	0.0072	+
WP4493	Cells and molecules involved in local acute inflammatory response	4	–	<0.001	–
WP5473	Cytokine receptor interaction	14	–	<0.001	–
WP530	Cytokines and inflammatory response	5	–	<0.001	–
WP75	Toll like receptor signaling	7	–	<0.001	–
WP4542	Leukocyte – intrinsic Hippo pathway functions	2	–	0.0334	–
	Hemostasis				
WP2806	Complement system	2	0.0135	–	–
WP272	Blood clotting cascade	1	0.018	–	–
WP558	Complement and coagulation cascades	1	0.0278	–	–
WP4462	Platelet mediated interactions with vascular and circulating cells	4	–	<0.001	–
	Circulatory system				
WP5036	Angiotensin II receptor type 1 pathway	1/2	0.0184	0.023	+
WP5158	Urotensin II mediated signaling	1/7	0.0278	<0.001	+
WP560	TGF beta receptor signaling	5	–	<0.001	–
WP3888	VEGFA VEGFR2 signaling	8	–	0.0155	–
WP4331	Neovascularization processes	2	–	0.0361	
	Metabolic activity and cell behavior (proliferation, differentiation, apoptosis)				
WP5156	Glyoxylate metabolism	1	0.0167	–	–
WP4172	PI3K Akt signaling	2	0.0206	–	–
WP5504	Disorders of mitochondrial homeostasis dynamics, protein import and quality control	1	0.0277	–	–
WP3680	Physicochemical features and toxicity-associated pathways	1	0.0278	–	–
WP4534	Mechanoregulation and pathology of YAP/TAZ via Hippo and non-Hippo mechanisms	4	–	<0.001	–
WP5477	Molecular pathway for oxidative stress	4	–	<0.001	–
WP3941	Oxidative damage response	3	–	0.0051	–
WP5046	NAD metabolism in oncogene-induced senescence and mitochondrial dysfunction-associated senescence	3	–	0.0012	–
WP2435	Quercetin and Nf kB AP 1- induced apoptosis	2	–	0.009	–
WP2911	miRNA targets in ECM and membrane receptors	2	–	0.0377	–

This is not surprising, since blood is a complex medium capable of wetting almost any artificial surface. Accordingly, *ex vivo* modification of the wettability of cardiovascular devices may not fulfill the useful practical role intended by materials scientists. At the same time, the technological minimization of surface topography is a more straightforward task in the manufacture of cardiovascular devices [77]. Consequently, it is necessary to determine a UV-laser treatment regimen that improves or does not affect the nanoscale roughness of stent substrates.

CONCLUSION

Metal stents, including those made of nitinol, are a modern tool of choice for cardiac surgeons in the minimally invasive treatment of arterial stenosis in various parts of the vascular bed. In turn, laser surface treatment can mitigate negative physicochemical properties (the corrosive activity of nitinol) and improve the bio- and hemocompatibility of cardiovascular devices. In this regard, UV laser modification of the nitinol surface (at an energy density of 0.1 J/cm^2) reduces the metabolic imbalance of cells adhering to the samples in an *in vitro* culture, which improves their survival rates according to the MTT test.

From the perspective of the experimental model and the bioinformatics prediction of the cause-and-effect relationships behind the obtained effect, the increased hydrophilicity and nanoscale roughness, but not the ζ-potential, of the nitinol substrates modified with UV laser radiation may underlie the induction of a cascade of intracellular signaling and metabolic pathways involved in the expression and transcription of genes regulating the cellular and tissue reactions of the blood system to implantable

materials. These reactions include the induction of inflammation, activation of hemostasis, angiospasm and regeneration of the vascular bed, as well as the metabolic activity of target cells. Further experimental verification of the actual expression of target genes and the response of target cells (endothelial cells, blood cells, mesenchymal stem cells, smooth muscle cells) to the physicochemical modification of the nitinol substrate surface is necessary.

REFERENCES

1. Usacheva E.V., Nelidova A.V., Kulikova O.M., Flyanku I.P. Mortality of Russian Able-bodied Population from Cardiovascular Diseases. *Hygiene and Sanitation*. 2021;100(2):159–165. (In Russ.). DOI: 10.47470/0016-9900-2021-100-2-159-165.
2. Camici G.G. What is an optimal stent? Biological requirements of drug eluting stents. *Kardiovaskuläre Medizin*. 2008;11(1):22–25.
3. Mani G., Feldman M.D., Patel D., Agrawal C.M. Coronary stents: a materials perspective. *Biomaterials*. 2007;28(9):1689–1710. DOI: 10.1016/j.biomaterials.2006.11.042.
4. U.S. Food and Drug Administration, Center for Devices and Radiological Health. Technical considerations for non-clinical assessment of medical devices containing Nitinol [draft guidance]. Silver Spring (MD): U.S. Food and Drug Administration; 2021 Jul 15 [updated 2021 Jul 15; cited 2024 Aug 10]. Available from: https://www.fda.gov/media/145294/download
5. Fukushima O., Yoneyama T., Doi H., Hanawa T. Corrosion resistance and surface characterization of electrolyzed Ti-Ni alloy. *Dental Materials Journal*. 2006;25(1):151–60. DOI: 10.4012/dmj.25.151.
6. Pequegnat A., Michael A., Wang J., Lian K., Zhou Y., Khan M.I. Surface characterizations of laser modified biomedical grade NiTi shape memory alloys. *Materials Science and Engineering: C*. 2015;50:367–378. DOI: 10.1016/j.msec.2015.01.085.
7. Chenrayan V., Vaishnav V., Shahapurkar K., Dhanabal P., Kalayarasan M., Raghunath S. et al. The effect of fs-laser micromachining parameters on surface roughness, bio-corrosion and biocompatibility of nitinol. *Optics & Laser Technology*. 2024;170:110200. DOI: 10.1016/j.optlastec.2023.110200.
8. Sablina T.Yu., Panchenko M.Yu., Zyatikov I.A., Puchikin A.V., Konovalov I.N., Panchenko Yu.N. Study of Surface Hydrophilicity of Metallic Materials Modified by Ultraviolet Laser Radiation. *Metal Working and Material Science*. 2024;26(4):218–233. (In Russ.). DOI: 10.17212/1994-6309-2024-26.4-218-233.
9. Panchenko M.Yu., Sablina T.Yu., Zyatikov I.A., Puchikin A.V., Panchenko Yu.N. Effect of UV laser treatment on wetting properties of TiNi alloy. *Russian Physics Journal*. 2024;67(10):1575–1582. DOI: 10.1007/s11182-024-03284-0.
10. Grenadyorov A.S., Chebodaeva V.V., Khlusov I.A., Semin V.O., Madzhara N.E., Solovyev A.A. Effect of a-C:H:SiOx coating thickness on corrosion resistance and zeta potential level of Ti-6Al-4V. *Journal of Vacuum Science & Technology A*. 2025;43(2):023401. DOI: 10.1116/6.0004085.
11. Evtushenko D.N., Fateev A.V., Khainovsky M.A., Polishchuk J., Kokorev O.V., Nasibov T.F. et al. Intermolecular interactions, regioselectivity, and biological activity of L-ascorbic acid, nicotinic acid and their cocrystal. *CrystEngComm*. 2024;26(46):6650–6666. DOI: 10.1039/d4ce00770k.
12. Nasibov T., Gorokhova A., Porokhova E., Shupletsova V., Yurova K., Avdeeva E. et al. A hypothesis of mesenchymal stem cell osteogenic differentiation mediated by chelidonic acid through the calcium import: original research and computer simulation. *Histochemistry and Cell Biology*. 2025;163(1):14. DOI: 10.1007/s00418-024-02342-5.
13. Nasibov T.F., Gorokhova A.V., Brazovsky K.S., Porokhova E.D., Avdeeva E.Yu., Belousov M.V. et al. The pipeline for in silico prediction of target genes and target metabolic pathways for small molecules, using chelidonic acid as an example. *Advanced targets in Biomedicine*. 2025;1(1):6–19. DOI: 10.5922/ATB-2025-1-1-1.
14. Korkmaz S., Goksuluk D., Zararsiz G. MVN: An R package for assessing multivariate normality. *The R Journal*. 2014;6(2):151–162.
15. PMCMRplus (version 1.9.12). Rdocumentation [Internet]. URL: https://www.rdocumentation.org/packages/PMCMRplus/versions/1.9.12.
16. brunnermunzel (version 2.0). Rdocumentation [Internet]. [cited 2024 Jul 21]. URL: https://www.rdocumentation.org/packages/brunnermunzel/versions/2.0
17. Royston P. Remark AS R94: A remark on algorithm AS 181: the W-test for normality. *Journal of the Royal Statistical Society. Series C (Applied Statistics)*. 1995;44(4):547–551. DOI: 10.2307/2986146.
18. Moser B.K., Stevens G.R. Homogeneity of variance in the two-sample means test. *The American Statistician*. 1992;46(1):19–21. DOI: 10.1080/00031305.1992.10475839.
19. Coombs W.T., Algina J., Oltman D.O. Univariate and multivariate omnibus hypothesis tests selected to control type I error rates when population variances are not necessarily equal. *Review of Educational Research*. 1996;66(2):137–179. DOI: 10.3102/00346543066002137.
20. Markowski C.A., Markowski E.P. Conditions for the effectiveness of a preliminary test of variance. *The American Statistician*. 1990;44(4):322–326. DOI: 10.1080/00031305.1990.10475752
21. Smith,H.F, The problem of comparing the results of two experiments with unequal errors. *Journal of the Council for Scientific and Industrial Research.* 1936;9:211–212.
22. Satterthwaite F.E. An approximate distribution of estimates of variance components. *Biometrics Bulletin*. 1946;2(6):110–114. DOI: 10.2307/3002019.
23. Welch B.L. The significance of the difference between two means when the population variances are unequal. *Biometrika*. 1938;29(3/4):350–362. DOI: 10.2307/2332010.
24. Moser B.K., Stevens G.R., Watts C.L. The two-sample *t* test versus Satterthwaite's approximate *F* test. *Communications in Statistics-Theory and Methods*. 1989;18(11):3963–3975. DOI: 10.1080/03610928908830135.
25. Zimmerman D.W., Zumbo B.D. Rank transformations and the power of the Student *t* test and Welch *t* test for non-normal populations with unequal variances. *Canadian Journal of Experimental Psychology / Revue canadienne de psychologie expérimentale*. 1993;47(3):523. DOI: 10.1037/h0078850.

26. Ruxton G.D. The unequal variance t-test is an underused alternative to Student's *t*-test and the Mann – Whitney *U*-test. *Behavioral Ecology*. 2006;17(4):688–690. DOI: 10.1093/beheco/ark016.
27. Munzel U., Brunner E. Nonparametric tests in the unbalanced multivariate one-way design. *Biometrical Journal*. 2000;42(7):837–854. DOI: 10.1002/1521-4036(200011)42:7<837::AID-BIMJ837>3.0.CO;2-S.
28. Brunner E., Munzel U. The nonparametric Behrens – Fisher problem: asymptotic theory and a small-sample approximation. *Biometrical Journal*. 2000;42(1):17–25. DOI: 10.1002/(SICI)1521-4036(200001)42:1<17::AID-BIMJ17>3.0.CO;2-U.
29. Karch J.D. Psychologists should use Brunner – Munzel's instead of Mann – Whitney's *U*- test as the default nonparametric procedure. *Advances in Methods and Practices in Psychological Science*. 2021;4(2): 2515245921999602. DOI: 10.1177/2515245921999602.
30. Noguchi K., Konietschke F., Marmolejo-Ramos F., Pauly M. Permutation tests are robust and powerful at 0.5% and 5% significance levels. *Behavior Research Methods*. 2021;53(6):2712–2724. DOI: 10.3758/s13428-021-01595-5.
31. Celik N. Welch's ANOVA: Heteroskedastic skew-t error terms. *Communications in Statistics-Theory and Methods*. 2022.;51(9):3065–3076. DOI: 10.1080/03610926.2020.1788084.
32. Delacre M., Lakens D., Leys C. Why psychologists should by default use Welch's *t*-test instead of Student's *t*-test. *International Review of Social Psychology*. 2017;30(1):92–101. DOI: 10.5334/irsp.82.
33. Tomarken A.J., Serlin R.C. Comparison of ANOVA alternatives under variance heterogeneity and specific noncentrality structures. *Psychological Bulletin*. 1986; 99(1):90. DOI: 10.1037/0033-2909.99.1.90.
34. Levy K.J. An empirical comparison of the ANOVA F-test with alternatives which are more robust against heterogeneity of variance. *Journal of Statistical Computation and Simulation*. 1978;8(1):49–57. DOI: 10.1080/00949657808810247.
35. Lix L.M., Keselman J.C., Keselman H.J. Consequences of assumption violations revisited: A quantitative review of alternatives to the one-way analysis of variance *F* test. *Review of Educational Research*. 1996;66(4):579–619. DOI: 10.3102/00346543066004579.
36. Tamhane A.C. A comparison of procedures for multiple comparisons of means with unequal variances. *Journal of the American Statistical Association*. 1979:74(366a):471–480. DOI: 10.1080/01621459.1979.10482541.
37. Shingala M.C., Rajyaguru A. Comparison of post hoc tests for unequal variance. *International Journal of New Technologies in Science and Engineering*. 2015;2(5):22–33.
38. Berridge M.V., Herst P.M., Tan A.S. Tetrazolium dyes as tools in cell biology: new insights into their cellular reduction. *Biotechnology Annual Review*. 2005;11:127–152. DOI: 10.1016/S1387-2656(05)11004-7.
39. Ghasemi M., Turnbull T., Sebastian S., Kempson I. The MTT Assay: Utility, Limitations, Pitfalls, and Interpretation in Bulk and Single-Cell Analysis. *International Journal of Molecular Sciences*. 2021;22(23):12827. DOI: 10.3390/ijms222312827.
40. Ren Q., Zhu X., Li W., Wu M., Cui S., Ling Y. et al. Fabrication of super-hydrophilic and highly open-porous poly (lactic acid) scaffolds using supercritical carbon dioxide foaming. *International Journal of Biological Macromolecules*. 2022;205:740–748. DOI: 10.1016/j.ijbiomac.2022.03.107.
41. Long J., Zhong M., Zhang H., Fan P. Superhydrophilicity to superhydrophobicity transition of picosecond laser microstructured aluminum in ambient air. *Journal of Colloid and Interface Science*. 2015;441:1–9. DOI: 10.1016/j.jcis.2014.11.015.
42. Razi S., Mollabashi M., Madanipour K. Improving the hydrophilicity of metallic surfaces by nanosecond pulsed laser surface modification. *Journal of Laser Applications*. 2015;27(4):042006-1–042006-9. DOI: 10.2351/1.4928290.
43. Zhu H.Z., Zhang H.C., Ni X.W., Shen Z.H., Lu J. Fabrication of superhydrophilic surface on metallic nickel by sub-nanosecond laser-induced ablation. *AIP Advances*. 2019;9(8):085308. DOI: 10.1063/1.5111069.
44. Ganash M.A. Anticancer potential of ascorbic acid and inorganic selenium on human breast cancer cell line MCF-7 and colon carcinoma HCT-116. *Journal of Cancer Research and Therapeutics*. 2021;17(1):122–129. DOI: 10.4103/jcrt.JCRT_989_17.
45. Mobasher M.A. Apoptotic activity and cytotoxic effect of convolvulus spicatus on human breast cancer cell line (MCF-7). *Pakistan Journal of Biological Sciences*. 2021;24(6):646–655. DOI: 10.3923/pjbs.2021.646.655.
46. Gambardella G., Viscido G., Tumaini B., Isacchi A., Bosotti R., di Bernardo D. A single-cell analysis of breast cancer cell lines to study tumour heterogeneity and drug response. *Nature Communications*. 2022;13(1):1714. DOI: 10.1038/s41467-022-29358-6.
47. Fayyad R.J., Ali A.N.M., Saeed N.A.A.A.H., Hamzah I.H., Dwaish A.S. Phycosynthesis of silver nanoparticles *using Cladophora glomerata* and evaluation of their ability to inhibit the proliferation of MCF-7 and L20B cell lines. *Asian Pacific Journal of Cancer Prevention: APJCP*. 2022;23(10):3563–3569. DOI: 10.31557/APJCP.2022.23.10.3563.
48. Komarova E.G., Akimova E.B., Kondranova A.M., Porokhova E.D., Nasibov T.F., Syrokvashin M.M. et al. Laser interference microscopy study of the morphometric features of MCF-7 cancer cells contacted with 5-Fluorouracil-loaded calcium phosphate coatings on titanium implants. *Materials Chemistry and Physics*. 2025;333:130299. DOI: 10.1016/j.matchemphys.2024.130299.
49. Zohrabi T., Habibi N., Zarrabi A., Fanaei M., Lee L.Y. Diphenylalanine peptide nanotubes self-assembled on functionalized metal surfaces for potential application in drug-eluting stent. *Journal of Biomedical Materials Research. Part A*. 2016;104(9):2280–2290. DOI: 10.1002/jbm.a.35764.
50. Pintor A.V.B., Queiroz L.D., Barcelos R., Primo L.S.G., Maia L.C., Alves G.G. MTT versus other cell viability assays to evaluate the biocompatibility of root canal filling materials: a systematic review. *International Endodontic Journal*. 2020;53(10):1348–1373. DOI: 10.1111/iej.13353.
51. Ohashi K., Fujiwara S., Mizuno K. Roles of the cytoskeleton, cell adhesion and rho signalling in mechanosensing and mechanotransduction. *The Journal of Biochemistry*. 2017;161(3):245–254. DOI: 10.1093/jb/mvw082.
52. Burridge K., Monaghan-Benson E., Graham D.M. Mechanotransduction: from the cell surface to the nucleus via

RhoA. *Philosophical Transactions of the Royal Society B*. 2019;374(1779):20180229. DOI: 10.1098/rstb.2018.0229.
53. Janota C.S., Calero-Cuenca F.J., Gomes E.R. The role of the cell nucleus in mechanotransduction. *Current Opinion in Cell Biology*. 2020;63:204–211. DOI: 10.1016/j.ceb.2020.03.001.
54. Khlusov I.A., Litvinova L.S., Yurova K.A., Khlusova M.Y. Precise tissue bioengineering and niches of mesenchymal stem cells: their size and hierarchy matter. *Biocell*. 2022;46(6):1365–1373. DOI: 10.32604/biocell.2022.018917.
55. Khlusov I.A., Khlusova M.Yu., Litvinova L.S. Native cell domains as stem cell regulatory microterritories for precise tissue engineering. *Next Materials*. 2023;1(3):100021. DOI: 10.1016/j.nxmate.2023.100021.
56. Spriano S., Sarath Chandra V., Cochis A., Uberti F., Rimondini L., Bertone E. How do wettability, zeta potential and hydroxylation degree affect the biological response of biomaterials? *Materials Science and Engineering: C*. 2017;74:542–555. DOI: 10.1016/j.msec.2016.12.107.
57. Song J., Gerecht S. Hydrogels to recapture extracellular matrix cues that regulate vascularization. *Arteriosclerosis, Thrombosis, and Vascular Biology*. 2023;43(8):e291–e302. DOI: 10.1161/ATVBAHA.122.318235.
58. Khlusov I.A., Grenadyorov A.S., Solovyev A.A., Semenov V.A., Zhulkov M.O., Sirota D.A. et al. Endothelial cell behavior and nitric oxide production on a-C:H:SiOx-coated Ti-6Al-4V substrate. *International Journal of Molecular Sciences*. 2023;24(7):6675. DOI: 10.3390/ijms24076675.
59. Zhang M., Zhao F., Zhu Y., Brouwer L.A., Van der Veen H., Burgess J.K. et al. Physical properties and biochemical composition of extracellular matrix-derived hydrogels dictate vascularization potential in an organ-dependent fashion. *ACS Applied Materials & Interfaces*. 2024;16(23):29930–29945. DOI: 10.1021/acsami.4c05864.
60. Grenadyorov A.S., Solovyev A.A., Oskomov K.V., Semenov V.A., Zhulkov M.O., Sirota D.A. et al. Morphofunctional reaction of leukocytes and platelets in in vitro contact with a-C:H:SiOx-coated Ti-6Al-4V substrate. *Journal of Biomedical Materials Research. Part A*. 2023;111(3):309–321. DOI: 10.1002/jbm.a.37470.
61. Belosludtsev K.N., Belosludtseva N.V., Agafonov A.V., Penkov N.V., Samartsev V.N., Lemasters J.J. et al. Effect of surface-potential modulators on the opening of lipid pores in liposomal and mitochondrial inner membranes induced by palmitate and calcium ions. *Biochimica et Biophysica Acta (BBA) – Biomembranes*. 2015;1848(10):2200–2205. DOI: 10.1016/j.bbamem.2015.05.013.
62. Oberleithner H. Quantifying salt sensitivity. *Biological Chemistry*. 2021;402(12):1597–1602. DOI: 10.1515/hsz-2021-0206.
63. Ghitescu L., Fixman A. Surface charge distribution on the endothelial cell of liver sinusoids. *The Journal of Cell Biology*. 1984;99(2):639–647. DOI: 10.1083/jcb.99.2.639.
64. Lee K.S., Lee J., Kim H.K., Yeom S.H., Woo C.H., Jung Y.J. et al. Extracellular vesicles from adipose tissue-derived stem cells alleviate osteoporosis through osteoprotegerin and miR-21-5p. *Journal of Extracellular Vesicles*. 2021;10(12):e12152. DOI: 10.1002/jev2.12152.
65. Ouyang L., Shaik R., Xu R., Zhang G., Zhe J. Mapping surface charge distribution of single-cell via charged nanoparticle. *Cells*. 2021;10(6):1519. DOI: 10.3390/cells10061519.
66. Mao A.W., Jiang T.H., Sun X.J., Peng J. Application of chemokine receptor antagonist with stents reduces local inflammation and suppresses cancer growth. *Tumor Biology*. 2015;36(11):8637–8643. DOI: 10.1007/s13277-015-3557-1.
67. Venault A., Hsu K.J., Yeh L.C., Chinnathambi A., Ho H.T., Chang Y. Surface charge-bias impact of amine-contained pseudozwitterionic biointerfaces on the human blood compatibility. *Colloids and Surfaces B: Biointerfaces*. 2017;151:372–383. DOI: 10.1016/j.colsurfb.2016.12.040.
68. Choi S.Y., Habimana O., Flood P., Reynaud E.G., Rodriguez B.J., Zhang N. et al. Material- and feature-dependent effects on cell adhesion to micro injection moulded medical polymers. *Colloids and Surfaces B: Biointerfaces*. 2016;145:46–54. DOI: 10.1016/j.colsurfb.2016.04.032.
69. Mirzadeh H., Moghadam E.V., Mivehchi H. Laser-modified nanostructures of PET films and cell behavior. *Journal of Biomedical Materials Research. Part A*. 2011;98(1):63–71. DOI: 10.1002/jbm.a.33097.
70. Anderson C.R., Gambinossi F., DiLillo K.M., Laschewsky A., Wischerhoff E., Ferri J.K. et al. Tuning reversible cell adhesion to methacrylate-based thermoresponsive polymers: effects of composition on substrate hydrophobicity and cellular responses. *Journal of Biomedical Materials Research Part A*. 2017;105(9):2416–2428. DOI: 10.1002/jbm.a.36100.
71. Lamichhane S., Anderson J.A., Remund T., Sun H., Larson M.K., Kelly P. et al. Responses of endothelial cells, smooth muscle cells, and platelets dependent on the surface topography of polytetrafluoroethylene. *Journal of Biomedical Materials Research. Part A*. 2016;104(9):2291–304. DOI: 10.1002/jbm.a.35763.
72. Tan L., Xie Q., Jia X., Guo M., Zhang Y., Tang H. et al. Dynamic measurement of the surface stress induced by the attachment and growth of cells on Au electrode with a quartz crystal microbalance. *Biosensors and Bioelectronics*. 2009;24(6):1603–1609. DOI: 10.1016/j.bios.2008.08.021.
73. Xie Y., Sproule T., Li Y., Powell H., Lannutti J.J., Kniss D.A. Nanoscale modifications of PET polymer surfaces via oxygen-plasma discharge yield minimal changes in attachment and growth of mammalian epithelial and mesenchymal cells in vitro. *Journal of Biomedical Materials Research: An Official Journal of The Society for Biomaterials, The Japanese Society for Biomaterials, and The Australian Society for Biomaterials and the Korean Society for Biomaterials*. 2002;61(2):234–245. DOI: 10.1002/jbm.10141.
74. Khorsandi L., Orazizadeh M., Niazvand F., Abbaspour M.R., Mansouri E., Khodadadi A. Quercetin induces apoptosis and necroptosis in MCF-7 breast cancer cells. *Bratislavske Lekarske Listy*. 2017;118(2):123–128. DOI: 10.4149/BLL_2017_025.
75. Zhu T., Wu J., Zhao N., Cai C., Qian Z., Si F. et al. Superhydrophobic / superhydrophilic Janus fabrics reducing blood loss. *Advanced Healthcare Materials*. 2018;7(7):e1701086. DOI: 10.1002/adhm.201701086.
76. Wu X.H., Liew Y.K., Mai C.W., Then Y.Y. Potential of superhydrophobic surface for bood-contacting medical devices. *International Journal of Molecular Sciences*. 2021;22(7):3341. DOI: 10.3390/ijms22073341.

77. Li H., Wang Y., Wu X., Zhou L., Liu L., Fang Y. Blood pump surface roughness: hemocompatibility and machining optimization. *ASAIO Journal*. 2025;10.1097. DOI: 10.1097/MAT.0000000000002501.

Author Contribution

Kokorev O.V. – developing the model, conducting co-cultivation of cells with nitinol samples, performing the MTT test. Gorokhova A.V. – morphometric processing and interpretation of experimental data, drafting and editing the article. Nasibov T.F. – conducting bioinformatics and statistical analysis, interpretation and visualization of data. Khlusov I.A. – collection and analysis of literary sources, drafting and editing of the article, coordination of the research. Krivoshchekov S.V. – measurement of cell zeta potential. Chebodaeva V.V. – measurement of the zeta potential of the flat surface of nitinol samples. Brazovsky K.S. – development of the algorithm for in silico modeling of intracellular signaling and metabolic pathways. Khlusova M.Yu. – collection and analysis of literary sources on the biology of the tested cells, participation in article editing. Sablina T.Yu. – collection and analysis of literary sources, conducting research after laser surface modification, interpretation and visualization of experimental data, drafting of a section of the article, editing of the article. Kandaurova M.Yu. – collection and analysis of literary sources, performing UV laser treatment of experimental samples, conducting physical research after laser surface modification, interpretation and visualization of experimental data, drafting of a section of the article. Zyatikov I.A. – performing UV laser treatment of experimental samples, conducting research after laser surface modification, interpretation and visualization of experimental data. Panchenko Yu.N. – coordination of research on laser surface modification of experimental samples, drafting and editing of the article.

Author Information

Khlusov Igor A. – Dr. Sci. (Med.), Professor, Division of Morphology and General Pathology, Siberian State Medical University, Tomsk; Head of the Laboratory of Cellular and Microfluidic Technologies, Siberian State Medical University, Tomsk; Senior Researcher, IHCE SB RAS, Tomsk, khlusov63@mail.ru, https://orcid.org/0000-0003-3465-8452

Kokorev Oleg V. – Dr. Sci. (Med.), Professor, Division of Biochemistry and Molecular Biology with a Course in Clinical Laboratory Diagnostics, Siberian State Medical University, Tomsk, https://orcid.org/0000-0003-3690-0177

Gorokhova Anna V. – Research Assistant, Division of Morphology and General Pathology, Siberian State Medical University, Tomsk; Engineer, IHCE SB RAS, Tomsk, a.gorokhova3062@gmail.com, https://orcid.org/0000-0001-8401-7181

Nasibov Temur F. – Research Assistant, Division of Morphology and General Pathology, Siberian State Medical University, Tomsk; Engineer, IHCE SB RAS, Tomsk, temur.nsbv@gmail.com, https://orcid.org/0000-0002-8056-3967

Krivoshchekov Sergey V. – Cand. Sci. (Chemistry), Associate Professor, Division of Pharmaceutical Analysis, Siberian State Medical University, Tomsk, krivoshchekov.sv@ssmu.ru, https://orcid.org/0000-0001-5505-7141

Chebodaeva Valentina V. – Cand. Sci. (Engineering), Researcher, ISPMS SB RAS, Tomsk; Junior Researcher, IHCE SB RAS, Tomsk, vtina5@mail.ru, https://orcid.org/0000-0002-1980-3941

Brazovsky Konstantin S. – Dr. Sci. (Engineering), Professor, Division of Medical and Biological Cybernetics, Siberian State Medical University, Tomsk, brazovsky.ks@ssmu.ru, https://orcid.org/ 0000-0002-4779-9820

Khlusova Marina Yu. – Cand. Sci. (Med.), Associate Professor, Pathophysiology Division, Siberian State Medical University, Tomsk, hlusova.my@ssmu.ru, https://orcid.org/0000-0001-9583-5358

Sablina Tatyana Yu. – Cand. Sci. (Engineering), Researcher, Gas Lasers Laboratory, IHCE SB RAS, Tomsk, sty@lgl.hcei.tsc.ru, https://orcid.org/0000-0002-5941-5732

Kandaurova Marina Yu. – Cand. Sci. (Physics and Mathematics), Researcher, Gas Lasers Laboratory, IHCE SB RAS, Tomsk, panchenko.marina4@gmail.com, https://orcid.org/0000-0003-0236-2227

Zyatikov Ilya A. – Junior Researcher, Gas Lasers Laboratory, IHCE SB RAS, Tomsk, zyatikov@lgl.hcei.tsc.ru, https://orcid.org/0000-0003-3219-9299

Panchenko Yuri N. – Dr. Sci. (Physics and Mathematics), Chief Researcher, Head of the Gas Lasers Laboratory, IHCE SB RAS, Tomsk, yu.n.panchenko@mail.ru, https://orcid.org/0000-0001-8017-7268

(✉) **Khlusov Igor A.,** khlusov63@mail.ru

Received on September 05, 2025;
approved after peer review on September 19, 2025;
accepted on September 25, 2025

УДК 575.112:004.94
https://doi.org/10.20538/1682-0363-2026-2-115-120

Computer Simulation of Xanthotoxin Interaction with Caspase 3

Chasovskikh N.Yu., Shestakova E.E., Novitsky D.E.

Siberian State Medical University
2 Moskovsky trakt, 634050 Tomsk, Russian Federation

ABSTRACT

Aim. To perform computer modeling and evaluate the interactions between caspase 3 and xanthotoxin.

Materials and methods. The structures of caspase 3 and xanthotoxin were extracted from the PDB protein database (ID 2J31) and the PubChem chemical compounds and mixtures database (ID 4114), respectively. PyMOL v. 2.5 was used to prepare the caspase 3 structure for docking, and OpenBabel was used to convert xanthotoxin to .pdb format. Molecular docking was performed in AutoDock Vina. Molecular dynamics was performed using GROMACS 2023.3. The CHARMM 36 force field was used to generate the protein topology, and the CHARMM General Force Field (CGenFF) server was used for the ligand topology. Xmgrace and PyMOL were used to analyze the results.

Results. Molecular docking of caspase 3 and xanthotoxin resulted in a stable complex with binding energy of -4.83 kcal/mol. The amino acid residues of caspase 3 involved in intermolecular interaction were identified: tyrosine 195 (TYR195), valine 266 (VAL266), lysine 137 (LYS137). The results of the molecular dynamics simulation confirmed the stability of the complex obtained as a result of docking.

Conclusion. The data obtained indicate the possible role of the studied furocoumarin in the implementation of programmed cell death and can be used for further experimental studies.

Keywords: docking, molecular dynamics, caspase 3, xanthotoxin

Conflict of interest. The authors declare the absence of obvious or potential conflicts of interest related to the publication of this article.

Source of financing. The authors declare that they received no funding for the study.

For citation: Chasovskikh N.Yu., Shestakova E.E., Novitsky D.E. Computer Simulation of Xanthotoxin Interaction with Caspase 3. *Bulletin of Siberian Medicine.* 2026;25(2):115–120. https://doi.org/10.20538/1682-0363-2026-2-115-120.

Компьютерное моделирование взаимодействия ксантотоксина с каспазой 3

Часовских Н.Ю., Шестакова Е.Е., Новицкий Д.Е.

Сибирский государственный медицинский университет (СибГМУ)
Россия, 634050, г. Томск, Московский тракт, 2

РЕЗЮМЕ

Цель – провести компьютерное моделирование и оценить взаимодействие каспазы 3 с ксантотоксином.

Материалы и методы. Структуры каспазы 3 и ксантотоксина извлечены из банка данных белков PDB (ID 2J31) и базы данных химических соединений и смесей PubChem (ID 4114) соответственно. Для подготовки структуры каспазы 3 к докингу применяли PyMOL v. 2.5, для конвертации ксантотоксина в формат .pdb использовали OpenBabel. Докинг проводили в AutoDock Vina. Молекулярно-динамическое моделирование выполняли с использованием GROMACS 2023.3. Для генерации топологии белка использовали силовое поле CHARMM 36, для топологии лиганда – сервер CHARMM General Force Field (CGenFF). Для анализа результатов применяли Xmgrace и PyMOL.

✉ *Shestakova Evgeniia E.,* evgenika06@gmail.com

Результаты. В результате проведенного молекулярного докинга каспазы 3 и ксантотоксина получен стабильный комплекс с энергией связывания –4,83 ккал/моль. Выявлены аминокислотные остатки каспазы 3, участвующие в межмолекулярном взаимодействии: тирозин 195 (TYR195), валин 266 (VAL266), лизин 137 (LYS137). Результаты проведенной симуляции молекулярной динамики подтвердили устойчивость комплекса, полученного в результате докинга.

Заключение. Полученные данные свидетельствуют о возможной роли изучаемого фурокумарина в реализации программируемой гибели клеток и могут быть использованы для дальнейших экспериментальных исследований.

Ключевые слова: докинг, молекулярная динамика, каспаза 3, ксантотоксин, апоптоз

Конфликт интересов. Авторы декларируют отсутствие явных и потенциальных конфликтов интересов, связанных с публикацией настоящей статьи.

Источник финансирования. Авторы заявляют об отсутствии финансирования при проведении исследования.

Для цитирования: Часовских Н.Ю., Шестакова Е.Е., Новицкий Д.Е. Компьютерное моделирование взаимодействия ксантотоксина с каспазой 3. *Бюллетень сибирской медицины.* 2026;25(2):115–120. https://doi.org/10.20538/1682-0363-2026-2-115-120.

INTRODUCTION

Socially sensitive diseases, particularly cancer, are the leading causes of disability and mortality in Russia. According to the Rosstat data for 2023, malignant tumors account for 16.4% of all deaths in Russia [1]. One of the key factors in the development of these pathologies is the dysregulation of apoptosis, which involves the activation or suppression of the cell death program [2].

Apoptosis is a form of cell death that eliminates excess or functionally abnormal cells to maintain tissue homeostasis in the body [3]. The main pathways that initiate apoptosis are the extrinsic (death receptor) pathway and the intrinsic (mitochondrial) pathway. Additionally, there are granzyme B-dependent, endoplasmic reticulum (ER) stress, perforin/granzyme, and nuclear apoptosis pathways. The induction of apoptosis and the activation of pro-apoptotic proteins trigger a cascade of caspases [4]. At the first stage of each pathway, an initiator caspase is activated (caspase 8 in the extrinsic pathway, caspase 9 in the intrinsic pathway, and caspase 10 in the perforin – granzyme pathway), which subsequently activates effector caspase 3. In the extrinsic (receptor) pathway, following the binding of a ligand to the corresponding receptor (a molecule from of the TNFα receptor superfamily) on the cell surface, a cascade of intracellular reactions is activated, resulting in the activation of caspases 8 and 10. These caspases then activate caspases 3, 6, and 7, which facilitate cell death [5].

In the intrinsic (mitochondrial) pathway, in response to stressors (such as DNA damage or a lack of growth factors), the mitochondrial protein p53 is activated. In turn, p53 suppresses Bcl-2 and activates Bax, whose dimeric form activates the serine protease Ich-1, leading to the induction of apoptosis and activation of effector caspases [5]. This process ultimately results in the cleavage of caspase 3, causing DNA fragmentation, degradation of cytoskeletal and nuclear proteins, formation of apoptotic bodies, and their subsequent engulfment by phagocytic cells [4].

Caspase 3 is one of the main effectors of apoptosis, making molecules that can modify its activity particularly interesting due to their potential therapeutic properties. Currently, furocoumarins, especially xanthotoxin (8-methoxypsoralen), are actively being studied as such molecules [6–8]. Xanthotoxin exhibits photosensitizing properties and can induce apoptosis in various tumor cell lines [9, 10]. It is hypothesized that xanthotoxin can activate caspase 3; however, the exact mechanism remains unknown [11, 12].

To predict and evaluate interactions between proteins and molecules with potential therapeutic properties (including those that can be valuable for studying apoptosis mechanisms), *in silico* methods are currently being used extensively [13, 14].

Given this context, the aim of this study was to conduct computer simulation and evaluate the interaction between caspase 3 and xanthotoxin.

MATERIALS AND METHODS

The experimental three-dimensional (3D) structure of caspase 3 (PDB identifier: 2J31) was extracted from the Protein Data Bank (PDB) [15]. The 3D structure of xanthotoxin (PubChem identifier: 4114) was retrieved from the PubChem Substance and Compound database [16].

The 3D structure of caspase 3 was cleaned of all water molecules and ligands, analyzed, and prepared for further simulation using PyMOL v. 2.5 [17].

The 3D structure of xanthotoxin from the PubChem database was retrieved in .sdf format and converted to .pdb format for molecular docking using the OpenBabel converter [18].

AutoDock Vina [19] was used to conduct the molecular docking of caspase 3 and xanthotoxin. AutoDock Vina employs an empirical and knowledge-based function to predict the binding affinity of compounds [19]. The dimensions of the calculation grid for caspase 3 were set to 25 x 25 x 25 Å, centered at the coordinates (31.0, 21.0, 55.0).

Molecular dynamics (MD) simulation of the caspase – xanthotoxin complex was performed using GROMACS 2023.3 [20]. The protein topology was generated using the CHARMM36 force field, while the ligand topology was created using the CHARMM General Force Field (CGenFF) server [21]. The complex was solvated in a cubic box with a dimension of 1.0 nanometer (nm) using the TIP3P water model, and neutralization was achieved with Cl^- ions. Energy minimization was conducted using the steepest descent method [22]. Equilibrium state simulations lasting 100 picoseconds (ps) were carried out using NVT (canonical ensemble, where N is the number of particles, V is the volume, and T is the temperature) and NPT (isothermal – isobaric ensemble, where N is the number of particles, P is the pressure, and T is the temperature) ensembles. The parameters for these ensembles were optimized for a temperature of 300 K and a pressure of 1 bar. The main phase of MD simulation was conducted over 50 nanoseconds (ns) with a time step of 2 femtoseconds (fs). The Xmgrace software was used to generate graphs illustrating the simulation results [23].

For further analysis of the obtained results, we evaluated the root mean square deviation (RMSD), root mean square fluctuation (RMSF), and radius of gyration (Rg) [24].

RESULTS AND DISCUSSION

Molecular docking of caspase 3 and xanthotoxin resulted in the most stable complex with a binding energy of –4.83 kcal/mol. The residues involved in intermolecular interaction were identified: tyrosine 195 (TYR195), valine 266 (VAL266), and lysine 137 (LYS137) (Fig. 1).

The obtained complex is stabilized due to several types of interactions: π-stacking (or π-π interactions) between the ligand and TYR195, π-cation interactions between the ligand and VAL266, and hydrophobic interactions between the ligand and both TYR195 and VAL266. π-stacking refers to the non-covalent interaction between aromatic systems (benzene rings) that occurs due to the overlap of their π-electron clouds. π-cation interactions represent a non-covalent bond between an aromatic system and a positively charged amino group of the protein. Hydrophobic interactions are characterized by the tendency of non-polar molecules to cluster together in an aqueous environment to minimize the contact area of their non-polar surfaces with water.

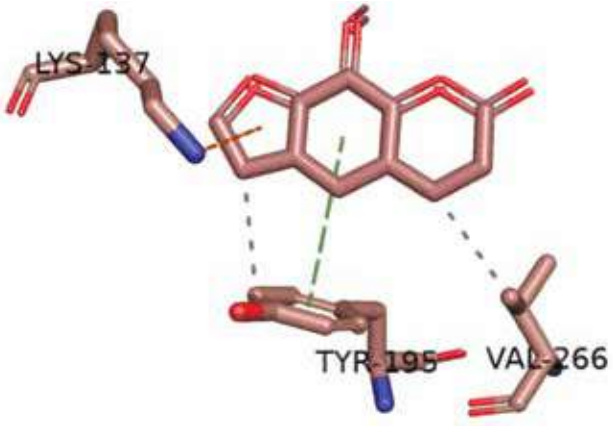

Fig. 1. This figure illustrates the amino acids of caspase 3 that are involved in interactions with xanthotoxin. Dashed lines indicate the following types of interactions: gray dashed lines represent hydrophobic interactions, green dashed lines indicate π-stacking, and orange dashed lines denote π-cation interactions

Subsequently, MD simulations were conducted, and their characteristics are described below.

RMSD is a commonly used metric for assessing the stability and conformational changes of a protein or protein – ligand complex during MD simulations. Constant RMSD values throughout the simulation process indicate that the initial conformation and structural stability of the system are maintained [25].

In our case, there was a sharp increase in RMSD during the first 10 ns, followed by values remaining within the range of 0.2–0.3 nm from 10 to 40 ns, indicating structural stability (Fig. 2).

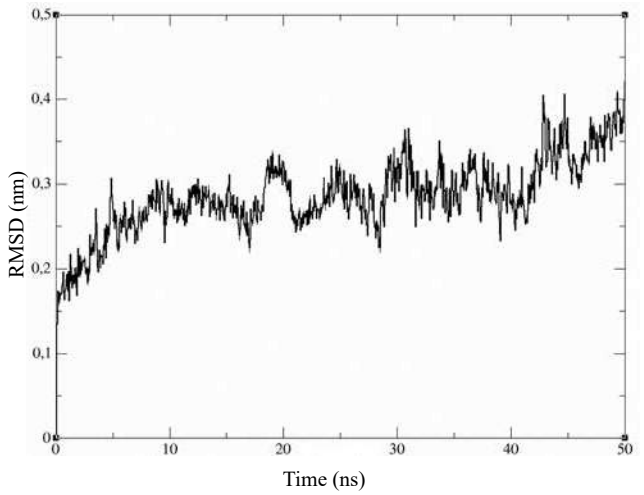

Fig. 2. The root mean square deviation of caspase 3 in complex with xanthotoxin

The RMSF metric is used to evaluate the mobility of amino acid residues in a protein and specific regions of the polypeptide chain. For the caspase 3 and xanthotoxin complex, the maximum RMSF value of 1.0 nm was observed in the first 30 residues, indicating high mobility in this region (Fig. 3). Beyond this point, RMSF values remained at around 0.05–0.15 nm, suggesting stability among these residues and indicating the presence of secondary structural elements of the protein (α-helices and β-sheets) in this zone. Peaks of approximately 0.3 nm were noted in the regions of amino acid residues 160–190, 200–220, and 250–270, indicating flexible loops.

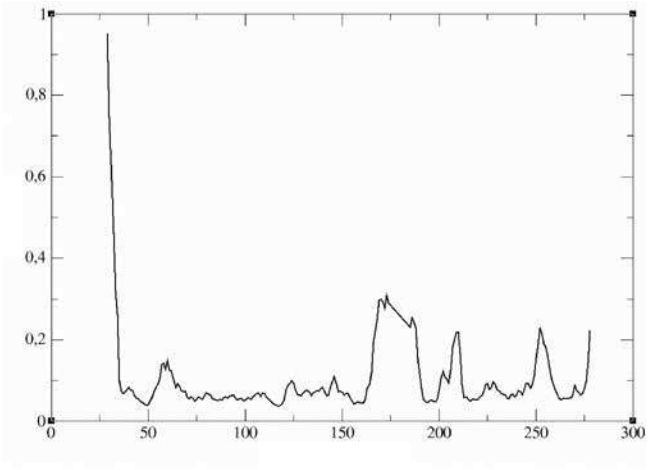

Fig. 3. Root mean square fluctuation (RMSF) of caspase 3

The radius of gyration is used to assess the compactness of the protein – ligand complex during simulation. A loss of compactness can impact the stability of the complex by introducing weak intermolecular interactions.

According to the findings, the radius of gyration ranged from 1.78 to 1.83 nm, indicating stability and compactness of the structure (Fig. 4). During the first 10 ns, the protein adopted a stable, compact form; the radius of gyration fluctuated between 1.74 and 1.78 nm without significant variations.

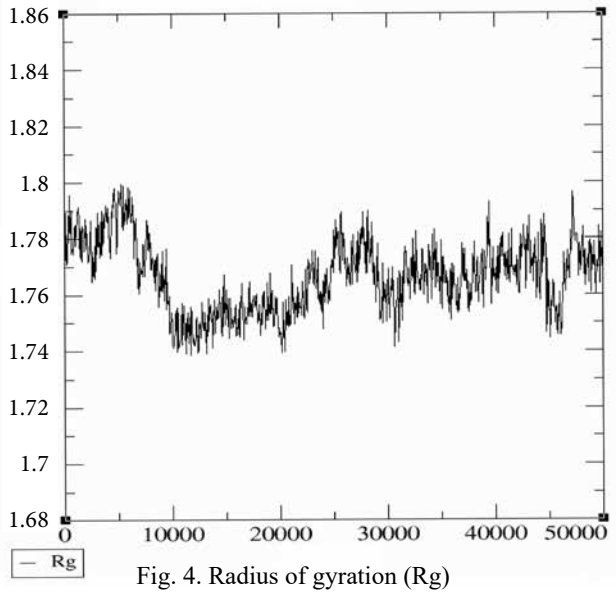

Fig. 4. Radius of gyration (Rg)

The findings suggest that a stable xanthotoxin – caspase 3 complex can form. It can be hypothesized that this interaction may alter the activity of caspase 3, which is involved in programmed cell death processes.

Experimental data indicate that programmed cell death in tumor cells is associated with the activation of caspase 3 in the presence of xanthotoxin. Caspase 3 is essential for transmitting apoptotic signals following exposure to DNA-damaging agents [26]. A study by G. Viola et al. shows that caspase 3 is activated after irradiation in the presence of xanthotoxin [12]. Additionally, apoptosis induction was noted in HepG2 cell line (a liver cancer cell line) after treatment with xanthotoxin [11]. However, the molecular mechanisms underlying this phenomenon remain unexplored.

CONCLUSION

The computer simulation of the interaction between caspase 3 and xanthotoxin, conducted through molecular docking followed by verification

using molecular dynamics demonstrated the presence of a stable intermolecular interaction. The resulting complex features a binding energy of -4.83 kcal/mol and several types of chemical bonds: π-stacking and π-π interactions between the ligand and TYR195, π-cation interactions between the ligand and VAL266, and hydrophobic interactions between the ligand and both TYR195 and VAL266. The results of molecular dynamics simulation confirmed the stability of the complex obtained from docking.

Thus, the findings of this study suggest that xanthotoxin has the potential to interact with caspase 3, forming a stable complex. These data indicate a possible role of the studied furocoumarin in the process of programmed cell death. Further experimental studies are necessary to validate the results of the computer simulation.

REFERENCES

1. Natural Movement of the Population of the Russian Federation for 2023 (Statistical Bulletin). Moscow: Rosstat, 2024. (In Russ.).
2. Glukhov A.I., Gryzunova G.K., Usay L.I., Aleynikova T.L., Chernikova N.V., Burt A.Yu. The Role of Apoptosis in the Pathogenesis of Some Critical Conditions. *General Reanimatology*. 2019;15(2):79-98. (In Russ.). DOI:10.15360/1813-9779-2019-2-79-98
3. Chasovskikh N.Yu. et al. Apoptosis and Oxidative Stress. Tomsk: Pechatnaya Manufaktura, 2009:148. (In Russ.).
4. Elmore S. Apoptosis: a review of programmed cell death. *Toxicol Pathol*. 2007;35(4):495-516. DOI: 10.1080/01926230701320337
5. Sokolov D.I. Immunological Mechanisms of Apoptosis in Placental Development. *Medical Immunology (Russia)*. 2008;10(2–3):125–138. (In Russ.). DOI:10.15789/1563-0625-2008-2-3-125-138
6. Fu K, Zhang J., Wang L., Zhao X., Luo Y. Xanthotoxin induced photoactivated toxicity, oxidative stress and cellular apoptosis in Caenorhabditis elegans under ultraviolet A. *Comp. Biochem. Physiol. C Toxicol. Pharmacol*. 2022;251:109217. DOI: 10.1016/j.cbpc.2021.109217.
7. Hähnel V., Brosig A.M., Ehrenschwender M., Burkhardt R., Offner R., Ahrens N. Apoptosis induction by extracorporeal photopheresis is enhanced by increasing the 8-methoxypsoralen concentration and by replacing plasma with saline. *Transfusion*. 2021;61(10):2991-2999. DOI: 10.1111/trf.16634.
8. Abdel Hafez O.M., Amin K.M., Abdel-Latif N.A., Mohamed T.K., Ahmed E.Y., Maher T. Synthesis and antitumor activity of some new xanthotoxin derivatives. *Eur. J. Med. Chem*. 2009;44(7):2967–2974. DOI: 10.1016/j.ejmech.2009.01.006
9. Yang H., Xiong J., Luo W., Yang J., Xi T. 8-Methoxypsoralen Induces Intrinsic Apoptosis in HepG2 Cells: Involvement of Reactive Oxygen Species Generation and ERK1/2 Pathway Inhibition. *Cell Physiol. Biochem*. 2015;37(1):361–374. DOI: 10.1159/000430360.
10. Choi E.K., Kim H.D., Park E.J., Song S.Y., Phan T.T., Nam M. et al. 8-Methoxypsoralen Induces Apoptosis by Upregulating p53 and Inhibits Metastasis by Downregulating MMP-2 and MMP-9 in Human Gastric Cancer Cells. *Biomol. Ther. (Seoul)*. 2023;31(2):219-226. DOI: 10.4062/biomolther.2023.004.
11. Kurita M., Shimauchi T., Kobayashi M., Atarashi K., Mori K., Tokura Y. Induction of keratinocyte apoptosis by photosensitizing chemicals plus UVA. *J. Dermatol. Sci*. 2007;45(2):105-12. DOI: 10.1016/j.jdermsci.2006.10.010.
12. Viola G., Fortunato E., Cecconet L., Disarò S., Basso G. Induction of apoptosis in Jurkat cells by photoexcited psoralen derivatives: Implication of mitochondrial dysfunctions and caspases activation. *Toxicol. In Vitro*. 2007;21(2):211-6. DOI: 10.1016/j.tiv.2006.09.016.
13. Issa M.Y., Elshal M.F., Fathallah N., Abdelkawy M.A., Bishr M., Salama O. et al. Potential Anticancer Activity of the Furanocoumarin Derivative Xanthotoxin Isolated from Ammi majus L. Fruits: In Vitro and In Silico Studies. *Molecules*. 2022;27(3):943. DOI: 10.3390/molecules27030943.
14. Ismail N.Z., Mohamed W.A.S., Ab Rahim N., Hashim N.M., Adebayo I.A., Mohamad Zain N.N., Arsad H. Molecular docking and molecular dynamic simulations of apoptosis proteins with potential anticancer compounds present in Clinacanthus nutans extract using gas chromatography-mass spectrometry. *J. Biomol. Struct. Dyn*. 2023;41(13):6104-6120. DOI: 10.1080/07391102.2022.2101530.
15. Berman H.M., Westbrook J., Feng Z., Gilliland G., Bhat T.N., Weissig H. et al. The Protein Data Bank. *Nucleic. Acids. Res*. 2000;28(1):235–242. DOI: 10.1093/nar/28.1.235.
16. Kim S., Chen J., Cheng T., et al. PubChem 2025 update. *Nucleic Acids Res*. 2025;53(D1):D1516-D1525. DOI:10.1093/nar/gkae1059
17. Schrödinger L., DeLano W. PyMOL. 2020. URL: http://www.pymol.org/pymol
18. O'Boyle N.M., Banck M., James C.A., Morley C., Vandermeersch T., Hutchison G.R.. Open Babel: An open chemical toolbox. *J. Cheminform*. 2011;3:33. DOI: 10.1186/1758-2946-3-33.
19. Trott O., Olson A.J. AutoDock Vina: Improving the speed and accuracy of docking with a new scoring function, efficient optimization, and multithreading. *J. Comput. Chem*. 2010;31:455–461. DOI: 10.1002/jcc.21334.
20. Abraham, M.J., Murtola, T., Schulz, R., Páll, S., Smith, J. C., Hess, B. et al. GROMACS: High performance molecular simulations through multi-level parallelism from laptops to supercomputers. *SoftwareX*. 2015;1–2:19–25. DOI: 10.1016/j.softx.2015.06.001.
21. Vanommeslaeghe K., Hatcher E., Acharya C. et al. CHARMM general force field: A force field for drug-like molecules compatible with the CHARMM all-atom additive biological force fields. *J. Comput. Chem*. 2010;31(4):671–690. DOI: 10.1002/jcc.21367.
22. Groningen Biomolecular Sciences and Biotechnology Institute. GROMACS 4.5 Manual. 2010.URL:https://becksteinlab.physics.asu.edu/pages/courses/2013/SimBioNano/14/gromacs_manual-4.5.pdf

23. Vaught A. Graphing with Gnuplot and Xmgr: Two graphing packages available under Linux. *Linux J*. 1996;1996:7.
24. Cheng X., Ivanov I. Molecular dynamics. *Methods Mol. Biol*. 2012;929:243–285. DOI: 10.1007/978-1-62703-050-2_11.
25. Liu K., Watanabe E., Kokubo H. Exploring the stability of ligand binding modes to proteins by molecular dynamics simulations. *J. Comput. Aided Mol. Des.* 2017;31(2):201–211. DOI: 10.1007/s10822-016-0005-2.
26. Oleinick N.L., Morris R.L., Belichenko I. The role of apoptosis in response to photodynamic therapy: what, where, why, and how. *Photochem. Photobiol. Sci*. 2002;1(1):1–21. DOI: 10.1039/B108586G.

Author Information

Chasovskikh Nataliya Yu. – Dr. Sci. (Med.), Associate Professor, Head of the Medical and Biological Cybernetics Division, Siberian State Medical University, Tomsk, chasovskih.ny@ssmu.ru, https://orcid.org/0000-0001-6077-0347

Shestakova Evgeniia E. – Assistant of the Medical and Biological Cybernetics Division, Siberian State Medical University, Tomsk, chizik.ee@ssmu.ru, http://orcid.org/ 0000-0003-4731-8449

Novitsky Dmitry E. – 6th-year Student, Siberian State Medical University, Tomsk, novitskydima07@mail.ru

(✉) **Shestakova Evgeniia E.,** chizik.ee@ssmu.ru

Received on June 23, 2025;
approved after peer review on July 4, 2025;
accepted on September 09, 2025

УДК 616-056.257(470+571)”2024”
https://doi.org/10.20538/1682-0363-2026-2-121-129

Assessment of Obesity Prevalence and Associated Factors in the Russian Federation Based on the 2024 Rosstat Sample Survey Data

Chigrina V.P.[1], Tyufilin D.S.[1], Kobyakova O.S.[1], Deev I.A.[2], Nikitina S.Yu.[3]

[1]*Russian Research Institute of Health*
11 Dobrolubov St., 127254 Moscow, Russian Federation

[2]*Pirogov Russian National Research Medical University*
1 Ostrovityanov St., 117513 Moscow, Russian Federation

[3]*Federal State Statistics Service*
39/1 Myasnitskaya St., 107450 Moscow, Russian Federation

ABSTRACT

Aim. To assess the prevalence of obesity and identify the factors associated with it among the adult population in the Russian Federation in order to determine the main directions for the development of measures for obesity prevention.

Materials and methods. We carried out a secondary analysis of the data from the selective monitoring of the population health status by the Federal State Statistics Service for 2024. The study included data from 95,887 respondents from all regions of the Russian Federation. Descriptive statistics, $\chi 2$ test, Mann – Whitney test, Kruskal – Wallis test, and multiple logistic regression analysis were used for statistical analysis.

Results. The prevalence of obesity among the adult population of the Russian Federation was 23.7% (class 1 – 17.9%, class 2 – 4.7%, and class 3 – 1.6%). Significant regional differences in the prevalence of obesity were revealed: from 6.6% in the Chukotka Autonomous Okrug to 34.3% in the Jewish Autonomous Oblast. The proportion of obese people was significantly higher among women (27.2% vs. 20.4% among men), rural residents (27.9% vs. 22.7% among urban residents), and respondents with low socioeconomic status. Multiple regression analysis revealed the most significant risk factors for obesity: lack of accessible sports infrastructure in the respondents' area of residence (odds ratio (OR) = 2.71; 95% confidence interval (95% CI): 1.608–4.471), retirement status (OR = 1.63; 95% CI: 1.548–1.707), low income (OR = 1.60; 95% CI: 1.014–2.477), and low awareness of balanced nutrition (OR = 1.44; 95% CI: 1.243–1.659).

Conclusion. Based on the results of the study, key areas for the development of measures for the prevention of obesity have been formulated: creating an environment that supports a healthy lifestyle; improving public health literacy; developing preventive healthcare; as well as developing and implementing measures taking into account regional specifics and the needs of various socio-demographic groups.

Keywords: obesity, prevalence, risk factors, body mass index, adult population, Russian Federation

Conflict of interest. The authors declare the absence of obvious or potential conflicts of interest related to the publication of this article.

Source of financing. The authors state that they received no funding for the study.

For citation: Chigrina V.P., Tyufilin D.S., Kobyakova O.S., Deev I.A., Nikitina S.Yu. Assessment of Obesity Prevalence and Associated Factors in the Russian Federation Based on the 2024 Rosstat Sample Survey Data. *Bulletin of Siberian Medicine.* 2026;25(2):121–129. https://doi.org/10.20538/1682-0363-2026-2-121-129.

✉ *Chigrina Valeriya P.,* chigrinavp@mednet.ru

Оценка уровня распространенности ожирения и факторов, ассоциированных с ним, в Российской Федерации по данным выборочного исследования Росстата, 2024 г.

Чигрина В.П.[1], Тюфилин Д.С.[1], Кобякова О.С.[1], Деев И.А.[2], Никитина С.Ю.[3]

[1] *Центральный научно-исследовательский институт организации и информатизации здравоохранения (ЦНИИОИЗ)*
Россия, 127254, г. Москва, ул. Добролюбова 11

[2] *Российский национальный исследовательский медицинский университет (РНИМУ им. Н.И. Пирогова)*
Россия, 117513, г. Москва, ул. Островитянова, 1

[3] *Федеральная служба государственной статистики*
Россия, 107450, г. Москва, ул. Мясницкая, 39/1

РЕЗЮМЕ

Цель. Оценить уровень распространенности ожирения и выявить факторы, ассоциированные с ним, среди взрослого населения в Российской Федерации для формирования основных направлений разработки мероприятий по профилактике ожирения.

Материалы и методы. Проведен вторичный анализ данных выборочного наблюдения состояния здоровья населения Федеральной служба государственной статистики за 2024 г. В исследование включены данные 95 887 респондентов из всех субъектов РФ. Для статистического анализа использовались методы описательной статистики, критерии χ^2, Манна – Уитни, Краскела – Уоллиса, множественный логистический регрессионный анализ.

Результаты. Распространенность ожирения среди взрослого населения Российской Федерации составляла 23,7% (1-1 степени – 17,9%, 2-й степени – 4,7%, 3-й степени – 1,6%). Выявлены значительные региональные различия в распространенности ожирения: от 6,6% в Чукотском автономном округе до 34,3% в Еврейской автономной области. Доля лиц с ожирением была статистически значимо выше среди женщин (27,2 против 20,4% среди мужчин), сельских жителей (27,9 против 22,7% среди жителей города) и респондентов с низким социально-экономическим статусом. Множественный регрессионный анализ выявил наиболее значимые факторы риска наличия ожирения: отсутствие доступной спортивной инфраструктуры в зоне проживания респондентов (отношение шансов (ОШ) = 2,71; 95%-й доверительный интервал (95%ДИ): 1,608–4,471), пенсионный статус (ОШ = 1,63; 95%ДИ: 1,548–1,707), низкий уровень дохода (ОШ = 1,60; 95%ДИ: 1,014–2,477) и низкий уровень осведомленности о рациональном питании (ОШ = 1,44; 95%ДИ: 1,243–1,659).

Заключение. На основании результатов проведенного исследования сформулированы ключевые направления разработки мероприятий по профилактике ожирения: создание среды, поддерживающей здоровый образ жизни; повышение санитарной грамотности населения; развитие профилактического звена здравоохранения; а также разработка и реализация мероприятий с учетом региональной специфики и потребностей различных социально-демографических групп.

Ключевые слова: ожирение, распространенность, факторы риска, индекс массы тела, взрослое население, Российская Федерация

Конфликт интересов. Авторы заявляют об отсутствии явных и потенциальных конфликтов интересов, связанных с публикацией настоящей статьи.

Источник финансирования. Авторы декларируют отсутствие внешнего финансирования для проведения исследования и публикации статьи.

Для цитирования: Чигрина В.П., Тюфилин Д.С., Кобякова О.С., Деев И.А., Никитина С.Ю. Оценка уровня распространенности ожирения и факторов, ассоциированных с ним, в Российской Федерации по данным выборочного исследования Росстата, 2024 г. *Бюллетень сибирской медицины.* 2026;25(2):121–129. https://doi.org/10.20538/1682-0363-2026-2-121-129.

INTRODUCTION

Obesity poses a grave challenge to global public health [1–4]. The prevalence of overweight and obesity is increasing worldwide. Based on the results of a meta-analysis conducted by S. Ibrahim et al. (2021), over the past three decades, the global prevalence of obesity among women has increased by 104.9% (95% confidence interval (95% CI): 100.9%–108.8%) from 10.2% (95% CI: 10.0%–10.3%) in 1990 to 20.8% (95% CI: 20.5%–21.1%) in 2021. Among men, it increased by 155.1% (95% CI: 149.8%–160.3%) from 5.8% (95% CI: 5.7%–5.9%) to 14.8% (95% CI: 14.6%–15.0%) [5]. According to M. Li et al. (2022), in 2017–2018, the prevalence of obesity among adults in the United States of America was 42.8% (95% CI: 39.5%–46.1%), which is more than 10% higher than in 2003–2004: 32.3% (95% CI: 29.9%–34.6%) [6].

Obesity prevention is crucial for combating chronic non-communicable diseases (NCDs), including type 2 diabetes mellitus, insulin resistance, metabolic syndrome with hyperinsulinemia, hyperlipidemia, hypertension, metabolic-associated fatty liver disease, coronary heart disease, etc. [7]. A prospective cohort study conducted by S. Ghosh et al. (2023) showed that obese adults had a 7-year shorter life expectancy compared to the rest of the population [8]. Similarly, according to S.T. Nyberg et al. (2018), people with class 2 obesity had a life expectancy of 8 years less than their peers with normal body weight, and people with class 1 obesity had a life expectancy of 4 years less [9].

There are several causes of overweight and obesity, including behavioral determinants (type of diet and level of physical activity), genetic (presence of obesity and related diseases in parents), as well as demographic (age, gender, place of residence, and levels of education and income) [10]. To develop measures aimed at combating obesity, it is necessary to have an insight into the prevalence of obesity and the factors associated with it.

The aim of the study was to assess the prevalence of obesity and identify factors associated with it among the adult population in the Russian Federation in order to determine the main directions for the development of measures for obesity prevention.

MATERIALS AND METHODS

The study used primary data from the sample observation of the health status of the population of the Federal State Statistics Service (Rosstat) for 2024 (Order of the Federal State Statistics Service dated June 28, 2024 No. 266 "On Approval of Forms of Federal Statistical Observation with Guidelines for the Completion of Sample Observation of the Population Health Status in 2024". URL: https://normativ.kontur.ru/document?moduleId=1&documentId=475320).

The monitoring unit was a private household and household members. The observation was conducted as personal interviews of household members (respondents) at their place of residence, as part of the household selected for observation. The number of households eligible for selection in the observational sample across Russia was 60,000 households in total. Selection of enumeration areas and households was centrally managed by Rosstat based on a territorial multi-purpose sampling frame. The number of households eligible for selection within an enumeration area was 54 households (including reserves), both in urban and rural areas. The respondents' body mass index (BMI) was calculated as the ratio of the body weight in kilograms (kg) to the square of height in meters (m^2).

The Statistica for Windows version 10.0, Stata, and R-studio software packages were used for statistical processing of the research results. Qualitative data were represented as absolute or relative (%) frequencies, quantitative data were represented as $X \pm x$, where X is the arithmetic mean and x is the standard deviation. In the case of an abnormal data distribution, the median and interquartile range of variables were also calculated. When comparing the distributions of qualitative features, the Pearson's test was used. When comparing qualitative characteristics, the odds ratio (OR) was calculated. The Mann – Whitney and Kruska – Wallis U-tests were used to evaluate differences in pairwise unrelated samples with abnormal distribution; Student's t-test was used for normal distribution. Multiple logistic regression analysis was used to determine the significant relationships between variables, as well as the directions of these relationships.

RESULTS

A total of 95,887 respondents aged 18 and over (40.4% of men and 58.2% of women) from all regions of the Russian Federation took part in the survey, the average age of participants was 51.1 (18–101) years. Table 1 provides detailed sociodemographic characteristics of the respondents.

Table 1

Characteristics

Parameter	*n*	%
Sex		
Male	38,692	40.4
Female	55,849	58.2
Skipped the question	1,346	1.4
Age, years		
18–24	5,516	5.8
25–34	12,778	13.3
35–44	19,508	20.3
45–54	16,380	17.1
55–64	16,044	16.7
65+	25,661	26.8
Type of Locality		
Urban	65,010	67.8
Rural	30,877	32.2
Education Level		
Elementary general (elementary)	770	0.80
Basic general (incomplete secondary)	4,074	4.24
Secondary general (complete secondary)	12,061	12.58
Secondary vocational	43,401	45.26
Undergraduate (incomplete higher)	1,929	2.01
Higher	31,592	32.95
Highly qualified personnel (postgraduate, academic degrees, and doctoral programs)	555	0.58
No education	119	0.12
Refused to respond	40	0.04
Skipped the question	1,346	1.40
Marital Status		
Registered marriage	48,209	50.28
Common-law marriage	4,191	4.37
Widower/widow	15,828	16.51
Divorced	13,180	13.75
Separated	1,976	2.06
The respondent has never been in a registered or common-law marriage	10,898	11.37
Refused to respond	259	0.27
Skipped the question	1,346	1.40
Employment Type		
Employee of the state or public sector	25,274	26.36
Employee of a private enterprise	27,772	28.96
Self-employed/individual entrepreneur	3,863	4.03
The respondent does not have a permanent job, but occasionally engages in temporary work	2,789	2.90
Unpaid work (volunteering, subsistence production for family needs, and domestic work)	1,520	1.59
Unemployed and able to work	1,304	1.36
Unemployed and unable to work (due to disability)	633	0.66
Student	2,269	2.37
Retiree	28,866	30.10
Refused to respond	251	0.26
Skipped the question	1,346	1.40

According to the results of the analysis, 1.0% of the respondents (n = 961) were underweight, 42.9% (n = 39,912) were overweight and 23.7% (n = 22,682) were obese. At the same time, 17.9% (n = 16,647) had class 1 obesity, 4.7% (n = 4,408) had class 2, and 1.6% (n = 1,483) had class 3 according to the Classification of Obesity of the World Health Organization (1997) [11].

According to a sample study by Rosstat in 2024, the average BMI level was 27.34 ± 0.67 kg/m^2. According to the results of the analysis, less than 10% of respondents were obese in only two regions of the Russian Federation (the Chechen Republic and the Chukotka Autonomous Okrug). In two regions of the Russian Federation (Moscow and Astrakhan regions), the percent of obese respondents varied from 10 to 15%, in nine regions – from 15.1 to 20%, in 32 subjects – from 20.1 to 25%, and in 30 regions, over 25% of the respondents were obese. The largest proportion of obese respondents was registered in the Jewish Autonomous Oblast (34.3%), the smallest -in the Chukotka Autonomous Okrug (6.6%) (Fig. 1).

The proportion of obese people was significantly higher among women (27.2% vs. 20.4% among men ($p < 0.05$)), as well as among rural residents (27.9% vs. 22.7% among urban residents, $p < 0.05$). In addition, among the respondents who underwent medical examinations over the past two years, the proportion of obese people was also significantly higher compared to the rest (25.9 vs. 22.3%, $p < 0.05$). This may be due to the fact that people who have already been diagnosed with diseases or risk factors that often accompany obesity are more likely to seek medical examination at doctor's recommendation. Therefore, this group initially includes more people with health problems.

When analyzing socioeconomic parameters, a statistically significantly greater proportion of obese people was found among widows and widowers (36.0%), the unemployed and unable to work (disabled) (26.9%), respondents with basic general education (30.2%), the smallest - among the higher professional category (15.6%), who have never been in a registered marriage (10.6%), engaged in unpaid work (volunteering, domestic work, subsistence production for the needs of the family, 17.1%), $p < 0.05$ for all comparisons (Fig. 2–4).

In addition, among the participants who lived alone (widower/widow, divorced, separated, and never been in a registered / common-law marriage), there were slightly more obese people (24.3%) compared to those who lived with a partner (in a registered marriage and is in a common-law marriage) – 23.8%, $p > 0.05$.

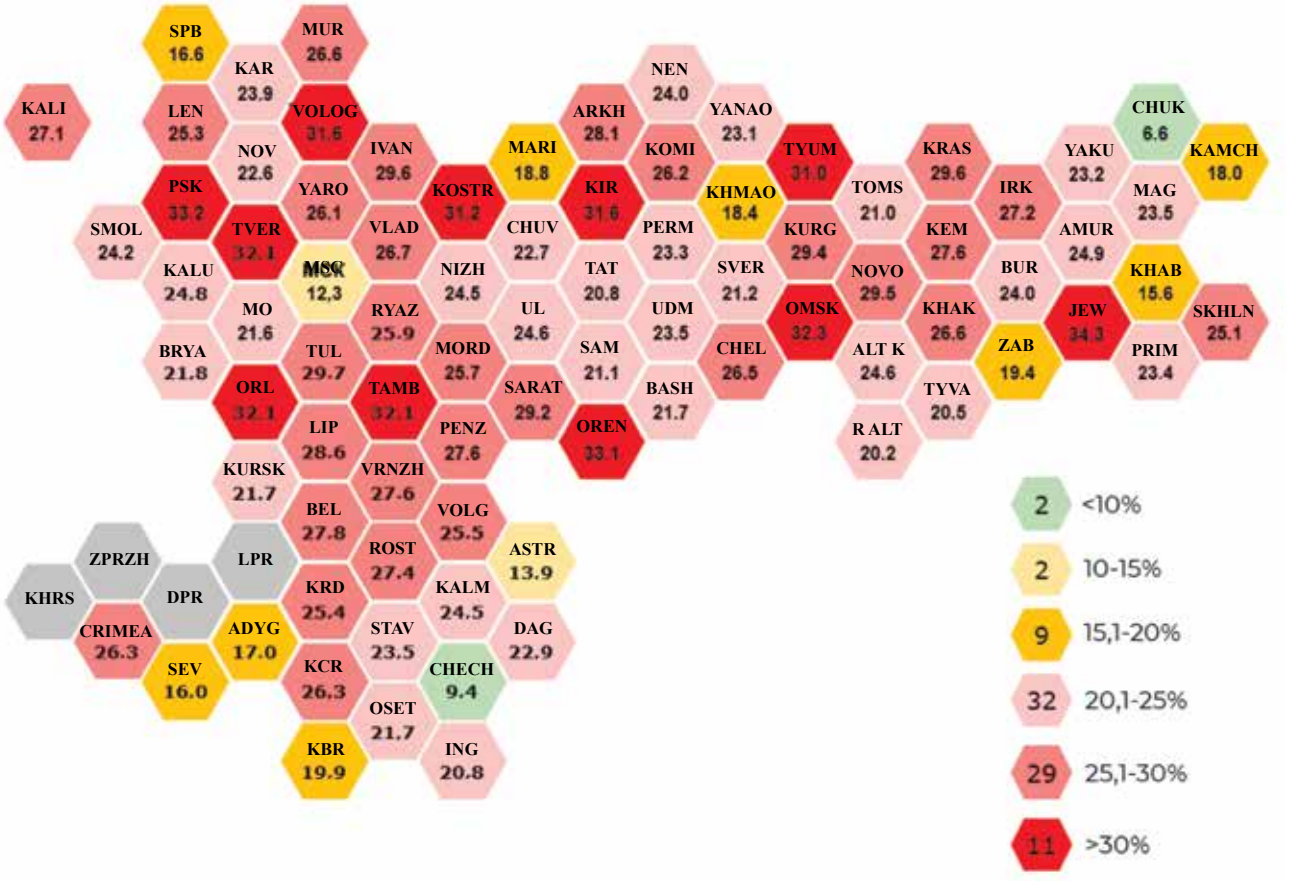

Fig. 1. The number of obese respondents in the regions of the Russian Federation, %

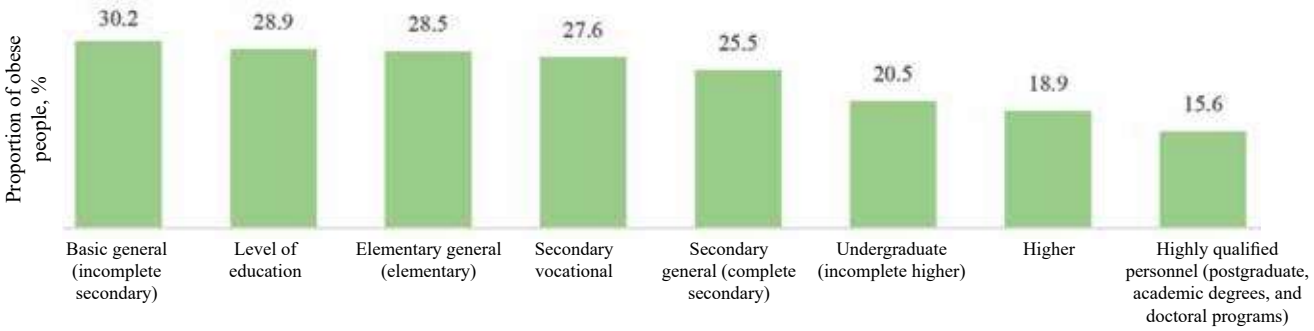

Fig. 2. The proportion of obese people depending on the level of education, %: $p < 0.05$ when comparing the group of basic general (incomplete secondary) education with highly qualified personnel

Fig. 3. The proportion of obese people depending on marital status, %: $p < 0.05$ when comparing groups with each other

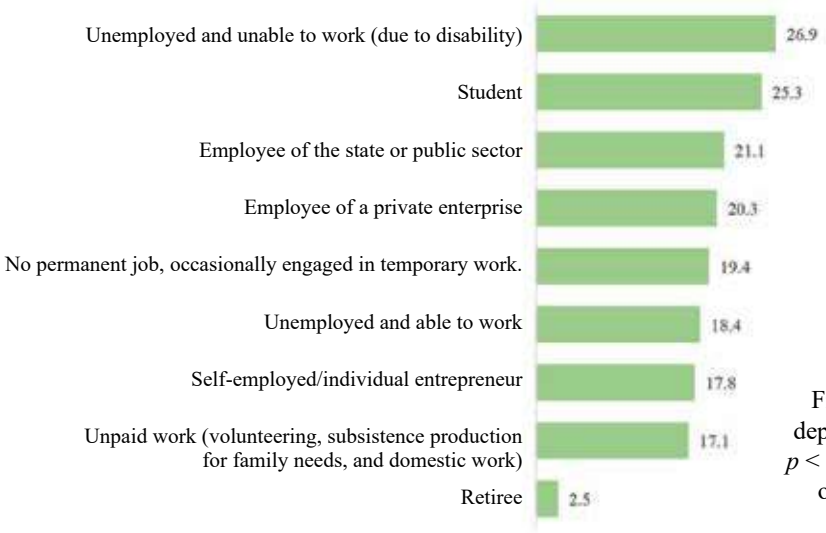

Fig. 4. The proportion of obese people depending on the type of employment, %: $p < 0.05$ when comparing groups with each other, except for the group of retirees

Fig. 5. The proportion of obese people depending on their financial situation, %: $p < 0.05$ when comparing all groups with each other, except for those respondents who chose the option "I live in extreme need"

A statistically significantly greater proportion of obese people (33.5%) was registered among participants with low income, while the lowest proportion was registered among citizens with high income (20.2%, $p < 0.05$). No statistically significant difference was found in other socioeconomic characteristics of the respondents, including age ($p > 0.05$), Fig. 5.

A statistically significantly bigger proportions of obese respondents were registered in the group of people who experienced severe anxiety or depression (32.9%), loneliness (30.9%), and a sense of uncertainty about the future (29.2%). Conversely, the smallest proportions were found among those not experiencing anxiety or depression (20.6%), loneliness (22.9%), and anxiety about the uncertain future (20.9%). No statistically significant difference was found in the proportion of obese people in terms of other personal characteristics of the respondents ($p > 0.05$).

The level of awareness of respondents about balanced nutrition was also associated with the presence of obesity. The biggest proportion of obese participants was registered among those who reported that they did not know anything about a balanced diet and eating regime (28.3%), while the smallest proportion was well-informed about these aspects of nutrition (20.5%, $p < 0.05$). In addition, among the respondents who always consumed foods with a high salt content, the greatest proportion of obese people (26.3%) was noted compared with those who had never done so ($p < 0.05$).

When analyzing the parameters characterizing the respondents' physical activity, it was revealed that a statistically significantly bigger proportion of obese participants was registered among those who spent less than one hour a week on physical activity (21.9%), and the smallest proportion was observed among those who spent more than two hours a week on physical activities (9.8%, $p < 0.05$).

The method of multiple logistic analysis was used to determine the factors associated with the presence of obesity. According to the regression results, it was revealed that if a respondent assessed their state of health as poor, the chance of being obese was almost five times higher than for those who considered

their health as excellent ($p < 0.05$). In addition, if a respondent assessed their health status worse than people of the same age, then the chance of being obese was 45.5% higher ($p < 0.05$). If there were no facilities for physical education and sports near the respondent's place of residence, or they did not use them, the chance of being obese was almost three times higher than for those who engaged in physical activity in specially designated public spaces ($p < 0.05$).

Other factors associated with obesity included higher education, belonging to a group of students and divorced people, lack of loneliness, and considering an interesting job as one of the most important values in life ($p < 0.05$). In addition, if a respondent stopped using non-smoking tobacco products, the chance of being obese decreased by 54.0% compared to the rest of the participants. If they did not use non-smoking tobacco products every day, the chance of being obese compared to those who consumed them daily was 85.7% lower. And if a respondent felt cheerful and in a good mood, it was 37.7% lower, and if a respondent has never been married, it would decrease by 43.3% ($p < 0.05$). All the factors associated with the respondent's obesity are listed in Table 2.

Table 2

Factors Associated with the Presence of Obesity in Respondents

Factor	Effect	OR (95% CI)
Evaluate their state of health as poor	↑ by 4.9 times	4.924 (4.406–5.511)
There are no suitable facilities for physical education and sports at the place of residence	↑ by 2.7 times	2.707 (1.608–4.471)
There are suitable facilities for physical education and sports at the place of residence, but the respondent does not use them	↑ by 81.4%	1.814 (1.165–2.798)
Children are the most important value in life (compared to material well-being)	↑ by 65.4%	1.654 (1.387–1.983)
Retiree	↑ by 62.5%	1.626 (1.548–1.707)
Lives in extreme need	↑ by 60.3%	1.603 (1.014–2.477)
The respondent thinks their health status is worse compared to people of the same age.	↑ by 45.5%	1.455 (1.355–1.562)
The respondent does not know anything about what a diet and eating regime are and what they should be like	↑ by 43.6%	1.436 (1.243–1.659)
The respondent is not worried about losing their current job	↑ by 40.3%	1.403 (1.263–1.561)
Almost the entire family's income is usually spent on food	↑ by 36.7%	1.367 (1.098–1.700)
Unemployed and able to work	↑ by 30.8%	1.308 (1.131–1.509)
The respondent is concerned by the feeling of uncertainty about the future	↑ by 29.4%	1.294 (1.232–1.359)
Widower or widow	↑ by 8.4%	1.084 (1.035–1.042)
With an increase in the portions of bread and bakery products consumed in one day	↑ by 4.0%	1.040 (1.018–1.062)
Does not consume non-smoking tobacco products every day (compared to daily consumption)	↓ by 85.7%	0.149 (0.048–0.418)
Student	↓ by 80.5%	0.195 (0.143–0.260)
Stopped using non-smoking tobacco products	↓ by 54.0%	0.460 (0.219–0.996)
Has never been in a registered marriage	↓ by 43.3%	0.567 (0.525–0.612)
Feels cheerful and in a good mood	↓ by 37.7%	0.623 (0.488–0.798)
No feeling of loneliness	↓ by 35.7%	0.643 (0.426–0.945)
An interesting job is the most important value in life (compared to material well-being)	↓ by 35.2%	0.648 (0.581–0.723)
Higher education	↓ by 32.0%	0.680 (0.651–0.710)
Never adds salt, salty seasonings, or salty sauce to prepared food immediately before eating it	↓ by 31.2%	0.688 (0.578–0.820)
A high level of education is the most important value in life (compared to material well-being)	↓ by 20.8%	0.792 (0.721–0.870)
Employee of a private enterprise (compared to a state-owned organization)	↓ by 16.7%	0.833 (0.794–0.874)
Separated	↓ by 16.2%	0.838 (0.735–0.952)
The respondent does not have a permanent job, but occasionally engages in temporary work	↓ by 12.6%	0.874 (0.769–0.991)
Never underwent a medical check-up in the last two years	↓ by 7.3%	0.927 (0.896–0.960)

Note. ↑– increase, ↓– decrease.

DISCUSSION

The results of the study revealed a high prevalence of obesity among the adult population of the Russian Federation, including in the context of its federal subjects. It is important to note that the morbidity index used in the framework of the federal project "Health for Everyone" and formed on the basis of data from citizens' visits to medical organizations was used to collect official statistics. Morbidity is

not similar to prevalence. Prevalence is a broader epidemiological indicator that makes it possible to identify cases of "hidden" obesity, when patients live with the disease but do not seek medical care and are not included in official reports.

We revealed some differences when comparing the results obtained with similar foreign studies. So, according to the results of an American study by D. Kim et al. (2019, $n = 4,118$), 44% of men and 66% of women had abdominal obesity, which is higher than in the Russian Federation [12]. In a nationwide survey conducted in South Korea in 2020, 48.0% of men and 27.3% of women aged 19 and over were obese [13].

According to S. Kaboré et al. (2020, $n = 4,800$), the prevalence of overweight and obesity in Burkina Faso (West Africa) was 13.8% and 4.8%, respectively, which is lower than in Russia. Among men, the chances of being overweight (obese) increased with living in a city ($p < 0.001$), older age ($p < 0.002$), and marital status other than single ($p < 0.007$), and decreased with smoking ($p = 0.009$). Among women, the chances of being overweight (obese) increased with living in a city ($p < 0.001$) and having elementary education ($p = 0.01$), and decreased with smoking ($p < 0.001$) [14].

According to the study, the main socioeconomic factors associated with obesity include female gender, living in rural areas, marital status other than single, and lack of higher education. Marital status other than single is a risk factor due to changes in the profile of consumption, the regularity of meals, as well as due to a reduction in time devoted to personal health and physical activity, especially after the birth of children, when priorities shift towards caring for the family.

The lack of higher education as a factor associated with obesity is explained by lower awareness of proper nutrition and professional employment in areas that are usually characterized by either high physical but monotonous work, or, conversely, low mobility. Low income was also associated with obesity, which can be explained by the fact that the diet of this group of respondents is based on cheaper but high-calorie foods, which include fast carbohydrates.

The personal and behavioral factors identified include the habit of salting food, eating baked goods, smoking, anxiety about job loss and uncertainty of the future, low awareness of the regime and diet, and low self-assessment of health status. The above factors are consistent with the data obtained in foreign studies.

So, in the Korean study conducted by G. Kim et al. (2024; $n = 5,262$), 38.3% of the respondents were obese. At the same time, the factors associated with obesity were as follows: male gender (OR = 2.318; 95% CI: 2.311–2.326), marital status (OR = 1.273; 95% CI: 1.269–1.277), rural residence (OR = 1.830; 95% CI: 1.813–1.847), sleep problems (OR = 1.310; 95% CI: 1.305–1.314), anxiety (OR = 1.217; 95% CI: 1.211–1.223), alcohol consumption (OR = 1.445; 95% CI: 1.433–1.458), and smoking (1.194; 95% CI: 1.192–1.197) [15].

Similar data was obtained by S. Shabu et al. (2019; $n = 1,480$) who revealed using a multifactorial analysis that age (OR = 2.36; 95% CI: 1.60–3.49), female gender (OR = 2.17; 95% CI: 1.53–3.08), and marital status (OR = 1.87; 95% CI: 1.20-2.90) were statistically significant factors associated with overweight and obesity [16].

CONCLUSION

Thus, the data obtained during the study not only confirm the high prevalence of obesity among the adult population of the Russian Federation, but also reveal a complex set of interrelated factors associated with it. The development of targeted prevention programs should take into account regional specifics and be aimed at the most vulnerable groups of the population (rural residents, people with low incomes and lack of higher education, and retirees).

Strategic directions for the development of preventive measures should include creating an environment that supports a healthy lifestyle, including the development of accessible infrastructure for physical activity and providing conditions for rational nutrition; improving public health literacy, including the implementation of information and communication campaigns on the principles of healthy eating and the importance of regular physical activity; development of preventive health care (strengthening the role of primary health care in the early detection, counseling and support of patients with risk factors, including the integration of psychological support); implementation of targeted programs (development and implementation of measures taking into account regional specifics and the needs of various socio-demographic groups).

REFERENCES

1. Reinbacher P., Draschl A., Smolle M.A., Hecker A., Gaderer F., Lanner K.B. et al. The impact of obesity on the health of the older population: a cross-sectional study on the relationship between health-related quality of life and body mass index across different age groups. *Nutrients*. 2023;16(1):51. DOI: 10.3390/nu16010051.
2. Coulman K.D., Blazeby J.M. Health-related quality of life in bariatric and metabolic surgery. *Curr. Obes. Rep.* 2020;9(3):307–314. DOI: 10.1007/s13679-020-00392-z.
3. Nagi M.A., Ahmed H., Rezq M.A.A., Sangroongruangsri S., Chaikledkaew U., Almalki Z. et al. Economic costs of obesity: a systematic review. *Int. J. Obes.* 2024;48(1):33–43. DOI: 10.1038/s41366-023-01398-y.
4. Hales C.M., Carroll M.D., Fryar C.D., Ogden C.L. Prevalence of obesity and severe obesity among adults: United States, 2017-2018. *NCHS Data Brief.* 2020;360:1–8.
5. Ibrahim S., Akram Z., Noreen A., Baig M.T. Overweight and obesity prevalence and predictors in people living in Karachi. *J. Pharm. Res. Int.* 2021:194–202. DOI: 10.9734/jpri/2021/v33i31B31708.
6. Li M., Gong W., Wang S., Li Z. Trends in body mass index, overweight and obesity among adults in the USA, the NHANES from 2003 to 2018: a repeat cross-sectional survey. *BMJ Open.* 2022;12(12):e065425. DOI: 10.1136/bmjopen-2022-065425.
7. Abbott L., Lemacks J., Greer T. Development and evaluation of a measure for social support provided by friends during lifestyle management programs. *Healthcare.* 2022;10(5):901. DOI: 10.3390/healthcare10050901.
8. Ghosh S., Paul M., Mondal K.K., Bhattacharjee S., Bhattacharjee P. Sedentary lifestyle with increased risk of obesity in urban adult academic professionals: an epidemiological study in West Bengal, India. *Sci. Rep.* 2023;13(1):4895. DOI: 10.1038/s41598-023-31977-y.
9. Nyberg S.T., Batty G.D., Pentti J., Virtanen M., Alfredsson L., Fransson E.I. et al. Obesity and loss of disease-free years owing to major non-communicable diseases: a multicohort study. *Lancet Public Health.* 2018;3(10):e490–e497. DOI: 10.1016/S2468-2667(18)30139-7.
10. Kerkadi A., Sadig A.H., Bawadi H., Al Thani A.A.M., Al Chetachi W., Akram H. et al. The relationship between lifestyle factors and obesity indices among adolescents in Qatar. *Int. J. Environ. Res. Public Health.* 2019;16(22):4428. DOI: 10.3390/ijerph16224428.
11. World Health Organization. Obesity: preventing and managing the global epidemic. Geneva, 1997: WHO.
12. Kim D., Hou W., Wang F., Arcan C. Factors affecting obesity and waist circumference among US adults. *Prev. Chronic. Dis.* 2019;16:180220. DOI: 10.5888/pcd16.180220.
13. Oh K., Kim Y., Kweon S., Kim S., Yun S., Park S. et al. Korea National Health and Nutrition Examination Survey, 20th anniversary: accomplishments and future directions. *Epidemiol. Health.* 2021;43:e2021025. DOI: 10.4178/epih.e2021025.
14. Kaboré S., Millogo T., Soubeiga J.K., Lanou H., Bicaba B., Kouanda S. Prevalence and risk factors for overweight and obesity: a cross-sectional countrywide study in Burkina Faso. *BMJ Open.* 2020;10(11):e032953. DOI: 10.1136/bmjopen-2019-032953.
15. Kim G., Woo H., Ji Y.A. Factors affecting abdominal obesity: analyzing national data. *Healthcare.* 2024;12(8):827. DOI: 10.3390/healthcare12080827.
16. Shabu S. Prevalence of overweight/obesity and associated factors in adults in Erbil, Iraq: A household survey. *Zanco J. Med. Sci.* 2019;23(1):128–134. DOI: 10.15218/zjms.2019.017.

Author Contribution

Chigrina V.P. – literature analysis, obtaining and interpretation of data, statistical processing of the data, and drafting of the manuscript. Tyufilin D.S., Kobyakova O.S., Deev I.A., Nikitina S.Yu. – editing of the manuscript, final approval of the manuscript for publication.

Author Information

Chigrina Valeriya P. – Senior Specialist, Health Care Strategic Development Management, Russian Research Institute of Health, Moscow, chigrinavp@mednet.ru, https://orcid.org/0000-0002-5044-4836

Tyufilin Denis S. – Head of Health Care Strategic Development Management, Russian Research Institute of Health, Moscow, tyufilinds@mednet.ru, https://orcid.org/0000-0002-9174-6419

Kobyakova Olga S. – Dr. Sci. (Med.), Professor, Corresponding Member of the Russian Academy of Sciences, Director, Russian Research Institute of Health, Moscow, kobyakovaos@mednet.ru, https://orcid.org/0000-0003-0098-1403

Deev Ivan A. – Dr. Sci. (Med.), Professor, Professor of the Department of Management, Economics of Healthcare and Medical Insurance, Pirogov Russian National Research Medical University, kafedra-rgmu@mail.ru, https://orcid.org/0000-0002-4449-4810

Nikitina Svetlana Yu. – Cand.Sci. (Econ.), Head of the Department for Population and Health Statistics, Federal State Statistics Service, mail@mednet.ru, https://orcid.org/0000-0003-0749-0965

(✉) **Chigrina Valeriya P.,** chigrinavp@mednet.ru

Received on November 6, 2025;
approved after peer review on December 8, 2025;
accepted on December 11, 2025

УДК 616.12-008.64-002.2:616.9
https://doi.org/10.20538/1682-0363-2026-2-130-138

Cytomegalovirus Infection Activity as a Predictor of Adverse Clinical Events in Chronic Heart Failure

Shilov S.N.[1], Berezikova E.N.[1], Pankova I.V.[1], Grakova E.V.[2], Kopyeva K.V.[2], Teplyakov A.T.[2], Mayanskaya S.D.[3], Kovalenko G.V.[4], Kolmakova A.M.[4], Kalyuzhin V.V.[4]

[1]*Novosibirsk State Medical University (NSMU)*
52 Krasny Ave., 630091 Novosibirsk, Russian Federation

[2]*Cardiology Research Institute, Tomsk National Research Medical Center (NRMC), Russian Academy of Sciences*
111a Kievskaya St., 634012 Tomsk, Russian Federation

[3]*Kazan State Medical University (KSMU)*
49 Butlerov St., 420012 Kazan, Russian Federation

[4]*Siberian State Medical University*
2 Moskovsky trakt, 634050 Tomsk, Russian Federation

ABSTRACT

Aim. To evaluate the impact of cytomegalovirus (CMV) infection on the course of chronic heart failure (CHF) over a 24-month prospective follow-up.

Material and methods. The study included patients (n = 151) hospitalized due to CHF decompensation. Based on a follow-up, they were divided into groups with favorable and adverse CHF course, underlying pathology, and their complications. The adverse CHF course group included patients who experienced at least one of the following events during the 24-month follow-up period: 1) hospitalization for CHF decompensation; 2) adverse clinical events (cardiovascular death, nonfatal myocardial infarction or acute cerebrovascular accident, and pulmonary embolism); 3) any deterioration in CHF class; 4) a decrease in left ventricular ejection fraction (LVEF) by more than 10% from baseline. Plasma CMV DNA levels were assessed at baseline and after 12 and 24 months of follow-up. To identify predictors of the development of adverse cardiovascular events, ROC analysis was used with the construction of characteristic curves and the calculation of the area under the curve (AUC).

Results. In patients with an adverse CHF course, CMV DNA levels at study inclusion were significantly higher (p < 0.001) compared to those with a favorable CHF course 2,232.0 copies/ml [1,687.0; 2,765.0] and 1,245 copies/ml [991.3; 1,592.0], respectively. The CMV DNA blood plasma level showed a direct correlation with CHF FC (r = 0.66; p = 0.001) and left ventricular end-diastolic dimension (r = 0.53; p = 0.01), while showing a inverse correlation with LVEF (r = –0.49; p = 0.001). The CMV DNA level greater than 1,687 copies/ml predicts adverse cardiovascular events (sensitivity 67%, specificity 81%, AUC = 0.763; p < 0.001) and death (sensitivity 68% and specificity 92%, AUC = 0.844, p < 0.001) in CHF patients over 24 months.

Conclusion. To stratify the risk of developing adverse cardiovascular events during a 24-month follow-up period after CHF decompensation, it is advisable to determine the concentration of cytomegalovirus DNA in the blood of patients with coronary heart disease.

Keywords: cytomegalovirus, herpes virus, heart failure, prognosis, biomarkers

Conflict of interest. The authors declare the absence of obvious or potential conflicts of interest related to the publication of this article.

Source of financing. The authors state that they received no funding for the study.

✉ *Shilov Sergey N.,* newsib54@gmail.com

Conformity with the principles of ethics. All patients signed an informed consent to participate in the study. The study was approved by the local Ethics Committee of the Novosibirsk Region Municipal Clinical Hospital No. 1 (Minutes No. 200 of January 31, 2019).

For citation: Shilov S.N., Berezikova E.N., Pankova I.V., Grakova E.V., Kopyeva K.V., Teplyakov A.T., Mayanskaya S.D., Kovalenko G.V., Kolmakova A.M., Kalyuzhin V.V. Cytomegalovirus infection activity as a predictor of adverse clinical events in chronic heart failure. *Bulletin of Siberian Medicine.* 2026;25(2):130–138. https://doi.org/10.20538/1682-0363-2026-2-130-138.

Активность цитомегаловирусной инфекции как предиктор неблагоприятных клинических событий при хронической сердечной недостаточности

Шилов С.Н.[1], Березикова Е.Н.[1], Панкова И.В.[1], Гракова Е.В.[2], Копьева К.В.[2], Тепляков А.Т.[2], Маянская С.Д.[3], Коваленко Г.В.[4], Колмакова А.М.[4], Калюжин В.В.[4]

[1] *Новосибирский государственный медицинский университет (НГМУ)*
Россия, 630091, г. Новосибирск, Красный пр., 52

[2] *Научно-исследовательский институт (НИИ) кардиологии, Томский национальный исследовательский медицинский центр (НИМЦ) Российской академии наук*
Россия, 634012, г. Томск, ул. Киевская, 111а

[3] *Казанский государственный медицинский университет (КГМУ)*
Россия, 420012, г. Казань, ул. Бутлерова, 49

[4] *Сибирский государственный медицинский университет (СибГМУ)*
Россия, 634050, г. Томск, Московский тракт, 2

РЕЗЮМЕ

Цель. Оценить в ходе 24-месячного проспективного исследования влияние цитомегаловирусной (ЦМВ) инфекции на течение хронической сердечной недостаточности (ХСН) у пациентов с ишемической болезнью сердца (ИБС).

Материал и методы. В исследование включены пациенты (n = 151), госпитализированные в связи с ухудшением течения ХСН, которые по результатам наблюдения были разделены на группы с благоприятным и неблагоприятным течением основного заболевания, фоновой патологии и их осложнений. В группу неблагоприятного течения вошли пациенты, у которых в течение 24 мес было зарегистрировано хотя бы одно из указанных событий: 1) госпитализация по поводу декомпенсации ХСН; 2) наступление неблагоприятных клинических событий (сердечно-сосудистая смерть, нефатальный инфаркт миокарда или острое нарушение мозгового кровообращения, тромбоэмболия легочной артерии); 3) любое нарастание функционального класса (ФК) ХСН; 4) уменьшение фракции выброса левого желудочка (ФВ ЛЖ) на 10% и более от исходного значения. Уровень ДНК ЦМВ инфекции в плазме крови оценивали исходно, через 12 и 24 мес наблюдения. Для выявления предикторов развития неблагоприятных сердечно-сосудистых событий использовали ROC-анализ с построением характеристических кривых и расчетом площади под кривой (AUC).

Результаты. У пациентов с неблагоприятным течением ХСН содержание ДНК ЦМВ инфекции в плазме крови на момент включения в исследование было существенно выше (p < 0,001) по сравнению с лицами с благоприятным течением ХСН: 2232,0 [1687,0; 2765,0] и 1245 [991,3; 1592,0] копий/мл соответственно. Уровень ДНК ЦМВ инфекции в плазме крови демонстрировал прямую взаимосвязь со значением ФК ХСН (r = 0,66; p = 0,001), а также с конечно-диастолическим размером левого желудочка (r = 0,53; p = 0,01) и обратную – с ФВ ЛЖ (r = –0,49; p = 0,001). Содержание ДНК ЦМВ инфекции в плазме крови более 1687 копий/мл позволило прогнозировать неблагоприятные сердечно-сосудистые события (чувствительность 67%, специфичность 81%, AUC = 0,763; p < 0,001) и летального исхода (чувствительность 68%, специфичность 92%, AUC = 0,844; p < 0,001) у пациентов с ХСН в течение 24 мес.

Заключение. Для стратификации риска развития неблагоприятных сердечно-сосудистых событий в течение 2 лет после декомпенсации ХСН в крови больных ИБС целесообразно определять концентрацию ДНК ЦМВ инфекции.

Ключевые слова: цитомегаловирус, вирус герпеса, сердечная недостаточность, прогноз, биомаркеры

Для цитирования: Шилов С.Н., Березикова Е.Н., Панкова И.В., Гракова Е.В., Копьева К.В., Тепляков А.Т., Маянская С.Д., Коваленко Г.В., Колмакова А.М., Калюжин В.В. Активность цитомегаловирусной инфекции как предиктор неблагоприятных клинических событий при хронической сердечной недостаточности. *Бюллетень сибирской медицины.* 2026;25(2):130–138. https://doi.org/10.20538/1682-0363-2026-2-130-138.

INTRODUCTION

Despite advances in the fight against coronary heart disease (CHD) thanks to active preventive and therapeutic measures that have led to a reduction in mortality, an alarming trend is observed as an increasing number of patients with CHD are experiencing the development of chronic heart failure (CHF) over time. This, in turn, significantly increases the risk of premature death [1, 2]. This situation makes it extremely important to conduct research aimed at thoroughly understanding the mechanisms of the onset and development of CHF in order to develop innovative and personalized strategies for the prevention of cardiovascular diseases in general, and CHF in particular.

Current concepts regarding the progression of CHF emphasize the role of immune activation and systemic inflammation as key markers of an adverse disease course and high cardiovascular risk [3, 4]. According to this concept, severe microcirculation disorders trigger nonspecific activation of mononuclear cells and monocytes, which triggers the synthesis of proinflammatory cytokines. These cytokines play a crucial role in the evolution of left ventricular dysfunction [5, 6]. It is believed that chronic inflammation can lead to structural changes in cardiomyocytes, including their apoptosis, which ultimately leads to the development of heart failure.

Thus, subclinical cytomegalovirus infection and the accompanying immune response may act as important triggers for the development and decompensation of CHF. This is likely due to the ability of CMV to induce the synthesis of inflammatory markers, such as interleukin (IL) 1β and tumor necrosis factor α (TNFα) [7]. Numerous scientific data obtained from animal experiments, epidemiological and molecular biological studies demonstrate a close association between CMV infection and the aggravation of the atherosclerotic process and the development of acute coronary syndrome (ACS) [8, 9]. Since atherosclerosis and CHD are integral components of the cardiovascular continuum leading to the development of CHF, the need for a detailed study of the influence of CMV on the mechanisms of formation and clinical course of heart failure becomes obvious.

The aim of the study was to analyze the impact of CMV infection on the development and course of CHF in patients with CHD in a 24-month prospective study.

MATERIALS AND METHODS

The study included 151 patients with chronic heart failure (CHF) of ischemic etiology admitted to the Cardiology Unit due to decompensated heart failure. Patients signed an informed consent to participate in the study after resolution of symptoms and signs of CHF decompensation prior to hospital discharge. Patients were then prospectively followed for 24 months. The study was conducted in accordance with the Declaration of Helsinki and received approval from the Ethics Committee of the State Budgetary Healthcare Institution of the Novosibirsk Region City Clinical Hospital No. 1 (Minutes No. 200 of January 31, 2019).

Exclusion criteria were as follows: acute cardiovascular events in the last six months (cerebrovascular accident, pulmonary embolism, stroke, myocarditis) or the presence of acute myocarditis at onset; heart valve pathology affecting hemodynamics: grade II mitral regurgitation (or higher), aortic stenosis with a pressure gradient > 25 mmHg, grade I aortic insufficiency (or higher), grade II tricuspid regurgitation (or higher); age over 70 years; confirmed COVID-19 (positive PCR test or the presence of IgG to SARS-CoV-2); severe comorbidity: liver disease, end-stage renal failure (glomerular filtration rate (GFR) <30 ml/min/1.73 m²), bronchial asthma or exacerbation of chronic obstructive pulmonary disease; the presence of

autoimmune pathology and malignant neoplasms; lack of informed consent.

Acute coronary syndrome as a reason for hospitalization of patients was excluded based on the absence of clinical, laboratory, and instrumental data (absence of pain syndrome, significant laboratory activity of necrosis markers, characteristic electrocardiographic signs, and the appearance of new zones of impaired local contractility according to echocardiography (EchoCG)) within six months prior to inclusion of patients in the study.

The combined endpoint for the 24-month follow-up period after the first episode of CHF decompensation was the total number of subsequent CHF decompensations requiring hospitalization, as well as major serious adverse events, such as cardiovascular death, nonfatal myocardial infarction, stroke, or pulmonary embolism.

The level of CMV deoxyribonucleic acid (DNA) in blood plasma was determined by the polymerase chain reaction with fluorescence *in situ* hybridization detection of amplification products in real-time mode during hospitalization of patients in the Cardiology Unit due to decompensation of CHF, as well as after 12 and 24 months.

Statistical analysis was performed using R software (version 4.4.3; R Foundation for Statistical Computing, Vienna, Austria). Quantitative variables were presented as minimum (*min*) and maximum (*max*) values, median and interquartile range *Me* [Q_{25}; Q_{75}], and qualitative variables - as absolute and relative *n* (%) frequencies. The prognostic value of parameters was assessed using ROC analysis: models were considered to be adequate if the area under the curve (AUC) was > 0.70. Relationships between features were identified using Spearman's rank correlation. Differences were considered as statistically significant at $p < 0.05$.

RESULTS

After 24 months of follow-up, patients were divided into two cohorts. The first group ($n = 84$) was characterized by an adverse course of the disease. The second group ($n = 67$) included patients with a favorable prognosis. The inclusion criteria in the first group (with an adverse course) were at least one of the following events within 24 months: hospitalization due to decompensated CHF, the development of cardiovascular events (death from cardiovascular causes, nonfatal MI, stroke, and pulmonary embolism), progression of CHF class, or a decrease in left ventricular ejection fraction (LVEF) by 10% or more compared to baseline.

The patient groups were comparable by most of the recorded parameters: gender, age, body mass index, time since the last MI, presence of post-infarction cardiosclerosis, and CHF class (Table 1). However, patients in group 2 were statistically significantly ($p = 0.038$) more likely to have stage 2 CHF compared to patients in group 1 (44.8% vs. 25%, respectively).

The distance measured during the 6-minute walk test at the time of inclusion in the study was significantly lower in group 1 patients compared to group 2 patients ($p = 0.041$), which is consistent with the fact that the number of patients with class 3 CHF was higher among patients with an adverse course of the pathology (68.7% vs. 53.6%). The number of patients seropositive for CMV in group 2 was significantly greater than in group 1 ($p = 0.024$).

Table 1

Clinical and Demographic Characteristics of Patients

Characteristic	Group 1, $n = 84$	Group 2, $n = 67$	p
Gender, male, *n* (%)	55 (65.5)	39 (58.2)	0.455
BMI, kg/m^2, *Me* [Q_{25}; Q_{75}]	30.1 [25.1; 33]	27.7 [24.5; 32.4]	0.146
Age, years, *Me* [Q_{25}; Q_{75}]	57 [52; 63]	59 [55; 63]	0.187
Prior myocardial infarction, *n* (%)	52 (61.9)	44 (65.7)	0.758
Duration of MI, years, *Me* [Q_{25}; Q_{75}]	3.0 [1.5; 4.0]	2.5 [2.0; 4.0]	0.363
CHF stage, *n* (%) Stage 1 Stage 2	 63 (75) 21 (25)	 37 (55.2) 30 (44.8)	0.038
CHF class, *n* (%) Class 2 Class 3	 39 (46.4) 45 (53.6)	 21 (31.3) 46 (68.7)	0.146
6-minute walk test, m, *Me* [Q_{25}; Q_{75}]	289.5 [188.0; 362.0]	233.0 [139.0; 331.5]	0.041
NT-proBNP, pg/ml, *Me* [Q_{25}; Q_{75}]	350.0 [284.0; 526.0]	607.0 [378.5; 920.5]	0.001
LVEF, %, *Me* [Q_{25}; Q_{75}]	44.5 [39.0; 54.8]	41.0 [36.0; 45.5]	0.116
EDD, mm, *Me* [Q_{25}; Q_{75}]	52.0 [49.0; 59.0]	57.0 [54.0; 61.6]	0.042
ESD, mm, *Me* [Q_{25}; Q_{75}]	41.0 [35.8; 47,0]	45.0 [40.0; 49.0]	0.059
Seropositive CMV patients, *n* (%)	34 (40.5)	45 (67.2)	0.024

Note. NT-proBNP – N-terminal pro-brain natriuretic peptide, EDD – end-diastolic dimension, ESD – end-systolic dimension (here and in Table 2).

When comparing CMV-seropositive and -seronegative patients, significant differences in CHF class and stage were revealed (Table 2). Thus, seropositive patients more often had class 3 CHF (70.9% vs. 48.6%, p = 0.042) and stage 2 CHF (41.8% vs. 25.0%, p = 0.043). The results of the 6-minute walk test also demonstrated significant differences: CMV-seropositive patients walked a shorter distance (p = 0.031). Also, CMV-seropositive patients had a significantly higher level of NT-proBNP (p = 0.001).

Table 2

Clinical and Demographic Characteristics of Patient Groups Formed Depending on CMV

Characteristic	CMV –, n = 72	CMV +, n = 79	p
Gender, male, n (%)	43 (59.7)	51 (64.6)	0.395
BMI, kg/m^2, *Me* [Q_{25}; Q_{75}]	30.3 [25.6; 34.4]	27.7 [24.5; 31.9]	0.132
Age, years, *Me* [Q_{25}; Q_{75}]	57.5 [53; 63]	59 [53; 63]	0.262
Prior myocardial infarction, n (%)	45 (62.5)	51 (64.6)	0.911
Duration of MI, years, *Me* [Q_{25}; Q_{75}]	2.5 [2.0; 4.0]	3.0 [2.0; 4.0]	0.489
CHF stage, n (%) Stage 1 Stage 2	 54 (75) 18 (25)	 46 (58.2) 33 (41.8)	0.043
CHF class, n (%) Class 2 Class 3	 37 (51.4) 35 (48.6)	 23 (29.1) 56 (70.9)	0.042
6-minute walk test, m, *Me* [Q_{25}; Q_{75}]	325.5 [208.5; 364.0]	230.0 [136.5; 324.0]	0.031
NT-proBNP, pg/ml, *Me* [Q_{25}; Q_{75}]	350.0 [281.0; 449.0]	580.0 [378.0; 735.5]	0.001
LVEF, %, *Me* [Q_{25}; Q_{75}]	44.0 [38.8; 57.0]	41.0 [37.0; 46.0]	0.095
EDD, mm, *Me* [Q_{25}; Q_{75}]	54.0 [50.0; 59.0]	56.0 [50.5; 61.5]	0.365
ESD, mm, *Me* [Q_{25}; Q_{75}]	41.0 [36.8; 47.0]	45.0 [38.5; 49.0]	0.07

Note. "+" stands for presence; "–" stands for absence

In patients with an adverse course of CHF during 24-month follow-up, the CMV DNA content at the time of inclusion in the study was significantly higher compared to patients who had positive dynamics of the clinical and instrumental characteristics of CHF – 2,232.0 [1,687.0; 2,765.0] copies/ml and 1,245 [991.3; 1,592.0] copies/ml, respectively (p < 0.001) (Fig. 1).

In adverse CHF course, the CMV DNA content did not change significantly, amounting to 2,438.0 copies/ml [1,902.8; 2,847.5] after one year of follow-up (p = 0.115) and 2,218.0 copies/ml [1,845.0; 2,578.5] after two years of follow-up (p = 0.811). In patients with a favorable course of pathology, there was an insignificant decrease in CMV DNA after one year of observation to 1,011.0 copies/ml [697.0; 1,275.5] (p = 0.137), which actually remained at the same level after the next year of observation 1,019.0 copies/ml [799.5; 1,319.0].

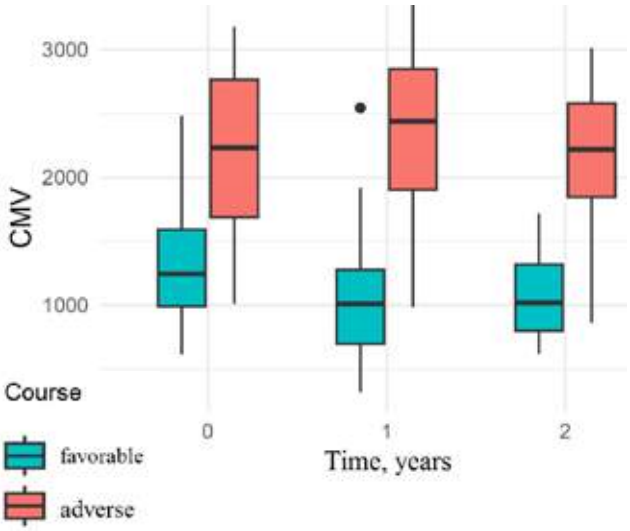

Fig. 1. Dynamics of the CMV DNA content in the blood plasma of patients with favorable and adverse course of CHF, copies/ml: *min* (lower vertical line), Q_{25} (bottom side of the rectangle), *Me* (horizontal line inside the rectangle), Q_{75} (top side of the rectangle), *max* (top vertical line)

Using ROC analysis, it was found that in seropositive patients, the CMV DNA content in blood plasma of more than 1,687 copies/ml allowed for the prediction of adverse cardiovascular events within 2 years after hospitalization for decompensated CHF with sensitivity of 67% and specificity of 81% (AUC = 0.763, p < 0.001) (Fig. 2, *a*). It was also found that the CMV DNA content in blood plasma of more than 1,687 copies/ml allowed for the prediction of death within the next 24 months with a sensitivity of 68% and a specificity of 92% (AUC = 0.844, p < 0.001) (Fig. 2, *b*).

The amount of CMV DNA in blood plasma directly correlated with CHF class (r = 0.66, p = 0.001) and with the EDD (r = 0.53, p = 0.01), and, on the contrary, showed a moderate inverse relationship with the distance covered in the six-minute walk test (r = –0.63, p = 0.001) and LVEF (r = –0.49, p = 0.001) (Table 3).

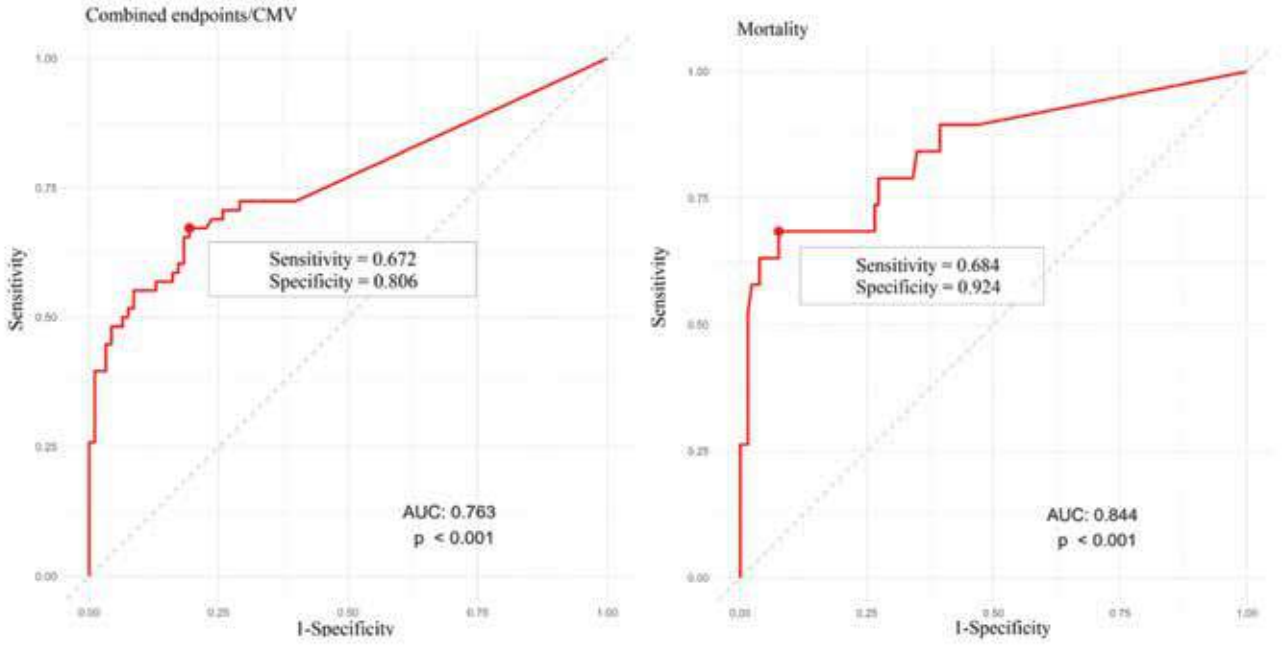

a *b*

Fig. 2. ROC curves of sensitivity and specificity of CMV DNA level in blood plasma in predicting the development of adverse cardiovascular events (*a*) and mortality (*b*) in CHF patients over 24 months: the area under the curve (AUC) value is presented together with the significance level estimate (*p*)

Table 3

Correlation Analysis of the Relationship between CMV DNA Content and Clinical, Instrumental, and Laboratory Parameters

Parameter	*r*	*p*
CHF class	0.66	0.001
6-minute walk test	–0.63	0.001
LVEF	–0.49	0.01
EDD	0.53	0.01
GFR	0.08	0.73
Total cholesterol	–0.15	0.62
LDL	–0.18	0.6

Note. LDL – low-density lipoprotein, *p* – statistical significance of the correlation coefficient.

DISCUSSION

The data obtained in this study confirm the pathogenetic role of CMV infection in the destabilization of patients with CHF secondary to CHD. The identified correlations between viral load and myocardial structural and functional remodeling indicate a direct link between CMV DNA levels and the risk of adverse cardiovascular events. These results suggest that viral concentration in the blood is a significant factor modulating the severity of heart failure.

Cytomegalovirus establishes deep and complex relationships with the host immune system, resulting in a variety of changes in the functional characteristics of lymphocytes. In immunocompetent individuals, CMV typically manifests as an asymptomatic latent infection with episodic reactivations. In contrast, in immunocompromised patients, it typically causes acute pathology. The host inflammatory response is essential for CMV reactivation and stimulation of its gene expression [10]. Some viral gene products, in turn, induce the host to produce a wide range of proinflammatory cytokines, including tumor necrosis factorα, interleukin-1β, and interleukin-6 [11]. Although CMV reactivation in immunocompromised individuals is associated with severe consequences, it has been established that in elderly patients with CHF, viral reactivation is often subclinical, which complicates timely diagnosis, despite its potential contribution to disease progression [12].

In vivo studies indicate a significant impact of CMV infection on the vascular wall, affecting various cell types. Among the most susceptible cells are monocytes/macrophages, smooth muscle cells, and, most importantly, endothelial cells [13]. The latter play a critical role in maintaining the health of the vascular system. Endothelial cells form the

inner layer of blood vessels, acting as a barrier that regulates vascular wall permeability and controls blood – tissue interactions. They not only passively separate blood from surrounding tissues but also actively participate in the regulation of vascular tone, as if orchestrating vascular processes.

Endothelial cells like a highly organized communication network receive and transmit signals, ensuring the integrity of the vascular system and maintaining normal blood flow. Various biologically active substances synthesized by the endothelium play a key role in this process. Among them are prostacyclin (a potent inhibitor of platelet aggregation), thromboxane A2, which has the opposite effect of stimulating platelet aggregation, endothelin (a regulator of vascular tone), and thrombomodulin, which modulates the blood coagulation system [14]. Thus, endothelial cells maintain a delicate balance between coagulation and fibrinolysis processes, preventing unwanted thrombus formation and maintaining the free flow of blood. In particular, the enzyme adenosine diphosphate (ADP) secreted by platelets plays a significant role in thrombus formation and cellular adhesion, while endothelial cells are actively involved in the regulation of its action [15]. They provide an antithrombotic surface, preventing uncontrolled activation of coagulation factors and platelets. Endothelial dysfunction leads to a chain reaction of pathological processes, triggering an inflammatory process, stimulating the production of cytokines and other inflammatory mediators. This leads to the expression of adhesion molecules on the surface of endothelial cells, which promotes the adhesion of leukocytes to the vessel wall and the further development of inflammation [15].

Studies by Y.J. Tang-Feldman et al. have shed light on the mechanism by which CMV provokes inflammatory processes that can lead to endothelial dysfunction [16]. A key link in this process is the release of arachidonic acid after infection of cells with CMV. This acid, in turn, triggers a cascade of reactions catalyzed by cyclooxygenase (COX). COX activated by early viral proteins IE-72/IE-86 leads to an increase in the production of reactive oxygen species (ROS). An increased concentration of ROS plays a crucial role in the activation of the transcription factor NF-κB, which is located in the cell cytoplasm in an inactive state.

Activation of NF-κB triggers the expression of proinflammatory cytokines, such as IL-6 and IL-8. Further studies by D. Prochnau et al. confirmed a significant increase in the levels of a number of inflammatory factors, including interleukins 6 and 8 and platelet-derived growth factor, in vascular smooth muscle cells 24 and 72 hours after CMV infection [17]. In addition to its direct damaging effect, interleukin 6 also stimulates endothelial cells to release monocyte chemoattractant protein-2 (CCL-2). CCL-2 attracts additional monocytes and lymphocytes to the intima, increasing inflammation in the affected area. Interleukin 8, in turn, activates neutrophils, which, in a process known as an oxidative burst, release a huge amount of ROS. This flow of ROS creates a vicious cycle, further stimulating the production of NF-κB and, consequently, even more inflammatory factors. Ultimately, the interaction of all these factors forms a complex network of interconnected processes, where factors affect each other, exacerbating inflammation and contributing to the development and progression of cardiovascular disease. CMV, through its influence on ROS production and NF-κB activation, plays a key role in this pathological cascade [17, 18], which can ultimately activate inflammation not only in the vascular wall but also in the myocardium, contributing to the progression of cardiac dysfunction.

Our findings confirmed that monitoring CMV viral load in the blood serves as an objective tool for assessing the severity of the condition and predicting the progression of CHF in patients with a history of ischemia. The established direct link between increased viral DNA concentration and the risk of decompensation supports the hypothesis that CMV plays a pathogenic role in the progression of heart failure and the development of adverse cardiovascular outcomes.

Thus, the results of our study highlight the importance of measuring plasma CMV levels for an objective assessment of heart failure severity. This may become an important prognostic test for determining the disease course in patients with coronary heart disease, which, in turn, will optimize the diagnosis and treatment of these patients. Understanding the immune – inflammatory mechanisms underlying ischemic CHF is critical for developing new approaches to studying the pathogenesis of heart failure. These results highlight the importance of developing a comprehensive approach to the prevention and treatment of heart failure that takes into account both infectious and inflammatory mechanisms, which may lead to

improved outcomes in patients with cardiovascular disease.

CONCLUSION

A relationship has been established between plasma CMV DNA concentration and the severity and course of CHF. To stratify the risk of developing adverse cardiovascular events within two years after CHF decompensation, it is advisable to measure plasma CMV DNA concentrations in patients with coronary heart disease.

However, it is important to note that, in our opinion, CMV is not the primary etiologic factor leading to the development of CHF. Patients with pre-existing CHF due to other causes, such as coronary artery disease or hypertension, exhibit decreased immune reactivity. This decrease may be associated with age and the development of systemic circulatory hypoxia, which is also a consequence of CHF. This process results in the activation of latent CMV infection, which, in turn, may lead to further activation of inflammatory processes in the myocardium. Therefore, it can be concluded that the presence of active or latent CMV infection in patients with pre-existing CHF may aggravate the disease and increase the risk of adverse cardiovascular events.

REFERENCES

1. Boytsov S.A. Chronic Heart Failure: Evolution of Etiology, Prevalence and Mortality over the Past 20 Years. *Terapevtichekii Arkhiv.* 2022;94(1):5–8. (In Russ.). DOI: 10.26442/00403660.2022.01.201317.
2. Fomin I.V., Belenkov Yu.N., Mareev V.Yu., Ageev F.T., Artemyeva E.G., Badin Yu.V. et al. EPOCH-CHF As A Mirror of the Current Problems in Cardiovascular Diseases Treatment in Real Clinical Practice. *Kardiologiia*.2024;64(11):48–61. (In Russ.). DOI: 10.18087/cardio.2024.11.n2808.
3. Ageev F.T., Ovchinnikov A.G. Diastolic Heart Failure: 20 Years Later. Current Issues of Pathogenesis, Diagnosis and Treatment of Heart Failure with Preserved LVEF. *Kardiologiia*. 2023;63(3):3–12. (In Russ.). DOI: 10.18087/cardio.2023.3.n2376.
4. Chen J., Zhu Z., Wang Y., Yu J., Zhang X., Xu Y. Cardiac resident macrophages in cardiovascular disease: from physiology to pathology. *Heart.* 2025;111(9):391–400. DOI: 10.1136/heartjnl-2024-324333.
5. Korotaeva a.A., Samoylova E.V., Mindzaev D.R., Nasonova S.N., Zhirov I.V., Tereshchenko S.N. Proinflammatory Cytokines in Chronic Cardiac Failure: State of Problem. *Terapevtichekii Arkhiv.* 2021;93(11):1389–1394. (In Russ.). DOI: 10.26442/00403660.2021.11.201170.
6. Tokmachev R.E., Budnevsky A.V., Kravchenko A.Ya. The Role of Inflammation in the Pathogenesis of Chronic Heart Failure. *Terapevtichekii Arkhiv*. 2016;88(9):106–110. (In Russ.). DOI: 10.17116/terarkh2016889106-110.
7. Cristescu C.V., Alain S., Ruță S.M. The role of CMV infection in primary lesions, development and clinical expression of atherosclerosis. *J. Clin. Med.* 2022;11(13):3832. DOI: 10.3390/jcm11133832.
8. Lebedeva A.M., Maryukhnich E.V., Grivel Zh.Sh., Nikitskaya E.A., Albakova T.M., Albakova R.M. et al. Cytomegalovirus Infection and Endothelial Function in Patients With Acute Myocardial Infarction. *Kardiologiia.* 2018;58(7):41–52. (In Russ.). DOI: 10.18087/cardio.2018.7.10155.
9. Nikitskaya E.A., Grivel Zh.Sh., Maryukhnich E.V., Lebedeva A.M., Ivanova O.I., Savvinova P.P. et al. Cytomegalovirus in Plasma of Acute Coronary Syndrome Patients. *ACTA NATURAE*. 2016;2(29):114–119. (In Russ.). DOI: 10.32607/20758251-2016-8-2-102-107.
10. Griffiths P., Reeves M. Pathogenesis of human cytomegalovirus in the immunocompromised host. *Nat. Rev. Microbiol.* 2021;19(12):759-773. DOI: 10.1038/s41579-021-00582-z.
11. Jackson S.E., Noor M., Lim E., Wills M. The immune response to human cytomegalovirus: impact of age, co-morbidities and the significance of anti-viral activity assessment. *Philos. Trans. R Soc. Lond. B. Biol Sci.* 2025;380(1938):20240408. DOI: 10.1098/rstb.2024.0408.
12. García-Torre A., Bueno-García E., López-Martínez R., Rioseras B., Díaz-Molina B., Lambert J.L. et al. CMV infection is directly related to the inflammatory status in chronic heart failure patients. *Front. Immunol.* 2021;12:687582. DOI: 10.3389/fimmu.2021.687582.
13. Styles J.N., Converse R.R., Griffin S.M., Wade T.J., Klein E., Nylander-French L.A. et al. Human cytomegalovirus infections are associated with elevated biomarkers of vascular injury. *Front. Cell Infect. Microbiol*. 2020;10:334. DOI: 10.3389/fcimb.2020.00334.
14. Yan R., Zhang X., Xu W., Li J., Sun Y., Cui S. et al. ROS-induced endothelial dysfunction in the pathogenesis of atherosclerosis. *Aging Dis*. 2024;16(1):250–268. DOI: 10.14336/AD.2024.0309.
15. Wang X., He B. Endothelial dysfunction: molecular mechanisms and clinical implications. *Med. Comm*. 2024;5(8):e651. DOI: 10.1002/mco2.651.
16. Tang-Feldman Y.J., Lochhead S.R., Lochhead G.R., Yu C., George M., Villablanca A.C. et al. Murine cytomegalovirus (MCMV) infection upregulates P38 MAP kinase in aortas of Apo E KO mice: a molecular mechanism for MCMV-induced acceleration of atherosclerosis. *J. Cardiovasc. Transl. Res*. 2013;6:54–64. DOI: 10.1007/s12265-012-9428-x.
17. Prochnau D., Straube E., Figulla H.R., Rodel J. Supra-additive expression of interleukin-6, interleukin-8 and basic fibroblast growth factor in vascular smooth muscle cells following coinfection with *Chlamydia pneumoniae* and cytomegalovirus as a novel link between infection and atherosclerosis. *Can. J. Infect. Dis. Med. Microbiol*. 2012;23:e26–e30. DOI: 10.1155/2012/987476.
18. Fulkerson H.L., Nogalski M.T., Collins-McMillen D., Yurochko A.D. Overview of human cytomegalovirus pathogenesis. *Methods Mol. Biol*. 2021;2244:1–18. DOI: 10.1007/978-1-0716-1111-1_1.

Author Contribution

Shilov S.N., Pankova I.V., Mayanskaya S.D. – conception and design, data analysis and interpretation, and drafting of the manuscript. Berezikova E.N., Grakova E.V. – conception and design, justification of the manuscript. Kopyeva K.V., Kovalenko G.V., Kolmakova A.M. – data analysis and interpretation. Teplyakov A.T., Kalyuzhin V.V. – final approval of the manuscript for publication.

Author Information

Shilov Sergey N. – Dr. Sci. (Med.), Professor, Department of Pathological Physiology and Clinical Pathological Physiology, NSMU, Novosibirsk, newsib54@gmail.com, http://orcid.org/0000-0002-7777-6419

Berezikova Ekaterina N. – Dr. Sci. (Med.), Professor, Department of Internal Medicine, NSMU, Novosibirsk, cardio@enberezikova.ru, http://orcid.org/0000-0002-9630-0213

Pankova Irina V. – Assistant Professor, Department of Pathological Physiology and Clinical Pathological Physiology, NSMU, Novosibirsk, pankovairin@mail.ru; http://orcid.org/0000-0001-7864-3194

Grakova Elena V. – Dr. Sci. (Med.), Leading Reasercher, Department of Myocardial Pathology, Cardiology Research Institute, Tomsk NRMC, Tomsk, Russian Federation, gev@cardio-tomsk.ru, http://orcid.org/0000-0003-4019-3735

Kopeva Kristina V. – Cand. Sci. (Med.), Senior Researcher, Department of Myocardial Pathology, Cardiology Research Institute, Tomsk NRMC, Tomsk, Kristin-kop@inbox.ru, http://orcid.org/0000-0002-2285-6438

Teplyakov Alexander T. – Dr. Sci. (Med.), Professor, Chief Researcher, Cardiology Research Institute, Tomsk NRMC, Tomsk, Vgelen1970@gmail.com, http://orcid.org/0000-0003-0721-0038

Mayanskaya Svetlana D. – Dr. Sci. (Med.), Professor, Hospital Therapy Department, KSMU, Kazan, smayanskaya@mail.ru, http://orcid.org/0000-0001-6701-5395

Kovalenko GeorgiyV. – 6th-year Student, General Medicine Department, Siberian State Medical University, Tomsk, kovageorgvlad@yandex.ru, http://orcid.org/0009-0005-0070-2111

Kolmakova Arina M. – 6th-year Student, General Medicine Department, Siberian State Medical University, Tomsk, arina.kolmakova.02@mail.ru, http://orcid.org/0009-0008-0480-7094

Kalyuzhin Vadim V. – Dr. Sci. (Med.), Professor, Head of the Advanced Therapy Division with a Course in Rehabilitation, Physiotherapy and Sports Medicine, Siberian State Medical University, Tomsk, kalyuzhinvv@mail.ru, http://orcid.org/0000-0001-9640-2028

(✉) **Shilov Sergey N.,** newsib54@gmail.com

Received on January 23, 2026;
approved after peer review on February 5, 2026;
accepted on February 26, 2026

УДК 616.33-006.6-08-047.72
https://doi.org/10.20538/1682-0363-2026-2-139-149

Molecular and Genetic Parameters of Prognosis and New Strategies for the Treatment of Peritoneal Carcinomatosis in Gastric Cancer

Zavyalova M.V.[1, 2], Zavyalov A.V.[2], Neklyudov A.A.[2], Belousova O.A.[2], Pismenny D.S.[1, 2], Miller S.V.[1], Perelmuter V.M.[1, 2]

[1] *Cancer Research Institute, Tomsk National Research Medical Center (NRMC), Russian Academy of Sciences*
5 Kooperativny St., 634009 Tomsk, Russian Federation

[2] *Siberian State Medical University*
2 Moskovsky trakt, 634050 Tomsk, Russian Federation

ABSTRACT

Despite advances in modern oncology, in Russia, 36% of gastric cancers are detected at an advanced stage, with a one-year mortality rate of 39.6%. One of the most common causes of death from gastric cancer is peritoneal carcinomatosis. Synchronous peritoneal carcinomatosis is diagnosed in 18–26% of cases. Metachronous carcinomatosis occurs in 7–39% of patients 8.5–26 months after the primary tumor is removed. To date, there are no effective treatments for peritoneal carcinomatosis. Tumors accompanied by peritoneal carcinomatosis are often resistant to systemic chemotherapy. Cytoreductive surgeries and intraperitoneal chemotherapy are not always possible or successful for all patients.

This review focuses on analyzing the molecular and genetic mechanisms of peritoneal carcinomatosis in gastric cancer and presents an original hypothesis suggesting that peritoneal carcinomatosis occurs when tumor cells acquire the ability to autonomously exist in a matrix-independent state in the ascitic fluid without undergoing apoptosis (anoeucsis). Using the PRISMA (Preferred Reporting Items for Systematic Reviews and Meta-Analyses) guidelines, 10,025 scientific papers were identified, of which 228 English-language and 323 Russian-language publications met the analysis criteria. Twenty-nine articles (including four Russian-language ones) relevant to the topic of this review were included in the review. It is assumed that the identification of key molecules associated with the matrix-independent existence of tumor cells could serve as the basis for the development of technologies for predicting peritoneal carcinomatosis, as well as for the development of new targeted therapy for metastatic gastric cancer.

Keywords: peritoneal carcinomatosis, stomach cancer, molecular and genetic mechanisms, matrix independence, metastasis

Conflict of interest. The authors declare the absence of obvious or potential conflicts of interest related to the publication of this article.

Source of financing. Priority 2030 program.

For citation: Zavyalova M.V., Zavyalov A.V., Neklyudov A.A., Belousova O.A., Pismenny D.S., Miller S.V., Perelmuter V.M. Molecular and Genetic Parameters of Prognosis and New Strategies for the Treatment of Peritoneal Carcinomatosis in Gastric Cancer. *Bulletin of Siberian Medicine.* 2026;25(2):139–149. https://doi.org/10.20538/1682-0363-2026-2-139-149.

✉ *Pismenny Dmitry S.,* pismenniy.dmitry@yandex.ru

Молекулярно-генетические параметры прогноза и новые стратегии терапии перитонеального канцероматоза при раке желудка

Завьялова М.В.[1, 2], Завьялов А.В.[2], Неклюдов А.А.[2], Белоусова О.А.[2], Письменный Д.С.[1, 2], Миллер С.В.[1], Перельмутер В.М.[1, 2]

[1] *Научно-исследовательский институт (НИИ) онкологии, Томский национальный исследовательский медицинский центр (НИМЦ) Российской академии наук Россия, 634009, г. Томск, пер. Кооперативный, 5*

[2] *Сибирский государственный медицинский университет (СибГМУ) Россия, 634050, г. Томск, Московский тракт, 2*

РЕЗЮМЕ

Несмотря на достижения современной онкологии, в России в 36% случаев рак желудка выявляется в запущенной стадии, при этом летальность в течение года с момента установления диагноза составляет 39,6%. Одной из частых причин летальных исходов при раке желудка является перитонеальный канцероматоз. Синхронный перитонеальный канцероматоз диагностируется в 18–26% случаев. Метахронный канцероматоз после удаления первичной опухоли наблюдается у 7–39% пациентов через 8,5–26 мес после операции. До настоящего времени не существует эффективных методов прогнозирования риска развития и лечения перитонеального канцероматоза. Опухоли, сопровождающиеся перитонеальным канцероматозом, нередко устойчивы к системной химиотерапии. Выполнение циторедуктивных операций и внутрибрюшинной химиотерапии возможно не для всех пациентов и не всегда является успешным.

Обзор посвящен анализу информации, касающейся молекулярно-генетических механизмов развития перитонеального канцероматоза при раке желудка, и содержит оригинальную гипотезу, согласно которой перитонеальный канцероматоз возникает в результате приобретения опухолевыми клетками матрикс-независимости и способности к автономному существованию в асцитической жидкости, не подвергаясь апоптозу (аноикису). С использованием руководства «Предпочтительные элементы отчетности для систематических обзоров и метаанализов» (PRISMA) было выявлено 10 025 научных работ, из которых 228 англоязычных и 323 русскоязычных публикаций соответствовали критериям анализа.

В обзор включено 35 статей (в том числе четыре русскоязычные), соответствующих теме настоящего обзора. Предполагается, что выявление ключевых молекул, ассоциированных с матрикс-независимым существованием опухолевых клеток, могло бы послужить основой для разработки технологий прогнозирования перитонеального канцероматоза, а также для разработки новой таргетной терапии метастатического рака желудка.

Ключевые слова: перитонеальный канцероматоз, рак желудка, молекулярно-генетические механизмы, матрикс-независимость, метастазирование

Конфликт интересов. Авторы заявляют об отсутствии конфликта интересов, связанных с публикацией настоящей статьи.

Источник финансирования. Программа «Приоритет 2030».

Для цитирования: Завьялова М.В., Завьялов А.В., Неклюдов А.А., Белоусова О.А., Письменный Д.С., Миллер С.В., Перельмутер В.М. Молекулярно-генетические параметры прогноза и новые стратегии терапии перитонеального канцероматоза при раке желудка. *Бюллетень сибирской медицины.* 2026;25(2):139–149. https://doi.org/10.20538/1682-0363-2026-2-139-149.

INTRODUCTION

Despite advances in modern oncology, in Russia, gastric cancer is detected at an advanced stage in 36% of cases, with one-year mortality rate from the time of diagnosis reaching 39.6% [1]. High mortality rates for gastric cancer are also recorded in global statistics, with the overall survival from the start of treatment being only 5–12 months [2–4].

Peritoneal carcinomatosis is considered as one of the most unfavorable forms of tumor progression with high lethality rates. Synchronous peritoneal carcinomatosis in gastric cancer is diagnosed in 18–26% of cases. The overall survival from the

time of diagnosis in these cases is only 2–9 months. Metachronous carcinomatosis, following the removal of the primary tumor, is observed in 7–39% of patients within 8.5–26 months after surgery, with the median overall survival from the detection of peritoneal recurrence being only 5 months. The success rate of therapy for peritoneal carcinomatosis in cases of its clinical manifestation is extremely low [5–7]. Therefore, the search for factors that can predict the occurrence of peritoneal carcinomatosis prior to its clinical manifestation is highly relevant.

MATERIALS AND METHODS

A search for original studies on the incidence, diagnosis, lethality, and therapy of peritoneal carcinomatosis in gastric cancer was conducted using the PubMed database and the eLIBRARY.ru scientific electronic library. This review includes original articles published between May 5, 2020 and August 3, 2025 in English and Russian. The selection of potential studies adhered to all requirements outlined in the Preferred Reporting Items for Systematic Reviews and Meta-Analyses (PRISMA) guidelines. The analysis was performed according to a four-stage algorithm (Figure).

Stage 1. Primary search for publications encompassed studies on gastric cancer and peritoneal carcinomatosis. The search utilized Boolean operators to combine the following keywords. In the PubMed database: peritoneal carcinomatosis, stomach cancer, molecular and genetic mechanisms, matrix independence, metastasis. In the eLIBRARY.ru scientific electronic library: peritoneal carcinomatosis, stomach cancer, molecular and genetic mechanisms, matrix independence, metastasis. The initial search yielded 10,025 publications: 9,624 articles in English and 401 articles in Russian.

Stage 2. From the total number of publications, 228 articles in English and 323 articles in Russian were selected, which contained the results of original research and were available in full text.

Stage 3. During the analysis of the abstracts of the selected articles, 201 publications from the PubMed database and 308 publications from the eLIBRARY.ru electronic library were excluded as they did not align with the topic of the present literature review.

Stage 4. A thorough analysis of the full texts of all publications was conducted. The selected articles were screened for compliance with the established inclusion criteria. Specifically, two studies investigated peritoneal carcinomatosis in cases of multiple primary malignant neoplasms, and two other published studies did not perform molecular analysis of the primary tumor tissue. One study with a small sample size (fewer than 30 patients) was also excluded, three publications did not present complete research results, and in one article, access to the results was restricted. For the preparation of this review, 35 articles (including four in Russian) that corresponded to the stated topic were included in the final analysis (Figure).

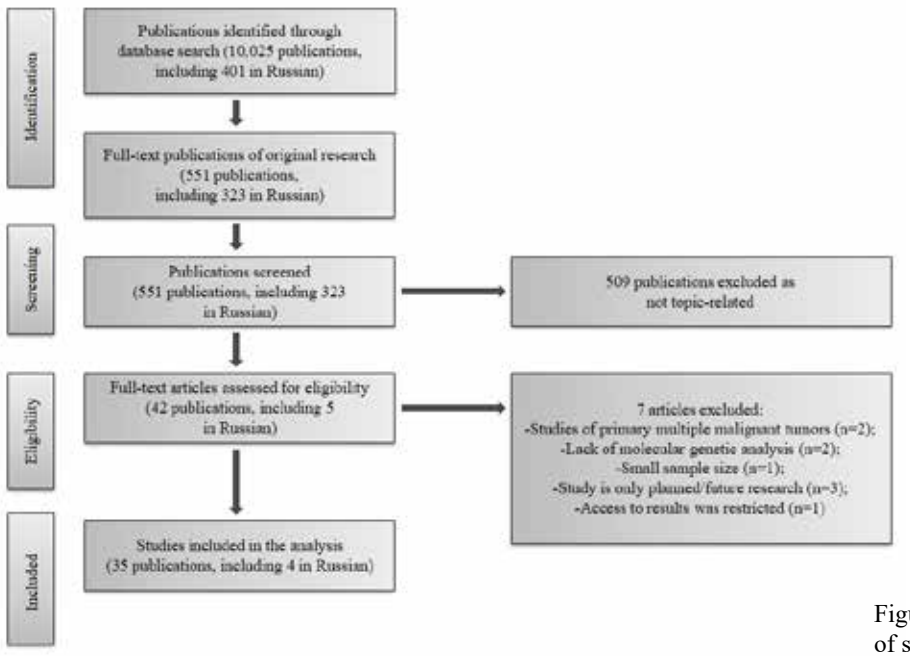

Figure. Algorithm for the identification of studies included in the review

CLINICAL AND MORPHOLOGICAL PARAMETERS ASSOCIATED WITH PERITONEAL CARCINOMATOSIS

The widely accepted prognostic parameters in gastric cancer associated with the risk of peritoneal carcinomatosis are T and N criteria, histological type, and the differentiation grade of a primary tumor. Based on the analysis of 17 studies, A.Rijken et al. identified the following parameters associated with the risk of synchronous peritoneal carcinomatosis: age, sex, tumor location, histological type, stage, and number of metastases. The prognosis was worse in younger patients, females, with non-cardia tumor location, locally advanced tumor process corresponding to the T4 stage, signet-ring cell or diffuse histological variant, and the presence of two or more metastatic foci. Furthermore, the authors noted increased incidence of synchronous peritoneal carcinomatosis in patients of Hispanic origin. However, the occurrence of peritoneal carcinomatosis does not always align with predictions, which is why current efforts are focused on developing mathematical models to assess the prognostic significance of a combination of factors, as well as incorporating additional parameters, including results from laboratory and instrumental diagnostic methods [8].

Based on a study involving 622 gastric cancer patients, D.J. Szor et al. developed a prognostic model to predict the risk of peritoneal carcinomatosis. The model included parameters such as patient sex, T stage, metastases detected on computed tomography, and diffuse or mixed histological type of gastric cancer according to the Lauren classification. However, the sensitivity of the model was not high, reaching only 82.8% [7, 9].

G. Guan et al. performed a meta-analysis of 21 case-control studies and one cohort study to identify the prognostic value of various clinical, morphological, and laboratory parameters in predicting peritoneal carcinomatosis in gastric cancer patients. The analysis confirmed the prognostic value of well-established criteria, such as T criterion (OR 2.96 (95% CI: 1.87–4.69)), N criterion (OR = 1.22 (95% CI: 0.86–1.73)), tumor differentiation grade (OR = 1.91 (95% CI: 1.42–2.56)), and Borrmann type IV (diffusely infiltrative form) primary tumor (OR = 7.68, 95% CI: 3.62–16.27) [10]. Furthermore, the highest risk of peritoneal carcinomatosis was associated with an elevated serum CA-125 level (OR = 19.45, 95% CI: 4.71–80.30); however, only a limited number of such studies have been conducted to date [11, 12].

These circumstances underscore the necessity of developing new approaches for the early diagnosis and effective therapy of peritoneal carcinomatosis, taking into account all possible factors and mechanisms of its occurrence.

ANATOMICAL AND PHYSIOLOGICAL FACTORS CONTRIBUTING TO PERITONEAL CARCINOMATOSIS

For a long time, it was believed that the anatomical and physiological features of the peritoneum contribute to the emergence and relentless spread of peritoneal carcinomatosis. Parietal and visceral layers of the peritoneum are a serous membrane comprising a single layer of mesothelial cells located on a basement membrane, and an underlying layer of connective tissue that includes collagen fibers, hyaluronic acid, proteoglycans, fibroblasts, immune cells, as well as blood vessels [13]. Significant importance was attributed to the stomata, which are spaces lacking a basement membrane, located between mesothelial cells. These spaces are necessary for the physiological circulation of fluid within the abdominal cavity. This specific structural feature of the peritoneum was linked to the potential for rapid progression of peritoneal carcinomatosis, as tumor cells spreading across the peritoneum can easily pass through the stomata, which expand during the respiratory movements of the diaphragm, directly into the connective tissue base of the peritoneum, bypassing the basement membrane. This significantly facilitates the progression of peritoneal carcinomatosis [14]. The potential for rapid and extensive dissemination of tumor cells, affecting the peritoneal layers in different parts of the abdominal cavity, was explained by the circulation of physiological fluid flows [15, 16].

One mechanism underlying peritoneal carcinomatosis with rapid and extensive involvement may be the spread of tumor cells through small lymphatic vessels of the peritoneum, known as carcinomatous lymphangitis. Carcinomatous lymphangitis, manifesting as massive embolism of small lymphatic vessels in the lung parenchyma and the visceral and parietal pleura, is also observed in

gastric cancer [17–20]. In a study by T. Shigenobu et al., carcinomatous lymphangitis with embolism of the lymphatic vessels and pleura was found in 31% of patients after radical gastrectomy. The peritoneum, like the pleura, is rich in lymphatic vessels; therefore, a similar mechanism may underlie peritoneal carcinomatosis that is prone to rapid and massive spread, which requires a separate in-depth study [2].

However, anatomical and physiological factors alone cannot explain high propensity of tumor cells to develop peritoneal carcinomatosis. This necessitates the study of the molecular genetic features of tumor cells and the conditions of their survival in ascitic fluid.

MOLECULAR GENETIC CHARACTERISTICS OF TUMOR CELLS ASSOCIATED WITH PERITONEAL CARCINOMATOSIS

The study of the molecular and genetic features of primary tumor cells that form lesions in the peritoneum and are detected in ascitic fluid could form the basis for understanding the mechanisms of peritoneal carcinomatosis and for identifying targets for targeted therapy.

J.J. Zhao et al. performed whole-exome sequencing, whole-transcriptome sequencing, and digital spatial profiling of samples from primary tumor tissue, peritoneal metastases, as well as healthy tissue from primary tumors and the peritoneum of 326 patients. It was found that the primary tumor tissue harbored mutations in ELF3, CDH1, and PIGR, along with an increased number of M2 macrophages. Furthermore, carcinomatosis lesions showed reduced expression of CLDN18.2 and FGFR2b, which are therapeutic targets for targeted therapy. The authors suggest that these conditions facilitate the formation of pre-metastatic niches prior to the clinical manifestation of peritoneal carcinomatosis [21]. The obtained results were confirmed in a mouse model of transcoelomic metastasis [12].

As a result of whole-exome sequencing and whole-transcriptome sequencing, R. Wang et al. demonstrated that tumor cells from carcinomatosis lesions differed from primary tumor cells by more frequent mutations in CDH1 and TAF1, loss of 6q, and gain of chr19. Tumor cells from metastatic foci of rapidly progressing peritoneal carcinomatosis showed an increased number of mutations in TP53, CDH1, TAF1, and KMT2C, microenvironment reprogramming, MYC activation, and impaired immune response [22].

Gastric cancer is characterized by intratumoral heterogeneity [23, 24]. X. Han et al. investigated the significance of intratumoral heterogeneity in the development of peritoneal carcinomatosis in patients with diffuse gastric cancer without microsatellite instability. The results of single-cell transcriptomic profiling of cells from peritoneal carcinomatosis lesions were compared with the Human Cell Landscape (HCL) database. This study identified 14 unique cellular clusters with differentially expressed genes and compiled a list of 12 genes associated with carcinomatosis and survival in gastric cancer patients. A common alteration in tumor cells was a gain of 17q copy number, associated with worse survival in gastric cancer patients with peritoneal carcinomatosis. The list of genes activated on 17q included genes involved in key signaling pathways (PI3K/AKT/mTOR, mTORC1, MYC, Wnt, NF-κB) or being potential therapeutic targets (HN1, GRB2, PSMB3) [25].

Improved survival rates were associated with immune mechanisms involving defensins, IL-7 signaling, the complement cascade, IL6/JAK/STAT3 signaling, and interferon alpha/gamma signaling [26].

Y. Fang et al. identified autocrine expression of laminin gamma-1 (LAMC1) in primary tumor cells and carcinomatosis lesions in gastric cancer. To investigate the role of autocrine LAMC1 expression in the initiation and progression of peritoneal carcinomatosis, the authors conducted a comprehensive study utilizing single-cell sequencing, co-culture modeling, RNA immunoprecipitation (RIP), and chromatin immunoprecipitation (ChIP). This approach revealed the palmitic acid/p-STAT3/miR-193a-3p/LAMC1 signaling pathway, which paracrinally regulated preadipocyte differentiation, pre-metastatic niche formation, and tumor cell invasion and proliferation within the peritoneum, leading to the development of carcinomatosis lesions. Furthermore, the authors established a correlation between high serum levels of LAMC1 in gastric cancer patients and a high risk of peritoneal carcinomatosis. According to ROC analysis data, the area under the curve (AUC) was 0.785 [27].

X.Z. Huang et al. discovered clusters of tumor cells with high plasticity in the ascitic fluid of patients with peritoneal carcinomatosis, exhibiting

propensity to transition into a highly proliferative phenotype. The authors attribute this transformation to a plasticity program driven by autophagy and paligenosis. Paligenosis is understood as the process where mature, quiescent cells revert to a stem cell-like progenitor state in response to injury. This high tumor cell plasticity was associated with autophagy-related genes — MARCKS and TXNIP [28].

Through spatial analysis, H. Peng et al. demonstrated that MUC1+ tumor cells with a high potential for epithelial – mesenchymal transition were located in proximity to macrophages and fibroblasts. Furthermore, the authors revealed that in cases of immunoresistance, MUC1+ tumor cells located near C1Q+ macrophages exhibited hyperexpression of TGFβ [29].

The necessity for a comprehensive approach to identifying the molecular and genetic features of tumor cells from the primary tumor, metastases, and ascitic fluid is emphasized in the meta-analysis by D. Ng et al. The authors express hope for the possibility of developing new strategies based on the accumulated knowledge about the combined involvement of various molecules and signaling pathways in the initiation and progression of peritoneal carcinomatosis [30].

Despite the discovery of molecular and genetic differences between primary tumor cells and the tumor cells forming carcinomatosis lesions, key molecules with prognostic significance or potential as therapeutic targets have not yet been identified.

THE ROLE OF THE INFLAMMATORY MICROENVIRONMENT IN THE DEVELOPMENT OF PERITONEAL CARCINOMATOSIS

In studying the mechanisms of peritoneal carcinomatosis, a significant emphasis is placed on the investigation of parenchymal – stromal interactions. Research into the tumor microenvironment of carcinomatosis lesions has revealed a number of patterns, leading Y. Li et al. to describe peritoneal carcinomatosis as a unique “ecosystem” with an immunosuppressive effect. This effect is attributed to the formation of a stromal – myeloid niche, composed of tumor-associated SPP1+ macrophages (TAMs), thrombospondin-2 (THBS2), and matrix cancer-associated fibroblasts (MCAFs). These very conditions are thought to explain the resistance of tumor tissue to therapy in patients with peritoneal carcinomatosis. According to the authors, niche formation is initiated by the accumulation of thrombospondin-2 and cancer-associated fibroblasts, which leads to the recruitment of peritoneum-specific tissue macrophages and their transformation into SPP1+ TAMs via complement C3 and its C3a receptor 1 (C3AR1). Ultimately, this results in the formation of a pro-tumor stromal – myeloid niche. Blocking the C3-C3AR1 axis significantly enhances the efficacy of immunotherapy for peritoneal carcinomatosis in *in vivo* models [14].

Recently, considerable attention has been paid to investigating the role of claudin 18 in determining indications for immunotherapy in metastatic gastric cancer [31–34]. There is evidence of an association between PD-L1 expression in the primary tumor and the risk of peritoneal carcinomatosis [35].

A more comprehensive understanding of the patterns governing microenvironment formation and its role in the development of peritoneal carcinomatosis could facilitate the development of methods to regulate cellular composition and the extent of inflammatory infiltration within the tumor microenvironment, aimed at treating peritoneal carcinomatosis.

CHARACTERISTICS OF ASCITIC FLUID IN PERITONEAL CARCINOMATOSIS

Ascitic fluid in peritoneal carcinomatosis contains not only tumor cells but also immune cells and cytokines. There is a view that ascitic fluid provides optimal conditions for the survival of tumor cells, contributing to the rapid and relentless progression of peritoneal carcinomatosis.

Studying the molecular composition of ascitic fluid could be useful for understanding the ligand – receptor mechanisms that activate the proliferative and invasive capabilities of tumor cells, and could also help identify target receptors for targeted therapy. However, most such studies focus on detecting markers indicating the presence of tumor cells, such as carcinoembryonic antigen (CEA), CA 19-9, CA 72-4, CA 125, and cytokeratin 20 (CK20), rather than investigating the conditions of their survival [36, 37].

The detection of tumor cells in ascitic fluid is often observed in advanced cases of peritoneal carcinomatosis from gastric cancer, when all possible

treatment options are no longer effective. Therefore, the search for markers that can predict the development of peritoneal carcinomatosis is highly relevant.

Z. Allan et al. proposed an effective marker detectable in ascitic fluid, associated with reduced 3-year progression-free survival and overall survival in gastric cancer patients: the detection of tumor-derived DNA, termed peritoneal tumor DNA (ptDNA) [38]. While this kind of approach holds high value for diagnosing early stages of peritoneal carcinomatosis development, it does not open prospects for understanding the molecular and genetic mechanisms of this process, nor does it allow for predicting the risk of developing peritoneal carcinomatosis or suggesting potential targets for targeted intervention.

X.Z. Huang et al., in a study of the single-cell transcriptome of ascitic fluid from 35 patients with peritoneal carcinomatosis from gastric cancer, discovered an increased number of monocyte-like dendritic cells (DCs) with pro-angiogenic activity and reduced antigen-presenting capacity [28]. H. Peng et al. found that macrophages present in the ascitic fluid of gastric cancer patients had significantly greater pro-angiogenic activity compared to macrophages from the primary tumor stroma and carcinomatosis lesions [29].

Significant importance is also placed on cytokines detected in the ascitic fluid of gastric cancer patients. O. Kersy et al. found that cytokines TNFα, IL-6, and IL-1β were present in the ascitic fluid of gastric cancer patients with peritoneal carcinomatosis. TNFα induce increased expression of adhesion molecules ICAM-1 and VCAM-1 on mesothelial cells, while interleukins 6 and 8 potentiate tumor cell motility and their chemoresistance [39].

Furthermore, cytokines CXCL12/CXCR4 and CCL22/CCR4 are detected in ascitic fluid; these are involved in migration, chemotaxis, adhesion, and metastasis. The interaction between the chemokine receptor CXCR4 on tumor cells and its ligand CXCL12, contained in the ascitic fluid, promotes tumor cell migration and carcinomatosis [30, 40, 41].

Experimental evidence confirms that soluble growth factors, such as VEGF and TGFβ, secreted by tumor cells, participate in preparing the peritoneum for metastasis by activating the vascular endothelium, leading to its remodeling, a process termed pre-metastatic angiogenesis [42, 43].

Analysis of the protein spectrum of ascitic fluid aimed at identifying ligand molecules associated with the acquisition of invasive and proliferative capabilities by tumor cells, as well as with creating conditions for the growth of metastatic foci, opens up possibilities for identifying prognostic factors and potential targets for targeted therapy.

NEW THERAPEUTIC STRATEGIES FOR PERITONEAL CARCINOMATOSIS

To date, there are no effective treatments for peritoneal carcinomatosis. Tumors accompanied by peritoneal carcinomatosis are often resistant to systemic chemotherapy. A significant reason for this resistance to systemic chemotherapy is considered to be the plasma – peritoneal barrier [44]. Cytoreductive surgery and intraperitoneal chemotherapy are not feasible for all patients and are not always successful [5, 45, 46].

Consequently, there is growing interest in intraperitoneal therapy for treating peritoneal carcinomatosis, which is performed in three modalities: hyperthermic intraperitoneal chemotherapy (HIPEC), neoadjuvant hyperthermic intraperitoneal chemotherapy, and pressurized intraperitoneal aerosol chemotherapy (PIPAC) [47]. When combining surgical intervention with prophylactic HIPEC, the three-year mortality rate was 32%, compared to 55% in the control group [48]. F. Tajik et al. believe that hyperthermic intraperitoneal chemotherapy combined with systemic therapy provides survival benefits for patients [49]. Personalized systemic and intraperitoneal chemotherapy is used in patients with gastric cancer and peritoneal carcinomatosis, based on determining the expression levels of eight genes in the primary tumor, lymph nodes, and peritoneal metastases [50].

Given the significant influence of the tumor microenvironment on the development and progression of peritoneal carcinomatosis, considerable attention is paid to optimizing immunotherapy. Whole-exome sequencing and whole-transcriptome sequencing have identified two main molecular subtypes of peritoneal carcinomatosis: a chemotherapy-resistant "mesenchyme-like" subtype and a chemotherapy-sensitive "epithelium-like" subtype. R. Wang et al. found that the "mesenchyme-like" subgroup exhibited high expression of potential targets for immunotherapy, such as TIM-3, galectin-9, VISTA,

and TGFβ [22]. Recently, significant attention has been given to investigating the role of claudin 18 in determining indications for immunotherapy in metastatic gastric cancer [31–34].

Intraperitoneal immunotherapy is also aimed at improving treatment efficacy. In 2009, catumaxomab, a trifunctional bispecific (anti-EpCAM × anti-CD3) antibody, was approved for clinical use.

Chemoresistance of carcinomatosis lesions is associated with features of the tumor microenvironment in metastases. H. Peng et al. discovered that in cases of tumor insensitivity to chemotherapy, there is a combination of a higher level of infiltration by C1Q+ macrophages with a low level of infiltration by GZMA+ T lymphocytes in the microenvironment of carcinomatosis lesions [29].

To enhance the efficacy of intraperitoneal therapy, a method using engineered CAR-T cells (M28z1XXPD1DNR) is being developed in mouse models of peritoneal carcinomatosis, achieving longer survival compared to systemic administration [51].

CONCLUSION

Peritoneal carcinomatosis in gastric cancer represents one of the most unfavorable variants of the disease course. Despite efforts to study the molecular and genetic characteristics of tumor cells underlying peritoneal carcinomatosis, the composition of ascitic fluid, features of immune and inflammatory responses, and the development of new combined regimens of local and systemic therapy, effective methods for predicting and treating peritoneal carcinomatosis are still lacking. This is largely due to an insufficient understanding of the mechanisms behind carcinomatosis generalization within the abdominal cavity.

Among the hypotheses proposing mechanisms for the development of peritoneal carcinomatosis, none fully explain how tumor cells lose connection with neighboring cells and the matrix, becoming capable of autonomous survival in ascitic fluid. Matrix-independent survival was studied by D.K. Lee et al. and termed adherent-to-suspension transition. Genes conferring these properties were identified in a model system. However, our evaluation of the expression of these genes in circulating tumor cells from breast cancer, performed using single-cell sequencing, revealed a low percentage of circulating tumor cells expressing these genes (unpublished data). This may indicate that intravasation and the emergence of matrix-independent circulating tumor cells can occur without the activation of these genes [52].

In our view, it is the matrix independence of tumor cells that is the key factor determining the very likelihood of developing peritoneal carcinomatosis. Elucidating the molecular basis of matrix independence would not only allow for predicting the risk of peritoneal carcinomatosis in gastric cancer but also identify targets for therapy. Corresponding markers could potentially be assessed in biopsy material from the primary tumor. Furthermore, the identified molecules could serve as targets for targeted intervention. The results of research aimed at identifying key molecules associated with the acquisition of matrix independence and the adherent-to-suspension transition could pave the way for developing novel targeted therapies for peritoneal carcinomatosis in gastric cancer.

REFERENCES

1. Cancer Care for the Population of Russia in 2024; ed. by A.D.Kaprin, V.V.Starinsky, A.O.Shakhzadova. Moscow.: P.A.Hertsen MNIOI M; 2025. (In Russ.).
2. Shigenobu T., Ohtsuka T., Hanawa R., Sakamaki H., Yoshizu A., Tajima A. Prognostic impact of visceral pleural invasion in resected solitary lung metastases from gastric cancer. *Ann. Thorac. Cardiovasc. Surg*. 2023;20;29(6):279−286. DOI: 10.5761/atcs.oa.23-00032.
3. Bray F., Laversanne M., Sung H., Ferlay J., Siegel R.L., Soerjomataram I. et al. Global cancer statistics 2022: GLOBOCAN estimates of incidence and mortality worldwide for 36 cancers in 185 countries. *CA Cancer J. Clin.* 2024;74:229–263. DOI: 10.3322/caac.21834.
4. Siegel R.L., Kratzer T.B., Giaquinto A.N., Sung H., Jemal A. Cancer statistics, 2025. *CA Cancer J. Clin*. 2025;75:10–45. DOI: 10.3322/caac.21871.
5. Chia D.K.A., Gwee Y.X., Sundar R. Resistance to systemic immune checkpoint inhibition in the peritoneal niche. *Journal for Immunotherapy of Cancer*. 2022;10(6):e004749. DOI: 10.1136/jitc-2022-004749.
6. Guan G., Li Z., Wang Q., Ying X., Shan F., Li Z. Risk factors associated with peritoneal carcinomatosis of gastric cancer in staging laparoscopy: A systematic review and meta-analysis. *Front. Oncol.* 2022;12:955181. DOI: 10.3389/fonc.2022.955181.
7. Szor D.J., Pereira M.A., Ramos M.F.K.P., Nigro B.C., Dias A.R., Rebeiro U. Jr. et al. Peritoneal recurrence in gastric cancer after curative gastrectomy: Risk factors and predictive score model. *Journal of Gastrointestinal Surgery*. 2025;29(1):101850. DOI: 10.1016/j.gassur.2024.10.005.
8. Rijken A., Lurvink R.J., Luyer M.D.P., Nieuwenhuijzen G.A.P., van Erning F.N., van Sandick J.W. et al. The burden of peritoneal metastases from gastric cancer: a systematic review on the

incidence, risk factors and survival. *Journal of Clinical Medicine*. 2021;10(21):4882. DOI: 10.3390/jcm10214882.
9. Díaz Del Arco C., Ortega Medina L., Estrada Muñoz L., García Gómez de Las Heras S., Fernández Aceñero M.J. Is there still a place for conventional histopathology in the age of molecular medicine? Laurén classification, inflammatory infiltration and other current topics in gastric cancer diagnosis and prognosis. *Histol. Histopathol.* 2021;36(6):587–613. DOI: 10.14670/HH-18-309.
10. Guan G., Li Z., Wang Q., Ying X., Shan F., Li Z. Risk factors associated with peritoneal carcinomatosis of gastric cancer in staging laparoscopy: A systematic review and meta-analysis. *Front. Oncol*. 2022;12:955181. DOI: 10.3389/fonc.2022.955181.
11. Li C., Oh S.J., Kim S., Hyung W.J., Yan M., Zhu Z.G. Macroscopic Borrmann type as a simple prognostic indicator in patients with advanced gastric cancer. *Oncology.* 2009;77(3):197–204. DOI: 10.1159/000236018.
12. Nakayama I. Therapeutic strategy for scirrhous type gastric cancer. *Jpn. J. Clin. Oncol*. 2025;55(8):860–870. DOI: 10.1093/jjco/hyaf081.
13. Van Baal J.O., Van de Vijver K.K., Nieuwland R., van Noorden .CJ., van Driel W.J., Sturk A. et al. The histophysiology and pathophysiology of the peritoneum. *Tissue Cell*. 2017;49(1):95–105. DOI: 10.1016/j.tice.2016.11.004.
14. Li Y., Zheng Y., Huang J., Nie R.C., Wu Q.N., Zuo Z. et al. CAF-macrophage crosstalk in tumour microenvironments governs the response to immune checkpoint blockade in gastric cancer peritoneal metastases. *Gut.* 2025. 6;74(3):350–363. DOI: 10.1136/gutjnl-2024-333617.
15. Gaballah A.H., Algazzar M., Kazi I.A., Badawy M., Guys N.P., Mohamed E.A.S. et al. The peritoneum: anatomy, pathologic findings, and patterns of disease spread. *Radiographics.* 2024;44(8):e230216. DOI: 10.1148/rg.230216.
16. Van der Speeten K., Stuart O.A., Sugarbaker P.H. Using pharmacologic data to plan clinical treatments for patients with peritoneal surface malignancy. *Curr. Drug. Discov. Technol*. 2009;6(1):72–81. DOI: 10.2174/157016309787581084.
17. Souza B.D.S., Bonamigo R.R., Viapiana G.L., Cartell A. Signet ring cells in carcinomatous lymphangitis due to gastric adenocarcinoma. *An. Bras. Dermatol.* 2020;95(4):490–492. DOI: 10.1016/j.abd.2019.12.004.
18. Otsuka N., Shirayama K. A case of gastric cancer with pulmonary carcinomatous lymphangitis and disseminated carcinomatosis of the bone marrow responding to s-1 plus cisplatin chemotherapy. *Gan To Kagaku Ryoho*. 2023;50(12):1319–1321.
19. Systemic Lymphangitic Carcinomatosis from Unknown Primary Cancer Mimicking Lung Disease in a New Coronavirus Infection (COVID-19): a Case Report. *Siberian Journal of Oncology*. 2023;22(5):180–189. (In Russ.). DOI: 10.21294/1814-4861-2023-22-5-180-189.
20. Zavyalova M.V., Zavyalov A.V., Pudova E.S., Kutsenko I.G., Egunova M.A., Klyaus K.A. et al. Generalized Lymphogenous Metastasis Involving Parenchymal Organs in Gastric Cancer (Case Report). *Siberian Journal of Oncology*. 2025;24(1):189–198. (In Russ.). DOI: 10.21294/1814-4861-2025-24-1-189-198.
21. Zhao J.J., Ong C.J., Srivastava S., Chia D.K.A., Ma H., Huang K. et al. Spatially resolved niche and tumor microenvironmental alterations in gastric cancer peritoneal metastases. *Gastroenterology.* 2024;167(7):1384–1398.e4. DOI: 10.1053/j.gastro.2024.08.007.
22. Wang R., Song S., Harada K., Ghazanfari Amlashi F., Badgwell B., Pizzi M.P. et al. Multiplex profiling of peritoneal metastases from gastric adenocarcinoma identified novel targets and molecular subtypes that predict treatment response. *Gut.* 2020;69(1):18–31. DOI: 10.1136/gutjnl-2018-318070.
23. Ma J., Shen H., Kapesa L., Zeng S. Lauren classification and individualized chemotherapy in gastric cancer. *Oncol. Lett.* 2016;11:2959–2964.
24. Thrift A.P., Wenker T.N., El-Serag H.B. Global burden of gastric cancer: epidemiological trends, risk factors, screening and prevention. *Nat. Rev. Clin. Oncol.* 2023;20:338–349. DOI: 10.3892/ol.2016.4337.
25. Han X., Zhou Z., Fei L., Sun H., Wang R., Chen Y. et al. Construction of a human cell landscape at single-cell level. *Nature.* 2020;581(7808):303–309. DOI: 10.1038/s41586-020-2157-4.
26. Wang R., Dang M., Harada K., Han G., Wang F., Pool Pizzi M. et al. Single-cell dissection of intratumoral heterogeneity and lineage diversity in metastatic gastric adenocarcinoma. *Nat. Med.* 2021;27(1):141–151. DOI: 10.1038/s41591-020-1125-8.
27. Fang Y., Dou R., Huang S., Han L., Fu H., Yang C., et al. LAMC1-mediated preadipocytes differentiation promoted peritoneum pre-metastatic niche formation and gastric cancer metastasis. *Int. J. Biol. Sci.* 2022;18(7):3082–3101. DOI: 10.7150/ijbs.70524.
28. Huang X.Z., Pang M.J., Li J.Y., Chen H.Y., Sun J.X., Song Y.X. et al. Single-cell sequencing of ascites fluid illustrates heterogeneity and therapy-induced evolution during gastric cancer peritoneal metastasis. *Nat. Commun.* 2023;14(1):822. DOI: 10.1038/s41467-023-36310-9.
29. Peng H., Jiang L., Yuan J., Wu X., Chen N., Liu D. et al. Single-cell characterization of differentiation trajectories and drug resistance features in gastric cancer with peritoneal metastasis. *Clin. Transl. Med.* 2024;14(10):e70054. DOI: 10.1002/ctm2.70054.
30. Ng D., Cyr D., Khan S., Dossa F., Swallow C., Kazazian K. Molecular mechanisms of metastatic peritoneal dissemination in gastric adenocarcinoma. *Cancer and Metastasis Review.* 2025;44(2):50. DOI: 10.1007/s10555-025-10265-3.
31. Shitara K., Xu R.H., Ajani J.A., Moran D., Guerrero A., Li R. et al. Global prevalence of claudin 18 isoform 2 in tumors of patients with locally advanced unresectable or metastatic gastric or gastroesophageal junction adenocarcinoma. *Gastric. Cancer*. 2024;27:1058–1068. DOI: 10.1007/s10120-024-01518-1.
32. Cao W., Xing H., Li Y., Tian W., Song Y., Jiang Z. et al. Claudin18.2 is a novel molecular biomarker for tumor-targeted immunotherapy. *Biomark. Res*. 2022;10:38. DOI: 10.1186/s40364-022-00385-1.
33. Inamoto R., Takahashi N., Yamada Y. Claudin18.2 in advanced gastric cancer. *Cancers*. 2023;15:5742. DOI: 10.3390/cancers15245742.

34. Shah M.A., Shitara K., Ajani J.A., Bang Y.J., Enzinger P., Ilsonet D., et al. Zolbetuximab plus CAPOX in CLDN18.2-positive gastric or gastroesophageal junction adenocarcinoma: the randomized, phase 3 GLOW trial. *Nat. Med.* 2023;29:2133–2141. DOI: 10.1038/s41591-023-02465-7.
35. Chen X.J., Wei C.Z., Lin J., Zhang R.P., Chen G.M., Li Y.F. et al. Prognostic significance of PD-L1 expression in gastric cancer patients with peritoneal metastasis. *Biomedicines.* 2023;11:2003. DOI: 10.3390/biomedicines11072003.
36. Miro M., Vives R., Farran L., Secanella L., Varela M., Baixeras N. et al. Utility of molecular analysis of peritoneal fluid in staging laparoscopy of advanced esophagogastric junction and gastric cancer prior to neoadjuvant treatment. *J. Gastrointest. Cancer.* 2023;54(2):651–661. DOI: 10.1007/s12029-022-00846-8.
37. Pinheiro J.L., Duarte L., Santos A.J., Tojal A., Canhoto C., Ferreira M. et al. Predicting peritoneal carcinomatosis in locally advanced gastric cancer: the significance of tumor markers in the peritoneal washing. *J. Gastrointest. Cancer.* 2024;55(1):427–434. DOI: 10.1007/s12029-023-00984-7.
38. Allan Z., Witts S., Wong D.J., Lee M.M., Tie J., Tebbutt N.C. et al. Peritoneal Tumor DNA as a Prognostic Biomarker in Gastric Cancer: A Systematic Review and Meta-Analysis. *JCO Precis. Oncol.* 2024;8:e2300546. DOI: 10.1200/PO.23.00546.
39. Kersy O., Loewenstein S., Lubezky N., Sher O., Simon N.B., Klausner J.M. et al. Omental Tissue-Mediated Tumorigenesis of Gastric Cancer Peritoneal Metastases. *Front. Oncol.* 2019;18;9:1267. DOI: 10.3389/fonc.2019.01267.
40. Daniel S.K., Seo Y.D., Pillarisetty V.G. The CXCL12-CXCR4/CXCR7 axis as a mechanism of immune resistance in gastrointestinal malignancies. *Semin. Cancer Biol.* 2020;65:176–188. DOI: 10.1016/j.semcancer.2019.12.007.
41. Qin Y., Wang F., Ni H., Liu Y., Yin Y., Zhou X. et al. Cancer-associated fibroblasts in gastric cancer affect malignant progression via the CXCL12-CXCR4 axis. *J. Cancer.* 2021;12(10):3011–3023. DOI: 10.7150/jca.49707.
42. Kit O.I., Frantsiyants E.M., Kaplieva I.V., Gevorkyan Yu.A., Soldatkina N.V., Dzhenkova E.A. at al. Level of Neoangiogenesis-related Factors in the Pathological Tissues of Patients with Gastric Cancer. *Experimental and Clinical Gastroenterology.* 2019;172(12):81–86. (In Russ.).
4. 3Ito Y., Sun T., Tawada M., Kinashi H., Yamaguchi M., Katsuno T. et al. Pathophysiological mechanisms of peritoneal fibrosis and peritoneal membrane dysfunction in peritoneal dialysis. *Int. J. Mol. Sci*. 2024;25(16):8607. DOI:10.3390/ijms25168607.
44. Jacquet P., Sugarbaker P.H. Peritoneal-plasma barrier. *Peritoneal Carcinomatosis: Principles of Management*. 1996;82:53–63.
45. Ishmuratova K.R., Gantsev K.Sh.. New Insights in the Pathogenesis and Diagnosis of Peritoneal Carcinomatosis. *Creative Surgery and Oncology.* 2022;12(4):328–336. (In Russ.). DOI: 10.24060/2076-3093-2022-12-4-328-336.
46. Brandl A., van Sandick J.W. Treatment of gastric cancer peritoneal metastases: role of cytoreductive surgery and hyperthermic intraperitoneal chemotherapy. *Br. J. Surg.* 2024;111(7). znae149. DOI: 10.1093/bjs/znae149.
47. Krell M., Ranjbar S., Gitlin S., Alvarez Vega D.R., Wilson R., Thrasher K. et al. Evolution in the surgical management of gastric cancer peritoneal metastases. *Cancers.* 2024;17(1):100. DOI: 10.3390/cancers17010100.
48. Stefano M., Perrina D., Vallicelli C., Ansaloni L., Fugazzola P., Coccolini F. et al. Prophylaxis and treatment of peritoneal carcinomatosis of gastric origin using hyperthermic intraperitoneal chemotherapy: a systematic review and meta-analysis of randomized trials. *J. Gastrointest. Surg.* 2024;28(7):1185–1193. DOI: 10.1016/j.gassur.2024.04.007.
49. Tajik F., Eyob B., Khan A.M., Radhakrishnan V.K., Senthil M. Iterative intraperitoneal chemotherapy in gastric cancer peritoneal carcinomatosis. *Cancers.* 2025;17(2):289. DOI: 10.3390/cancers17020289.
50. Markovich V.A., Tuzikov S.A., Rodionov E.O., Popova N.O., Tsyganov M.M., Miller S.V. et al. Gene expression profile-guided personalized intraperitoneal chemotherapy for gastric cancer peritoneal carcinomatosis. *World J. Oncol.* 2024;15(2):298–308. DOI: 10.14740/wjon1578.
51. Restle D., Amador-Molina A., Misawa K., Banerjee S., Ku G., Adusumilli P.S. Intraperitoneal CAR T-cell therapy for peritoneal carcinomatosis from gastroesophageal cancer: preclinical investigations to a phase I clinical trial (NCT06623396). *J. Immunother. Cancer*. 2025;13(9):e012292. DOI: 10.1136/jitc-2025-012292.
52. Lee D.K., Oh J., Park H.W., Gee H.Y. Anchorage dependence and cancer metastasis. *J. Korean Med. Sci.* 2024;39(19):e156. DOI:10.3346/jkms.2024.39.e156.

Author Contribution

Zavyalova M.V., Miller S.V., Perelmuter V.M. – conception and design. Zavyalov A.V., Neklyudov A.A., Belousova O.A., Pismenny D.S. – literature collection and analysis.

Author Information

Zavyalova Marina V. – Dr. Sci. (Med.), Professor, Leading Researcher, Department of General and Molecular Pathology, Cancer Research Institute, Tomsk NRMC of RAS; Head of Pathology Division, Siberian State Medical University, Tomsk, zavyalovamv@mail.ru, https://orcid.org/0000-0001-9429-9813

Zavyalov Aleksandr V. – Student, General Medicine Department, Siberian State Medical University, Tomsk, zavyalov.av@ssmu.ru, https://orcid.org/0009-0009-0266-6707

Neklyudov Alexey A. – Postgraduate Student, Pathology Division, Siberian State Medical University, Tomsk, neklyudov.aa@ssmu.ru, https://orcid.org/0000-0003-2133-5064

Belousova Olga A. – Postgraduate Student, Pathology Division, Siberian State Medical University, Tomsk, belousova.oab@yandex.ru, https://orcid.org/0000-0001-6082-6136

Pismenny Dmitry S. – Cand. Sci. (Med.), Clinical Laboratory Diagnostics Physician, Department of General and Molecular Pathology, Cancer Research Institute, Tomsk NRMC of RAS; Associate Professor, Pathology Division, Siberian State Medical University, Tomsk, pismenniy.dmitry@yandex.ru, https://orcid.org/0000-0001-8973-8439

Miller Sergey V. – Dr. Sci. (Med.), Head of Thoracic Department, Cancer Research Institute, Tomsk NRMC of RAS, Tomsk, millersv1309@gmail.com, https://orcid.org/0000-0002-5365-9840

Perelmuter Vladimir M. – Dr. Sci. (Med.), Professor, Chief Researcher, Department of General and Molecular Pathology, Cancer Research Institute, Tomsk NRMS of RAS, Tomsk, pvmngs@yandex.ru, https://orcid.org/0000-0002-7633-9620

(✉) **Pismenny Dmitry S.,** pismenniy.dmitry@yandex.ru

Received on October 11, 2025;
approved after peer review on October 23, 2025;
accepted on October 30, 2025

УДК 616.831-005.1-005.4-073.756.8
https://doi.org/10.20538/1682-0363-2026-2-150-160

Multimodal Magnetic Resonance Imaging of the Brain at Different Stages of Rehabilitation after Ischemic Stroke

Kurazhov A.P.[1], Alifirova V.M.[1], Koroleva E.S.[1], Degtyarev I.Yu.[1], Loiko Yu.N.[2], Kucherova K.S.[1], Sukhanova K.S.[1], Zavadovskaya V.D.[1]

[1] *Siberian State Medical University*
2 Moscovsky trakt, 634050 Tomsk, Russian Federation

[2] *Treatment and Diagnostic Center, Dr. Berezin Medical Institute*
105 Michurin St., 634063 Tomsk, Russian Federation

ABSTRACT

Stroke is an important medical and social problem in the world and in the Russian Federation, which is due to high rates of morbidity, mortality, and disability. The basis for the development of innovative approaches to the accelerated rehabilitation of individuals after an ischemic stroke is the study of neuroplasticity using modern neuroimaging methods, such as multimodal magnetic resonance imaging (MRI).

The present literature review describes diagnostic capabilities of different multimodal MRI modalities, such as functional MRI (fMRI), ASL MR perfusion, and diffusion tensor MRI, including their advantages and drawbacks in assessing rehabilitation potential of patients after ischemic stroke. These MRI modalities can be successfully utilized to study the mechanisms of neuroplasticity and identify reliable markers of a response to therapy in context of rehabilitation measures in stroke patients.

It was shown that broad implementation of multimodal MRI in clinical practice is hindered by a lack of profound knowledge about its diagnostic capabilities in certain clinical settings, complexity of its use, and insufficient evidence base.

Keywords: acute cerebrovascular accident, functional magnetic resonance imaging, neuroplasticity, rehabilitation

Conflict of interest. The authors declare the absence of obvious or potential conflicts of interest related to the publication of this article.

Source of financing. The authors state that they received no funding for the study.

For citation: Kurazhov A.P., Alifirova V.M., Koroleva E.S., Degtyarev I.Yu., Loiko Yu.N., Kucherova K.S., Sukhanova K.S., Zavadovskaya V.D. Multimodal Magnetic Resonance Imaging of the Brain at Different Stages of Rehabilitation after Ischemic Stroke. *Bulletin of Siberian Medicine.* 2026;25(2):150–160. https://doi.org/10.20538/1682-0363-2026-2-150-160.

✉ *Kurazhov Alexei P.,* kurazhovap@mail.ru

Мультимодальная магнитно-резонансная томография головного мозга в оценке реабилитационного потенциала у пациентов после перенесенного ишемического инсульта

Куражов А.П.[1], Алифирова В.М.[1], Королёва Е.С.[1], Дегтярев И.Ю.[1], Лойко Ю.Н.[2], Кучерова К.С.[1], Суханова К.С.[1], Завадовская В.Д.[1]

[1] *Сибирский государственный медицинский университет (СибГМУ)*
Россия, 634050, г. Томск, Московский тракт, 2

[2] *Лечебно-диагностический центр (ЛДЦ) Медицинского института им. Березина Сергея (МИБС)*
Россия, 634063, г. Томск, ул. Мичурина, 105

РЕЗЮМЕ

Острые нарушения мозгового кровообращения являются важной медико-социальной проблемой как в мире, так и в Российской Федерации, что обусловлено высокими показателями заболеваемости, смертности и инвалидизации. Основу разработки инновационных подходов ускоренной реабилитации лиц после перенесенного ишемического инсульта составляет исследование нейропластичности с использованием методов современной нейровизуализации, таких как мультимодальная магнитно-резонансная томография (МРТ).

Представлен обзор литературы, в котором рассматриваются диагностические возможности различных компонентов мультипараметрической МРТ, таких как функциональная МРТ, ASL-МРТ и диффузионно-тензорная МРТ, включая их потенциальные преимущества и недостатки применительно к оценке реабилитационного потенциала у пациентов после перенесенного ишемического инсульта. Показано, что данные компоненты мультипараметрической МРТ могут быть успешно использованы для изучения механизмов нейропластичности и определения ответа на терапию в ходе реабилитационных мероприятий у пациентов после ишемического инсульта. Обозначены проблемные аспекты активного внедрения мультипараметрической МРТ в широкую клиническую практику, главными из которых являются отсутствие глубоких знаний о диагностических возможностях того или иного компонента данной технологии в конкретной клинической ситуации, сложность ее использования и недостаточная емкость доказательной научной базы.

Ключевые слова: ишемический инсульт, мультимодальная магнитно-резонансная томография, нейропластичность, реабилитация

Конфликт интересов. Авторы декларируют отсутствие явных и потенциальных конфликтов интересов, связанных с публикацией настоящей статьи.

Источник финансирования. Авторы заявляют об отсутствии источника финансирования при проведении исследования.

Для цитирования: Куражов А.П., Алифирова В.М., Королёва Е.С., Дегтярев И.Ю., Лойко Ю.Н., Кучерова К.С., Суханова К.С., Завадовская В.Д. Мультимодальная магнитно-резонансная томография головного мозга в оценке реабилитационного потенциала у пациентов после перенесенного ишемического инсульта. *Бюллетень сибирской медицины.* 2026;25(2):150–160. https://doi.org/10.20538/1682-0363-2026-2-150-160.

INTRODUCTION

Cerebral vascular diseases represent a significant medical and social problem for modern society. Acute cerebrovascular accidents (ACVA) are the leading cause of death and severe disability among nervous system disorders both globally and in the Russian Federation (RF). They are a leading cause of mortality and severe disability in patients. More than 450,000 new cases of stroke are registered annually in the RF, with the annual stroke mortality rate being 374 cases per 100,000 population. During the acute phase of stroke, which lasts 28 days from its clinical manifestation, the mortality rate reaches 35%, but increases by another 15% over the following year [1–3].

According to various authors, the initial disability rate in individuals who have suffered ACVA reaches 40% [4, 5]. Thus, improving medical care for patients with this disease is one

of the most pressing scientific and practical issues in modern medicine. At the same time, timely rehabilitation and a comprehensive assessment of anatomical and functional changes in the brain tissue of patients who have suffered ACVA can reduce the severity of neurological deficits and improve their social adaptation [6].

According to current concepts, neurological deficits in patients with ACVA are caused by both irreversible focal damage to brain tissue that develops during the infarction and changes in peri-infarction zones in the form of structural and functional conduction pathway impairments. Moreover, the extent of damage to brain conduction pathways is a stronger predictor of patient treatment outcomes and functional recovery compared to the infarct size or the initial functional status. This is due to the fact that in response to damage, structural and functional reorganization processes, primarily affecting the conduction pathways, begin to activate in the human brain [7].

Scientific advances in recent decades have indicated that neuroplasticity mechanisms play a key role in brain tissue restoration processes after ACVA [6, 8]. Neuroplasticity is the ability of various parts of the central nervous system (CNS) to undergo structural and functional reorganization, including qualitative and quantitative neuronal rearrangements, as well as changes in neuronal connections and glial elements, allowing for adaptive response implementation [9, 10].

The cerebral cortex has a high level of neuroplasticity. The restoration of motor, sensory, and cognitive functions in patients after ACVA is largely associated with neural network reorganization, as well as with changes in the strength and number of formed synaptic connections [11]. This reorganization was first demonstrated in 1991 using positron emission tomography (PET). Subsequently, PET and fMRI have repeatedly demonstrated changes in brain hemispheres at all stages of stroke, caused by neuroplasticity [12].

Along with functional plasticity, which implies restoration of certain functional capabilities of the brain tissue, structural neuroplasticity is of particular interest. This is due to the fact that axonal degeneration in areas structurally connected to the lesion triggers the development of new synapses with denervated neurons, which likely determines motor function restoration in patients. Despite progress in neuroplasticity studies, the relationships and interactions between functional reorganization and structural changes occurring in the CNS after stroke remain incompletely understood [13]. However, a thorough understanding of the mechanisms of neuroplasticity in the brain pathways will allow us to predict the outcome of ACVA and the effectiveness of rehabilitation measures in each individual patient. Although the significance of the structural integrity of the brain pathways in motor function recovery after stroke currently remains largely unclear and insufficiently covered in Russian and world literature, in recent years, researchers have increasingly focused their attention on the search for markers of the structural and functional state of the brain pathways that can act as rehabilitation potential indicators in patients after ACVA.

MODERN NEUROIMAGING METHODS FOR THE CONSEQUENCES OF ISCHEMIC STROKE

Modern neuroimaging methods provide a wide range of diagnostic information necessary for assessing the state of brain tissue at various stages of ACVA, including determining its viability, predicting a hemorrhagic transformation risk, and understanding the natural evolution of neuroplasticity, neurodegeneration, diaschisis, vicariance, and disinhibition [5, 8]. Neuroimaging methods have also been used to develop and utilize prognostic models that predict ACVA treatment effectiveness and determine the rehabilitation potential in patients after ACVA.

MRI currently plays a key role in addressing these challenges. The evolution of this method – from MRI angiography of cerebral vessels (including contrast-enhanced angiography) to MR tissue perfusion imaging using endogenous (arterial spin labeling (ASL), blood oxygenation level-dependent (BOLD)) and exogenous (gadolinium preparations) markers, as well as diffusion-weighted imaging (DWI) with apparent diffusion coefficient (ADC), tractography, and

spectroscopy combined with functional testing – has significantly increased its diagnostic potential [14].

Another MRI advantage is the ability to conduct multiple studies of the whole brain, which makes it an ideal modality for studying neuroplasticity at the level of interconnected neural pathways over a large area [15]. Currently, structural and functional changes after stroke are widely studied using functional magnetic resonance imaging (fMRI), diffusion tensor MRI (DT-MRI) [12], and contrast-enhanced MRI. However, the inconsistent use of modern MR technologies does not allow for a comprehensive study of structural and functional changes in the brain in patients after ACVA. Therefore, recently, most studies have used an integrated approach involving various MR modalities.

In this regard, today, diagnostic multimodal MRI is gaining primary importance in assessing brain condition in patients after stroke [16–19], since this approach makes it possible to obtain a huge amount of information about stroke severity and stage [16]. According to K. Atchaneeyasakul, D.S., Liebeskind et al. [20], multimodal MRI remains the most optimal method for assessing the morphofunctional state of the brain in patients after ACVA due to its more accurate identification of brain damage after stroke and excellent spatial resolution.

Other studies have shown that multimodal MRI results may influence the outcomes of thrombolytic and endovascular therapy in patients with a wake-up stroke subtype. Moreover, it is possible that multimodal MRI will become the best neuroimaging method, providing the necessary information for deciding on treatment strategies for ACVA.

Based on multimodal MRI results, in 2020, H. Lee and K. Jung [21] developed and presented a fully automated algorithm for segmenting the main zones of ischemic stroke. They demonstrated that this algorithm can be applied to decide on the use of reperfusion therapy, providing fast and reliable processing of clinical information. All this indicates that multimodal MRI can be one of the best radiological methods for determining the rehabilitation potential in patients who experienced ACVA and can greatly influence the treatment strategy [7, 16].

FUNCTIONAL MRI CAPABILITIES

Functional MRI (fMRI) is a non-invasive neuroimaging technique used to detect changes in the bioactivity of various brain structures. This method is based on recording differences in the magnetic properties of oxyhemoglobin and deoxyhemoglobin, whose ratios in the brain vary depending on local changes in blood flow caused by neuronal activity. Thus, the construction of fMRI images is influenced by the dependence of the MR signal on the degree of oxygen saturation in the brain tissue (blood-oxygenation-level-dependent (BOLD) imaging).

When neurons in a brain region become active, blood flow in that region increases to meet the increased oxygen demand of functioning neurons. This allows for the recording and quantification of neuronal activity in response to a stimulus, using BOLD signal intensity as a neuronal activity indicator.

Since fMRI does not involve radiation exposure, does not require the administration of contrast agents, is non-invasive, and is currently recognized as one of the optimal radiation methods for assessing the structural and functional state of brain pathways, it is an ideal radiation modality for clinical ACVA studies and its consequences [11]. Measurements carried out in the context of fMRI can provide qualitative and quantitative information on the state of neurons remaining after stroke and undergoing recovery, including dynamic monitoring of the activation degree of various areas in the cerebral cortex and changes in their volume [15].

The same opinion is shared by X. Xiao, Q. Lin, J. Liu, and Q. Wang [22, 23], who believe that fMRI is a promising method for the quantitative assessment of brain recovery predictors after ACVA. This is confirmed by C.W. Wu and S.N. Lin [24], who, studying patients after ACVA using fMRI, revealed that their primary state of conduction pathways largely determined the success of rehabilitation and could subsequently serve as a neurorehabilitation marker of the treatment effectiveness.

Many other modern studies have also demonstrated high potential of fMRI in predicting ACVA outcomes when used in conjunction with other diagnostic approaches. Thus, according to the results of J. Du and F. Yang [25], a prognostic model incorporating fMRI results at early stages of ACVA made it possible to predict the degree of motor activity recovery after ischemic stroke in the long term. Moreover, the best outcome of motor function recovery statistically significantly correlated with lesser initial motor impairments, a lesser extent of damage to the corticospinal tract (CST), the initial presence of motor evoked potentials, as well as with stronger initial motor cortex activation.

Incorporating fMRI data into multivariate analysis improved the accuracy of predicting ischemic stroke outcomes compared to clinical and neurophysiological assessments alone [25]. This is explained by the fact that new pathways are initially activated to compensate for the function of the damaged brain region during recovery, which, according to fMRI data, is manifested by an increase in the MR signal, the intensity of which depends on the blood oxygen saturation (BOLD) degree. Moreover, patients after ACVA typically exhibit a greater increase in the MR signal in the region of interest during task performance than in the control group, represented by healthy volunteers. Subsequently, the MR signal intensity in the region of interest decreases to baseline levels, as the pathways become more efficient, similar to the learning process typically observed during normal brain development [11].

New scientific data obtained using fMRI on the motor function recovery dynamics in patients after ACVA are of considerable interest for modern clinical neurology. These studies revealed that within 24 hours of ACVA, a reorganized motor network emerged in the CNS, enabling the bypass of damaged pathways through the alternative pathway activation. It was also shown that damaged hemisphere reorganization and neuronal activity restoration around the affected area were the next important rehabilitation stage, during which the activity of these new, but less effective, connections was maintained [11]. Another study, based on the fMRI results of patients after stroke, demonstrated dynamic changes in neuronal activity in brain areas adjacent to infarcted areas. Therefore, rehabilitation measures should be aimed at intensifying activation of the areas where functional reorganization processes are taking place [7].

A number of fMRI studies describe motor function recovery progression at a single time point after stroke, typically 3–6 months [11]. However, these results indicate that changes in neural activity and regional cerebral blood flow after stroke occur in both hemispheres. Therefore, monitoring recovery requires long-term dynamic studies, typically beginning within the first few weeks after clinical manifestations of ACVA and continuing from several months to one year thereafter. Therefore, it is advisable to conduct fMRI in such patients at least at the acute stage, then after 3 weeks, and after 6 months.

However, it should be noted that systematic brain fMRI studies that cover time intervals in both early and various delayed periods after stroke in the same patients are lacking. This highlights the need for research that takes the above into account to better understand neural tissue restoration processes and to efficiently systematize fMRI data.

Another application of fMRI is the study of cerebrovascular reactivity (CVR) in patients with ACVA. CVR is the ability of cerebral blood vessels to dilate or constrict in response to external or internal stimuli. Assessing CVR is crucial for identifying latent cerebral circulatory failure and brain maladaptation depth under extreme conditions [26]. CVR along with traditional parameters, such as cerebral blood flow velocity and volume (CBF and CBV, respectively), is one of the most valuable cerebral perfusion indicators and provides important information about vascular reserves [24]. Measuring CVR helps assess neurovascular uncoupling, which is manifested by false-negative or false-positive cerebral cortex activation in response to fMRI tasks. It has been established that assessing CVR can help optimize treatment strategies for patients with ACVA [27].

Thus, the implementation of fMRI into clinical practice can significantly improve the prediction of the rehabilitation potential in patients after ACVA and significantly influence their rehabilitation treatment algorithm.

ASL PERFUSION MRI CAPABILITIES FOR ASSESSING CEREBRAL BLOOD FLOW

To understand the processes occurring in the nervous tissue after stroke and to predict rehabilitation measure outcomes, it is essential to assess the state of cerebral collateral circulation. Studying cerebral vascular collaterals and determining their functioning are crucial for assessing reperfusion severity, bleeding risk, and recovery degree of lost brain function.

Currently, various medical imaging modalities are used to determine the state of collateral circulation, including ultrasound technologies (primarily carotid artery duplex scanning and transcranial Doppler sonography), as well as CT and MRI. However, traditional static MR technologies for assessing blood flow have significant limitations, while MR perfusion with arterial spin labeling (ASL), or ASL MRI, enables the study of cerebral hemodynamics at a qualitatively higher level [28, 29].

ASL MRI is based on the fact that under the action of radiofrequency pulses applied proximal to the area of interest, an inversion of hydrogen atom spins contained in arterial blood occurs, which ultimately allows for obtaining information about the cerebral perfusion state without any contrast agents administered to the patient's body [29]. To date, there are many scientific papers demonstrating the important applied aspects of ASL MRI at various stages of ACVA. Thus, a study carried out by G. Crisi et al. [29] revealed that ASL MRI can become an integral part of the MR examination protocol for patients with stroke who have not received treatment for 24–36 hours based on the possibility of recording the positive effects of reperfusion after recanalization. In another recent work by S.S. Lu and Y.Z. Cao [28], it was found that changes in cerebral perfusion parameters detected using ASL MRI correlated with the recanalization results. Therefore, the authors proposed using quantitative ASL MRI parameters as an independent favorable prognostic marker of neurological outcomes in patients with ACVA 90 days after thrombectomy.

J. Wang et al. [22] investigated ASL MRI capabilities in assessing cerebral perfusion in patients with crossed cerebellar diaschisis and concluded that CBF calculated using ASL MRI can be a valuable predictor of the development of this condition in patients with supratentorial stroke, and the risk of developing crossed cerebellar diaschisis was significantly associated with an increase in the volume of ischemic cerebral damage and a higher baseline NIHSS score (National Institutes of Health Stroke Scale) [29].

In the meantime, S. Verclytte and O. Fisch concluded that ASL MRI should not be used as a routine technology due to the long duration of the examination, despite the fact that it provides valuable information for differential diagnosis in specific clinical situations, assessing the treatment effectiveness at early stages of ACVA and non-invasively assessing the penumbra size [30].

One of the serious problems arising in the treatment of patients with ACVA is its hemorrhagic transformation, which develops after reperfusion therapy. Thus, early detection of hyperperfusion zones in the brain after reperfusion therapy may reduce the risk of this condition through more carefully selected treatment [31]. There are studies in the modern literature indicating that hyperperfusion detected by ASL MRI in patients with ACVA after intravenous thrombolysis or endovascular intervention can be a reliable predictor of ACVA hemorrhagic transformation.

In 2019, J. Lyu and N. Ma [32] demonstrated unique capabilities of ASL MRI in the non-invasive assessment of cerebral hemodynamics, including in patients after ischemic stroke, using a new technology of post-labeling delay (PLD). At the same time, the authors of this study emphasize that the use of PLD requires an individualized approach to each patient, since the delay should correspond as closely as possible to the time required for the labeled protons to reach the region of interest and, ultimately, generate an MR signal. If the PLD is too short, the entire labeled bolus may not have time to fully distribute throughout the brain tissue under

study, especially in areas important for diagnosis. This can lead to significant local loss of the MR signal, which may be erroneously interpreted as a consequence of hypoperfusion [31].

Falsely identified hypoperfusion areas can also be caused by patient-specific factors (e.g., stenosis of major arterial trunks originating from the aorta), which increases the delivery time of labeled protons to the region of interest. In this case, distinguishing between false and true hypoperfusion can be quite difficult. Artifacts associated with structural features of the circle of Willis can also be observed when using PLD technology. Therefore, PLD is an important parameter that must be adjusted according to the patient's circulatory status to avoid diagnostic errors [32].

Summarizing the significance of ASL MRI, it should be noted that this technology is currently not a generally accepted method for predicting neurological status, susceptibility to ACVA hemorrhagic transformation and its outcomes. Moreover, large-scale studies of the ASL MRI potential for investigating diaschisis in the brain have not been carried out yet [33].

Furthermore, the global literature has not paid sufficient attention to analyzing the CBF value calculated using ASL MRI data as a predictor of cerebellar diaschisis development. Additionally, large patient cohorts have not demonstrated that hyperperfusion detected by ASL MRI can predict ACVA hemorrhagic transformation, and the issue of the procedure duration remains unresolved. Therefore, further studies are needed, examining larger cohorts of patients at early and late time points after stroke, to integrate ASL MRI into the diagnostic algorithm for this patient population.

DIFFUSION TENSOR MRI POTENTIAL IN ASSESSING CEREBRAL BLOOD FLOW

Another non-invasive MRI technique used in patients with a history of stroke is diffusion tensor MRI (DT-MRI) [34]. DT-MRI is a method that allows for an *in vivo* measurement of the water molecule movement direction, providing information on the degree of its anisotropy in various tissues. Based on the diffusion anisotropy occurring in CNS tissues, DT-MRI allows for the study of the conduction pathway structure and the reconstruction of three-dimensional images of commissural, association, and projection tracts [35].

DT-MRI results are vector maps that use color to encode the water molecule diffusion direction. Most commonly, red denotes «right – left» movement of water molecules, green denotes «forward – backward», and blue denotes «up – down» [36]. It is believed that DT-MRI (also known as tractography) can provide valuable information about the state of both the main pathways damaged by ischemic stroke and the pathways that compensate for lost brain functions.

R.M Umarova et al. (2017) [33], using tractography, found that large lesions of interconnected cortex areas cause large-scale structural reorganization of neural connections and determine various symptoms and neurological deficits. M.M. Visser et al. (2019) [35], studying patients with ACVA during the first week after the cerebrovascular accident, as well as after one and three months, came to the conclusion that changes in the white brain matter after ischemic stroke may be a localized rather than a global phenomenon.

Therefore, the analysis of white matter tracts using DT-MRI data is a key aspect in studying brain tissue processes after stroke [37, 38]. When studying motor function recovery after ischemic stroke, the primary pathway studied is the CST. In recent years, a growing body of evidence suggests that combining clinical assessments with information on the integrity of the CST obtained using DT-MRI can improve the accuracy of predicting motor function recovery. Moreover, according to many scientists, the degree of CST damage on DT-MRI is the main prognostic factor determining motor function recovery after ischemic stroke [39, 40].

One of the most important quantitative parameters reflecting structural brain integrity and its structural and functional organization is fractional anisotropy coefficient (FAC). T. Koyama et al. [41] showed that FAC in the CST can be a potential marker for limb motor function recovery. The authors determined that the CFA measured in the superior longitudinal fasciculus

(SLF) can be used to predict the cognitive state in patients after ischemic stroke. Similar results were obtained in 2024 by L.M. Moura et al. [42]. In 2019, J. Puig et al. proposed basic strategies for quantifying CST damage in ischemic stroke, which included measuring FAC distal to the stroke site, measuring the number of fibers passing through the tract, and comparing changes in the CST state in the stroke site in stroke patients with that in healthy volunteers of the same age and gender [43].

Currently, in addition to CST, DT-MRI can also be used to study other CNS tracts. However, there are relatively few studies in this field, although their results are quite interesting. Thus, Z. Keser (2020) and E.L. Meier (2024) [44, 45] analyzed the arcuate fasciculus (AF), inferior longitudinal fasciculus (ILF), inferior fronto-occipital fasciculus (IFOCF), and uncinate fasciculus (UF) in patients with aphasia after left-sided ischemic stroke. The authors concluded that DT-MRI can provide valuable clinical information for predicting speech function recovery, and the degree of ILF integrity, in particular, is a prognostic marker for the extent of speech comprehension recovery.

During the same period, M. Blom-Smink et al. (2020) [39], using DT-MRI to study the state of the ILF, IFOCF, UF, SLF, and the middle longitudinal fasciculus (MLF) in the same category of patients, came to a similar conclusion about the influence of the ILF integrity on the processes of speech function restoration in aphasia. Z. Gong et al. (2020) [45] also studied the predicting capabilities of DT-MRI for motor function restoration but in patients with poor hand function after hypertensive intracerebral hemorrhage and came to the conclusion that this radiation technology can be used to visualize damage to the CST fibers of the hand. In addition, the same authors found that rehabilitation measures carried out to restore hand function after hypertensive intracerebral hemorrhage were most effective in patients with only partially damaged CST.

However, DT-MRI technology, used to diagnose the consequences of stroke, currently has a number of challenges. The most important of them is its dependence on the volume and location of the lesion, which affect the recording, post-processing, and presentation of visual data. Secondary expansion of cerebrospinal fluid-filled spaces can also distort the obtained information about white matter tracts.

Therefore, when interpreting DT-MRI data, it is necessary to consider distortions in typical brain anatomy after ischemic stroke, and standardizing this assessment is quite difficult. Consequently, despite the encouraging prospects for using DT-MRI in clinical practice, this technology has not yet found widespread application for assessing the rehabilitation potential of patients after stroke. On the other hand, despite the relatively widespread evaluation of CST, other tracts, such as the SLF, AF, ILF, IFOCF, UF, and MLF, have not been adequately studied in patients after stroke. Meanwhile, based on the results of the few studies presented in the literature, their integrity may also be a potential predictor of the degree of brain function recovery after stroke.

CONCLUSION

Therefore, when discussing the treatment of patients after ischemic stroke, it becomes clear that multimodal MRI is required to assess brain neuroplasticity and, consequently, the rehabilitation potential of such patients. Although multimodal MRI can identify predictors of brain function recovery after stroke, the number of large-scale, long-term studies of structural and functional changes in the brain after ischemic stroke is currently insufficient to understand its role in routine clinical practice. Furthermore, the clinical significance of each diagnostic component of multimodal MRI in a specific clinical situation has not been determined.

So, there is currently no generally accepted diagnostic algorithm for examining patients after ischemic stroke using multimodal MRI [16]. Therefore, the development of an accessible algorithm for assessing the rehabilitation potential of patients after ischemic stroke, including multimodal MRI, should be the goal of further large-scale studies aimed at a more in-depth study of the information value of individual MRI modalities, their combinations with one another and with clinical assessments, in parallel with overcoming the problems of implementing this radiation technology into routine clinical practice.

REFERENCES

1. Osborne A.G., Zaltsman K.L., Assure M.D. Radiation diagnostics. *Brain.* 2018;248.
2. Campbell B.C.V., De Silva D.A., Macleod M.R. Ischaemic stroke. *Nat. Rev. Dis. Primers* 5. 2019;70. DOI: 10.1038/s41572-019-0118-8.
3. Zhao Y., Zhang X., Chen X., Wei Y. Neuronal injuries in cerebral infarction and ischemic stroke: From mechanisms to treatment (Review). *Int. J. Mol. Med*. 2022;49(2):15. DOI: 10.3892/ijmm.2021.5070.
4. Feigin V.L., Brainin M., Norrving B., Martins S., Sacco R.L., Hacke W. et al. World Stroke Organization (WSO): Global Stroke Fact Sheet 2022. *Int. J. Stroke*. 2022;17(1):18–29. DOI: 10.1177/17474930211065917.
5. Saini V., Guada L., Yavagal D.R. Global epidemiology of stroke and access to acute ischemic stroke interventions. *Neurology*. 2021;16(97):S6–S16. DOI: 10.1212/WNL.0000000000012781.
6. Zhang J., Lu C., Wu X., Nie D., Yu H. Neuroplasticity of Acupuncture for Stroke: An Evidence-Based Review of MRI. *Neural. Plast.* 2021;2021:2662585. DOI: 10.1155/2021/2662585.
7. Guggisberg A.G., Koch P.J., Hummel F.C., Buetefisch C.M. Brain networks and their relevance for stroke rehabilitation. *Clin. Neurophysiol*. 2019;130(7):1098–1124. DOI: 10.1016/j.clinph.2019.04.004.
8. Hartwigsen G., Volz L.J. Probing rapid network reorganization of motor and language functions via neuromodulation and neuroimaging. *Neuroimage*. 2021;224:117449. DOI: 10.1016/j.neuroimage.2020.117449.
9. Innocenti G.M. Defining neuroplasticity. *Handb. Clin. Neurol*. 2022;184:3–18. DOI: 10.1016/B978-0-12-819410-2.00001-1. PMID: 35034744.
10. Joy M.T., Carmichael S.T. Encouraging an excitable brain state: mechanisms of brain repair in stroke. *Nat. Rev. Neurosci*. 2021;22(1):38–53. DOI: 10.1038/s41583-020-00396-7.
11. Johnson B.P., Cohen L.G. Applied strategies of neuroplasticity. *Handb. Clin. Neurol*. 2023;196:599–609. DOI: 10.1016/B978-0-323-98817-9.00011-9.
12. Xing Y., Bai Y. A Review of Exercise-Induced Neuroplasticity in Ischemic Stroke: Pathology and Mechanisms. *Mol. Neurobiol*. 2020;57(10):4218–4231. DOI: 10.1007/s12035-020-02021-1.
13. Włodarczyk L., Cichon N., Saluk-Bijak J., Bijak M., Majos A., Miller E. Neuroimaging techniques as potential tools for assessment of angiogenesis and neuroplasticity processes after stroke and their clinical implications for rehabilitation and stroke recovery prognosis. *J. Clin. Med*. 2022;11(9):2473. DOI: 10.3390/jcm11092473.
14. Bhasin A., Srivastava P., Kumaran S.S. Correlation of DTI-derived measures to therapy-mediated recovery after stroke: preliminary findings. *Neurol. India*. 2021;69(5):1210–1216. DOI: 10.4103/0028-3886.329584.
15. Yang H.E., Kyeong S., Kang H., Kim D.H. Multimodal magnetic resonance imaging correlates of motor outcome after stroke using machine learning. *Neurosci. Lett.* 2021;741:135451. DOI: 10.1016/j.neulet.2020.135451.
16. Ball E.L., Shah M., Ross E., Sutherland R., Squires C., Mead G.E. et al. Predictors of post-stroke cognitive impairment using acute structural MRI neuroimaging: A systematic review and meta-analysis. *Int. J. Stroke*. 2023;18(5):543–554. DOI: 10.1177/17474930221120349.
17. Nael K., Yoo B., Salamon N., Liebeskind D.S. Acute ischemic stroke: MR imaging-based paradigms. *Neuroimaging Clin. N. Am*. 2021;31(2):177–192. DOI: 10.1016/j.nic.2021.01.002. PMID: 33902873.
18. Garcia-Esperon C., Raposo N., Seners P., Spratt N., Parsons M., Olivot J.M. Role of neuroimaging before reperfusion therapy. Part 1 – IV thrombolysis – Review. *Rev. Neurol. (Paris).* 2021;177(8):908–918. DOI: 10.1016/j.neurol.2020.10.007.
19. Zhang Y.L., Zhang J.F., Wang X.X., Wang Y., Anderson C.S., Wu Y.C. Wake-up stroke: imaging-based diagnosis and recanalization therapy. *J. Neurol.* 2021;268(11):4002–4012. DOI: 10.1007/s00415-020-10055-7.
20. Atchaneeyasakul K., Liebeskind D.S., Jahan R., Starkman S., Sharma L., Yoo B. et al. UCLA reperfusion therapy investigators. Efficient multimodal MRI evaluation for endovascular thrombectomy of anterior circulation large vessel occlusion. *J. Stroke Cerebrovasc. Dis.* 2020;29(12):105271. DOI: 10.1016/j.jstrokecerebrovasdis.2020.105271.
21. Lee H., Jung K., Kang D.W., Kim N. Fully Automated and real-time volumetric measurement of infarct core and penumbra in diffusion- and perfusion-weighted mri of patients with hyper-acute stroke. *J. Digit. Imaging.* 2020;33(1):262–272. DOI: 10.1007/s10278-019-00222-2.
22. Xiao Z.P., Jin K., Wan J.Q., Lin Y., Pan Y.H., Jin Y.C. et al. Measurement of cerebrovascular reserve by multimodal imaging for cerebral arterial occlusion or stenosis patients: protocol of a prospective, randomized, controlled clinical study. *Trials*. 2020;21(1):49. DOI: 10.1186/s13063-019-3967-2.
23. Liu J., Wang Q., Liu F., Song H., Liang X., Lin Z. et al. Altered functional connectivity in patients with post-stroke memory impairment: A resting fMRI study. *Exp. Ther. Med.* 2017;14(3):1919–1928. DOI: 10.3892/etm.2017.4751.
24. Wu C.W., Lin S.N., Hsu L.M., Yeh S.C., Guu F., Lee S.H., Chen C.C. Synchrony Between Default-Mode and Sensorimotor Networks Facilitates Motor Function in Stroke Rehabilitation: A Pilot fMRI Study. *Front. Neurosci.* 2020;14:548. DOI: 10.3389/fnins.2020.00548.
25. Du J., Yang F., Zhang Z. et al. Early functional MRI activation predicts motor outcome after ischemic stroke: a longitudinal, multimodal study. *Brain Imaging and Behavior.* 2018;12:1804–1813. DOI: 10.1007/s11682-018-9851-y.
26. Belani P., Kihira S., Pacheco F., Pawha P., Cruciata G., Nael K. Addition of arterial spin-labelled MR perfusion to conventional brain MRI: clinical experience in a retrospective cohort study. *BMJ Open.* 2020;10(6):e036785. DOI: 10.1136/bmjopen-2020-036785.
27. Wang J., Pan L.J., Zhou B., Zu J.Y., Zhao YX, Li Y. et al. Crossed cerebellar diaschisis after stroke detected noninvasively by arterial spin-labeling MR imaging. *BMC Neurosci.* 2020;21(1):46. DOI: 10.1186/s12868-020-00595-z.
28. Lu S.S., Cao Y.Z., Su C.Q., Xu X.Q., Zhao L.B., Jia Z.Y. et al. Hyperperfusion on arterial spin labeling MRI predicts the 90-day functional outcome after mechanical thrombectomy in

ischemic stroke. *J. Magn. Reson. Imaging.* 2021;53(6):1815–1822. DOI: 10.1002/jmri.27455.
29. Crisi G., Filice S., Scoditti U. Arterial spin labeling mri to measure cerebral blood flow in untreated ischemic stroke. *J. Neuroimaging*. 2019;29(2):193–197. DOI: 10.1111/jon.12569.
30. Verclytte S., Fisch O., Colas L., Vanaerde O., Toledano M., Budzik J.F. ASL and susceptibility-weighted imaging contribution to the management of acute ischaemic stroke. *Insights Imaging.* 2017;8(1):91–100. DOI: 10.1007/s13244-016-0529-y.
31. Santos L.A., Sullivan B., Kvist O., Jambawalikar S., Mostoufi-Moab S., Raya J.M. et al. Diffusion tensor imaging of the physis: the ABC's. *Pediatr. Radiol*. 2023;53(12):2355–2368. DOI: 10.1007/s00247-023-05753-z.
32. Lyu J., Ma N., Tian C. et. al. Perfusion and plaque evaluation to predict recurrent stroke in symptomatic middle cerebral artery stenosis. *Stroke and Vascular Neurology.* 2019;4(3):129–134. DOI: 10.1136/svn-2018-000228.
33. Umarova R.M., Beume L., Reisert M., Kaller C.P., Klöppel S., Mader I. et al. Distinct white matter alterations following severe stroke: Longitudinal DTI study in neglect. *Neurology.* 2017;88(16):1546–1555. DOI: 10.1212/WNL.0000000000003843.
34. Levashkina I.M., Serebryakova S.V., Efimtsev A. Yu. Diffusion-tensor MRI – the most up-to-date method to research microstructual changes in white matter (publications' review). *Vestnik SPbSU. Series 11. Medicine.* 2016;4:39–54. DOI: 10.21638/11701/spbu11.2016.404.
35. Visser M.M., Yassi N., Campbell B.C.V., Desmond P.M., Davis S.M., Spratt N. et al. White Matter Degeneration after Ischemic Stroke: A Longitudinal Diffusion Tensor Imaging Study. *J. Neuroimaging.* 2019;29(1):111–118. DOI: 10.1111/jon.12556.
36. Egorova-Brumley N., Dhollander T., Khan W., Khlif M.S., Ebaid D., Brodtmann A. Changes in white matter microstructure over 3 years in people with and without stroke. *Neurology.* 2023;100(16):e1664–e1672. DOI: 10.1212/WNL.0000000000207065.
37. Lewis A.F., Myers M., Heiser J., Kolar M., Baird J.F., Stewart J.C. Test-retest reliability and minimal detectable change of corticospinal tract integrity in chronic stroke. *Hum. Brain Mapp.* 2020;41(9):2514–2526. DOI: 10.1002/hbm.24961.
38. Liu J., Wang C., Qin W., Ding H., Guo J., Han T. et al. Corticospinal fibers with different origins impact motor outcome and brain after subcortical stroke. *Stroke*. 2020;51(7):2170–2178. DOI: 10.1161/STROKEAHA.120.029508.
39. Blom-Smink M., Verly M., Spielmann K., Smits M., Ribbers G.M., van de Sandt-Koenderman M.W.M.E. Change in right inferior longitudinal fasciculus integrity is associated with naming recovery in subacute poststroke aphasia. *Neurorehabil. Neural Repair.* 2020;34(9):784–794. DOI: 10.1177/1545968320940982.
40. Keser Z., Meier E.L., Stockbridge M.D., Hillis A.E. The role of microstructural integrity of major language pathways in narrative speech in the first year after stroke. *J. Stroke Cerebrovasc. Dis.* 2020;29(9):105078. DOI: 10.1016/j.jstrokecerebrovasdis.2020.105078.
41. Mochizuki M., Uchiyama Y., Domen K. et al. Associations between stroke outcome assessments and automated tractography fractional anisotropy incorporating age. *Ann. Rehabil. Med*. 2025;49(1):15–22. DOI: 10.5535/arm.240073.
42. Mahmoud B.E., Mohammad M.E., Serour D.K. What can DTI add in acute ischemic stroke patients? *Egypt J. Radiol. Nucl. Med.* 2019;50:67. DOI: 10.1186/s43055-019-0058-z.
43. Puig J., Blasco G., Schlaug G. et al. Diffusion tensor imaging as a prognostic biomarker for motor recovery and rehabilitation after stroke. *Neuroradiology.* 2017;59:343–351. DOI: 10.1007/s00234-017-1816-0.
44. Keser Z. et al. The role of microstructural integrity of major language pathways in narrative speech in the first year after stroke. *Journal of Stroke and Cerebrovascular Diseases*. 2020;29(9). DOI: 1016/j.jstrokecerebrovasdis.2020.105078.
45. Nägele F.L., Petersen M., Mayer C. et al. Longitudinal microstructural alterations surrounding subcortical ischemic stroke lesions detected by free-water imaging. *Hum. Brain Mapp.* 2024;45(8):e26722. DOI: 10.1002/hbm.26722.
46. Gong Z., Zhang R., Jiang W. et al. Integrity of the hand fibers of the corticospinal tract shown by diffusion tensor imaging predicts hand function recovery after hemorrhagic stroke. *J. Stroke Cerebrovasc. Dis.* 2021;30(1):105447. DOI: 10.1016/j.jstrokecerebrovasdis.2020.105447.

Author Information

Kurazhov Alexei P. – Radiologist, Dr. Sci. (Med.), Professor of the Division of Radiodiagnostics and Radiation Therapy, Siberian State Medical University, Tomsk, kurazhovap@mail.ru, https://orcid.org/0000-0003-1316-5421

Alifirova Valentina M. – Neurologist, Dr. Sci. (Med.), Professor, Head of the Neurology and Neurosurgery Division, Siberian State Medical University, Tomsk, v_alifirova@mail.ru, http://orcid.org/0000-0002-4140-3223

Koroleva Ekaterina S. – Neurologist, Dr. Sci. (Med.), Associate Professor, Neurology and Neurosurgery Division, Siberian State Medical University, Tomsk, kattorina@list.ru, http://orcid.org/0000-0003-1911-166X

Degtyarev Ilya Y. – Radiologist, Post-graduate Student, Division of Radiodiagnostics and Radiation Therapy, Siberian State Medical University, Tomsk, ilya.degtyarev.4201@mail.ru, http://orcid.org/0000-0002-8812-4168

Loiko Yulia N. – Radiologist, S. Berezin Treatment and Diagnostic Center of the International Institute of Biological Systems, Tomsk, loikojulian@gmail.com, http://orcid.org/0000-0002-1889-4554

Kucherova Kristina S. – Neurologist, Post-graduate Student, Neurology and Neurosurgery Division, Siberian State Medical University, Tomsk, kristyajka@ya.ru, http://orcid.org/0000-0003-4968-4012

Sukhanova Kristina S. – Radiologist, Computed Tomography Department, Clinics of Siberian State Medical University, Tomsk, athos227930@gmail.com, http://orcid.org/0000-0001-9449-8564

Zavadovskaya Vera D. – Radiologist, Dr. Sci. (Med.), Professor, Head of the Division of Radiodiagnostics and Radiation Therapy, Siberian State Medical University, Tomsk, wdzav@mail.ru, http://orcid.org/0000-0001-6231-7650

(✉) **Kurazhov Alexei P.,** kurazhovap@mail.ru

Received on October 28, 2025;
approved after peer review on November 12, 2025;
accepted on November 20, 2025

УДК 616.94-092
https://doi.org/10.20538/1682-0363-2026-2-161-172

Modern Aspects of Separate Mechanisms of Sepsis Pathogenesis

Naumova L.A., Yallyev M.B.

Surgut State University
1 Lenin St., 628412 Surgut, Russian Federation

ABSTRACT

The objective of the review is to analyze the continuously developing and changing ideas about the numerous interrelated mechanisms of sepsis pathogenesis, new research directions, and potential approaches to treatment that are formed on their basis. A search was conducted using keywords in the PubMed database of relevant scientific publications for the period after the Third International Consensus Definition of Sepsis and Septic Shock (Sepsis-3).

The review considers modern concepts of the main pathophysiological mechanisms of sepsis development, which remains a pressing health problem. The data accumulated to date on various pathophysiological mechanisms of sepsis reflect the complexity of its pathogenesis, caused by the development and coexistence of a large number of diverse pathological reactions with wide overlap and interaction of various signaling cellular pathways responsible for both cell survival and death. In this case, the outcome of the process is determined by the delicate balance of developing reactions, in particular the balance between activation of the immune response and immunosuppression. New research directions into the pathogenesis of sepsis focus not only on the mechanisms of modulation of the immune system activity, but also on the study of a wide range of pathophysiological processes associated with the development of multiple organ failure syndrome. Accordingly, there is a search for new therapeutic strategies, and with the recognition of sepsis as a heterogeneous syndrome, a transition to more personalized approaches in its treatment.

Keywords: sepsis, immunosuppression, mitochondrial dysfunction, cellular exhaustion, endothelial dysfunction, platelets

Conflict of interest. The authors declare the absence of obvious or potential conflicts of interest related to the publication of this article.

Source of financing. The authors state that they recieved no funding for the study.

For citation: Naumova L.A., Yallyev M.B. Modern Aspects of Separate Mechanisms of Sepsis Pathogenesis. *Bulletin of Siberian Medicine.* 2026;25(2):161–172. https://doi.org/10.20538/1682-0363-2026-2-161-172.

Современные аспекты отдельных механизмов патогенеза сепсиса

Наумова Л.А., Яллыев М.Б.

Сургутский государственный университет (СурГУ)
Россия, 628412, г. Сургут, ул. Ленина, 1

РЕЗЮМЕ

Цель обзора – анализ непрерывно развивающихся и меняющихся представлений о многочисленных взаимосвязанных механизмах патогенеза сепсиса, формирующихся на их основе новых направлениях исследований и потенциальных подходах к лечению. Проведен поиск с использованием ключевых слов в базе дан-

✉ *Naumova Liudmila A.,* naumovala@yandex.ru

ных PubMed релевантных научных публикаций за период после Третьего международного консенсусного определения сепсиса и септического шока (Sepsis-3).

В обзоре рассматриваются современные представления об основных патофизиологических механизмах развития сепсиса, остающегося актуальной проблемой здравоохранения. Накопленные к настоящему времени данные о различных патофизиологических механизмах сепсиса отражают сложность его патогенеза, обусловленную развитием и сосуществованием большого количества разнообразных патологических реакций с широким перекрытием и взаимодействием различных сигнальных клеточных путей, отвечающих как за выживание, так и гибель клеток. При этом исход процесса определяется тонким балансом развивающихся реакций, в частности, балансом между активацией иммунного ответа и иммуносупрессией. Новые направления исследований патогенеза сепсиса сосредоточиваются не только на механизмах модуляции активности иммунной системы, но и на изучении широкого спектра патофизиологических процессов, ассоциирующихся с развитием синдрома полиорганной недостаточности. Соответственно, идет поиск новых терапевтических стратегий, а с признанием сепсиса гетерогенным синдромом – переход к более персонализированным подходам в его лечении.

Ключевые слова: сепсис, иммуносупрессия, митохондриальная дисфункция, клеточное истощение, эндотелиальная дисфункция, тромбоциты

Конфликт интересов. Авторы декларируют отсутствие явных и потенциальных конфликтов интересов, связанных с публикацией настоящей статьи.

Источник финансирования. Авторы заявляют об отсутствии источника финансирования при проведении исследования.

Для цитирования: Наумова Л.А., Яллыев М.Б. Современные аспекты отдельных механизмов патогенеза сепсиса. *Бюллетень сибирской медицины.* 2026;25(2):161–172. https://doi.org/10.20538/1682-0363-2026-2-161-172.

INTRODUCTION

Currently, sepsis is defined as a pathological condition caused by the introduction of an infectious pathogen and the subsequent unregulated response of the macroorganism, threatening life as a result of the development of multiple organ failure [1–4]. Despite advancing the understanding of its molecular pathophysiology and an increasing number of studies, including those devoted to a wide range of targeted therapies, sepsis remains a disease with a high mortality rate [5–8], and in patients who survive it, it causes an increased risk of death or a health-related decrease in quality of life [7, 9]. The World Health Organization has declared sepsis a global health priority [2, 10].

The development of a definition of sepsis and the search for its diagnostic criteria has have continued over the past 30 yearsand reflect both the growing understanding of its pathophysiological mechanisms and the successes and failures in its diagnosis and treatment [2, 3, 11]. The concept of sepsis has evolved in recent years from its understanding as a systemic inflammatory response syndrome (SIRS) caused by infection (Sepsis-1) to severe and potentially fatal organ dysfunction due to an inadequate or unregulated host response to infection (Sepsis-3). The concept has also emerged that systemic manifestations of infection can be caused by inflammatory mediators in the absence of dissemination of infection [2].

In the early 2000s, an alternative concept to the classical theory of sepsis pathogenesis (hyperinflammation) emerged, focusing on the importance of immunosuppression developing at later stages of the process [2, 4]. At the same time, the concept was emerging that excessive inflammation and immunosuppression develop simultaneously, rather than sequentially, and their balance determines the outcome. With the predominance of hyperinflammation, early death is possible from an intractable cytokine storm and multiple organ damage, often with the development of persistent inflammation, immunosuppression, and catabolism syndrome (PICS), characterized by prolonged immunoparalysis, recurrent infections, and prolonged multiple organ dysfunction, whereas with successful regulation of the immune response, a rapid recovery from the critical condition is possible [12, 13].

Today, it is becoming clear that sepsis is a very complex response of the macroorganism, in which there is simultaneous development, coexistence, and complex interrelationship of a large number of diverse pathological reactions: systemic inflammation, metabolic and hemostatic disorders,

dysfunction of the immune system, disturbances of nervous regulation and others, and the outcome of the process depends on the delicate balance of these reactions and their counter-reactions, in particular the balance between activation of the immune response and immunosuppression [11, 14]. Sepsis is also characterized by long-term effects of developing reactions and difficulties in restoring homeostasis [12], the complexity of differentiating reactions into protective and those that enhance damage [2, 3, 11], as well as assessing their temporal sequence [7].

The complexity of the pathophysiology of sepsis, based on the simultaneous involvement, intersection, and interaction of a large number of signaling cellular pathways that determine the existence of various clinical phenotypes of the disease, determines the difficulty of its diagnosis, the absence of specific clinical symptoms and biomarkers with sufficient sensitivity and specificity [7, 9]. Such clinical diversity of sepsis explains not only the contradictory characteristics of the process, in particular in the spectrum of expressed cytokines, but also the ineffectiveness of many targeted drugs in the clinical setting that have shown good effect in the experiment or in certain subgroups of patients [15, 16]. At the same time, it is the early diagnosis and treatment of sepsis that ensure its favorable outcome [7, 9].

New areas of sepsis research focus not only on mechanisms modulating immune system activity, including epigenomic reprogramming of immune cells, but also on the study of a wide range of pathophysiological processes associated with the development of multiple organ dysfunction syndrome (MODS), including mitochondrial dysfunction, cellular exhaustion, and endothelial dysfunction. The recognition of sepsis as a heterogeneous syndrome determines the need for its deeper phenotyping using bioinformatics technologies with subsequent personalized approaches to treatment [4, 15].

The aim of this review is to analyze the continually evolving and changing understanding of the numerous interrelated mechanisms of sepsis pathogenesis, the emerging new research areas, and potential treatment approaches.

MATERIALS AND METHODS

A search of the PubMed database for scientific publications on sepsis published in the 9 years following the Third International Consensus Definition of Sepsis and Septic Shock (Sepsis-3) was conducted [1]. A total of 1,210 abstracts were analyzed during the initial search, and the leading concepts of sepsis pathogenesis and current research areas were identified, which became potential thematic sections of the review. The following keywords were used for the search: sepsis, immunosuppression, mitochondrial dysfunction, cellular exhaustion, endothelial dysfunction, and thrombocytopenia. Seventy full-text papers were analyzed. The inclusion criterion was relevance, while the exclusion criterion was sepsis in children. This review includes 54 studies that reflect recent advances in the research of the least understood aspects of sepsis pathogenesis.

RESULTS

Pathophysiological Basis of the Modern Concept of Sepsis

The trigger event for the development of sepsis is an infectious pathogen that causes a local inflammatory response involving, first of all, antigen-presenting cells of the innate immune system (IIS) – resident macrophages and dendritic cells (DCs), which provide the first line of defense [2–4, 10]. Activation of specific receptors (PRRs) in these cells through molecular patterns associated with both infectious pathogens (PAMPs) and those released during damage to host cells (DAMPs) leads to the inclusion of complex metabolic cascades responsible for the formation of the inflammasome, primarily in monocytes/macrophages, which are considered the primary source of inflammatory cytokines in response to activating stimuli and cells that maintain a delicate balance between the expression of pro- and anti-inflammatory cytokines [3, 10, 17].

The inflammasome is a protein oligomeric complex responsible for the inflammatory response by activating biologically inactive molecules, in particular pro-IL-1β and pro-IL-18, through autoproteolytic cleavage by caspase-1 (CASP1). Overactivation of the inflammasome can lead to cytokine storm with accompanying fever, shock, and multiple organ dysfunction [2, 4, 10]. A secondary multiple release of **cytokines** caused by the destruction of cell membranes during the initial cytokine storm also occurs, which serves as an additional immune trigger [10]. High levels of expression of inflammasome components have been

detected not only in professional immune cells of the IIS, but also in the endothelium and epithelial cells of barrier tissues of the body (in particular, in mucous membranes) [18].

Activation of PRRs also causes a cascade of reactions leading to the nuclear translocation of nuclear factor kappa B (NFκB) in immune cells and the induction of transcription of target genes involved in the synthesis of a number of proinflammatory cytokines (including IL-1β and IL-6) and some chemokines (CXCL8) [10, 12]. The second most important signaling cascade of IIS activation is triggered by interferons (IFNs). In both cascades, molecules of the small ubiquitin-like modifier (SUMO) play an important regulatory role, binding to target proteins and modulating their function (sumoylation) [12].

The inflammatory microenvironment is necessary for the release of complement proteins involved in direct pathogen lysis and for the active recruitment of effector cells of the innate and adaptive immune system (AIS) involved in the destruction of the pathogen [10]. At the same time, the secretion of proinflammatory cytokines can induce a special type of programmed cell death – pyroptosis, and inflammasomes involved in larger complexes (panaptosomes) can cause cell death by panoptosis, with cell survival and death signaling pathways (networks) intersecting. Programmed cell death (PCD) networks are critical mechanisms in the host response to infection, allowing for both the elimination of infected cells and the induction of inflammation, and are considered as key factors in immune dysregulation in sepsis [19].

In addition to the release of DAMPs, neutrophil extracellular traps (NETs) contribute to the inflammatory response. NETs are formed during neutrophil cell death (netosis) and consist of extracellular chromatin, histones, unfolded nuclear double-stranded DNA (dsDNA), and numerous granular proteins (such as elastase, cathepsin G, myeloperoxidase (MPO), among others). While NETs provide blood bactericidal activity, their excessive formation exacerbates tissue damage [4, 7, 10].

For instance, high levels of S100a8/a9 (released by neutrophils) suppress the expression of Ndufa3 (a subunit of NADH dehydrogenase) in mitochondrial complex I by inhibiting the expression of Nrf1 (nuclear respiratory factor 1). The deficiency in mitochondrial complex I promotes NAD+-dependent suppression of Sirt1 (sirtuin 1), leading to mitochondrial impairments – excessive mitochondrial fission and blocked mitophagy. In turn, mtDNA released from damaged mitochondria activates ZBP1 (Z-DNA-binding protein 1, which also binds Z-RNA)-mediated panoptosis in endothelial cells. Based on comprehensive RNA sequencing (scRNA-seq, RNA-seq) data, a strong correlation has been demonstrated between S100A8/A9hi neutrophils and the number of circulating endothelial cells (a useful marker of endothelial damage), establishing S100A8 as an independent risk factor for an unfavorable prognosis in septic patients [20].

The recently discovered IL-40 is primarily responsible for the influx of S100A8/9^{hi} neutrophils, particularly into the peritoneal cavity, and the formation of NETs. High levels of IL-40 in sepsis are positively correlated with the NET-related MPO/dsDNA ratio, procalcitonin, C-reactive protein, lactate dehydrogenase, and the sequential organ failure assessment (SOFA). Genetic knockout of IL-40 (IL-40$^{-/-}$) prevents multiorgan damage in experimental sepsis by blocking netosis, therefore IL-40 may become a new therapeutic target in sepsis [21].

Signals emanating from the IIS in response to the presence of DAMPs also activate the autonomic nervous system with a reflex loop at the brainstem level and lead to the activation of a special population of lymphocytes (ChAT^{+}) expressing the enzyme choline acetyltransferase and, as shown experimentally, playing a role in the regulation of blood pressure and the inhibition of macrophages producing proinflammatory cytokines. Such biological feedback allows for the suppression of the inflammatory reaction and the prevention of immune response “evasion” [10]. Adrenergic receptors in primary and secondary lymphoid organs are responsible for the suppression of the immune response. Among IIS cells, adrenergic receptors are actively expressed by neutrophils, especially beta-2 receptors, the activation of which is responsible for a decrease in the production of reactive oxygen species (ROS), neutrophil migration, and the formation of NETs [10].

A controlled immune response to infection is characterized by the appearance of anti-inflammatory factors (IL-4, IL-10, IL-11, IL-13, TGFβ, GM-CSF, and IL-1 receptor antagonist), which help balance

the inflammatory response after the initial phase. This is achieved by reducing the production of inflammatory cytokines by monocytes/macrophages and activating T-cells, while simultaneously preserving the capacity for phagocytosis and microbial killing through the generation of ROS and nitric oxide. This process leads to the restoration of homeostasis and clinical recovery [2, 7, 10, 22]. The mechanisms of a balanced inflammatory response and recovery from organ dysfunction are included in the concept of compensatory anti-inflammatory response syndrome (CARS) [2]. In an uncontrolled inflammatory response, dysregulation of the innate and adaptive immune response occurs, with dysfunction and/or depletion of immune cells, primarily $CD4^+$ T lymphocytes. Regulatory T cells (Tregs) avoid apoptosis and contribute to immune suppression [12].

Thus, it is now becoming clear that the inflammatory response caused by infection must be tightly regulated and that mechanisms for controlling this response are triggered during the development of sepsis [2, 12, 23].

Dysregulation of the Immune Response

Dysregulation of the immune response in sepsis is reflected in the multidirectional nature of inflammasome activation and in the characteristics of the clinical phenotype of the disease. For example, compared to SIRS, some studies have found decreased expression of the NALP1 and CASP1 genes (responsible for processing the proinflammatory cytokines IL-1β and IL-18) in patients with septic shock. Conversely, other studies have noted increased expression of these genes, particularly in patients with sepsis and acute respiratory distress syndrome compared to SIRS. Upregulation of the NOD-like receptors NLRP3 and NLRC4 and downregulation of NOD1 or NLRP1 have also been found in fatal sepsis outcomes [2]. *In vitro*, it has been shown that a macrophage-derived transmembrane protein belonging to the tumor necrosis factor receptor (GITR) superfamily enhances macrophage uptake of lysophosphatidylcholine and NLRP3-inflammasome-mediated macrophage pyroptosis. Conditional knockout of GITR in myeloid cells or NLRP3/caspase-1/IL-1β deficiency reduces the severity/lethality of sepsis [24].

Immunosuppression that develops in sepsis is associated with the release of anti-inflammatory cytokines (IL-4, IL-10, IL-37, and TGF-β), immune cell death, T-cell exhaustion, and excessive production of immunomodulatory cells, including Tregs and myeloid-derived suppressor cells (MDSCs) [4, 23]. Increased expression of immune checkpoint receptors PD-1, TIM-3, and BTLA and decreased expression of IL-7 (lymphocyte growth factor) receptors in CD4+ and CD8+ splenic lymphocytes also leads to the progression of immunosuppression [3, 4, 23]. Thus, in sepsis, both IIS and AIS responses can be either suppressed or enhanced [3]. Therapeutic strategies aimed at preventing the development of immunosuppression include the use of GM-CSF to increase neutrophil activity, anti-PD-L1 antibodies to reduce T-cell exhaustion, and IFNγ to enhance macrophage function [4].

Immune disorders are also manifested by a decrease in chemotaxis, phagocytosis, and ROS formation in young neutrophils [2, 3]. At the same time, high ROS production by neutrophils is observed in patients with septic shock, and high expression of elastase, cathepsin G, and MPO by young neutrophils, and high frequency of NETs are associated with the development of organ failure, DIC syndrome, and higher mortality. The study of neutrophil phenotypes may be useful for the early recognition of various clinical scenarios in patients with sepsis [3]. Thus, depletion of neutrophils with the $Siglec\text{-}F^+$ phenotype, which are the primary producers of IL-10, leads to an increase in T-lymphocyte function and a noticeable improvement in the survival of mice with secondary infections, which does not exclude the potential therapeutic value of this discovery [25].

Decreased HLA-DR expression in monocytes is considered as a reliable biomarker of the immune status in patients with sepsis and a predictor of the development of secondary infectious complications. Decreased HLA-DR expression on the DC surface also correlates with the severity of sepsis and is characteristic of septic shock. The immunosuppressive activity of monocytes/macrophages also partially depends on the expression of Nod-like receptor protein-3 (NALP-3), which is the main component of the eponymous type of inflammasome multiprotein complex. NALP-3 expression in macrophages is regulated by T-cell immunoglobulin and the mucin domain (Tim4); in patients with septic shock, the expression of Tim4 and NALP-3 decreases, which leads to dysfunction of phagocytosis and immunosuppression [3]. Currently, the importance

of the balance of two macrophage profiles – MHCII$^+$ F4/80$^+$ Tim4- and CD206$^+$ F4/80$^+$ Tim4$^+$, which have a proinflammatory and anti-inflammatory effect, respectively, and the need for early (before the development of a cytokine storm) administration of drugs (in particular, liposomal clodronate) that stop the accumulation of MHCII$^+$ F4/80$^+$ Tim4 has been shown [26].

At the same time, monocytes from patients with sepsis demonstrate functional plasticity and the possibility of reprogramming under the influence of the expression of HIF1α (hypoxia-inducible factor 1α), a key factor in the reprogramming of monocytes with the development of so-called "lipopolysaccharide tolerance", which can also be the result of epigenetic (in particular, during DNA methylation of monocytes) suppression of inflammatory genes (for example, NF-kB, IRAK-1, TLR-4 and TREM-1) and, conversely, an increase in transcription factors, such as IL-1 receptor-associated kinase-M (IRAK-M) and SH2-containing inositol phosphatase (SHIP) [3, 27].

Transcription factor-mediated reprogramming can also occur in DCs, for example, by downregulating the expression of interferon regulatory factor 4 (IRF4), which promotes antigen presentation to CD4$^+$ lymphocytes by dendritic cells, or by upregulating Blimp-1 (B-lymphocyte-induced maturation protein-1) expression, which induces DC tolerance *in vitro*. Transcription factor-mediated DC reprogramming can also result from autocrine TGFβ inflammatory signaling and local Treg regulation [3]. Blimp-1 can function as an activator/repressor and determine the fate of different T cell lines, it also enhances the production of IL-2, IL-21 and IL-10 in effector T lymphocytes, regulating the degree of inflammation and cell damage, therefore, the regulatory mechanisms of immune homeostasis determined by Blimp-1 may become an important therapeutic target in sepsis [28, 29].

Apoptosis of T and B cells in patients with sepsis leads to lymphopenia, which is observed during the first week of septic shock and is associated with more severe organ dysfunction and a worse prognosis. In contrast, in surviving patients, the absolute number of CD3$^+$ CD4$^+$- lymphocytes is restored [3]. The immunosuppressive state, especially in patients with septic shock, is maintained by a decrease in the expression of transcription factors, such as T-bet, GATA3, and Foxp3 in lymphocytes, as well as through a number of mechanisms in Treg CD4$^+$ CD25$^+$ FoxP3$^+$ (Forkhead/winged helix transcription factor P3). In severe sepsis, an increase in the number of Tregs, especially Treg CD39$^+$, is observed. Tregs can eliminate target cells or modulate target cell signaling through direct contact, via anti-inflammatory cytokines (IL-10, TGFβ, or IL-35) or exosomes containing microRNAs. The complex balance between pro- and anti-inflammatory responses in sepsis may disrupt the Th17/Treg ratio and lead to increased resistance of Tregs to apoptosis or to inhibitory effects in the adaptive immune response [3].

Severe suppression of the immune response, which causes the development of secondary infections and high mortality, develops in patients with PICS, associated with high expression of, in particular, PD-1, CTLA-4, BTLA, TLR-2, TLR-4, and TLR-5 and excessive production of such cytokines as IFNγ, IL-6, TNFα, and IL-10 [3]. The pathophysiological mechanisms of PICS are not fully understood, but a link has been noted with mitochondrial dysfunction (MD), cellular exhaustion and an increase in the number of MDSCs, which regulate and limit inflammation at the beginning of the septic process, and later (after day 14) lead to the development of an anti-inflammatory response, and PICS [12, 30]. Glycemic variability and low levels of high-density lipoprotein cholesterol are also considered as independent risk factors for the development of secondary PICS in sepsis [31, 32].

Thus, both pro- and anti-inflammatory genomic storms arise in the earliest stages of infection, and the balance between them determines the development of clinically excessive inflammation or immunosuppression. Immunomodulation (particularly the use of PD-1/PD-L inhibitors) could potentially become a new strategy for treating sepsis [12].

Mitochondrial Dysfunction

Mitochondrial dysfunction and bioenergetic failure are recognized as important pathophysiological mechanisms of sepsis, particularly the development of MODS and immunosuppression, and early mitochondrial biogenesis and antioxidant defense are considered as critical factors for the survival of patients with sepsis [33–37].

Mitochondria are dynamic networks that constantly adapt to cellular needs. Their morphology and function depend on a delicate balance between fusion processes, which create an extensive network, and, conversely, disintegration, which is necessary to remove damaged mitochondria and utilize them through autophagy, or mitophagy. Inadequate mitophagy leads to the accumulation of dysfunctional mitochondria in cells [34, 37, 38]. The PINK1/Parkin (PTEN-activated kinase/ parkin) mitophagy pathway, which is activated in the heart and kidneys during sepsis, plays a crucial role in the protection and preservation of their mitochondria. When one of these pathways is deficient in experimental mice, myocardial contractile dysfunction and renal dysfunction increase. Suppression of mitophagy receptors, as well as impaired fusion of autophagosomes containing dysfunctional mitochondria with lysosomes, may play a significant role in skeletal muscle dysfunction and the development of fatty liver disease. A large group of membrane transport proteins (SNAREs), including STX17, SNAP29, VAMP8, and VAMP7, is involved in the complex process of autophagosome – lysosome fusion [34].

Factors causing structural damage to mitochondria include proinflammatory cytokines, bacterial LPS, and ROS, leading to decreased ATP production, disruption of the redox balance, followed by accumulation of ROS and the formation of a vicious cycle [36]. MD is induced by poly(ADP-ribose) polymerase 1, or PARP1, the main isoform of the enzyme family catalyzing poly-ADP-ribosylation. Hyperactivation of PARP1 leads to depletion of NAD^+ and ATP and the development of MD. Experimentally, mice with PARP1 deficiency exhibit reduced mortality in response to high doses of LPS [2].

Research aimed at further studying MD in sepsis, mitophagy pathways, and the search for therapeutic effects on mitochondrial dynamics remains relevant [34]. Thus, it has been shown that the severity of kidney damage in sepsis correlates well with the expression of the transient receptor potential ankyrin 1 (TRPA1) in the renal tubular epithelium, which can serve as a "sensor" of oxidative stress and an important regulator of the activation of MAPK (mitogen-activated protein kinase)/NF-κB signaling pathways, and also contribute to the subsequent transcriptional regulation of IL-8 [39]. The use of the drug A-967079 (TRPA1 antagonist) prevents the development of MODS and increased secretion of proinflammatory cytokines and reduces the level of lipid peroxidation in mitochondria and MD, in particular in renal tissue [40].

Also of interest are studies examining the mechanisms of insulin influence on oxidative stress in the kidneys of rats with experimental sepsis. Insulin administration is accompanied by an increase in the expression of superoxide dismutase and uncoupling protein (UCP2) and a decrease in the severity of structural and functional disorders in the kidneys [41].

Since intracellular metabolic pathways modulate immune cell function, mitochondria, which are metabolic and signaling organelles, have come to be regarded as important participants in immune activation. When exposed to LPS, mitochondrial components, through ROS and HIF1α activation, promote the production of inflammatory cytokines via activation of the NLRP3 inflammasome. The field of study of these processes is called immunometabolism [2].

Analysis of data from numerous studies confirms the significant efficacy of mitochondrial cofactors – α-lipoic acid, coenzyme Q10, and carnitine – in sepsis and other acute illnesses, including COVID-19 pneumonia. These cofactors have a pronounced antioxidant effect and play different but complementary roles in mitochondrial function [33, 37]. The natural flavonoid eriocitrin, which has anti-inflammatory and antioxidant properties, increases mitochondrial biosynthesis and mtDNA content, activates the mitochondrial biogenesis-associated NRF1/PGC-1/TFAM signaling pathway, has a therapeutic effect on acute lung injury in sepsis *in vitro* and *in vivo*, reduces the manifestations of liver steatosis, and suppresses mitochondrial glycolysis through regulation of the MKP1 (mitogen-activated protein kinase 1 phosphatase)/MAPK pathway [37].

The use of notoginsenoside R1 (NGR1) as a mitochondrial protector in experimental sepsis showed that, acting through Drp1 (dynamin-like protein 1), which is responsible for mitochondrial homeostasis in cells under hypoxic – ischemic conditions, it prevents mitochondrial fragmentation and causes the restoration of the morphology and function of the vascular endothelium in the

microcirculatory bed, thereby increasing the barrier function of the intestinal mucosa [36].

Cellular Exhaustion

Cellular exhaustion is observed not only in immune cells, causing immunosuppression, but also forms the structural basis for the development of multiple organ failure in sepsis and is closely pathogenetically linked to the previously discussed MD and PICS [19, 23, 30, 42]. The pathophysiology of sepsis-associated cell death is characterized not only by the diversity of factors triggering this process (DAMPs, PAMPs, cytokines, MD, oxidative stress, transcriptional changes), but also by a complex network of intersecting mechanisms aimed at both cell survival and cell death. Proteins involved in cell death also play a key role in immune signaling in sepsis.

Thus, PCD networks are both components of the host defense response to infection and are associated with the development of inflammation aimed at survival (production of cytokines, activation of inflammasomes, changes in gene transcription), and various mechanisms of cell death, including apoptosis (activation of the caspase cascade); necroptosis with the participation of kinases and pseudokinases (RIPK1, RIPK3, MLKL), accompanied by a pronounced immune response; pyroptosis with excessive activation of inflammasomes with the participation of CASP1 and GSDMD (gasdermin D) [20].

Ferroptosis is now being actively investigated as a novel type of cell death in sepsis. It is driven by iron-dependent lipid peroxidation and is characterized by unique morphological, biochemical, and genetic features. Ferroptotic cells can be immunogenic, enhance inflammatory responses, cause massive cell death, and lead to multiple organ failure [43].

Targeting cell death mediators with new treatments may be able to eliminate uncontrolled inflammation in sepsis and improve patient outcomes [19]. Thus, preliminary administration of BRL37344, a β3-adrenergic receptor (β3-AR) agonist, and preliminary treatment of H9c2 cells with the same drug during experimental sepsis in rats inhibits LPS-induced cardiomyocyte apoptosis, suppresses the activation of caspases-3, -8, and -9, and increases the level of PI3K (phosphoinositide 3-kinase), p-Akt Ser473 (phosphorylated serine/threonine-specific protein kinase at Ser473), and p-eNOS Ser1177 (phosphorylated endothelial nitric oxide synthase at Ser1177) proteins in H9c2 cells [44].

Currently, there is a search for and evaluation of mediators that suppress immune system imbalances, or so-called specialized pro-resolving mediators (SPMs). In particular, resolvin D2 (RvD2), which has an anti-inflammatory effect without the effect of immunosuppression, is being tested [42]. In a model of macrophage depletion by repeated administration of LPS, RvD2 attenuates the suppression of macrophages *in vitro* and *in vivo*, increases NF-κB activity, TNFα release, and bacterial clearance compared to the control [42]. Fludarabine, which suppresses the effects of DnaK, or Hsp70 of *Escherichia coli*, the main regulator of the bacterial proteostasis network that promotes the depletion of T cells, macrophages and osteoclasts, may be potentially effective in the treatment of sepsis [45].

In general, the wide overlap and interaction of PCD networks, based, in turn, on the participation of caspase cascades [19] and intercellular communication via exosomes (the contents of which, including exosomal microRNAs, significantly influence cellular metabolism) [46], greatly complicate attempts to control network interactions [10, 19].

Endothelial Dysfunction and Hemostasis Disorders

Endothelial cells (ECs) are among the first targets in sepsis. They become activated and change their phenotype when exposed to ROS, inflammatory cytokines, and bacterial endotoxins [7, 10, 17]. The consequences of endothelial dysfunction are determined by the physiological role of the endothelium in regulating various systems and are manifested through disruption of regional microcirculation and hemostasis, the development of ischemia/reperfusion, oxidative stress, microthrombosis and tissue hypoxia, and activation of proapoptotic mechanisms, reflecting the intersection of many pathophysiological reactions in sepsis [7, 10, 17, 47].

Under physiological conditions, the endothelium maintains a balance between coagulation and fibrinolysis, and its interaction with leukocytes is modulated by the glycocalyx, the damage of which under conditions of a cytokine storm exposes adhesion molecules (P-selectin, E-selectin, VCAM-1),

enhancing the activation, adhesion, and extravasation of leukocytes [7]. Activated endothelial cells express von Willebrand factor (VWF), tissue factor, and plasminogen activator inhibitor type 1 (PAI-1). The development of the thrombotic phenotype is also promoted by proteolytic inactivation of tissue factor pathway inhibitor (TFPI) and decreased activation of protein C. These defects, as well as a decrease in the level of ADAMTS13 (a protease that cleaves VWF), increase the formation of fibrin-rich microvascular clots, leading to the development of DIC syndrome in sepsis [7, 10].

Changes in vascular permeability and leukocyte recruitment occur primarily at the level of capillaries and postcapillary venules, which have organ-specific structural differences determined by the characteristics of interendothelial connections and, accordingly, the presence of continuous capillaries, discontinuous capillaries, or sinusoids, and capillaries with fenestrated endothelium, or an intermediate type. ScRNA-seq studies have demonstrated the existence of a continuum of transcriptional states in ECs in different branches of the vascular bed [17].

Under physiological conditions, ECs, by releasing nitric oxide, regulate arteriolar tone and local blood flow distribution. Sepsis-activated nitric oxide synthase (iNOS) is expressed heterogeneously in the vascular bed, including due to its organ specificity, which leads to the formation of areas of both hypo- and hyperperfusion. A decrease in capillary functional density and an increase in capillary stasis, including due to a decrease in erythrocyte deformability and platelet/fibrin plugging, as well as the loss of vascular tone regulation, lead to a disruption of convective oxygen transport, a transition of cells to anaerobic glycolysis, and the development of lactic acidosis. In recent years, it has become clear that microvascular ECs play an important role in the pathophysiology of MODS in sepsis [7, 48].

A special place in the initiation of microcirculation disorders is occupied by damage to the glycocalyx, the levels of biomarkers of which in the blood (syndecan-1, soluble CD44 and thrombomodulin) and urine (sulfated glycosaminoglycans) correlate with disturbances in microvascular parameters – perfused vessel density (PVD), perfused border region (PBR), which is the inverse of the glycocalyx thickness, and an indicator of microvascular health [48]. These data determine the development of a new therapeutic approach to the restoration of the endothelial glycocalyx, in particular, a pronounced therapeutic effect, assessed by the stabilization of PVD and PBR, was obtained using liposomal nanocarriers with glycocalyx [49].

New data on the mechanisms of EC involvement in leukodiapaedesis, microvascular permeability control, and hemostasis regulation are forming new understanding of the pathogenesis of sepsis, but cannot yet be transformed into effective methods of its treatment, to a certain extent due to the organotypic characteristics of the endothelium. Results of single-cell RNA sequencing and spatial transcriptomics may help to reveal the full spatiotemporal signature of EC responses in sepsis, better understand the molecular pathways used by EC, and develop therapeutic methods for suppressing the processes leading to the development of MODS [17, 47].

Platelets, Thrombocytopenia, and Immunothrombosis

Various indicators of platelets status, such as thrombocytopenia, P-selectin expression, aggregation with neutrophils, increased mean platelet volume (MPV), and thrombopoietin levels, correlate with the severity of sepsis and are used as its biomarkers [7, 50–52]. By releasing a wide range of biologically active substances (adenosine diphosphate, thromboxane A2, and platelet activating factor (PAF)), including cytokines (IL-1, IL-6, and TNFα) and possessing an equally wide range of receptors, platelets actively participate in two important synchronously developing and interconnected protective reactions during infection – activation of coagulation and the IIS response, which determines their important role in the course of sepsis. [51].

One of the forms of interaction of platelets with cells of the immune system is the formation of platelet –leukocyte, in particular, platelet – neutrophil complexes [51]. Platelets bind to neutrophils through the platelet Toll-like receptor 4 (TLR4), which stimulates the formation of NETs, an excessive amount of which shifts the hemostatic balance towards coagulation and thrombus formation [7, 52]. It has been shown that the introduction of deoxyribonuclease, which destroys circulating free DNA, which is a marker of NETs and enhances thrombin production through activation of the intrinsic coagulation pathway, reduces mortality in sepsis. Thus,

platelets and neutrophils in sepsis are participants in an interconnected immunothrombotic mechanism, which is defined as immunothrombosis [7, 51].

Inflammatory cytokines and the complement system suppress anticoagulant pathways in sepsis. The initial increase in tissue plasminogen activator during the acute phase of inflammation is subsequently overridden by a powerful and sustained upregulation of plasminogen activator inhibitor-1 (PAI-1) production by endothelial cells. This leads to a blockade of fibrinolysis, and thrombus formation in small and medium-sized vessels contributes to MODS. In turn, the administration of recombinant activated protein C suppresses leukocyte – endothelial interaction, the production of inflammatory cytokines and PAI-1, which modulates fibrinolysis, and protects against thrombus formation [7].

Thrombocytopenia in sepsis may be a consequence of sequestration and consumption of Plt by microthrombi [50], Plt pyroptosis caused by S100A8/A9 released from NETs [20], suppression of hematopoiesis in the bone marrow by inflammatory cytokines and bacterial toxins; in particular, a negative correlation of thrombocytopenia with IL-18 and IL-35 has been established [53]. In turn, the use of recombinant human thrombopoietin (rhTPO) in sepsis reduces the severity of inflammation and endothelial cell damage by regulating the PI3K/Akt pathway [54].

CONCLUSION

Thus, the data accumulated to date on the various pathophysiological mechanisms of sepsis reflect the complexity of its pathogenesis, conditioned by the development and coexistence of a large number of diverse pathological reactions with extensive interactions between various cellular signaling pathways. This determines the diversity of clinical phenotypes of the disease, the difficulty of diagnosis (the absence of an ideal biomarker), and the impossibility of universal therapy [2, 7, 15]. Hopes for solving the problem of sepsis are placed on its deep phenotyping using omics technologies, as well as artificial intelligence in the analysis of a vast amount of information on the course of this process [15].

REFERENCES

1. Singer M., Deutschman C.S., Seymour C.W., Shankar-Hari M., Annane D., Bauer M. et al. The third international consensus definitions for sepsis and septic shock (Sepsis-3). *JAMA.* 2016;315(8):801–810. DOI: 10.1001/jama.2016.0287.
2. Salomão R., Ferreira B.L., Salomão M.C., Santos S.S., Azevedo L.C.P., Brunialti M.K.C. Sepsis: evolving concepts and challenges. *Braz. J. Med. Biol. Res*. 2019;52(4):e8595. DOI: 10.1590/1414-431X20198595.
3. Vázquez A.C., Arriaga-Pizano L., Ferat-Osorio E. Cellular markers of immunosuppression in sepsis. *Arch. Med. Res.* 2021;52(8):828–835. DOI: 10.1016/j.arcmed.2021.10.001.
4. Kim M.J., Choi E.J., Choi E.J. Evolving Paradigms in Sepsis Management: A Narrative Review. *Cells.* 2024;13(14):1172. DOI: 10.3390/cells13141172.
5. Rudd K.E., Johnson S.C., Agesa K.M., Shackelford K.A., Tsoi D., Kievlan D.R. et al. Global, regional, and national sepsis incidence and mortality, 1990-2017: analysis for the Global Burden of Disease Study. *Lancet.* 2020;395(10219):200–211. DOI: 10.1016/S0140-6736(19)32989-7.
6. Farrah K., McIntyre L., Doig C.J., Talarico R., Taljaard M., Krahn M. et al. Sepsis-Associated Mortality, Resource Use, and Healthcare Costs: A Propensity-Matched Cohort Study. *Crit. Care Med.* 2021;49(2):215–227. DOI: 10.1097/CCM.0000000000004777.
7. Arora J., Mendelson A.A., Fox-Robichaud A. Sepsis: network pathophysiology and implications for early diagnosis. *Am. J. Physiol. Regul. Integr. Comp. Physiol.* 2023;324(5):R613–R624. DOI: 10.1152/ajpregu.00003.2023.
8. Zhong X., Xie H., Wang S., Ren T., Chen J., Huang Y. et al. TIGIT regulates $CD4^+$ T cell immunity against polymicrobial sepsis. *Front. Immunol.* 2024;15:1290564. DOI: 10.3389/fimmu.2024.1290564.
9. Prescott H.C., Ostermann M. What is new and different in the 2021 Surviving Sepsis Campaign guidelines. *Med. Klin. Intensivmed. Notfmed.* 2023;118(Suppl. 2):75–79. DOI: 10.1007/s00063-023-01028-5.
10. Daniel M., Bedoui Y., Vagner D., Raffray L., Ah-Pine F., Doray B. et al. Pathophysiology of sepsis and genesis of septic shock: the critical role of mesenchymal stem cells (MSCs). *Int. J. Mol. Sci.* 2022;23(16):9274. DOI: 10.3390/ijms23169274.
11. Falcão-Holanda R.B., Brunialti M.K.C., Jasiulionis M.G., Salomão R. Epigenetic regulation in sepsis, role in pathophysiology and therapeutic perspective. *Front. Med. (Lausanne).* 2021;8:685333. DOI: 10.3389/fmed.2021.685333.
12. Nakamori Y., Park E.J., Shimaoka M. Immune deregulation in sepsis and septic shock: reversing immune paralysis by targeting PD-1/PD-L1 pathway. *Front. Immunol*. 2021;11:624279. DOI: 10.3389/fimmu.2020.624279.
13. Cao M., Wang G., Xie J. Immune dysregulation in sepsis: experiences, lessons and perspectives. *Cell Death Discov.* 2023;9(1):465. DOI: 10.1038/s41420-023-01766-7.
14. Zhang W., Li J., Qi G., Tu G., Yang C., Xu M. Myeloid-derived suppressor cells in transplantation: the dawn of cell therapy. *J. Transl. Med.* 2018;16(1):19. DOI: 10.1186/s12967-018-1395-9.
15. Baillie J.K., Angus D., Burnham K., Calandra T., Calfee C., Gutteridge A. et al. Causal inference can lead us to modifiable mechanisms and informative archetypes in sepsis. *Intensive Care Med.* 2024;50(12):2031–2042. DOI: 10.1007/s00134-024-07665-4.
16. Zhang X., Zhang Y., Yuan S., Zhang J. The potential im-

munological mechanisms of sepsis. *Front. Immunol.* 2024;15:1434688. DOI: 10.3389/fimmu.2024.1434688.
17. Cleuren A., Molema G. Organotypic heterogeneity in microvascular endothelial cell responses in sepsis-a molecular treasure trove and pharmacological Gordian knot. *Front. Med. (Lausanne).* 2023;10:1252021. DOI: 10.3389/fmed.2023.1252021.
18. Winsor N., Krustev C., Bruce J., Philpott D.J., Girardin S.E. Canonical and noncanonical inflammasomes in intestinal epithelial cells. *Cell Microbiol.* 2019;21(11):e13079. DOI: 10.1111/cmi.13079.
19. Yang C.S., Coopersmith C.M., Lyons J.D. Cell death proteins in sepsis: key players and modern therapeutic approaches. *Front. Immunol.* 2024;14:1347401. DOI: 10.3389/fimmu.2023.1347401.
20. Wang Y., Shi Y., Shao Y., Lu X., Zhang H., Miao C. S100A8/A9^{hi} neutrophils induce mitochondrial dysfunction and PANoptosis in endothelial cells via mitochondrial complex I deficiency during sepsis. *Cell Death Dis.* 2024;15(6):462. DOI: 10.1038/s41419-024-06849-6.
21. Cai S., Li X., Zhang C., Jiang Y., Liu Y., He Z., et al. Inhibition of Interleukin-40 prevents multi-organ damage during sepsis by blocking NETosis. *Crit Care.* 2025;29(1):29. DOI: 10.1186/s13054-025-05257-2.
22. Melis M.J., Miller M., Peters V.B.M., Singer M. The role of hormones in sepsis: an integrated overview with a focus on mitochondrial and immune cell dysfunction. *Clin. Sci. (Lond.).* 2023;137(9):707–725. DOI: 10.1042/CS20220709.
23. Liu D., Huang S.Y., Sun J.H., Zhang H.C., Cai Q.L., Gao C. et al. Sepsis-induced immunosuppression: mechanisms, diagnosis and current treatment options. *Mil. Med. Res.* 2022;9(1):56. DOI: 10.1186/s40779-022-00422-y.
24. Liang S., Zhou J., Cao C., Liu Y., Ming S., Liu X. et al. GITR exacerbates lysophosphatidylcholine-induced macrophage pyroptosis in sepsis via posttranslational regulation of NLRP3. *Cell Mol. Immunol.* 2024;21(7):674–688. DOI: 10.1038/s41423-024-01170-w.
25. Liao C., Luo S., Liu X., Zhang L., Xie P., Zhou W. et al. Siglec-F^{+} neutrophils in the spleen induce immunosuppression following acute infection. *Theranostics.* 2024;14(6):2589–2604. DOI: 10.7150/thno.93812.
26. Khanna K., Eul E., Yan H., Faccio R. Delayed macrophage targeting by clodronate liposomes worsens the progression of cytokine storm syndrome. *Front. Immunol.* 2024;15:1477449. DOI: 10.3389/fimmu.2024.1477449.
27. Caldwell B.A., Wu Y., Wang J., Li L. Altered DNA methylation underlies monocyte dysregulation and immune exhaustion memory in sepsis. *Cell Rep.* 2024;43(3):113894. DOI: 10.1016/j.celrep.2024.113894.
28. Fu S.H., Yeh L.T., Chu C.C., Yen B.L., Sytwu H.K. New insights into Blimp-1 in T lymphocytes: a divergent regulator of cell destiny and effector function. *J. Biomed. Sci.* 2017;24(1):49. DOI: 10.1186/s12929-017-0354-8.
29. Zou Z., Deng X., Zhang J., Dong J., Xu F., Zhang H. et al. B-lymphocyte-induced maturation protein-1 inhibits inflammation and pyroptosis to alleviate sepsis injury. *J. Investig. Med.* 2024;72(6):553–566. DOI: 10.1177/10815589241249994.
30. Chadda K.R., Puthucheary Z. Persistent inflammation, immunosuppression, and catabolism syndrome (PICS): a review of definitions, potential therapies, and research priorities. *Br. J. Anaesth.* 2024;132(3):507–518. DOI: 10.1016/j.bja.2023.11.052.
31. Barker G., Winer J.R., Guirgis F.W., Reddy S. HDL and persistent inflammation immunosuppression and catabolism syndrome. *Curr. Opin. Lipidol.* 2021;32(5):315–322. DOI: 10.1097/MOL.0000000000000782.
32. Yao J., Chen K., Tong H., Liu R. Predictive value of glycemic variability and HDL-C for secondary persistent inflammatory immunosuppressed catabolic syndrome in patients with sepsis. *J. Inflamm. Res.* 2023;16:5299–5307. DOI: 10.2147/JIR.S433895.
33. Pagano G., Manfredi C., Pallardó F.V., Lyakhovich A., Tiano L., Trifuoggi M. Potential roles of mitochondrial cofactors in the adjuvant mitigation of proinflammatory acute infections, as in the case of sepsis and COVID-19 pneumonia. *Inflamm. Res.* 2021;70(2):159–170. DOI: 10.1007/s00011-020-01423-0.
34. Sedraoui S., Leduc-Gaudet J.P., Mayaki D., Moamer A., Huck L., Gouspillou G. et al. Lack of compensatory mitophagy in skeletal muscles during sepsis. *J. Physiol.* 2024;602(12):2823–2838. DOI: 10.1113/JP286216.
35. Hou D., Liu R., Hao S., Dou Y., Chen G., Liu L. et al. Notoginsenoside R1 improves intestinal microvascular functioning in sepsis by targeting Drp1-mediated mitochondrial quality imbalance. *Pharm. Biol.* 2024;62(1):250–260. DOI: 10.1080/13880209.2024.2318349.
36. Wu M., Huang Z., Akuetteh P.D.P., Huang Y., Pan J. Eriocitrin prevents Sepsis-induced acute kidney injury through anti-inflammation and anti-oxidation via modulating Nrf2/DRP1/OPA1 signaling pathway. *Biochim. Biophys. Acta Gen. Subj.* 2024;1868(7):130628. DOI: 10.1016/j.bbagen.2024.130628.
37. Keshani M., Alikiaii B., Babaei Z., Askari G., Heidari Z., Sharma M. et al. The effects of L-carnitine supplementation on inflammation, oxidative stress, and clinical outcomes in critically Ill patients with sepsis: a randomized, double-blind, controlled trial. *Nutr. J.* 2024;23(1):31. DOI: 10.1186/s12937-024-00934-4.
38. Rahmani S., Roohbakhsh A., Pourbarkhordar V., Hayes A.W., Karimi G. Melatonin regulates mitochondrial dynamics and mitophagy: Cardiovascular protection. *J. Cell Mol. Med.* 2024;28(18):e70074. DOI: 10.1111/jcmm.70074.
39. Wu C.K., Wu C.L., Lee T.S., Kou Y.R., Tarng D.C. Renal tubular epithelial TRPA1 Acts as an oxidative stress sensor to mediate ischemia-reperfusion-induced kidney injury through MAPKs/NF-κB signaling. *Int. J. Mol. Sci.* 2021;22(5):2309. DOI: 10.3390/ijms22052309.
40. Zhu J., Zhang S., Geng Y., Song Y. Transient receptor potential ankyrin 1 protects against sepsis-induced kidney injury by modulating mitochondrial biogenesis and mitophagy. *American Journal of Translational Research.* 2018;10(12):4163–4172.
41. Chen G.D., Zhang J.L., Chen Y.T., Zhang J.X., Wang T., Zeng Q.Y. Insulin alleviates mitochondrial oxidative stress involving upregulation of superoxide dismutase 2 and uncoupling protein 2 in septic acute kidney injury. *Exp. Ther. Med.* 2018;15(4):3967–3975. DOI: 10.3892/etm.2018.5890.

42. Padovani C.M., Wilson R.M., Rodriguez A., Spur B.W., Yin K. Resolvin D2 attenuates LPS-induced macrophage exhaustion. *FASEB J.* 2024;38(7):e23569. DOI: 10.1096/fj.202302521R.
43. Huang Q., Ding Y., Fang C., Wang H., Kong L. The emerging role of ferroptosis in sepsis, opportunity or challenge? *Infect Drug Resist.* 2023;16:5551–5562. DOI: 10.2147/IDR.S419993.
44. Xing Y., Tian T., Zhang X., Yang D., Zhang C., Wang M. et al. Endogenous β3-adrenergic receptor activation alleviates sepsis-induced cardiomyocyte apoptosis via PI3K/AKT signaling patway. *Shock.* 2024;61(6):915–923. DOI: 10.1097/SHK.0000000000002354.
45. Yin S., Peng Y., Lin Y., Wu H., Wang B., Wang X. et al. Bacterial heat shock protein: A new crosstalk between T lymphocyte and macrophage via JAK2/STAT1 pathway in bloodstream infection. *Microbiol. Res.* 2024;282:127626. DOI: 10.1016/j.micres.2024.127626.
46. Gebeyehu G.M., Rashidiani S., Farkas B., Szabadi A., Brandt B., Pap M. et al. Unveiling the role of exosomes in the pathophysiology of sepsis: insights into organ dysfunction and potential biomarkers. *Int. J. Mol. Sci.* 2024;25(9):4898. DOI: 10.3390/ijms25094898.
47. Afshar Y., Ma F., Quach A., Jeong A., Sunshine H.L., Freitas V. et al. Transcriptional drifts associated with environmental changes in endothelial cells. *Elife.* 2023;12:e81370. DOI: 10.7554/eLife.81370.
48. Soubihe Neto N., de Almeida M.C.V., Couto H.O., Miranda C.H. Biomarkers of endothelial glycocalyx damage are associated with microvascular dysfunction in resuscitated septic shock patients. *Microvasc. Res.* 2024;154:104683. DOI: 10.1016/j.mvr.2024.104683.
49. Ishiko S., Huang A., Sun D. Long-term efficacy of liposomal nanocarriers of preassembled lycocalyx in restoring cerebral endothelial glycocalyx in sepsis. *Microvasc. Res.* 2024;154:104684. DOI: 10.1016/j.mvr.2024.104684.
50. Fogagnolo A., Taccone F.S., Campo G., Montanari G., Capatti B., Ferraro G. et al. Impaired platelet reactivity in patients with septic shock: a proof-of-concept study. *Platelets.* 2020;31(5):652–660. DOI: 10.1080/09537104.2019.1663807.
51. Vardon-Bounes F., Gratacap M.P., Groyer S., Ruiz S., Georges B., Seguin T. et al. Kinetics of mean platelet volume predicts mortality in patients with septic shock. *PLoS One*. 2019;14(10):e0223553. DOI: 10.1371/journal.pone.0223553.
52. Chen S., Wu A., Shen X., Kong J., Huang Y. Disrupting the dangerous alliance: Dual anti-inflammatory and anticoagulant strategy targets platelet-neutrophil crosstalk in sepsis. *J. Control. Release.* 2025;379:814–831. DOI: 10.1016/j.jconrel.2025.01.053.
53. Zhu M., Rong X., Li M., Wang S. IL-18 and IL-35 in the serum of patients with sepsis thrombocytopenia and the clinical significance. *Exp. Ther. Med.* 2020;19(2):1251–1258. DOI: 10.3892/etm.2019.8347.
54. Xie Y., Lv H., Chen D., Huang P., Wu S., Shi H. et al. Recombinant human thrombopoietin in alleviating endothelial cell injury in sepsis. *J. Intensive Med.* 2024;4(3):384–392. DOI: 10.1016/j.jointm.2023.12.006.

Autor Information

Naumova Liudmila A. – Dr. Sci. (Med.), Professor, Department of Pathophysiology and General Pathology, Medical Institute, Surgut State University, Surgut, naumovala@yandex.ru, https://orcid.org/0000-0003-1145-3710

Yallyev Mudrinat B. – Postgraduate Student, Department of Pathophysiology and General Pathology, Medical Institute, Surgut State University, Surgut, mudrinat@gmail.com, https://orcid.org/0009-0001-0518-1213

(✉) **Naumova Liudmila A.,** naumovala@yandex.ru

Received on June 18, 2025;
approved after peer review on November 6, 2025;
accepted on November 20, 2025

УДК 616-056.257+616.153.915]:616.718.4-002.4
https://doi.org/10.20538/1682-0363-2026-2-173-183

The Role of Dyslipidemia and Obesity in the Pathogenesis of Osteonecrosis of the Femoral Head

Poryadin G.V.[1], Zakhvatov A.N.[2], Yasnetsov V.V.[3], Mosina L.M.[2], Khaydar D.A.[4], Zakharkin I.A.[2], Tarasova T.V.[2], Shaev A.A.[2]

[1]Pirogov Russian National Research Medical University
1 Ostrovityanov St., 117997 Moscow, Russian Federation

[2]National Research Ogarev Mordovia State University
68 Bolshevistskaya St., 430005 Saransk, Russian Federation

[3]Institute of Biomedical Problems of the Russian Academy of Sciences
76a Khoroshyovskoe Highway, 123007 Moscow, Russian Federation

[4]RUDN University
6 Miklouho-Maclay St., 117198 Moscow, Russian Federation

ABSTRACT

The review focuses on current concepts of the role of obesity, the chronic systemic inflammation it induces, and lipid metabolism disorders in the pathogenesis of osteonecrosis of the femoral head (ONFH) in order to substantiate new approaches to its prevention and treatment. This review analyzes modern fundamental and clinical studies focusing on the relationship between metabolic disorders, chronic inflammation, and osteonecrosis. Specifically, we examined research investigating the molecular mechanisms of adipose tissue dysfunction, lipotoxicity, oxidative stress, and their impact on bone tissue homeostasis.

The analysis established that obesity acts as a systemic risk factor for ONFH development, functioning not merely as a source of mechanical load but also as an initiator of a pathogenic cascade. Dysfunctional adipose tissue leads to chronic low-grade systemic inflammation and oxidative stress. Together, these factors provoke endothelial dysfunction, impair perfusion of the femoral head bone tissue, and induce lipotoxicity in the bone marrow. Consequently, at the local level, this cascade suppresses osteogenesis, simultaneously enhances bone resorption, and triggers osteocyte apoptosis.

Systemic metabolic and inflammatory disruptions initiated by obesity underlie impaired bone remodeling, ischemia, and necrosis of the femoral head subchondral bone. Therefore, the correction of body weight and associated metabolic disorders should be considered as an integral part of a comprehensive strategy for treating ONFH and preventing its progression. This integrated approach may improve the outcomes of joint-preserving interventions and delay the need for total hip arthroplasty in young patients.

Keywords: avascular necrosis of the femoral head, obesity, chronic systemic inflammation, dyslipidemia, oxidative stress, pathogenesis

Conflict of interest. The authors declare the absence of obvious or potential conflicts of interest related to the publication of this article.

Source of financing. The authors state that they received no funding for this study.

For citation: Poryadin G.V., Zakhvatov A.N., Yasnetsov V.V., Mosina L.M., Khaydar D.A., Zakharkin I.A., Tarasova T.V., Shaev A.A. The Role of Dyslipidemia and Obesity in the Pathogenesis of Osteonecrosis of the Femoral Head. *Bulletin of Siberian Medicine.* 2026;25(2):173–183. https://doi.org/10.20538/1682-0363-2026-2-173-183.

✉ *Shaev Aleksey A.,* schaev.leha2017@yandex.ru

Роль дислипидемии и ожирения в патогенезе асептического некроза головки бедренной кости

Порядин Г.В.[1], Захватов А.Н.[2], Яснецов В.В.[3], Мосина Л.М.[2], Хайдар Д.А.[4], Захаркин И.А.[2], Тарасова Т.В.[2], Шаев А.А.[2]

Российский национальный исследовательский медицинский университет (РНИМУ) им. Н.И. Пирогова
Россия, 117997, г. Москва, ул. Островитянова, 1

Национальный исследовательский Мордовский государственный университет (МГУ) им. Н.П. Огарёва
Россия, 430005, г. Саранск, ул. Большевистская, 68

Государственный научный центр РФ «Институт медико-биологических проблем Российской академии наук» (ГНЦ РФ – ИМБП РАН)
Россия, 123007, г. Москва, Хорошёвское шоссе, 76а

Российский университет дружбы народов (РУДН) им. П. Лумумбы
Россия, 117198, г. Москва, ул. Миклухо-Маклая, 6

РЕЗЮМЕ

Представлен обзор современных данных о роли ожирения, индуцированного им хронического системного воспаления и нарушений липидного обмена в патогенезе асептического некроза головки бедренной кости (АНГБК) для обоснования новых подходов к профилактике и лечению. Проведен анализ современных фундаментальных и клинических исследований, посвященных взаимосвязи метаболических нарушений, хронического воспаления и остеонекроза. Рассмотрены работы, изучающие молекулярные механизмы дисфункции жировой ткани, липотоксичности, окислительного стресса и их влияния на гомеостаз костной ткани.

Установлено, что ожирение выступает системным фактором риска развития АНГБК, действуя не только как источник механической нагрузки, но и как инициатор патогенетического каскада. Дисфункциональное состояние жировой ткани приводит к развитию хронического вялотекущего системного воспаления и окислительного стресса. В совокупности эти факторы провоцируют развитие эндотелиальной дисфункции, ухудшают перфузию костной ткани головки бедренной кости и вызывают явления липотоксичности в костном мозге. Следствием этого на локальном уровне становится угнетение остеогенеза, одновременное усиление резорбции кости и апоптоз остеоцитов.

Инициируемые ожирением системные метаболические и воспалительные сбои формируют основу для нарушения костного ремоделирования, ишемии и некроза субхондральной кости головки бедренной кости. Следовательно, коррекция массы тела и сопутствующих метаболических расстройств должна рассматриваться как неотъемлемая часть комплексной стратегии лечения и вторичной профилактики прогрессирования АНГБК. Такой подход может улучшить результаты органосохраняющих вмешательств и отсрочить необходимость эндопротезирования у молодых пациентов.

Ключевые слова: асептический некроз головки бедренной кости, ожирение, хроническое системное воспаление, дислипидемия, окислительный стресс, патогенез

Конфликт интересов. Авторы декларируют отсутствие явных и потенциальных конфликтов интересов, связанных с публикацией настоящей статьи.

Источник финансирования. Авторы заявляют об отсутствии финансирования при проведении исследования.

Для цитирования: Порядин Г.В., Захватов А.Н., Яснецов В.В., Мосина Л.М., Хайдар Д.А., Захаркин И.А., Тарасова Т.В., Шаев А.А. Роль дислипидемии и ожирения в патогенезе асептического некроза головки бедренной кости. *Бюллетень сибирской медицины.* 2026;25(2):173–183. https://doi.org/10.20538/1682-0363-2026-2-173-183.

INTRODUCTION

Osteonecrosis of the femoral head (ONFH) remains one of the most common and difficult-to-treat pathologies in orthopedic practice, primarily affecting young and middle-aged patients. In different countries, the incidence of ONFH ranges from 1.5 to 3.0 per 100,000 population with a continuing upward trend. The disease is characterized by rapid progression: without effective treatment, 94% of patients develop femoral head collapse within 5 years followed by loss of hip joint function [1–3]. Despite certain advances in the development of organ-preserving methods, the difficulties of early diagnosis as well as the presence of unfavorable prognostic factors often lead to ineffective treatment and the need for total hip arthroplasty. In the USA and Europe, 2–10% of all hip arthroplasty surgeries are performed for ONFH, while in Asian countries, this figure reaches 60%. Although total hip arthroplasty improves the quality of life, it creates serious medical, social, and economic problems due to the limited service life of endoprostheses and the high probability of reoperations, especially considering that most patients with ONFH are young people [4, 5]. The need for an in-depth study of the pathogenetic mechanisms of ONFH and the search for fundamentally new ways to prevent it are becoming obvious.

The causes of ONFH are divided into traumatic, most often caused by fractures of the proximal femur, and non-traumatic, among which conditions associated with metabolic syndrome occupy a special place. Obesity as one of the key components of metabolic syndrome is not only a global health problem, but also a potential modifiable pathogenetic factor that requires detailed consideration in ONFH development. By 2035, almost two billion people are expected to suffer from obesity. It underlies the development of a cascade of complications, including type 2 diabetes mellitus, cardiovascular diseases, non-alcoholic fatty liver disease, malignant neoplasms, musculoskeletal diseases, and psychological disorders, leading to increased morbidity, mortality, and healthcare costs worldwide [6].

The key pathogenetic link between obesity and these complications is the chronic low-grade systemic inflammation induced by obesity. Dysfunctional adipose tissue produces excess proinflammatory adipokines and cytokines, while simultaneously suppressing the synthesis of anti-inflammatory factors. This process is accompanied by severe lipid metabolism disorders, insulin resistance, and oxidative stress, creating a vicious cycle of metabolic and inflammatory damage [7].

In terms of ONFH pathogenesis, obesity in addition to the mechanical load factor is a condition that systemically disrupts metabolic and immune homeostasis. It directly contributes to the key pathogenetic mechanisms of ONFH: it exacerbates endothelial dysfunction, dyslipidemia, and hypercoagulation, promotes intravascular fat embolism, increases intraosseous pressure due to adipocyte hyperplasia, and creates persistent chronic systemic inflammation. This inflammation mediated by altered secretion of adipokines and cytokines damages the vascular endothelium, disrupts bone remodeling, and accelerates osteocyte apoptosis. Therefore, studying the causal relationships between obesity-induced metabolic inflammation and the development of ONFH is important to identify new potential biomarkers and therapeutic strategies aimed at correcting the metabolic and inflammatory status as part of a comprehensive approach to ONFH treatment [8–10] (Fig. 1).

The review aims to systematize current knowledge on the relationship between obesity, lipid metabolism disorders, chronic systemic inflammation and the development of ONFH. The article will discuss the molecular basis of obesity-induced inflammation as well as the integrated pathways through which these systemic disorders lead to ischemia, impaired remodeling, and necrosis of the femoral head.

SEARCH STRATEGY

A comprehensive systematic search was performed in electronic databases indexed in PubMed to identify relevant publications. The search covered the period from January 2020 to December 2025. The search strategy was based on using combinations of key terms and their synonyms: (“avascular necrosis” OR “osteonecrosis” OR “aseptic necrosis”) AND (“femoral head” OR “hip head”) AND (“obesity” OR “adipose tissue” OR “metabolic syndrome” OR “lipid metabolism” OR “dyslipidemia” OR “hyperlipidemia”). A manual search was also conducted on the reference lists of included articles and relevant review papers.

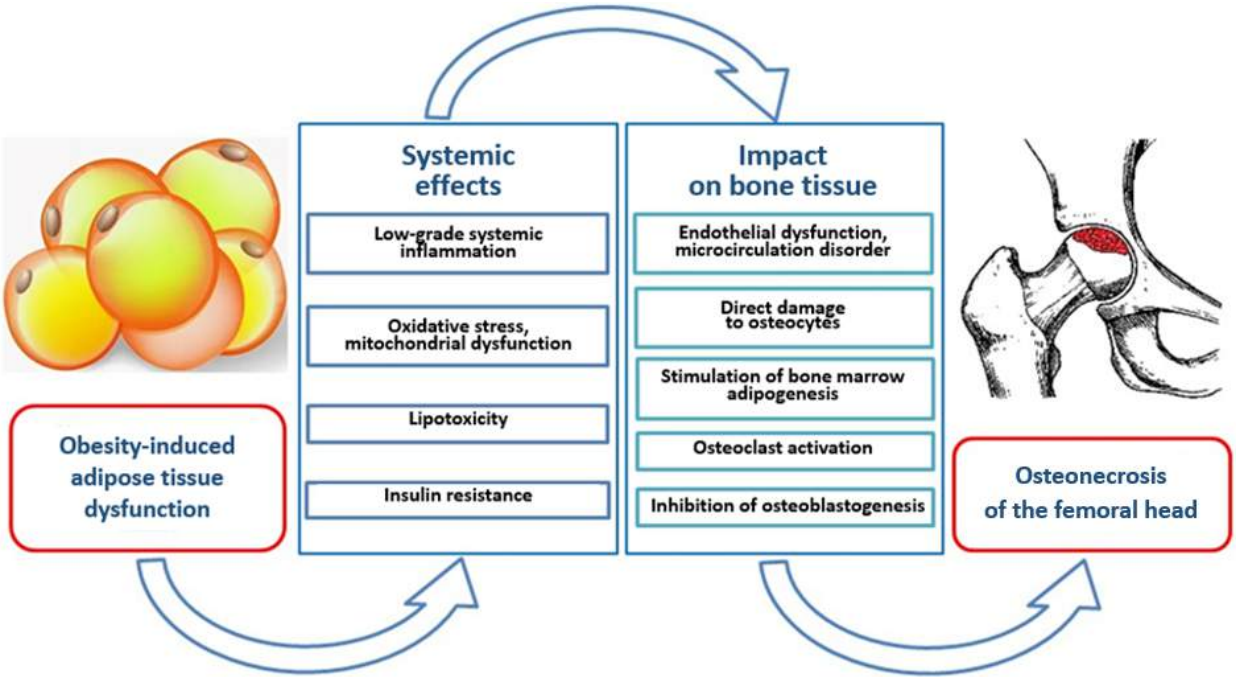

Fig. 1. The role of dyslipidemia and obesity in the pathogenesis of osteonecrosis of the femoral head

INCLUSION AND EXCLUSION CRITERIA

The inclusion criteria were original studies (clinical and experimental in animals), systematic reviews, and case reports focusing on the relationship between obesity, lipid metabolism parameters, and the development or progression of ONFH, as well as the description of the pathogenetic mechanisms linking metabolic disorders to bone damage. The exclusion criteria were articles devoted to secondary ONFH solely due to trauma, decompression sickness, and corticosteroid use (without analyzing concomitant metabolic factors); articles that mention obesity or dyslipidemia only as a demographic characteristic without analyzing their pathogenetic role; isolated case reports without analyzing mechanisms; letters to the editor, conference abstracts; and the absence of a full-text article.

DATA EXTRACTION

The authors independently extracted the following data from the selected studies: first author's last name and year of publication, study design, biomarkers examined, experimental models used, the strength of the association between metabolic parameters and ONFH risk, described pathogenetic pathways, and the authors' conclusions about the role of obesity and dyslipidemia in the pathogenesis of the disease. Any disagreements that arose between the co-authors during the data extraction phase were resolved through a joint discussion.

RESULTS

The initial search using the developed strategy revealed 101 records. After applying a time filter (excluding publications published before 2020), 48 papers were excluded, leaving 53 studies for further consideration. At the title and abstract screening stage, 25 articles were excluded because their subject matter did not match the aim of this review. Evaluating the full text of each of the remaining 28 articles to determine whether they met the inclusion criteria resulted in the exclusion of six studies. An additional manual search of the reference lists of relevant publications allowed us to include 28 more studies that met all the criteria. Thus, the final set of analyzed works consisted of 50 full-text articles, which ensured a comprehensive coverage of the topic and representative data for subsequent qualitative synthesis.

DISCUSSION

Adipose tissue dysfunction, lipid metabolism disorders, and chronic inflammation form a single pathogenetic pathway. Its final result is a combined damage to the vascular network and cell populations

of the femoral head, which is confirmed as a mechanism of ONFH development. Research has demonstrated that specific changes in the lipid profile collectively contribute to the progression of ONFH by disrupting the integrity of cell membranes, causing oxidative stress, leading to endothelial dysfunction, and impairing the regulation of signaling pathways involved in bone cell survival and function [11, 12].

DISORDERS OF LIPID METABOLISM

The relationship between dyslipidemia and ONFH is bidirectional, as the presence of necrotized bone tissue leads to destabilization of systemic lipid metabolism, which aggravates the pathological process in the bone and makes it self-sustaining [13, 14]. Severe disorders of systemic lipid metabolism manifested by hypercholesterolemia, hypertriglyceridemia, increased levels of low-density lipoprotein cholesterol (LDL-C) and apolipoprotein B, as well as decreased levels of high-density lipoprotein cholesterol (HDL-C) and adiponectin, contribute to the formation of fat emboli, which, in combination with endothelial dysfunction exacerbated by dyslipidemia, disrupts the microcirculation of subchondral bone tissue and leads to its ischemia, triggering osteonecrosis [15]. X. Yu et al. (2024) demonstrate that non-HDL-C and apolipoprotein B levels are risk factors for the progression of ONFH, serving as a clinically accessible reflection of the role of lipid metabolism disorders in the development of this pathology [16].

Excess lipids and free fatty acids affecting the differentiation of mesenchymal stem cells, which are common precursors of adipocytes and osteoblasts, lead to an imbalance between adipogenesis and osteogenesis in the bone marrow in favor of the former. Excessive accumulation of adipocytes in the bone marrow caused by both excess lipid production and impaired lipid elimination mechanisms leads to intraosseous hypertension and reduced bone tissue perfusion. R. Toribio-Fernández et al. (2024) demonstrated that apolipoprotein E gene polymorphism may increase the likelihood of subclinical atherosclerosis progression due to impaired reverse cholesterol transport [17]. Moreover, a study conducted by Y. Chen et al. (2025) showed a decrease in the expression of apolipoprotein E in articular cartilage samples of the hip joint in patients with ONFH compared to intact cartilage, which may indicate common mechanisms for the development of ONFH and vascular pathology [18].

During lipolysis of bone marrow adipocytes, saturated fatty acids (SFA) are released, which are key mediators of damage. In particular, palmitic acid has multiple negative effects on bone metabolism. Palmitate inhibits the expression of key osteogenic transcription factors (Runx2, DLX5) and enhances adipogenesis through activation of peroxisome proliferator-activated receptor gamma (PPARγ) and CCAAT/enhancer-binding protein alpha (C/EBPα). In addition, palmitate induces the secretion of proinflammatory cytokines (interleukin-6 (IL-6) and -8 (IL-8)), which activate the RANK/RANKL/OPG (receptor activator of nuclear transcription factor kappa B / receptor activator of nuclear transcription factor kappa B ligand / osteoprotegerin) ligand – receptor system, promoting the differentiation and activation of osteoclasts and enhancing bone resorption [19].

Activation of the ERK signaling pathway in response to palmitate leads to apoptosis of mesenchymal stem cells and osteoblasts. In this case, the critical factor is not the absolute amount of SFA, but the balance between saturated and monounsaturated fatty acids (MUFA). In particular, oleic acid has a protective effect, neutralizing the lipotoxicity of palmitate due to its esterification into triglycerides and deposition into lipid droplets. A high intracellular SFA/MUFA ratio in bone marrow may potentially act as a prognostic marker for the risk of developing ONFH [20].

Different lipids have opposing causal relationships with this disease. Phosphatidylcholine and phosphatidylethanolamine provide a protective effect being key components of cell membranes that ensure their integrity, participating in lipid transport, and possessing anti-inflammatory activity. Elevated levels of these may reflect compensatory mechanisms aimed at membrane restoration. Conversely, elevated levels of triacylglycerols and sterol esters are associated with an increased risk of ONFH due to lipotoxicity and adipocyte hypertrophy, which further exacerbates tissue damage and promotes the progression of osteonecrosis. The accumulation of sterol esters reflects a disturbance in the reverse transport of cholesterol, which brings the pathogenesis of ONFH closer to atherosclerosis [21–23].

Thus, lipid metabolism disorders play a multifaceted role in the pathogenesis of ONFH acting both as a cause and a consequence of osteonecrosis. The identification of specific lipid markers opens new perspectives for early diagnosis, screening of at-risk groups, and the development of targeted therapeutic strategies. Further research focusing on the mechanisms of local lipid metabolism in hip joint tissue is needed to fully elucidate the role of lipid biomarkers and their potential as therapeutic targets.

ADIPOSE TISSUE DYSFUNCTION AS A CAUSAL FACTOR FOR SYSTEMIC INFLAMMATION

Accumulated data indicate that in the adipose tissue of individuals with normal body weight, the majority of resident macrophages are of the anti-inflammatory M2 phenotype. Macrophages maintain tissue homeostasis by promoting repair and increasing insulin sensitivity, releasing anti-inflammatory cytokines, such as interleukin-4, -10, -11, and -13 (IL-4, IL-10, IL-11, IL-13), IL-1 receptor antagonist (IL-1Ra), arginase-1, and transforming growth factor-β (TGFβ), as well as anti-inflammatory adipokines, such as adiponectin and apelin [24]. As excess lipids accumulate, adipocytes undergo hypertrophy, which results in the development of local hypoxia zones, as the enlarged cells become distant from the capillary network. Hypoxia induces the expression of the transcription factor HIF-1α, which triggers metabolic reprogramming of cells associated with the activation of glycolytic pathways, and also causes increased production of proinflammatory cytokines and chemotactic factors, including monocyte chemotactic protein-1 (MCP-1), which attract monocytes from the bloodstream to adipose tissue and promote their activation [25].

Polarization of adipose tissue macrophages towards the proinflammatory M1 phenotype occurs. Activated macrophages become a source of proinflammatory mediators: tumor necrosis factor-alpha (TNFα), IL-6, and interleukin-1β (IL-1β), as well as plasminogen activator inhibitor-1 (PAI-1) and adipokines, such as leptin, visfatin, and resistin [26]. Thus, a vicious cycle of inflammation develops: dysfunctional adipocytes attract macrophages, which, upon activation, intensify inflammation and further exacerbate adipocyte dysfunction and insulin resistance. This localized inflammatory process in adipose tissue is the primary source of chronic low-grade systemic inflammation, which determines the metabolic and vascular complications of obesity.

Dysregulation of adipokine secretion in obesity generates a powerful endocrine signal aimed at damaging the vascular endothelium. Despite differences in their primary receptors and signaling pathways, leptin, visfatin, and resistin converge in activating key proinflammatory transcription factors, primarily nuclear factor kappa-B (NF-κB) [27, 28]. This leads to the induction of oxidative stress and suppression of endothelial antioxidant protection, a decrease in the bioavailability of nitric oxide (II) (NO) due to the suppression of endothelial NO synthase expression, and the creation of a proadhesive and prothrombotic state through an increase in the expression of adhesion molecules. Elevated levels of IL-1β promote the recruitment of a large number of immune cells and enhance local inflammation by increasing the expression of vascular cell adhesion molecule-1 (VCAM-1), intercellular adhesion molecule-1 (ICAM-1), and MCP-1 [29, 30]. Hypercoagulation caused by high PAI-1 levels and platelet activation creates the preconditions for microthrombosis. The resulting endothelial dysfunction includes loss of vasodilatory properties, increased permeability, and adhesion, which directly predisposes to microthrombosis, impaired perfusion, and subchondral bone ischemia.

Proinflammatory cytokines (TNFα, IL-1β, and IL-6) act as direct mediators of insulin resistance by disrupting the insulin receptor signal transduction. IL-1β leads to activation of the serine/threonine kinase, Janus kinase (JAK-1), which inactivates insulin receptor substrates (IRS-1,2), resulting in suppression of insulin signaling and subsequent elevation of blood glucose levels. TNFα directly interferes with peripheral glucose uptake by enhancing serine phosphorylation of IRS-1, inhibits translocation of glucose transporter-4 (GLUT-4) to the plasma membrane, and leads to peripheral insulin resistance [31]. These molecular mechanisms determine the development of persistent peripheral insulin resistance, linking chronic inflammation to metabolic dysfunction.

A study by H. Zhang et al. (2023) demonstrated that the microRNA miR-22-3p contained in adipocyte exosomes affects skeletal muscle and promotes the development of insulin resistance by reducing the levels of signaling molecules, such

as phosphorylated protein kinase B (p-AKT) and IRS-1 (p-IRS-1) [32]. Resistance of dysfunctional adipocytes to the antilipolytic effect of insulin leads to the uncontrolled breakdown of triglyceride stores, resulting in an increased release of free fatty acids (FFA) into the systemic circulation, a key component of lipotoxicity. Thus, adipose tissue dysfunction in obesity manifested through mechanisms of endocrine dysregulation and immune activation creates a systemic metabolic and inflammatory environment that is a risk factor for ONFH development and progression.

Other factors in the chronic inflammatory process observed in metabolic syndrome are receptors of the innate immune system, such as Toll-like receptors (TLR). TLR are involved in pathogen recognition and modulate the innate immune response by activating downstream inflammatory signaling pathways that lead to the release of various cytokines (TNFα, IL-6, IL-1β, and monocyte chemotactic protein-1 (MCP-1)). The immune response is triggered by TLR recognition of ligands, which include pathogen-associated molecular patterns (PAMPs) released by pathogens (e.g. lipopolysaccharides) and damage-associated molecular patterns (DAMPs) released by damaged inflamed tissues [33]. Among DAMPs, many endogenous ligands – SFA, modified LDL-C, advanced glycation end products, extracellular matrix degradation products, and heat shock proteins – are recognized by TLRs, especially TLR2 and TLR4, and activate the proinflammatory cascade [34].

A systemic inflammatory response causes a hypercoagulable state, accompanied by endothelial damage, which also increases the likelihood of ONFH. Endothelial cells respond to injury by producing proinflammatory molecules, including IL-1β, interferons, TNFα, colony-stimulating factors, and vascular cell adhesion molecule-1 (VCAM-1). The proinflammatory background at the site of osteonecrosis induces macrophages, neutrophils, and other immune cells to migrate to damaged endothelial cells and promote further development of inflammation, which leads to acute and chronic changes in vascular permeability. Normally, resolution of inflammation eliminating the consequences of damage promotes tissue regeneration. However, endothelial dysfunction causes prolonged inflammation, impeding bone tissue restoration. Damaged endothelium activated platelet-derived factors and disrupted extracellular matrix serve as sources of DAMPs.

Various immune cells recognize these stimuli via pattern recognition receptors (PRR) and further activate a cascade of inflammatory responses, exacerbating endothelial damage. In addition to intensive secretion of reactive oxygen species and proteolytic enzymes, activated neutrophils are capable of releasing DNA into the extracellular space with the formation of neutrophil extracellular traps (NETs), creating a prothrombotic state [35]. The scaffold formed by DNA fibers and histone networks activates platelets, leukocytes, erythrocytes, and plasma proteins. The microvessels of the femoral head contain significant numbers of neutrophils and NETs in patients with ONFH. NET-mediated activation of the coagulation pathway and inhibition of anticoagulation potentially play a role in the pathogenesis of ONFH. M. Nonokawa et al. (2020) showed that intravenous administration of NET-forming neutrophils is associated with ischemic changes in femoral head osteocytes [36].

Chronic systemic inflammation is not simply an accompanying phenomenon, but a significant pathogenetic factor determining the progression of ONFH and affecting the outcomes of organ-preserving surgeries. Systemic inflammation creates an unfavorable background impairing the processes of neoangiogenesis and osteogenesis necessary for successful repair after decompression and contributing to microcirculatory disorders and bone resorption. C. Li et al. (2025) found that preoperative systemic immune-inflammatory index (SII), which comprehensively reflects the activity of neutrophils, lymphocytes, and platelets, serves as an independent prognostic marker of increased risk of failure after medullary canal decompression [37].

Thus, experimental and clinical studies consistently confirm that disturbances occurring in dysfunctional adipose tissue through mechanisms of endotheliopathy, lipotoxicity, and chronic inflammation create a pathological environment in the femoral head leading to ischemia, suppressed repair, and necrosis. Dyslipidemia, free fatty acid flux, oxidative stress, and lipotoxicity act synergistically, damaging the femoral head vasculature, inhibiting bone formation, and triggering bone cell death. These systemic metabolic disturbances create a foundation for local risk factors to induce ischemic necrosis.

OXIDATIVE STRESS

Oxidative stress is a fundamental pathobiochemical mechanism that mediates the transformation of systemic signals into direct cellular damage in the subchondral region of the femoral head. Reactive oxygen species (ROS) are natural byproducts of aerobic respiration in the mitochondria. During oxidative phosphorylation, which includes the Krebs cycle and the respiratory chain enzyme complexes, most of the oxygen is used for the synthesis of ATP, and only a small proportion is inevitably converted into ROS due to a small leakage of electrons, which leads to the direct reduction of oxygen to radicals. Low concentrations of ROS produced by osteocyte mitochondria are either neutralized by the antioxidant system or can perform signaling functions, for example, by activating the transcription factor Nrf2 and promoting osteoblast differentiation during osteogenesis [38]. However, excessive intake of free fatty acids leads to their increased oxidation in mitochondria, which is accompanied by increased ROS formation and the development of oxidative stress.

Adiponectin and apelin act as protective factors in maintaining metabolic homeostasis and redox balance. Adiponectin has an insulin-sensitizing effect; a decrease in its level deprives tissues of the ability to effectively enhance fatty acid oxidation by activating AMP-activated protein kinase (AMPK) and peroxisome proliferator-activated receptor alpha (PPARα) [39–41]. Apelin promotes the synthesis of antioxidant enzymes via the Ras/Raf/mitogen-activated protein kinase (MAPK/ERK) and AMPK pathways and suppresses the expression of pro-oxidant enzymes [42, 43]. Their reduction in obesity and chronic inflammation directly contributes to the development and worsening of insulin resistance and oxidative stress.

Excess of ROS leads to a reduction in the population of viable osteocytes in several pathways. First, excessive ROS production is one of the mechanisms of programmed osteocyte death. High levels of ROS increase the phosphorylation of p66(shc), a key mediator of osteocyte apoptosis. Phosphorylated p66(shc) at Ser-36 is transported into the mitochondria, triggering an oxidative stress cascade and the release of cytochrome C, which ultimately activates caspases and leads to programmed osteocyte death. Notably, p66(shc) also has oxidoreductase activity, creating a vicious cycle by further increasing mitochondrial ROS production [44]. Secondly, excessive ROS production inhibits the differentiation of mesenchymal stem cells into osteoblasts by blocking the Wnt/beta-catenin pathway. The retention of the beta-catenin-binding transcription factor FoxO in the nucleus blocks its interaction with the TCF/LEF signaling pathway, suppressing the expression of key early osteoblastogenesis genes Runx2 and Osterix. It should be noted that the same ROS, while suppressing osteoblastogenesis, simultaneously stimulate the activity and proliferation of osteoclasts. It has been shown that the removal of ROS inhibits osteoclastogenesis induced by the receptor activator of NF-κB ligand (RANKL) [45].

Mitochondria being the centers of ROS production under pathological conditions are themselves most sensitive to them. Exceeding the compensatory potential of the antioxidant system causes oxidative stress and creates conditions for mitochondrial membrane damage, causing massive electron leakage in the respiratory enzyme chain, which reinforces the intracellular redox imbalance. Free radicals also attack mitochondria, affecting the activity of enzymatic complexes in the membrane of these organelles and reducing their efficiency. This, in turn, disrupts oxidative phosphorylation and leads to a decrease in ATP synthesis. Mitochondrial membrane damage promotes the leakage of Ca^{2+} and cytochrome C into the cytosol and triggers apoptosis by activating the caspase cascade [46].

Some mitochondrial components due to their similarity to bacterial and viral molecules can act as PAMPs and, consequently, as ligands for PRRs, for example, cyclic mitochondrial DNA. In addition, mitochondrial DNA, N-formyl peptide, cardiolipin, mitochondrial RNA, and fumarate can act as DAMPs that activate PRRs and induce an inflammatory response [47, 48]. Mitochondrial DNA leakage into the cytoplasm that occurs during mitochondrial damage leads to activation of the cGAS-STING pathway, which can activate the NF-κB signaling pathway, and activated NF-κB induces the production of proinflammatory stimulators, including TNFα, IL-1β, and IL-6 [49]. Mitochondrial DNA is rich in CpG islands, a structure that can be recognized by TLR9 and directly activate the NF-κB signaling pathway, thereby triggering inflammation. Unlike

nuclear DNA, it is more susceptible to mutations and oxidation. The accumulation of damaged mitochondrial DNA disrupts the homeostasis of these organelles, exacerbating mitochondrial damage and leading to their inability to control the inflammatory response in bone tissue [50]. As a result, a decrease in osteoblast numbers coupled with increased osteoclast activity leads to bone resorption rates exceeding the rate of bone formation. This microenvironment is unable to support healthy bone tissue. Therefore, maintaining proper mitochondrial function to prevent excessive ROS production is critical for both bone health and the treatment of associated metabolic diseases.

Oxidative stress is also a causative factor in endothelial dysfunction, which disrupts the regulation of vascular tone and blood flow, leading to bone ischemia. Modulation of the vascular system is crucial for initiating the angiogenesis – osteogenesis process, which is necessary for the complete regeneration and restoration of osteocytes in necrotic areas. Therefore, blocking oxidative stress processes represents a potentially important therapeutic target in the comprehensive treatment and prevention of ONFH progression.

CONCLUSION

The analysis suggests that obesity is not simply a mechanical overload factor, but a systemic metabolic and inflammatory disease that forms a universal pathogenic basis for the development and progression of ONFH. Adipose tissue dysfunction, acting as a driver of chronic low-grade systemic inflammation, through a complex set of interconnected mechanisms – endocrine dysregulation (adipokine imbalance), oxidative stress, lipotoxicity, and endothelial dysfunction – creates an environment in the femoral head that leads to ischemia, suppression of bone remodeling, and osteocyte death. Dyslipidemia exacerbates these processes, contributing to microthrombosis, fat embolism, and disruption of intraosseous lipid homeostasis.

Thus, it can be concluded that the pathogenesis of ONFH in obesity appears to be a cascade of processes initiated at the systemic level and resulting in localized bone damage. Integrating measures aimed at correcting body weight and lipid metabolism into comprehensive prevention and treatment regimens will not only improve the immediate results of organ-preserving surgeries but also, by addressing the underlying causes of the disease, improve the long-term prognosis and delay or avoid the need for hip arthroplasty, which is especially important for young patients. Overall, improving our understanding of the role of metabolic factors in ONFH opens new opportunities for prevention, early diagnosis, and the development of personalized treatments.

REFERENCES

1. Quan H., Ren C., He Y., Wang F., Dong S., Jiang H. Application of biomaterials in treating early osteonecrosis of the femoral head: research progress and future perspectives. *Acta Biomater.* 2023;164:15–73. DOI: 10.1016/j.actbio.2023.04.005.
2. Quan H., Ren C., Xie H., He Z., Ding H., Li J. et al. An injectable hydrogel loaded with miRNA nanocarriers promotes vessel-associated osteoclast (VAO)-mediated angiogenesis and bone regeneration in osteonecrosis of the rat femoral head. *Biomaterials.* 2025;320:123252. DOI: 10.1016/j.biomaterials.2025.123252.
3. Konarski W., Poboży T., Śliwczyński A., Kotela I., Krakowiak J., Hordowicz M. et al. Avascular necrosis of femoral head-overview and current state of the art. *Int. J. Environ. Res. Public Health*. 2022 ;19(12):7348. DOI: 10.3390/ijerph19127348.
4. Zheng C., Wu Y., Xu J., Liu Y., Ma J. Exosomes from bone marrow mesenchymal stem cells ameliorate glucocorticoid-induced osteonecrosis of femoral head by transferring microRNA-210 into bone microvascular endothelial cells. *J. Orthop. Surg. Res.* 2023;18(1):939. DOI: 10.1186/s13018-023-04440-x.
5. Konarski W., Poboży T., Konarska K., Śliwczyński A., Kotela I., Hordowicz et al. Osteonecrosis related to steroid and alcohol use-an update on pathogenesis. *Healthcare (Basel).* 2023;11(13):1846. DOI: 10.3390/healthcare11131846.
6. Müller T.D., Blüher M., Tschöp M.H., DiMarchi R.D. Anti-obesity drug discovery: advances and challenges. *Nat. Rev. Drug Discov.* 2022;21(3):201–223. DOI: 10.1038/s41573-021-00337-8.
7. Khanna D., Khanna S., Khanna P., Kahar P., Patel B.M. Obesity: a chronic low-grade inflammation and its markers. *Cureus.* 2022;14(2):e22711. DOI: 10.7759/cureus.22711.
8. Lin X., Li H. Obesity: epidemiology, pathophysiology, and therapeutics. *Front. Endocrinol. (Lausanne).* 2021;12:706978. DOI: 10.3389/fendo.2021.706978.
9. Peng W., Zhang L., Wen F., Tang X., Zeng L., Chen J. et al. Trends and disparities in non-communicable diseases in the Western Pacific region. *Lancet Reg. Health West Pac.* 2023;43:100938. DOI: 10.1016/j.lanwpc.2023.100938.
10. Müller T.D., Blüher M., Tschöp M.H., DiMarchi R.D. Anti-obesity drug discovery: advances and challenges. *Nat. Rev. Drug. Discov.* 2022;21(3):201–223. DOI: 10.1038/s41573-021-00337-8.
11. Yan Y., Wang J., Wang Y., Wu W., Chen W. Research on lipidomic profiling and biomarker identification for osteonecrosis of the femoral head. *Biomedicines.* 2024;12(12):2827. DOI: 10.3390/biomedicines12122827.

12. Yu X., Zhang S., Zhang B., Dai M. Relationship of idiopathic femoral head necrosis with blood lipid metabolism and coagulation function: A propensity score-based analysis. *Front. Surg.* 2023;9:938565. DOI: 10.3389/fsurg.2022.938565.
13. Baek S.H., Kim K.H., Lee W.K., Hong W., Won H., Kim S.Y. Abnormal lipid profiles in nontraumatic osteonecrosis of the femoral head: a comparison with osteoarthritis using propensity score matching. *J. Bone Joint Surg. Am.* 2022;104(Suppl. 2):19–24. DOI: 10.2106/JBJS.20.00520.
14. Wang C., Cen C., Su H., Peng Y., Wang T., Li J. et al.. Integrated multi-omics analysis identifies lipid metabolism biomarkers in ONFH and reveals therapeutic potential of retinoic acid. *Sci .Rep.* 2025;15(1):30716. DOI: 10.1038/s41598-025-13703-y.
15. George G., Lane J.M. Osteonecrosis of the femoral head. *J. Am. Acad. Orthop. Surg. Glob. Res. Rev.* 2022;6(5):e21.00176. DOI: 10.5435/JAAOSGlobal-D-21-00176.
16. Yu X., Dou S., Lu L., Wang M., Li Z., Wang D. Relationship between lipid metabolism, coagulation and other blood indices and etiology and staging of non-traumatic femoral head necrosis: a multivariate logistic regression-based analysis. *J. Orthop. Surg. Res.* 2024;19(1):251. DOI: 10.1186/s13018-024-04715-x.
17. Toribio-Fernández R., Tristão-Pereira C., Carlos Silla-Castro J., Callejas S., Oliva B., Fernandez-Nueda I. et al. Apolipoprotein E-ε2 and Resistance to Atherosclerosis in Midlife: The PESA Observational Study. *Circ. Res.* 2024;134(4):411–424. DOI: 10.1161/CIRCRESAHA.123.323921.
18. Chen Y., Zhou Z., Che H., Li D. Lipid metabolism and osteonecrosis: unraveling causal mechanisms via multi-omics and mendelian randomization. *Front. Physiol.* 2025;16:1642153. DOI: 10.3389/fphys.2025.1642153.
19. Ren Y., Deng Z., Gokani V., Kutschke M., Mitchell T.W., Aruwajoye O. et al. Anti-interleukin-6 therapy decreases hip synovitis and bone resorption and increases bone formation following ischemic osteonecrosis of the femoral head. *J. Bone Miner. Res.* 2021;36(2):357–368. DOI: 10.1002/jbmr.4191.
20. Li L., Zhao S., Leng Z., Chen S., Shi Y., Shi L. et al. Pathological mechanisms and related markers of steroid-induced osteonecrosis of the femoral head. *Ann. Med.* 2024;56(1):2416070. DOI: 10.1080/07853890.2024.2416070.
21. Posor Y., Jang W., Haucke V. Phosphoinositides as membrane organizers. *Nat. Rev. Mol. Cell Biol.* 2022;23(12):797–816. DOI: 10.1038/s41580-022-00490-x.
22. Motta F., Timilsina S., Gershwin M.E., Selmi C. Steroid-induced osteonecrosis. *J. Transl. Autoimmun.* 2022;5:100168. DOI: 10.1016/j.jtauto.2022.100168.
23. Yan Y., Wang J., Huang D., Lv J., Li H., An J. et al. Plasma lipidomics analysis reveals altered lipids signature in patients with osteonecrosis of the femoral head. *Metabolomics.* 2022;18(2):14. DOI: 10.1007/s11306-022-01872-0.
24. Taylor E.B. The complex role of adipokines in obesity, inflammation, and autoimmunity. *Clin. Sci. (Lond.).* 2021;135(6):731–752. DOI: 10.1042/CS20200895.
25. Singh S., Anshita D., Ravichandiran V. MCP-1: Function, regulation, and involvement in disease. *Int. Immunopharmacol.* 2021;101(Pt. B):107598. DOI: 10.1016/j.intimp.2021.107598.
26. Planat-Benard V., Varin A., Casteilla L. MSCs and inflammatory cells crosstalk in regenerative medicine: concerted actions for optimized resolution driven by energy metabolism. *Front. Immunol.* 2021;12:626755. DOI: 10.3389/fimmu.2021.626755.
27. Romacho T., Valencia I., Ramos-González M., Vallejo S., López-Esteban M., Lorenzo O. et al. Visfatin/eNampt induces endothelial dysfunction *in vivo*: a role for toll-like receptor 4 and NLRP3 inflammasome. *Sci. Rep.* 2020;10(1):5386. DOI: 10.1038/s41598-020-62190-w.
28. Obradovic M., Sudar-Milovanovic E., Soskic S., Essack M., Arya S., Stewart A.J. et al. Leptin and obesity: role and clinical implication. *Front. Endocrinol. (Lausanne).* 2021;12:585887. DOI: 10.3389/fendo.2021.585887.
29. Ghanbari M., Momen Maragheh S., Aghazadeh A., Mehrjuyan S.R., Hussen B.M., Abdoli Shadbad M. et al.Interleukin-1 in obesity-related low-grade inflammation: from molecular mechanisms to therapeutic strategies. *Int. Immunopharmacol.* 2021;96:107765. DOI: 10.1016/j.intimp.2021.107765.
30. Calabrese L., Fiocco Z., Satoh T.K., Peris K., French L.E. Therapeutic potential of targeting interleukin-1 family cytokines in chronic inflammatory skin diseases. *Br. J. Dermatol.* 2022;186(6):925–941. DOI: 10.1111/bjd.20975.
31. Lee S.H., Park S.Y., Choi C.S. Insulin Resistance: From Mechanisms to Therapeutic Strategies. *Diabetes Metab. J.* 2022;46(1):15–37. DOI: 10.4093/dmj.2021.0280.
32. Zhang H., Zhang X., Wang S., Zheng L., Guo H., Ren Y. et al. Adipocyte-derived exosomal miR-22-3p modulated by circadian rhythm disruption regulates insulin sensitivity in skeletal muscle cells. *J. Biol. Chem.* 2023;299(12):105476. DOI: 10.1016/j.jbc.2023.105476.
33. Ma M., Jiang W., Zhou R. DAMPs and DAMP-sensing receptors in inflammation and diseases. *Immunity.* 2024;57(4):752–771. DOI: 10.1016/j.immuni.2024.03.002.
34. Fahed G., Aoun L., Bou Zerdan M., Allam S., Bou Zerdan M., Bouferraa Y. et al. Metabolic syndrome: updates on pathophysiology and management in 2021. *Int. J. Mol. Sci.* 2022;23(2):786. DOI: 10.3390/ijms23020786.
35. Xiang M., Yin M., Xie S., Shi L., Nie W., Shi B. et al. The molecular mechanism of neutrophil extracellular traps and its role in bone and joint disease. *Heliyon.* 2023;9(12):e22920. DOI: 10.1016/j.heliyon.2023.e22920.
36. Nonokawa M., Shimizu T., Yoshinari M., Hashimoto Y., Nakamura Y., Takahashi D. et al. Association of neutrophil extracellular traps with the development of idiopathic osteonecrosis of the femoral head. *Am. J. Pathol.* 2020;190(11):2282–2289. DOI: 10.1016/j.ajpath.2020.07.008.
37. Li C., Guo H., Han Z., Wang T., Wu D., Yang Z. et al. Association of the systemic immune inflammation index with failure after core decompression for osteonecrosis of the femoral head: a prospective time-to-event analysis. *Ann. Med.* 2025;57(1):2566867. DOI: 10.1080/07853890.2025.2566867.
38. Sánchez-de-Diego C., Pedrazza L., Pimenta-Lopes C., Martinez-Martinez A., Dahdah N., Valer J.A. et al. NRF2 function in osteocytes is required for bone homeostasis and drives osteocytic gene expression. *Redox. Biol.* 2021;40:101845. DOI: 10.1016/j.redox.2020.101845.
39. Szumilas K., Szumilas P., Słuczanowska-Głąbowska S., Zgutka K., Pawlik A. Role of adiponectin in the pathogenesis of rheumatoid arthritis. *Int. J. Mol. Sci.* 2020;21(21):8265. DOI: 10.3390/ijms21218265.
40. Zorena K., Jachimowicz-Duda O., Ślęzak D., Robakowska M.,

Mrugacz M. Adipokines and obesity. Potential link to metabolic disorders and chronic complications. *Int. J. Mol. Sci.* 2020;21(10):3570. DOI: 10.3390/ijms21103570.
41. Al-Mansoori L., Al-Jaber H., Prince M.S., Elrayess M.A. Role of inflammatory cytokines, growth factors and adipokines in adipogenesis and insulin resistance. *Inflammation.* 2022;45(1):31–44. DOI: 10.1007/s10753-021-01559-z.
42. Li C., Cheng H., Adhikari B.K., Wang S., Yang N., Liu W. et al. The role of apelin-APJ system in diabetes and obesity. *Front. Endocrinol. (Lausanne).* 2022;13:820002. DOI: 10.3389/fendo.2022.820002.
43. Fibbi B., Marroncini G., Naldi L., Peri A. The yin and yang effect of the apelinergic system in oxidative stress. *Int. J. Mol. Sci.* 2023;24(5):4745. DOI: 10.3390/ijms24054745.
44. Lebiedzinska-Arciszewska M., Pakula B., Bonora M., Missiroli S., Potes Y., Jakubek-Olszewska P. et al. Distribution of the p66Shc adaptor protein among mitochondrial and mitochondria-associated membranes fractions in normal and oxidative stress conditions. *Int. J. Mol. Sci.* 2024;25(23):12835. DOI: 10.3390/ijms252312835.
45. Li J., Deng C., Liang W., Kang F., Bai Y., Ma B. et al. Mn-containing bioceramics inhibit osteoclastogenesis and promote osteoporotic bone regeneration via scavenging ROS. *Bioact. Mater.* 2021;6(11):3839–3850. DOI: 10.1016/j.bioactmat.2021.03.039.
46. Shimasaki M., Ueda S., Ichiseki T., Hirata H., Kawahara N., Ueda Y. Resistance of bone marrow mesenchymal stem cells in a stressed environment – comparison with osteocyte cells. *Int. J. Med. Sci.* 2021;18(6):1375–1381. DOI: 10.7150/ijms.52104.
47. Marchi S., Guilbaud E., Tait S.W.G., Yamazaki T., Galluzzi L. Mitochondrial control of inflammation. *Nat. Rev. Immunol.* 2023;23(3):159–173. DOI: 10.1038/s41577-022-00760-x.
48. Harapas C.R., Idiiatullina E., Al-Azab M., Hrovat-Schaale K., Reygaerts T., Steiner A. et al. Organellar homeostasis and innate immune sensing. *Nat. Rev. Immunol.* 2022;22(9):535–549. DOI: 10.1038/s41577-022-00682-8.
49. Decout A., Katz J.D., Venkatraman S., Ablasser A. The cGAS-STING pathway as a therapeutic target in inflammatory diseases. *Nat. Rev. Immunol.* 2021;21(9):548–569. DOI: 10.1038/s41577-021-00524-z.
50. Iliushchenko D., Efimenko B., Mikhailova A.G., Shamanskiy V., Saparbaev M.K., Matkarimov B.T. et al. Deciphering the foundations of mitochondrial mutational spectra: replication-driven and damage-induced signatures across chordate classes. *Mol. Biol. Evol.* 2025;42(2):msae261. DOI: 10.1093/molbev/msae261.

Author Information

Poryadin Gennadiy V. – Dr. Sci. (Med.), Professor, Corresponding Member of the RAS, Professor of the Department of Pathophysiology and Clinical Pathophysiology, Pirogov Russian National Research Medical University, Moscow, poryadin_gv@rsmu.ru, http://orcid.org/0000-0003-2010-3296

Zakhvatov Aleksey N. – Dr. Sci. (Med.), Professor, Department of General Surgery named after N. I. Atyasov, National Research Ogarev Mordovia State University, Saransk, zachvatan78@mail.ru, http://orcid.org/0000-0003-1433-0337

Yasnetsov Viktor V. – Dr. Sci. (Med.), Leading Researcher, Head of the Laboratory of Experimental and Clinical Pharmacology, Deputy Head of the Department of Space Radiobiology and Pharmacology; State Research Center of the Russian Federation – Institute of Biomedical Problems of the Russian Academy of Sciences, Moscow, vicyas@yandex.ru, http://orcid.org/0000-0002-6399-3703

Mosina Larisa M. – Dr. Sci. (Med.), Professor, Department of Hospital Therapy, National Research Ogarev Mordovia State University, Saransk, larisamosina97@yandex.ru, http://orcid.org/0000-0001-6831-3116

Khaydar Dalila A. – Assistant, Department of General and Clinical Dentistry; RUDN University, Moscow, dhaidarA@mail.ru, http://orcid.org/0000-0002-8519-3408

Tarasova Tat′yana V. – Dr. Sci. (Biol.), Professor, Department of Psychology; National Research Ogarev Mordovia State University, Saransk, 9023060@mail.ru, http://orcid.org/0000-0001-9745-9739

Zakharkin Il′ya A. – Senior Lecturer, Department of Dentistry; National Research Ogarev Mordovia State University, Saransk, zakharkinas@mail.ru, http://orcid.org/0000-0001-7132-4887

Shaev Aleksey A. – National Research Ogarev Mordovia State University, Saransk, schaev.leha2017@yandex.ru, https://orcid.org/0009-0007-5151-123X

(✉) **Shaev Aleksey A.,** schaev.leha2017@yandex.ru

Received on February 4, 2026;
approved after peer review on February 12, 2026;
accepted on February 26, 2026

УДК 616.61-002.2-047.36-07-082
https://doi.org/10.20538/1682-0363-2026-2-184-190

Chronic Kidney Disease Registries as a Tool for Monitoring, Diagnosis, and Quality Improvement in Medical Care

Yurastova K.A.[1,2], Yarovoy N.D.[2], Bespalova I.D.[1], Teteneva A.V.[1,2]

[1] *Siberian State Medical University*
2 Moskovsky trakt, 634050 Tomsk, Russian Federation

[2] *City Clinical Hospital No. 1*
3 Bela Kun St., 634040 Tomsk, Russian Federation

ABSTRACT

Chronic kidney disease (CKD) is a leading cause of morbidity and mortality worldwide. CKD registries serve as an effective tool for the systematic collection and analysis of data, facilitating early detection, monitoring, and improvement in the quality of medical care. This lectute presents international and Russian experience in using CKD registries, analyzing their structure, variables, and data sources. Particular attention is paid to the organizational and methodological aspects of implementing CKD registries at the regional level. The results of the analysis make it possible to identify key directions for the development and implementation of regional registries. Their maintenance will contribute to increasing the effectiveness of follow-up and, consequently, to improving the epidemiological indicators of socially significant diseases.

Keywords: chronic kidney disease, patient registry, healthcare organization, quality of medical care, epidemiological monitoring

Conflict of interest. The authors declare the absence of obvious or potential conflicts of interest related to the publication of this article.

Source of financing. The authors declare they received no funding for the study.

For citation: Yurastova K.A., Yarovoy N.D., Bespalova I.D., Teteneva A.V. Chronic Kidney Disease Registries as a Tool for Monitoring, Diagnosis, and Quality Improvement in Medical Care. *Bulletin of Siberian Medicine.* 2026;25(2):184–190. https://doi.org/10.20538/1682-0363-2026-2-184-190.

Регистры хронической болезни почек как инструмент мониторинга, диагностики и улучшения качества медицинской помощи

Юрастова К.А.[1, 2], Яровой Н.Д.[2], Беспалова И.Д.[1], Тетенева А.В.[1, 2]

[1] *Сибирский государственный медицинский университет (СибГМУ)*
Россия, 634050, г. Томск, Московский тракт, 2

[2] *Городская клиническая больница № 1 (ГКБ № 1)*
Россия, 634040, г. Томск, ул. Бела Куна, 3

РЕЗЮМЕ

Хроническая болезнь почек (ХБП) является одной из ведущих причин заболеваемости и смертности во всем мире. Регистры ХБП служат эффективным инструментом для систематического сбора и анализа дан-

✉ *Bespalova Inna D.,* innadave@mail2000.ru

ных, что способствует раннему выявлению, мониторингу и повышению качества медицинской помощи. В лекции представлен международный и отечественный опыт использования регистров ХБП, проанализированы их структура, переменные и источники данных. Особое внимание уделено организационно-методическим аспектам внедрения регистров ХБП на региональном уровне. Результаты анализа позволяют определить ключевые направления для разработки и внедрения региональных регистров, ведение будет способствовать повышению эффективности диспансерного наблюдения, и, как следствие, улучшению эпидемиологических показателей социально значимых заболеваний.

Ключевые слова: хроническая болезнь почек, регистр пациентов, организация медицинской помощи, качество медицинской помощи, эпидемиологический мониторинг

Конфликт интересов. Авторы декларируют отсутствие явных и потенциальных конфликтов интересов, связанных с публикацией настоящей статьи.

Источник финансирования. Авторы заявляют об отсутствии финансирования при проведении исследования.

Для цитирования: Юрастова К.А., Яровой Н.Д., Беспалова И.Д., Тетенева А.В. Регистры хронической болезни почек как инструмент мониторинга, диагностики и улучшения качества медицинской помощи. *Бюллетень сибирской медицины.* 2026;25(2):184–190. https://doi.org/10.20538/1682-0363-2026-2-184-190.

INTRODUCTION

Chronic kidney disease (CKD) is a major public health concern, with a prevalence ranging from 11% to 13%, with most cases occurring at stage 3 of the disease [1]. In 2017, the global prevalence of CKD was estimated at 9.1%, corresponding to approximately 700 million cases worldwide [2]. From 1990 to 2017, global mortality attributable to CKD increased by 41.5%, highlighting the need for more active control and preventive strategies [3]. Progression of CKD is associated with a high risk of cardiovascular complications and premature mortality, making it one of the leading causes of death worldwide [3]. The main risk factors for CKD development are diabetes mellitus and arterial hypertension, which account for the majority of cases [4].

In addition, genetic factors, environment, lifestyle, and the availability and quality of healthcare also play a significant role. CKD registries are organized databases that systematize information on this patient population. They play a crucial role in studying epidemiological indicators of the disease, analyzing trends, evaluating treatment effectiveness, and developing preventive strategies. In Russia, as in several other countries, the true prevalence of CKD may be underestimated due to the absence of a unified national registry, which highlights the importance of data systematization and the implementation of regional registries within the healthcare system.

IMPORTANCE OF REGISTRIES FOR THE HEALTHCARE SYSTEM

CKD registries play a crucial role in healthcare systems by enabling systematic collection and analysis of patient data, which contributes to improving medical care, developing prevention strategies, and increasing treatment effectiveness. One of the key objectives of registries is monitoring the epidemiological situation, including assessing the prevalence and trends of CKD across different regions and population groups. This allows for identification of major risk factors and causes of disease development, as well as detection of geographic and socio-demographic differences in morbidity, which is particularly important for developing targeted preventive measures [5].

In addition to epidemiological monitoring, CKD registries provide in-depth analysis of clinical outcomes and trends, enabling tracking of disease progression from early stages to end-stage renal disease. An important task is the evaluation of the effectiveness of different treatment approaches and their impact on patient survival, allowing healthcare professionals to develop optimal management strategies. For example, registry data help determine how successfully patients with different stages of CKD respond to conservative therapy, when initiation of dialysis or kidney transplantation becomes necessary, and how treatment strategies affect prognosis [6].

Furthermore, registries serve an important function in supporting clinical decision-making and healthcare planning. They provide an evidence base for the development of clinical guidelines and standards of care, facilitate optimization of healthcare resource allocation based on real-world patient needs, and support the development of early detection and prevention programs for CKD. For instance, registry data can help identify patient groups at higher risk of rapid disease progression and enable the development of targeted monitoring and treatment strategies for these populations [7].

Comprehensive analysis of registry data and the resulting timely management decisions form the foundation for improving the quality of medical care, including through the implementation of personalized treatment approaches. Patient data allow clinicians to select evidence-based strategies, reducing the risk of complications and improving treatment effectiveness. The implementation of electronic medical registries and integration of big data into clinical practice have made it possible to improve CKD diagnosis and management, identify patients at earlier stages of disease, and adjust therapy according to individual characteristics. These systems also help assess the impact of various treatment approaches on long-term outcomes and improve patients′ quality of life [8].

Thus, CKD registries represent a powerful tool for improving the effectiveness of diagnosis, treatment, and prevention of this condition. They enable identification of risk factors, development of optimal therapeutic strategies, improved planning of healthcare resources, and establishment of an evidence base for informed healthcare management decisions. Through these systems, it becomes possible not only to improve the quality of medical care but also to reduce the overall burden of CKD at the population level, which is particularly important given the increasing global prevalence of the disease.

INTERNATIONAL AND NATIONAL EXPERIENCE IN THE USE OF REGISTRIES FOR CHRONIC KIDNEY DISEASE

One of the most well-known international registries is the United States Renal Data System (USRDS), a national data collection system for patients with end-stage renal disease (ESRD) in the United States. This registry provides valuable information on the prevalence, treatment patterns, mortality, and economic burden of CKD, as well as evaluates the effectiveness of different therapeutic strategies. USRDS data are widely used in scientific research and healthcare policy development, supporting programs for early detection and prevention of the disease [9].

Another major international initiative is the European Renal Association − European Dialysis and Transplant Association (ERA-EDTA) registry, which includes data on patients with CKD across Europe. This registry tracks outcomes in patients undergoing dialysis or kidney transplantation and analyzes factors affecting disease progression. ERA-EDTA actively collaborates with national registries, creating large-scale databases that enable international comparisons and contribute to the development of unified standards of care [10].

CKD.QLD, the chronic kidney disease registry in Australia, should be highlighted among national registries. It was designed to collect data on patients in the pre-dialysis stages of CKD and served as the foundation for the establishment of the Center for Kidney Disease Research in Australia. The registry supports assessment of disease prevalence, identification of risk factors, and development of treatment strategies aimed at reducing the burden of CKD [11].

In Romania, the ReNal national CKD registry collects demographic and clinical data on patients at all stages of the disease. The registry is used to improve the quality of medical care, analyze causes of CKD, and develop prevention programs. Preliminary data indicate that the main causes of CKD in Romania are arterial hypertension and diabetes mellitus, which is consistent with global trends [7]. In the United States, electronic health record-based registry systems are also actively developing, integrating CKD patient data at a national level. Such approaches allow healthcare providers to exchange information efficiently, monitor disease progression, and optimize patient management [8].

In Russia, several registries collect and analyze CKD data at both national and regional levels. However, a unified federal registry focused on early detection and case monitoring of CKD patients is currently lacking. The Russian Dialysis Society maintains a federal registry of patients with end-stage renal disease receiving kidney replacement

therapy (KRT) (https://nephro.ru/index.php?r=site/main). In addition, regional initiatives for CKD monitoring have been implemented. For example, in Yekaterinburg, the Registry of the Kidney Disease and Dialysis Center at City Clinical Hospital No. 40 provides data on CKD prevalence in the region [12].

CKD REGISTRY VARIABLES

CKD registries include a wide range of variables that allow for monitoring of patient status, disease progression, and treatment effectiveness. Demographic data typically include age, sex, ethnicity, body mass index (BMI), and health insurance status [9]. Clinical and laboratory parameters include glomerular filtration rate (GFR), serum creatinine, proteinuria/albuminuria, and concentrations of urea, sodium, potassium, calcium, and phosphorus, as well as hemoglobin levels, blood glucose, and lipid profile indicators [13]. Patient medical history commonly includes the presence of diabetes mellitus, arterial hypertension, cardiovascular diseases, obesity, hyperphosphatemia, and mineral and bone disorders [14].

Information on treatment includes data on medication use (angiotensin-converting enzyme inhibitors, angiotensin II receptor blockers, diuretics, and erythropoiesis-stimulating agents), their dosages, and duration of therapy, as well as information on the use of hemodialysis or peritoneal dialysis and history of kidney transplantation [15]. In addition, CKD registries often capture risk factors, such as smoking status, family history of kidney disease, level of physical activity, and patient-reported quality of life [3]. Collection and analysis of these data allow clinicians and researchers to better understand disease progression, predict outcomes, and develop more effective strategies for treatment and prevention.

DATA SOURCES FOR CKD REGISTRIES

CKD registries are typically developed using information obtained from multiple medical, laboratory, and administrative systems. The primary data sources include healthcare institutions and clinical databases, such as electronic health records, inpatient and outpatient records, and hospital information systems containing patient medical histories, including diagnoses, results of laboratory and instrumental examinations, prescribed treatments, and other clinical information [16]. Laboratory and diagnostic sources include blood and urine test results, such as glomerular filtration rate (GFR), serum creatinine, urea, electrolytes, and the presence and level of albuminuria, as well as data from ultrasound examinations and kidney biopsy findings [13]. Governmental and insurance medical databases also represent important sources of information, providing data on treated patients, prescribed medications, and drug reimbursement programs [3].

Specialized registries of patients receiving dialysis treatment or undergoing kidney transplantation provide detailed information on treatment modality, frequency of procedures, complications, and use of immunosuppressive therapy [15]. Databases on prescribed medications and pharmacotherapy monitoring play an important role in assessing treatment effectiveness, including its impact on creatinine levels and blood pressure control [9]. In addition, patient-reported data and lifestyle information collected through validated questionnaires are increasingly incorporated into registries, along with data obtained from mobile health applications and wearable devices that monitor blood pressure, blood glucose levels, and physical activity. Scientific studies and clinical trials also provide valuable data for evaluating new treatment approaches and understanding epidemiological characteristics of CKD [16]. Comprehensive analysis of these diverse data sources enables not only monitoring of disease progression but also development of personalized treatment strategies and improvement of the quality of healthcare provided to patients with CKD.

CHALLENGES AND LIMITATIONS

Chronic kidney disease registries play an important role in patient monitoring, development of treatment strategies, and healthcare policy planning. However, their implementation and maintenance face several challenges, including issues related to data quality, ethical considerations, and funding. One of the major limitations is incomplete or unreliable data. Studies have shown that registries often suffer from insufficient data standardization and data entry errors [17]. Limited integration with electronic health records may result in duplication of information and inconsistencies across databases [8].

In low- and middle-income countries, maintaining accurate and up-to-date registries is particularly challenging due to limited resources and a shortage of trained personnel [18]. Ethical considerations also represent an important challenge. Issues related to patient data confidentiality and protection of personal information are critical when developing registries. For example, the European pediatric registry CERTAIN maintains high standards of data protection, but this requires substantial resources [19]. Ethical concerns may also arise due to inequalities in access to treatment for patients with CKD in underfunded healthcare systems [20]. Patient participation in research and obtaining informed consent may be difficult, particularly in settings with limited health literacy [21].

Funding is another significant challenge. The development and maintenance of registries require considerable financial investment. In many countries, funding for clinical research and registry maintenance remains limited. For example, in some African countries, only about 7% of research funding is allocated to nephrology-related studies [22]. Unequal distribution of financial resources across regions may lead to disparities in access to high-quality healthcare services [23]. In low-income countries, registry implementation and CKD patient management are often supported primarily through charitable organizations and international grants [24]. Thus, despite the importance of CKD registries in improving the quality of healthcare, their implementation and sustainability require addressing challenges related to data quality, ethical issues, and funding. Improving data standards, strengthening personal data protection, and expanding financial support will contribute to making these registries more effective and accessible.

FUTURE PERSPECTIVES

Modern technologies are opening new horizons for the development of CKD registries, improving diagnosis, monitoring, and personalized treatment of patients. Key perspective directions include digitalization, the application of artificial intelligence, and global initiatives. The implementation of digital healthcare solutions, such as electronic registries, cloud-based platforms, and telemedicine services, significantly simplifies patient monitoring and disease management [25]. Intelligent mobile health applications allow patients to track their health status, receive personalized recommendations, and communicate with healthcare professionals in real time [26]. The development of remote monitoring technologies for patients with CKD improves disease control, reduces the burden on healthcare institutions, and increases access to medical care [27].

The use of artificial intelligence (AI) in data analysis and CKD diagnostics also provides new opportunities. Advances in machine learning and deep learning algorithms enable prediction of renal function decline and support early adaptation of treatment strategies [28]. AI-based systems can analyze kidney biopsy and ultrasound findings to improve CKD staging and increase diagnostic accuracy [29].

Global initiatives in CKD management also play an important role. The creation of international databases and standardized approaches to medical data exchange contributes to more accurate monitoring of disease prevalence and development of effective treatment strategies [30]. Several countries are already implementing national and regional CKD patient registry systems, improving healthcare resource planning and allocation [31]. In the future, global AI-supported monitoring systems for CKD patients may help predict disease burden trends and improve healthcare delivery worldwide [32]. The future of CKD registries is connected with digitalization, the use of AI, and the development of global initiatives. These technologies will facilitate improvements in diagnosis, enhance prognosis accuracy, and make treatment personalized. International cooperation and data standardization also play a crucial role in establishing effective kidney disease management systems.

Analysis of international and Russian experience in maintaining CKD patient registries demonstrates that registries as structured systems for data collection, storage, and analysis represent an effective tool for monitoring patient health status and providing evidence for evaluation of quality of care, healthcare costs, scientific research, and health policy development. They enable not only analysis of disease trends but also the development of personalized treatment approaches, which is particularly important given the increasing global prevalence of CKD. Future research directions include integration of artificial intelligence and machine learning into registry data analysis,

enabling early prediction of disease progression and prevention of adverse outcomes.

Further digitalization and automation of data collection processes will improve data quality and ensure accessibility for the medical community. Global initiatives aimed at data harmonization and development of international registries will enhance comparative analyses across countries and regions, facilitating more efficient healthcare resource management. The establishment and development of regional CKD registries in the Russian Federation may improve long-term patient monitoring, enhance prognosis, and support rational healthcare planning. Thus, the continued development of CKD registries, implementation of advanced technologies, and international collaboration will contribute to improved diagnostics, higher quality of care, and reduction of the overall burden of CKD for both patients and healthcare systems.

CONCLUSION

Characterizing the chronic kidney disease course should become an integral part of the clinical diagnosis based on an appropriate classification system. Such a classification can be an effective tool in clinical practice only if the terms it includes have clear definitions and well-defined boundaries for their proper application. However, despite ongoing discussions regarding the delineation of key concepts and repeated attempts to develop unified positions, experts from leading international professional communities have not yet reached full consensus, and definitions of terms used to describe the course of CKD differ across clinical guidelines.

REFERENCES

1. Hill N.R., Fatoba S.T., Oke J.L., Hirst J.A., O'Callaghan C.A., Lasserson D.S. et al. Global Prevalence of Chronic Kidney Disease – A Systematic Review and Meta-Analysis. *PLoS One.* 2016 Jul 6;11(7):e0158765. DOI: 10.1371/journal.pone.0158765.
2. Cockwell P., Fisher L.A. The global burden of chronic kidney disease. *Lancet.* 2020;395(10225):662–664. DOI: 10.1016/S0140-6736(19)32977-0.
3. GBD Chronic Kidney Disease Collaboration. Global, regional, and national burden of chronic kidney disease, 1990–2017: a systematic analysis for the Global Burden of Disease Study 2017. *Lancet*. 2020;395(10225):709–733. DOI: 10.1016/S0140-6736(20)30045-3.
4. Webster A.C., Nagler E.V., Morton R.L., Masson P. Chronic kidney disease. *Lancet.* 2017;389(10075):1238–1252. DOI: 10.1016/S0140-6736(16)32064-5.
5. Van den Wyngaert I., Mamouris P., Vaes B., Van Pottelbergh G. An exploration of under-registration of chronic kidney disease stages 3-5 in Belgian general practices using logistic regression. *PLoS One*. 2022;17(12):e0279291. DOI: 10.1371/journal.pone.0279291.
6. Jain P., Calvert M., Cockwell P., McManus R.J. The need for improved identification and accurate classification of stages 3-5 chronic kidney disease in primary care: retrospective cohort study. *PLoS One.* 2014;9(8):e100831. DOI: 10.1371/journal.pone.0100831.
7. Peride I., Andronesi A., Niculae A., Căldăraru C., Mihailescu E., Busila I. et al. P0787 the importance and benefits of the predialysis patients – Romanian Experience. *Nephrol. Dial. Transplant.* 2020;35(Suppl.3):gfaa142.P0787. DOI: 10.1093/ndt/gfaa142.P0787.
8. Mendu M.L., Ahmed S., Maron J.K., Rao S.K., Chaguturu S.K., May M.F. et al. Development of an electronic health record-based chronic kidney disease registry to promote population health management. *BMC Nephrol.* 2019;20(1):72. DOI: 10.1186/s12882-019-1260-y.
9. Navaneethan S.D., Jolly S.E., Schold J.D., Arrigain S., Saupe W., Sharp J. et al. Development and validation of an electronic health record-based chronic kidney disease registry. *Clin. J. Am. Soc. Nephrol.* 2011;6(1):40–49. DOI: 10.2215/CJN.04230510.
10. Boenink R., Astley M.E., Huijben J.A., Stel V.S., Kerschbaum J., Ots-Rosenberg M. et al. The ERA Registry Annual Report 2019: summary and age comparisons. *Clin. Kidney J.* 2021;15(3):452–472. DOI: 10.1093/ckj/sfab273.
11. Venuthurupalli S.K., Hoy W.E., Healy H.G., Cameron A., Fassett R.G. CKD.QLD: establishment of a chronic kidney disease [CKD] registry in Queensland, Australia. *BMC Nephrol.* 2017;18(1):189. DOI: 10.1186/s12882-017-0607-5.
12. Nazarov A.V., Zhdanova T.V., Sadykova Yu.R., Nikitina D.V., Serkova V.V. Prevalence of Chronic Kidney Disease according to the Register Centre of Dialisys and Kidney Diseases Clinical Hospital No. 40 MAU in Ekaterinburg. *Nephrology*. 2012;16(3–1):88–92. (In Russ.).
13. Romagnani P., Remuzzi G., Glassock R., Levin A., Jager K.J., Tonelli M. et al. Chronic kidney disease. *Nat. Rev. Dis. Primers.* 2017;3:17088. DOI: 10.1038/nrdp.2017.88.
14. Rucci P., Mandreoli M., Gibertoni D., Zuccalà A., Fantini M.P., Lenzi J. et al. Prevention of Renal Insufficiency Progression (PIRP) Project. A clinical stratification tool for chronic kidney disease progression rate based on classification tree analysis. *Nephrol. Dial. Transplant.* 2014;29(3):603–610. DOI: 10.1093/ndt/gft444.
15. Cantarovich M., Tchervenkov J., Paraskevas S., Ghali P., Wong P., Deschênes M. et al. Early changes in kidney function predict long-term chronic kidney disease and mortality in patients after liver transplantation. *Transplantation.* 2011;92(12):1358–1363. DOI: 10.1097/TP.0b013e3182384aff.
16. Tuot D.S., McCulloch C.E., Velasquez A., Schillinger D., Hsu C.Y., Handley M. et al. Impact of a Primary Care CKD Registry in a US Public Safety-Net Health Care Delivery System: A Pragmatic Randomized Trial. *Am. J. Kidney Dis.* 2018;72(2):168–177. DOI: 10.1053/j.ajkd.2018.01.058.
17. Grams M.E., Plantinga L.C., Hedgeman E., Saran R., Myers G.L., Williams D.E. et al. CDC CKD Surveillance

Team. Validation of CKD and related conditions in existing data sets: A systematic review. *Am. J. Kidney Dis.* 2011;57(1):44–54. DOI: 10.1053/j.ajkd.2010.05.013.
18. Talbot B., Athavale A., Jha V., Gallagher M. Data challenges in addressing chronic kidney disease in low- and lower-middle-income countries. *Kidney Int. Rep.* 2021;6(6):1503–1512. DOI: 10.1016/j.ekir.2021.03.901.
19. Plotnicki L., Kohl C.D., Höcker B., Krupka K., Rahmel A., Pape L. et al. The CERTAIN Registry: a novel, web-based registry and research platform for pediatric renal transplantation in Europe. *Transplant. Proc.* 2013;45(4):1414–1417. DOI: 10.1016/j.transproceed.2013.01.007.
20. Flood D., Wilcox K., Ferro A.A., Mendoza Montano C., Barnoya J., Garcia P. et al. Challenges in the provision of kidney care at the largest public nephrology center in Guatemala: a qualitative study with health professionals. *BMC Nephrol.* 2020;21(1):71. DOI: 10.1186/s12882-020-01732-w.
21. Molnar A.O., Barua M., Konvalinka A., Schick-Makaroff K. Patient engagement in kidney research: opportunities and challenges ahead. *Can. J. Kidney Health Dis.* 2017;4:2054358117740583. DOI: 10.1177/2054358117740583.
22. Okpechi I.G., Alrukhaimi M., Ashuntantang G.E., Bellorin-Font E., Benghanem Gharbi M., Braam B. et al. Global capacity for clinical research in nephrology: a survey by the International Society of Nephrology. *Kidney Int. Suppl.* (2011). 2018;8(2):82–89. DOI: 10.1016/j.kisu.2017.10.012.
23. Bello A.K., Levin A., Tonelli M., Okpechi I.G., Feehally J., Harris D. et al. Assessment of Global Kidney Health Care Status. *JAMA.* 2017;317(18):1864–1881. DOI: 10.1001/jama.2017.4046.
24. Rodriguez R.A., Hsiao L.L., Tucker J.K., Pugsley D. Kidney disease in disadvantaged populations. *Int. J. Nephrol.* 2012;2012:427589. DOI: 10.1155/2012/427589.
25. Canaud B., Davenport A., Leray-Moragues H., Morena-Carrere M., Cristol J.P., Kooman J. et al. Digital Health Support: current status and future development for enhancing dialysis patient care and empowering patients. *Toxins (Basel).* 2024;16(5):211. DOI: 10.3390/toxins16050211.
26. Liu W., Yu X., Wang J., Zhou T., Yu T., Chen X. et al. Improving Kidney Outcomes in Patients with Nondiabetic Chronic Kidney Disease Through an Artificial Intelligence-Based Health Coaching Mobile App: Retrospective Cohort Study. *JMIR Mhealth Uhealth*. 2023;11:e45531. DOI: 10.2196/45531.
27. Yi T.W., Laing C., Kretzler M., Nkulikiyinka R., Legrand M., Jardine M. et al. Digital health and artificial intelligence in kidney research: a report from the 2020 Kidney Disease Clinical Trialists (KDCT) meeting. *Nephrol. Dial Transplant.* 2022;37(4):620–627. DOI: 10.1093/ndt/gfab320.
28. Khan A.H., Khan M.A., Abbas S., Siddiqui S.Y., Saeed M.A., Alfayad M. et al. Simulation, modeling, and optimization of intelligent kidney disease prediction empowered with computational intelligence approaches. *Comput. Mater. Contin.* 2021;67(2):1399–1415. DOI: 10.32604/cmc.2021.014370.
29. Rashidi P., Bihorac A. Artificial intelligence approaches to improve kidney care. *Nat. Rev. Nephrol.* 2020;16(2):71–72. DOI: 10.1038/s41581-019-0243-3.
30. Irish G., Caskey F.J., Davids M.R., Tonelli M., Yang C.W., Arruebo S. et al. Global data monitoring systems and early identification for kidney diseases. *Nephrol. Dial Transplant.* 2024;39(Suppl. 2):ii49–ii55. DOI: 10.1093/ndt/gfae127.
31. See E.J., Alrukhaimi M., Ashuntantang G.E., Bello A.K., Bellorin-Font E., Benghanem Gharbi M. et al. Global coverage of health information systems for kidney disease: availability, challenges, and opportunities for development. *Kidney Int. Suppl.* (2011). 2018;8(2):74–81. DOI: 10.1016/j.kisu.2017.10.011.
32. Wu C.C., Islam M.M., Poly T.N., Weng Y.C. Artificial Intelligence in Kidney Disease: A Comprehensive Study and Directions for Future Research. *Diagnostics (Basel).* 2024;14(4):397. DOI: 10.3390/diagnostics14040397.

Author Information

Yurastova Kristina A. – Assistant, Propaedeutics of Internal Diseases Division with Therapy Course of the Pediatrics Department, Siberian State Medical University; General Practitioner, Head of the Adult Polyclinic, City Clinical Hospital No. 1, Tomsk, kristinarakina@mail.ru, https://orcid.org/0009-0001-1660-1770

Yarovoy Nikolay D. – Statistician Physician, City Clinical Hospital No. 1, Tomsk, koly-yarovoy@yandex.ru, https://orcid.org/0000-0003-3619-6095

Bespalova Inna D. – Dr. Sci. (Med.), Head of the Propaedeutics of Internal Diseases Division with Therapy Course of the Pediatrics Department, Siberian State Medical University, Tomsk, innadave@mail2000.ru, http://orcid.org/0000-0002-4513-6329

Teteneva Anna V. – Dr. Sci (Med.), Professor, Propaedeutics of Internal Diseases Division with Therapy Course of the Pediatrics Department, Siberian State Medical University, Deputy Chief Physician for Clinical and Expert Work of the City Clinical Hospital No. 1, Tomsk, anna.dubodelova@mail.ru, ORCID 0000-0002-4323-2798

(✉) **Bespalova Inna D.,** innadave@mail2000.ru

Received on February 6, 2026;
approved after peer review on February 17, 2026;
accepted on February 26, 2026

Platform Technology Regulation as a Tool for Accelerating Drug Development: Analysis and Prospects for Russia

Galyamova M.R.[1], Valieva O.V.[2, 3], Andrianov V.V.[1, 4], Osipenko A.N.[5], Alexandrovich E.A.[1, 3], Popova M.A.[1]

[1] Center for the National Technology Initiative HealthNet (NTI Healthnet)
12 Nikolaev St., 630090 Novosibirsk, Russian Federation

[2] Institute of Economics and Industrial Engineering, Siberian Branch of the Russian Academy of Sciences
17 Acad. Lavrentiev Ave., 630090 Novosibirsk, Russia

[3] Novosibirsk State University (NSU)
1 Pirogov St., 630090 Novosibirsk, Russian Federation

[4] JSC R-Pharm
19/1 Berzarin St., 123154 Moscow, Russian Federation

[5] Siberian State Medical University
2 Moskovsky trakt, 634050 Tomsk, Russian Federation

ABSTRACT

The **aim** of this study was to demonstrate the potential of the platform approach in the regulation of biotechnological drug development supported by specific examples and case studies from FDA practice. The study examines the Platform Technology Designation Program (PTDD) of the U.S. Food and Drug Administration (FDA) launched in 2024. This program serves as a regulatory mechanism for granting platform technology status and has practical value for accelerating drug development and review through the justified data reuse. Obtaining platform technology status entitles the developer to partially reuse CMC (Chemistry, Manufacturing, and Controls) data from an already approved drug when submitting applications for subsequent products based on the same backbone.

The article discusses the mechanisms for granting such status, examples from FDA practice, as well as Russian companies possessing similar technologies and the potential for their development. Based on the analysis, a conclusion is drawn regarding the feasibility of implementing similar regulatory mechanisms in Russia.

Keywords: platform technology, FDA, PTDD, gene therapy, CAR-T, AAV vectors, regulatory review, NTI Healthnet

Conflict of interest. The authors declare the absence of obvious or potential conflicts of interest related to the publication of this article.

Source of financing. This publication was prepared with the support of the Technopark of Novosibirsk Akademgorodok Foundation (Scientific and Technological Park of Novosibirsk Akademgorodok) participating in the National Technology Initiative with the support of the National Technology Initiative (NTI) Project Support Fund and the Ministry of Industry and Trade of the Russian Federation as part of the Program for the Development of the HealthNet direction of the National Technology Initiative.

For citation: Galyamova M.R., Valieva O.V., Andrianov V.V., Osipenko A.N., Alexandrovich E.A., Popova M.A. Platform Technology Regulation as a Tool for Accelerating Drug Development: Analysis and Prospects for Russia. *Bulletin of Siberian Medicine.* 2026;25(2):192–194. https://doi.org/10.20538/1682-0363-2026-2-191-194.

✉ *Valieva Olga V.,* innadave@mail2000.ru

Программа по регулированию платформенных технологий как инструмент ускорения разработки лекарственных средств: анализ и перспективы для России

Галямова М.Р.[1], Валиева О.В.[2, 3], Андрианов В.В.[1, 4], Осипенко А.Н.[5], Александрович Е.А.[1, 3], Попова М.А.[1]

[1] *Центр национальной технологической инициативы по направлению «Хелснет»*
Россия, 630090, г. Новосибирск, ул. Николаева, 12

[2] *Институт экономики и организации промышленного производства (ИЭОПП) СО РАН*
Россия, 630090, г. Новосибирск, ул. Акад. Лаврентьева, 17

[3] *Новосибирский государственный университет (НГУ)*
Россия, 630090, г. Новосибирск, ул. Пирогова,1

[4] *Акционерное общество (АО) «Р-Фарм»*
Россия, 123154, г. Москва, ул. Берзарина, 19/ 1

[5] *Сибирский государственный медицинский университет (СибГМУ)*
Россия, 634050, г. Томск, Московский тракт, 2

РЕЗЮМЕ

Цель работы: продемонстрировать возможности платформенного подхода в регулировании биотехнологических разработок фармацевтических препаратов, подкрепив это конкретными примерами и кейсами из практики FDA. В исследовании разбирается программа PTDD (Platform Technology Designation Program) Управления по санитарному надзору за качеством пищевых продуктов и медикаментов США (Food and Drug Administration), запущенной в 2024 г. в США. Эта программа выполняет роль регуляторного механизма присвоения статуса платформенной технологии и имеет практическое значение для ускорения разработки и экспертизы лекарственных средств за счет обоснованного переиспользования данных. Получение статуса «платформенной технологии» дает разработчику право частично переиспользовать данные CMC (Chemistry, Manufacturing, Controls) от уже зарегистрированного препарата при подаче заявок на последующие продукты на той же «матрице».

Представлены механизмы присвоения такого статуса, примеры из практики FDA, а также российские компании, имеющие похожие технологии и потенциал их развития. На основании анализа делается вывод о целесообразности использования в России аналогичных регуляторных механизмов.

Ключевые слова: платформенная технология, FDA, PTDD, генная терапия, CAR-T, AAV-векторы, регуляторная экспертиза, НТИ Хелснет

Конфликт интересов. Авторы декларируют отсутствие явных и потенциальных конфликтов интересов, связанных с публикацией настоящей статьи.

Источники финансирования. Публикация подготовлена при поддержке Фонда «Научно-технологический парк Новосибирского Академгородка», участвующем в Национальной технологической инициативе при поддержке Фонда поддержки проектов Национальной технологической инициативы и Министерства промышленности и торговли Российской Федерации, в рамках реализации Программы по развитию отдельного направления Национальной технологической инициативы «Хелснет».

Для цитирования: Галямова М.Р., Валиева О.В., Андрианов В.В., Осипенко А.Н., Александрович Е.А., Попова М.А. Программа по регулированию платформенных технологий как инструмент ускорения разработки лекарственных средств: анализ и перспективы для России. *Бюллетень сибирской медицины.* 2026;25(2):191–194. https://doi.org/10.20538/1682-0363-2026-2-191-194.

INTRODUCTION

The modern pharmaceutical industry faces a systemic challenge: the cost of bringing an innovative drug to market exceeds $2–3 billion, and development timelines are 10–15 years. The traditional «one compound – one product» model is becoming economically unsustainable, particularly in the development of drugs for orphan diseases and cancers, gene therapy, and personalized medicine.

The response to this challenge has been the platform approach – the creation of reproducible technological systems that standardize processes from preclinical studies to market approval, minimize data duplication, and ensure manufacturing scalability. Platforms represent a solution relevant to developers, regulators, and the entire industry alike. They provide a technological breakthrough that could transition drug manufacturing to a «conveyor» mode in biopharmaceutical development. A more detailed review is presented in the analytical report «Review of the FDA Platform Technology Designation Program for Drug Development» prepared by experts from the NTI Healthnet Infrastructure Center [1].

In 2024, the U.S. Food and Drug Administration (FDA) launched the Platform Technology Designation Program (PTDD). The program is established by Section 506K of the U.S. Food, Drug, and Cosmetic Act (FD&C Act) [2] and is described by the FDA as part of the implementation of the PREVENT Pandemics Act (enacted as part of the major 2023 law). The program was conceived, in part, as a means to accelerate the scaling of platform technology development (e.g., for infectious threats), but the mechanism itself is broader as it applies to drugs and biologics with a repeating technological architecture. It is important to note that this is only a draft guidance that outlines Section 506K of the FD&C Act and contains recommendations that are not legally binding.

The PTDD program aims to improve the efficiency of drug development, manufacturing, and regulatory review. According to FDA guidance (May 2024), designation may be granted to a technology that is «well-understood and reproducible,» essential to the structure or function of the drug, applicable to more than one product, and facilitates manufacturing through standardized processes.

Key criteria to be granted platform technology designation:

– the technology must be embedded into the drug and essential to its structure or function;

– the technology must be usable across multiple products sharing common structural elements (demonstrable technological commonality);

– the technology must facilitate the development and manufacturing of multiple products through a standardized process (if each product requires a fully unique process, platform status collapses).

The FDA reviews the request within 90 days. The designation does not automatically grant access to expedited approval programs but provides advantages: early consultations with the regulator, the ability to reuse stability and preclinical safety data, and consideration of prior manufacturing facility inspections.

CASE STUDY ANALYSIS: SAREPTA THERAPEUTICS AND KRYSTAL BIOTECH

PTDD practice includes two officially known cases of designation. The case of Sarepta Therapeutics (June 2025) was landmark: the company received designation for the AAV vector rAAVrh74 used in the drug Elevidys (Duchenne muscular dystrophy) and the experimental SRP-9003. However, in July 2025, after three patients died from acute liver failure, the FDA revoked the designation, calling into question the platform's reliability. This precedent demonstrated that platform status is not a «permanent benefit» but a mechanism with feedback loops: new safety data can nullify previously recognized tolerability. Ultimately, Elevidys remained approved, but with safety updates [3].

In October 2025, Krystal Biotech successfully utilized the FDA's Platform Technology Designation. The company received it for a non-replicating HSV-1-vector used in the drug Vyjuvek (epidermolysis bullosa). The platform was then applied to KB801 eye drops for the treatment of neurotrophic keratitis, which confirmed the reproducibility of the technology across different tissues and local delivery forms. The company views PTDD as an opportunity to accelerate the development pipeline of genetic medicines [4].

POTENTIAL PLATFORM TECHNOLOGIES IN RUSSIA

The Russian biotechnology market has formed a pool of companies and research centers developing products based on platform solutions including:

Artgen Biotech PJSC – the Betusphere (betulin) recombinant protein vaccine platform and the Nextgen gene therapy platform (plasmid DNA for therapeutic angiogenesis);

BIOCAD JSC – MabNEXT (recombinant antibodies) and GeneNEXT (AAV vectors for gene therapy of hemophilia B) platforms;

Federal State Budgetary Institution National Medical Research Center for Hematology — a

hospital-based CAR-T production platform (drug Utzhefra);

Federal State Budgetary Institution National Medical Research Radiological Center with partners — a personalized mRNA vaccine platform (Neoonkovac).

The analysis reveals that although Russia already possesses the technological foundations for platform-based regulation, it still lacks a formal equivalent of the PTDD.

CONCLUSION

The FDA PTDD program represents an innovative regulatory tool that translates the platform approach from a scientific concept into a formalized evidence regime. The Sarepta case demonstrated the vulnerability of the designation to new safety data, while the Krystal case showed its promise for local and repeat-dose therapies. For Russia, it is critically important not to copy the American experience but to develop an adapted national program, building on existing technological groundwork (AAV, mRNA, and CAR-T) and current mechanisms (hospital exemption and conditional approval). A pilot project lasting 1.5–2 years would allow for refining the criteria for platform qualification and data reuse, which would become the basis for harmonizing regulation within the EAEU and achieving technological sovereignty in biopharmaceuticals.

REFERENCES

1. The Analysis of Platform Technology Regulation in Biomedicine, NTI HealthNet, May 31, 2026. URL: https://healthnet.academpark.com/analytics/analiz-regulirovaniya-platformennyh-tehnologij-v-biomediczine/ (In Russ.)
2. FEDERAL FOOD, DRUG, AND COSMETIC ACT. As Amended Through P.L. 119–175, Enacted February 3, 2026. URL: https://www.govinfo.gov/content/pkg/COMPS-973/pdf/COMPS-973.pdf
3. ELEVIDYS, FDA, 11/14/2025. URL: https://www.fda.gov/vaccines-blood-biologics/tissue-tissue-products/elevidys
4. FDA Grants Krystal Biotech Platform Technology Designation, Marking Strategic Shift in Gene Therapy Oversight. URl: https://fairsonline.org/fda-grants-krystal-biotech-platform-technology-designation-marking-strategic-shift-gene-therapy

Author Information

Galyamova Maria R. – Head of the Center for National Technological Initiative in the HealthNet Direction, Novosibirsk, maria@mgalyamova.ru

Valieva Olga V. – Cand. Sci. (Econ.), Senior Researcher, Institute of Economics and Industrial Engineering, Siberian Branch of the Russian Academy of Sciences; Associate Professor, Department of Management, NSU, Novosibirsk, o_valieva@mail.ru, https://orcid.org/0000-0002-7831-0581

Andrianov Vladimir V. – Director of Partnerships, Deputy Leader of the NTI HealthNet Working Group; R-Pharm JSC, Moscow, Andrianov@rpharm.ru

Osipenko Anton N. – Assistant Professor, Pharmacology Division, Siberian State Medical University, Tomsk, osipenko.an@ssmu.ru, https://orcid.org/0000-0002-4763-3214

Aleksandrovich Elizaveta A. – Expert, Center for National Technological Initiative in the HealthNet Direction; Institute of Medical and Technical Technologies, NSU, Novosibirsk, eksandrovich@g.nsu.ru

Popova Maria A. – Expert, Center for National Technological Initiative in the HealthNet Direction, Novosibirsk, karma.m.p.@ya.ru

(✉) **Valieva Olga V.,** o_valieva@mail.ru

Received on June 10, 2026

СИБИРСКИЙ ГОСУДАРСТВЕННЫЙ МЕДИЦИНСКИЙ УНИВЕРСИТЕТ

МИНИСТЕРСТВО ЗДРАВООХРАНЕНИЯ РОССИЙСКОЙ ФЕДЕРАЦИИ

ФЕДЕРАЛЬНОЕ ГОСУДАРСТВЕННОЕ БЮДЖЕТНОЕ ОБРАЗОВАТЕЛЬНОЕ УЧРЕЖДЕНИЕ ВЫСШЕГО ОБРАЗОВАНИЯ «СИБИРСКИЙ ГОСУДАРСТВЕННЫЙ МЕДИЦИНСКИЙ УНИВЕРСИТЕТ» МИНИСТЕРСТВА ЗДРАВООХРАНЕНИЯ РОССИЙСКОЙ ФЕДЕРАЦИИ

Кафедра факультетской терапии с курсами эндокринологии и клинической фармакологии

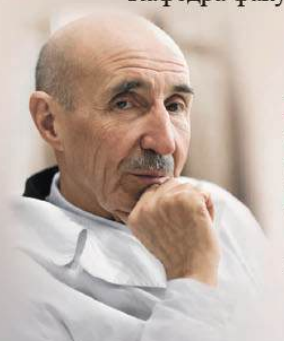

ИНФОРМАЦИОННОЕ ПИСЬМО-ПРИГЛАШЕНИЕ

ВСЕРОССИЙСКАЯ НАУЧНО-ПРАКТИЧЕСКАЯ КОНФЕРЕНЦИЯ «СИБИРСКАЯ ТЕРАПЕВТИЧЕСКАЯ ШКОЛА: ИСТОКИ И ПЕРСПЕКТИВЫ», ПОСВЯЩЁННАЯ **130-ЛЕТИЮ СО ДНЯ РОЖДЕНИЯ АКАДЕМИКА АМН СССР Д.Д. ЯБЛОКОВА**

г. Томск, 19–20 ноября 2026 г.

Уважаемые коллеги!

Приглашаем принять активное участие в работе Всероссийской научно-практической конференции «Сибирская терапевтическая школа: истоки и перспективы», посвящённой 130-летию со дня рождения академика АМН СССР Дмитрия Дмитриевича Яблокова (13.11.1896 – 18.02.1993 гг.), которая состоится в гибридном формате в г. Томске с 19 по 20 ноября 2026 года.

Конференция станет профессиональной площадкой, объединившей специалистов из разных регионов РФ в сфере практического здравоохранения, ведущих ученых, педагогов и общественных деятелей для всестороннего обсуждения инициатив совершенствования медицинской помощи взрослому населению, обмена опытом и выработки конструктивных решений, направленных на сохранение и укрепление здоровья населения.

Научная программа конференции охватывает широкий спектр актуальных тем, включая вопросы организации и совершенствования медицинской помощи взрослому населению, а также практические шаги к решению ключевых проблем.

Программа конференции аккредитована в системе непрерывного медицинского образования на сайте Министерства здравоохранения РФ (1 день участия в работе конференции - 6 баллов, всего 12 баллов). Получить баллы смогут врачи из любых регионов РФ.

Участие в конференции бесплатное. В рамках конференции состоится конкурс молодых учёных. Итоги конкурса будут объявлены на церемонии закрытия конференции –20.11.2026,

В завершение конференции 20.11.2026 состоится презентация книги, посвященной академику Д.Д. Яблокову

НАУЧНЫЕ НАПРАВЛЕНИЯ КОНФЕРЕНЦИИ

Терапия	Эндокринология	Кардиология
Ревматология	Пульмонология	Гастроэнтерология
Фтизиатрия	Физиотерапия и курортология	Рентгенология
Профессиональная медицинская коммуникация		

ОРГАНИЗАТОРЫ:

ФГБОУ ВО «Сибирский государственный медицинский университет» Минздрава России, кафедра факультетской терапии с курсами эндокринологии и клинической фармакологии

ОРГАНИЗАЦИОННЫЙ КОМИТЕТ:

Председатель – Долгалёв Игорь Владимирович, доктор медицинских наук, профессор, заведующий кафедрой факультетской терапии с курсами эндокринологии и клинической фармакологии.

Заместитель председателя – Саприна Татьяна Владимировна, доктор медицинских наук, врач эндокринолог, заведующий эндокринологическим отделением клиник, профессор кафедры факультетской терапии с курсами эндокринологии и клинической фармакологии, руководитель НКЦ

ВРЕМЯ И МЕСТО ПРОВЕДЕНИЯ:

г. Томск, 19.11.2026 – Московский тракт, 2, главный корпус СибГМУ, актовый зал
Время регистрации с 8.30 до 8.55. Время конференции с 9.00 до 18.00.
20.11. 2026 – ул.Советская 45, Дом учёных, время: с 9.00 до 18.00 часов
Онлайн-трансляция состоится на web-платформе Pruffme.com

Ссылки для подключения:
Актовый зал https://pruffme.com/landing/u4767539/tmp1773826184
Башенная аудитория https://pruffme.com/landing/u4767539/tmp1774234830

КОНТАКТЫ: E-mail: kaf.fak.ter@ssmu.ru. Тел.: +7 (3822)901-101 доп. 1902

С уважением, ОРГКОМИТЕТ

bulletin.ssmu.ru

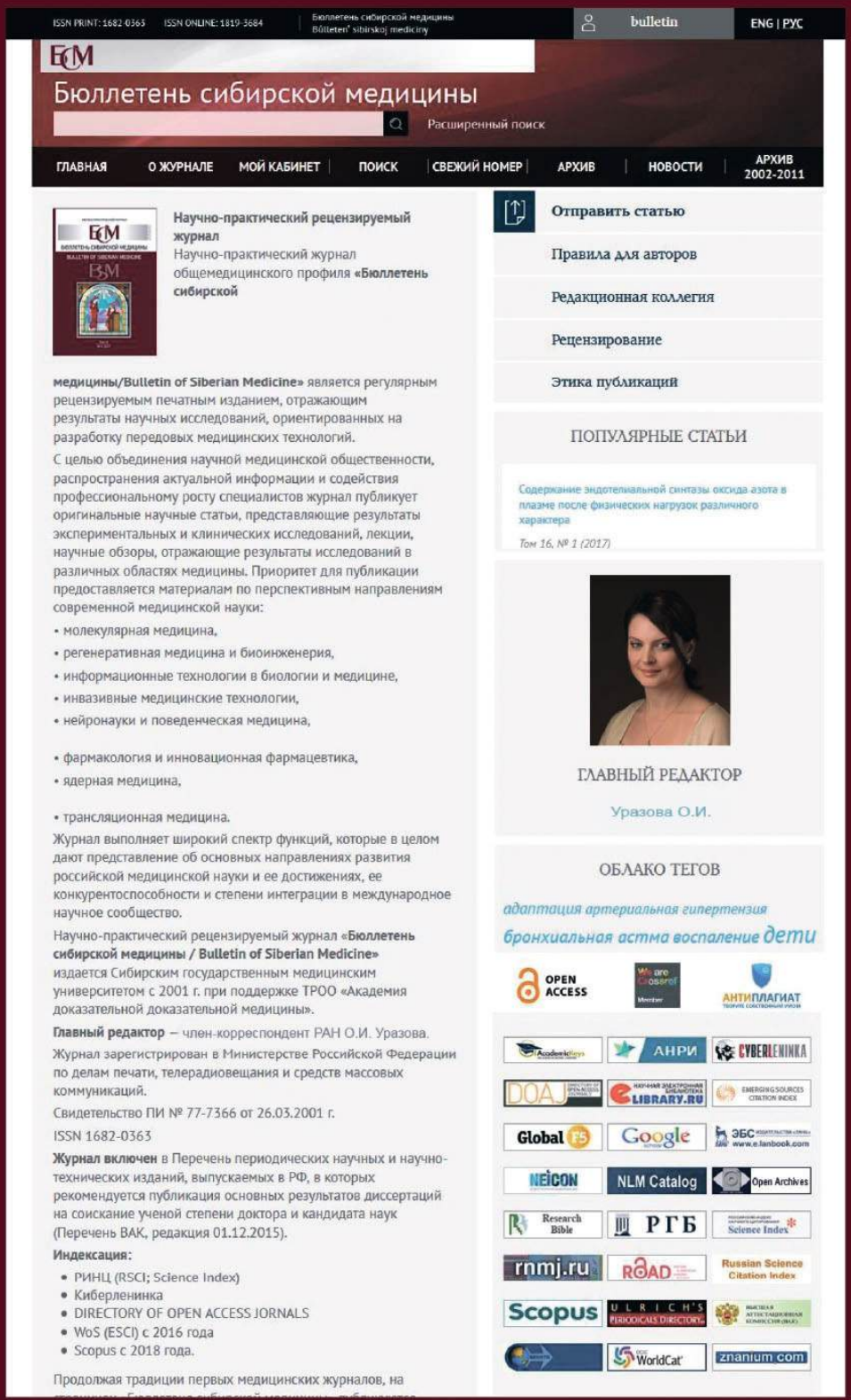

ISSN 1682-0363 (print)
ISSN 1819-3684 (online)
БЮЛЛЕТЕНЬ СИБИРСКОЙ МЕДИЦИНЫ
2026. Т. 25. № 2. 1–194